frontiers | Research Topics

Crosstalk between cancer-associated fibroblasts and tumor cells in the tumor microenvironment: An emerging target of anti-cancer immunotherapy

Edited by
Bo Kong, Rong Hu, Runbin Sun and Qianming Du

Published in
Frontiers in Pharmacology
Frontiers in Oncology
Frontiers in Immunology

ISSN 1664-8714
ISBN 978-2-8325-3270-6
DOI 10.3389/978-2-8325-3270-6

About Frontiers

Frontiers is more than just an open access publisher of scholarly articles: it is a pioneering approach to the world of academia, radically improving the way scholarly research is managed. The grand vision of Frontiers is a world where all people have an equal opportunity to seek, share and generate knowledge. Frontiers provides immediate and permanent online open access to all its publications, but this alone is not enough to realize our grand goals.

Frontiers journal series

The Frontiers journal series is a multi-tier and interdisciplinary set of open-access, online journals, promising a paradigm shift from the current review, selection and dissemination processes in academic publishing. All Frontiers journals are driven by researchers for researchers; therefore, they constitute a service to the scholarly community. At the same time, the *Frontiers journal series* operates on a revolutionary invention, the tiered publishing system, initially addressing specific communities of scholars, and gradually climbing up to broader public understanding, thus serving the interests of the lay society, too.

Dedication to quality

Each Frontiers article is a landmark of the highest quality, thanks to genuinely collaborative interactions between authors and review editors, who include some of the world's best academicians. Research must be certified by peers before entering a stream of knowledge that may eventually reach the public - and shape society; therefore, Frontiers only applies the most rigorous and unbiased reviews. Frontiers revolutionizes research publishing by freely delivering the most outstanding research, evaluated with no bias from both the academic and social point of view. By applying the most advanced information technologies, Frontiers is catapulting scholarly publishing into a new generation.

What are Frontiers Research Topics?

Frontiers Research Topics are very popular trademarks of the *Frontiers journals series*: they are collections of at least ten articles, all centered on a particular subject. With their unique mix of varied contributions from Original Research to Review Articles, Frontiers Research Topics unify the most influential researchers, the latest key findings and historical advances in a hot research area.

Find out more on how to host your own Frontiers Research Topic or contribute to one as an author by contacting the Frontiers editorial office: frontiersin.org/about/contact

Crosstalk between cancer-associated fibroblasts and tumor cells in the tumor microenvironment: An emerging target of anti-cancer immunotherapy

Topic editors

Bo Kong — Rutgers University, Newark, United States
Rong Hu — China Pharmaceutical University, China
Runbin Sun — Nanjing Drum Tower Hospital, China
Qianming Du — Nanjing Medical University, China

Citation

Kong, B., Hu, R., Sun, R., Du, Q., eds. (2023). *Crosstalk between cancer-associated fibroblasts and tumor cells in the tumor microenvironment: An emerging target of anti-cancer immunotherapy*. Lausanne: Frontiers Media SA.
doi: 10.3389/978-2-8325-3270-6

Table of contents

frontiers | Frontiers in Pharmacology

TYPE Editorial
PUBLISHED 04 August 2023
DOI 10.3389/fphar.2023.1256643

OPEN ACCESS

EDITED AND REVIEWED BY
Olivier Feron,
Université Catholique de Louvain,
Belgium

*CORRESPONDENCE
Qianming Du,
duqianming@njmu.edu.cn
Rong Hu,
ronghu@cpu.edu.cn

†These authors have contributed equally to this work

RECEIVED 11 July 2023
ACCEPTED 31 July 2023
PUBLISHED 04 August 2023

CITATION
Zhang C, Sun R, Kong B, Hu R and Du Q (2023), Editorial: Crosstalk between cancer-associated fibroblasts and tumor cells in the tumor microenvironment: an emerging target of anti-cancer immunotherapy.
Front. Pharmacol. 14:1256643.
doi: 10.3389/fphar.2023.1256643

Editorial: Crosstalk between cancer-associated fibroblasts and tumor cells in the tumor microenvironment: an emerging target of anti-cancer immunotherapy

Chunxue Zhang[1†], Runbin Sun[2,3†], Bo Kong[4†], Rong Hu[5*] and Qianming Du[6*]

[1]School of Basic Medicine and Clinical Pharmacy, China Pharmaceutical University, Nanjing, China, [2]Phase I Clinical Trials Unit, Nanjing Drum Tower Hospital, Affiliated Hospital of Medical School, Nanjing University, Nanjing, China, [3]Nanjing Drum Tower Hospital, Clinical College of Nanjing, University of Chinese Medicine, Nanjing, China, [4]Department of Pharmacology and Toxicology, Rutgers, The State University of New Jersey, Piscataway, NJ, United States, [5]State Key Laboratory of Natural Medicines, Department of Physiology, China Pharmaceutical University, Nanjing, Jiangsu, China, [6]General Clinical Research Center, Nanjing First Hospital, Nanjing Medical University, Nanjing, China

KEYWORDS

tumor microenvironment (TME), cancer-associated fibroblasts (CAFs), immune cells, CAF-targeted therapy, cancer

Editorial on the Research Topic
Crosstalk between cancer-associated fibroblasts and tumor cells in the tumor microenvironment: an emerging target of anti-cancer immunotherapy

Extensive researches have been conducted on Cancer Associated Fibroblasts (CAFs) during the past several years. As a key component of the tumor microenvironment with crucial functions, CAFs regulate tumor progression, malignant transformation and immune response by interacting with tumor cells and the other cellular components. Extensive studies on CAFs will help to discover new targets for individualized treatments.

This Research Topic, titled "*Crosstalk Between Cancer-Associated Fibroblasts and Tumor Cells in the Tumor Microenvironment: An Emerging Target of Anti-cancer Immunotherapy*," focuses on the roles of specific subpopulations of CAFs in different types of tumors. Although most studies have highlighted the tumor-promoting effects of CAFs in this Research Topic, it is worth to note that CAFs exhibit various phenotypes and functions in different tumor types and individuals. Further investigations on these subgroup identification and functional characterization, and the associated potential therapeutic targets will benefit the development of targeted therapeutic strategies and the efficacy of cancer treatment. In this Research Topic, Zhang et al. conducted a comprehensive analysis by integrating multiple single-cell RNA sequencing (scRNA-seq) datasets from various tumors and adjacent normal tissues, which discovered that COL11A1$^+$ fibroblasts only present in tumor tissue but not normal tissue fibroblasts. These fibroblasts might promote tumor progression by regulating extracellular matrix (ECM) remodeling and anti-tumor

10.3389/fphar.2023.1256643

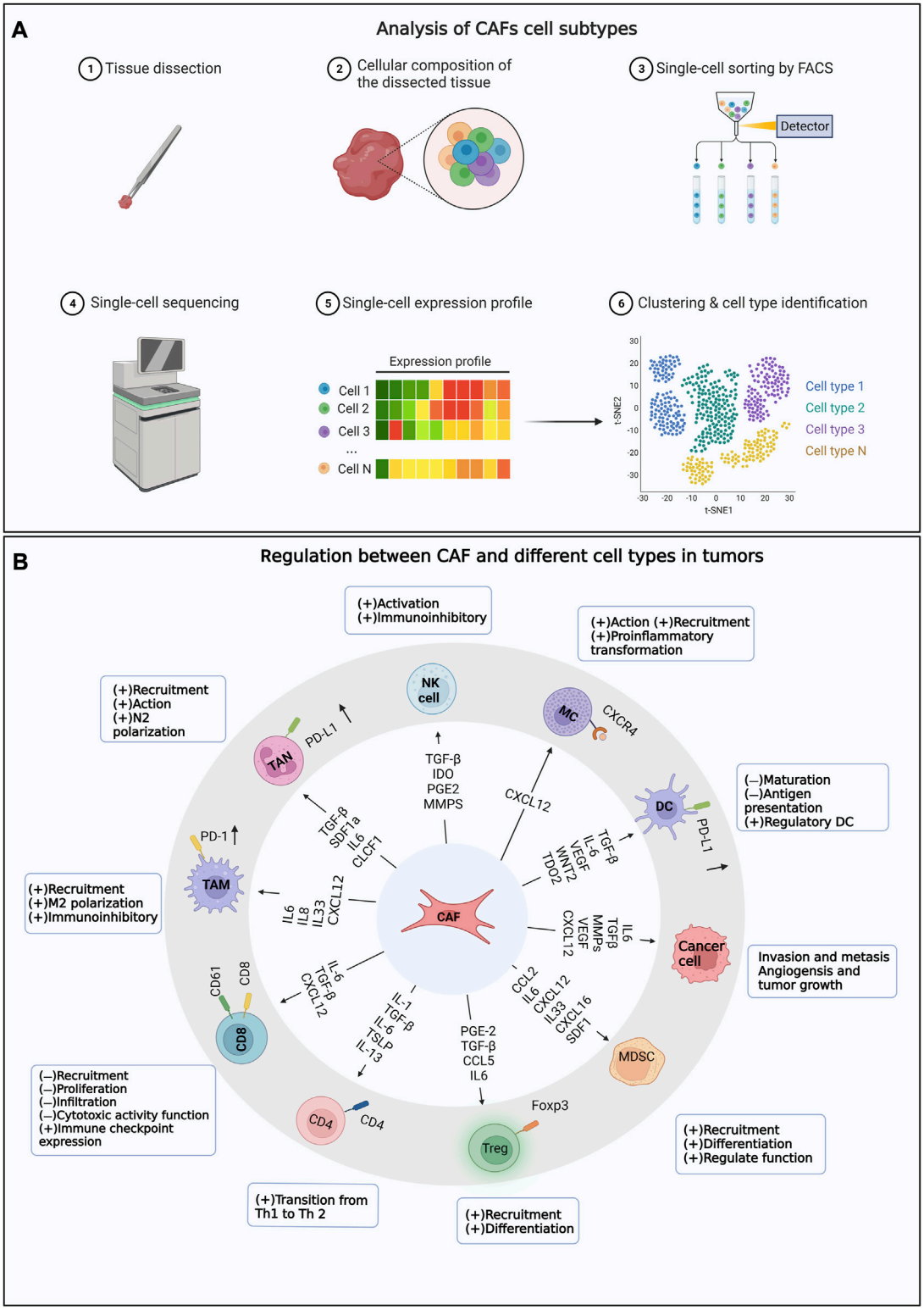

FIGURE 1
The Research Topic mainly includes the content. **(A)** Analysis of CAFs cell subtypes. **(B)** Regulation between CAF and different cell types in tumors.

immune response (Zhang et al.). Research has shown that CAFs exhibit multiple functions in epithelial ovarian cancer and are closely related to tumor progression. Zou et al. identified multiple subtypes of CAFs through extensive tumor data analysis and found that these subtypes are closely related to the clinical outcomes and immunotherapy response of epithelial ovarian cancer. This breakthrough enhances the understanding of CAF heterogeneity in ovarian cancer and provides guidance for

personalized treatment (Zou et al.). In addition, Zhihao et al. revealed that there are differences in the expression of CAFs subtypes and pathways in Osteosarcoma, and these differences are related to tumor progression and immunosuppression (Zhihao et al.). These studies expand our understanding of the tumor diversity and complexity, and provide new insights into specific CAF subgroups. Through the integration of data from multiple cancer types, researchers discovered that NT5E is associated with upregulated expression of CAFs in various cancers, potentially serving as a novel prognostic biomarker linked to specific tumor microenvironments. The increased expression of NT5E may be related to enhanced epithelial-mesenchymal transition (EMT) function in CAFs, presenting new possibilities for immunotherapy by targeting CAFs with high NT5E expression (Xue et al.). Similarly, in gastrointestinal cancer, RAB6B shows promise as a prognostic marker associated with alterations in the tumor immune microenvironment (Peng et al.). These findings contribute to the identification of new prognostic markers crucial for assessing tumor prognosis and individualized treatment.

This Research Topic also covers recent advances in the functions of CAFs' in tumor progression and treatment. CAFs influence tumor cell proliferation, migration, and invasive capabilities through secreted growth factors, extracellular matrix remodeling, and immune regulation (Wu et al.). For instance, CAFs derived from cholangiocarcinoma (CCA) promote cell viability and enhance gemcitabine resistance in CCA cells by activating IL-6/STAT3 signaling. Inhibition of IL-6R on CCA cells using tocilizumab, an IL-6R humanized antihuman monoclonal antibody, impedes the CAF-CCA interaction, leading to increased gemcitabine sensitivity in CCA cells (Kittirat et al.). Halofuginone inhibits migration and invasion of oral squamous cell carcinoma (OSCC) by targeting CAFs, reducing the malignancy of CAFs, and decreasing the viability and proliferation of OSCC-derived CAFs (Wang et al.).

Current advances regarding the efficacy of immunotherapy by targeting CAFs are also included in this Research Topic. A systematic review and meta-analysis demonstrated the effectiveness of PD-1 inhibitors in treating recurrent/metastatic nasopharyngeal carcinoma, particularly in patients with CAF infiltration, suggesting the influence of CAFs on immunotherapy (Yan et al.). The overview of possible therapeutic strategies including inhibition of CAFs' immunomodulatory function, suppression of immunosuppressive factors produced by CAFs, and modification of the extracellular matrix secreted by CAFs are discussed by Zhang et al.

In summary, CAFs play crucial roles in tumor progression and treatment. Extensive studies on CAFs facilitate the understanding of tumor biology, identification of new prognostic markers, and development of novel therapeutic strategies as well. However, further researches are necessary to broaden the understanding of CAF functions and regulatory mechanisms for better cancer therapy. The main content of the research topic is shown in Figure 1.

Author contributions

CZ: Writing–original draft, Writing–review and editing. RS: Writing–original draft, Writing–review and editing. BK: Supervision, Validation, Writing–review and editing. RH: Supervision, Writing–review and editing. QD: Writing–original draft, Writing–review and editing.

Conflict of interest

The authors declare that the research was conducted in the absence of any commercial or financial relationships that could be construed as a potential conflict of interest.

Publisher's note

frontiers | Frontiers in Immunology

TYPE Original Research
PUBLISHED 10 August 2022
DOI 10.3389/fimmu.2022.956224

OPEN ACCESS

EDITED BY
Antonella Sistigu,
Agostino Gemelli University Polyclinic (IRCCS), Italy

REVIEWED BY
Mei Luo,
Huazhong University of Science and Technology, China
Qianming Du,
Nanjing Medical University, China

*CORRESPONDENCE
Hongda Ding
dhd1987@163.com
Liangqing Yao
yaoliangqing@163.com

SPECIALTY SECTION
This article was submitted to Cancer Immunity and Immunotherapy, a section of the journal Frontiers in Immunology

RECEIVED 30 May 2022
ACCEPTED 15 July 2022
PUBLISHED 10 August 2022

CITATION
Zou R, Jiang Q, Jin T, Chen M, Yao L and Ding H (2022) Pan-cancer analyses and molecular subtypes based on the cancer-associated fibroblast landscape and tumor microenvironment infiltration characterization reveal clinical outcome and immunotherapy response in epithelial ovarian cancer. *Front. Immunol.* 13:956224. doi: 10.3389/fimmu.2022.956224

Pan-cancer analyses and molecular subtypes based on the cancer-associated fibroblast landscape and tumor microenvironment infiltration characterization reveal clinical outcome and immunotherapy response in epithelial ovarian cancer

Ruoyao Zou[1], Qidi Jiang[1], Tianqiang Jin[2], Mo Chen[1], Liangqing Yao[1]* and Hongda Ding[2]*

[1]Department of Gynecologic Oncology, Obstetrics and Gynecology Hospital of Fudan University, Shanghai, China, [2]Department of General Surgery, ShengJing Hospital of China Medical University, Shenyang, China

Background: Cancer-associated fibroblasts (CAFs) are essential components of the tumor microenvironment (TME). These cells play a supportive role throughout cancer progression. Their ability to modulate the immune system has also been noted. However, there has been limited investigation of CAFs in the TME of epithelial ovarian cancer (EOC).

Methods: We comprehensively evaluated the CAF landscape and its association with gene alterations, clinical features, prognostic value, and immune cell infiltration at the pan-cancer level using multi-omic data from The Cancer Genome Atlas (TCGA). The CAF contents were characterized by CAF scores based on the expression levels of seven CAF markers using the R package "GSVA." Next, we identified the molecular subtypes defined by CAF markers and constructed a CAF riskscore system using principal component analysis in the EOC cohort. The correlation between CAF riskscore and TME cell infiltration was investigated. The ability of the CAF riskscore to predict prognosis and immunotherapy response was also examined.

Results: CAF components were involved in multiple immune-related processes, including transforming growth factor (TGF)-β signaling, IL2-STAT signaling, inflammatory responses, and Interleukin (IL) 2-signal transducer and activator of transcription (STAT) signaling. Considering the positive correlation between CAF scores and macrophages, neutrophils, and mast cells, CAFs may exert immunosuppressive effects in both pan-cancer and ovarian cancer

cohorts, which may explain accelerated tumor progression and poor outcomes. Notably, two distinct CAF molecular subtypes were defined in the EOC cohort. Low CAF riskscores were characterized by favorable overall survival (OS) and higher efficacy of immunotherapy. Furthermore, 24 key genes were identified in CAF subtypes. These genes were significantly upregulated in EOC and showed a strong correlation with CAF markers.

Conclusions: Identifying CAF subtypes provides insights into EOC heterogeneity. The CAF riskscore system can predict prognosis and select patients who may benefit from immunotherapy. The mechanism of interactions between key genes, CAF markers, and associated cancer-promoting effects needs to be further elucidated.

KEYWORDS

cancer-associated fibroblast, epithelial ovarian cancer, tumor microenvironment, prognosis, immunotherapy

Introduction

Epithelial ovarian cancer (EOC) is the fifth leading cause of cancer-related deaths in women and is the most lethal gynecological malignancy (1). Globally, the incidence of EOC is increasing annually, with approximately 310,000 newly diagnosed cases and 210,000 deaths (2). Up to 75% of patients are diagnosed at an advanced stage, manifesting with extensive intra-abdominal metastases. The 5-year survival rate is only 15%–25%, even after optimal surgical reduction with standard treatment using platinum/paclitaxel (3). Moreover, EOC is characterized by a high degree of heterogeneity, which makes it challenging to effectively characterize and optimize treatment, especially for high-grade serous ovarian cancer. Extensive heterogeneity also contributes to persistent drug resistance and poor oncological outcomes (4, 5). Hence, identifying EOC molecular subtypes is crucial for guiding personalized therapy.

The tumor microenvironment (TME) has received much attention as a critical element in tumor evolution. This highly complex system contains many components, including tumor cells, infiltrating immune cells, stromal cells, endothelial cells, lipid cells, extracellular matrix (ECM), and various signaling molecules (6). Cancer-associated fibroblasts (CAFs) play a significant role in the TME as stromal components that affect tumor behavior (7). By the production of growth factors and cytokines, remodeling ECM, and promoting angiogenesis, these cells facilitate malignant cell invasion and migration; they may also contribute to therapeutic resistance and tumor recurrence (8–10). Recent studies highlighted the emerging role of CAFs in immune regulation, since they modulate immune cell recruitment in the TME and mediate immune evasion (11, 12).

CAFs are typically derived from local resident fibroblasts that undergo myofibroblast differentiation during wound healing and tumor development (13). The conversion of other cell types, such as mature adipocytes, endothelial cells, and mesenchymal stem cells, into CAFs explains their phenotypic heterogeneity and functional diversity (14–16). Currently, phenotypically distinct CAF subtypes have been identified. Preclinical and early clinical research on immunotherapy targeting CAFs has focused on various tumor types, but little has been done regarding EOC (17–21). Therefore, determining the molecular characteristics of CAFs and understanding therole of CAF isoforms in the TME may help clarify EOC heterogeneity and enhance the development of immunotherapeutic regimens.

The present study comprehensively evaluated the clinical and genomic characteristics of CAF components in 33 solid tumors. We stratified 480 patients with EOC into two distinct subtypes based on the expression levels of seven CAF markers. Subtype-specific survival and immune infiltration differences were also determined. Furthermore, a scoring system was developed to quantitatively evaluate the CAF landscape for patients with EOC, which will permit accurate prediction of patient outcomes and responses to immunotherapy.

Materials and methods

Dataset sources

The Cancer Genome Atlas (TCGA) cancer samples from 33 types were included in the pan-cancer study. RNA sequencing (RNA-seq) data and clinical information from TCGA and

Genotype-Tissue Expression (GTEx) were downloaded from the UCSC Xena database (http://xenabrowsernet/datapages/). A single-cell RNA-seq dataset of ovarian cancer (OV_GSE118828) was obtained from the tumor Immune Single Cell Hub (TISCH) database (22). The GSE40595 dataset from the GEO database provides gene expression profiles of 31 cancer stromal samples and eight normal ovarian stromal samples from patients with high-grade serous ovarian cancer (https://www.ncbi.nlm.nih.gov/geo/query/acc.cgi? acc=GSE40595). The EOC samples used for clustering were obtained from TCGA_OV (RNA-seq FPKM dataset) and the GSE63885 dataset (https://www.ncbi.nlm. nih.gov/gds/?term=GSE63885).

Molecular markers

To quantify the relative abundance of fibroblasts in pan-cancer samples and identity CAF subpopulations in EOC, we adopted seven classical CAF molecular markers, including platelet-derived growth factor receptor alpha (PDGFRA), platelet-derived growth factor receptor-beta (PDGFRB), α-smooth muscle actin (ACTA2, α-SMA), thy-1 cell surface antigen (THY1), podoplanin (PDPN), fibroblast activation protein (FAP), and collagen 1A1 (COL1A1). These seven markers were combined to identify triple-negative breast cancer (TNBC) samples with different levels of CAF infiltration (23).

Genetic alteration analysis

Gene set cancer analysis (GSCA), a comprehensive database of cancer genomics, was used to analyze genetic alterations in CAF markers, including copy number variation (CNV), single-nucleotide variation (SNV), and methylation (http://bioinfo.life.hust.edu.cn/GSCA/#/) (24).

Clinical relevance and prognostic analysis of the cancer-associated fibroblast score

The CAF score was calculated by the single-sample gene set enrichment analysis (ssGSEA) function of R package "GSVA" across all samples within each cancer type (including 9,784 from tumor tissue, (Table S1). We compared CAF scores for 33 cancer types and evaluated their correlations with tumor stage and prognosis. Using the surv cutoff function in the "Survminer" R package, we calculated the optimal cutoff value and divided samples from each tumor type into low- and high-CAF score groups based on the calculated cutoff value.

Functional and pathway enrichment analysis

The R package "GSVA" was used to perform gene set variation analysis (GSVA) enrichment to explore the relevance of CAF score to Hallmark pathways in the pan-cancer and TCGA_OV cohorts. Relevant gene sets were downloaded from the MSigDB database (http://software.broadinstitute.org/gsea/msigdb/index.jsp).

Tumor microenvironment and immune infiltrating analysis

For each TCGA patient, we calculated the immuneScore, stromalScore, and tumor purity using the "ESTIMATE" algorithm and assessed the correlation with the CAF score using Spearman's correlation analysis. To determine the ESTIMATEScore, we summed the immuneScore and stromalScore, which reflect the relative abundances of immune and stromal components, respectively. A higher ESTIMATEScore indicates poorer tumor purity (25). Data on immune cell infiltration in TCGA cohorts were obtained from the Immune Cell Abundance Identifier (ImmuCellAI) database (http://bioinfo.life.hust.edu.cn/ImmuCellAI#!/) and the TIMER2 database (http://timer.cistrome.org/). Then, the relative proportion of 22 TME immune cells in the EOC cohort was evaluated using the "CIBERSORT" algorithm.

Consensus clustering for cancer-associated fibroblast subtypes in epithelial ovarian cancer samples

The EOC samples were analyzed by hierarchical agglomerative clustering using consensus clustering algorithm according to the expression of seven CAF markers. The EOC cohort contained the complete TCGA_OV (379 tumor samples, 377 with survival data) and GSE63885 (101 tumor samples, 75 with survival data) clinical datasets. Batch effects were eliminated using the "limma" and "sva" R packages. The associated clinical information is shown in Table S2. The "ConsensusClusterPlus" R package was used to perform cluster analysis and to identify two CAF subtypes (clusters A and B). The algorithm was repeated 1,000 times to ensure that the classification was stable. We also compared the associations between subtypes, tumor grade, tumor stage, and prognosis to examine the role of the two CAF subtypes in clinical practice. Additionally, GSVA was performed to compare the relevant Hallmark and Kyoto Encyclopedia of Genes and Genomes (KEGG) pathways in the CAF subtypes.

Differentially expressed genes related to cancer-associated fibroblast subtypes

A total of 613 differentially expressed genes (DEGs) in the two CAF subtypes were identified using the R package "limma" with $|\log_2 \text{foldchange}| > 0.5$ and adjusted p-values <0.05 (26). The "clusterProfiler" R package was used to investigate the potential function of CAF-related DEGs *via* KEGG enrichment analysis and Gene Ontology (GO) annotation (27). Differences were considered statistically significant at $p < 0.05$.

Differentially expressed gene clustering and construction of the cancer-associated fibroblast riskscore

We performed a univariate Cox regression analysis to identify DEGs that were associated with overall survival (OS) ($p < 0.05$). Based on these prognostic DEG expression values, consensus clustering was performed to categorize the patients into two genomic clusters (gene clusters A and B). We then conducted principal component analysis (PCA) to calculate the CAF riskscore. Principal component (PC) 1 and PC2 were selected as the feature scores. The score of each EOC sample was calculated using the formula: CAF riskscore = $\sum(PC1i + PC2i)$, where i represents the expression of each prognostic feature gene (28). Patients were divided into low- and high-CAF riskscore groups based on the optimal cutoff value. To assess the impact of riskscore on prognosis, we performed survival analysis and Cox regression analysis of the EOC cohort.

Immunophenoscore analysis

To predict the sensitivity of immunotherapy, we downloaded immunophenoscore (IPS) data for EOC patients from the The Cancer Immunome Atlas (TCIA) database (https://tcia.at/). IPS scores were positively associated with immunogenicity. Higher scores represent better outcomes after treatment with immune checkpoint inhibitors (29). We compared the IPS values between the high- and low-riskscore groups to evaluate immunotherapy decisions. Finally, the Tumor Immune Dysfunction and Exclusion (TIDE) algorithm was applied to investigate immune evasion in the EOC cohort (30).

Statistical analyses

R (version 4.1.1) was used for all statistical analyses. Differences between two groups were analyzed using Wilcoxon tests or t-tests. Kaplan–Meier survival analysis and log-rank tests were performed using the "survival" and "survminer" R packages to evaluate the survival divergence of different subtypes and riskscore groups. We computed the 95% confidence interval (CI) and hazard ratio (HR) using a Cox regression model. Correlation coefficients were determined using Spearman's correlation analysis. Statistical significance was set at $p < 0.05$.

Results

The expression of seven cancer-associated fibroblast markers in ovarian cancer

Initially, we investigated the OV_GSE118828 dataset to explore which OV cell subpopulations of these marker genes are predominantly expressed. We found that the expression of PDGFRA, THY1, PDPN, FAP, and COL1A1 was the highest in fibroblasts compared to that of other cell subpopulations. The expression of PDGFRB and ACTA2 expression was highest in myofibroblasts, followed by fibroblasts (Figure 1A). In addition, we observed that these seven genes were significantly upregulated in cancer stroma compared with that of normal ovarian stroma in high-grade serous OV, indicating their competence as CAF-specific markers in OV and their critical function in tumor stroma (Figure 1B).

A protein–protein interaction (PPI) network was constructed to assess the associations among these seven CAF marker-related proteins using the search tool for the retrieval of interacting genes/proteins (STRING) online database (https://cn.string-db.org/, Figure S1A). The correlation between the mRNA expression levels of CAF markers based on TCGA pan-cancer data and TCGA_OV cohort was also examined, both of which showed a strong positive correlation (Figures S1B, S1C).

Genomic alterations of cancer-associated fibroblast markers at the pan-cancer level

We next obtained details of CNVs for the seven CAF markers. The CNV distribution showed that heterozygous amplification and heterozygous deletion were the main CNV types in pan-cancers (Figure 2A). Correlation analysis indicated that the CNV of PDPN was positively correlated with its mRNA level in 10 of the 33 tumor types, especially in low-grade glioma (LGG; $r = 0.57$) and cholangiocarcinoma (CHOL; $r = 0.44$). The CNV of PDGFRA was positively correlated with its mRNA levels in glioblastoma multiforme (GBM) ($r = 0.43$). However, there was a negative correlation for COL1A1 in five of the 33 tumor types (Figure 2B). SNV was also analyzed to determine the variation frequency and type for each TCGA cancer subtype. Our analysis revealed that most genetic aberrations were

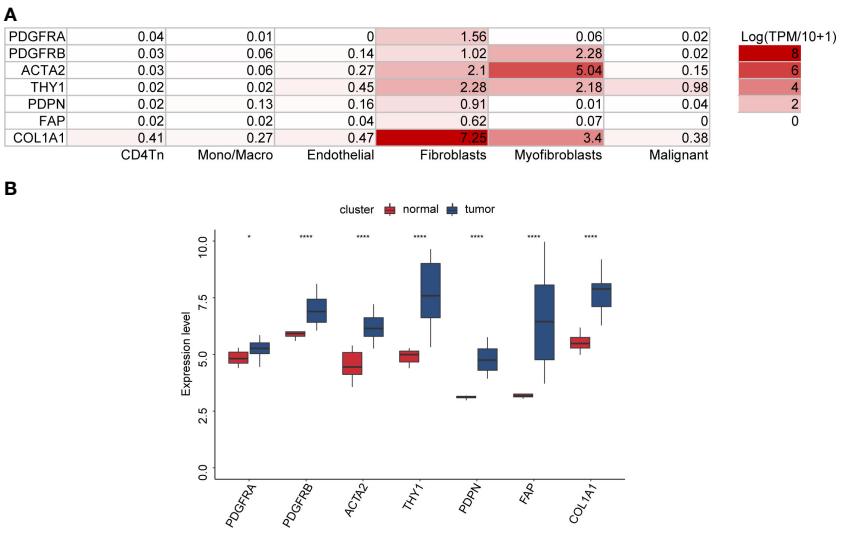

FIGURE 1
The expression of seven CAF markers in OV. **(A)** The distribution of seven CAF markers in OV cell subpopulations through the TISCH database (OV_GSE118828 dataset). **(B)** Seven CAF markers were upregulated in ovarian cancer stroma compared with normal ovarian stroma (GSE40595 dataset).

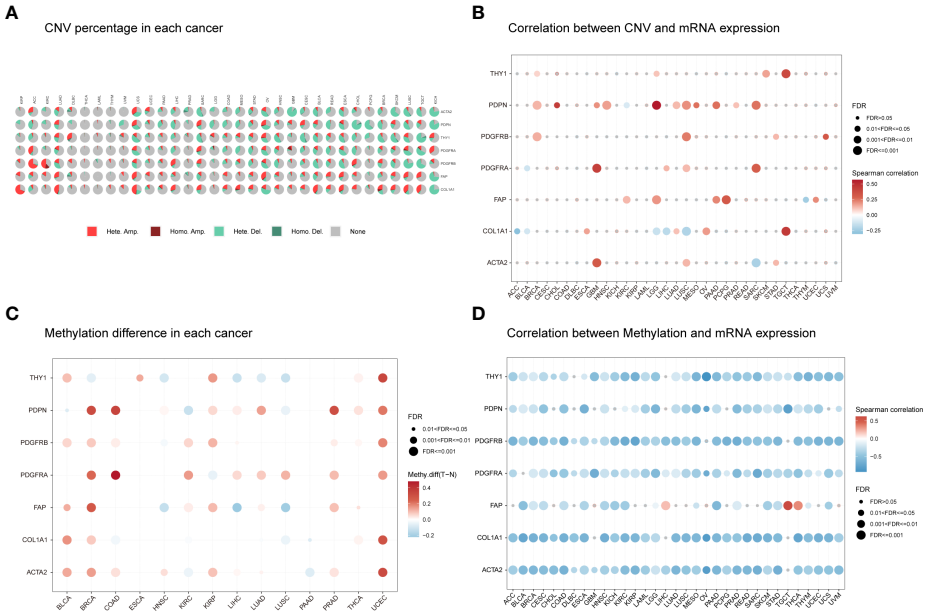

FIGURE 2
The CNV distribution and methylation levels of seven CAF markers in pan-cancer. **(A)** Pie charts illustrating the proportion of multiple CNV types for each marker across each cancer type. The color represents different CNV types. Hete Amp, heterozygous amplification; Hete Del, heterozygous deletion; Homo Amp, homozygous amplification; Homo Del, homozygous deletion; None, no CNV. **(B)** The correlation between CNV and mRNA expression for each marker in the selected cancer types. **(C)** Marker gene methylation status between tumor and normal samples in the selected cancer types. The red and blue dots represent increased and decreased methylation in tumors compared to normal tissues, respectively. The darker the color, the larger the methylation difference. **(D)** Correlation between methylation and mRNA expression for each marker in the selected cancer types. The red and blue dots represent positive and negative correlations, respectively. Gray dots indicate no significant correlation. Darker colors indicate stronger correlations. The dot size represents statistical significance (larger dot sizes indicate increased statistical significance).

missense mutations. The SNV frequency for these CAF markers was 100% (850 of 850 tumors). Of these, PDGFRA had the highest mutation rate (34%) among CAF markers. In skin cutaneous melanoma (SKCM), COL1A1 mutations were the most prevalent (71%; Figure S2).

Next, we explored CAF marker gene methylation to identify epigenetic regulation in pan-cancer. Our results revealed a highly heterogeneous methylation status in different tumors. Hypermethylated genes were more frequently observed than hypomethylated genes in bladder urothelial carcinoma (BLCA), breast invasive carcinoma (BRCA), colon adenocarcinoma (COAD), kidney renal papillary cell carcinoma (KIRP), prostate adenocarcinoma (PRAD), and uterine corpus endometrioid carcinoma (UCEC). In contrast, hypomethylated genes were more common in lung squamous cell carcinoma (LUSC) and head and neck squamous cell carcinoma (HNSC). Most cancers presented PDGFRA, PDGFRB, PDPN, ACTA2, and FAP hypermethylation compared to normal samples. However, most cancers showed THY1 and COL1A1 hypomethylation compared to normal samples (Figure 2C). The methylation levels of CAF markers were generally negatively correlated with their mRNA levels (Figure 2D). These results indicate that the CNV distribution, SNV alterations, and methylation status of CAF markers mediate abnormal marker gene expression.

The expression levels and prognostic significance of the cancer-associated fibroblast score

A comparison of CAF scores for the 33 tumor types in TCGA cohorts showed that pancreatic adenocarcinoma (PAAD) had the highest CAF score, while acute myeloid leukemia (LAML) had the lowest score and OV had a moderate score (Figure 3A) Additionally, we examined the relevance of CAF score with tumor stage and found a significant correlation between CAF score and tumor stage in nine cancer types. CAF scores were generally higher in advanced tumor stages (stage IV or III) in patients with BLCA, BRCA, esophageal cancer (ESCA), kidney renal clear cell carcinoma (KIRC), KIRP, OV, gastric adenocarcinoma (STAD), thyroid carcinoma (THCA), and uterine carcinosarcoma (UCS) but were lower in early tumor stages (stage II or I) (Figure 3B). Intriguingly, CAF scores in ESCA and STAD were higher in stage II than that in stage I but decreased in stage II compared to stage I in patients with KIRC and THCA. The CAF scores did not differ between stage I and II in patients with the remaining tumor types. We also observed no differences in CAF scores between stage III and IV in pan-cancer.

To evaluate the prognostic value of the CAF score in various tumor types, we conducted a Kaplan–Meier analysis. We observed that high CAF scores were correlated with poor OS in 21 tumor types, including adrenocortical carcinoma (ACC), BLCA, COAD, GBM, kidney chromophobe (KICH), KIRC, KIRP, LGG, LUSC, mesothelioma (MESO), OV, PAAD, sarcoma (SARC), SKCM, STAD, testicular germ cell tumor (TGCT), THCA, thymoma (THYM), UCEC, UCS, and uveal melanoma (UVM; Figure 4).

Functional enrichment analyses of the cancer-associated fibroblast score

We performed GSVA from the HALLMARK pathway database to determine how pathways within the CAF landscape are involved in pan-cancer. The results showed that the CAF scores were positively linked to pathways such as epithelial–mesenchymal transition, TGF-β signaling, IL2-STAT signaling, hypoxia, inflammatory response, and IL6-JAK-STAT3 signaling (Figure 5A). In TCGA_OV cohort, CAF enrichment analysis showed enrichment similar to that of pan-cancer analysis (Figure 5B). These tumor-related pathways, particularly immune-related pathways, might lead to poor survival in patients with malignancy.

Association of the cancer-associated fibroblast score with the tumor microenvironment

We investigated the relationship between the CAF score and the TME and found a significant positive correlation between CAF scores and stromalScores in all 33 tumor types, demonstrating that CAF scores calculated using CAF markers may influence stromal cell infiltration and contribute to stromal function. Furthermore, CAF scores were positively correlated with immuneScores in most tumor types except for MESO, UCS, THYM, TGCT, and lymphoid neoplasm diffuse large B-cell lymphoma (DLBC), indicating that elevated CAF scores may facilitate immune cell infiltration and modulate immune responses. In addition, CAF scores were negatively and positively correlated with tumor purity and ESTIMATEScores, respectively, in pan-cancer, excluding LAML. Since low purity indicates a poor prognosis for cancer, the above findings are consistent with our survival prediction results that high CAF scores correspond to poor prognosis (31) (Figure 6A). The scatter plot in Figure 6B highlights the association between CAF scores and the TME in TCGA_OV cohort.

Association of the cancer-associated fibroblast score with immune cell infiltration in the tumor microenvironment

To assess the role of the CAF score in predicting immune cell infiltration, we explored the association between CAF scores and

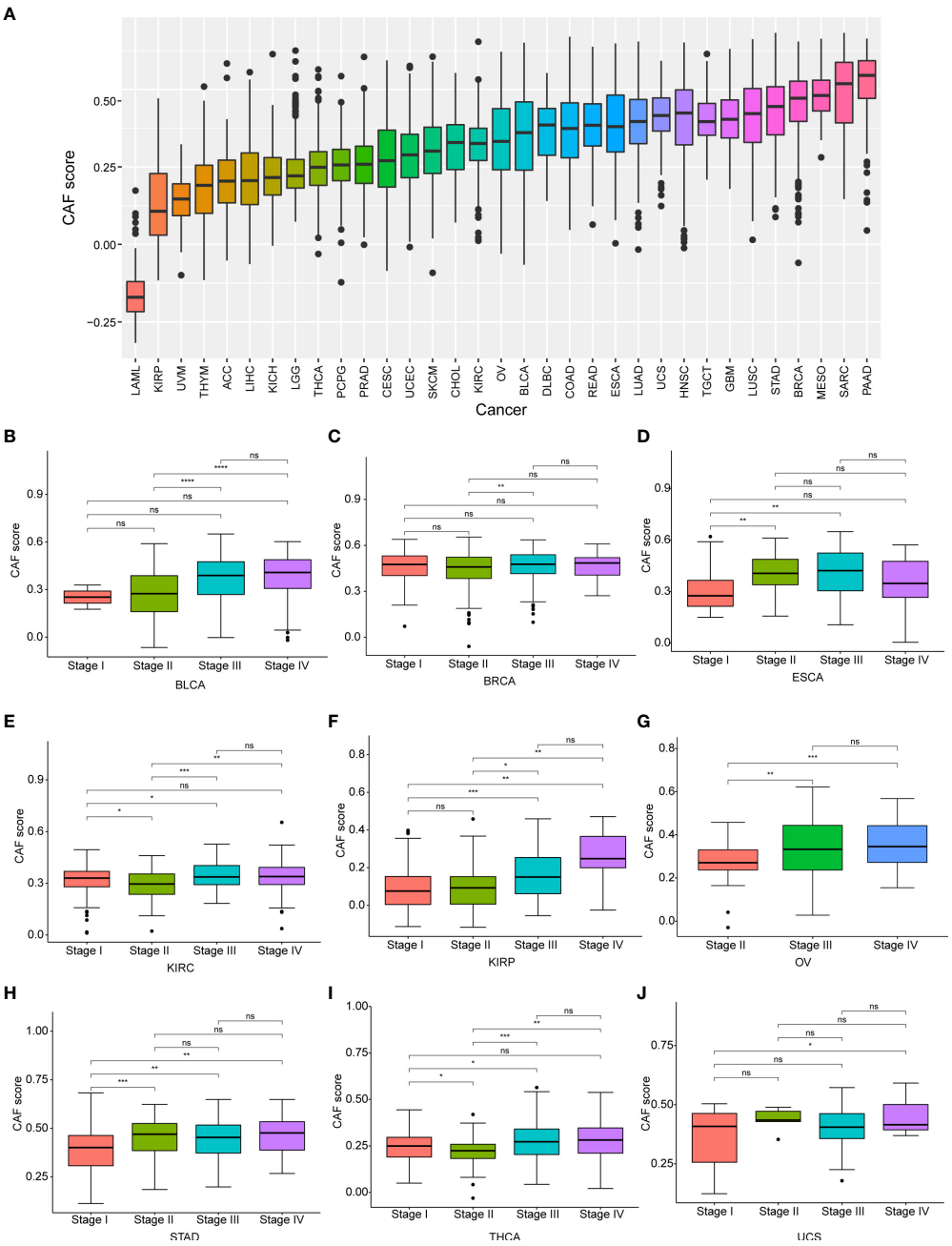

FIGURE 3
The differential distribution of CAF score. **(A)** The CAF score distribution in pan-cancer. **(B)** The differential distribution of CAF score in various tumor stages in pan-cancer. Only significant results were shown. *p < 0.05, **p < 0.01, ***p < 0.001, ****p < 0.0001.

immune cells in the TME. Using data from the ImmuCellAI database, we found that the CAF scores were significantly positively correlated with macrophages, monocytes, and induced T regulatory cells (iTregs) and negatively correlated with CD8 T cells, CD4-naive cells, B cells, and natural T regulatory cells (nTregs) (Figure 7A). In addition, our CAF score and CAFs showed a significant positive correlation according to the TIMER2 database, which confirmed that scoring reflects CAF features. Meanwhile, the CAF scores were positively correlated with macrophages, myeloid-derived suppressor cells (MDSCs), neutrophils, and mast cells (MCs). In contrast, CAF scores were negatively correlated with plasma B cells and Th1 CD4 T cells (Figure 7B, Table S3). These results indicate that CAFs may act in an immunosuppressive manner. Previous studies showed that in

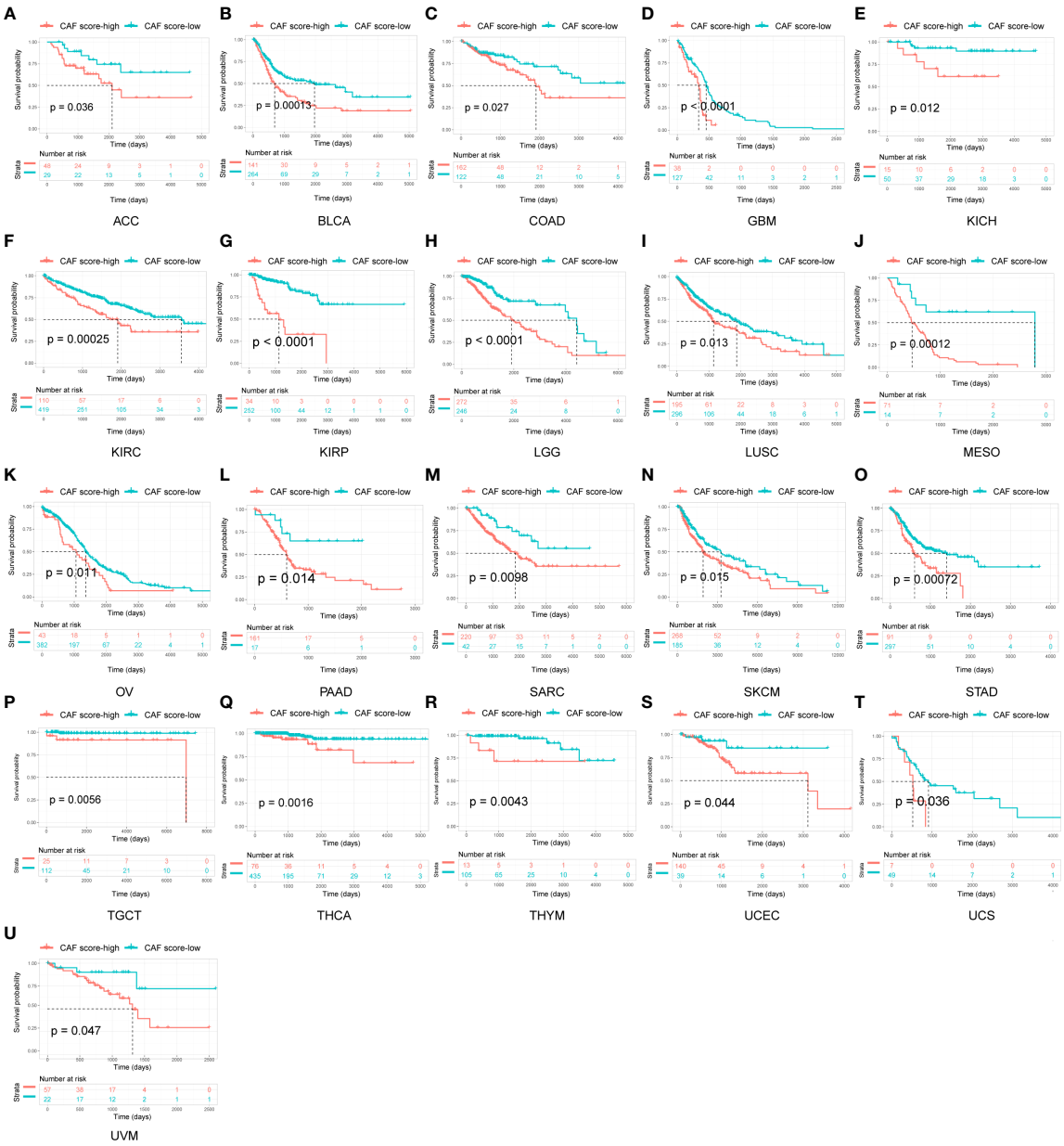

FIGURE 4
Survival analysis between CAF score group and overall survival in pan-cancer. Only significant results were shown.

tumors with immune checkpoint gene overexpression, immune checkpoint blockade could effectively enhance the antitumor effect of T cells and help the immune system identify and eliminate cancer cells (32). Accordingly, we investigated the correlation between CAF scores and immune checkpoints in TCGA_OV cohort and found that CAF scores were significantly positively correlated with programmed cell death protein 1 (PD-1), programmed cell death-ligand 1 (PD-L1), cytotoxic T lymphocyte-associated antigen-4 (CTLA-4), T-cell immunoreceptor with immunoglobulin and immunoreceptor tyrosine-based inhibition motif domains (TIGIT), and lymphocyte activation gene 3 (LAG-3) (Figure 7C). These results suggested that tumor immune escape may be involved in CAF-mediated tumorigenesis in OV.

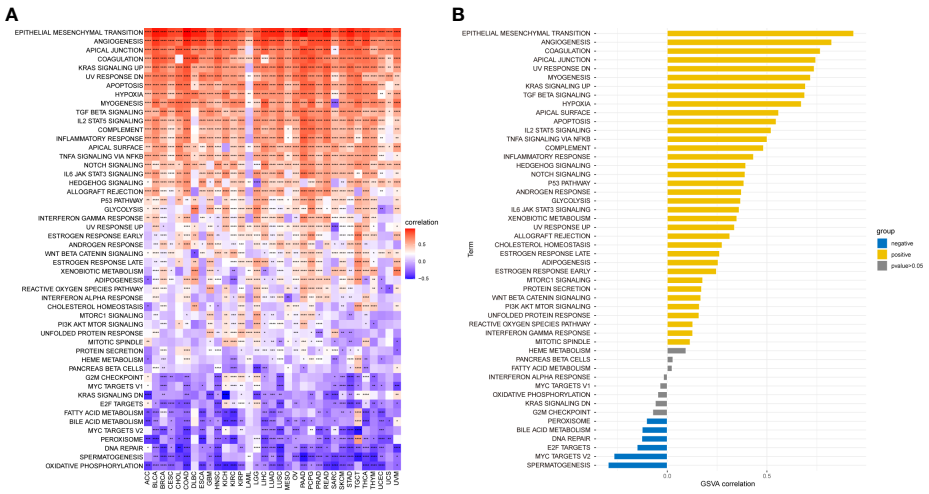

FIGURE 5
GSVA of CAF score. **(A)** The top 50 HALLMARK pathways in pan-cancer. **(B)** The top 50 HALLMARK pathways in TCGA_OV cohort. The red and blue colors represent positive and negative correlations, respectively. *p < 0.05, **p < 0.01, ***p < 0.001, ****p < 0.0001.

Identification of cancer-associated fibroblast subtypes in the epithelial ovarian cancer cohort

To determine the characteristics of CAF molecular subtypes in tumorigenesis, we performed further analysis on 480 patients from two eligible EOC cohorts. With the two datasets integrated, PCA evaluated the batch effect before and after the conversion and found it to be remarkably reduced after conversion (Figures 8A, B). The network map shown in Figure 8C provides a comprehensive landscape of the interactions among CAF markers in EOC patients and the prognostic value for each marker. Survival analysis showed that the high expression of these markers corresponded to poor prognosis in patients with EOC (Figures 8D–J, $p < 0.05$).

We categorized the entire cohort based on the expression profiles of the seven CAF markers. Cluster analysis showed that $k = 2$ was the best cutoff for dividing the entire cohort into cluster A ($n = 301$) and cluster B ($n = 179$) (Figure 9A). PCA revealed a remarkable transcriptome difference between the two CAF subtypes (Figure 9B). Kaplan–Meier analysis showed that patients in cluster A had longer OS than that in patients in cluster B ($p = 0.022$; Figure 9C). The relationship between the expression of CAF markers and clinical characteristics of two CAF subtypes was visualized (Figure 9D). Furthermore, GSVA enrichment analysis was conducted to examine functional and biological differences between subtypes. HALLMARK analysis showed that cluster B was significantly enriched in epithelial mesenchymal transition, TGF-β signaling, TGF-β signaling *via* Nuclear factor-k-gene binding (NF-κB), inflammatory response, and IL6-JAK-STAT3 signaling, whereas cluster A was mainly enriched in DNA repair (Figure 9E). KEGG analysis showed that cluster B was enriched in immune-related pathways, such as complement and coagulation cascades, leukocyte transendothelial migration, and chemokine signaling pathways, whereas cluster A was mainly related to mismatch repair and nucleotide excision repair (Figure 9F, Table S4).

Characteristics of the tumor microenvironment cell infiltration in cancer-associated fibroblast subtypes

We then explored the composition of the TME-infiltrating cells among the two subtypes. The infiltration of memory B cells, T-follicular helper cells, T regulatory cells (Tregs), activated natural killer (NK) cells, and activated dendritic cells (DCs) was remarkably higher in cluster A than that in cluster B, while the infiltration of memory resting CD4 T cells, M2 macrophages, and neutrophils was significantly lower in cluster A than that in cluster B (Figure 10A).

Identification of gene subtypes based on prognostic differentially expressed genes

We identified 613 CAF subtype-related DEGs, visualized by volcano plots (Figure 10B). Functional enrichment analysis was performed to understand the potential behavior of DEGs in EOC (Table S5). GO annotation showed that the DEGs were involved in ECM organization, collagen-containing ECM, and ECM structural constituent (Figure 10C). KEGG analysis revealed

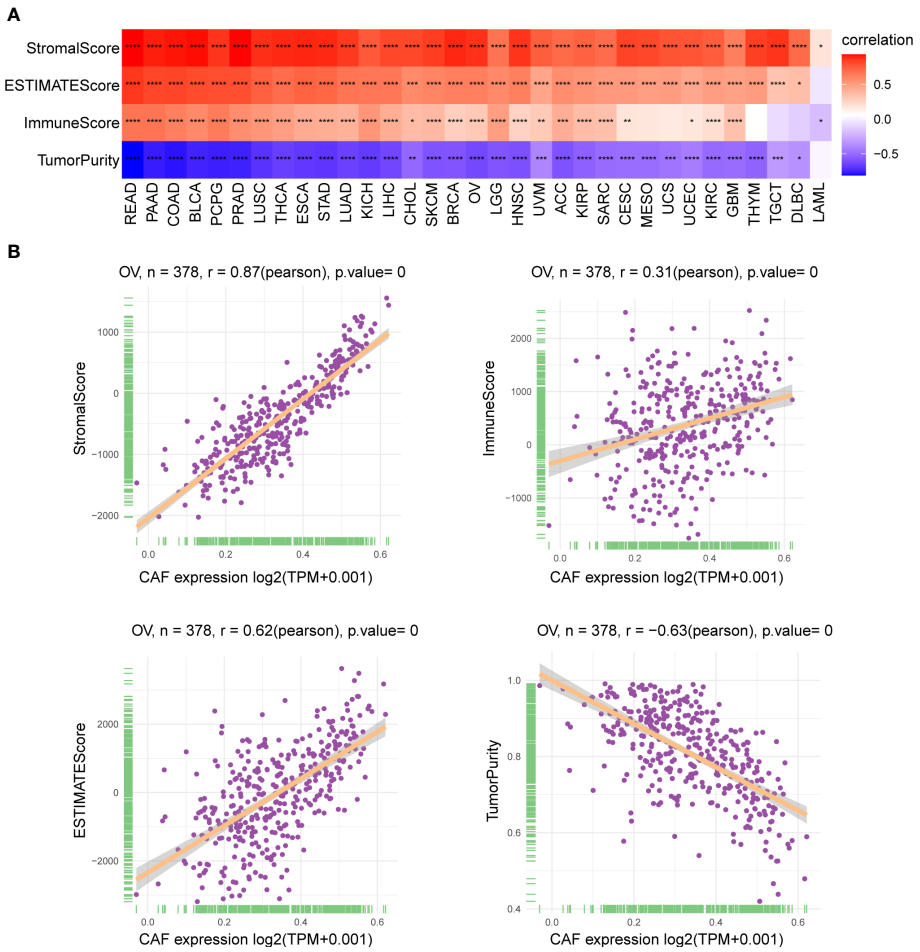

FIGURE 6
Association of CAF score with the TME. **(A)** Heatmap showed the correlation between CAF score and stromalScore, ESTIMATEScore, immuneScore, and tumor purity score in pan-cancer. **(B)** The correlation between CAF score and stromalScore, ESTIMATEScore, immuneScore, and tumor purity score in TCGA_OV cohort. The correlation coefficients were calculated by Spearman correlation analysis. The red and blue colors represent positive and negative correlations, respectively. The darker the color, the stronger the correlation. *p < 0.05, **p < 0.01, ***p < 0.001, ****p < 0.0001.

enrichment in the PI3K-Akt signaling pathway, ECM–receptor interaction, and immune-related pathways such as the TGF-β signaling pathway, leukocyte transendothelial migration, cytokine–cytokine receptor interaction, NF-κB signaling pathway, and IL-17 signaling pathway (Figures 10D, E). Univariate Cox regression analysis showed that 118 DEGs were associated with OS. We screened these genes (Table S6) and observed that two genomic subtypes (gene clusters A and B) were separated based on the expression of these prognostic genes (Figure 11A). Kaplan–Meier analysis suggested that patients with gene cluster B had worse OS than those with gene cluster A (p = 0.005; Figure 11B). The two gene subtypes showed significant differences in the expression of the seven CAF markers, which was consistent with the results for the CAF subtypes (Figure 11C). Figure 11D depicts a heat map that illustrates DEG expression in different CAF clusters and gene clusters. To quantify the CAF landscape, we established a scoring system based on these prognostic DEGs using PCA. We defined this score as the CAF riskscore. A Sankey diagram was used to illustrate the distribution of the survival differences among the distinct clusters, gene clusters, and two CAF riskscore groups (Figure 11E). Next, we explored the relationship between the CAF riskscore and CAF clusters as well as CAF gene clusters. The CAF riskscore was significantly higher in cluster B than that in cluster A. Similar results were observed for the two genetic subtypes (Figures 11F, G).

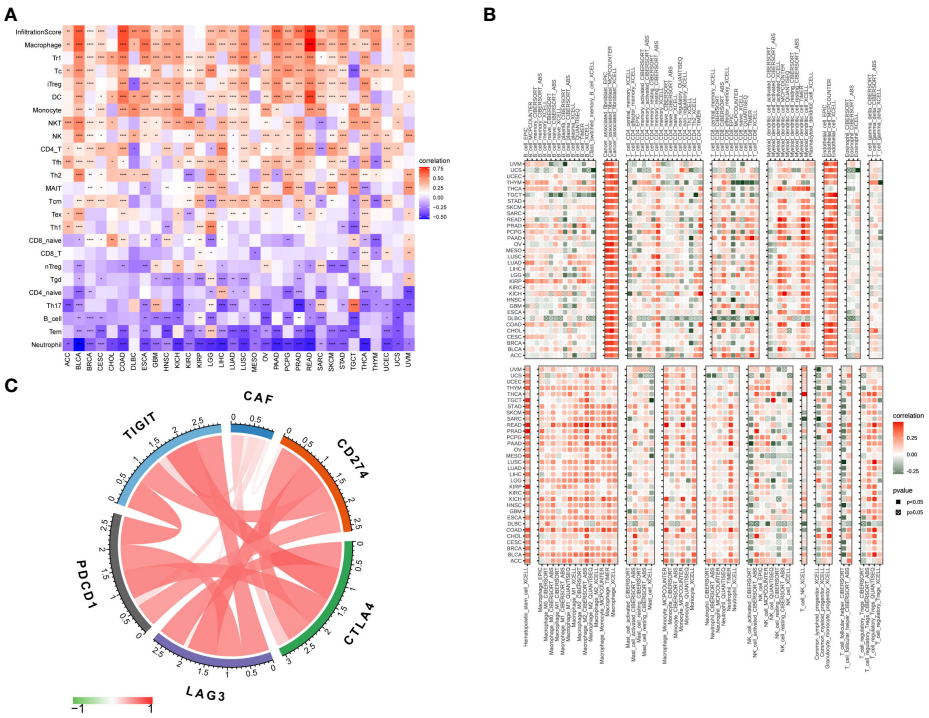

FIGURE 7
Association of CAF score with immune cell infiltration. **(A)** Association of CAF score with immune cell infiltration in pan-cancer based on ImmuCellAI (The red and blue colors represent positive and negative correlations, respectively) and **(B)** TIMER2 database. **(C)** Association of CAF scores with immune checkpoints in TCGA_OV cohort. The correlation coefficients were calculated by Spearman correlation analysis. The red and green colors represent positive and negative correlations, respectively. The darker the color, the stronger the correlation. *p < 0.05, **p < 0.01, ***p < 0.001, ****p < 0.0001.

Clinicopathological and prognostic characteristics of the cancer-associated fibroblast riskscore in the epithelial ovarian cancer cohort

To investigate the impact of CAF riskscore on clinical characteristics, we explored the correlation between CAF riskscore, tumor stage, and survival status. Patients in the stage III–IV subgroup had significantly higher CAF riskscores than patients in the stage I–II subgroup. Moreover, patients in the high-riskscore group tended to have more advanced diseases (Figures 12A, B). The CAF riskscores were significantly higher in patients who died than those in patients who survived. A larger proportion of tumor-related deaths occurred in patients with a high riskscore (Figures 12C, D). Furthermore, the OS of the high-riskscore group was worse than that of the low-riskscore group ($p < 0.001$, Figure 12E). Based on the data from TCGA_OV cohort, multivariate Cox regression revealed that the presence of residual tumors and high CAF riskscore were independent risk factors (HR = 2.285, p = 0.000407; and HR = 1.438, p =0.025, respectively; Figure 12F).

Relationship between the cancer-associated fibroblast riskscore and the tumor microenvironment cell infiltration

Figure S3 and Table S7 based on GSVA showed that there was also a significant positive correlation between CAF riskscore and epithelial–mesenchymal transition, TGF-β signaling, IL2-STAT signaling, hypoxia, inflammatory response, and IL6-JAK-STAT3 signaling pathways. Subsequently, we examined the correlation between the CAF riskscore and the abundance of immune cells. We found that in the EOC cohort, the CAF riskscores were positively correlated with the infiltration of resting memory CD4 T cells, M0 macrophages, and resting DCs. The CAF riskscores were negatively correlated with the infiltration of memory B cells, T-follicular helper cells, Tregs, monocytes, M1 macrophages, and activated DCs (Figure 13A). To examine whether the CAF riskscore could predict immunotherapy outcomes, we analyzed the association between the CAF riskscore and IPS in EOC. The results showed that IPS-CTLA4-/PD-L1-, IPS-CTLA4-/PD-L1+, IPS-CTLA4+/PD-L1-, and IPS-CTLA4+/PD-L1+ were significantly higher in the low-riskscore group than that in the high-riskscore

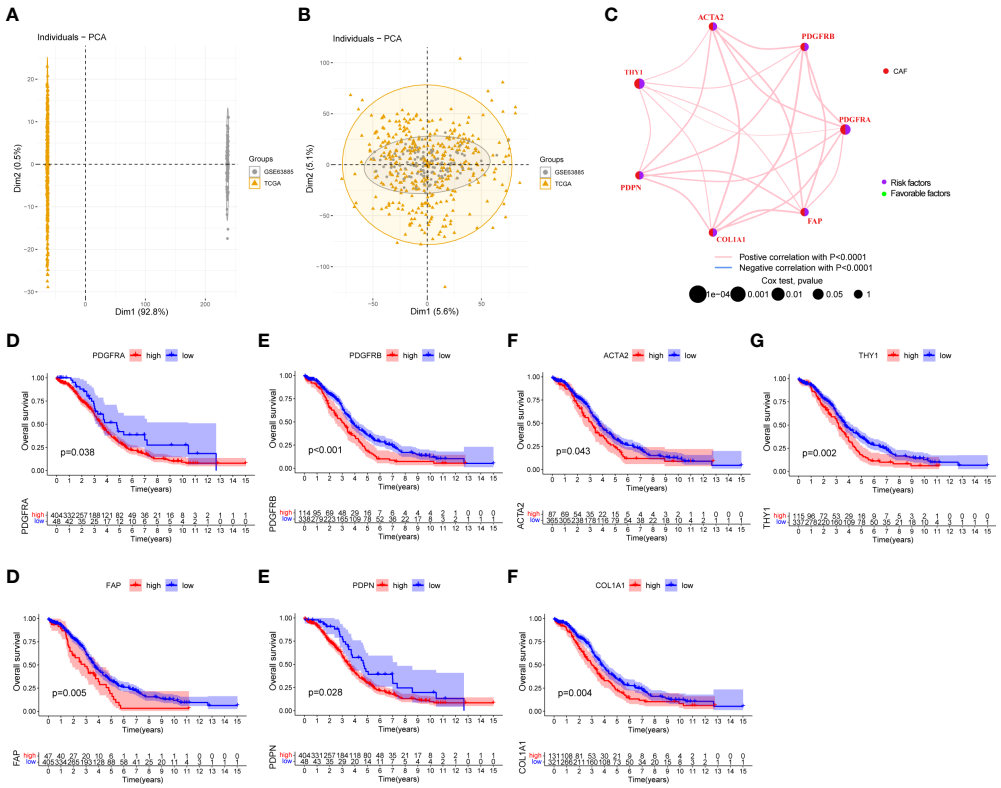

FIGURE 8
Survival analysis of seven CAF markers in the EOC cohort. **(A)** Before the removal of batch effects through principal component analysis, the differences between samples obtained from two datasets are illustrated. **(B)** After the removal of batch effects, the differences among samples obtained from two datasets are reduced. **(C)** Interactions and interconnection among CAF markers in EOC. The connecting lines represent their interactions, and the thickness of the lines indicates the strength of the association. The pink and blue lines represent positive and negative correlations, respectively. The green and purple dots in the circle indicate favorable and risk factors, respectively. **(D–J)** Survival analysis between seven CAF markers and overall survival in EOC patients.

group, indicating that patients in the low-riskscore group would likely achieve a better response to immunotherapy (Figures 13B–E). The TIDE value was significantly higher in the high-riskscore group than that in the low-riskscore group, indicating that the high-riskscore group had a greater potential for immune evasion and lower responses to immunotherapy (Figure 13F).

Identification of key genes with differential expression in epithelial ovarian cancer samples

We integrated tumor samples from TCGA database with normal ovarian samples from the GTEx database and analyzed the difference in expression levels of these prognostic DEGs among the two groups. Then, we obtained 24 key genes that were significantly upregulated in EOC (Figure 14A). Meanwhile, immunohistochemical results acquired from the Human Protein Atlas (HPA) database showed that DEG expression was relatively stronger in the tumor group compared to that in the normal ovary group (Figure 14B). Most genes exhibited significantly strong correlations with CAF markers, except for anterior gradient protein 2 (AGR2), forkhead box A2 (FOXA2), and SAM pointed domain-containing ETS transcription factor (SPDEF), which had a significant negative correlation (Figure 14C).

Discussion

The TME is a multicellular system characterized by complex tumor–stroma interactions. CAFs have recently been recognized as essential components of the cancer stroma. These cells are widely distributed in human solid tumors and play a significant role in cancer pathogenesis (33). PDGFRA, PDGFRB, ACTA2, THY1, PDPN, FAP, and COL1A1 were previously considered CAF markers. However, these cell surface markers are not exclusively expressed by CAFs. For example, ACTA2 also serves as a general marker for vascular muscle cells and pericytes. Thus, the selective expression patterns of these markers could be used to characterize the phenotypic

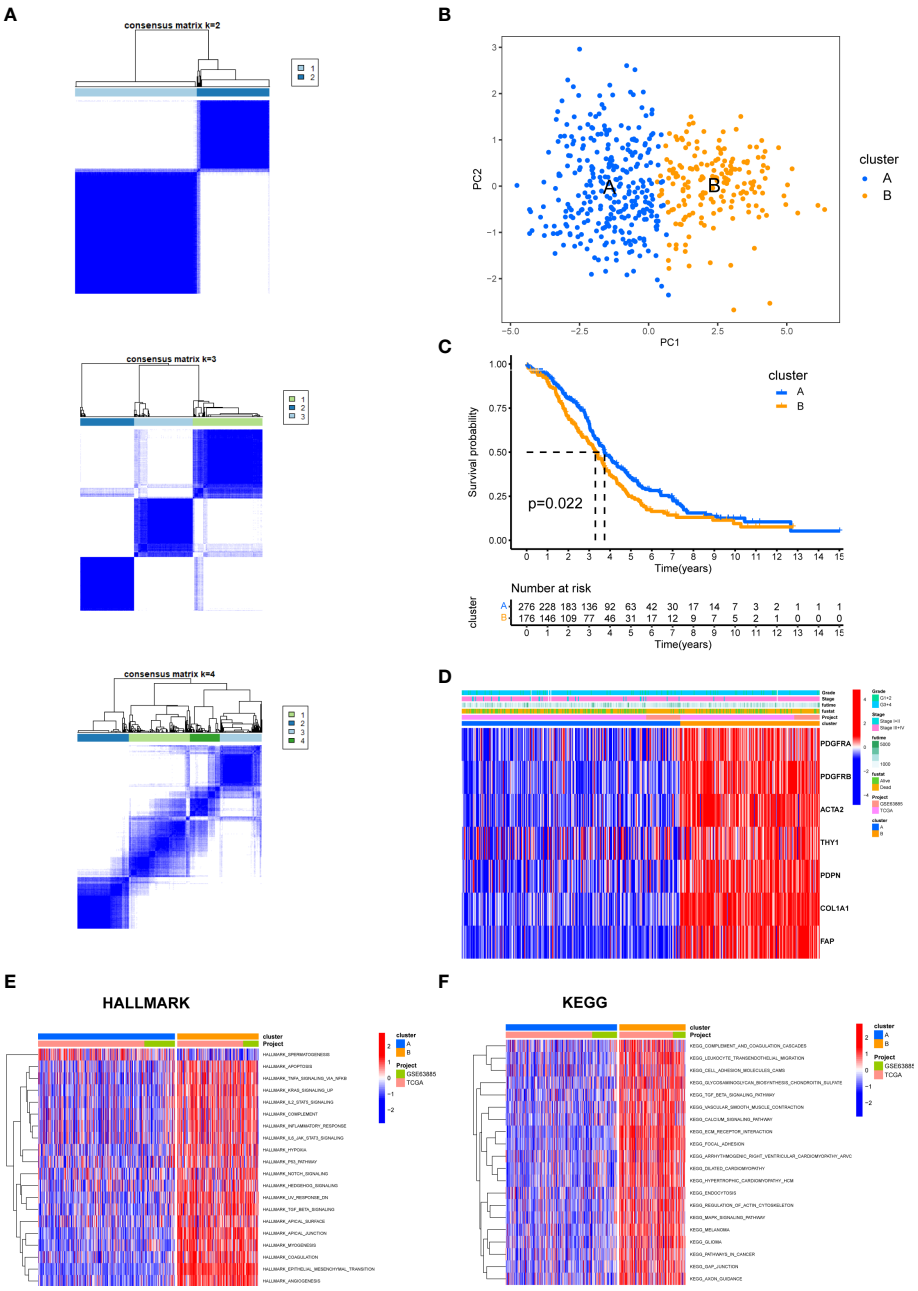

FIGURE 9
The biological characteristics between two CAF subtypes in the EOC cohort. **(A)** Two clusters (k = 2) were identified by consistent clustering. **(B)** The transcriptomes of the two CAF subtypes differed significantly. **(C)** Kaplan–Meier curves of overall survival between cluster A and B. **(D)** The heat map depicted the relationship between the expression of CAF markers and clinical characteristics of two CAF subtypes. **(E)** HALLMARK pathways between two CAF subtypes. **(F)** KEGG pathways between two CAF subtypes. The red and blue colors represent pathways that are active and inhibitory, respectively.

heterogeneity and functional diversity of activated CAFs within the specific TME (7, 34–38). Furthermore, the combination of these markers may enhance the differentiation of CAF subgroups, and different CAF subgroups have specific prognostic significance and exert different roles in efficacy. An analysis of ACTA2, FAPα, PDGFRA, PDGFRB, CD26, and PDPN revealed the coexistence of multiple CAF subpopulations in murine TNBC (39). Based on the expression of FAP, CD29, ACTA2, PDGFRA, and PDPN, four CAF subpopulations were detected in metastatic breast cancer

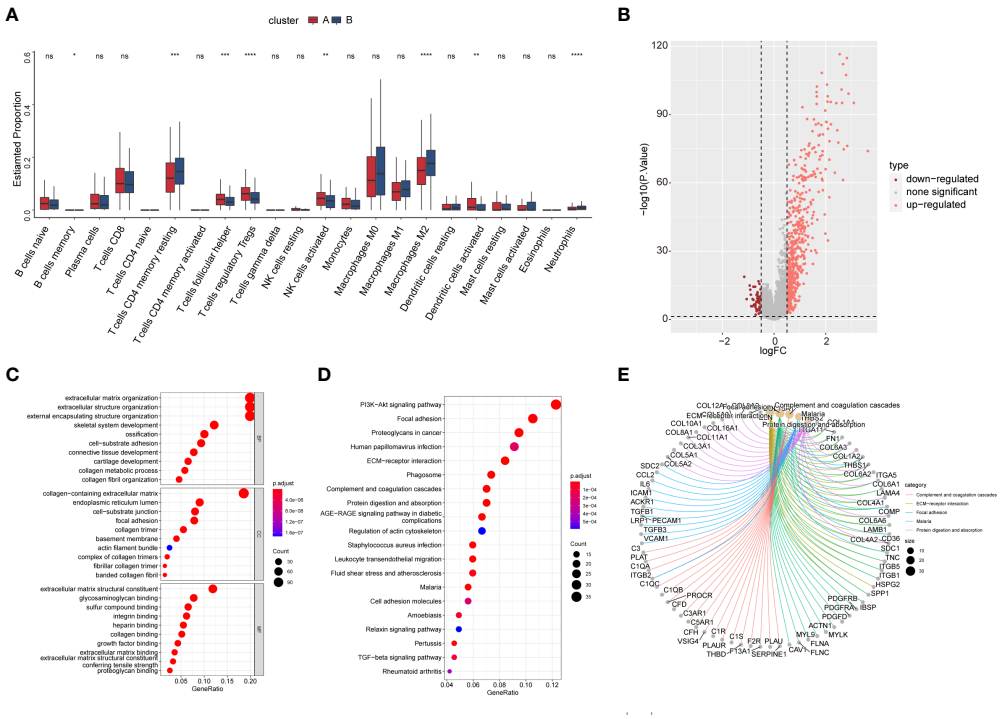

FIGURE 10
The TME cell infiltration of CAF subtype and biological characteristics of CAF subtype-related DEGs. **(A)** The abundance of the 22 TME infiltration cell subsets in two CAF subtypes based on the CIBERSORT algorithm. **(B)** Volcano map showing CAF subtype-related DEGs. Pink and red colors represent upregulated and downregulated, respectively. **(C)** GO enrichment analysis of DEGs. **(D)** KEGG enrichment analysis of DEGs. The size of the bubbles represents the amount of gene enrichment. The depth of color represents the FDR value. **(E)** Circle diagram showing the relationship between DEGs and pathways in KEGG.

axillary lymph nodes and these subpopulations contribute to metastasis through distinct mechanisms (17). The human PDAC-derived CAF subtype B population may be associated with poor prognosis, whereas subtype C CAFs appear to be associated with good clinical prognosis (40). Additionally, CAF-S1 in human BC is a key player in immunosuppression, as this subtype enhances the differentiation, recruitment, and activation of Tregs. In contrast, CAF-S4 does not exhibit these properties (41). Nonetheless, studies investigating CAF subgroups in EOC remain limited (42). In this study, we performed a comprehensive and systematic characterization of CAF markers in pan-cancer and identified CAF subgroups in EOC. Our results elucidate the tumor-promoting profile of CAFs, identify multiple potential CAF-related mechanisms in the TME, confirm their critical role in immune infiltration, and provide a basis for developing innovative therapies targeting specific CAF subgroups in EOC.

Genetic alterations lead to aberrant gene expression and cancer progression (43). CNVs are an important form of genetic structural variation and are crucial for cancer diagnosis, prevention, and treatment. Furthermore, CNV-induced gene mutations may lead to immune escape (44, 45). In our study, we observed a high CNV frequency in CAF markers and a correlation between CNV and marker expression, suggesting that CNV may affect CAF function and contribute to tumorigenesis. Previous studies detected PDGFRA amplification in GBM, consistent with our findings (46). Among the epigenetic modifications in mammalian genomes, DNA methylation plays a fundamental role in regulating gene expression and tumorigenesis. Tumors are usually accompanied by oncogene hypomethylation and tumor-suppressor gene hypermethylation (47, 48). Hypomethylation in our study corresponds to abnormally high CAF marker expression in most tumors (except for FAP in THCA and TGCT), which indicates that CAF markers underlie a tumor-promoting behavior and may be potential new targets for epigenetic regulation.

By interacting with several signaling pathways, such as TGF-β, NF-κB, IL6-JAK-STAT3, and PI3K-Akt signaling pathways, CAFs contribute to TME formation and maintenance. TGF-β signaling has been implicated as a mediator of immune contexts within the TME, with its ability to influence the ECM structure, which excludes immune cells and possibly generates immunotherapy resistance (49). Recent studies emphasize the

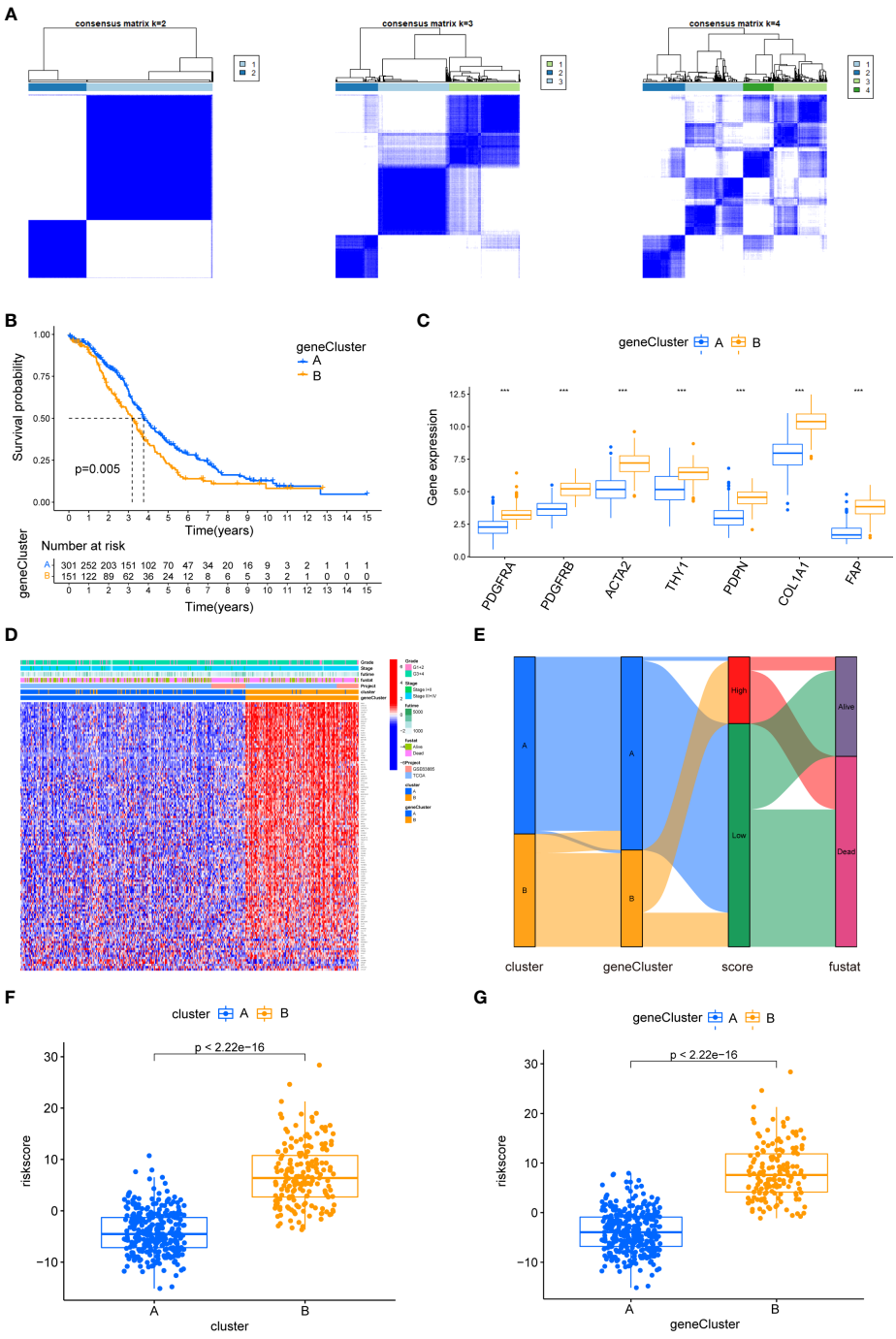

FIGURE 11
The biological characteristics of CAF gene cluster and construction of CAF riskscore system. **(A)** Two gene clusters (k = 2) were identified by consistent clustering based on prognostic DEGs. **(B)** Kaplan–Meier curves of overall survival between gene clusters A and B. **(C)** Differences in the expression of seven CAF markers among the two gene clusters. **(D)** The heat map was drawn to visualize the expression of prognostic DEGs in distinct CAF clusters and gene clusters. **(E)** Sankey diagram illustrating the distribution of survival outcomes among the distinct clusters, gene clusters, and CAF riskscore groups. **(F)** Differences in CAF riskscore among two clusters in EOC cohorts. **(G)** Differences in CAF riskscore among two gene clusters in EOC cohorts.

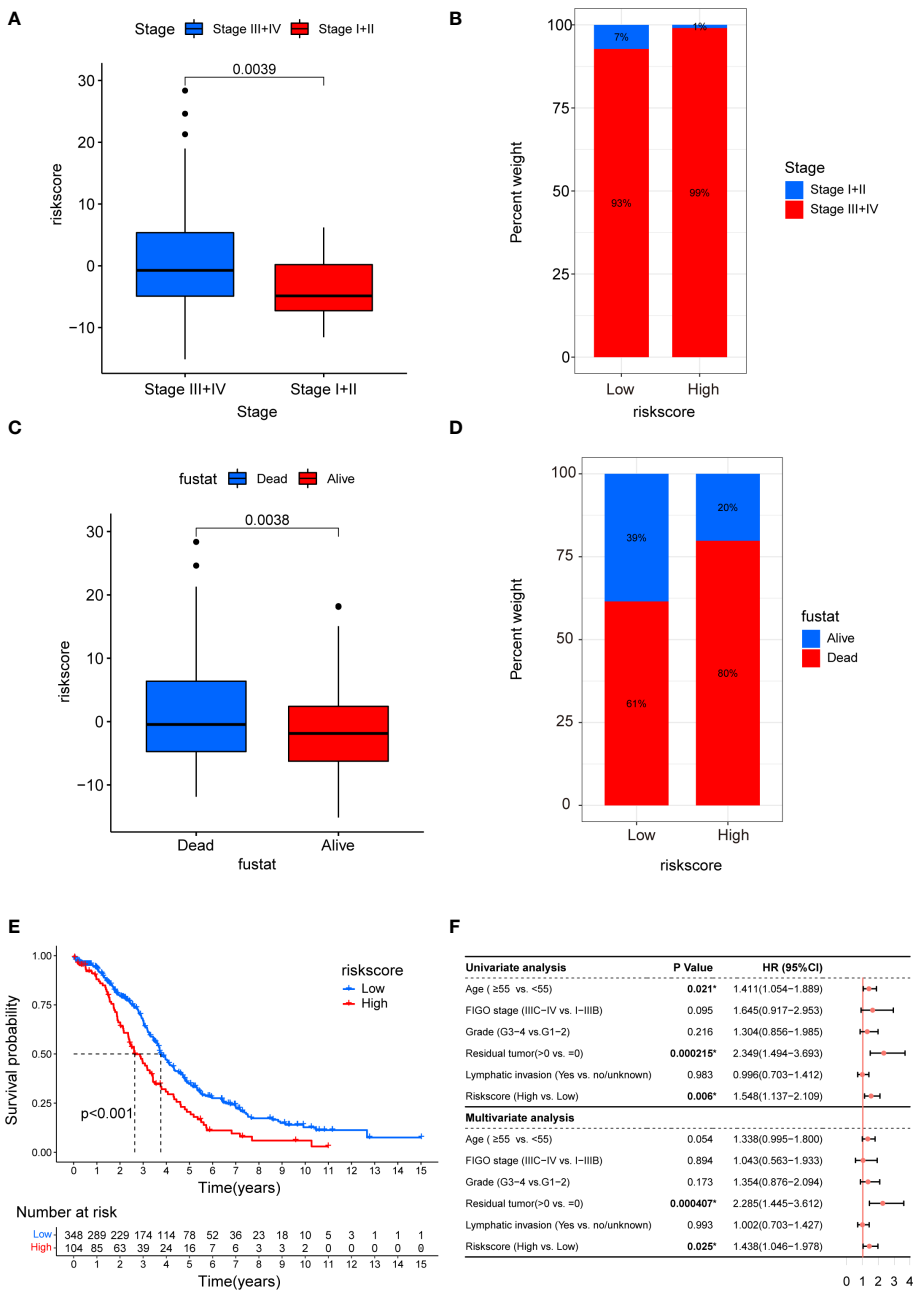

FIGURE 12
Clinicopathological and prognostic characteristics of CAF riskscore. **(A)** Correction between CAF riskscore and tumor stage. **(B)** Proportions of tumor stage in high- and low-riskscore groups. **(C)** Correction between CAF riskscore and survival status. **(D)** Proportions of survival status in high- and low-riskscore groups. **(E)** Kaplan–Meier curves of overall survival between high- and low-riskscore groups. **(F)** Forest map of CAF riskscore and clinicopathological parameters in TCGA_OV cohort.

role of NF-κB signaling in mediating interactions between cancer cells and stroma. In various tumor types, continuous NF-κB signaling pathway activation in CAFs facilitates tumor progression and triggers inhibitory immune cell infiltration by secreting IL6, IL8, and other inflammatory molecules (33, 50). The JAK/STAT3 and PI3K/AKT signaling pathways could be considered potential targets for combating CAF-induced chemotherapy resistance in gastric cancer (51, 52). Additionally, a complex crosstalk exists between CAFs and immune cells. Tumor-associated macrophages are the most prominent immune cells in the vicinity of CAF aggregation, suggesting an intimate interplay between the two cell types (12).

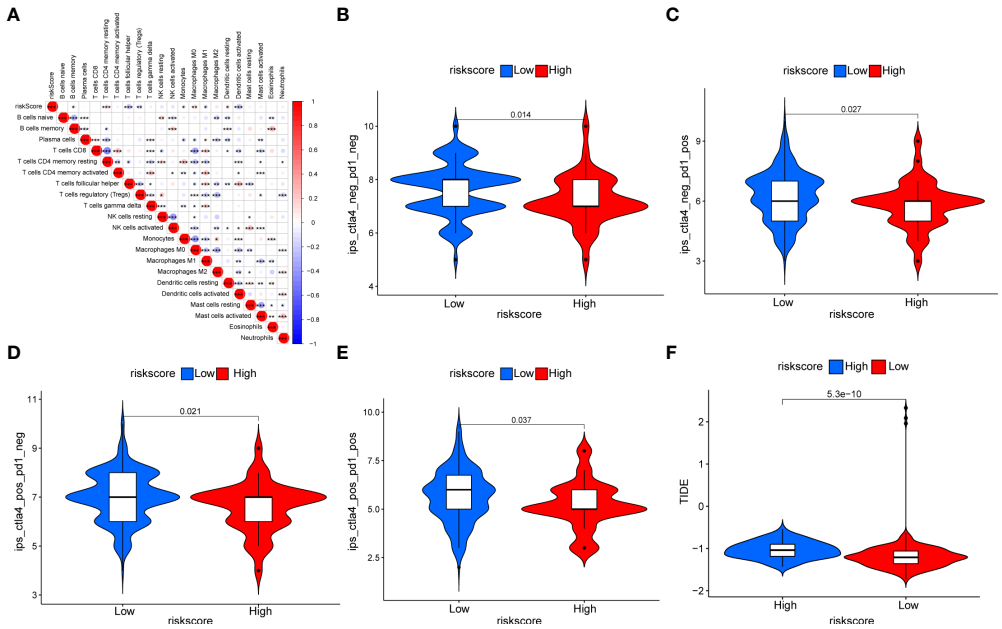

FIGURE 13
Relationship between the CAF riskscore and immunity. **(A)** The correction between the CAF riskscore and the 22 TME infiltration cells based on the CIBERSORT algorithm. **(B–E)** The relationship between IPS and CAF riskscore groups in EOC patients. The IPS-CTLA4-/PD-L1- **(B)**, IPS-CTLA4-/PD-L1+ **(C)**, IPS-CTLA4+/PD-L1- **(D)**, and IPS-CTLA4+/PD-L1+ **(E)** were higher in the low-riskscore group than in the high-riskscore group (all $p < 0.05$). **(F)** The TIDE prediction value was significantly higher in the high-riskscore group than that in the low-riskscore group.

Reactive oxygen species and pro-inflammatory cytokines are produced by M1 macrophages to kill tumor cells (53), while M2 macrophages facilitate tumor growth and inhibit tumor immunity by secreting anti-inflammatory cytokines (54, 55). Activated CAFs promote the adhesion of monocytes (macrophage precursors) and their transformation into M2 macrophages *via* multiple regulatory pathways, thereby inhibiting immune responses in the TME (56, 57). Cardiotrophin-like cytokine factor 1 (CLCF1) derived from CAFs induces N2 neutrophil polarization to facilitate hepatocellular carcinoma (HCC) progression (58). In HCC, IL6 secreted by CAFs inhibits T-cell activity and induces immune tolerance by triggering the JAK-STAT3 pathway in tumor-associated neutrophils (59). CAF-secreted IL6 is also responsible for the generation and activation of MDSCs, which weakens the antitumor immune response and promotes HCC progression (60, 61). Recent research in esophageal squamous cell carcinoma demonstrated that CAF-derived exosome-packed microRNA-21 *via* activating STAT3 signaling promoted the generation of monocyte-MDSCs, thereby causing resistance to cisplatin (62). Cooperation between MCs and CAFs is an influential microenvironmental driver of prostate cancer progression that results in the transformation of benign epithelial cells into early malignant cells (63). In HCC, CAFs induce indoleamine 2,3-dioxygenase(IDO)-producing regulatory DCs to acquire a tolerogenic phenotype through IL6-mediated STAT3 activation (64). Furthermore, CAFs significantly inhibit NK cell function by reducing their proliferation rates, cytotoxic capacity, and stimulatory receptor expression (65). As demonstrated in our study, the CAF score was highly correlated with multiple immune pathways and immunosuppressive cells, which is in agreement with previous research. The effects of CAFs on immune cells in the TME suggest that they induce immune evasion by tumor cells and exert immunosuppressive effects in pan-cancer and OV cohorts.

Next, we categorized the EOC samples into two distinct CAF molecular subtypes and constructed a CAF riskscore system. We found that a higher CAF riskscore was associated with cluster B, which corresponded to a worse prognosis and advanced stage. In contrast, a lower CAF riskscore was associated with cluster A and corresponded to a better prognosis and predicted early-stage disease. We then performed an enrichment analysis among the subtypes to explore the reasons for these differences. Cluster B was significantly enriched in immune-related pathways, whereas cluster A was mainly associated with DNA repair-related pathways. The TME immune infiltration analysis showed that memory resting CD4 T cells, M2 macrophages, neutrophils, and resting DCs had a higher probability of infiltration in cluster B and high-riskscore groups. Increasing evidence has shown that intratumoral CD4 T cells upregulate various inhibitory immune checkpoint proteins such as PD-1, CTLA-4, T-cell immunoglobulin and mucin domain-containing protein 3

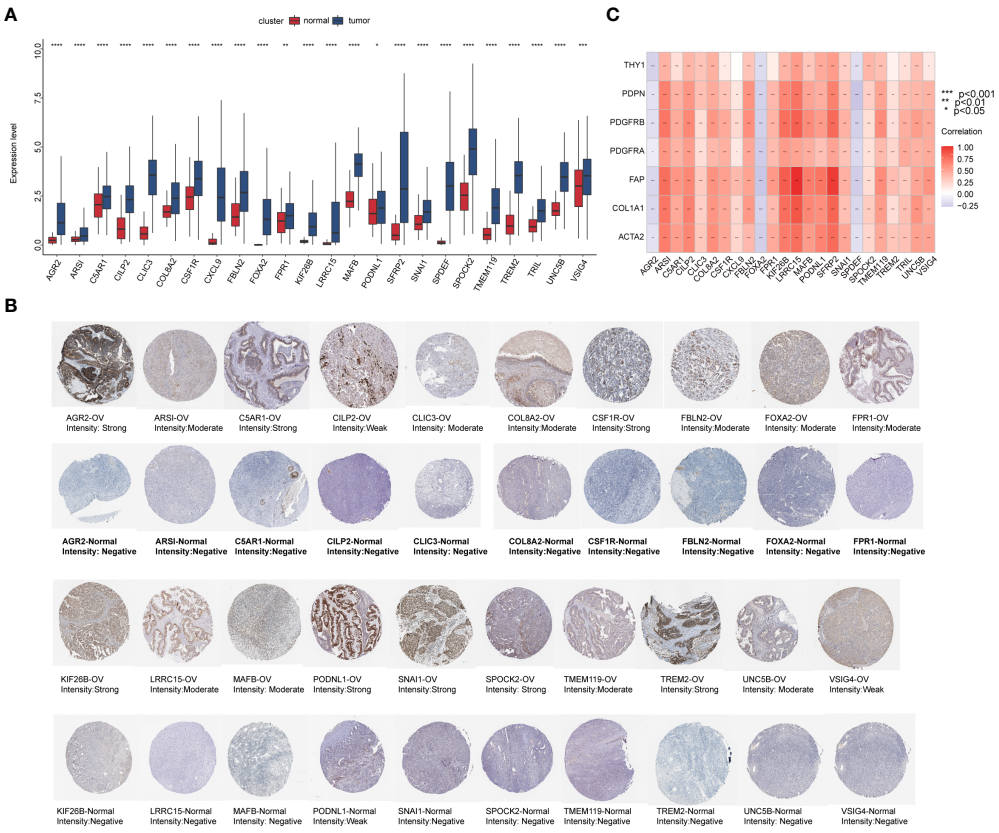

FIGURE 14
The preliminary screened key genes in EOC. **(A)** The 24 key genes were significantly upregulated in EOC samples compared to normal ovarian samples (The statistical differences were compared by t-test). **(B)** Immunohistochemical staining for indicated key genes in EOC tissues and normal ovarian tissues (Human Protein Atlas database). **(C)** Correlation analysis of 24 key genes with seven CAF markers.

(TIM-3), and LAG-3, which contribute to negative immune responses against tumors (66). As a result of their immunosuppressive properties, tumor cells within this group may escape the immune system. In addition, memory B cells, activated NK cells, activated DCs, and M1 macrophages infiltrated more frequently in cluster A and the low-riskscore group. It is reported that B-cell enrichment is associated with a better response to PD-1 blockade in soft tissue sarcoma and is the most predictive prognostic indicator for prolonged survival (67–69). Since this group was associated with immune activation characteristics, we hypothesize that patients in this group would benefit from immunotherapy. We subsequently found that the low-risk subgroup was more immunogenic than the high-risk subgroup, indicating that patients in this group may be more sensitive to immune checkpoint inhibitors and may have better clinical outcomes, which is consistent with our predictions. Eventually, we identified prognostic DEGs associated with CAF subtypes and determined 24 key genes that were upregulated in EOC with certain correlations to CAF markers. Some of these genes, such as colony-stimulating factor 1 receptor (CSF1R), snail (SNAI1), and uncoordinated-5 homolog B (UNC5B), influence CAF function. However, limited information is available on EOC (70–72).

Our study has some limitations. First, more samples from independent cohorts are required to validate the accuracy and predictability of the CAF riskscore system that we applied to EOC. In addition, the role of CAFs in the EOC immune system and their potential as immunotherapy targets for intervention need further investigation. Finally, additional experiments are necessary to explore the biological behavior of these key genes and the exact mechanisms associated with CAFs in EOC.

Conclusions

In the present study, we determined that CAFs are critical for tumor immune evasion and outcomes at the pan-cancer level and in the OV cohort by comprehensively stratifying and quantifying the CAF landscape. CAF subtypes contribute to a better understanding of EOC heterogeneity. The CAF riskscore

system we developed could be used to predict prognosis and provide new insights into the potential of CAF status as an immunotherapeutic approach for EOC.

Data availability statement

The datasets presented in this study can be found in online repositories. The names of the repository/repositories and accession number(s) can be found in the article/Supplementary Material.

Author contributions

RZ wrote the draft of the manuscript. QJ and MC designed the study. TJ conducted the analysis of the data. LY supervised the execution of the study. HD provided all the funding for this study. All authors contributed to the article and approved the submitted version.

Funding

This work was supported by Liaoning Province Natural Science Fund Plan (No.2019-MS-358), and 345 Talent Project.

Conflict of interest

The authors declare that the research was conducted in the absence of any commercial or financial relationships that could be construed as a potential conflict of interest.

Publisher's note

Supplementary material

The Supplementary Material for this article can be found online at: https://www.frontiersin.org/articles/10.3389/fimmu.2022.956224/full#supplementary-material

SUPPLEMENTARY TABLE 1
The CAF score for TCGA pan-cancer samples.

SUPPLEMENTARY TABLE 2
The clinical information from GSE63885 and TCGA_OV cohort.

SUPPLEMENTARY TABLE 3
The correlation of CAF score with immune cells in TME (based on ImmuCellAI and TIMER2 database).

SUPPLEMENTARY TABLE 4
GSVA enrichment analysis for two CAF subtypes in EOC cohort.

SUPPLEMENTARY TABLE 5
The details of DEGs and functional enrichment analysis.

SUPPLEMENTARY TABLE 6
118 DEGs associated with OS for EOC patients.

SUPPLEMENTARY TABLE 7
GSVA enrichment analysis for CAF riskscore in EOC cohort.

SUPPLEMENTARY FIGURE 1
The correlation of seven CAF markers. **(A)** The PPI networks among seven CAF markers. **(B)** The correlation of seven CAF markers based on TCGA pan-cancer data. **(C)** The correlation of seven CAF marker based on TCGA_OV cohort. The darker the color, the stronger the correlation.

SUPPLEMENTARY FIGURE 2
The SNV alteration of seven CAF markers in pan-cancer. **(A)** The information of variant classification, variant type, SNV class, variants per sample, variant classification summary, and variant count and percentage of seven CAF markers across the cancer type. **(B)** The waterfall plot presents the mutation distribution and a classification of SNV types of each marker in selected caner types. **(C)** The heat map presents the mutation frequency of each marker in selected caner types. The number represents the number of samples with the corresponding mutated gene for a given cancer type.

SUPPLEMENTARY FIGURE 3
GSVA enrichment analysis for CAF riskscore in EOC cohort.

References

1. Siegel RL, Miller KD, Jemal A. Cancer statistics, 2019. *Ca-Cancer J Clin* (2019) 69:7–34. doi: 10.3322/caac.21551

2. Sung H, Ferlay J, Siegel RL, Laversanne M, Soerjomataram I, Jemal A, et al. Global cancer statistics 2020: GLOBOCAN estimates of incidence and mortality worldwide for 36 cancers in 185 countries. *Ca-Cancer J Clin* (2021) 71(3):209–49. doi: 10.3322/caac.21660

3. Raja FA, Chopra N, Ledermann JA. Optimal first-line treatment in ovarian cancer. *Ann Oncol* (2012) 23(suppl 10):x118–27. doi: 10.1093/annonc/mds315

4. Rojas V, Hirshfield KM, Ganesan S, Rodriguez-Rodriguez L. Molecular characterization of epithelial ovarian cancer: Implications for diagnosis and treatment. *Int J Mol Sci* (2016) 17(12):2113. doi: 10.3390/ijms17122113

5. Kossaï M, Leary A, Scoazec JY, Genestie C. Ovarian cancer: A heterogeneous disease. *Pathobiology* (2018) 85:41–9. doi: 10.1159/000479006

6. Anderson NM, Simon MC. The tumor microenvironment. *Curr Biol* (2020) 30(16):R921–5. doi: 10.1016/j.cub.2020.06.081

7. Chen X, Song E. Turning foes to friends: targeting cancer-associated fibroblasts. *Nat Rev Drug Discov* (2019) 18(2):99–115. doi: 10.1038/s41573-018-0004-1

8. Sahai E, Astsaturov I, Cukierman E, DeNardo DG, Egeblad M, Evans RM, et al. A framework for advancing our understanding of cancer-associated fibroblasts. *Nat Rev Cancer* (2020) 20(3):174–86. doi: 10.1038/s41568-019-0238-1

9. Fiori ME, Di Franco S, Villanova L, Bianca P, Stassi G, De Maria R. Cancer-associated fibroblasts as abettors of tumor progression at the crossroads of EMT and therapy resistance. *Mol Cancer* (2019) 18(1):70. doi: 10.1186/s12943-019-0994-2

10. Chandra Jena B, Kanta Das C, Banerjee I, Das S, Bharadwaj D, Majumder R, et al. Paracrine TGF-β1 from breast cancer contributes to chemoresistance in cancer associated fibroblasts *via* upregulation of the p44/42 MAPK signaling pathway. *Biochem Pharmacol* (2021) 186:114474. doi: 10.1016/j.bcp.2021.114474

11. Barrett R, Puré E. Cancer-associated fibroblasts: key determinants of tumor immunity and immunotherapy. *Curr Opin Immunol* (2020) 64:80–7. doi: 10.1016/j.coi.2020.03.004

12. Liu T, Han C, Wang S, Fang P, Ma Z, Xu L, et al. Cancer-associated fibroblasts: an emerging target of anti-cancer immunotherapy. *J Hematol Oncol* (2019) 12(1):86. doi: 10.1186/s13045-019-0770-1

13. Kobayashi H, Enomoto A, Woods SL, Burt AD, Takahashi M, Worthley DL. Cancer-associated fibroblasts in gastrointestinal cancer. *Nat Rev Gastroenterol Hepatol* (2019) 16(5):282–95. doi: 10.1038/s41575-019-0115-0

14. Strong AL, Pei DT, Hurst CG, Gimble JM, Burow ME, Bunnell BA. Obesity enhances the conversion of adipose-derived Stromal/Stem cells into carcinoma-associated fibroblast leading to cancer cell proliferation and progression to an invasive phenotype. *Stem Cells Int* (2017) 2017:9216502. doi: 10.1155/2017/9216502

15. Raz Y, Cohen N, Shani O, Bell RE, Novitskiy SV, Abramovitz L, et al. Bone marrow-derived fibroblasts are a functionally distinct stromal cell population in breast cancer. *J Exp Med* (2018) 215(12):3075–93. doi: 10.1084/jem.20180818

16. Yeon JH, Jeong HE, Seo H, Cho S, Kim K, Na D, et al. Cancer-derived exosomes trigger endothelial to mesenchymal transition followed by the induction of cancer-associated fibroblasts. *Acta Biomater* (2018) 76:146–53. doi: 10.1016/j.actbio.2018.07.001

17. Pelon F, Bourachot B, Kieffer Y, Magagna I, Mermet-Meillon F, Bonnet I, et al. Cancer-associated fibroblast heterogeneity in axillary lymph nodes drives metastases in breast cancer through complementary mechanisms. *Nat Commun* (2020) 11(1):404. doi: 10.1038/s41467-019-14134-w

18. Givel AM, Kieffer Y, Scholer-Dahirel A, Sirven P, Cardon M, Pelon F, et al. miR200-regulated CXCL12β promotes fibroblast heterogeneity and immunosuppression in ovarian cancers. *Nat Commun* (2018) 9(1):1056. doi: 10.1038/s41467-018-03348-z

19. Faivre S, Santoro A, Kelley RK, Gane E, Costentin CE, Gueorguieva I, et al. Novel transforming growth factor beta receptor I kinase inhibitor galunisertib (LY2157299) in advanced hepatocellular carcinoma. *Liver Int* (2019) 39(8):1468–77. doi: 10.1111/liv.14113

20. Duperret EK, Trautz A, Ammons D, Perales-Puchalt A, Wise MC, Yan J, et al. Alteration of the tumor stroma using a consensus DNA vaccine targeting fibroblast activation protein (FAP) synergizes with antitumor vaccine therapy in mice. *Clin Cancer Res* (2018) 24(5):1190–201. doi: 10.1158/1078-0432.Ccr-17-2033

21. Winer A, Adams S, Mignatti P. Matrix metalloproteinase inhibitors in cancer therapy: Turning past failures into future successes. *Mol Cancer Ther* (2018) 17(6):1147–55. doi: 10.1158/1535-7163.Mct-17-0646

22. Sun D, Wang J, Han Y, Dong X, Ge J, Zheng R, et al. TISCH: a comprehensive web resource enabling interactive single-cell transcriptome visualization of tumor microenvironment. *Nucleic Acids Res* (2021) 49:D1420–30. doi: 10.1093/nar/gkaa1020

23. Zheng S, Zou Y, Tang Y, Yang A, Liang JY, Wu L, et al. Landscape of cancer-associated fibroblasts identifies the secreted biglycan as a protumor and immunosuppressive factor in triple-negative breast cancer. *Oncoimmunology* (2022) 11(1):2020984. doi: 10.1080/2162402x.2021.2020984

24. Liu CJ, Hu FF, Xia MX, Han L, Zhang Q, Guo AY. GSCALite: a web server for gene set cancer analysis. *Bioinformatics* (2018) 34(21):3771–2. doi: 10.1093/bioinformatics/bty411

25. Yoshihara K, Shahmoradgoli M, Martínez E, Vegesna R, Kim H, Torres-Garcia W, et al. Inferring tumour purity and stromal and immune cell admixture from expression data. *Nat Commun* (2013) 4:2612. doi: 10.1038/ncomms3612

26. Ritchie ME, Phipson B, Wu D, Hu Y, Law CW, Shi W, et al. Limma powers differential expression analyses for RNA-sequencing and microarray studies. *Nucleic Acids Res* (2015) 43(7):e47. doi: 10.1093/nar/gkv007

27. Yu G, Wang LG, Han Y, He QY. clusterProfiler: an r package for comparing biological themes among gene clusters. *OMICS* (2012) 16(5):284–7. doi: 10.1089/omi.2011.0118

28. Zhang B, Wu Q, Li B, Wang D, Wang L, Zhou YL. mA regulator-mediated methylation modification patterns and tumor microenvironment infiltration characterization in gastric cancer. *Mol Cancer* (2020) 19(1):53. doi: 10.1186/s12943-020-01170-0

29. Charoentong P, Finotello F, Angelova M, Mayer C, Efremova M, Rieder D, et al. Pan-cancer immunogenomic analyses reveal genotype-immunophenotype relationships and predictors of response to checkpoint blockade. *Cell Rep* (2017) 18(1):248–62. doi: 10.1016/j.celrep.2016.12.019

30. Jiang P, Gu S, Pan D, Fu J, Sahu A, Hu X, et al. Signatures of T cell dysfunction and exclusion predict cancer immunotherapy response. *Nat Med* (2018) 24(10):1550–8. doi: 10.1038/s41591-018-0136-1

31. Aran D, Sirota M, Butte AJ. Systematic pan-cancer analysis of tumour purity. *Nat Commun* (2015) 6:8971. doi: 10.1038/ncomms9971

32. Mahoney KM, Rennert PD, Freeman GJ. Combination cancer immunotherapy and new immunomodulatory targets. *Nat Rev Drug Discov* (2015) 14(8):561–84. doi: 10.1038/nrd4591

33. Su S, Chen J, Yao H, Liu J, Yu S, Lao L, et al. CD10GPR77 cancer-associated fibroblasts promote cancer formation and chemoresistance by sustaining cancer stemness. *Cell* (2018) 172(4):841–856.e16. doi: 10.1016/j.cell.2018.01.009

34. Öhlund D, Handly-Santana A, Biffi G, Elyada E, Almeida AS, Ponz-Sarvise M, et al. Distinct populations of inflammatory fibroblasts and myofibroblasts in pancreatic cancer. *J Exp Med* (2017) 214(3):579–96. doi: 10.1084/jem.20162024

35. Strell C, Paulsson J, Jin SB, Tobin NP, Mezheyeuski A, Roswall P, et al. Impact of epithelial-stromal interactions on peritumoral fibroblasts in ductal carcinoma *in situ*. *J Natl Cancer Inst* (2019) 111(9):983–95. doi: 10.1093/jnci/djy234

36. Elyada E, Bolisetty M, Laise P, Flynn WF, Courtois ET, Burkhart RA, et al. Cross-species single-cell analysis of pancreatic ductal adenocarcinoma reveals antigen-presenting cancer-associated fibroblasts. *Cancer Discov* (2019) 9(8):1102–23. doi: 10.1158/2159-8290.Cd-19-0094

37. Hesterberg AB, Rios BL, Wolf EM, Tubbs C, Hurley PJ. A distinct repertoire of cancer-associated fibroblasts is enriched in cribriform prostate cancer. *J Pathol Clin Res* (2021) 7:271–86. doi: 10.1002/cjp2.205

38. Mano Y, Yoshio S, Shoji H, Tomonari S, Aoki Y, Aoyanagi N, et al. Bone morphogenetic protein 4 provides cancer-supportive phenotypes to liver fibroblasts in patients with hepatocellular carcinoma. *J Gastroenterol* (2019) 54(11):1007–18. doi: 10.1007/s00535-019-01579-5

39. Venning FA, Zornhagen KW, Wullkopf L, Sjölund J, Rodriguez-Cupello C, Kjellman P, et al. Deciphering the temporal heterogeneity of cancer-associated fibroblast subpopulations in breast cancer. *J Exp Clin Cancer Res* (2021) 40(1):175. doi: 10.1186/s13046-021-01944-4

40. Neuzillet C, Tijeras-Raballand A, Ragulan C, Cros J, Patil Y, Martinet M, et al. Inter- and intra-tumoural heterogeneity in cancer-associated fibroblasts of human pancreatic ductal adenocarcinoma. *J Pathol* (2019) 248(1):51–65. doi: 10.1002/path.5224

41. Costa A, Kieffer Y, Scholer-Dahirel A, Pelon F, Bourachot B, Cardon M, et al. Fibroblast heterogeneity and immunosuppressive environment in human breast cancer. *Cancer Cell* (2018) 33(3):463–79.e10. doi: 10.1016/j.ccell.2018.01.011

42. Hussain A, Voisin V, Poon S, Karamboulas C, Bui NHB, Meens J, et al. Distinct fibroblast functional states drive clinical outcomes in ovarian cancer and are regulated by TCF21. *J Exp Med* (2020) 217(8):e20191094. doi: 10.1084/jem.20191094

43. Mhaskar DN, Goodman MF. On the molecular basis of transition mutations. frequency of forming 2-aminopurine-cytosine base mispairs in the G X c--A X T mutational pathway by T4 DNA polymerase *in vitro*. *J Biol Chem* (1984) 259(19):11713–7. doi: 10.1016/S0021-9258(20)71268-8

44. Shao X, Lv N, Liao J, Long J, Xue R, Ai N, et al. Copy number variation is highly correlated with differential gene expression: a pan-cancer study. *BMC Med Genet* (2019) 20(1):175. doi: 10.1186/s12881-019-0909-5

45. Chen X, Lin Y, Qu Q, Ning B, Chen H, Cai L. A multi-source data fusion framework for revealing the regulatory mechanism of breast cancer immune evasion. *Front Genet* (2020) 11:595324. doi: 10.3389/fgene.2020.595324

46. Bidinotto LT, Torrieri R, Mackay A, Almeida GC, Viana-Pereira M, Cruvinel-Carloni A, et al. Copy number profiling of Brazilian astrocytomas. *G3 (Bethesda Md.)* (2016) 6(7):1867–78. doi: 10.1534/g3.116.029884

47. Das PM, Singal R. DNA Methylation and cancer. *J Clin Oncol* (2004) 22(22):4632–42. doi: 10.1200/jco.2004.07.151

48. Meng H, Cao Y, Qin J, Song X, Zhang Q, Shi Y, et al. DNA Methylation, its mediators and genome integrity. *Int J Biol Sci* (2015) 11(5):604–17. doi: 10.7150/ijbs.11218

49. Ghahremanifard P, Chanda A, Bonni S, Bose P. TGF-β mediated immune evasion in cancer-spotlight on cancer-associated fibroblasts. *Cancers (Basel)* (2020) 12(12):3650. doi: 10.3390/cancers12123650

50. Gu J, Li X, Zhao L, Yang Y, Xue C, Gao Y, et al. The role of PKM2 nuclear translocation in the constant activation of the NF-κB signaling pathway in cancer-associated fibroblasts. *Cell Death Dis* (2021) 12(4):291. doi: 10.1038/s41419-021-03579-x

51. Ham IH, Wang L, Lee D, Woo J, Kim TH, Jeong HY, et al. Curcumin inhibits the cancer–associated fibroblast–derived chemoresistance of gastric cancer through the suppression of the JAK/STAT3 signaling pathway. *Int J Oncol* (2022) 61(1):85. doi: 10.3892/ijo.2022.5375

52. Zhao ZX, Zhang YQ, Sun H, Chen ZQ, Chang JJ, Wang X, et al. Calcipotriol abrogates cancer-associated fibroblast-derived IL-8-mediated oxaliplatin resistance in gastric cancer cells *via* blocking PI3K/Akt signaling. *Acta Pharmacol Sin* (2022). doi: 10.1038/s41401-022-00927-1

53. Shapouri-Moghaddam A, Mohammadian S, Vazini H, Taghadosi M, Esmaeili SA, Mardani F, et al. Macrophage plasticity, polarization, and function in health and disease. *J Cell Physiol* (2018) 233(9):6425–40. doi: 10.1002/jcp.26429

54. Jeannin P, Paolini L, Adam C, Delneste Y. The roles of CSFs on the functional polarization of tumor-associated macrophages. *FEBS J* (2018) 285 (4):680–99. doi: 10.1111/febs.14343

55. Chen Y, Song Y, Du W, Gong L, Chang H, Zou Z. Tumor-associated macrophages: an accomplice in solid tumor progression. *J BioMed Sci* (2019) 26 (1):78. doi: 10.1186/s12929-019-0568-z

56. Tan B, Shi X, Zhang J, Qin J, Zhang N, Ren H, et al. Inhibition of rspo-Lgr4 facilitates checkpoint blockade therapy by switching macrophage polarization. *Cancer Res* (2018) 78(17):4929–42. doi: 10.1158/0008-5472.Can-18-0152

57. Zhang R, Qi F, Zhao F, Li G, Shao S, Zhang X, et al. Cancer-associated fibroblasts enhance tumor-associated macrophages enrichment and suppress NK cells function in colorectal cancer. *Cell Death Dis* (2019) 10(4):273. doi: 10.1038/s41419-019-1435-2

58. Song M, He J, Pan QZ, Yang J, Zhao J, Zhang YJ, et al. Cancer-associated fibroblast-mediated cellular crosstalk supports hepatocellular carcinoma progression. *Hepatology* (2021) 73(5):1717–35. doi: 10.1002/hep.31792

59. Cheng Y, Li H, Deng Y, Tai Y, Zeng K, Zhang Y, et al. Cancer-associated fibroblasts induce PDL1+ neutrophils through the IL6-STAT3 pathway that foster immune suppression in hepatocellular carcinoma. *Cell Death Dis* (2018) 9(4):422. doi: 10.1038/s41419-018-0458-4

60. Deng Y, Cheng J, Fu B, Liu W, Chen G, Zhang Q, et al. Hepatic carcinoma-associated fibroblasts enhance immune suppression by facilitating the generation of myeloid-derived suppressor cells. *Oncogene* (2017) 36(8):1090–101. doi: 10.1038/onc.2016.273

61. Liu H, Shen J, Lu K. IL-6 and PD-L1 blockade combination inhibits hepatocellular carcinoma cancer development in mouse model. *Biochem Biophys Res Commun* (2017) 486(2):239–44. doi: 10.1016/j.bbrc.2017.02.128

62. Zhao Q, Huang L, Qin G, Qiao Y, Ren F, Shen C, et al. Cancer-associated fibroblasts induce monocytic myeloid-derived suppressor cell generation *via* IL-6/exosomal miR-21-activated STAT3 signaling to promote cisplatin resistance in esophageal squamous cell carcinoma. *Cancer Lett* (2021) 518:35–48. doi: 10.1016/j.canlet.2021.06.009

63. Pereira BA, Lister NL, Hashimoto K, Teng L, Flandes-Iparraguirre M, Eder A, et al. Tissue engineered human prostate microtissues reveal key role of mast cell-derived tryptase in potentiating cancer-associated fibroblast (CAF)-induced morphometric transition *in vitro*. *Biomaterials* (2019) 197:72–85. doi: 10.1016/j.biomaterials.2018.12.030

64. Cheng JT, Deng YN, Yi HM, Wang GY, Fu BS, Chen WJ, et al. Hepatic carcinoma-associated fibroblasts induce IDO-producing regulatory dendritic cells through IL-6-mediated STAT3 activation. *Oncogenesis* (2016) 5:e198. doi: 10.1038/oncsis.2016.7

65. Yang N, Lode K, Berzaghi R, Islam A, Martinez-Zubiaurre I, Hellevik T. Irradiated tumor fibroblasts avoid immune recognition and retain immunosuppressive functions over natural killer cells. *Front Immunol* (2020) 11:602530. doi: 10.3389/fimmu.2020.602530

66. Toor SM, Murshed K, Al-Dhaheri M, Khawar M, Abu Nada M, Elkord E. Immune checkpoints in circulating and tumor-infiltrating CD4 T cell subsets in colorectal cancer patients. *Front Immunol* (2019) 10:2936. doi: 10.3389/fimmu.2019.02936

67. Tanaka A, Sakaguchi S. Regulatory T cells in cancer immunotherapy. *Cell Res* (2017) 27(1):109–18. doi: 10.1038/cr.2016.151

68. Cabrita R, Lauss M, Sanna A, Donia M, Skaarup Larsen M, Mitra S, et al. Tertiary lymphoid structures improve immunotherapy and survival in melanoma. *Nature* (2020) 577(7791):561–5. doi: 10.1038/s41586-019-1914-8

69. Helmink BA, Reddy SM, Gao J, Zhang S, Basar R, Thakur R, et al. B cells and tertiary lymphoid structures promote immunotherapy response. *Nature* (2020) 577 (7791):549–55. doi: 10.1038/s41586-019-1922-8

70. Herrera A, Herrera M, Alba-Castellón L, Silva J, García V, Loubat-Casanovas J, et al. Protumorigenic effects of snail-expression fibroblasts on colon cancer cells. *Int J Cancer* (2014) 134(12):2984–90. doi: 10.1002/ijc.28613

71. Sung PJ, Rama N, Imbach J, Fiore S, Ducarouge B, Neves D, et al. Cancer-associated fibroblasts produce netrin-1 to control cancer cell plasticity. *Cancer Res* (2019) 79(14):3651–61. doi: 10.1158/0008-5472.Can-18-2952

72. Kumar V, Donthireddy L, Marvel D, Condamine T, Wang F, Lavilla-Alonso S, et al. Cancer-associated fibroblasts neutralize the anti-tumor effect of CSF1 receptor blockade by inducing PMN-MDSC infiltration of tumors. *Cancer Cell* (2017) 32(5):654–68.e5. doi: 10.1016/j.ccell.2017.10.005

Glossary

ACC	Adrenocortical carcinoma
ACTA2	Smooth muscle actin 2
AGR2	Anterior gradient protein 2
BLCA	Bladder Urothelial Carcinoma
BRCA	Breast invasive carcinoma
CAFs	Cancer associated fibroblasts
CESC	Cervical squamous cell carcinoma and endocervical adenocarcinoma
CHOL	Cholangiocarcinoma
CI	Confidence interval
CNV	Copy number variation
COAD	Colon adenocarcinoma
COL1A1	https://pubmed.ncbi.nlm.nih.gov/29906404/Collagen 1A1
CSF1R	Colony-stimulating factor 1 receptor
DCs	Dendritic cells
DEGs	Differentially expressed genes
DLBC	Lymphoid Neoplasm Diffuse Large B-cell Lymphoma
ECM	Extracellular matrix
EOC	Epithelial ovarian cancer
ESCA	Esophageal carcinoma
FAP	Fibroblast activation protein
FDR	False Discovery Rate
FOXA2	Forkhead box A2
GBM	Glioblastoma multiforme
GEO	Gene Expression Omnibus data base
GO	Gene ontolog
GSCA	Gene Set Cancer Analysis
GSVA	Gene set variation analysis
GTEx	Genotype-Tissue Expression
HCC	Hepatocellular carcinoma
HNSC	Head and Neck squamous cell carcinoma
HR	Hazards ratio
IL2-STAT	Interleukin 2-Signal transducer and activator of transcription
IPS	Immunophenoscores
iTreg	induced Treg
KEGG	Kyoto encyclopedia of genes agenomes
KICH	Kidney Chromophobe
KIRC	Kidney renal clear cell carcinoma
KIRP	Kidney renal papillary cell carcinoma
LAML	Acute Myeloid Leukemia
LGG	Lower Grade Glioma
LIHC	Liver hepatocellular carcinoma
LUAD	Lung adenocarcinoma
LUSC	Lung squamous cell carcinoma
MCs	Mast cells
MDSCs	Myeloid-derived suppressor cells
MESO	Mesothelioma
NF-kB	Nuclear factor-k-gene binding

(Continued)

Continued

NK	Natural killer
nTreg	natural Treg
OS	Overall survival
OV	Ovarian cancer
PAAD	Pancreatic adenocarcinoma
PCA	Principal component analysis
PCPG	Pheochromocytoma and Paraganglioma
PDGFRA	Platelet-derived growth factor receptor alpha
PDGFRB	Platelet-derived growth factor receptor-beta
PDPN	Podoplanin
PPI	Protein-protein interaction
PRAD	Prostate adenocarcinom
READ	Rectum adenocarcinoma
SARC	Sarcoma
SKCM	Skin Cutaneous Melanoma
SNAI1	Snail
SNV	Single nucleotide variation
SPDEF	SAM pointed domain-containing ETS transcription factor
ssGSEA	Single-sample gene set enrichment analysis
STAD	Stomach adenocarcinoma
STRING	Search tool for the retrieval of interacting genes/proteins
TCGA	The Cancer Genome Atlas
TCIA	The Cancer Immunome Atlas
TGCT	Testicular Germ Cell tumours
TGF-β	Transforming growth factor-β
THCA	Thyroid carcinoma
THY1	https://pubmed.ncbi.nlm.nih.gov/20599951/Thy-1 cell surface antigen
THYM	Thymoma
TIDE	Tumor Immune Dysfunction and Exclusion
TISCH	tumour Immune Single Cell Hub
TME	tumour microenvironment
Tregs	T regulatory cells
UCEC	Uterine Corpus Endometrial Carcinoma
UCS	Uterine Carcinosarcoma
UCSC	University of California Santa Cruz
UNC5B	Uncoordinated-5 homolog B
UVM	Uveal Melanoma

frontiers | Frontiers in Pharmacology

TYPE Original Research
PUBLISHED 26 August 2022
DOI 10.3389/fphar.2022.897368

OPEN ACCESS

EDITED BY
Wang Lingzhi,
Cancer Science Institute of Singapore, National University of Singapore, Singapore

REVIEWED BY
Nguan Soon Tan,
Nanyang Technological University, Singapore
Stéphane Chabaud,
Centre de Recherche du CHU de Québec, Canada
Yiheng Du,
Suzhou Kowloon Hospital, China

*CORRESPONDENCE
Nisana Namwat,
nisana@kku.ac.th

SPECIALTY SECTION
This article was submitted to Pharmacology of Anti-Cancer Drugs, a section of the journal Frontiers in Pharmacology

RECEIVED 16 March 2022
ACCEPTED 01 August 2022
PUBLISHED 26 August 2022

CITATION
Kittirat Y, Suksawat M, Thongchot S, Padthaisong S, Phetcharaburanin J, Wangwiwatsin A, Klanrit P, Sangkhamanon S, Titapun A, Loilome W, Saya H and Namwat N (2022), Interleukin-6-derived cancer-associated fibroblasts activate STAT3 pathway contributing to gemcitabine resistance in cholangiocarcinoma. *Front. Pharmacol.* 13:897368. doi: 10.3389/fphar.2022.897368

Interleukin-6-derived cancer-associated fibroblasts activate STAT3 pathway contributing to gemcitabine resistance in cholangiocarcinoma

Yingpinyapat Kittirat[1,2], Manida Suksawat[2,3], Suyanee Thongchot[4,5], Sureerat Padthaisong[6], Jutarop Phetcharaburanin[1,2,3], Arporn Wangwiwatsin[1,2,3], Poramate Klanrit[1,2,3], Sakkarn Sangkhamanon[2,7], Attapol Titapun[2,8], Watcharin Loilome[1,2,3], Hideyuki Saya[9] and Nisana Namwat[1,2,3]*

[1]Department of Biochemistry, Faculty of Medicine, Khon Kaen University, Khon Kaen, Thailand, [2]Cholangiocarcinoma Research Institute, Faculty of Medicine, Khon Kaen University, Khon Kaen, Thailand, [3]Khon Kaen University International Phenome Laboratory, Khon Kaen University Science Park, Innovation and Enterprise Affairs, Khon Kaen University, Khon Kaen, Thailand, [4]Department of Immunology, Faculty of Medicine Siriraj Hospital, Mahidol University, Bangkok, Thailand, [5]Siriraj Center of Research Excellence for Cancer Immunotherapy (SiCORE-CIT), Research Department, Faculty of Medicine Siriraj Hospital, Mahidol University, Bangkok, Thailand, [6]Faculty of Allied Health Sciences, Burapha University, Chonburi, Thailand, [7]Department of Pathology, Faculty of Medicine, Khon Kaen University, Khon Kaen, Thailand, [8]Department of Surgery, Faculty of Medicine, Khon Kaen University, Khon Kaen, Thailand, [9]Division of Gene Regulation, Fujita Cancer Center, Fujita Health University, Tokyo, Japan

Cancer-associated fibroblasts (CAFs) are the dominant component of the tumor microenvironment (TME) that can be beneficial to the generation and progression of cancer cells leading to chemotherapeutic failure *via* several mechanisms. Nevertheless, the roles of CAFs on anti-cancer drug response need more empirical evidence in cholangiocarcinoma (CCA). Herein, we examined the oncogenic roles of CAFs on gemcitabine resistance in CCA cells mediated *via* IL-6/STAT3 activation. Our findings showed that CCA-derived CAFs promote cell viability and enhance gemcitabine resistance in CCA cells through the activation of IL-6/STAT3 signaling. High expression of IL-6R was correlated with a poor overall survival rate and gemcitabine resistance in CCA, indicating that IL-6R can be a prognostic or predictive biomarker for the chemotherapeutic response of CCA patients. Blockade of IL-6R on CCA cells by tocilizumab, an IL-6R humanized antihuman monoclonal antibody, contributed to inhibition of the CAF-CCA interaction leading to enhancement of gemcitabine sensitivity in CCA cells. The results of this study should be helpful for modifying therapeutic regimens aimed at targeting CAF interacting with cancer cells resulting in the suppression of the tumor progression but enhancement of drug sensitivity.

KEYWORDS
cholangiocarcinoma, IL-6, gemcitabine, cancer-associated fibroblasts, tocilizumab

Introduction

Cholangiocarcinoma (CCA) is a bile duct cancer originating from cholangiocytes lining of biliary tract. CCA is the second most common primary liver cancer worldwide (Banales et al., 2016). This cancer occurs prevalently in mainland Southeast Asian countries, especially in Northeast Thailand which has the world's highest incidence rates (Sriplung et al., 2006; Hughes et al., 2017). A poor prognosis and low survival rate are burdens for CCA treatment (Khan et al., 2012; Khuntikeo et al., 2014). Surgical resection has been the mainstay remedy in CCA treatment. CCA patients with unresectable cancer often received chemotherapy as a palliative treatment (Thongprasert, 2005; Butthongkomvong et al., 2013). However, CCA is resistant to common chemotherapy and has a poor response based on the characteristics of its multidrug resistant phenotypes, leading to complex mechanisms of chemoresistance (Marin et al., 2018). The lack of sensitivity of CCA cells to chemotherapeutic drugs is still dismal. The mechanisms of chemoresistance are composed of drug metabolism (such as its uptake, export, and intracellular biotransformation), the expression of molecular targets on cancer cells, and the ability of repair mechanisms to avoid apoptosis or programmed cell death (Banales et al., 2016). Moreover, the extensive desmoplastic microenvironment surrounding the neoplastic ducts, termed tumor reactive stroma, act as a key determinant of decreased sensitivity of CCA to drug-induced cytotoxicity (Cadamuro et al., 2017). To improve the potential of anti-cancer drugs for CCA treatment we should consider their mechanisms of chemoresistance.

The etiology of Thai CCA is strongly associated with chronic infection by the liver fluke (*Opisthorchis viverrini*), resulting in chronic inflammation that contributes to biliary damage (Sripa and Pairojkul, 2008; Songserm et al., 2009). Repeated infection causes tissue injury followed by chronic wound healing of host repair resulting in the generation of cancerous lesions that contains heterotypic tumor and stromal cells. The tumor microenvironment (TME) or tumor stroma consists of heterogeneous stromal cell populations. A complex network of extracellular matrix (ECM) surrounding cancer cells is beneficial to cancer development and progression (Pietras and Ostman, 2010; Quail and Joyce, 2013). A dominant component of TME is activated fibroblasts that are termed cancer-associated fibroblasts (CAFs). Several previous studies suggested functional roles for these cells in cancer progression and drug resistance mediated by secretory molecules such as cytokines or chemokines and physical contact *via* cell-cell adhesion molecules resulting in cancer cell growth and ECM remodeling toward migration and invasive outgrowth (Kalluri and Zeisberg, 2006; Ohlund et al., 2014). The alteration of pathways associated with the interaction of CAFs and cancer cells, including ECM adhesion and paracrine signaling, also facilitates mechanisms for cancer resistance (Meads et al., 2009; Paraiso and Smalley, 2013). Hence, the tumor stroma is the major causes of cancer development and progression toward chemoresistance presenting a clinical challenge. (Hogdall et al., 2018). Moreover, CAFs promote a migration of CCA cells *via* interleukin-6 (IL-6) secretion driving epithelial-to-mesenchymal transition (Thongchot et al., 2018). High expression of IL-6 in fibrotic stromal cells is associated with a poor prognosis and chemoresponse in CCA patients (Thongchot et al., 2021). The inhibitor related to the blockage of IL-6 and IL-6R such as tocilizumab is considered as an effective anti-cancer therapeutic approach (Masjedi et al., 2018). Therefore, improved understanding of interaction between CCA cells and their microenvironment might be effective strategies to overcome limitations on CCA treatment.

The development of drug resistance and CAFs are influential in promoting cancer cell evasion of anti-cancer therapies. However, the mechanisms involved in drug resistance are still poorly defined. Taking all data together, they suggest that CAFs play important roles in CCA progression and drug resistance. Understanding the mechanism by which CAFs communicate or interact with CCA cells is likely to be useful in the discovery of predictors of chemotherapeutic response toward drug targeting. In this study, we aimed at investigating the roles of CCA-derived CAFs on gemcitabine resistance in CCA cells and the inhibition of CAF-CCA interactions by blocking IL-6R on CCA cells to enhance gemcitabine sensitivity. These findings will be helpful for unraveling more secrets of CAFs on their pro-oncogenic effects in CCA chemoresistance, as well as modifying the therapeutic regimen aimed at targeting their interaction resulting in suppression of the tumor progression and enhancement of drug sensitivity.

Materials and methods

Patients, samples, and ethical issues

CCA tissue microarray (CCA-TMAs) of paraffin-embedded cases originated from primary tumors of 146 patients who admitted to surgical wards of Srinagarind Hospital, Khon Kaen University, Khon Kaen, Thailand, collected between 2014–2016. CAF samples were also collected from CCA tissues of patients who underwent surgical resection in Srinagarind Hospital. Written informed consent was obtained from all patients in accordance with the Declaration of Helsinki and its later revision. The Human Research Ethics Committee, Khon Kaen University, approved the research protocol (#HE571283 and #HE611544).

Reagents

MTT (3-(4,5-dimethylthiazol-2-yl)-2,5-diphenyltetrazolium bromide) formazan and dimethyl sulfoxide (DMSO) were purchased from Sigma-Aldrich (St. Louis, MO). Human IL-6 Quantikine ELISA Kit was purchased from R&D system (Minnesota, United States). Recombinant IL-6 was purchased from ImmunoTools (Friesoythe; DE), Gemcitabine was purchased from Fresenius Kabi (Maharashtra, IN), IL-6R inhibitor (Tocilizumab) was purchased from Roche (Basel, CH).

Cell culture

CCA cell lines, KKU-055 and KKU-213A, were obtained from the Japanese Collection of Research Bioresources Cell Bank (Osaka, Japan). The KKU-055 and KKU-213A cell lines were isolated from the tissue of 56- and 58-year-old male CCA patients, respectively. Both cell lines are established and characterized as poorly differentiated cells (Sripa et al., 2020). Primary normal adult human dermal fibroblast (NF) (ATCC® PCS-201–012™) was purchased from American Type Culture Collection (ATCC) (Virginia, US). Cells were cultured in Dulbecco's Modified Eagle Medium (DMEM) supplemented with 10% heat-inactivated fetal bovine serum (FBS) and 100 IU/ml of penicillin-streptomycin, at 37°C in a humidified atmosphere containing 5% CO_2.

Primary cultured cancer-associated fibroblasts isolation and culture

The samples from 8 CCA patient's tissues were cut into small pieces, digested with 0.5% collagenase, and filtered through the cell strainer. The isolated cells were cultured in DMEM containing 10% fetal bovine serum with 100 U/ml penicillin, 100 μg/ml streptomycin. CAFs were identified by morphology and staining for a CAF marker, α-smooth muscle actin (α-SMA). The patients' clinical information was presented in Supplementary Table S1.

Immunofluorescence assay

Primary CAF culture (6×10^4 cells/ml) were plated in a slide chamber and incubated at 37°C in a humidified 5% CO_2 atmosphere. After 24 h incubation, CAFs were fixed by 4% paraformaldehyde and blocked with 5% bovine serum albumin (BSA) followed by incubation with primary specific antibodies including anti-α-SMA (Abcam, Cambridge, United Kingdom) and anti-cytokeratin-19 (CK-19) (Abcam, Cambridge, United Kingdom). After incubation, the secondary antibody Alexa Fluor® 488 and 555 (Invitrogen, Massachusetts, United States) were added into cells. The slides were mounted with 50% glycerol in phosphate buffered saline (PBS) contained Hoechst 33342 (Invitrogen, Massachusetts, United States) nucleic acid stain.

Transwell co-culture system

Non-contact co-culture of CCA cells (KKU-055 and KKU-213A) and primary isolated CAFs was performed using a Transwell assay by plating CAFs into the 6.5 mm insert while plating CCA cells in the bottom of 24-well plates. After 16 h incubation, the inserts containing CAFs were placed on the CCA cells. A DMEM containing 1% FBS was used in this experiment. Cell viability of CCA cells in a co-culture plate was measured using MTT assay.

MTT assay

After experiments, the cell viability was determined by adding the 0.5 mg/ml of MTT solution into each well and incubated at 37°C for 1 h. After incubation, dimethyl sulfoxide (DMSO) was added to dissolve formazan. The absorbance was determined at 540 nm using a microplate reader (Tecan, Männedorf, CH).

Gemcitabine and IL-6R inhibitor treatment in the co-culture

After co-culturing CAFs and CCA cells for 72 h, gemcitabine was added into the co-culture at a final concentration based on the half maximal inhibitory concentration (IC_{50}) of CCA cells for 48 h. Additionally, for the IL-6R inhibitor treatment, CCA cells were pre-treated with the IL-6R inhibitor for 6 h followed by co-culturing with CAFs and gemcitabine treatment. Cell viability of CCA cells was measured using an MTT assay after 48-h post-treatment.

Enzyme-linked immunosorbent assay

Conditioned media (CM) from CAFs and the co-cultures were collected after incubation with and without gemcitabine. CM were centrifuged to remove the debris and the ELISA was immediately performed following the manufacturer's protocol for the human IL-6 ELISA kit (R&D system).

Western blot analysis

CCA cells were harvested and then lysed with RIPA lysis buffer (150 mM NaCl, 0.5 M Tris-HCl pH 7.4, 1% (v/v) Tween-

20, 1% (w/v) sodium deoxycholate, 0.1% (w/v) SDS). Protein concentration was determined using the Pierce BCA™ Protein Assay kit (Pierce Biotechnology, Rockford, United States). The 20 µg of protein extracts were electrophoresed by 10% (w/v) sodium dodecyl sulfate polyacrylamide gel electrophoresis (SDS-PAGE), transferred to a PVDF membrane, and blocked with 5% (w/v) skimmed milk. The membranes were probed at 4°C overnight with the following antibodies: rabbit anti-pSTAT3 (Abcam, Cambridge, United Kingdom), rabbit anti-STAT3 (Cell Signaling Technology, Massachusetts, US), mouse anti-IL-6R (OriGene, Maryland, US), rabbit anti-Bcl-2 (Proteintech, Illinois, US) and rabbit anti-Cyclin D1 (Cell Signaling Technology, Massachusetts, US) antibodies and β-actin antibody (Proteintech, Illinois, US) was used as an internal loading control. After incubation with secondary antibodies the band intensity was measured using ECL™ Prime Western Blotting Detection Reagent for chemiluminescent detection (GE Healthcare, Illinois, US). The apparent density of the bands on the membranes was captured by Image Quant Imager (GE Healthcare, Illinois, US).

Immunohistochemical analysis

IL-6R was detected on the CCA tissue microarray (TMA) of 146 paraffin embedded sections using standard immunohistochemistry protocols. Firstly, tissue sections were de-paraffinized and rehydrated with stepwise xylene followed by a series of concentrations of ethanol. Antigen retrieval was performed by microwaving sections in 10 mM sodium citrate pH 6 for 10 min. After that, the tissue sections were treated with 0.3% H_2O_2 for 30 min to block endogenous peroxidase activity. Nonspecific binding was blocked by 10% skim milk in phosphate-buffered saline (PBS) for 1 h. Sections were incubated with primary antibody (IL6R Antibody #CF506859; Thermo Fisher, Massachusetts, United States) for 1 h at room temperature followed by 4°C overnight. Thereafter, the sections were washed in PBS containing 0.1% tween 20 and incubated with peroxidase-conjugated Envision secondary antibody (DAKO, Glostrup, Denmark) for 1 h. The color was developed with a 3,3′diaminobenzidine tetrahydrochloride (DAB) substrate kit (Vector Laboratories, Inc., CA) for 5 min and the sections were counterstained with Mayer's hematoxylin for 2 min and dehydrated stepwise with a series of concentrations of ethanol and xylene. Finally, sections were mounted with permount and observed under a light microscope (Eclipse, Ni-U, Nikon Instru-ments Inc. Missouri, United States). The protein expression was analyzed according to staining frequency and intensity. The staining frequency of proteins was semiquantitatively scored based on the percentages of positive cells, 0% = negative; 1–25% = +1; 26–50% = +2; and >50% = +3. The intensity of protein staining was scored as weak = 1, moderate = 2, and strong = 3. The final immunohistochemical score was determined by multiplying the intensity with the frequency score. The median value was calculated by grading the scores of all patients and was used as a cut-off point. The patients with grading score lower than the median were classified as the low expression group and those with a grading score equal to or higher than the median was classified as the high expression group (Namwat et al., 2011).

Statistical analysis

The data were collected from at least 3 independent experiments and processed using GraphPad Prism 5.0 software (GraphPad. Software Inc.). The statistical analysis was performed using ANOVA and Student's t-test. Immunohistochemical analyses were carried out using Statistical Package for the Social Sciences; SPSS software (version 27.0; SPSS Inc., Chicago, IL, United States). A survival curve was calculated using the Kaplan-Meier (log-rank) analysis. The analyses of factors predicting overall survival was determined using Cox proportion hazard regression. The correlation between IL-6R expression score and HDRA data was performed using a Pearson's correlation. A p-value of less than 0.05 was considered statistically significant.

Results

Isolation and characterization of cancer-associated fibroblasts

To investigate the effect of CAFs on the gemcitabine response of CCA cells, we isolated CAFs from 8 CCA patients' tissues. Since the isolated CAFs present a spindle-like morphology, we performed western blotting to examine the expression level of a CAF marker, i.e., α-SMA. CK-19, an epithelial cell marker, was used to confirm non-contamination with epithelial cells. The results showed that all isolated CAFs expressed α-SMA. The 3 isolated CAFs showed no expression of CK-19 indicating that these CAFs were not contaminated with epithelial cells including CAF1, CAF5 and CAF6 (Figure 1A). Moreover, these 3 CAFs were further verified by immunofluorescence staining. In Figure 1B, CAFs showed positive staining with α-SMA presenting as a red color, but they were not stained with CK-19 (green). In sub-culturing passages, CAF1 stopped dividing and it could not be subsequently cultured. Therefore, the 2 isolated CAFs (CAF5 and CAF6) were collected for experiments.

IL-6 induced gemcitabine resistance of cholangiocarcinoma cells

We determined the level of IL-6 secreted from NF and CAFs using a human IL-6 ELISA kit. The NF was used as a

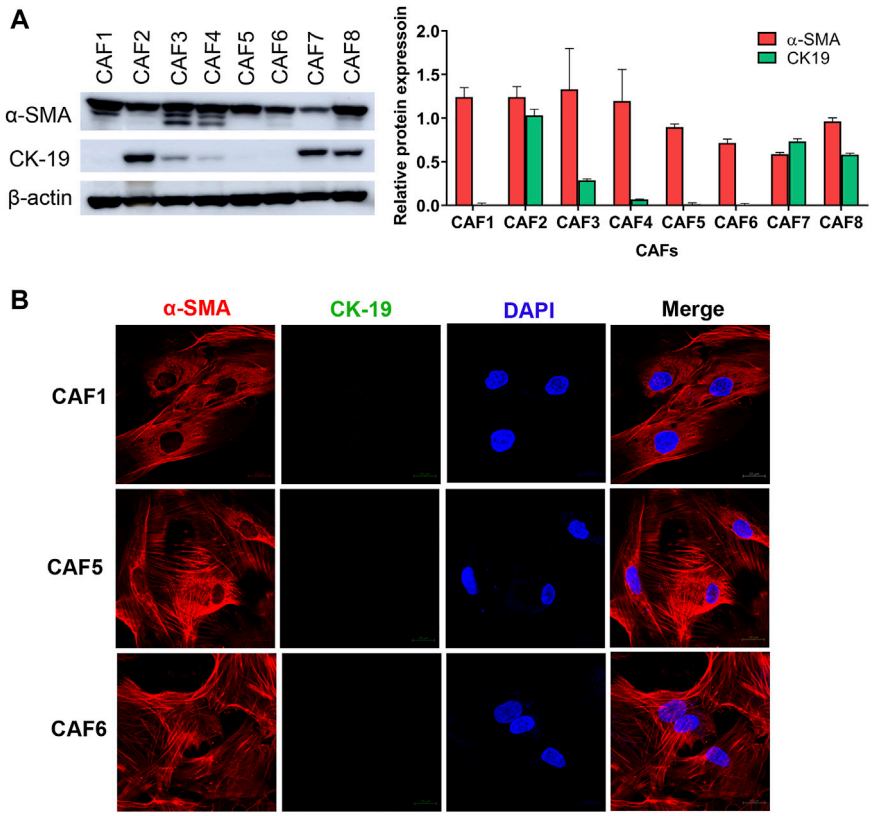

FIGURE 1
Characterization of CAFs by western blotting and immunofluorescence staining. **(A)** Western blot analysis shows the levels of α-SMA and CK-19 in primarily isolated CAFs. **(B)** CAFs displayed a spindle-like morphology by α-SMA staining observed under confocal microscopy. Hoechst 33342 was used for visualizing the nuclei of CAFs. Green, stained with cytokeratin-19 (CK-19); red, stained with α-SMA and blue, stained with Hoechst 33342. Original magnification is ×630.

control for determining the basal level of IL-6 in normal fibroblasts. The 1% (v/v) FBS-conditioned media was used as a reference value for comparison. The result showed that the level of IL-6 in CAFs was significantly higher than NF. It was noted that the IL-6 level in CAF5 was significantly higher than that in CAF6 (Figure 2A). Therefore, CAF5 was selected to perform further experiments. In addition, rhIL-6 was used for examining the effect of IL-6 on the gemcitabine response of CCA cells. CCA cells were pre-treated with 15 ng/ml of rhIL-6 for 72 h and then treated with gemcitabine at 5, 20 and 80 μM for 48 h. The half-maximal inhibitory concentrations (IC_{50}) at 48 h of gemcitabine on CCA cells including KKU-055 and KKU213A were 3.50 ± 1.0 and 10.1 ± 14.0 μM, respectively. The IC_{50} of gemcitabine on KKU-055 and KKU-213A cells in presence of rhIL-6 were 54.4 ± 18.0 and 705.1 ± 18.6 μM, respectively. The result showed that rhIL-6 treated CCA cells had a significant higher IC_{50} and percentage of cell viability than untreated cells upon gemcitabine treatment (Figures 2B,C).

Cholangiocarcinoma-derived cancer-associated fibroblasts induced gemcitabine resistance of cholangiocarcinoma cells

We investigated the effect of CCA-derived CAFs on gemcitabine response in CCA cells. CCA cells were co-cultured with CAF5 cells for 72 h. After incubation, the co-cultures were treated with gemcitabine for 48 h and cell viability measured by MTT assay. We found that the co-cultures significantly increased their viability up to 1.5- and 1.9-fold in KKU-055 and KKU-213A, respectively when compared to the monoculture. The co-cultures treated gemcitabine significantly increased cell viability in KKU-055 and KKU-213A up to 0.5- and 0.8-fold, respectively when compared to monoculture treated with gemcitabine (Figure 3A), indicating that CAFs induced CCA cells to be resistant against gemcitabine. The molecular changes were also investigated in gemcitabine treated CCA cells after incubation with or without CAFs using western blot analysis. The results showed that co-cultures treated with

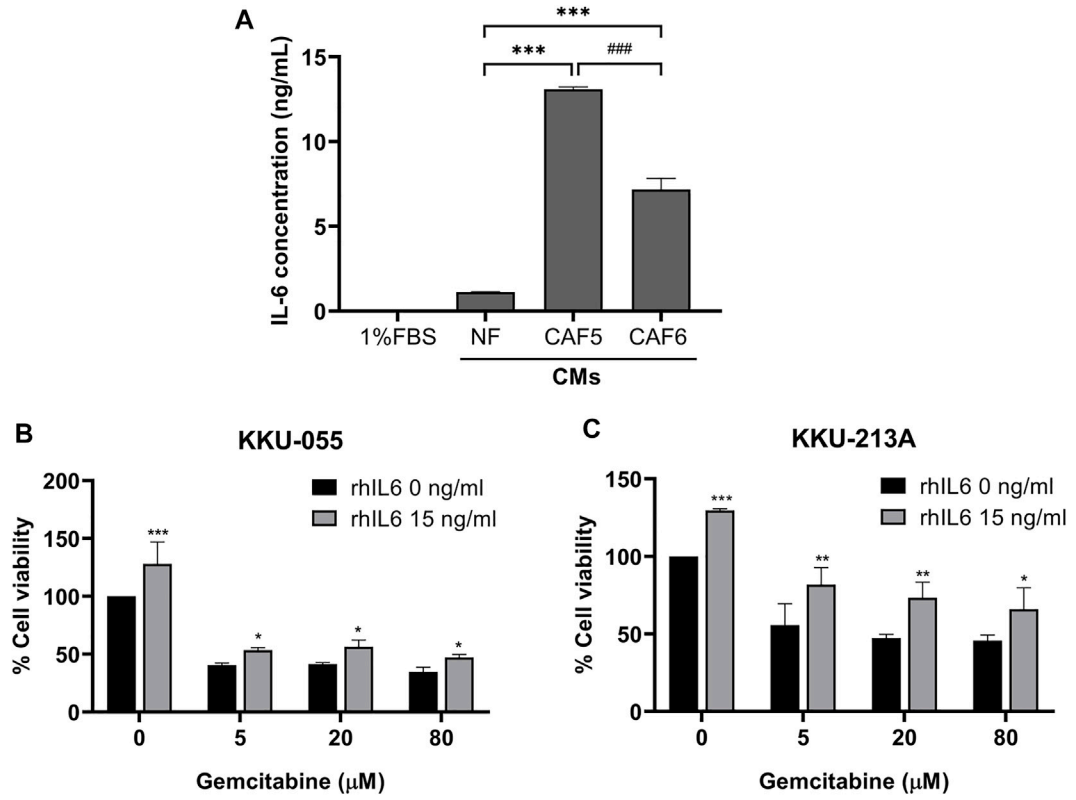

FIGURE 2
The level of IL-6 secreted from NF, CAFs and efficacy of rhIL-6 on gemcitabine response of CCA cells. **(A)** A human IL-6 ELISA kit was used for analyzing the level of IL-6 in conditioned medium (CMs) from NF and CAFs. **(B,C)** Cell viability was measured in CCA cells (KKU-055 and KKU-213A) by MTT assay upon treatment with rhIL-6 and gemcitabine. Error bars represent the standard deviation (SD) of triplicate experiments. A significant difference was determined using ANOVA and unpaired t-test (*$p < 0.05$, **$p < 0.01$, ***$p < 0.001$ compared to the control groups, $^{###}p < 0.001$ compared between CAF5 and CAF6).

gemcitabine significantly activated the STAT3 phosphorylation level and induced the expression of Bcl-2 and Cyclin D1 compared to the treated monoculture groups in KKU-055 (Figure 3B, lane 2 and 4) and KKU-213A (Figure 3C, lane 2 and 4). The results imply that CAFs interact and promote gemcitabine resistance mediated by the STAT3 signaling in CCA cells.

IL-6R inhibitor suppressed pSTAT3 level in rhIL-6-treated cholangiocarcinoma cells

To disrupt the interaction between CCA cells and CAFs *via* IL-6 signal transduction the IL-6R inhibitor (Tocilizumab; TCZ) was used. CCA cells were pre-incubated with rhIL-6 to induce pSTAT3 levels. After incubation, TCZ (1, 10 and 25 μg/ml) was added into the CCA cell culture for 6 h. The results showed that TCZ at concentrations of 10 and 25 μg/ml significantly suppressed pSTAT3 levels in rhIL-6-treated KKU-055 cells (Figure 4A, lane 4 and 5) and KKU-213A (Figure 4B, lane 4 and 5), indicating that TCZ inhibited the interaction of CAFs and CCA cells mediated by IL-6/STAT3 axis.

Blocking IL-6/STAT3 axis suppressed IL-6 secretion from cancer-associated fibroblasts-cholangiocarcinoma interaction and enhanced gemcitabine sensitivity in cholangiocarcinoma cells

To investigate the effect of TCZ on IL-6 secretion from the CAF-CCA interaction, we pre-treated TCZ to suppress the IL-6 signaling through IL-6R on CCA cells. CCA cells were cultured with and without adding CAFs followed by gemcitabine treatment. The levels of IL-6 in conditioned media of CCA cells in monoculture and co-culture were measured using ELISA. The results showed that the IL-6 level in CCA cells under co-culture was significantly higher than those under monoculture of both cells. Besides, TCZ significantly suppressed IL-6 levels in the monoculture and co-culture in

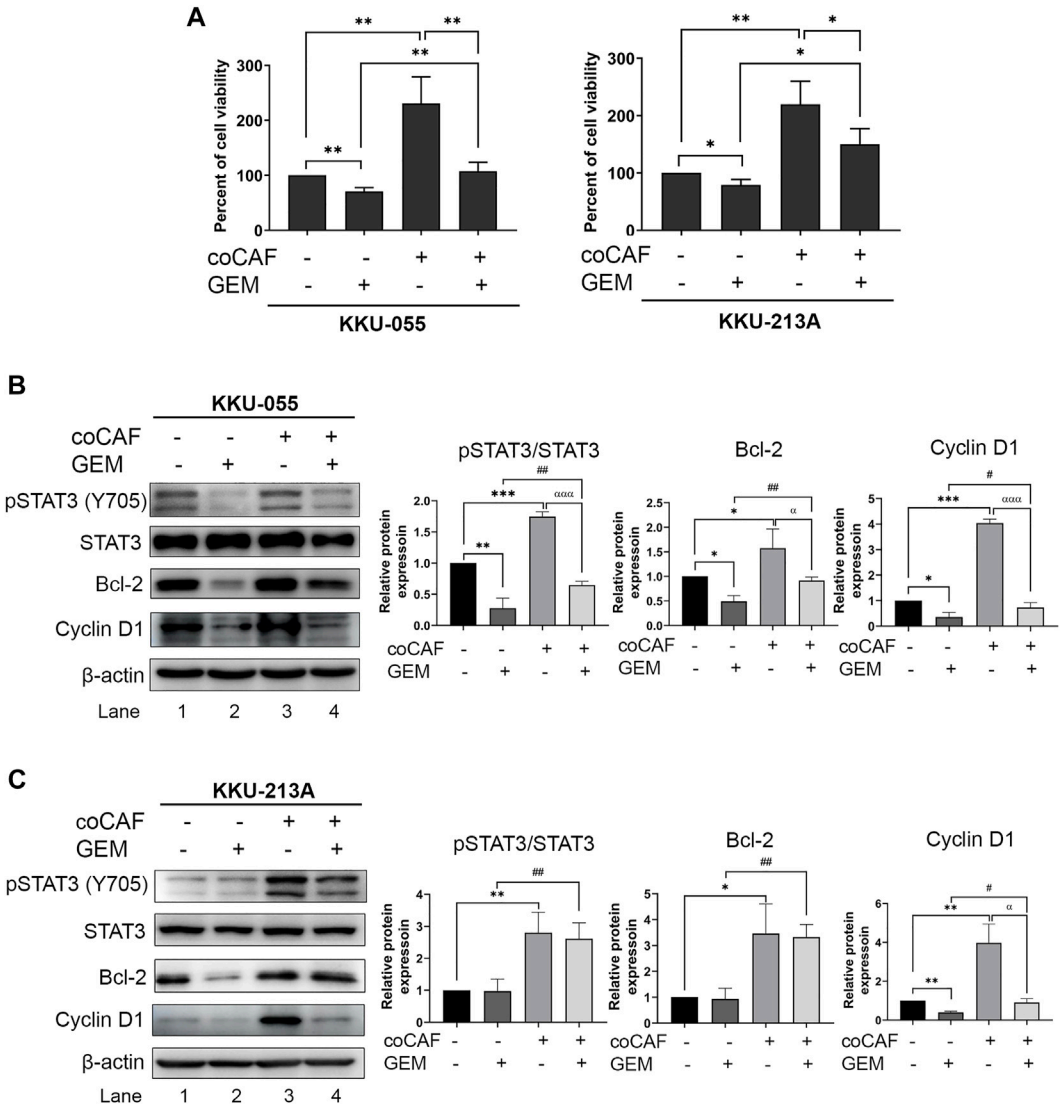

FIGURE 3
The effects of CAFs and molecular changes on gemcitabine response of CCA cells. **(A)** CCA cell viability after incubation with and without CAFs and gemcitabine were determined by MTT assay. Western blotting shows the molecular mechanisms of **(B)** KKU-055 and **(C)** KKU-213A assessed after monoculture or co-culture with CAFs and treatment with or without gemcitabine. Graphical plots represent the relative protein expressions. Error bars represent the standard deviation (SD) of triplicate experiments. A significant difference was determined using ANOVA and unpaired t-test (*$p < 0.05$, **$p < 0.01$, ***$p < 0.001$) compared to those control groups (black bars), $^{\#}p < 0.05$, $^{\#\#}p < 0.01$ compared to those gemcitabine-treated groups (dark grey bars), $^{\alpha}p < 0.05$, $^{\alpha\alpha\alpha}p < 0.001$ compared to those co-cultures (grey bars).

both CCA cells when compared to the untreated groups (Figure 5A). In Figures 5B,C, TCZ did not affect the viability in either CCA cell line. TCZ-treated co-cultured cells significantly reduced cell viability in gemcitabine treatment. These results indicated that blocking the CAF-CCA interaction *via* the IL-6/STAT3 axis enhanced gemcitabine sensitivity in KKU-213A and KKU-055.

The molecular mechanisms of TCZ on the inhibition of the CAF-CCA interaction mediated by IL-6/STAT3 toward the gemcitabine response of CCA cells were demonstrated by western blotting. After co-culture and treatment, CCA cells were collected to evaluate the molecular changes. In KKU-213A cells, TCZ significantly suppressed the pSTAT3 level when compared to the untreated co-culture (Figure 6B, lane 5 and 7). Likewise, a combination of TCZ and gemcitabine significantly decreased pSTAT3 level and cyclin D1 when compared to the untreated and TCZ treated-co-culture groups (Figure 6B, lane 5 and 8). This result indicates that TCZ can attenuate CAF-induced KKU-213A gemcitabine resistance through the inhibition of IL-6/STAT3 signaling leading to

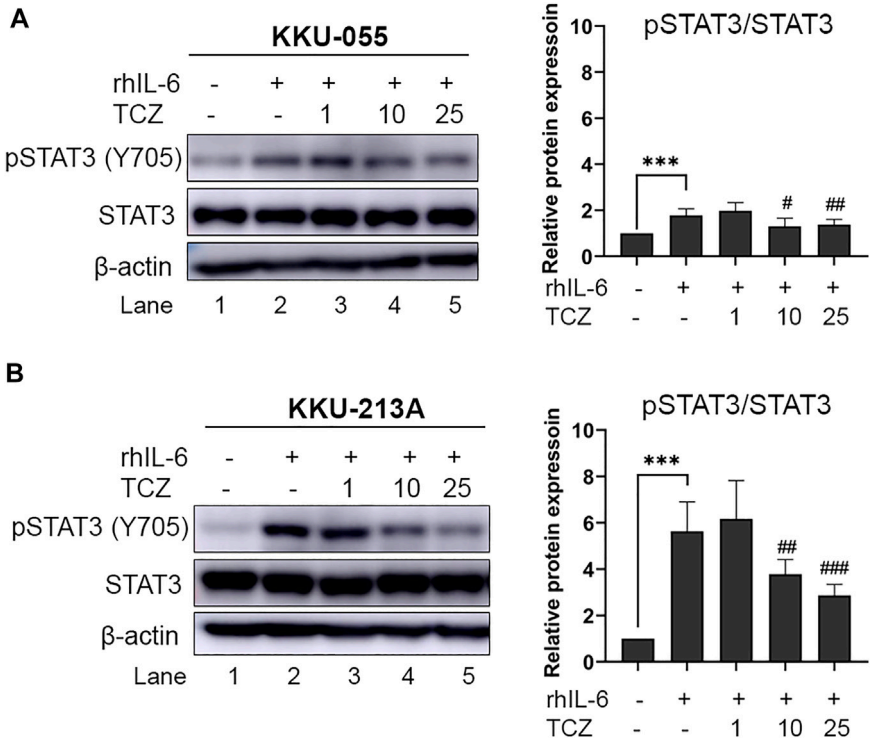

FIGURE 4
The efficacy of IL-6R inhibitor (Tocilizumab) on pSTAT3 levels of rhIL-6-treated CCA cells. The level of pSTAT3 in **(A)** KKU-055 and **(B)** KKU-213A after treatment with different concentrations of TCZ was assessed by western blot analysis. The graphical plots demonstrate relative protein expression of pSTAT3 and total STAT3. TCZ; tocilizumab. Error bars represent the standard deviation (SD) of triplicate experiments. A significant difference was determined using ANOVA and unpaired t-test (***$p < 0.001$ compared to untreated groups, $^{\#}p < 0.05$, $^{\#\#}p < 0.01$, $^{\#\#\#}p < 0.001$ compared to rhIL-6 treated groups).

gemcitabine sensitivity. In contrast, the TCZ treated-co-culture did not significantly affect signaling in KKU-055 cells (Figure 6A, lane 5 and 7). However, TCZ combined with gemcitabine significantly suppressed pSTAT3 level and cyclin D1 when compared to the untreated co-culture group, which is consistent with the result in Figure 5B. These results suggest that KKU-055 and KKU-213A have different response mechanisms. It was noted that the expression level of IL-6R in KKU-055 was lower than that of KKU-213A, suggesting a lower response of KKU-055 cells to gemcitabine and TCZ.

The prognostic significance of IL-6R expression and clinicopathological features

Immunohistochemical (IHC) staining of IL-6R was performed in a CCA tissue microarray. The intensity of IHC staining were scored in the CCA area and ranged from negative (score = 0) to strong (score = 3). A total of 146 cases of CCA patients were studied with 56 (38%) female cases and 90 (62%) male cases. The ages ranged between 42 and 82 years (median = 61 years). Positive staining of IL-6R protein was seen in the cytoplasm and cell membrane in the tissue sections. To examine the association of IL-6R expression and the chemo-response in CCA patients, the patients were divided into those with IL-6R low expression, who were or were not subjected to any chemotherapy (34 cases), and those with IL-6R high expression who were subjected to chemotherapy (44 cases) and those with IL-6R high expression who were not subjected to chemotherapy (68 cases). The representative figures of negative control, IL-6R low and high expression in CCA are shown in Figure 7A. Log-rank analysis was carried out to determine the overall survival rate of patients with CCA according to the expression of IL-6R. The Kaplan-Meier plot demonstrated that a high expression of IL-6R in CCA patients who were not subjected to chemotherapy was significantly associated with a shortest overall survival when compared to other groups ($p = 0.005$) (Figure 7B). Additionally, the correlation between the expression level of IL-6R and clinicopathological features including sex, age, histological types, tumor staging, tumor site, lymph node metastasis and distant metastasis showed no significant correlation with IL-6R expression. All clinicopathological features were also analyzed

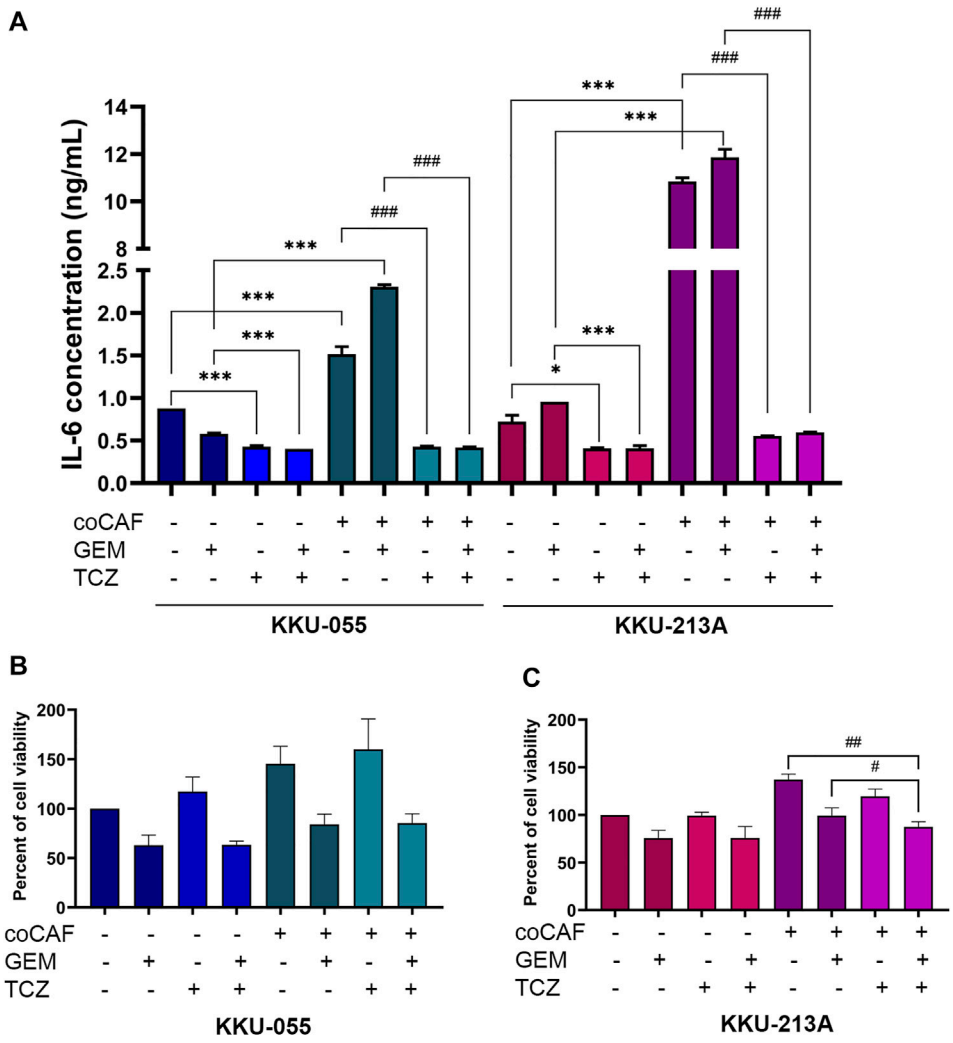

FIGURE 5
Effect of IL-6R inhibitor (TCZ) on gemcitabine response of CCA cells. **(A)** IL-6 levels in CMs from KKU-055 and KKU-213A in both mono- and co-culture were determined by human IL-6 ELISA kit. **(B,C)** CCA cell viability in culture with or without CAFs and after (or not after) gemcitabine and TCZ treatment was determined by MTT assay. TCZ; Tocilizumab. Error bars represent the standard deviation (SD) of triplicate experiments. A significant difference was determined using ANOVA and unpaired t-test (*$p < 0.05$, ***$p < 0.001$ compared to those monocultured groups, $^{\#}p < 0.05$, $^{\#\#}p < 0.01$, $^{\#\#\#}p < 0.001$ compared to co-cultured groups).

by univariate Cox proportional hazards regression to identify prognostic factors for CCA patients. The results demonstrated that high expression of IL-6R without chemotherapy, high tumor staging, and intrahepatic site were significantly correlated with a shorter overall survival rate compared with those individuals with a low expression with chemotherapy, low tumor staging and extrahepatic site ($p = 0.002$, $p = 0.034$ and $p = 0.010$, respectively) (Table 1). In addition, multivariate analysis showed that a high expression of IL-6R and high tumor staging could be used as independent prognostic factors of clinicopathological characteristics for overall survival of CCA patients ($p = 0.017$; HR = 1.731; CI = 1.103–2.716 and $p = 0.014$; HR = 1.548; CI = 1.093–2.192, respectively) (Table 2).

Correlation between IL-6R expression and gemcitabine response in cholangiocarcinoma

To determine the correlation between IL-6R expression and the gemcitabine response in CCA patients, we performed IHC staining in CCA samples in which tumor tissues were treated with gemcitabine by histoculture drug response assay (HDRA) as previously described (Suksawat et al., 2019). Tumor tissues were treated with gemcitabine at concentrations of 1,000 and 1,500 μg/ml. After the experiments, CCA patients were evaluated according to their response to classify the tumor tissues of patients into

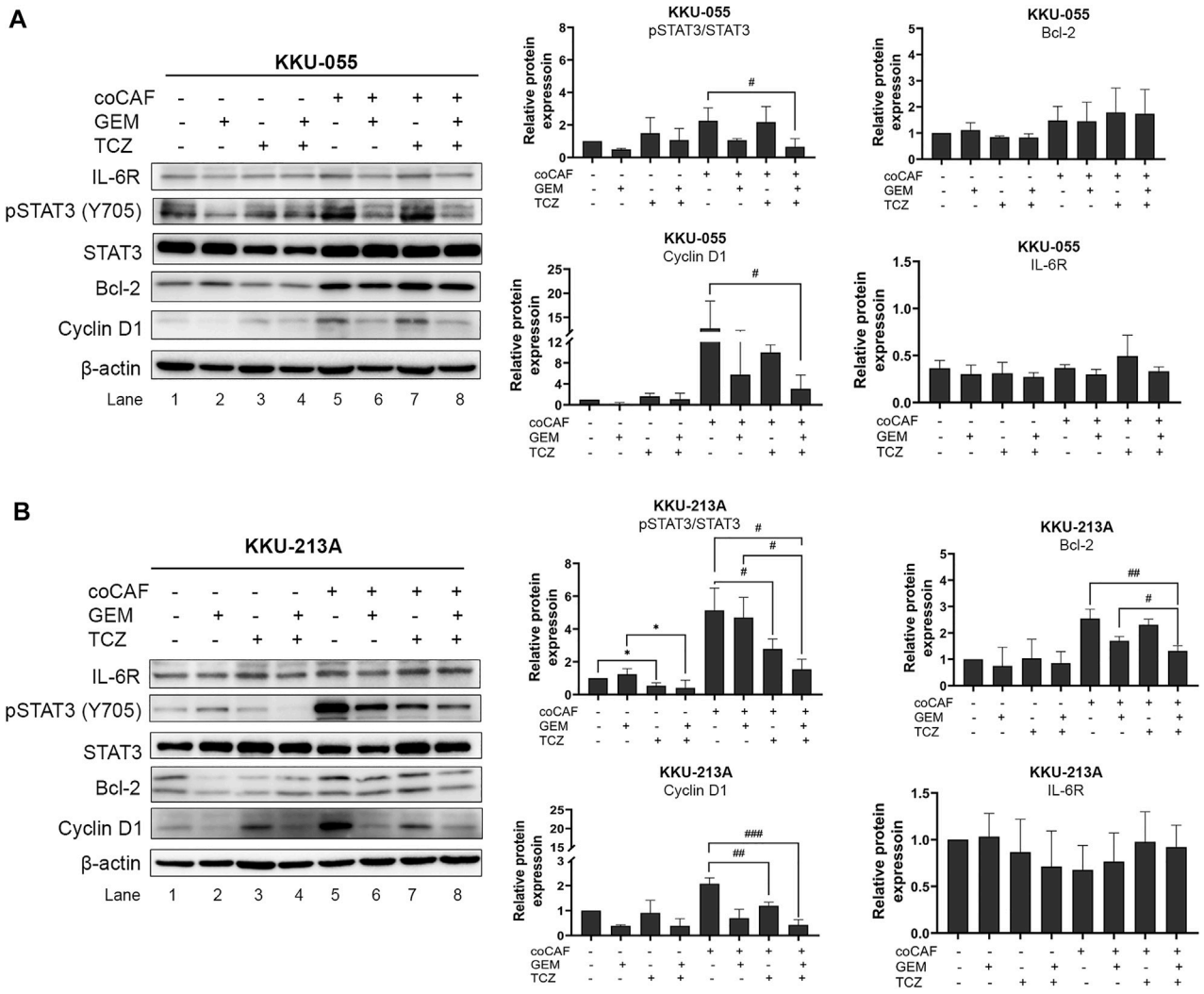

FIGURE 6
Effect of IL-6R inhibitor (TCZ) on molecular changes of CCA cells. The molecular mechanisms of **(A)** KKU-055 and **(B)** KKU-213A after co-culture with and without CAFs and then, incubation with and without gemcitabine and TCZ were assessed by western blotting. Error bars represent the standard deviation (SD) of triplicate experiments. A significant difference was determined using ANOVA and unpaired t-test (*$p < 0.05$ compared to those monocultured groups, $^{\#}p < 0.05$, $^{\#\#}p < 0.01$, $^{\#\#\#}p < 0.001$ compared to co-cultured groups).

response and non-response. The 40 CCA samples were divided into 3 groups including the patients who were responders (n = 5) and non-responders (n = 27) in low and high concentrations of gemcitabine and who had different responses in both doses (n = 8). Fisher's exact test demonstrated a significant correlation of IL-6R with high expression and patients with non-response to gemcitabine (p = 0.014) (Table 3). IHC scores for IL-6R protein and HDRA results were analyzed for their correlation using bivariate analysis. The result revealed that IL-6R expression was positively correlated with patients with non-response to gemcitabine (r = 0.444; p = 0.004) (Table 4).

Discussion

Adjuvant chemotherapy after surgical treatment is crucial for improving the survival of patients with CCA. The difficulty is the patient's poor response to available chemotherapy due to the high heterogeneity of CCA at the molecular level reducing or blocking the efficacy of therapies. Understanding the mechanism of the chemoresponse of this cancer might help to improve patients' outcomes (Marin et al., 2018; Banales et al., 2020). CAFs are prominent cells in TME that can stimulate matrix stiffening through remodeling of the ECM, secretion of cytokines, chemokines, and growth factors, facilitating a state of chemoresistance (Hogdall et al., 2018). IL-6 is an inflammatory

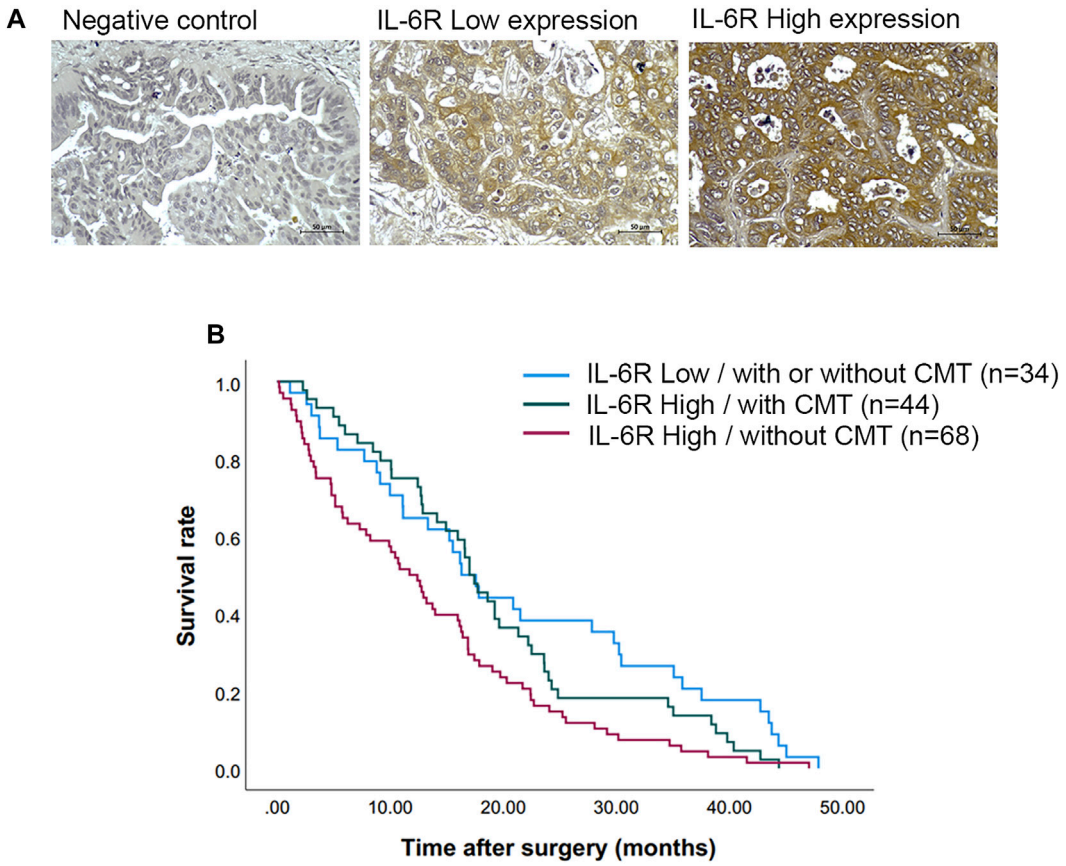

FIGURE 7
The expression of IL-6R in CCA tissues and correlation with overall survival rates of CCA patients. **(A)** Representative images demonstrated the expression of IL-6R by immunohistochemical staining in CCA tissues. Original magnification is ×200. **(B)** The Kaplan-Meier survival plot according to IL-6R expression and the chemotherapy regimen of CCA patients showed that the patients with IL-6R high expression without chemotherapy have a shorter survival time than those with low IL-6R expression and high IL-6R expression with chemotherapy (log-rank test, $p = 0.005$). CMT, chemotherapy.

molecule which is produced and secreted by various cell types that confer an aggressive behavior and poor response to therapies in many cancers as well as CCA (Frampton et al., 2012; Kumari et al., 2016; Thongchot et al., 2018; Thongchot et al., 2021). The study from Sripa et al. revealed that the concentration of plasma IL-6 is significantly higher in CCA patients than healthy groups (Sripa et al., 2012). Moreover, CCA-derived CAFs can induce cell growth and migration ability of CCA cells *via* IL-6 secretion (Thongchot et al., 2018). Taken together, CAFs in CCA environment would be one of the TME that involved in IL-6 production and contribute to CCA development and progression. Consistently, in this study, we revealed the effect of CCA-derived CAFs on the gemcitabine resistance of CCA cells. CAFs were successfully isolated from CCA tissues and were selected upon their potential extracellular IL-6 secretion. CCA cells treated with rhIL-6 sustained their viability and increased resistance to gemcitabine treatment. Additionally, CCA-derived CAFs induced CCA cell viability and resistance to gemcitabine by activation of pSTAT3 and the proteins involved in cell viability, as well as inducing IL-6 secretion in CCA cells. These results suggested that the IL-6 secreted from CAF plays roles in the gemcitabine resistance of CCA cells mediated by the IL-6/STAT3 signaling pathway. Supporting this finding, the efflux of the gemcitabine and conversion to gemcitabine monophosphate effects were examined. We found that these mechanisms were not involved in CAF-induced CCA gemcitabine resistance (Supplementary Figure S1). Furthermore, a previous study found that the conditioned medium of CCA-derived CAFs containing IL-6 stimulated the secretion of IL-6 (Thongchot et al., 2018). The IL-6-mediated STAT3 activation has been reported to cause therapeutic resistance in tumors by inducing several pro-survival pathways. The literature on the IL-6 functions on cancers reports that IL-6 binds to its receptor (IL-6R) and forms a complex with glycoprotein 130 (IL-6Rβ) to activate the downstream protein kinases, and subsequently activates STAT1, 3, and 5 (Heinrich et al., 2003; Babon et al., 2014; Jones and Jenkins, 2018) contributing to promotion of malignancy in colon cancer and hepatocellular carcinoma (HCC) (Ahmad et al.,

TABLE 1 Univariate analysis of factors predicting overall survival of CCA patients.

Factors	No. of patients	Hazard ratio (HR)	95% Confidence Interval (CI)	*p*-value
IL-6R				
Low with/without CMT	34	1		
High with CMT	44	1.295	0.818–2.050	0.269
High without CMT	68	1.945	1.269–2.983	0.002*
Sex				
Female	56	1		
Male	90	0.946	0.673–1.330	0.752
Age				
<61	66	1		
≥61	80	1.174	0.845–1.631	0.338
Histological types				
Papillary	75	1		
Non-papillary	71	1.231	0.884–1.714	0.218
Tumor staging				
I/II	52	1		
III/IV	94	1.448	1.029–2.038	0.034*
Tumor site				
Intrahepatic	94	1		
Extrahepatic	52	0.632	0.445–0.898	0.010*
Lymph node metastasis				
No	129	1		
Yes	17	0.721	0.433–1.200	0.208
Distant metastasis				
No	103	1		
Yes	43	0.717	0.501–1.027	0.070

Univariate analysis by Cox proportion hazard regression. HR, indicates hazard ratio. 95% CI, refers to the 95% confidence interval. CMT, refers to chemotherapy. *p-values less than 0.05 were considered as a statistical significance.

TABLE 2 Multivariate analysis of factors predicting overall survival of CCA patients.

Factors	No. of patients	Hazard ratio (HR)	95% Confidence Interval (CI)	*p*-value
IL-6R				
Low with/without CMT	34	1		
High with CMT	44	1.157	0.724–1.849	0.541
High without CMT	68	1.731	1.103–2.716	0.017*
Tumor staging				
I/II	52	1		
III/IV	94	1.548	1.093–2.192	0.014*
Tumor site				
Intrahepatic	94	1		
Extrahepatic	52	0.704	0.485–1.022	0.065

Multivariate analysis by Cox proportion hazard regression. HR, indicates hazard ratio. 95% CI, refers to the 95% confidence interval. *p-values less than 0.05 were considered as a statistical significance.

TABLE 3 Correlation of IL-6R expression with clinicopathological characteristics of CCA patients with gemcitabine response from HDRA results.

Factors	No. of patients (n = 40)	IL-6R expression		
		Low	High	p-value
Gemcitabine				
Response or non-response	8	7	1	
Response	5	2	3	
Non-response	27	8	19	0.014*
Sex				
Female	17	8	9	
Male	23	9	14	0.429
Age				
<61	16	7	9	
≥61	17	8	9	
N/A	7	2	5	0.701
Histological types				
Papillary	12	7	5	
Non-papillary	19	7	12	
N/A	9	3	6	0.409
Tumor site				
Intrahepatic	20	9	11	
Extrahepatic	11	5	6	
N/A	9	3	6	0.819
Tumor morphology				
Mass forming	7	3	4	
Intraductal growth	5	2	3	
Mixed	19	9	10	
N/A	9	3	6	0.917

Correlation between IHC, staining score of IL-6R, and clinicopathological features by Fisher's exact test. *p-values less than 0.05 were considered as a statistical significance.

TABLE 4 Pearson correlation coefficients between IHC scores of IL-6R expression and gemcitabine response from HDRA result.

	CCA patients with non-response to gemcitabine
Pearson Correlation	0.444
p-value	0.004*
No. of patients	40

*p-values less than 0.05 were considered as a statistical significance.

2017; Sun et al., 2018). Additionally, IL-6 acts as a stromal driver of therapeutic resistance by activating epithelial-to-mesenchymal transition in esophageal adenocarcinoma (EAC) which enhances the treatment. Likewise, inhibition of IL-6 restored drug sensitivity in the patient-derived organoid culture of EAC cells (Ebbing et al., 2019). IL-6-induced STAT3 phosphorylation in pancreatic ductal adenocarcinoma (PDAC) was suppressed by blocking IL-6R leading to the attenuation of STAT3 activation in TME toward enhanced sensitivity of cancer cells to chemotherapy (Long et al., 2017). In colorectal cancer, IL-6 promoted cell proliferation and drug resistance through its downstream signaling molecules, such as STAT3, representing potential molecular targets for cancer therapy (Ying et al., 2015). Therefore, inhibition of CAF-CCA interaction could be considered as a potent therapeutic approach for cancers associated with IL-6/STAT3 activation (Masjedi et al., 2018). Blockade of IL-6R with a humanized monoclonal antibody (Tocilizumab; TCZ) is sufficient to inhibit Bmi-1 expression and overcome the intrinsic chemoresistance of head and neck cancer stem cells (Herzog et al., 2021). Hence, again, targeting the IL-6/STAT3 axis might be a promising outcome in cancers.

TCZ, anti-IL-6R mAbs, was used in this study to inhibit the ligation of IL-6/IL-6R in CAFs and CCA cells. We found that TCZ suppressed pSTAT3 levels in rhIL-6-induced CCA cells. A

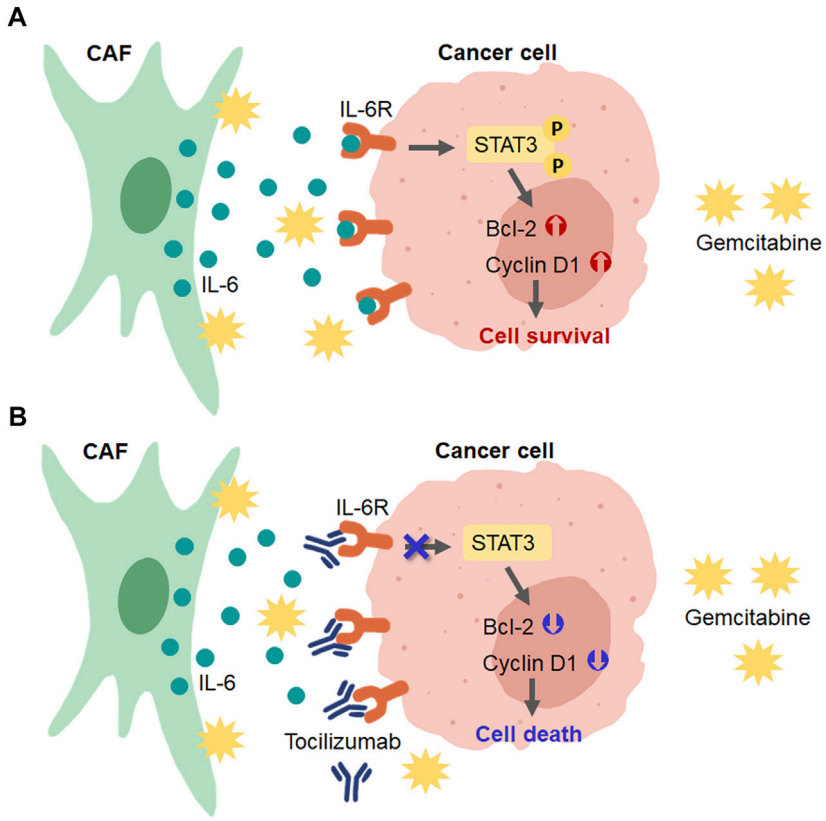

FIGURE 8
Schematic diagram for the role of CAFs in CCA cell resistance to gemcitabine and the presence of IL-6R blockage by tocilizumab. **(A)** CAFs secreted IL-6 to induce IL-6R/STAT3 signaling and upregulated the expression of proteins involved in the cell survival mechanism in CCA cells. **(B)** Blocking the IL-6-IL-6R binding in CCA cells by tocilizumab inhibited CAF-CCA interaction overcame the gemcitabine resistance and induced CCA cell death.

combination of TCZ and gemcitabine can enhance the sensitivity of CAF-induced gemcitabine resistance in KKU-213A cells by suppressing of pSTAT3 levels and Cyclin D1, with decreased levels of IL-6 secretion in the co-culture conditions. Consistent with non-small cell lung cancer (NSCLC) cells, TCZ decreased cell proliferation and induced the accumulation of sub-G1 phase in the cell cycle as well as possibly activating the NFκB pathway (Kim et al., 2015). However, TCZ could not affect cell viability and molecular changes in KKU-055 cells. To prove this finding, we focused on the expression level of IL-6R in both CCA cell lines and its correlation with the clinicopathological features of CCA patients. We found that KKU-055 displayed a lower level of IL-6R expression than KKU-213A. In addition, CCA patients who had a high expression of IL-6R without receiving any chemotherapy had the shortest overall survival rate when compared to other patient groups. Moreover, IL-6R can be used as an independent prognostic factor for the clinicopathological characteristics used to predict the overall survival rate of CCA patients. In colon cancer, in which IL-6R was correlated with the tumor size of the patients, a role of IL-6R in colorectal cancer progression was suggested and its possible roles as a biomarker could be useful in the follow-up disease and as potential targets for the therapy (Waldner et al., 2012; Turano et al., 2021). In epithelial ovarian cancer (EOC), the expression of IL-6 and IL-6R was increased in therapy-resistant cells and correlated with chemoresistance of EOC cells. The authors suggested that blockade of the IL-6 signaling pathways might reduce production and secretion of IL-6 leading to an increase in the potential effect of the agent involving inhibition of IL-6 or IL-6R in cancer (Yousefi et al., 2019). In breast cancer, high levels of soluble IL-6R (sIL-6R) in a patient's sera are likely to be associated with recurrence-free survival when compared to those patients with low levels of sIL-6R (Won et al., 2013). High expression of IL-6R was also observed and indicated a poor prognosis for overall survival and metastasis-free survival in patients with soft tissue sarcomas (Nakamura et al., 2020).

Subsequently, we analyzed the correlation between IL-6R expression and gemcitabine response from the HDRA results to confirm that the IL-6R expression level was correlated with the gemcitabine response in CCA patients. The results showed a positive correlation of IL-6R with a high expression in the patients who were

non-responders to gemcitabine. These findings confirmed that CCA with a high level of IL-6R has a poor response to gemcitabine treatment, which is consistent with cell studies. As mentioned, KKU-213A cells with a high IL-6R expression level indicate a high gemcitabine resistance ability rather than KKU-055 cells and the combination with the IL-6R inhibitor can enhance gemcitabine sensitivity in KKU-213A cells. In contrast to CCA with a low level of IL-6R, gemcitabine strongly affects CCA cells (KKU-055) and the combination with IL-6R inhibitor is not necessary. The IL-6R expression, therefore, is useful as a predictive marker for a personalized therapy in CCA patients.

In conclusion, our findings show that CCA-derived CAFs induced gemcitabine resistance in CCA cells *via* the activation of IL-6/STAT3 signaling. IL-6R can be a prognostic factor for the overall survival rate of CCA patients. IL6R-blocking antibody can induce chemosensitivity by attenuating the STAT3 activation in high IL-6R expressing CCA cells (Figure 8). Therefore, the IL-6/STAT3 axis could be a potential targeting pathway for CCA treatment. IL-6R expression, therefore, is useful as a predictive marker for a personalized therapy in CCA patients.

Data availability statement

The original contributions presented in the study are included in the article/Supplementary Material, further inquiries can be directed to the corresponding author.

Ethics statement

The studies involving human participants were reviewed and approved the research protocol by The Human Research Ethics Committee, Khon Kaen University (#HE571283 and #HE611544). The patients/participants provided their written informed consent to participate in this study.

Author contributions

NN provided the concept for the research; YK and NN designed the study; YK performed the main experiments; YK, MS and SP analyzed the clinical data; YK and NN wrote the paper; all authors discussed the data.

Funding

This work was supported by the Thailand Research Fund through Khon Kaen University and The Royal Golden Jubilee Ph.D. Program (Grant No. PHD/0215/2560) to YK and NN, a grant from Faculty of Medicine, Khon Kaen University (grant. no. IN63234 and AS64206) and the NSRF under the Basic Research Fund of Khon Kaen University under through Cholangiocarcinoma Research Institute to NN.

Acknowledgments

We would like to acknowledge Prof. Trevor N. Petney, for editing the MS *via* Publication Clinic KKU, Thailand.

Conflict of interest

The authors declare that the research was conducted in the absence of any commercial or financial relationships that could be construed as a potential conflict of interest.

Publisher's note

Supplementary material

The Supplementary Material for this article can be found online at: https://www.frontiersin.org/articles/10.3389/fphar.2022.897368/full#supplementary-material

References

Ahmad, R., Kumar, B., Chen, Z., Chen, X., Muller, D., Lele, S. M., et al. (2017). Loss of claudin-3 expression induces IL6/gp130/Stat3 signaling to promote colon cancer malignancy by hyperactivating Wnt/β-catenin signaling. *Oncogene* 36 (47), 6592–6604. PubMed PMID: 28783170; PubMed Central PMCID: PMCPMC6512312. doi:10.1038/onc.2017.259

Babon, J. J., Lucet, I. S., Murphy, J. M., Nicola, N. A., and Varghese, L. N. (2014). The molecular regulation of Janus kinase (JAK) activation. *Biochem. J.* 462 (1), 1–13. PubMed PMID: 25057888; PubMed Central PMCID: PMCPMC4112375. doi:10.1042/BJ20140712

Banales, J. M., Cardinale, V., Carpino, G., Marzioni, M., Andersen, J. B., Invernizzi, P., et al. (2016). Expert consensus document: Cholangiocarcinoma: Current knowledge and future perspectives consensus statement from the European network for the study of cholangiocarcinoma (ENS-CCA). *Nat. Rev. Gastroenterol. Hepatol.* 13 (5), 261–280. doi:10.1038/nrgastro.2016.51

Banales, J. M., Marin, J. J. G., Lamarca, A., Rodrigues, P. M., Khan, S. A., Roberts, L. R., et al. (2020). Cholangiocarcinoma 2020: The next horizon in mechanisms and management. *Nat. Rev. Gastroenterol. Hepatol.* 17 (9), 557–588. PubMed PMID: 32606456; PubMed Central PMCID: PMCPMC7447603. doi:10.1038/s41575-020-0310-z

Butthongkomvong, K., Sirachainan, E., Jhankumpha, S., Kumdang, S., and Sukhontharot, O. U. (2013). Treatment outcome of palliative chemotherapy in inoperable cholangiocarcinoma in Thailand. *Asian pac. J. Cancer Prev.* 14 (6), 3565–3568. PubMed PMID: 23886146. doi:10.7314/apjcp.2013.14.6.3565

Cadamuro, M., Brivio, S., Spirli, C., Joplin, R. E., Strazzabosco, M., and Fabris, L. (2017). Autocrine and paracrine mechanisms promoting chemoresistance in cholangiocarcinoma. *Int. J. Mol. Sci.* 18 (1), E149. PubMed PMID: 28098760; PubMed Central PMCID: PMCPMC5297782. doi:10.3390/ijms18010149

Ebbing, E. A., van der Zalm, A. P., Steins, A., Creemers, A., Hermsen, S., Rentenaar, R., et al. (2019). Stromal-derived interleukin 6 drives epithelial-to-mesenchymal transition and therapy resistance in esophageal adenocarcinoma. *Proc. Natl. Acad. Sci. U. S. A.* 116 (6), 2237–2242. PubMed PMID: 30670657; PubMed Central PMCID: PMCPMC6369811. doi:10.1073/pnas.1820459116

Frampton, G., Invernizzi, P., Bernuzzi, F., Pae, H. Y., Quinn, M., Horvat, D., et al. (2012). Interleukin-6-driven progranulin expression increases cholangiocarcinoma growth by an Akt-dependent mechanism. *Gut* 61 (2), 268–277. PubMed PMID: 22068162; PubMed Central PMCID: PMCPMC4498955. doi:10.1136/gutjnl-2011-300643

Heinrich, P. C., Behrmann, I., Haan, S., Hermanns, H. M., Muller-Newen, G., and Schaper, F. (2003). Principles of interleukin (IL)-6-type cytokine signalling and its regulation. *Biochem. J.* 374, 1–20. PubMed PMID: 12773095; PubMed Central PMCID: PMCPMC1223585. doi:10.1042/BJ20030407

Herzog, A. E., Warner, K. A., Zhang, Z., Bellile, E., Bhagat, M. A., Castilho, R. M., et al. (2021). The IL-6R and Bmi-1 axis controls self-renewal and chemoresistance of head and neck cancer stem cells. *Cell. Death Dis.* 12 (11), 988. PubMed PMID: 34689150; PubMed Central PMCID: PMCPMC8542035. doi:10.1038/s41419-021-04268-5

Hogdall, D., Lewinska, M., and Andersen, J. B. (2018). Desmoplastic tumor microenvironment and immunotherapy in cholangiocarcinoma. *Trends Cancer* 4 (3), 239–255. PubMed PMID: 29506673. doi:10.1016/j.trecan.2018.01.007

Hughes, T., O'Connor, T., Techasen, A., Namwat, N., Loilome, W., Andrews, R. H., et al. (2017). Opisthorchiasis and cholangiocarcinoma in Southeast Asia: An unresolved problem. *Int. J. Gen. Med.* 10, 227–237. doi:10.2147/IJGM.S133292

Jones, S. A., and Jenkins, B. J. (2018). Recent insights into targeting the IL-6 cytokine family in inflammatory diseases and cancer. *Nat. Rev. Immunol.* 18 (12), 773–789. PubMed PMID: 30254251. doi:10.1038/s41577-018-0066-7

Kalluri, R., and Zeisberg, M. (2006). Fibroblasts in cancer. *Nat. Rev. Cancer* 6 (5), 392–401. PubMed PMID: 16572188. doi:10.1038/nrc1877

Khan, S. A., Davidson, B. R., Goldin, R. D., Heaton, N., Karani, J., Pereira, S. P., et al. (2012). Guidelines for the diagnosis and treatment of cholangiocarcinoma: An update. *Gut* 61 (12), 1657–1669. PubMed PMID: 22895392. doi:10.1136/gutjnl-2011-301748

Khuntikeo, N., Pugkhem, A., Titapun, A., and Bhudhisawasdi, V. (2014). Surgical management of perihilar cholangiocarcinoma: A Khon kaen experience. *J. Hepatobiliary. Pancreat. Sci.* 21 (8), 521–524. PubMed PMID: 24464976. doi:10.1002/jhbp.74

Kim, N. H., Kim, S. K., Kim, D. S., Zhang, D., Park, J. A., Yi, H., et al. (2015). Anti-proliferative action of IL-6R-targeted antibody tocilizumab for non-small cell lung cancer cells. *Oncol. Lett.* 9 (5), 2283–2288. PubMed PMID: 26137057; PubMed Central PMCID: PMCPMC4467318. doi:10.3892/ol.2015.3019

Kumari, N., Dwarakanath, B. S., Das, A., and Bhatt, A. N. (2016). Role of interleukin-6 in cancer progression and therapeutic resistance. *Tumour Biol.* 37 (9), 11553–11572. PubMed PMID: 27260630. doi:10.1007/s13277-016-5098-7

Long, K. B., Tooker, G., Tooker, E., Luque, S. L., Lee, J. W., Pan, X., et al. (2017). IL6 receptor blockade enhances chemotherapy efficacy in pancreatic ductal adenocarcinoma. *Mol. Cancer Ther.* 16 (9), 1898–1908. PubMed PMID: 28611107; PubMed Central PMCID: PMCPMC5587413. doi:10.1158/1535-7163.MCT-16-0899

Marin, J. J. G., Lozano, E., Herraez, E., Asensio, M., Di Giacomo, S., Romero, M. R., et al. (2018). Chemoresistance and chemosensitization in cholangiocarcinoma. *Biochim. Biophys. Acta. Mol. Basis Dis.* 1864, 1444–1453. PubMed PMID: 28600147. doi:10.1016/j.bbadis.2017.06.005

Masjedi, A., Hashemi, V., Hojjat-Farsangi, M., Ghalamfarsa, G., Azizi, G., Yousefi, M., et al. (2018). The significant role of interleukin-6 and its signaling pathway in the immunopathogenesis and treatment of breast cancer. *Biomed. Pharmacother.* 108, 1415–1424. PubMed PMID: 30372844. doi:10.1016/j.biopha.2018.09.177

Meads, M. B., Gatenby, R. A., and Dalton, W. S. (2009). Environment-mediated drug resistance: A major contributor to minimal residual disease. *Nat. Rev. Cancer* 9 (9), 665–674. PubMed PMID: 19693095. doi:10.1038/nrc2714

Nakamura, K., Nakamura, T., Iino, T., Hagi, T., Kita, K., Asanuma, K., et al. (2020). Expression of interleukin-6 and the interleukin-6 receptor predicts the clinical outcomes of patients with soft tissue sarcomas. *Cancers (Basel)* 12 (3), E585. PubMed PMID: 32138303; PubMed Central PMCID: PMCPMC7139480. doi:10.3390/cancers12030585

Namwat, N., Puetkasichonpasutha, J., Loilome, W., Yongvanit, P., Techasen, A., Puapairoj, A., et al. (2011). Downregulation of reversion-inducing-cysteine-rich protein with Kazal motifs (RECK) is associated with enhanced expression of matrix metalloproteinases and cholangiocarcinoma metastases. *J. Gastroenterol.* 46 (5), 664–675. PubMed PMID: 21076843. doi:10.1007/s00535-010-0345-y

Ohlund, D., Elyada, E., and Tuveson, D. (2014). Fibroblast heterogeneity in the cancer wound. *J. Exp. Med.* 211 (8), 1503–1523. PubMed PMID: 25071162; PubMed Central PMCID: PMCPMC4113948. doi:10.1084/jem.20140692

Paraiso, K. H., and Smalley, K. S. (2013). Fibroblast-mediated drug resistance in cancer. *Biochem. Pharmacol.* 85 (8), 1033–1041. PubMed PMID: 23376122. doi:10.1016/j.bcp.2013.01.018

Pietras, K., and Ostman, A. (2010). Hallmarks of cancer: Interactions with the tumor stroma. *Exp. Cell. Res.* 316 (8), 1324–1331. PubMed PMID: 20211171. doi:10.1016/j.yexcr.2010.02.045

Quail, D. F., and Joyce, J. A. (2013). Microenvironmental regulation of tumor progression and metastasis. *Nat. Med.* 19 (11), 1423–1437. PubMed PMID: 24202395; PubMed Central PMCID: PMCPMC3954707. doi:10.1038/nm.3394

Songserm, N., Prasongwattana, J., Sithithaworn, P., Sripa, B., and Pipitkool, V. (2009). Cholangiocarcinoma in experimental hamsters with long-standing Opisthorchis viverrini infection. *Asian pac. J. Cancer Prev.* 10 (2), 299–302. PubMed PMID: 19537899.

Sripa, B., and Pairojkul, C. (2008). Cholangiocarcinoma: Lessons from Thailand. *Curr. Opin. Gastroenterol.* 24 (3), 349–356. PubMed PMID: 18408464; PubMed Central PMCID: PMCPMC4130346. doi:10.1097/MOG.0b013e3282fbf9b3

Sripa, B., Seubwai, W., Vaeteewoottacharn, K., Sawanyawisuth, K., Silsirivanit, A., Kaewkong, W., et al. (2020). Functional and genetic characterization of three cell lines derived from a single tumor of an Opisthorchis viverrini-associated cholangiocarcinoma patient. *Hum. Cell.* 33 (3), 695–708. PubMed PMID: 32207095. doi:10.1007/s13577-020-00334-w

Sripa, B., Thinkhamrop, B., Mairiang, E., Laha, T., Kaewkes, S., Sithithaworn, P., et al. (2012). Elevated plasma IL-6 associates with increased risk of advanced fibrosis and cholangiocarcinoma in individuals infected by Opisthorchis viverrini. *PLoS Negl. Trop. Dis.* 6 (5), e1654. PubMed PMID: 22629477; PubMed Central PMCID: PMCPMC3358341. doi:10.1371/journal.pntd.0001654

Sriplung, H., Wiangnon, S., Sontipong, S., Sumitsawan, Y., and Martin, N. (2006). Cancer incidence trends in Thailand, 1989-2000. *Asian pac. J. Cancer Prev.* 7 (2), 239–244.

Suksawat, M., Klanrit, P., Phetcharaburanin, J., Namwat, N., Khuntikeo, N., Titapun, A., et al. (2019). *In vitro* and molecular chemosensitivity in human cholangiocarcinoma tissues. *PLoS One* 14 (9), e0222140. PubMed PMID: 31504065; PubMed Central PMCID: PMCPMC6736243. doi:10.1371/journal.pone.0222140

Sun, L., Feng, L., and Cui, J. (2018). Increased expression of claudin-17 promotes a malignant phenotype in hepatocyte via Tyk2/Stat3 signaling and is associated with poor prognosis in patients with hepatocellular carcinoma. *Diagn. Pathol.* 13 (1), 72. PubMed PMID: 30219077; PubMed Central PMCID: PMCPMC6138900. doi:10.1186/s13000-018-0749-1

Thongchot, S., Ferraresi, A., Vidoni, C., Loilome, W., Yongvanit, P., Namwat, N., et al. (2018). Resveratrol interrupts the pro-invasive communication between cancer associated fibroblasts and cholangiocarcinoma cells. *Cancer Lett.* 430, 160–171. PubMed PMID: 29802929. doi:10.1016/j.canlet.2018.05.031

Thongchot, S., Vidoni, C., Ferraresi, A., Loilome, W., Khuntikeo, N., Sangkhamanon, S., et al. (2021). Cancer-associated fibroblast-derived IL-6 determines unfavorable prognosis in cholangiocarcinoma by affecting autophagy-associated chemoresponse. *Cancers (Basel)* 13 (9), 2134. PubMed PMID: 33925189; PubMed Central PMCID: PMCPMC8124468. doi:10.3390/cancers13092134

Thongprasert, S. (2005). The role of chemotherapy in cholangiocarcinoma. *Ann. Oncol.* 16 Suppl 2, ii93–6. PubMed PMID: 15958484. doi:10.1093/annonc/mdi712

Turano, M., Cammarota, F., Duraturo, F., Izzo, P., and De Rosa, M. (2021). A potential role of IL-6/IL-6R in the development and management of colon cancer. *Membr. (Basel)* 11 (5), 312. PubMed PMID: 33923292; PubMed Central PMCID: PMCPMC8145725. doi:10.3390/membranes11050312

Waldner, M. J., Foersch, S., and Neurath, M. F. (2012). Interleukin-6--a key regulator of colorectal cancer development. *Int. J. Biol. Sci.* 8 (9), 1248–1253. PubMed PMID: 23136553; PubMed Central PMCID: PMCPMC3491448. doi:10.7150/ijbs.4614

Won, H. S., Kim, Y. A., Lee, J. S., Jeon, E. K., An, H. J., Sun, D. S., et al. (2013). Soluble interleukin-6 receptor is a prognostic marker for relapse-free survival in estrogen receptor-positive breast cancer. *Cancer Invest.* 31 (8), 516–521. PubMed PMID: 23902164. doi:10.3109/07357907.2013.826239

Ying, J., Tsujii, M., Kondo, J., Hayashi, Y., Kato, M., Akasaka, T., et al. (2015). The effectiveness of an anti-human IL-6 receptor monoclonal antibody combined with chemotherapy to target colon cancer stem-like cells. *Int. J. Oncol.* 46 (4), 1551–1559. PubMed PMID: 25625841. doi:10.3892/ijo.2015.2851

Yousefi, H., Momeny, M., Ghaffari, S. H., Parsanejad, N., Poursheikhani, A., Javadikooshesh, S., et al. (2019). IL-6/IL-6R pathway is a therapeutic target in chemoresistant ovarian cancer. *Tumori* 105 (1), 84–91. PubMed PMID: 30021477. doi:10.1177/0300891618784790

frontiers | Frontiers in Pharmacology

TYPE Original Research
PUBLISHED 02 September 2022
DOI 10.3389/fphar.2022.989655

OPEN ACCESS

EDITED BY
Runbin Sun,
Nanjing Drum Tower Hospital, China

REVIEWED BY
Xiuting Liu,
Washington University in St. Louis, United States
Wei Song,
Nanjing Drum Tower Hospital, China

*CORRESPONDENCE
Meng Yang,
yangmeng_pumch@126.com
Yewei Zhang,
zhangyewei@njmu.edu.cn

†These authors have contributed equally to this work

SPECIALTY SECTION
This article was submitted to Pharmacology of Anti-Cancer Drugs, a section of the journal Frontiers in Pharmacology

RECEIVED 08 July 2022
ACCEPTED 15 August 2022
PUBLISHED 02 September 2022

CITATION
Peng H, Zhu E, Wang J, Du X, Wang C, Yang M and Zhang Y (2022), RAB6B is a potential prognostic marker and correlated with the remolding of tumor immune microenvironment in hepatocellular carcinoma. *Front. Pharmacol.* 13:989655. doi: 10.3389/fphar.2022.989655

RAB6B is a potential prognostic marker and correlated with the remolding of tumor immune microenvironment in hepatocellular carcinoma

Hao Peng[1†], Erwei Zhu[2†], Jitao Wang[1,3], Xuanlong Du[1], Chonggao Wang[1], Meng Yang[4*] and Yewei Zhang[5*]

[1]Medical School, Southeast University, Nanjing, China, [2]The Second People's Hospital of Lianyungang (The Oncology Hospital of Lianyungang), Lianyungang, China, [3]Xingtai Institute of Cancer Control, Xingtai People's Hospital, Xingtai, China, [4]State Key Laboratory of Complex Severe and Rare Diseases, Department of Ultrasound, Peking Union Medical College Hospital, Chinese Academy of Medical Sciences and Peking Union Medical College, Beijing, China, [5]Hepatopancreatobiliary Center, The Second Affiliated Hospital of Nanjing Medical University, Nanjing, China

Backgrounds: Hepatocellular carcinoma (HCC) is the most common type of primary liver cancer and the second leading cause of death among all cancers. The Ras-associated binding (Rab) proteins constitute the largest family of the Ras superfamily of small GTPases, which mainly mediate membrane trafficking processes. RAB6B is a member of Rab GTPases, and it has been found to be dysregulated in various tumors. However, the clinical significance, correlations with immune cells, and stroma infiltration of RAB6B in HCC remain unclear.

Methods: RAB6B mRNA and protein expression in HCC were examined using the TIMER, HCCDB, UALCAN, and HPA databases. The genetic alterations of RAB6B were analyzed by cBioPortal and COSMIC databases. The correlations between RAB6B and tumor-infiltrating immune cells and cancer-associated fibroblasts were explored by using TIMER, TISIDB, and GEPIA databases. Co-expression networks of RAB6B were investigated based on LinkedOmics. Drug sensitivity was analyzed through the GDSC and CTRP databases. RAB6B was knocked down with siRNA in HCC cell lines. EdU assay was performed to detect the cell proliferation ability, flow cytometry was used to compare the differences in the ability of apoptosis, and MTT was used to evaluate the drug sensitivity *in vitro*.

Results: RAB6B mRNA and protein expression were upregulated in the HCC tissues. Kaplan–Meier and Cox regression analyses suggested that highly expressed RAB6B was an independent prognostic factor for poor survival in HCC patients. Moreover, we found that RAB6B expression was positively correlated with the infiltration of immune cells in HCC, including some immunosuppressive cells, chemokines, and receptors, meanwhile RAB6B expression was associated with CD8+T cells exhaustion, resulting in an immunosuppressive microenvironment. Additionally, functional enrichment analysis indicated that RAB6B may be involved in ECM remodeling in the TME, and RAB6B expression was positively associated with CAFs infiltration.

Furthermore, RAB6B presented a positive association with sensitivity to GDSC and CTRP drugs. RAB6B knockdown inhibited the cell proliferation and promoted apoptosis and sensitivity to cisplatin of HCC cells *in vitro*.

Conclusion: Our study revealed that RAB6B is a potential biomarker for poor prognosis in HCC patients and correlates with the formation of the immunosuppressive microenvironment in HCC.

KEYWORDS

HCC, immune infiltration, RAB6B, CAFs, TME

Introduction

Hepatocellular carcinoma (HCC), the most common type of liver cancer, mainly develops from chronic liver diseases, such as hepatitis B infection, hepatitis C infection, and liver fibrosis (Craig et al., 2020). Most HCC patients were diagnosed at an advanced stage and lost the opportunity for optimal surgical resection, so it is urgent to discover new reliable HCC markers for diagnosis and prognosis of HCC. Currently, emerging research focus on the role of the tumor microenvironment (TME) on tumor progression. TME or tumor stroma includes various tumor-associated immune cells, vascular endothelial cells, cancer-associated fibroblasts (CAFs), and extracellular matrix (ECM). The stroma components continuously communicate with tumor cells to provide nutrients and growth factors for tumor occurrence and development (Lu et al., 2019). Moreover, it has been recently reported that oncogenic mutations in tumor cells can also influence tumor-stroma interactions by altering the expression of chemokines, cytokines, immune checkpoint molecules, and ECM remodeling in the TME, thereby fostering a more conducive microenvironment for tumor growth (Nishida and Kudo, 2018).

The Rab GTPase is a family of proteins that mediate membrane trafficking, and distinct Rab proteins located in specific organelles are involved in the regulation of cell growth, survival, and death (Gopal Krishnan et al., 2020). Additionally, accumulating studies have reported that dysregulated expression or mutation of several Rab proteins may affect tumor migration, invasion, metastasis, stromal cell communication, and drug resistance in HCC (Yang et al., 2021). RAB6B is an isoform protein of the RAB6 subfamily, mainly located in the Golgi complex (Opdam et al., 2000). Recently, studies have shown that RAB6B expression in gastric cancer can promote tumor cells proliferation, while RAB6B is low expressed and associated with poor prognosis in pancreatic cancer patients, suggesting that the role of RAB6B is context-specific (Anand et al., 2020; Zhao et al., 2020). However, the role and mechanism of RAB6B expression on the prognosis, progression, and immune infiltration in HCC have not been investigated.

In this study, we comprehensively investigated the expression level, genetic alterations, and prognostic and diagnostic significance of RAB6B in HCC patients in various public databases. Moreover, the association between RAB6B and infiltrating immune cells and CAFs in TME was also analyzed. To explore the potential biological functions of RAB6B, the functional enrichment analysis of co-expressed genes with RAB6B was performed. Meanwhile, we analyzed the drug responsiveness of RAB6B in HCC through GDSC and CTRP databases. Finally, a series of functional assays were performed to further evaluate the roles of RAB6B knockdown on HCC cell proliferation, apoptosis, and drug sensitivity.

Materials and methods

RAB6B gene expression analysis

TIMER2 (http://timer.cistrome.org/) was used to examine the expression of RAB6B in liver cancer and corresponding normal liver tissues through The Cancer Genome Atlas (TCGA) data (Li et al., 2017). The HCCDB database (http://lifeome.net/database/hccdb/home.html), which contains 15 public HCC datasets from Gene Expression Omnibus (GEO), TCGA, and International Cancer Genome Consortium (ICGC) databases, was used to further validate the differential expression of RAB6B in liver cancer and normal tissues (Ferlay et al., 2015). Besides, the mRNA and protein expression levels of RAB6B were also detected from the UALCAN (http://ualcan.path.uab.edu) (Chandrashekar et al., 2017). Immunohistochemistry (IHC) analysis of RAB6B in liver cancer samples and normal liver samples was explored from the Human Protein Atlas (HPA) (http://www.proteinatlas.org/) (Asplund et al., 2012). Correlation analysis of RAB6B and clinical parameters, including T stage and histological grade were performed with R using the ggplot2 package.

Survival prognosis analysis and nomogram establishment

The Kaplan- Meier plotter database (http://kmplot.com/analysis/) was used to evaluate the association of RAB6B expression with the survival of the HCC cohort (Lanczky and

Gyorffy, 2021). Furthermore, the prognostic value of RAB6B in HCC *via* univariate and multivariate Cox regression analysis was analyzed by using the R survival package. To assess the diagnostic value of RAB6B in HCC, a receiver operating characteristic (ROC) curve was performed and the area under the curve (AUC) was calculated by using the "pROC package." Besides, to predict the survival risk of HCC patients, the prognostic nomograms were constructed based on the multivariate Cox model by using the R package "rms".

Genetic alteration analysis

The cBioPortal database (http://cbioportal.org) was used to analyze the RAB6B gene alteration. Liver Hepatocellular Carcinoma (LIHC) (TCGA, Firehose Legacy) dataset was selected for subsequent analysis (Gao et al., 2013). The Catalogue of Somatic Mutations in Cancer (COSMIC) database (https://cancer.sanger.ac.uk/cosmic) was used to explore the different mutant types of RAB6B in HCC (Forbes et al., 2015).

Immune infiltration analysis

The relationship between RAB6B expression and ImmuneScore, StromalScore, and ESTIMATEScore was analyzed based on R packages "estimate" through the website of "http://sangerbox.com/Tool." TISIDB (http://cis.Hku.hk/TISIDB/) database was used to analyze the correlation between the RAB6B expression and various tumor-infiltrating immune cells, immunoinhibitors, immunostimulators, chemokines, and receptors (Ru et al., 2019). The correlation between RAB6B expression and infiltrating levels of regulatory T cells (Tregs), myeloid-derived suppressor cells (MDSC), Macrophages, and cancer-associated fibroblasts cells (CAFs) in HCC was analyzed by "gene modules" from TIMER2.0 database. Meanwhile, analysis of RAB6B expression combined with various immune infiltrating cells to predict patient survival was performed by "outcome modules" through the TIMER2.0 database. GEPIA2 (http://gepia2.cancer-pku.cn/) was used to compare the correlation between RAB6B expression and TGFB1, and IL10 (Tang et al., 2019). RAB6B expression was further evaluated the expression differences between different immune cell subsets by using single-cell RNA-sequencing results of six HCC patients through http://cancer-pku. Cn:3838/HCC/(Zhang et al., 2019).

Functional enrichment analysis

The LinkedOmics database (http://www.linkedomics.org/login. php) was used to search for the differentially expressed genes related to RAB6B in HCC using the LinkFinder module. Genes positively and negatively associated with RAB6B were analyzed and visualized by volcano plot and heat maps (Vasaikar et al., 2018). Gene Ontology (GO) analysis and Kyoto Encyclopedia of Genes and Genomes (KEGG) pathway enrichment analysis were performed to annotate the differentially expressed genes related to RAB6B.

Correlation between RAB6B and drug response

Gene Set Cancer Analysis (GSCA) (http://bioinfo.life.hust.edu.cn/GSCA/#/) was used to explore the correlation between the RAB6B expression and drug sensitivity. The module "GDSC drug sensitivity and expression correlation" and "CTRP drug sensitivity and expression correlation" were selected to analyze the correlation. The detailed information on the differential drug was annotated from Genomics of Drug Sensitivity in Cancer (GDSC) and Cancer therapeutics Response Portal (CTRP).

Cell culture and siRNA transfection

Human liver cancer cell lines (Huh7, MHCC97L, Hep3B, and HepG2) were purchased from the Shanghai Institute for Biological Science, Chinese Academy of Science (Shanghai, China), SMMC7721 cells were purchased from Xiamen Immocell Biotechnology Co., Ltd, all cells were cultured in Dulbecco's modified Eagle's medium (DMEM, Gibco, Thermo Fisher Scientific, United States) containing 10% fetal bovine serum (FBS, Invitrogen, United States) and 1% penicillin-streptomycin at 37°C in humidified air with 5% CO2. The RAB6B-specific siRNAs and negative control (NC) were designed from RIBOBIO (Guangzhou, China). Transfection was performed with Lipofectamine 2000 (Invitrogen, United States), and cells were collected for the further experiment after transfecting for 48 h.

qRT-PCR

Total RNA from cultured HCC cell lines was extracted with Trizol reagent (Invitrogen, United States) according to the manufacturer's instructions. 1 μg RNA samples were reverse transcribed into cDNA using a SweScript RT I First Strand cDNA Synthesis Kit (Servicebio, China). The qRT-PCR was carried out using 2 × SYBR Green qPCR Master Mix (High ROX) (Servicebio, China). All primers were listed as follows: RAB6B Forward: AGAGGCAGATAACCATCGAGG, Reverse: CTTCGCACTGGTCTCAATGAA. GAPDH Forward: GGA GCGAGATCCCTCCAAAAT, and Reverse: GGCTGTTGT

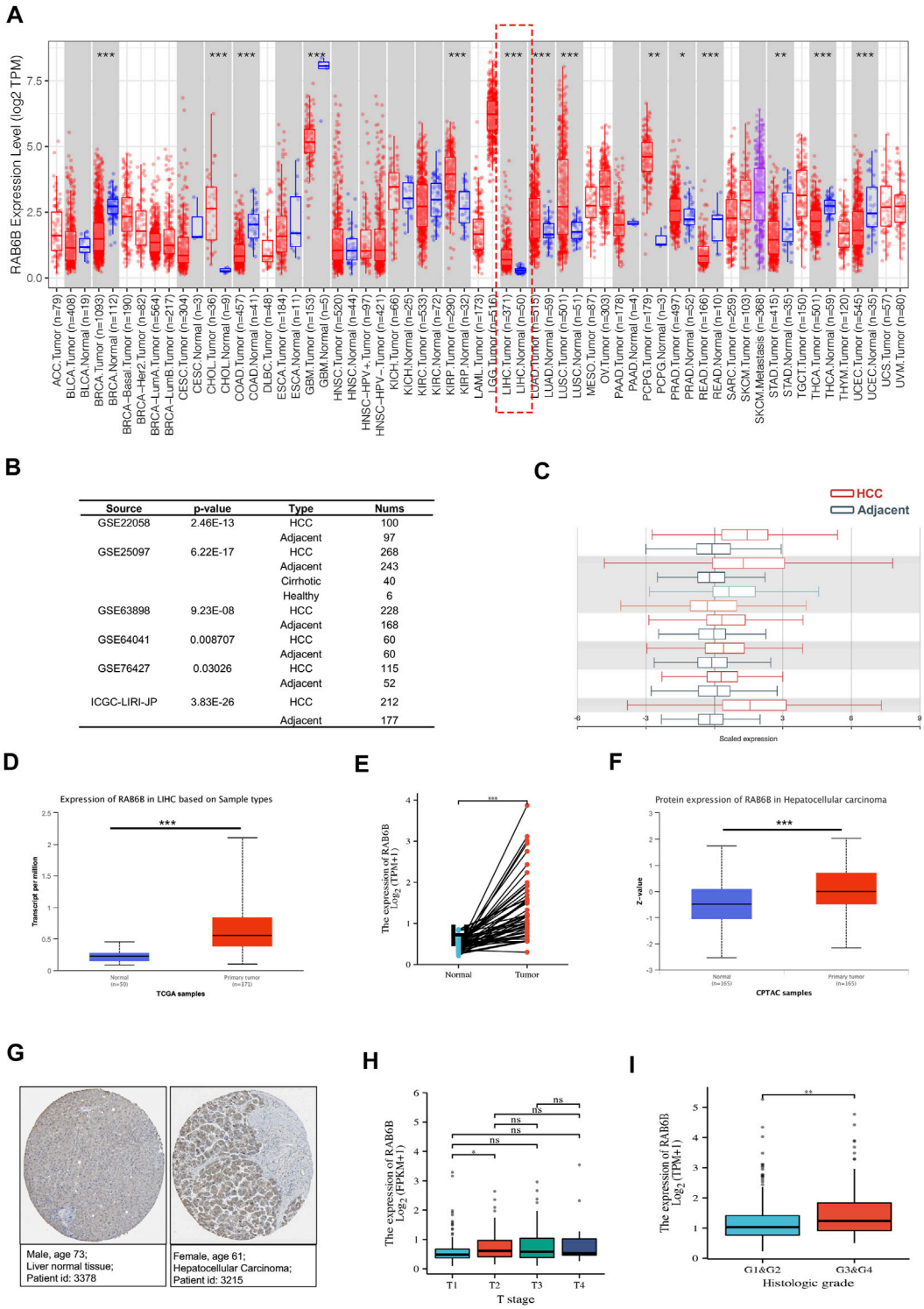

FIGURE 1
The expression level of RAB6B in HCC tissues. **(A)** RAB6B expression level in various tumor tissues and corresponding normal tissues in the TIMER2.0 database. RAB6B was upregulated in liver hepatocellular carcinoma (LIHC). *$p < 0.05$, **$p < 0.01$, and ***$p < 0.001$. **(B,C)** RAB6B was highly expressed in HCC tissues compared to the adjacent liver tissues in six HCC cohorts from the HCCDB database. **(D)** RAB6B mRNA expression level was increased in HCC tissues compared to normal liver tissues based on the UALCAN database. ***$p < 0.001$. **(E)** RAB6B expression was higher in 50 HCC tissues than in their paired adjacent normal liver tissues based on the TCGA database. ***$p < 0.001$. **(F)** RAB6B protein level in HCC tissues and normal tissues were obtained from the CPTAC dataset. ***$p < 0.001$. **(G)** Representative immunohistochemistry (IHC) images of RAB6B in HCC tissues (right image) and normal liver tissues (left image) from the HPA database. **(H)** Boxplot indicated that RAB6B expression was significantly associated with HCC patients' T stage. *$p < 0.05$, ns = no significance. **(I)** Boxplot showed that RAB6B expression was correlated with histologic grade. **$p < 0.01$.

CATACTTCTCATGG. GAPDH was utilized as the internal control.

Ethynyl deoxyuridine incorporation assay

After transfection with siRAB6B for 48 h, SMMC7721 and MHCC97L cells were seeded in 96-well plates (2,000 cells/well). After incubation overnight, cells were labeled with EdU and performed according to the manufacturer's instructions (Beyotime, China). The cells were visualized with a Zeiss Axio Observer microscope, and images were captured in at least three random fields for further analysis.

Cell apoptosis assays

After transfection with siRAB6B for 48 h, SMMC7721 and MHCC97L cells were seeded in 24-well plates (20,000 cells/well). Cells were cultured overnight and induced apoptosis with 20 μM cisplatin for 18 h. Then, cells were isolated with EDTA-free trypsin, washed with cold PBS three times, and resuspended in a binding buffer. After incubation with PI and Annexin V-FITC (Vazyme, China) in dark for 10 min, the cell apoptosis was examined through the flow cytometer (Thermo AttuneNxt, United States) and analyzed by FlowJo software.

MTT assay

Transfected cells were seeded into the 96-well plate (4,000 cells/well), after overnight attachment, the medium was changed to 100 μl fresh medium with dosage cisplatin (Selleck, China) and cultured for another 24 h or 48 h 5 mg/ml MTT (Beyotime, China) was added to each well and continued to incubate for 4 h, then discarded the supernatant, added 150 μl DMSO, and detected the OD value at 490 nm by a microplate reader (ThermoFisher, United States).

Statistical analysis

The Wilcoxon test was used to examine the RAB6B mRNA expression levels between pairs of groups. Logistic regression was conducted to analyze the association of the RAB6B expression and clinicopathological parameters. The Kaplan–Meier method and log-rank tests were performed to analyze the overall survival (OS) and disease-specific survival (DSS). Correlation analyses were performed by the Spearman correlation test. Univariate and multivariate analyses were applied to establish a Cox proportional hazard regression model and a nomogram model. The time-dependent receiver operating characteristic (ROC) curves were generated to compare various survival factors. One-way ANOVA tests and Kruskal–Wallis tests were utilized to compare the difference between more than two groups. For experimental data, Student's *t*-test was used to evaluate the differences between the two groups. Each experiment was performed three times, and all data were presented as the mean ± standard deviation (SD). Statistical significance was described as follows: ns, not significant; $^{*}p < 0.05$; $^{**}p < 0.01$; $^{***}p < 0.001$.

Results

RAB6B expression and its relationship with clinical parameters in hepatocellular carcinoma

To explore the potential roles of RAB6B in HCC, we first evaluated the expression difference of RAB6B in HCC tissues and normal liver tissues. Analyzing TCGA data from the TIMER2.0 database, we found that the RAB6B expression was significantly elevated in HCC tissues relative to normal liver tissues (Figure 1A). Meanwhile, based on the HCCDB database analysis, the other five HCC GEO datasets (GSE22058, GSE25097, GSE63898, GSE64041, and GSE76427) and ICGC databases also showed that RAB6B was highly expressed in HCC tissues relative to adjacent tissues (Figures 1B,C). We also confirmed that the RAB6B mRNA expression level was upregulated in HCC tissues by using the UCLCAN database (Figure 1D). Furthermore, RAB6B expression was highly expressed in 50 paired HCC tissues (Figure 1E). In addition, using the CPTAC database, we found that the RAB6B protein expression level in HCC tissues was also higher than that in normal liver tissue (Figure 1F). Immunohistochemistry assays from the HPA database further verified that the RAB6B protein expression was significantly elevated in HCC tissues (Figure 1G).

Then, we explored the association between RAB6B expression and clinicopathological variables. As is shown in Table 1, RAB6B expression was higher in advanced T stages. Besides, RAB6B expression increased with the T classification and the histological grade (Figures 1H,I). Altogether, the above results indicated that the mRNA and protein levels of RAB6B were highly expressed in HCC tissues, and RAB6B expression was related to the T stages and grades in HCC patients.

The prognostic and diagnostic value of RAB6B in patients with hepatocellular carcinoma

Then, we wondered whether the high expression of RAB6B in HCC tissues affects the prognosis of HCC patients. Kaplan–Meier survival curves demonstrated that patients with high RAB6B expression tended to have poor overall survival (OS)

TABLE 1 Correlations between the RAB6B expression and clinical characteristics of patients with HCC from the TCGA.

Characteristic	Total	High expression	Low expression	Pvalue
Age				0.4771
<=65	235 (62.83%)	121 (64.71%)	114 (60.96%)	
>65	138 (36.9%)	65 (34.76%)	73 (39.04%)	
Gender				0.1847
female	121 (32.35%)	67 (35.83%)	54 (28.88%)	
male	253 (67.65%)	120 (64.17%)	133 (71.12%)	
AFP				0.2226
high	117 (31.28%)	59 (31.55%)	58 (31.02%)	
normal	163 (43.58%)	69 (36.9%)	94 (50.27%)	
Stage				0.0337
stage I	173 (46.26%)	73 (39.04%)	100 (53.48%)	
stage II	87 (23.26%)	52 (27.81%)	35 (18.72%)	
stage III	85 (22.73%)	47 (25.13%)	38 (20.32%)	
stage IV	5 (1.34%)	3 (1.6%)	2 (1.07%)	
T				0.0211
T1	183 (48.93%)	77 (41.18%)	106 (56.68%)	
T2	95 (25.4%)	57 (30.48%)	38 (20.32%)	
T3	80 (21.39%)	45 (24.06%)	35 (18.72%)	
T4	13 (3.48%)	7 (3.74%)	6 (3.21%)	
M				1
M0	268 (71.66%)	138 (73.8%)	130 (69.52%)	
M1	4 (1.07%)	2 (1.07%)	2 (1.07%)	
N				0.67
N0	254 (67.91%)	131 (70.05%)	123 (65.78%)	
N1	4 (1.07%)	3 (1.6%)	1 (0.53%)	
Grade				0.089
G1	55 (14.71%)	23 (12.3%)	32 (17.11%)	
G2	178 (47.59%)	82 (43.85%)	96 (51.34%)	
G3	124 (33.16%)	71 (37.97%)	53 (28.34%)	
G4	12 (3.21%)	8 (4.28%)	4 (2.14%)	

(hazard ratio (HR) = 1.56, $p = 0.015$) and disease-specific survival (DSS) (HR = 1.68, $p = 0.025$) (Figures 2A,B). Meanwhile, univariate regression analysis revealed a relationship between prognosis with T stage, M stage, and RAB6B expression (Figure 2C). Furthermore, multivariate Cox regression analysis indicated that RAB6B expression (HR = 1.497, $p = 0.001$), and T stage (HR = 2.727, $p < 0.001$) were independent prognostic factors for HCC patients (Figure 2D).

In addition, a ROC curve analysis was conducted to evaluate the diagnostic performance of RAB6B in HCC. Area Under Curve (AUC) was found to be 0.946, which indicated that RAB6B expression was a highly reliable predictor (Figure 2E). The Time-dependent survival ROC curve of RAB6B was created to predict 1-, 3-, and 5-years survival rates. Relative to predicting 3-years (AUC = 0.548) and 5-years (AUC = 0.531) survival rates, the AUC value for predicting 1-year survival rate was 0.682, which showed a suitable predictive ability (Figure 2F). Furthermore, a nomogram model was performed according to the findings of multivariate Cox regression, which can be used to predict the survival probabilities at 1-, 3-, and 5-years for HCC patients (Figure 2G). Collectively, our results suggested that RAB6B may act as an independent prognosis factor and accurate diagnosis index in predicting OS among patients with HCC.

RAB6B mutation landscape in hepatocellular carcinoma

We then investigated the genetic alteration types and frequency of RAB6B in HCC based on the cBioPortal database. The TCGA-Firehose Legacy dataset, which contained 379 samples, was utilized for analysis. The alteration frequency of RAB6B was 5% in HCC, which

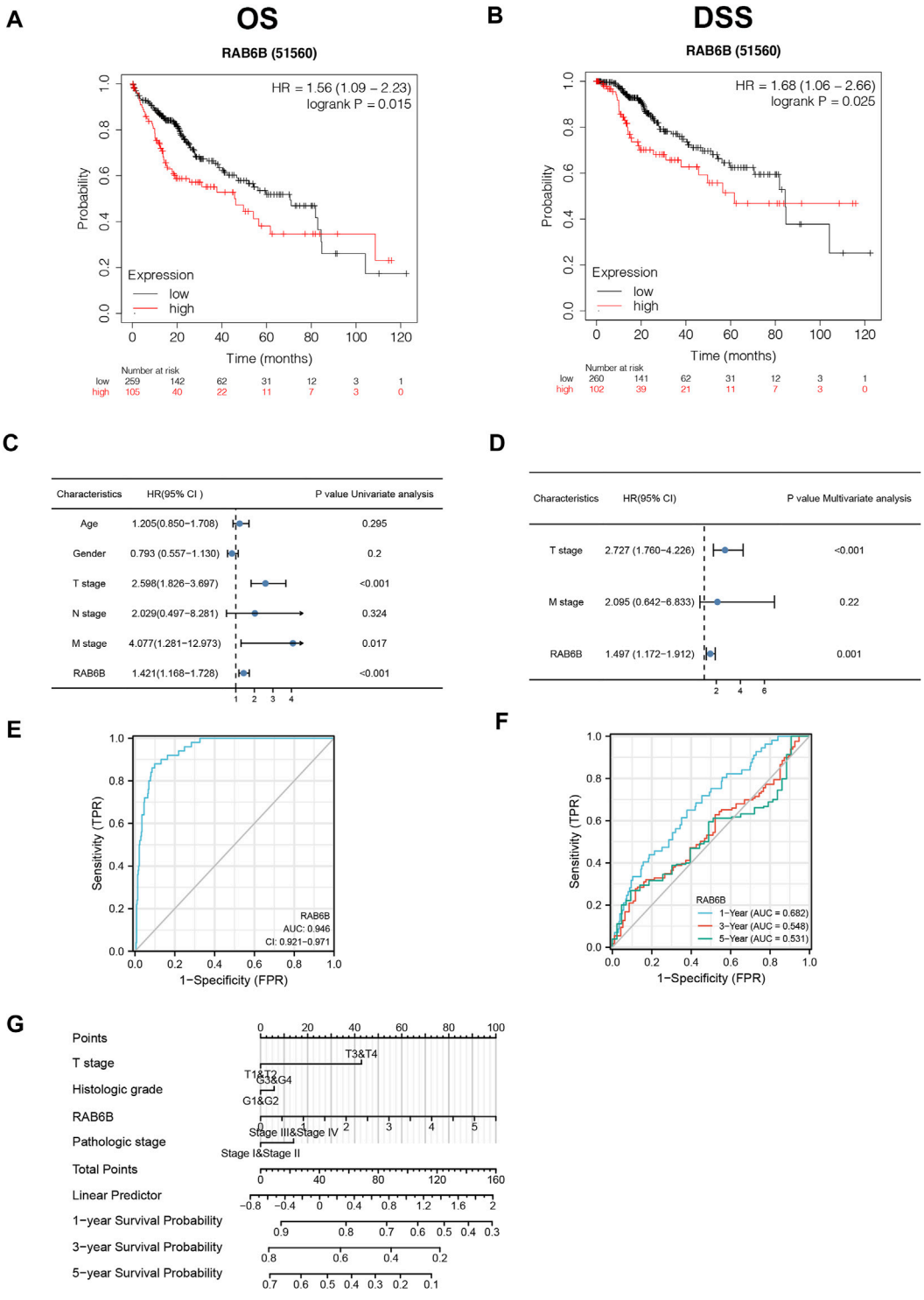

FIGURE 2
The prognostic and diagnostic value of RAB6B in patients with HCC. **(A,B)** Kaplan–Meier survival analysis showed that HCC patients with high RAB6B expression exhibited a shorter overall survival (OS) **(A)** and disease specific survival (DSS) **(B)** than those with low RAB6B expression. **(C)** Univariate COX analysis revealed that T stage, M stage, and RAB6B expression were significant factors affecting the survival rate of HCC patients. **(D)** Multivariate COX analysis showed that T stage and RAB6B expression were independent prognostic factors in HCC patients. **(E)** ROC curve was used to evaluate the diagnostic value of high RAB6B level for HCC patients in TCGA. **(F)** Time-dependent survival ROC curve analysis was used to predict 1-, 3- , and 5-years survival rates. **(G)** Nomogram integrating clinicopathologic features and RAB6B level was constructed to predict prognostic probabilities at 1-, 3-, and 5-years in the TCGA dataset.

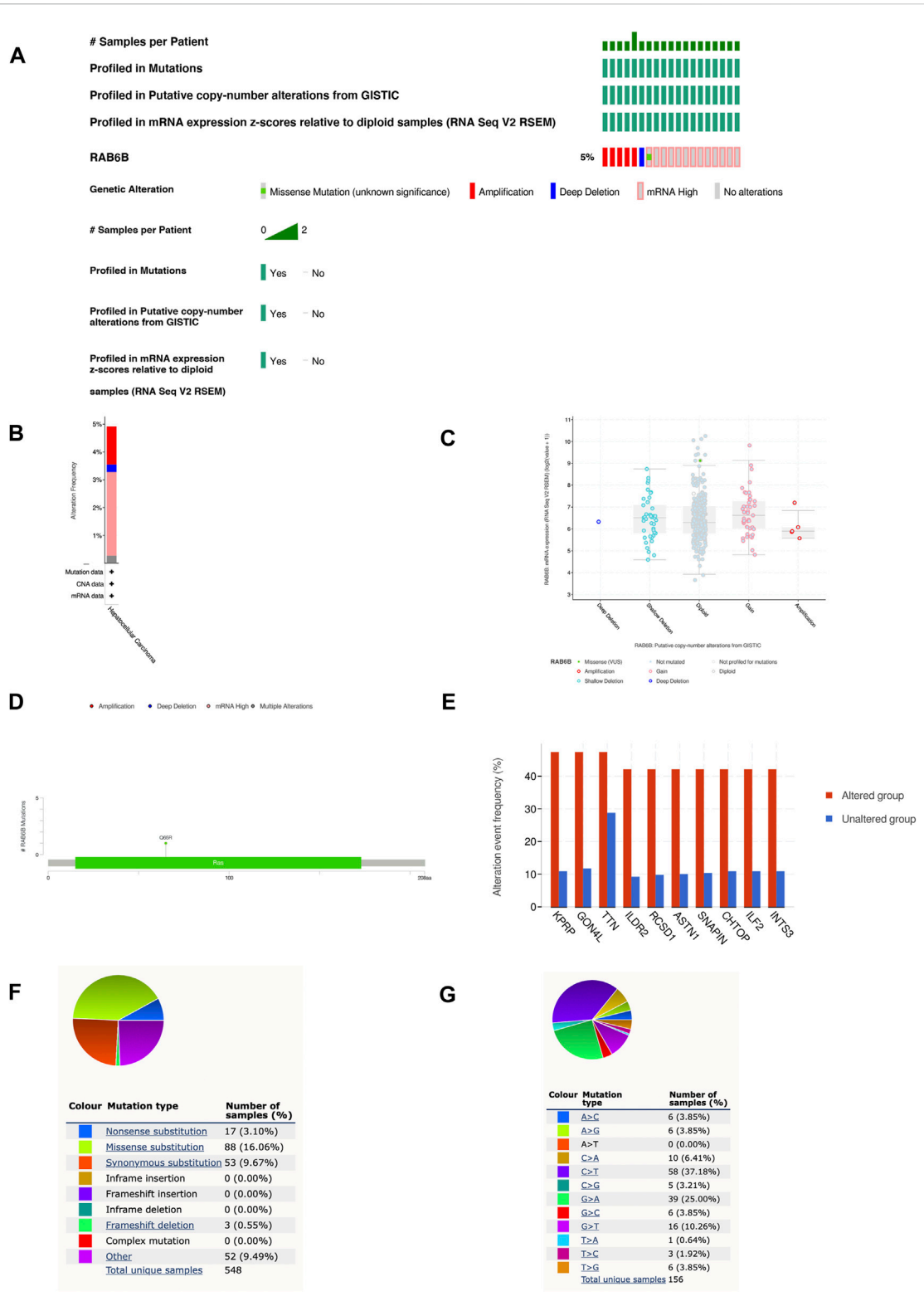

FIGURE 3
RAB6B mutation landscape in HCC. **(A)** OncoPrint summarized the genetic alterations in RAB6B based on LIHC (TCGA, Firehose Legacy, 379 samples) from the cBioPortal database. **(B)** RAB6B mutation frequency in HCC according to TCGA data. **(C)** The dot plot showed the correlation between RAB6B copy number and mRNA expression by cBioPortal. **(D)** Mutation diagram of RAB6B in HCC across protein domains. **(E)** The histogram showed the top 10 genes with the highest frequency in the genetic altered and unaltered group. **(F,G)** The pie chart showed the proportion of various mutation types of RAB6B in HCC based on the COSMIC database.

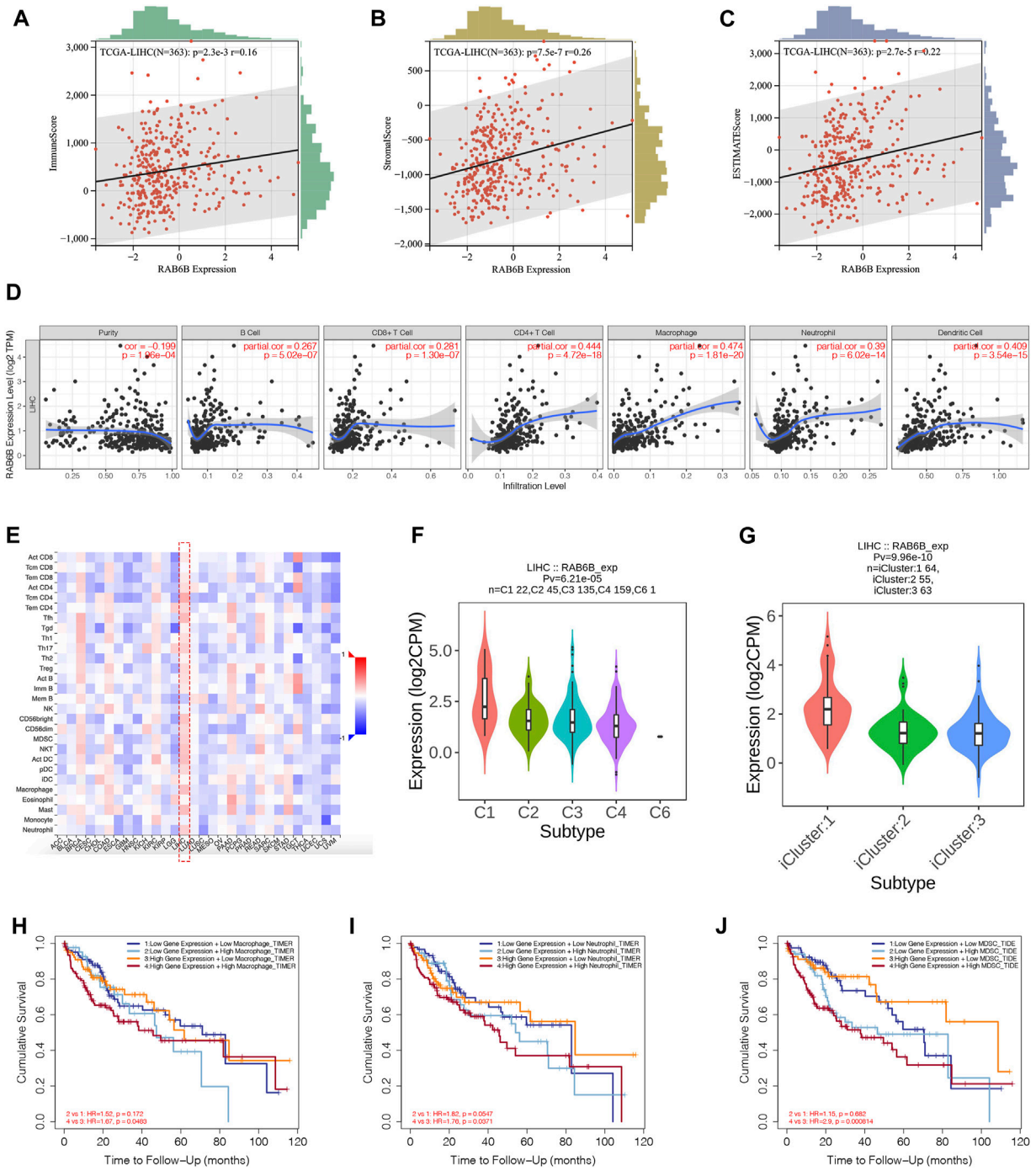

FIGURE 4
RAB6B expression correlated with tumor-infiltrating immune cells in HCC. **(A–C)** RAB6B expression was positively associated with the immune scores **(A)**, stromal scores **(B)**, and estimate scores **(C)** in HCC patients from the TCGA database. **(D)** Correlation between RAB6B expression and the tumor-infiltrating immune cells in HCC from the TIMER database. **(E)** Heatmap showed the relationship between RAB6B and various types of immune cells in HCC (red dashed rectangle) from the TISIDB database. **(F)** Correlation between RAB6B expression and immune subtypes in HCC from TISIDB database. C1 (wound healing); C2 (IFN-gamma dominant); C3 (inflammatory); C4 (lymphocyte depleted); C5 (immunologically quiet); C6 (TGF-b dominant). **(G)** Association between RAB6B expression and various molecular subtypes in HCC from TISIDB database. **(H–J)** Cumulative survival analysis of combinations of RAB6B expression and the abundance of macrophage cells **(H)**, neutrophil cells **(I)**, and MDSC **(J)** in HCC from the TIMER2.0 database. MDSC, myeloid-derived suppressor cells.

TABLE 2 The correlation between RAB6B expression and tumor lymphocyte infiltration in HCC (TISIDB).

	LIHC	
	r	p
Activated CD8 T cell	0.097	6.04E-02
Central memory CD8 T cell	−0.025	6.31E-01
Effector memory CD8 T cell	0.077	1.37E-01
Activated CD4 T cell	0.132	**1.05E-02**
Central memory CD4T cell	0.319	**3.52E-10**
Effector memory CD4 T cell	0.152	**3.38E-03**
T follicular helper cell	0.258	**4.65E-07**
Gamma delta T cell	0.055	2.86E-01
Type 1 T helper cell	0.127	**1.40E-02**
Type 17 T helper cell	0.18	**5.00E-04**
Type 2 T helper cell	0.055	2.85E-01
Regulatory T cell	0.143	**5.68E-03**
Activated B cell	0.123	**1.73E-02**
Immature B cell	0.077	1.38E-01
Memory B cell	−0.21	**4.63E-05**
natural killer cell	−0.044	0.398
CD56bright natural killer cell	0.22	**1.98E-05**
CD56dim natural killer cell	0.153	**3.06E-03**
Myeloid derived suppressor cell	0.175	**6.75E-04**
Natural killer T cell	0.221	**1.71E-05**
Activated dendtritic cell	0.241	**2.74E-06**
Plasmacytoid dendtritic cell	0.154	**2.95E-03**
Immature dendtritic cell	0.031	0.553
Macrophage	0.241	**2.75E-06**
Eosinophil	0.027	0.597
Mast	0.252	**8.86E-07**
Monocyte	−0.046	0.371
Neutrophil	0.182	**4.26E-04**

Data are bolded to highlight that these data are statistically different..

TABLE 3 Correlation analysis between RAB6B expression and immune cell markers in HCC.

	Biomarker	Cor	p value
CD8+T	CD8A	0.21	1.00E-06
	CD8B	0.23	1.00E-07
Th1	T-bet (TBX21)	0.035	0.42
	STAT4	0.081	0.064
	STAT1	0.44	1.40E-26
	IFN-g (IFNG)	0.049	0.26
	TNF-a (TNF)	0.14	0.0016
Th2	GATA3	0.16	0.00015
	STAT5A	0.48	4.10E-32
	CCR3	0.35	2.10E-16
Tfh	BCL6	−0.012	0.78
	IL21	0.11	0.014
	CXCR5	0.31	2.10E-13
	ICOS	0.36	2.20E-17
Th17	STAT3	0.11	0.012
	IL17A	0.076	0.082
	IL-21R	0.33	7.00E-15
Treg	FOXP3	0.14	0.00094
	CCR8	0.47	3.60E-30
	TGFb (TGFB1)	0.56	2.00E-44
	IL2RA	0.4	3.80E-22
M1	INOS (NOS2)	0.41	2.10E-23
	IRF5	0.42	1.40E-24
	COX2 (PTGS2)	0.00018	1
M2	ARG1	−0.29	8.10E-12
	CD206 (MRC1)	−0.1	0.02
	CD115 (CSF1R)	0.32	6.50E-14
N	CD66b (CEACAM8)	−0.14	0.00084
	CD11b (ITGAM)	0.38	1.20E-19
	CCR7	0.2	5.00E-06
	FUT4	0.42	1.90E-24
NK	CD7	0.24	4.4-e08
	XCL1	0.15	7.00E-04
	KIR3DL1	−0.091	0.037
DC	HLA-DPB1	0.45	6.80E-28
	HLA-DQB1	0.35	2.80E-16
	HLA-DRA	0.46	2.10E-28
	HLA-DPA1	0.43	1.80E-25
	BDCA-1 (CD1C)	0.3	1.50E-12
	BDCA-4 (NRP1)	0.5	2.30E-34
	CD11c	0.32	2.00E-14
B	CD19	0.24	1.30E-08
	CD79A	0.13	0.0027
TAM	CCL2	0.22	2.40E-07
	CD68	0.32	2.10E-14
	IL10	0.1	0.021

included amplification, deep deletion, missense mutation, and mRNA high (Figure 3A). The histogram summarized the different types of genetic alterations of RAB6B in HCC samples (Figure 3B). Meanwhile, the relationship between different mutation types of RAB6B and mRNA expression was compared. HCC with RAB6B amplification had lower expression of mRNA relative to other type alterations of RAB6B (Figure 3C). The detailed mutation landscapes revealed that the Q65R missense mutation was the most frequent mutation site (Figure 3D). Additionally, we analyzed the top 10 significantly up-regulated genes in the gene-altered group relative to the unaltered group, including KPRP, GON4L, TTN, ILDR2, RCSD1, ASTN1, SNAPIN, CHTOP, ILF2, and INTS3

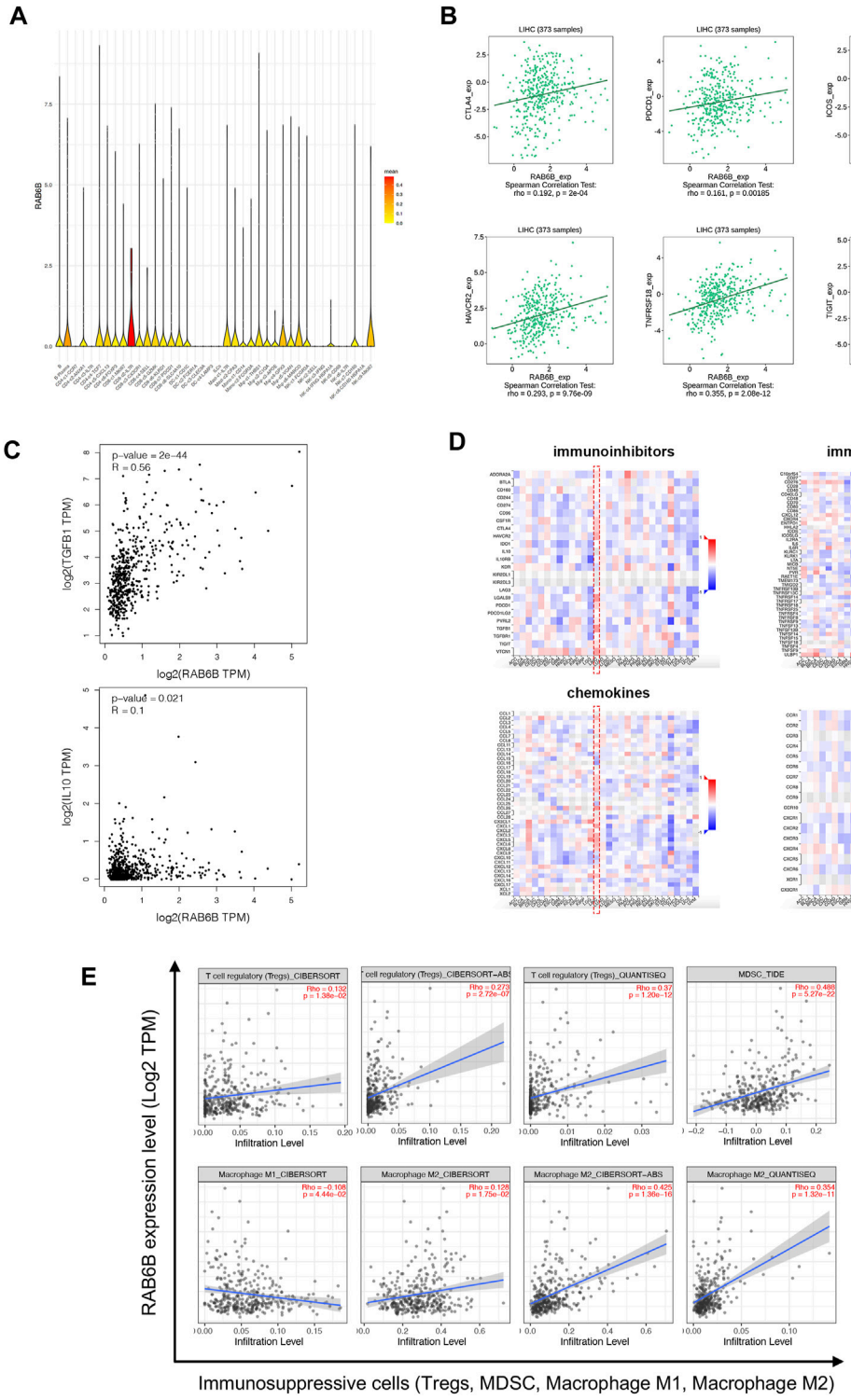

FIGURE 5
Relationship between RAB6B expression and immune-related molecules and cells. **(A)** RAB6B was mainly enriched in CD8+T cells according to single-cell RNA-sequencing results, which were analyzed by SMART-seq2. **(B)** Scatter plot showed that RAB6B expression was positively correlated with various immune checkpoint molecules, including CTLA4, PDCD1, ICOS, HAVCR2, TNFRSF18, and TIGIT. **(C)** RAB6B expression was positively correlated with TGFB1 and IL10 based on the GEPIA database. **(D)** The heatmap (red dashed rectangle) showed the correlation between RAB6B expression and various immunoinhibitors, immunostimulators, chemokines, and receptors in HCC from the TISIDB database. **(E)** RAB6B was positively correlated with Tregs, MDSC, and M2 macrophages infiltration, but negatively correlated with M1 macrophages infiltration by using the TIMER2.0 database. Tregs, regulatory T cells; MDSCs, myeloid-derived suppressor cells.

TABLE 4 The correlation between RAB6B expression and major genes of various stages of T cell exhaustion.

Stage	Gene	p value	R
Tex Prog1	CD28	6.20E-17	0.35
	CXCR5	2.10E-13	0.31
	ICOS	2.20E-17	0.36
	MYB	2.10E-19	0.38
	OAS1	2.80E-02	0.095
	SELL	8.50E-09	0.25
	STAT1	1.40E-26	0.44
	TCF7	9.50E-08	0.23
Tex Prog2	ALCAM	3.10E-24	0.42
	ANXA2	8.10E-59	0.63
	ITGB7	1.20E-03	0.14
	MKI67	1.10E-44	0.56
Tex Int	CX3CR1	1.20E-07	0.23
	GZMA	1.10E-06	0.21
	GZMB	8.60E-02	0.075
	KLRK1	1.20E-01	−0.068
	PRDM1	4.60E-26	0.44
	PRF1	4.90E-01	0.03
	ZEB2	1.30E-07	0.23
Tex Term	CD38	5.70E-04	0.15
	CD101	1.20E-26	0.44
	ENTPD1	2.20E-80	0.7

(Figure 3E). Using another database, COSMIC, we further assessed mutation types in RAB6B. As shown in the pie chart, missense substitutions accounted for the highest proportion at 16.06%, followed by synonymous substitutions at 9.67%, nonsense substitutions at 3.10%, and frameshift deletion at 0.55%, and other mutation types at 9.49% (Figure 3F). The top three substitution mutations were C > T (37.18%), G > A (25.00%), G > T (10.26%) (Figure 3G).

RAB6B influence the infiltration of various tumor-associated immune cells in hepatocellular carcinoma

Accumulating studies have demonstrated that tumor progression is regulated by its surrounding immune microenvironment (Fu et al., 2019). Therefore, the relationship between RAB6B expression and tumor immune-infiltrating immune cells in HCC was explored. We first analyzed the association between RAB6B expression and immune score and stromal score of HCC patients, respectively, by using the ESTIMATE algorithm. The results showed that RAB6B expression was positively correlated with immune scores (r = 0.16, p = 2.3e-3), stromal scores (r = 0.26, p = 7.5e-7), as well as with estimate scores (r = 0.22, p = 2.7e-5) (Figures 4A–C). Additionally, the correlation between RAB6B expression and immune cell infiltration was further validated through TIMER database. We found that RAB6B expression was significantly positively correlated with infiltration level of B cells (r = 0.267, p = 5.02e-07), $CD8^+$ T cells (r = 0.281, p = 1.30e-07), $CD4^+$ T cells (r = 0.444, p = 4.72e-18), Macrophages (r = 0.474, p = 1.81e-20), Neutrophils (r = 0.39, p = 6.02e-14), and Dendritic cells (r = 0.409, p = 3.54e-15) but negatively correlated with tumor purity (r = −0.199, p = 1.96e-04) in HCC (Figure 4D). Consistently, using the TISIDB database, we found that RAB6B expression was positively correlated with the infiltrating abundance of most immune cells (Figure 4E), the corresponding r and p values were summarized in Table 2. Moreover, the GEPIA database was employed to confirm the relationship between the RAB6B expression and various immune cells markers in HCC, the r and p values were listed in Table 3.

According to the TISIDB database, HCC samples were divided into six immune subtypes: C1, wound healing; C2, IFN-gamma dominant; C3, inflammatory; C4, lymphocyte depleted; C5, immunologically quiet; and C6, TGF-b dominant. RAB6B expression was significantly correlated with the immune subtypes in HCC (p = 6.21e-05) (Figure 4F). Furthermore, RAB6B expression was also correlated with different molecular subtypes (p = 9.96e-10) (Figure 4G). Finally, we investigated the prognostic effect of RAB6B expression combined with different abundances of immune cell infiltration in HCC patients. Kaplan-Meier analysis showed that the survival rate of HCC patients with high expression of RAB6B and high infiltration of macrophages, neutrophils, and MDSCs was significantly reduced (Figures 4H–J). In conclusion, the above results indicated that RAB6B affected the infiltration of various immune cells in HCC and influenced the prognosis of HCC patients.

RAB6B positively correlated with immunosuppressive microenvironment in hepatocellular carcinoma

To further explore the effect of RAB6B on immune regulation in HCC, we analyzed single-cell RNA-sequencing data of HCC to investigate the relationship. The result showed that RAB6B was highly expressed on $CD8^+$ T cells (Figure 5A). Since the HCC microenvironment is immunosuppressive, and the above results also indicated that RAB6B could also promote the infiltration of $CD8^+$ T cells, we speculated that RAB6B might be involved in the induction of $CD8^+$ T cells exhaustion. According to a recent study, exhausted $CD8^+$ T cells could be divided into four stages (Beltra et al., 2020), and the correlation analysis was used to find that RAB6B expression was positively correlated with the main markers of each stage through the GEPIA database (Table 4). Moreover, RAB6B was also positively

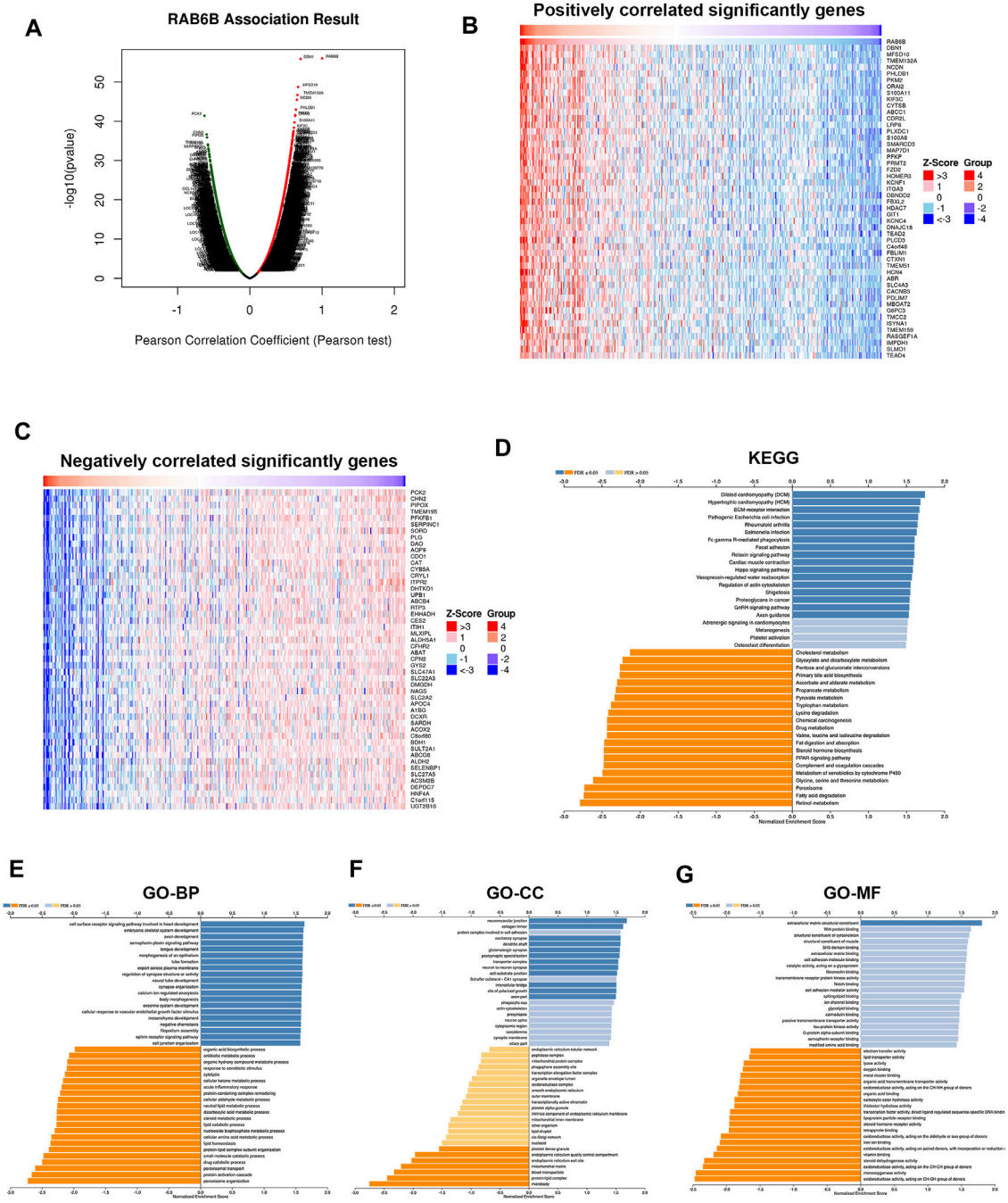

FIGURE 6
Functional enrichment analysis of RAB6B-related genes. **(A)** The Volcano plot showed RAB6B co-expressed gene profile in HCC bythe LinkedOmics database. **(B,C)** Heatmap showed 50 positively **(B)** and 50 negatively **(C)** correlated genes with RAB6B expression in HCC. **(D)** KEGG analysis of RAB6B co-expressed genes in HCC. KEGG, Kyoto Encyclopedia of Genes and Genomes. **(E–G)** Various types of GO analysis of RAB6B co-expressed genes in HCC. GO, Gene Ontology; BP, Biological Process; CC, Cellular Component; MF, Molecular Function.

associated with the expression of immune checkpoint molecules, such as CTLA-4, PDCD1, ICOS, HAVCR2, TNFRSF18, and TIGIT (Figure 5B). Immunosuppressive cytokines, such as IL10 and TGF-β, are also involved in the regulation of $CD8^+$ T cells exhaustion (Ejrnaes et al., 2006; Tinoco et al., 2009). Using the GEPIA database, we found that RAB6B was positively correlated with the expression of IL10 and TGF-b (Figure 5C). Besides, RAB6B was significantly associated with immunoinhibitors,

immunostimulators, chemokines, and receptors in HCC (Figure 5D). Finally, we analyzed the association of RAB6B with various immunosuppressive lymphocytes in the TME using the TIMER2.0 database, including regulatory T cells (Tregs), myeloid-derived suppressor cells (MDSCs), and macrophages (M1 and M2). The analysis indicated that RAB6B was positively correlated with Tregs, MDSCs, and M2 macrophages, but negatively associated with M1 macrophages (Figure 5E). Taken together, RAB6B, which may be highly expressed in $CD8^+$ T cells, participated in the regulation of CD8+T cells exhaustion by up-regulating the expression of immune checkpoint molecules, the secretion of immunosuppressive cytokines, and the recruitment of various immunosuppressive cells into HCC, thereby creating an immunosuppressive tumor microenvironment in HCC.

RAB6B co-expression networks in hepatocellular carcinoma

To investigate the biological role of RAB6B, the co-expression pattern of RAB6B was explored in TCGA- LIHC cohort through LinkedOmics. The results showed that 9,100 genes were positively correlated with RAB6B, while 3451 genes were negatively correlated with RAB6B (Figure 6A). The top 50 positively and negatively correlated genes were presented in heat maps (Figures 6B,C). KEGG pathway analysis indicated that enrichment mainly in the extracellular matrix (ECM)-receptor interaction, Fc-gamma R-mediated phagocytosis, Focal adhesion, and Hippo signaling pathway (Figure 6D). The results of GO enrichment analysis suggested that RAB6B co-expressed genes involved mainly in calcium ion regulated exocytosis, collagen trimer, and extracellular matrix structural constituent (Figures 6E–G). All these results indicated that the RAB6B co-expression network may influence the tumor stroma in the TME of HCC.

RAB6B is correlated with cancer-associated fibroblasts in hepatocellular carcinoma

The above results showed a positive correlation between RAB6B expression and stromal score, concerning cancer-associated fibroblasts (CAFs) were the main components of tumor stroma (Yin et al., 2019), so we explored the relationship between RAB6B and tumor-infiltrating CAFs. Through the TIMER2.0 database, the results showed that RAB6B expression was positively correlated with the abundance of CAFs infiltration in HCC by using different algorithms, including EPIC, TIDE, and MCPCOUNTER (Figure 7A). Then, we analyzed the relationship between the main markers of CAFs and RAB6B expression, the results revealed that RAB6B was positively correlated with ACTA2 (r = 0.37, p = 1.33e-12), Vimentin (r = 0.543, p = 8.29e-28), FAP (r = 0.524, p = 9.66e-26), S100A4 (r = 0.361, p = 4.46e-12), PDGFRB (r = 0.46, p = 2e-19). Moreover, RAB6B was also positively associated with collagen-related genes, including ELN (r = 0.245, p = 4.06e-06), FLNA (r = 0.538, p = 2.99e-27), COL1A1 (r = 0.513, p = 1.61e-24), COL1A2 (r = 0.527, p = 4.83e-26) (Figure 7B). We also performed GSEA to explore the potential biological process of RAB6B expression in HCC. The top 10 pathways significantly positively and negatively associated with RAB6B expression in HCC were presented in Supplementary Figure S1. The GSEA results confirmed that collagen formation and extracellular matrix organization were significantly gathered in the high-RAB6B expression group (Figure 7C). Finally, the co-expressed proteins network of RAB6B was investigated by using the HCCDB database, the results showed that RAB6B may participate in regulating the expression of LOXL2, CD248, and MPP2 et al., thereby affecting the homeostasis of ECM (Figure 7D). Collectively, these findings indicated that RAB6B may promote the infiltration of CAFs and ECM remolding, thereby reshaping the TME of HCC.

Correlation between RAB6B expression and drug response

Next, we wanted to explore the responsiveness of RAB6B to chemotherapy, the RAB6B mRNA expression and drug sensitivity were integrated through GDSC and CTRP databases. The results showed that in the GDSC database, RAB6B was positively correlated to IC50 of AICAR, AT-7519, AZD8055, BEZ235, CAL-101, CGP-60474, DMOG, EKB-569, GDC0941, GSK2126458, KIN001-102, KIN001-236, LY317615, MK-2206, OSU-03012, PAC-1, Paclitaxel, PHA-793887, PIK-93, SNX-2112, S-Trityl-L-cysteine, Sunitinib, TAK-715, and THZ-2–49, Vinblastine, ZSTK474, while was negatively associated with Dabrafenib, PD-0325901, PLX4720, SB590885 (Figure 8A). Based on the CTRP database, RAB6B displayed a positive relationship to IC50 of AZD7762, BRD-K63431240, BYL-719, MK-2206, NSC632839, PIK-93, SNX-2112, bleomycin A2, bosutinib, ciclopirox, decitabine, neratinib, tanespimycin, tosedostat but was negatively correlated to IC50 of BRD-K99006945, CIL70, ML239, SB-525334, niclosamide (Figure 8B). The specific correlation coefficients and targets with drugs of GDSC and CTRP were summarized respectively in Tables 5, 6. Taken together, most of these drugs were positively associated with RAB6B expression based on the IC50.

Knockdown of RAB6B inhibits hepatocellular carcinoma cells proliferation, promotes apoptosis, and enhances the sensitivity to cisplatin

Based on the above bioinformatics analysis results, the effect of RAB6B on the biological behavior of HCC was invalidated *in vitro*. The RAB6B mRNA expression in five HCC cell lines was

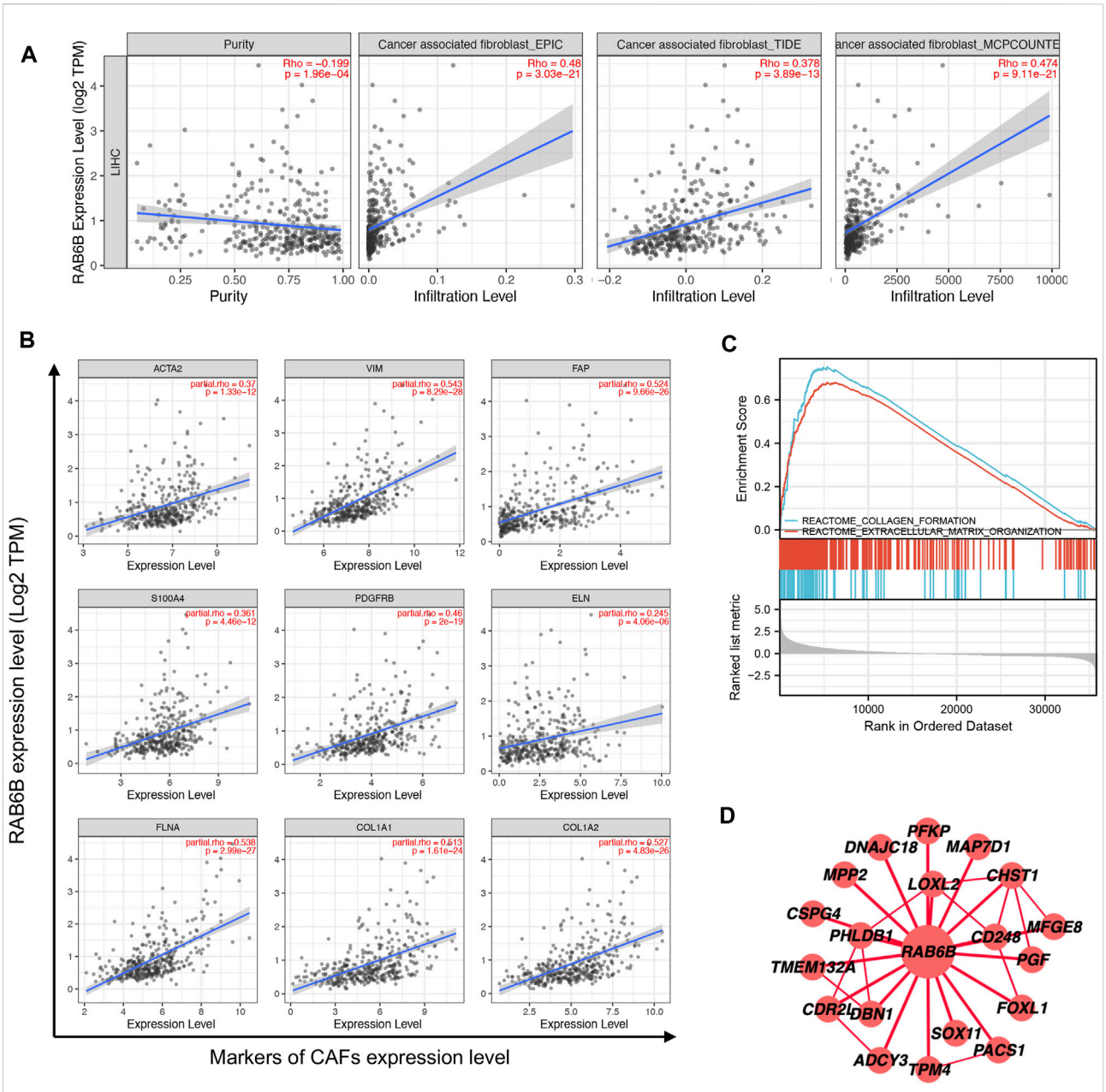

FIGURE 7
Correlation between the infiltration of CAFs and RAB6B expression in HCC. **(A)** RAB6B expression was positively correlated with the infiltration of CAFs in HCC based on the TIMER2.0 database. **(B)** RAB6B expression was positively associated with the main markers of CAFs, including ACTA2, VIM, FAP, S100A4, and PDGFRB, and was positively correlated with the expression of collagen-related proteins, including ELN, FLNA, COL1A1, and COL1A2. CAFs, cancer-associated fibroblasts. **(C)** The enrichment results of GSEA showed that upregulated RAB6B was positively correlated with "collagen formation" and "extracellular matrix organization." **(D)** The RAB6B PPI network was performed from the HCCDB database. PPI, protein-protein interaction.

compared, and the results showed that SMMC772 and MHCC97L had relatively higher RAB6B expression levels (Figure 9A). Therefore, RAB6B was knockdown in MHCC97L and SMMC7721 cells by transfection with siRNAs for subsequent experiments *in vitro*. qRT-PCR was performed to examine the knockdown efficiency of various siRNAs. The results showed that siRAB6B-2 significantly inhibited the RAB6B mRNA expression level in MHCC97L cells, while both siRAB6B-1 and siRAB6B-2 decreased the RAB6B mRNA expression in SMMC7721 cells (Figures 9B,C). To avoid off-target effects of siRNA, siRAB6B-2 and siRAB6B-1 were used to transfect MHCC97 L and SMMC7721 cells, respectively.

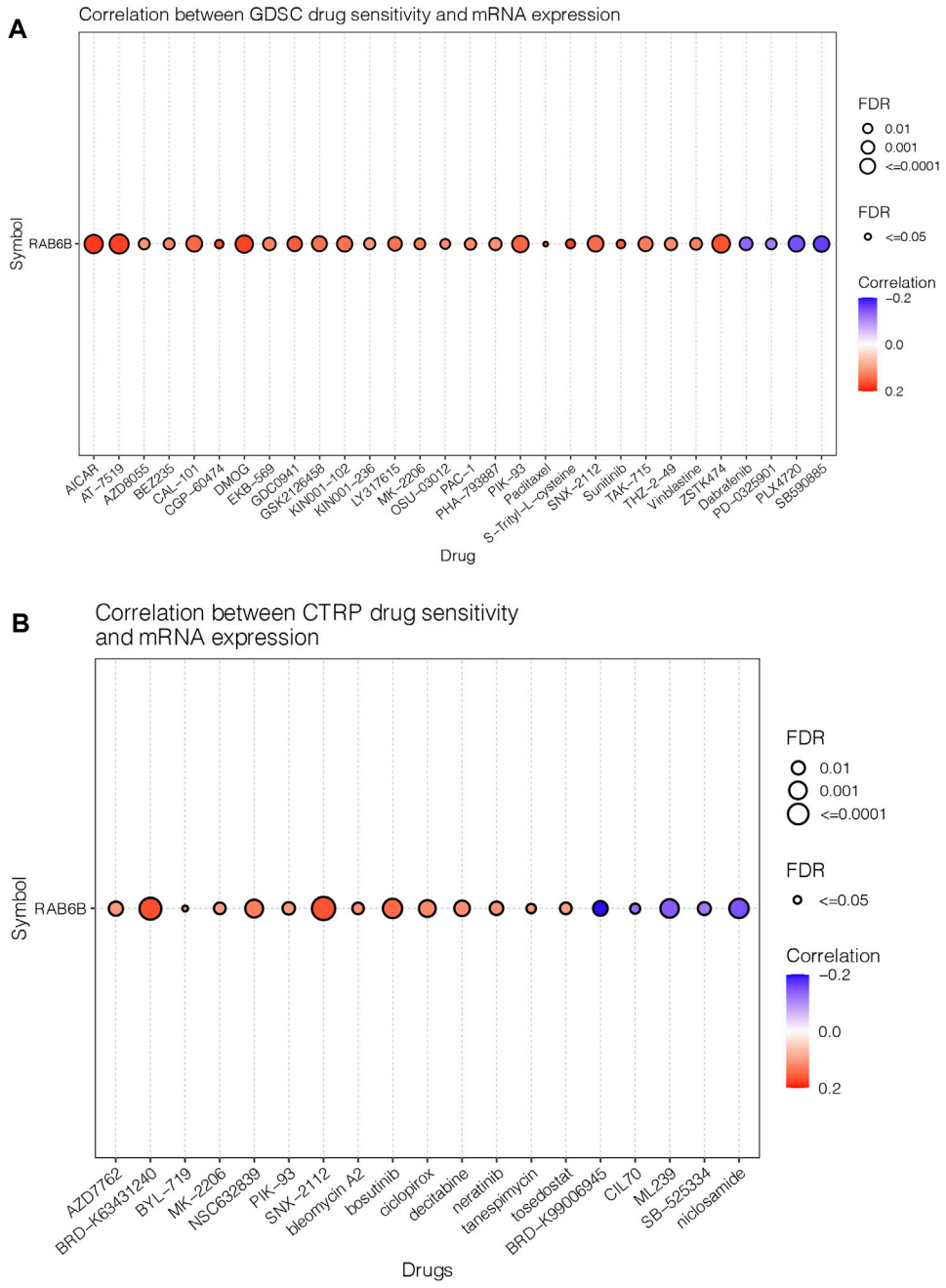

FIGURE 8
Correlation between RAB6B expression and drug response. **(A)** Dot plot summarized the relationship between RAB6B mRNA expression and the sensitivity of GDSC drugs (top 30) in pan-cancer. GDSC, Genomics of Drug Sensitivity in Cancer. **(B)** RAB6B mRNA expression and the sensitivity of CTRP drugs (top 30) in pan-cancer. CTRP, Cancer therapeutics Response Portal.

The EdU assay was performed to investigate the role of RAB6B knockdown on HCC cell proliferation, and the results revealed that the proliferation of MHCC97L and SMMC7721 cells was significantly decreased after RAB6B inhibition (Figures 9D–G). Moreover, after the knockdown of RAB6B, the percentage of apoptotic MHCC97L and SMMC7721 cells was significantly increased by using flow cytometry (Figure 9H). Finally, MHCC97L and SMMC7721 cells were treated with gradient doses of cisplatin for 24 and 48 h, and the results found that knockdown of RAB6B significantly reduced the resistance to cisplatin by MTT assay (Figures 9I,J). Overall, these results suggested that RAB6B may be

TABLE 5 Correlation between GDSC drug sensitivity and RAB6B mRNA expression.

Gene Symbol	Drug	Cor	Fdr	Target	Target pathway
RAB6B	AICAR	0.18188208	1.108421522E-06	AMPK agonist	Metabolism
	AT-7519	0.176693098	3.240025473E-07	CDK1, CDK2, CDK4, CDK6, CDK9	Cell cycle
	AZD8055	0.111224671	0.003751073	MTORC1, MTORC2	PI3K/MTOR signaling
	BEZ235	0.122117559	0.003652679	PI3K (class 1), MTORC1, MTORC2	PI3K/MTOR signaling
	CAL-101	0.148743384	3.2573E-05	PI3Kdelta	PI3K/MTOR signaling
	CGP-60474	0.167396186	0.01465139	CDK1,CDK2,CDK5,CDK7,CDK9, PKC	Cell cycle
	DMOG	0.175839264	4.559166636E-06	HIF-PH	Metabolism
	EKB-569	0.124046127	0.000954349	EGFR	EGFR signaling
	GDC0941	0.15762539	0.000172875	PI3K (class 1)	PI3K/MTOR signaling
	GSK2126458	0.139609616	0.000101231	PI3K (class 1), MTORC1, MTORC2	PI3K/MTOR signaling
	KIN001-102	0.138786462	6.7699E-05	AKT1, AKT2, AKT3	PI3K/MTOR signaling
	KIN001-236	0.106615078	0.003261655	Angiopoietin-1 receptor	RTK signaling
	LY317615	0.138465471	0.000371265	PKCB	Other, kinases
	MK-2206	0.129034024	0.004032457	AKT1, AKT2	PI3K/MTOR signaling
	OSU-03012	0.114852773	0.007637659	PDK1 (PDPK1)	Metabolism
	PAC-1	0.117320981	0.002803922	Procaspase-3, Procaspase-7	Apoptosis regulation
	Paclitaxel	0.171294461	0.032168205	Microtubule stabiliser	Mitosis
	PHA-793887	0.111571589	0.001409063	CDK2, CDK7, CDK5	Cell cycle
	PIK-93	0.150308436	1.4104E-05	PI3Kgamma	PI3K/MTOR signaling
	SNX-2112	0.145501484	3.6887E-05	HSP90	Protein stability and degradation
	S-Trityl-L-cysteine	0.178037205	0.010851251	KIF11	Mitosis
	Sunitinib	0.157548895	0.01407095	PDGFR, KIT, VEGFR, FLT3, RET, CSF1R	RTK signaling
	TAK-715	0.131352173	0.000203855	p38alpha, p38beta	JNK and p38 signaling
	THZ-2-49	0.116025378	0.001302119	CDK9	Cell cycle
	Vinblastine	0.124267764	0.00192142	Microtubule destabiliser	Mitosis
	ZSTK474	0.164483126	2.662594419E-06	PI3K (class 1)	PI3K/MTOR signaling
	Dabrafenib	-0.129933621	0.000794279	BRAF	ERK MAPK signaling
	PD-0325901	-0.109929629	0.00436616	MEK1, MEK2	ERK MAPK signaling
	PLX4720	-0.151194872	3.6483E-05	BRAF	ERK MAPK signaling
	SB590885	-0.164353004	4.4315E-05	BRAF	ERK MAPK signaling

involved in the regulation of HCC cell proliferation, apoptosis, and sensitivity to cisplatin.

Discussion

Rab GTPases are a highly conserved family of regulatory genes involved in vesicular transport (Li and Marlin, 2015). Each Rab GTPases localizes in a specific subcellular structure and exerts its respective membrane trafficking functions (Stenmark, 2009). Previous studies have reported that several Rab GTPases are involved in HCC progression, including modulating proliferation, migration, invasion, and metastasis (Yang et al., 2021). RAB6B, an isoform of RAB6, is mainly located in the Golgi apparatus and plays a role in Golgi-to-ER retrograde transport (Wanschers et al., 2007). Prior study has shown that high RAB6B expression promoted cell proliferation and the cell cycle G1/S phase transition through AKT/JNK signaling pathways in gastric cancer (Zhao et al., 2020). By contrast, RAB6B was low expressed in pancreatic and colorectal cancers, and correlated with poorer prognosis in patients (Anand et al., 2020; Jiang et al., 2022). These results suggested that RAB6B may play specific roles in different TME. Besides, few studies have reported the role of the Rab GTPases in the tumor immune microenvironment (TIME) of HCC. Therefore, we here mainly explored the potential functions of RAB6B in HCC based on public databases, including its role in tumor-associated immune cells infiltration and tumor stroma remodeling.

In this study, we found that RAB6B mRNA and protein expression levels were significantly upregulated in HCC compared to normal liver tissues across various public databases. Clinical association analyses demonstrated that increased RAB6B expression was correlated with higher T stage, and histological grade. Moreover, HCC patients with high RAB6B expression showed worse OS and DSS based on

TABLE 6 Correlation between CTRP drug sensitivity and RAB6B mRNA expression.

Gene symbol	Drug	Cor	Fdr	Target
RAB6B	AZD7762	0.105141148	0.006363712	inhibitor of checkpoint kinases 1 and 2
	BRD-K63431240	0.167889073	3.1119E-05	product of diversity oriented synthesis
	BYL-719	0.118366783	0.045070757	inhibitor of PI3K catalytic subunit alpha
	MK-2206	0.101297324	0.017278249	inhibitor of AKT1
	NSC632839	0.127547938	0.00082705	inhibitor of USP2, USP7 和 SENP2
	PIK-93	0.101684596	0.013107972	inhibitor of PI3K catalytic subunit gamma
	SNX-2112	0.16503565	8.467415545E-06	inhibitor of HSP90alpha and HSP90beta
	bleomycin A2	0.115929242	0.018053065	inducer of DNA damage
	bosutinib	0.145373518	0.000265119	inhibitor of SRC and ABL1
	ciclopirox	0.119001893	0.001514873	inhibitor of the iron-dependent enzyme ribonucleotide reductase
	decitabine	0.111592642	0.003158139	inhibitor of DNA methyltransferase
	neratinib	0.109379465	0.008598225	inhibitor of EGFR and HER2
	tanespimycin	0.105157895	0.031245529	inhibitor of HSP90
	tosedostat	0.10017112	0.017191426	inhibitor of ANPEP;LAP3;NPEPPS
	BRD-K99006945	−0.194235972	0.004936331	inhibitor of TP53
	CIL70	−0.125656697	0.026917134	Unknown
	ML239	−0.139809968	0.000518539	inhibitor of breast cancer stem cell proliferation
	SB-525334	−0.117023472	0.010787288	inhibitor of the transforming growth factor beta type 1 receptor
	niclosamide	−0.148197981	0.000276337	inhibitor of STAT3 signaling

Kaplan–Meier analysis. Univariate and multivariate Cox regression analyses further revealed that high RAB6B expression was an independent risk factor to predict poor OS for HCC patients. Additionally, ROC curve analysis showed that RAB6B has excellent diagnostic value in HCC.

Uncontrolled proliferation of tumor cells caused by key driver gene mutations often leads to tumorigenesis (El Tekle et al., 2021). Moreover, recent studies have found that there exist context-dependent genetic mutations, where a specific mutation plays a major role in a certain tumor type (Hoadley et al., 2018). Therefore, we explored the proportion and types of RAB6B mutations in liver cancer. The percentage of RAB6B genetical alterations reached 5%, of which missense substitutions accounted for the highest proportion of 16.06%. Meanwhile, we analyzed the top 10 genes that were significantly upregulated in the genetically altered group, including KPRP, GON4L, TTN, ILDR2, RCSD1, ASTN1, SNAPIN, CHTOP, ILF2, and INTS3. Among them, GON4L is a transcriptional regulator gene that has been reported to drive tumor growth through the YY1-androgen receptor-CD24 pathway (Agarwal et al., 2016). ILF2 (Interleukin enhancer binding factor 2), a transcription factor, is upregulated in HCC and can promote HCC tumorigenesis *in vivo* and *in vitro* (Cheng et al., 2016). INTS3 (integrator complex subunit 3), is found to be significantly overexpressed in HCC tissues and may be involved in HCC development (Inagaki et al., 2008). These results suggested that the genetic alterations of RAB6B in HCC may potentially activate the expression of the above-mentioned oncogenes or pathways to promote the progression of HCC.

According to the "seed and soil" theory, tumor cells act as seeds and continuously interact with the surrounding microenvironment to jointly promote tumor progression (Quail and Joyce, 2013). Targeting cancer cells alone usually cannot acquire a satisfactory effect. Recently, accumulating studies have focused on the research of TME. The TME is composed of various noncancer cellular components surrounding tumor cells, including tumor-infiltrating lymphocytes (TILs), CAFs, ECM, and endothelial cells (Chen and Song, 2019). Therefore, we explored the effect of RAB6B on the TME based on public databases. Our results revealed that RAB6B expression was positively correlated with immune scores and stromal scores by using the ESTIMATE algorithm. Meanwhile, RAB6B expression was related to the infiltrating abundance of various tumor-associated immune cells in HCC, including B cells, $CD8^+$ T cells, $CD4^+$ T cells, macrophages, neutrophils, and DCs. Furthermore, the survival analysis in combination with gene expression and immune cells infiltration abundance showed that HCC patients with high RAB6B expression and macrophages or neutrophils or MDSC cells infiltration tend to have a worse prognosis in HCC.

TILs can be divided into anti-tumor immune cells and immunosuppressive cells. The former include $CD8^+$ T cells, natural killer (NK) cells, DC cells, type 1-polarized macrophages (M1) and the latter includes myeloid-derived suppressor cells (MDSCs), regulatory T cells (Tregs), and type 2-polarized macrophages (M2) (Lu et al., 2019). We analyzed the single-cell sequencing data of HCC and found that RAB6B was significantly overexpressed in $CD8^+$ T cells, considering the TME of HCC is an

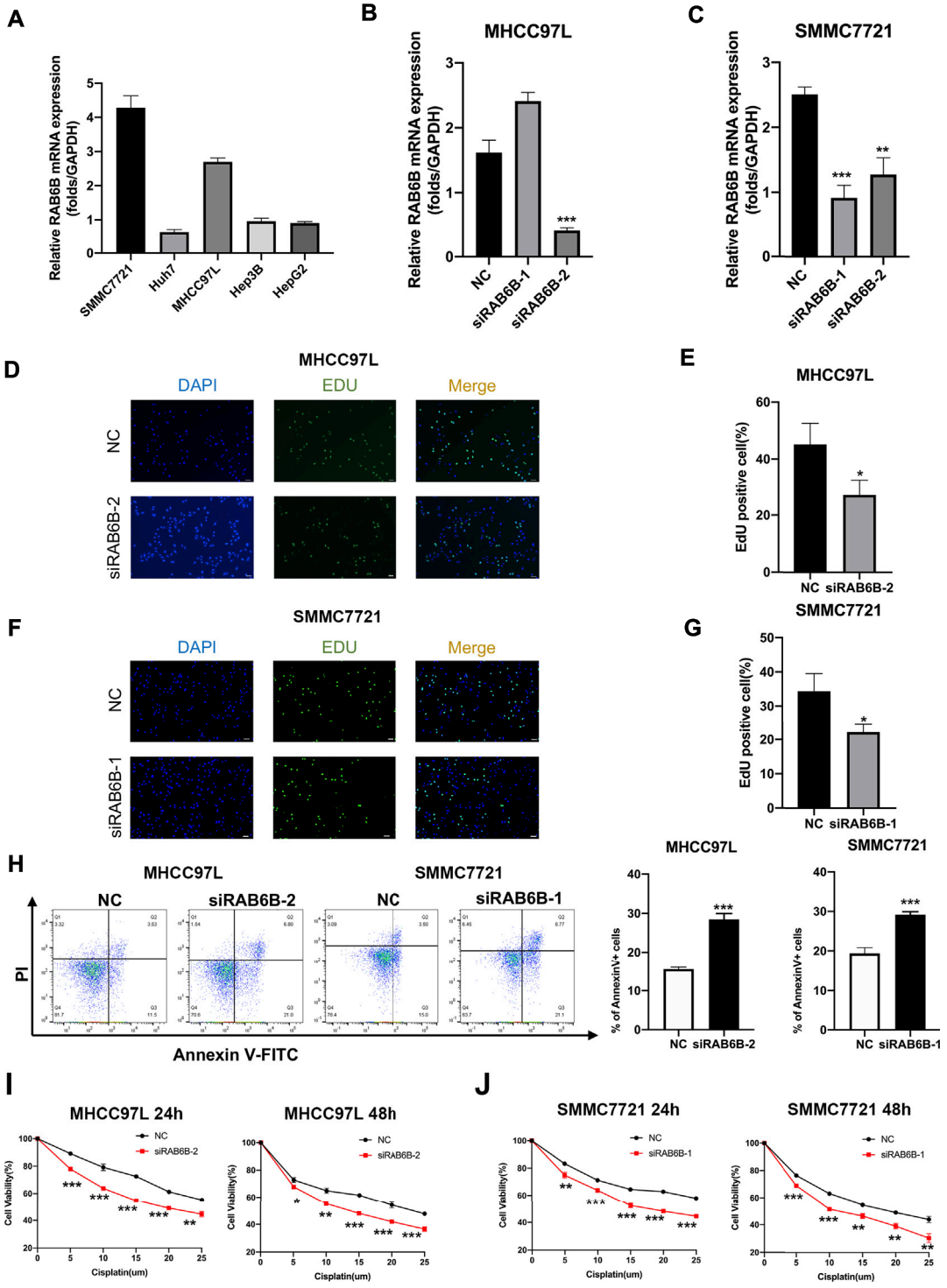

FIGURE 9
Effects of RAB6B knockdown on cell proliferation, apoptosis, and drug sensitivity in HCC cells. **(A)** The qRT-PCR result showed the RAB6B mRNA Expression in various HCC cell lines. **(B)** The qRT-PCR result showed the knockdown efficiency of RAB6B after transfection of MHCC97L cells with two different siRNAs. **(C)** Knockdown efficiency of RAB6B after transfection of SMMC7721 cells with two different siRNAs. **(D,E)** The effect of RAB6B knockdown on cell proliferation in MHCC97L cells was performed by EdU assay. Scale bar, 20um. **(F,G)** The effect of RAB6B knockdown on cell proliferation in SMMC7721 cells was performed by EdU assay. Scale bar, 20 μm. **(H)** The effect of RAB6B knockdown on cell apoptosis in MHCC97L and SMMC7721 cells performed by flow cytometry. **(I,J)** Gradient doses of cisplatin were used to treat MHCC97L cells **(I)** or SMMC7721 cells **(J)** for 24 and 48 h, and the cell viability was measured by MTT assay. All above data were presented as the mean ± SD, $n = 3$. NC, negative control. *$p < 0.05$; **$p < 0.01$; ***$p < 0.001$.

immunosuppressive state, we speculated that RAB6B may be involved in the regulation of $CD8^+$ T cell exhaustion in HCC. According to a newly published study, exhausted $CD8^+$ T cells can be divided into four stages, namely T cell exhaustion progenitors 1 (Tex Prog1), T cell exhaustion progenitors 2 (TexProg2), T cell exhaustion intermediate (TexInt), and T cell exhaustion terminally (Tex Term) (Beltra et al., 2020). By using the GEPIA database, we found that RAB6B was positively correlated with each exhausted stage of CD8+T cells. Previous studies have shown that the upregulation of immune checkpoint molecules can regulate T cells exhaustion, such as CTLA-4, PDCD1, ICOS, HAVCR2, TNFRSF18, and TIGIT (Wherry, 2011). Our results suggested that RAB6B was also positively associated with the aforementioned immune checkpoint molecules. In addition, we found that RAB6B may promote the production of immunosuppressive cytokines, such as IL10 and TGF-β, which have been reported to inhibit T cells function in TME (Ejrnaes et al., 2006; Tinoco et al., 2009). Finally, based on the TIMER database, our results revealed that RAB6B was positively correlated with immunosuppressive cells, such as MDSCs, Tregs, and M2 macrophages, but negatively correlates with M1 macrophages. All these findings indicated that RAB6B may induce the exhaustion of $CD8^+$ T cells, recruiting various immunosuppressive cells and cytokines into the TME, thereby promoting the formation of the immunosuppressive microenvironment of HCC.

Next, to further investigate the role of RAB6B in the progression of HCC, we identified genes co-expressed with RAB6B and performed functional enrichment analysis based on the group of differential co-expressed genes. The KEGG results revealed that the enrichment was primarily associated with ECM-receptor interaction, immune-related diseases (pathogenic *Escherichia coli* infection, *Salmonella* infection, Rheumatoid arthritis), Fc-gamma R-mediated phagocytosis, Focal adhesion, Hippo signaling pathway, regulation of actin cytoskeleton. GO analysis displayed that RAB6B expression was mainly involved in collagen trimer, cell adhesion, and ECM structural constituent. The functional enrichment results showed that RAB6B may be associated with ECM remodeling in the TME, so we explored the regulatory role of RAB6B on tumor stroma. Increasing studies have shown that CAFs, as the main components of tumor stroma, promote tumor progression by interacting with various cell components in the TME (Jia et al., 2021). ECM is a noncellular component of TME and is mainly produced by CAFs (Chaudhuri et al., 2014). During the tumor development, ECM continuously undergoes cross-linking, rearrangement, and degradation, thereby influencing tumor invasion, drug resistance, and metastasis (Elosegui-Artola et al., 2016). Using the TIMER2.0 database, different algorithms were used to find that RAB6B expression was positively correlated with the infiltration levels of CAFs in HCC. Previous studies have reported that α-smooth muscle actin (α-SMA), fibroblast activation protein (FAP), vimentin, platelet-derived growth factor (PDGF) receptor (PDGFR)-β, and fibroblast-specific protein 1 (FSP-1) can be served as the markers to identify CAFs. Our correlation analysis suggested that RAB6B was positively correlated with the genes encoding these proteins in HCC. Meanwhile, we also found that RAB6B was positively correlated with ECM-related genes, such as ELN, FLNA, COL1A1, and COL1A2. Through PPI network construction, several proteins, such as LOXL2, CD248, MPP2 et, al. Were found to be co-expressed with RAB6B in HCC. Lysyl oxidase-like 2 (LOXL-2), a collagen-modifying enzyme, has been found to increase the stiffness of tumor tissue by modifying the ECM components in the TME in HCC, thereby promoting intrahepatic metastasis (Wong et al., 2014). CD248, also known as Endosialin, is a transmembrane glycoprotein, that has been reported to be expressed mainly in CAFs in HCC, involved in the recruitment and M2 polarization of macrophages to promote HCC progression (Yang et al., 2020). In addition, Tropomyosin4 (TPM4), a member of actin-binding proteins, was also found to be highly expressed in HCC and correlated with poor prognosis in HCC patients (Li et al., 2021). These potentially interacting proteins suggested that RAB6B may be involved in remodeling the TME in HCC.

Most HCC patients are diagnosed at an advanced stage, and the treatment options are limited, usually targeted therapy, radiotherapy, and chemotherapy (Chen et al., 2019). Therefore, the potential RAB6B-responsive drugs based on GDSC and CTRP databases were mined. We found RAB6B positively correlated with IC50 of most drugs, most of which targeted PI3K/mTOR signaling. Recently, immunotherapy has emerged as a promising therapy in the treatment of several solid tumors, and various immune checkpoint molecules, such as PD-1/PD-L1 and CTLA-4, have been found to play an imperial role in tumor immune escape (Chang et al., 2017). Furthermore, the application of immune checkpoint inhibitors (ICIs) can enhance the immune response of tumors and inhibit tumor progression. Since we found that RAB6B was highly correlated with the expression of various immune checkpoint molecules and promoted the formation of the immunosuppressive microenvironment. Thus, the combination of ICIs and chemotherapeutics targeting RAB6B can provide a potent rationale for the treatment of HCC.

Based on the above bioinformatics findings, a series of functional assays were carried out *in vitro* by downregulating the RAB6B expression. The results showed that RAB6B knockdown inhibited cell proliferation and promoted apoptosis of HCC cells *in vitro*. In addition, inhibition of RAB6B enhanced the sensitivity to chemotherapeutic drugs such as cisplatin. However, our study also has some limitations, such as our findings were based on the analysis of public databases data, and the role of RAB6B in immune infiltration in TME needs to be examined *in vitro* and *in vivo*, meanwhile, the mechanism of RAB6B on HCC needs to be further studied.

Conclusion

Overall, in this study, we found that RAB6B was highly expressed in HCC tissues and was associated with poor

prognosis in HCC patients. Furthermore, RAB6B expression promotes the formation of an immunosuppressive microenvironment in HCC through recruiting various immune cells and inducing CD8+T cells exhaustion. Meanwhile, genomic alterations, functional enrichment analysis, and potential targeted drugs of RAB6B were analyzed. *In vitro* experiments have shown that knockdown of RAB6B inhibited cell proliferation, promoted cell apoptosis, and enhanced the sensitivity to cisplatin.

Data availability statement

The datasets presented in this study can be found in online repositories. The names of the repository/repositories and accession number(s) can be found in the article/Supplementary Material.

Author contributions

HP and EZ designed the study and wrote the manuscript. HP, XD, CW, and JW analyzed the data and did *in vitro* experiments. MY and YZ revised the manuscript.

Funding

This study was supported by the National Natural Science Foundation of China (Nos 81872255, 62141109), the Leading-edge Technology Programme of Jiangsu Natural Science Foundation: BK20212021.

Acknowledgments

We are grateful to the staff in the Public Scientific Research Platform of Zhongda Hospital Affiliated with Southeast University for technical assistance.

Conflict of interest

The authors declare that the research was conducted in the absence of any commercial or financial relationships that could be construed as a potential conflict of interest.

Publisher's note

All claims expressed in this article are solely those of the authors and do not necessarily represent those of their affiliated organizations, or those of the publisher, the editors and the reviewers. Any product that may be evaluated in this article, or claim that may be made by its manufacturer, is not guaranteed or endorsed by the publisher.

Supplementary material

The Supplementary Material for this article can be found online at: https://www.frontiersin.org/articles/10.3389/fphar.2022.989655/full#supplementary-material

References

Agarwal, N., Dancik, G. M., Goodspeed, A., Costello, J. C., Owens, C., Duex, J. E., et al. (2016). GON4L drives cancer growth through a YY1-androgen receptor-CD24 Axis. *Cancer Res.* 76, 5175–5185. doi:10.1158/0008-5472.Can-16-1099

Anand, S., Khan, M. A., Khushman, M., Dasgupta, S., Singh, S., and Singh, A. P. (2020). Comprehensive analysis of expression, clinicopathological association and potential prognostic significance of RABs in pancreatic cancer. *Int. J. Mol. Sci.* 21, 5580. doi:10.3390/ijms21155580

Asplund, A., Edqvist, P. H. D., Schwenk, J. M., and Ponten, F. (2012). Antibodies for profiling the human proteome-The Human Protein Atlas as a resource for cancer research. *Proteomics* 12, 2067–2077. doi:10.1002/pmic.201100504

Beltra, J. C., Manne, S., Abdel-Hakeem, M. S., Kurachi, M., Giles, J. R., Chen, Z., et al. (2020). Developmental relationships of four exhausted CD8(+) T cell subsets reveals underlying transcriptional and epigenetic landscape control mechanisms. *Immunity* 52, 825–841. doi:10.1016/j.immuni.2020.04.014

Chandrashekar, D. S., Bashel, B., Balasubramanya, S. a. H., Creighton, C. J., Ponce-Rodriguez, I., Chakravarthi, B., et al. (2017). Ualcan: A portal for facilitating tumor subgroup gene expression and survival analyses. *Neoplasia* 19, 649–658. doi:10.1016/j.neo.2017.05.002

Chang, H., Jung, W., Kim, A., Kim, H. K., Kim, W. B., Kim, J. H., et al. (2017). Expression and prognostic significance of programmed death protein 1 and programmed death ligand-1, and cytotoxic T lymphocyte-associated molecule-4 in hepatocellular carcinoma. *APMIS* 125, 690–698. doi:10.1111/apm.12703

Chaudhuri, O., Koshy, S. T., Branco Da Cunha, C., Shin, J. W., Verbeke, C. S., Allison, K. H., et al. (2014). Extracellular matrix stiffness and composition jointly regulate the induction of malignant phenotypes in mammary epithelium. *Nat. Mat.* 13, 970–978. doi:10.1038/nmat4009

Chen, S. Z., Cao, Q. Q., Wen, W., and Wang, H. Y. (2019). Targeted therapy for hepatocellular carcinoma: Challenges and opportunities. *Cancer Lett.* 460, 1–9. doi:10.1016/j.canlet.2019.114428

Chen, X., and Song, E. (2019). Turning foes to friends: Targeting cancer-associated fibroblasts. *Nat. Rev. Drug Discov.* 18, 99–115. doi:10.1038/s41573-018-0004-1

Cheng, S., Jiang, X., Ding, C., Du, C., Owusu-Ansah, K. G., Weng, X., et al. (2016). Expression and critical role of interleukin enhancer binding factor 2 in hepatocellular carcinoma. *Int. J. Mol. Sci.* 17, 1373. doi:10.3390/ijms17081373

Craig., A. J., Von Felden, J., Garcia-Lezana, T., Sarcognato, S., and Villanueva, A. (2020). Tumour evolution in hepatocellular carcinoma. *Nat. Rev. Gastroenterol. Hepatol.* 17, 139–152. doi:10.1038/s41575-019-0229-4 (

Ejrnaes, M., Filippi, C. M., Martinic, M. M., Ling, E. M., Togher, L. M., Crotty, S., et al. (2006). Resolution of a chronic viral infection after interleukin-10 receptor blockade. *J. Exp. Med.* 203, 2461–2472. doi:10.1084/jem.20061462

El Tekle, G., Bernasocchi, T., Unni, A. M., Bertoni, F., Rossi, D., Rubin, M. A., et al. (2021). Co-Occurrence and mutual exclusivity: What cross-cancer mutation patterns can tell us. *Trends Cancer* 7, 823–836. doi:10.1016/j.trecan.2021.04.009

Elosegui-Artola, A., Oria, R., Chen, Y., Kosmalska, A., Perez-Gonzalez, C., Castro, N., et al. (2016). Mechanical regulation of a molecular clutch defines force transmission and transduction in response to matrix rigidity. *Nat. Cell Biol.* 18, 540–548. doi:10.1038/ncb3336

Ferlay, J., Soerjomataram, I., Dikshit, R., Eser, S., Mathers, C., Rebelo, M., et al. (2015). Cancer incidence and mortality worldwide: Sources, methods and major patterns in GLOBOCAN 2012. *Int. J. Cancer* 136, E359–E386. doi:10.1002/ijc.29210

Forbes, S. A., Beare, D., Gunasekaran, P., Leung, K., Bindal, N., Boutselakis, H., et al. (2015). Cosmic: Exploring the world's knowledge of somatic mutations in human cancer. *Nucleic Acids Res.* 43, D805–D811. doi:10.1093/nar/gku1075

Fu, Y., Liu, S., Zeng, S., and Shen, H. (2019). From bench to bed: The tumor immune microenvironment and current immunotherapeutic strategies for hepatocellular carcinoma. *J. Exp. Clin. Cancer Res.* 38, 396. doi:10.1186/s13046-019-1396-4

Gao, J., Aksoy, B. A., Dogrusoz, U., Dresdner, G., Gross, B., Sumer, S. O., et al. (2013). Integrative analysis of complex cancer genomics and clinical profiles using the cBioPortal. *Sci. Signal.* 6, pl1. doi:10.1126/scisignal.2004088

Gopal Krishnan, P. D., Golden, E., Woodward, E. A., Pavlos, N. J., and Blancafort, P. (2020). Rab GTPases: Emerging oncogenes and tumor suppressive regulators for the editing of survival pathways in cancer. *Cancers (Basel)* 12, 259. doi:10.3390/cancers12020259

Hoadley, K. A., Yau, C., Hinoue, T., Wolf, D. M., Lazar, A. J., Drill, E., et al. (2018). Cell-of-Origin patterns dominate the molecular classification of 10, 000 tumors from 33 types of cancer. *Cell* 173, 291–304. doi:10.1016/j.cell.2018.03.022

Inagaki, Y., Yasui, K., Endo, M., Nakajima, T., Zen, K., Tsuji, K., et al. (2008). CREB3L4, INTS3, and SNAPAP are targets for the 1q21 amplicon frequently detected in hepatocellular carcinoma. *Cancer Genet. cytogenet.* 180, 30–36. doi:10.1016/j.cancergencyto.2007.09.013

Jia, W., Liang, S., Cheng, B., and Ling, C. (2021). The role of cancer-associated fibroblasts in hepatocellular carcinoma and the value of traditional Chinese medicine treatment. *Front. Oncol.* 11, 763519. doi:10.3389/fonc.2021.763519

Jiang, X., Yang, L., Gao, Q., Liu, Y., Feng, X., Ye, S., et al. (2022). The role of RAB GTPases and its potential in predicting immunotherapy response and prognosis in colorectal cancer. *Front. Genet.* 13, 828373. doi:10.3389/fgene.2022.828373

Lanczky, A., and Gyorffy, B. (2021). Web-based survival analysis tool tailored for medical research (KMplot): Development and implementation. *J. Med. Internet Res.* 23, e27633. doi:10.2196/27633

Li, G., and Marlin, M. C. (2015). Rab family of GTPases. *Methods Mol. Biol.* 1298, 1–15. doi:10.1007/978-1-4939-2569-8_1

Li, L., Ye, T., Zhang, Q., Li, X., Ma, L., and Yan, J. (2021). The expression and clinical significance of TPM4 in hepatocellular carcinoma. *Int. J. Med. Sci.* 18, 169–175. doi:10.7150/ijms.49906

Li, T., Fan, J., Wang, B., Traugh, N., Chen, Q., Liu, J. S., et al. (2017). Timer: A web server for comprehensive analysis of tumor-infiltrating immune cells. *Cancer Res.* 77, e108–e110. doi:10.1158/0008-5472.CAN-17-0307

Lu, C., Rong, D., Zhang, B., Zheng, W., Wang, X., Chen, Z., et al. (2019). Current perspectives on the immunosuppressive tumor microenvironment in hepatocellular carcinoma: Challenges and opportunities. *Mol. Cancer* 18, 130. doi:10.1186/s12943-019-1047-6

Nishida, N., and Kudo, M. (2018). Immune checkpoint blockade for the treatment of human hepatocellular carcinoma. *Hepatol. Res.* 48, 622–634. doi:10.1111/hepr.13191

Opdam, F. J. M., Echard, A., Croes, H. J. E., Van Den Hurk, J. a. J. M., Van De Vorstenbosch, R. A., Ginsel, L. A., et al. (2000). The small GTPase Rab6B, a novel Rab6 subfamily member, is cell-type specifically expressed and localised to the Golgi apparatus. *J. Cell Sci.* 113, 2725–2735. doi:10.1242/jcs.113.15.2725

Quail, D. F., and Joyce, J. A. (2013). Microenvironmental regulation of tumor progression and metastasis. *Nat. Med.* 19, 1423–1437. doi:10.1038/nm.3394

Ru, B., Wong, C. N., Tong, Y., Zhong, J. Y., Zhong, S. S. W., Wu, W. C., et al. (2019). Tisidb: An integrated repository portal for tumor-immune system interactions. *Bioinformatics* 35, 4200–4202. doi:10.1093/bioinformatics/btz210

Stenmark, H. (2009). Rab GTPases as coordinators of vesicle traffic. *Nat. Rev. Mol. Cell Biol.* 10, 513–525. doi:10.1038/nrm2728

Tang, Z., Kang, B., Li, C., Chen, T., and Zhang, Z. (2019). GEPIA2: An enhanced web server for large-scale expression profiling and interactive analysis. *Nucleic Acids Res.* 47, W556–W560. doi:10.1093/nar/gkz430

Tinoco, R., Alcalde, V., Yang, Y., Sauer, K., and Zuniga, E. I. (2009). Cell-intrinsic transforming growth factor-beta signaling mediates virus-specific CD8+ T cell deletion and viral persistence *in vivo*. *Immunity* 31, 145–157. doi:10.1016/j.immuni.2009.06.015

Vasaikar, S. V., Straub, P., Wang, J., and Zhang, B. (2018). LinkedOmics: Analyzing multi-omics data within and across 32 cancer types. *Nucleic Acids Res.* 46, D956–D963. doi:10.1093/nar/gkx1090

Wanschers, B. F., Van De Vorstenbosch, R., Schlager, M. A., Splinter, D., Akhmanova, A., Hoogenraad, C. C., et al. (2007). A role for the Rab6B Bicaudal-D1 interaction in retrograde transport in neuronal cells. *Exp. Cell Res.* 313, 3408–3420. doi:10.1016/j.yexcr.2007.05.032

Wherry, E. J. (2011). T cell exhaustion. *Nat. Immunol.* 12, 492–499. doi:10.1038/ni.2035

Wong, C. C. L., Tse, A. P. W., Huang, Y. P., Zhu, Y. T., Chiu, D. K. C., Lai, R. K. H., et al. (2014). Lysyl oxidase-like 2 is critical to tumor microenvironment and metastatic niche formation in hepatocellular carcinoma. *Hepatology* 60, 1645–1658. doi:10.1002/hep.27320

Yang, C. C., Meng, G. X., Dong, Z. R., and Li, T. (2021). Role of Rab GTPases in hepatocellular carcinoma. *J. Hepatocell. Carcinoma* 8, 1389–1397. doi:10.2147/JHC.S336251

Yang, F., Wei, Y., Han, D., Li, Y., Shi, S., Jiao, D., et al. (2020). Interaction with CD68 and regulation of GAS6 expression by Endosialin in fibroblasts drives recruitment and polarization of macrophages in hepatocellular carcinoma. *Cancer Res.* 80, 3892–3905. doi:10.1158/0008-5472.CAN-19-2691

Yin, Z., Dong, C., Jiang, K., Xu, Z., Li, R., Guo, K., et al. (2019). Heterogeneity of cancer-associated fibroblasts and roles in the progression, prognosis, and therapy of hepatocellular carcinoma. *J. Hematol. Oncol.* 12, 101. doi:10.1186/s13045-019-0782-x

Zhang, Q., He, Y., Luo, N., Patel, S. J., Han, Y., Gao, R., et al. (2019). Landscape and dynamics of single immune cells in hepatocellular carcinoma. *Cell* 179, 829–845. doi:10.1016/j.cell.2019.10.003

Zhao, L., Xue, M., Zhang, L., Guo, B., Qin, Y., Jiang, Q., et al. (2020). MicroRNA-4268 inhibits cell proliferation via AKT/JNK signalling pathways by targeting Rab6B in human gastric cancer. *Cancer Gene Ther.* 27, 461–472. doi:10.1038/s41417-019-0118-6

frontiers | Frontiers in Oncology

TYPE Review
PUBLISHED 08 September 2022
DOI 10.3389/fonc.2022.1008843

OPEN ACCESS

EDITED BY
Qianming Du,
Nanjing Medical University, China

REVIEWED BY
Tao Li,
China Pharmaceutical University, China
Jinzi Ji,
Nanjing Medical University, China

*CORRESPONDENCE
Runbi Ji
runbiji@163.com

†These authors have contributed equally to this work

SPECIALTY SECTION
This article was submitted to Pharmacology of Anti-Cancer Drugs, a section of the journal Frontiers in Oncology

RECEIVED 01 August 2022
ACCEPTED 18 August 2022
PUBLISHED 08 September 2022

CITATION
Wu C, Gu J, Gu H, Zhang XX, Zhang X and Ji R (2022) The recent advances of cancer associated fibroblasts in cancer progression and therapy. *Front. Oncol.* 12:1008843. doi: 10.3389/fonc.2022.1008843

The recent advances of cancer associated fibroblasts in cancer progression and therapy

Chenxi Wu[1,2†], Jianmei Gu[3†], Hongbing Gu[1], XiaoXin Zhang[2], Xu Zhang[2] and Runbi Ji[1,2*]

[1]Department of Clinical Laboratory Medicine, the Affiliated People's Hospital of Jiangsu University, Zhenjiang, China, [2]Jiangsu Key Laboratory of Medical Science and Laboratory Medicine, School of Medicine, Jiangsu University, Zhenjiang, China, [3]Department of Clinical Laboratory Medicine, Nantong Tumor Hospital, Nantong, China

As an abundant component of tumor microenvironment, cancer-associated fibroblasts (CAFs) are heterogeneous cell populations that play important roles in tumor development, progression and therapeutic resistance. Multiple sources of cells can be recruited and educated to become CAFs, such as fibroblasts, mesenchymal stem cells and adipocytes, which may explain the phenotypic and functional heterogeneity of CAFs. It is widely believed that CAFs regulate tumor progression by remodeling extracellular matrix, promoting angiogenesis, and releasing soluble cytokines, making them a promising cancer therapy target. In this review, we discussed about the origin, subpopulation, and functional heterogeneity of CAFs, with particular attention to recent research advances and clinical therapeutic potential of CAFs in cancer.

KEYWORDS

cancer-associated fibroblasts, tumor microenvironment, heterogeneity, tumor progression, tumor therapy

Introduction

As an important component of tumor microenvironment, CAFs are described as activated fibroblasts located in the vicinity of cancer cells without the phenotype of epithelial, cancerous, endothelial, and immune cells (1). They are elongated and spindle-shaped in morphology and have some positive markers, such as alpha-smooth muscle actin (α-SMA), fibroblast activation protein (FAP) and fibroblast specific protein 1 (FSP-1) (2). CAFs have merged as the hot-spot of cancer study; however, their phenotypic and functional heterogeneity hinders the clinical application (3). Studies have shown that CAFs could secrete a variety of chemokines, cytokines, and growth factors to facilitate tumor growth, chemotherapy resistance and immunosuppression (4). On the contrary, some studied have reported the tumor-suppressive function of CAFs in certain tumor

models (5). This review summarized the heterogeneity of biological origins, phenotypic markers, and biological functions of CAFs, as well as uncovered how their heterogeneity made identification, subtypes classification and clinical therapy challenging. Our review provided a new perspective for CAF research and personalized therapy.

The origin and transition of CAFs

Increasing evidence suggest that CAFs have different cellular origins. Though precise lineage tracing study has shown the origin of fibroblasts in healthy or injured tissues, the origins and specific activation processes of CAFs are still lacking (6, 7). Several cells may be predecessors of CAFs, such as normal fibroblasts (8), mesenchymal stem cells (MSCs) (9), pancreatic stellate cells (PSCs) (10), epithelial cells (11), endothelial cells (12), adipocytes (13), pericytes (14), hematopoietic stem cells (15) and cancer stem cells (CSCs) (16). The changes in the microenvironment where these precursor cells exist in may be a primary inducer of CAF transition (3).

As the major source of CAFs, normal fibroblasts can transform to CAFs by cytokines secreted by stromal or tumor cells. Transforming growth factor-β (TGF-β) can induce the CAF phenotype through SMAD-dependent or independent pathway (17). For example, bladder cancer cells released exosomes contain TGF-β, leading to the activation of SMAD-dependent signaling and the stimulation of normal fibroblasts to CAFs (8). Platelet-derived growth factor-D (PDGF-D) secreted by cholangiocarcinoma cells could stimulate surrounding fibroblasts to produce VEGF-C and VEGF-A, resulting in the expansion of lymphatic vasculature and tumor cell intravasation (18). In addition to cytokines, non-coding RNAs from cancer cells can also induce the conversion of resident fibroblasts to CAFs. Exosomes derived from hepatocellular carcinoma cells were rich in miR-1247-3p, which activated β1-integrin-NF-κB signaling through targeting B4GALT3 in fibroblasts (19). In lung adenocarcinoma, miR-200 deficiency in cancer cells promoted the expression of Jagged1/2 and the activation of Notch in adjacent CAFs, which reprogrammed CAFs from a quiescent state into an active pro-tumorigenic state (20). Additionally, the hypoxia microenvironment also contributes to the activation of resident fibroblasts. Hypoxia was related to the accumulation of ROS, the activation of the HIF-1α signaling pathway in hepatocellular carcinoma cells, and the enhanced expression of FAP in surrounding fibroblasts (21).

MSCs are another important source of CAFs. The transformational potential of MSCs into CAFs was first proved in breast cancer (9). TGF-β secreted by cancer cells recruited MSCs and maintained the differentiation of MSCs into CAFs (22). In colorectal cancer, the high level of stromal cell-derived factor-1 (SDF-1) upregulated the expression of chemokine receptor 4 (CXCR4) and TGF-β in MSCs, leading to the transformation of MSCs (23). In epithelial ovarian cancer, the elevated expression of STAT4 in epithelial cells induced MSCs derived from adipose and bone marrow to obtain CAF-like features, which in turn promoted EMT and peritoneal metastasis of ovarian cancer by secreting CXCL12, IL-6 and VEGF-A (24). In addition to the stimulation of cancer cells, changes in tumor microenvironment like pH can also stimulate the transformation of MSCs. PH induced activation of MSCs to CAFs was decreased by upregulating the expression of proton-sensing G-protein-coupled receptor68 (GPCR68) and activating downstream effector-Yes-associated protein (YAP) in MSCs (25).

The other cellular origins of CAFs have been reported. For example, PSCs could transform to CAFs in pancreatic cancer (10). In pancreatic ductal adenocarcinoma, the IL-1 signaling cascade led to JAK/STAT activation and induced an inflammatory CAF state (26). Epithelial or endothelial cells are found to be the probable origins of CAFs through epithelial-to-mesenchymal transition (EMT) or endothelial-to-mesenchymal transition (EndMT). The human nasal epithelial cells were activated and displayed CAF phenotypes such as FSP or FAP through EMT when they were exposed to matrix metalloproteinase (MMP)-9 (11). TGF-β could induce proliferating endothelial cells into fibroblast-like cells (12). In addition, a recent study reported that tumor cells induced adipocytes to CAFs by activating Wnt/β-catenin signaling in ovarian cancer (13). Cancer cells, especially cancer stem cells, have also been demonstrated to be a source of CAFs through the action of TGF-β (15). Besides these sources of CAFs mentioned above, there also exist some uncommon origins, such as pericytes, hematopoietic stem cells, which needs further exploration (14, 16).

In brief, the activation of CAFs is mainly regulated by different cytokines and signaling pathways of cancer niche (Figure 1). Although the origins of CAFs in solid tumors were not fully elucidated, using lineage tracing technologies to track CAF transition may provide a solution in the future.

Phenotypic identification and subtype classification of CAFs

The altered protein profiles can be used to identify or isolate CAFs. According to the distinct phenotypic markers, CAFs can be divided into several subpopulations and some of them partially overlap. In this part, we will present the phenotypic differences and subtype classification of CAFs, and provide some suggestions for identifying different CAF populations.

There are several typical CAF markers, such as FAP, α-SMA, FSP-1, PDGFR-α, PDGFR-β, and Thy-1 (27). Despite the diversity of biomarkers, the isolation of CAFs from cells remains a challenge due to low specificity. For example, α-

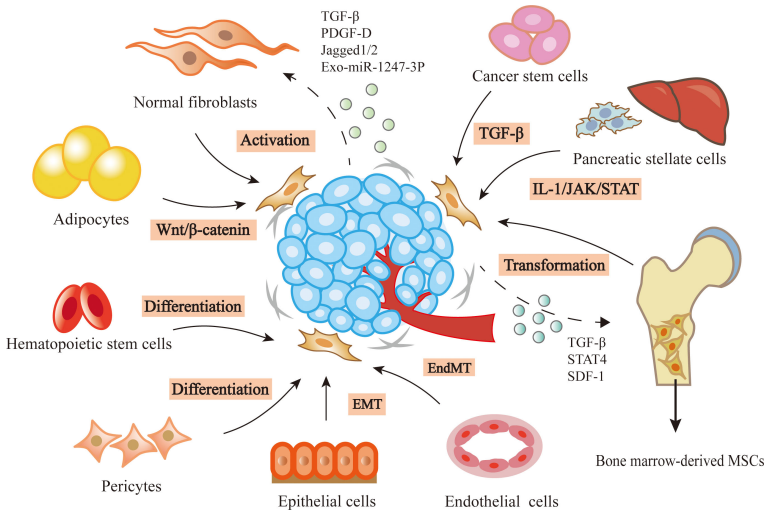

FIGURE 1
Heterogenous origins of CAFs. In the tumor microenvironment, lots of precursor cells can be transformed into CAFs by the stimulation of cancer cells, such as normal fibroblasts, bone marrow-derived MSCs, pancreatic stellate cells, epithelial cells, endothelial cells, adipocytes, caner stem cells, hematopoietic stem cells and pericytes.

SMA and FAP were highly presented in pericytes, lymphatic endothelial cells and fibroblast reticular cells. Similarly, vimentin was present in endothelial cells, smooth cells and tumor cells (28). Additionally, with the continuous optimization of detection technology, the researchers identified uncommon PSC-derived CAF subsets in pancreatic ductal adenocarcinoma tissues. These CAFs located away from cancer cells, lacked elevated α-SMA expression, and secreted IL-6 and other inflammatory mediators (10). The results highlighted the importance of considering multiple indicators in CAF identification. In addition to classical phenotypic markers, some new ones are studied in recent years. In pancreatic cancer, the high expression of caveolin-1 (Cav-1) in CAFs was associated with the invasiveness of cancer cells and poor prognosis of patients (29). The same results were further proved in lung adenocarcinoma (30). Similarly, a recent study reported that the melanoma cell adhesion molecule+ (MCAM+) CAFs induced by TGF-β in colorectal cancer patients were associated with poor prognosis (31). Another study concluded that focal adhesion kinase (FAK) activity in CAFs was increased in PDAC tissues compared with healthy ones and the FAK+ CAFs could be an independent prognostic marker (32).

Based on surface markers, CAFs are classified into different subtypes that display distinctive secretory phenotypes and perform specific biological functions in dynamic tumor environment, as summarized in Table 1 (33). In a mouse model of pancreatic ductal carcinoma, the researchers demonstrated the existence of myofibroblastic CAFs (myCAFs), inflammatory CAFs (iCAFs) and antigen-presenting CAFs (apCAFs) by single-cell RNA sequencing. MyCAFs were characterized by the expression of α-SMA, TAGLN, MYL9, TPM1, TPM2, MMP11, POSTN and HOPX, which could promote the proliferation, invasion and metastasis of tumor cells. ICAFs could promote metastasis and angiogenesis by producing inflammatory cytokines and chemokines such as IL-6, IL-8, CXCL1, CXCL2, CCL2, CXCL12 and Ly6c. ApCAFs had immunomodulatory capacity in pancreatic ductal adenocarcinoma. They expressed MHC II, Saa3, Slp and could activate CD4+ T cells in an antigen-specific manner in the model system (34). Another study reported four CAF subtypes in pancreatic ductal adenocarcinoma based on transcriptomic analysis. These four subgroups, named A-D, could be distinguished by differential expression of three markers, periostin (POSTN), myosin-11 (MYH11) and podoplanin (PDPN). Patients with the dominant subtype-C had prolonged survival, whereas those with the dominant subtype D had the worst prognosis, suggesting that specific tumor-stromal interactions are associated with adverse outcomes (35). Furthermore, a novel subtype of CAFs with a highly activated metabolic state (meCAFs) was identified in PDAC. MeCAFs had highly activated glycolysis, and patients with abundant meCAFs had a higher risk of metastasis and poor prognosis, but showed a dramatically better response to immunotherapy (36).

In human breast cancer, four CAF subgroups, known as S1-S4, have been identified by flow cytometry, immunohistochemistry, and RNA sequencing. They can be distinguished according to the expression of FAP, CD29, αSMA, PDPN and PDGFRβ. CAF-S1 stimulated cancer cell migration and mediated EMT transition through the activation of CXCL12 and TGF-β. CAF-S4 induced

TABLE 1 CAF subtypes and their markers.

CAF subtypes	Phenotypic markers	Functions	Detecting techniques	Cancer types	Refs
• myCAF (myofibroblastic CAF) • iCAF (inflammatory CAF) • apCAF (antigen-presenting CAF)	• α-SMA, TAGLN, MYL9, TPM1, TPM2, MMP11, POSTN, HOPX • IL6, IL8, CXCL1, CXCL2, CCL2, CXCL12, Ly6c • MHC II, Saa3, Slpi	• Promoting proliferation, invasion and metastasis • Promoting metastasis and angiogenesis • Activating CD4+ T cells	Single-cell RNA sequence	Pancreatic ductal carcinoma (mouse)	(34)
• CAF-A • CAF-B • CAF-C • CAF-D	• POSTN • POSTN, MYH11, PDPN • PDPN • Not determined	• Associated with intermediate prognosis • Associated with intermediate prognosis • Associated with better prognosis • Associated with poorer prognosis	Single-cell RNA sequence	Pancreatic ductal carcinoma (human)	(35)
• meCAF (Metabolic state CAF)	• CD74 and HLA-DRA	• Promoting metastasis	Single-cell RNA sequence	Pancreatic ductal carcinoma (human)	(36)
• CAF-S1 • CAF-S2 • CAF-S3 • CAF-S4	• FAP^{High}, $CD29^{Med-High}$, αSMA^{High}, $PDPN^{High}$, $PDGFR\beta^{High}$ • FAP^{Neg}, $CD29^{Low}$, $\alpha SMA^{Neg-Low}$, $PDPN^{Low}$, $PDGFR\beta^{Low}$ • $FAP^{Neg-Low}$, $CD29^{Med}$, $\alpha SMA^{Neg-Low}$, $PDPN^{Low}$, $PDGFR\beta^{Low-Med}$ • $FAP^{Low-Med}$, $CD29^{High}$, αSMA^{High}, $PDPN^{Low}$, $PDGFR\beta^{Med}$	• Mediating EMT • Making up of healthy tissues • Making up of healthy tissues • Inducing cancer invasion	Flow cytometry, immunohistochemistry and RNA-sequencing	Breast cancer (human)	(37)
• CD10+ GPR77+ CAF	• CD10, GPR77	• Promoting tumor formation and chemoresistance	Single-cell RNA sequence	Breast and lung cancer (human)	(38)
• vCAF (vascular CAF) • mCAF (matrix CAF) • cCAF (cycling CAF) • dCAF (developmental CAF)	• Desmin • Fibulin-1, PDGFR-α • Similar with vCAF • Scrg1	• Invading tumor stroma • Regulating tumor immune response • Similar with vCAF • Promoting tumor formation	Single-cell RNA sequence	Breast cancer (human)	(39)
• CAF-C1 • CAF-C2	• BMP4 • α-SMA	• Modulating cancer cells proliferation and stemness • Inhibiting cancer proliferation	Single-cell RNA sequence	Oral carcinoma (human)	(40)
• eCAF (extracellular matrix CAF)	• POSTN	• Promoting cancer invasion	Single-cell RNA sequence	Gastric cancer (human)	(41)
• CAF-A • CAF-B	• MMP2, DCN, COL1A2 • ACTA2, TAGLN, PDGFA	• Remodeling extracellular matrix • Expressing cytoskeletal genes	Reference component analysis(RCA)	Colorectal cancer (human)	(42)
• Subtype I • Subtype II • Subtype III	• HGF, FGF7 • FGF7 • Low HGF and FGF7	• Broad tumor promotion • Modest tumor promotion • Minimal tumor promotion	Single-cell RNA sequence	Non-small lung cancer (human)	(43)
• Activated myofibroblast • Phenotype • Mesenchymal stromal cell phenotype	• α-SMA, vimentin, FAP, collagen 1α, PDGFRα • CD90, CD73, CD105, CD29, CD44, CD166	• Enhancing the stemness of cancer cells • Regulating immunosuppression	Flow cytometry	Hepatocellular carcinoma (human)	(44)
• FAP-high CAF • FAP-low CAF	• FAP, TGF-β, IL-6, COL11A1, SULF1, CXCL12 • DLK1, COLEC11, TCF21	• Regulating cancer invasion and immune regulation • Regulating glucose homeostasis and lipid metabolism	Quantitative RT-PCR	High-grade serous ovarian cancer (human)	(45)

10.3389/fonc.2022.1008843

cancer invasion through NOTCH signaling. The study also found that patients with high levels of CAF-S4 in lymph nodes were prone to late distant metastases, which could be a potential prognostic marker for breast cancer (37). Furthermore, two new cell surface molecules, CD10 and GPR77, can define a CAF subset associated with chemoresistance and low survival in patients with breast cancer and lung cancer. CD10+ GPR77+ CAFs accelerated cancer progression by providing a survival niche for cancer stem cells, and the functional CAF subset could be specifically recognized and isolated, suggesting an effective therapeutic strategy for CSC-driven solid tumors (38). Bartoschek and colleagues defined four spatially and functionally distinct CAF subpopulations through single-cell RNA sequencing in breast cancer. According to different functions, these subgroups were named as vascular CAFs (vCAFs), matrix CAFs (mCAFs), cycling CAFs (cCAFs) and developmental CAFs (dCAFs). VCAFs originated from perivascular location, expressed genes controlling angiogenesis, and invaded tumor stroma during tumor progression. MCAFs were offspring of resident fibroblasts and regulated the tumor immune response. CCAFs were proliferative fragment of vCAFs and had different expression of cell cycle genes. DCAFs underwent EMT and shared expression patterns with tumor epithelium. Thus, the phenotypic and functional heterogeneity of CAFs can be attributed to their different origins (39).

In oral carcinoma, CAFs were grouped into two distinct clusters based on the expression difference of α-SMA. CAF-C1 had low α-SMA-scores and was more supportive for cell proliferation but suppressive for the growth of stem-like cancer cells (SLCCs). BMP4 played a determinant role in C1-type CAF-mediated suppression of SLCCs. However, CAF-C2 had the opposite effects on tumor cells (40). In gastric cancer, the researchers identified a new CAF subset defined as extracellular matrix CAFs (eCAFs). The subset had high expression of POSTN, which could support the adhesion and migration of epithelial cells, as well as be a prognostic marker for gastric cancer (41). In colorectal cancer, two distinct CAF subtypes, named CAF-A and CAF-B, were identified depending on their differential expressions. CAF-A expressed markers related to extracellular matrix remodeling, such as Matrix metalloproteinase-2 (MMP2), decorin (DCN) and collagen 1A2 (COL1A2). CAF-B cells expressed markers of myofibroblasts such as actin alpha 2 (ACTA2), transgelin (TAGLN) and platelet-derived growth factor A (PDGFA) (42). Hu and colleagues identified three subtypes of CAFs in non-small lung cancer. Subtype I highly expressed hepatocyte growth factor (HGF) and fibroblast growth factor 7 (FGF7), and had strong protective effects against cancer. Subtype II expressed FGF7 and had moderate protection against cancer. Subtype III had minimal protection (43). In hepatocellular carcinoma, CAFs isolated from fresh tumor tissues could be divided into activated myofibroblast phenotype and a mesenchymal stromal cell phenotype. They could enhance the stemness of cancer cells and modulate immunosuppression, respectively (44). In high-grade serous ovarian cancer, the CD49e+ CAF population was divided into two subgroups, FAP-high and FAP-low group. The FAP-high subgroup could regulate cancer invasion and immunomodulation, whereas the FAP-low group could regulate glucose homeostasis and lipid metabolism (45).

In summary, CAFs can be divided into several specific subpopulations in different tumor models based on surface markers and protein profiles (Table 1). These studies suggest that CAFs are a cell state rather than end-point of differentiation. Because the subtypes are dynamic, they can be mutually transformed under the influence of cancer status and drug treatment. For example, when CAFs are isolated from cancer tissues and cultured *in vitro*, CAF subpopulations may change their phenotype. Furthermore, the transition could also occur in different tumor types, even in different parts of the same tissue, so more advanced detection techniques and strategies are needed to further identification. Single-cell RNA sequencing is a cutting-edge technology that can investigate the transcriptome and related markers of individual cells, which may help to more accurately classify CAF subtypes in further studies (46). Additionally, new technologies such as mass spectrometry-based time-of-flight flow cytometry (CyTOF) (47), multiple flow cytometry (48) and multiple immunostaining (49) are helpful to identify CAF subtypes. During the detection of CAF subtypes, it is necessary to guarantee the number of patients to ensure the production of several cell subsets. Second, fresh samples are crucial in the current single-cell RNA sequencing strategy. Finally, batch effects may be involved between batch loaded samples (50). In addition to the inclusion of more molecular markers, the different functions, different positions in cancer tissues, and even different tumor stages of CAFs should also be considered to achieve a more detailed classification of CAFs.

Functional heterogeneity of CAFs in cancer biology

CAFs promote tumorigenesis and metastasis

CAFs play a dynamic role in proliferation, invasion and metastasis of tumors, and its mechanism is gradually elucidated. In lung adenocarcinoma, CAFs secreted SDF-1 to promote the expression of CXCR4, β-catenin and peroxisome proliferator activated receptor δ (PPARδ) in tumor cells, and enhance cancer invasiveness and EMT (51). In breast cancer, CAFs secreted IL-32 to induce an interaction between integrin β3 and the RGD motif, activate p38 MAPK in tumor cells, leading to increased expression of EMT markers (52). TGF-β and inflammatory cytokines secreted by breast cancer cells induced CAFs to express gremlin 1 (GREM1), abrogating BMP/SMAD signaling

and promoting stemness and invasion of cancer cells (53). In gastric cancer, downregulation of miR-214 in CAFs resulted in a high expression of Fibroblast Growth Factor 9 (FGF9), promoting EMT and tumor metastasis (54). In human colorectal cancer, CAFs promoted cancer proliferation, EMT and metastasis by secreting pro-inflammatory factors, such as IL-6, IL-8 and exosomal miRNA-92a-3p to activate Wnt/β-catenin pathway as well as inhibit mitochondrial apoptosis (55, 56).

CAFs induce chemoresistance

Tumor matrix is not only the material support but also an important regulator of cancer cells. They create a complex signaling network to promote drug resistance in tumor cells after drug treatment (57). In patients with breast and lung cancer, phosphorylation and acetylation of p65 activated NF-κB to produce CD10+GPR77+ CAFs. They provided a survival niche for cancer stem cells to achieve tumor formation and chemoresistance (37). Similarly, IL-11 secreted by CAFs induced STAT3 phosphorylation and increased the expression of anti-apoptotic proteins Bcl-2 and Survivin in lung adenocarcinoma. These protected cancer cells from cisplatin-induced apoptosis, thereby promoting chemoresistance (58). Exosomes derived from CD63+ CAFs contained miR-22 and mediated tamoxifen resistance in breast cancer by targeting ERα and PTEN (59). In gastric cancer, the USP7/hnRNPA1 axis was activated and miR-522 was expressed in CAFs after cisplatin and paclitaxel treatment, leading to ALOX15 inhibition and reduced lipid-ROS accumulation in cancer cells, ultimately resulting in decreased chemosensitivity (60). CAFs could also secrete IL-8 and activate the NF-κB signaling pathway in gastric cancer to mediate chemoresistance (61). In pancreatic ductal carcinoma, CAFs secreted SDF-1 to upregulate the expression of SATB-1 in cancer cells and mediate gemcitabine resistance (62). Similarly, CAFs promoted pancreatic cell proliferation and drug resistance by releasing exosomes containing the chemoresistance inducing factor, Snail (63).

CAFs mediate immunosuppression

CAFs can promote the immunosuppression of cancer cells by secreting TGF-β, IL-6, CXCL12 and CCL2, thereby preventing cytotoxic T cell activity and recruiting immunosuppressive populations (64). There was a significant increase in regulatory T cells (Tregs) in paracancerous tissues, which secreted TGF-β and IL-10 to inhibit the activation of tumor-site effector T cells. In breast cancer, CAF-S1 enhanced the ability of Tregs to suppress T effector proliferation, and then promoted immunosuppressive (65). A new subset of CAFs that expressed CD68 was found in esophageal squamous cell carcinoma. The recurrence rate of patients with low-CD68 CAFs was higher. Knockdown of CD68 in CAFs upregulated the secretion of CCL17 and CCL22 by tumor cells to enhance Treg recruitment (66). MiR-92-containing exosomes from CAFs induced the expression of programmed cell death receptor ligand 1 (PD-L1) in breast cancer and raised the apoptosis of T cells (67). Similarly, in melanoma and colorectal cancer cells, CAFs led to the high expression of PD-L1 and the activation of PI3K/AKT signaling, resulting in the disappearance of T cells in the anti-tumor immune response (68). Furthermore, CAFs could inhibit an anti-tumor immune response by inhibiting dendritic cells which are necessary for T lymphocytes activation. In a recent study, CAFs secreted WNT2 in esophageal squamous cell carcinoma and colorectal cancer. WNT2 suppressed the dendritic cells to act on the anti-tumor T cell response *via* SOCS3/p-JAK2/p-STAT3 signaling (69). Additionally, CAFs could also reduce immune efficiency by recruiting granulocytes and monocytes, and suppressing dendritic cell functions (70, 71). For example, increased expression of IL-33 in metastases-associated fibroblasts stimulated type 2 immunity and mediated the recruitment of eosinophils, neutrophils and inflammatory monocytes, influencing the function of these immune cells in tumor tissues (72).

CAFs exert tumor suppression effect

Although the studies mentioned above have revealed the cancer-promoting function of CAFs, some studies have also reported the tumor suppression effects of CAFs. In a mouse model of pancreatic ductal carcinoma, ablation of CAFs was first proven to be associated with worse tumor progression, further supporting the concept of CAFs heterogeneity in the tumor microenvironment (73). In mice with pancreatic cancer, the absence of α-SMA+ myofibroblasts led to hypoxia enhanced and EMT turnover. In patients with pancreatic ductal carcinoma, fewer myofibroblasts were related to increased drug resistance and reduced survival. Another study reported that deletion of sonic hedgehog (SHH) decreased the formation of fibroblast-rich desmoplastic stroma, increased vascularity and enhanced tumor proliferation (74). In estrogen receptor-positive (ER+) breast cancer, CD146+ CAFs could maintain ER expression, estrogen-dependent proliferation and tamoxifen sensitivity (75). Furthermore, a recent study reported the presence of two populations of CAFs with different functions, namely, cancer-promoting and cancer-restraining. Meflin, a marker of mesenchymal stromal cells to maintain their undifferentiated state, was expressed on pancreatic stellate cells in pancreatic ductal carcinoma. The results of situhybridization analysis of 71 human pancreatic ductal carcinoma tissues showed that the infiltration of Meflin-positive CAFs was related to good prognosis. In a mouse model of pancreatic ductal carcinoma,

Meflin deficiency led to significant tumor progression in poorly differentiated histology (76). The functional heterogeneity of CAFs in certain cancer types was highlighted in Figure 2.

Treatment strategies for CAFs

CAFs play a vital role in cancer occurrence and development by regulating the proliferation, invasion and chemoresistance of tumor cells. The abundance in tumor microenvironment and the diverse tumor-supportive roles of CAFs make them an ideal therapeutic target (77). The recent advances in cancer therapy by targeting CAFs were summarized in Table 2 and Figure 3.

CAF-targeted ablation

Targeting CAFs by inhibiting surface markers such as FAP and α-SMA has been extensively explored in pre-clinical studies. Sibrotuzumab, an antibody against FAP, has been tested in phase I clinical trials of colorectal cancer and non-small cell lung carcinoma. In patients with advanced FAP-positive cancer, repeat infusions of sibrotuzumab were safe, but the efficiency in Phase II trials was limited (78). The first clinical inhibitor against FAP activity, Val-boroPro, was used in phase II trials in patients with metastatic colorectal cancer. However, the results were not satisfactory and Val-boroPro had minimal clinical activity (79). In a mouse model, SynCon, a novel FAP DNA vaccine, was able to break tolerance and induce CD8+ and CD4+ immune responses (80). Similarly, the FAP-targeting immunotoxin αFAP-PE38 was used to deplete FAP+ CAFs in a metastatic breast cancer model, thereby decreasing the recruitment of tumor-infiltrating immune cells in the tumor microenvironment and suppressing tumor growth (81). Similar to the depletion of FAP+ CAFs, reduction of α-SMA+ content of stroma through Cellax therapy was confirmed to have effects in inhibiting tumor progression (82). Furthermore, CD10+GPR77 + CAFs were a novel subset that was identified in breast cancer. A neutralizing anti-GPR77 antibody could restore the chemosensitivity of cancer cells (37). Although CAF ablation is effective in some tumor models, the reduction of FAP+ stromal cells are proved to have a relationship with the loss of muscle mass and anemia (83). In addition, CAFs lack specific markers and alter phenotypes at different stage, making targeted therapy

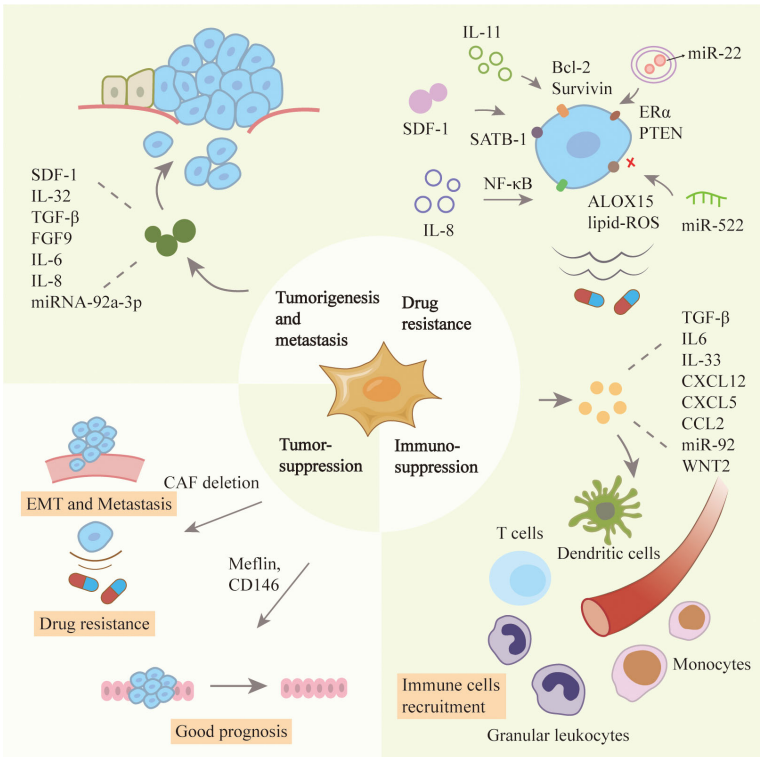

FIGURE 2
Roles of CAFs in tumor progression. CAFs have heterogenous functions in the tumor microenvironment including tumor promotion and suppression ones. CAFs can stimulate the proliferation, metastasis and drug resistance of cancer cells, and inhibit the effect of immune cells. CAFs have also been reported to inhibit tumors because their absence can affect the prognosis of patients.

TABLE 2 Treatment strategies based on CAFs.

Drugs	Mechanism	Cancer models	Biological effects	State	Refs
CAF-targeted ablation					
Sibrotuzumab	Deplete FAP+ CAFs	Colorectal cancer and non-small cell lung cancer	Inhibit tumor growth	Phase l	(78)
Val-boroPro	Deplete FAP+ CAFs	Colorectal cancer	Inhibit tumor growth	Phase II	(79)
SynCon FAP DNA vaccine	Deplete FAP+ CAFs	Lung, prostate, breast cancer	Enhance immune response	Preclinical	(80)
αFAP-PE38	Deplete FAP+ CAFs	Breast cancer	Inhibit tumor growth	Preclinical	(81)
Cellax	Deplete αSMA+ CAFs	Breast cancer	Deplete tumor stroma	Preclinical	(82)
Neutralizing anti-GPR77 antibody	Deplete CD10+ GPR77+ CAFs	Breast and lung cancer	Inhibit tumor growth	Preclinical	(37)
Restoring CAFs to a quiescent state					
Dasatinib	Inhibit PDGFR	Lung cancer	Reduce tumor cells proliferation	Preclinical	(84)
Artemisinin	Suppress TGF-β signaling	Breast cancer	Inhibit cancer cells growth and metastasis	Preclinical	(85)
Ruxolitinib and 5-azacytidine	Restore the fibroblast phenotype of CAFs	Lung and head and neck carcinomas	Reverse invasiveness of CAFs	Preclinical	(86)
GKT137831 [Setanaxib]	Inhibit NOX4	A broad range of cancers	Reverse immune resistance	Preclinical	(87)
Minnelide	Decrease viability of CAFs	Pancreatic cancer	Inhibit tumor growth	Phase l	(88)
Losartan and FOLFIRINOX	Suppress TGF-β signaling	Pancreatic cancer	Reverse tumor immunosuppression	Phase II	(89)
Blocking the interaction between CAFs and cancer cells					
LY2109761	Inhibit CTGF and TGF-β signal	Hepatocellular carcinoma	Inhibit tumor growth, intravasation and metastasis	Preclinical	(90)
7E3	Inhibit NRG1 and AKT/MAPK signals	Pancreatic cancer	Inhibit tumor growth and metastasis	Preclinical	(91)
AG490	Inhibit IL-17a and JAK2/STAT3 signaling pathway	Gastric cancer	Inhibit cancer cells growth	Preclinical	(92)
GDC-0449	Inhibit SHH signaling	Pancreatic cancer	Reverse doxorubicin resistance	Preclinical	(93)
RvD1	Inhibit CAFs-derived COMP	Hepatocellular carcinoma	Repress EMT and cancer stemness	Preclinical	(94)
AMD3100 and TN14003	Inhibit CXCR4	HER2 breast cancer	Inhibit cancer cells growth and metastasis	Preclinical	(95)
CAFs-derived WNT2 interference	Restore DC differentiation	Oesophageal squamous cell and colorectal cancer	Enhance immune response	Preclinical	(69)
Ruxolitinib	Suppress JACK/STAT pathway	Pancreatic cancer	Inhibit tumor growth	Phase II	(96)
Nab-paclitaxel and atezolizumab	Disrupt the stroma	Breast cancer	Block pathological collagen accumulation	Phase III	(97)

difficult. In conclusion, ablation of CAFs in cancer therapy needs cautious consideration, as non-selective removal may have the opposite effect, and the combined application of markers may contribute to more accurate subtype localization.

Restoring CAFs to a quiescent state

Sustained stimulation of tumor cells will activate some signaling pathways in progenitors, and promote their acquisition of CAF phenotypes and tumor-promoting functions. Strategies to inhibit the expression of some genes in activated CAFs may restore them to a quiescent state, which fails to promote tumor growth and even has tumor-suppressive effects (98). TGF-β and PDGF play crucial roles in the activation of CAFs. Dasatinib, the inhibitor of PDGFR, could reverse the phenotype of CAFs into normal fibroblasts. The proliferation of lung cancer cells was reduced if they were incubated with conditioned medium from CAFs pre-incubated with Dasatinib (84). Similarly, artesunate and dihydroartemisinin from Artemisinin (ART) were shown to suppress TGF-β signaling in CAFs and inhibit tumor growth and metastasis (85). The combination of JAK inhibitor (ruxolitinib) and DNMT inhibitor (5-azacytidine) could restore the fibroblast phenotype and reverse the pro-invasive activity of CAFs in lung cancer and head and neck carcinomas (86). The ROS-producing enzyme NOX4 was upregulated by CAFs in many human cancers, and gene inhibitors convert fibroblasts to CAFs, preventing CAF accumulation and slowing tumor growth (98). Pharmacologic inhibition of NOX4 by GKT137831 [Setanaxib] reversed CAFs to a quiescent state, overcame cancer immune resistance, and improved the

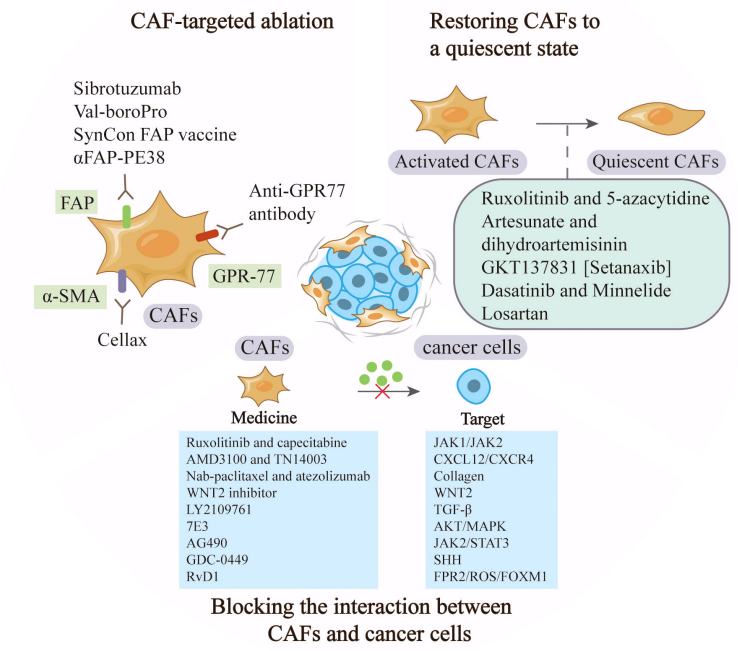

FIGURE 3
Anti-cancer strategies based on CAFs. CAF-based therapy can be achieved by targeting the markers to ablate CAFs, restoring activated CAFs to quiescent ones, and blocking the signaling between CAFs and tumor cells such as JAK1/JAK2 and CXCL12/CXCR.

prognosis of multiple cancers in a CAF-rich mouse tumor model (87). Minnelide is a water-soluble triptolide prodrug in phase I clinical trials. It is effective in multiple animal models of pancreatic cancer. Minnelide was observed to decrease the viability of CAFs and reduce ECM components such as hyaluronan and collagen, resulting in the suppression of cancer cells (88). Additionally, the use of angiotensin receptor blockers (ARBs) like losartan, converted myofibroblast CAFs to a quiescent state by decreasing the activation of TGF-β, and then alleviated immunosuppression and improved T lymphocyte activity (99). In a phase II clinical trial, the researchers combined losartan with FOLFIRINOX to assess the efficiency of locally advanced pancreatic cancer, and the results showed that the treatment prolonged the prognosis of patients (89).

Blocking the interaction between CAFs and cancer cells

Compared with depletion of CAFs or reversion of their state, other treatments, such as blocking the interaction between CAFs and cancer cells may be more practical. TGF-β signaling pathway has been proven to be vital in CAF activation and tumor promotion. LY2109761, the TGF-β receptor inhibitor, could suppress tumor growth and metastasis by inhibiting the release of connective tissue growth factor (CTGF) and interrupting the cross-talk between cancer cells and CAFs (90). In preclinical models of pancreatic tumor, neuregulin 1 (NRG1), the ligand of HER3 and HER4 receptors, was secreted by both cancer cells and CAFs. 7E3, as an antibody to NRG1, was demonstrated to prevent tumor growth and metastasis by inhibiting NRG1-mediated HER3 and AKT/MAPK signaling pathways, providing a novel therapeutic option for pancreatic cancer (91). In gastric cancer, IL-17a secreted by CAFs promoted the migration and invasion of cancer cells by activating JAK2/STAT3 signaling pathway. As a neutralizing antibody against IL-17a or JAK2 inhibitors, AG490, could significantly inhibit the effect of CAFs on cancer progression and improve prognosis (92). Furthermore, CAFs in pancreatic cancer were found to interact with tumor cells and hyperactive SHH signaling. A commercial SHH inhibitor, GDC-0449 was reported to reverse fibroblast-induced resistance to doxorubicin in smoothened-positive pancreatic cancer cells. Importantly, the synergistic combination of GDC-0449 with PEG-PCL-

Dox exhibited robust antitumor efficiency in a BxPC-3 tumor xenograft model, suggesting a potential strategy for the treatment of fibroblast-enriched pancreatic cancer (93). In hepatocellular carcinoma, the utilize of Resolvin D1 (RvD1) inhibited the paracrine of CAFs-derived cartilage oligomeric matrix protein (COMP) by targeting FPR2/ROS/FOXM1 signaling pathway, and repressed EMT and cancer stemness feature, which might be a potential agent contributing to treatment outcomes (94). The expression of CXCL12 in fibroblasts was considered to be associated with the presence of axillary metastases in HER2 breast cancer, and the suppression of its receptor provided some therapeutic potential. Researchers inhibited CXCR4, the receptor of CXCL12, through the administration of AMD3100 and TN14003, and found the effective suppression of tumor growth and metastasis (95). Similarly, in primary esophageal squamous cell carcinoma and colorectal cancer, WNT2+ CAFs were negatively correlated with active CD8+ T cells. Direct interference with CAF-derived WNT2 could restore DC differentiation and DC-mediated antitumor T-cell response (69). In a phase II clinical trial of pancreatic cancer, ruxolitinib combined with capecitabine was used in patients with metastatic pancreatic cancer who had failed to respond to gemcitabine. The results showed that patients treated with ruxolitinib had longer overall survival and better prognosis, supporting the potential clinical benefit of JAK1/JAK2 inhibitor ruxolitinib (96). Additionally, the stromal-disrupting effect of Nab-paclitaxel was reported in pancreatic cancer therapy (100). In a phase III clinical trial, nab-paclitaxel combined with atezolizumab was tested in patients with unrespectable, locally advanced or metastatic triple-negative breast cancer and showed longer overall survival (97).

Conclusions

Since the concept of CAFs was proposed in the early 1990s, CAFs have attracted extensive attention in cancer biology. Previous studies have led to a better understanding of the heterogeneity of CAF origins, phenotypes and functions. CAFs are the main cell types in tumor microenvironment which affect the occurrence, and development of cancer cells. They have rich cellular sources and precursor cells such as normal fibroblasts and mesenchymal stem cells have been shown to be the major sources. CAFs are not a cell type but heterogeneous functional subpopulations. Based on the surface markers, CAFs are divided into several subtypes, which have different biological functions. CAF subtypes identified in different cancer types may play opposite roles in cancer progression, such as tumor-promoting and tumor-suppressive functions. CAFs have great potential in clinical applications. Several preclinical studies and ongoing clinical trials have shown that strategies targeting CAFs are possible in cancer therapy. However, there are still some challenges in translating CAF research into clinical benefit. First, the concrete origins of CAFs in specific cancer types remains elusive. In addition, most studies on the origin of CAFs have been performed *in vitro* and lack appropriate clinical validation. The use of lineage tracing methods will greatly solve these problems in future studies. Second, the lack of uniform nomenclature for CAF subpopulations in different cancer types makes it difficult to compare CAF subgroups in distinct tumors. It would be useful to name them by combining analysis of cell lineage, surface markers, functions and clinical relevance. Additionally, there is still a lack of curate classification of CAF subtypes. Advanced strategies, such as single-cell RNA sequencing, mass spectrometry-based time-of-flight flow cytometry (CyTOF), multiple flow cytometry and multiple immunostaining, may be helpful to accurately classify CAF subtypes. Finally, although many experiments targeting CAFs to improve cancer therapy have been conducted in preclinical models and clinical trials, most of them have failed to pass phase II clinical trials. It has not yet reached practical application. To overcome this limitation, more detailed experimental designs and more clinical samples are needed, and the combination of these CAF-targeting approaches with existing therapies may be beneficial. Overall, it is critical to accurately understand the underlying mechanisms of action between CAFs and tumor cells. It is also important to understand CAF-targeting therapies at the molecular, cellular, and systemic levels based on the interactions between CAFs and tumor cells, to find the most appropriate strategies and avoid adverse effects. In addition, tracing the origins of CAFs may be a key factor in achieving the clinical application of CAF-targeting strategies and avoiding side effects. With the resolution of these problems, CAF-derived therapies are expected to provide new support for clinical cancer therapy in the near future.

Author contributions

CW wrote the manuscript and designed the figures. JG, HG, and XXZ assisted in the manuscript writing and figures drawing. XZ and RJ revised the manuscript. All authors contributed to the article and approved the submitted version.

Funding

The present study was supported by Distinguished Young Scholar Project of Jiangsu Natural Science Foundation (BK20200043), the National Natural Science Foundation of China (Grant no. 81702429, 81672416, 81972310), Natural Science Foundation of the Jiangsu Province (Grant No. BK20170561), Zhenjiang Science & Technology Program (Grant No. SH2019051).

Acknowledgments

The authors would like to thank literature support from Jiangsu University library and the support from fundings.

Conflict of interest

The authors declare that the research was conducted in the absence of any commercial or financial relationships that could be construed as a potential conflict of interest.

Publisher's note

All claims expressed in this article are solely those of the authors and do not necessarily represent those of their affiliated organizations, or those of the publisher, the editors and the reviewers. Any product that may be evaluated in this article, or claim that may be made by its manufacturer, is not guaranteed or endorsed by the publisher.

References

1. Chen Y, McAndrews KM, Kalluri R. Clinical and therapeutic relevance of cancer-associated fibroblasts. *Nat Rev Clin Oncol* (2021) 18:792–804. doi: 10.1038/s41571-021-00546-5

2. Sahai E, Astsaturov I, Cukierman E, DeNardo DG, Egeblad M, Evans RM, et al. A framework for advancing our understanding of cancer-associated fibroblasts. *Nat Rev Cancer* (2020) 20:174–86. doi: 10.1038/s41568-019-0238-1

3. Liao Z, Tan ZW, Zhu P, Tan NS. Cancer-associated fibroblasts in tumor microenvironment - accomplices in tumor malignancy. *Cell Immunol* (2019) 343:103729. doi: 10.1016/j.cellimm.2017.12.003

4. von Ahrens D, Bhagat TD, Nagrath D, Maitra A, Verma A. The role of stromal cancer-associated fibroblasts in pancreatic cancer. *J Hematol Oncol* (2017) 10:76. doi: 10.1186/s13045-017-0448-5

5. Miyai Y, Esaki N, Takahashi M, Enomoto A. Cancer-associated fibroblasts that restrain cancer progression: Hypotheses and perspectives. *Cancer Sci* (2020) 111:1047–57. doi: 10.1111/cas.14346

6. Driskell RR, Lichtenberger BM, Hoste E, Kretzschmar K, Simons BD, Charalambous M, et al. Distinct fibroblast lineages determine dermal architecture in skin development and repair. *Nature* (2013) 504:277–81. doi: 10.1038/nature12783

7. Dulauroy S, Di Carlo SE, Langa F, Eberl G, Peduto L. Lineage tracing and genetic ablation of ADAM12(+) perivascular cells identify a major source of profibrotic cells during acute tissue injury. *Nat Med* (2012) 18:1262–70. doi: 10.1038/nm.2848

8. Ringuette Goulet C, Bernard G, Tremblay S, Chabaud S, Bolduc S, Pouliot F. Exosomes induce fibroblast differentiation into cancer-associated fibroblasts through TGFβ signaling. *Mol Cancer Res* (2018) 16:1196–204. doi: 10.1158/1541-7786.Mcr-17-0784

9. Karnoub AE, Dash AB, Vo AP, Sullivan A, Brooks MW, Bell GW, et al. Mesenchymal stem cells within tumour stroma promote breast cancer metastasis. *Nature* (2007) 449:557–63. doi: 10.1038/nature06188

10. Öhlund D, Handly-Santana A, Biffi G, Elyada E, Almeida AS, Ponz-Sarvise M, et al. Distinct populations of inflammatory fibroblasts and myofibroblasts in pancreatic cancer. *J Exp Med* (2017) 214:579–96. doi: 10.1084/jem.20162024

11. Suzuki M, Ramezanpour M, Cooksley C, Li J, Nakamaru Y, Homma A, et al. Sirtuin-1 controls poly (I:C)-dependent matrix metalloproteinase 9 activation in primary human nasal epithelial cells. *Am J Respir Cell Mol Biol* (2018) 59:500–10. doi: 10.1165/rcmb.2017-0415OC

12. Zeisberg EM, Potenta S, Xie L, Zeisberg M, Kalluri R. Discovery of endothelial to mesenchymal transition as a source for carcinoma-associated fibroblasts. *Cancer Res* (2007) 67:10123–8. doi: 10.1158/0008-5472.Can-07-3127

13. Iyoshi S, Yoshihara M, Nakamura K, Sugiyama M, Koya Y, Kitami K, et al. Pro-tumoral behavior of omental adipocyte-derived fibroblasts in tumor microenvironment at the metastatic site of ovarian cancer. *Int J Cancer* (2021) 149:1961–72. doi: 10.1002/ijc.33770

14. Ning X, Zhang H, Wang C, Song X. Exosomes released by gastric cancer cells induce transition of pericytes into cancer-associated fibroblasts. *Med Sci Monitor* (2018) 24:2350–9. doi: 10.12659/msm.906641

15. Nair N, Calle AS, Zahra MH, Prieto-Vila M, Oo AKK, Hurley L, et al. A cancer stem cell model as the point of origin of cancer-associated fibroblasts in tumor microenvironment. *Sci Rep* (2017) 7:6838. doi: 10.1038/s41598-017-07144-5

16. McDonald LT, Russell DL, Kelly RR, Xiong Y, Motamarry A, Patel RK, et al. Hematopoietic stem cell-derived cancer-associated fibroblasts are novel contributors to the pro-tumorigenic microenvironment. *Neoplasia (New York NY)* (2015) 17:434–48. doi: 10.1016/j.neo.2015.04.004

17. Bhowmick NA, Chytil A, Plieth D, Gorska AE, Dumont N, Shappell S, et al. TGF-beta signaling in fibroblasts modulates the oncogenic potential of adjacent epithelia. *Science* (2004) 303:848–51. doi: 10.1126/science.1090922

18. Cadamuro M, Brivio S, Mertens J, Vismara M, Moncsek A, Milani C, et al. Platelet-derived growth factor-d enables liver myofibroblasts to promote tumor lymphangiogenesis in cholangiocarcinoma. *J Hepatol* (2019) 70:700–9. doi: 10.1016/j.jhep.2018.12.004

19. Fang T, Lv H, Lv G, Li T, Wang C, Han Q, et al. Tumor-derived exosomal miR-1247-3p induces cancer-associated fibroblast activation to foster lung metastasis of liver cancer. *Nat Commun* (2018) 9:191. doi: 10.1038/s41467-017-02583-0

20. Xue B, Chuang CH, Prosser HM, Fuziwara CS, Chan C, Sahasrabudhe N, et al. miR-200 deficiency promotes lung cancer metastasis by activating notch signaling in cancer-associated fibroblasts. *Genes Dev* (2021) 35:1109–22. doi: 10.1101/gad.347344.120

21. Zou B, Liu X, Zhang B, Gong Y, Cai C, Li P, et al. The expression of FAP in hepatocellular carcinoma cells is induced by hypoxia and correlates with poor clinical outcomes. *J Cancer* (2018) 9:3278–86. doi: 10.7150/jca.25775

22. Barcellos-de-Souza P, Comito G, Pons-Segura C, Taddei ML, Gori V, Becherucci V, et al. Mesenchymal stem cells are recruited and activated into carcinoma-associated fibroblasts by prostate cancer microenvironment-derived TGF-β1. *Stem Cells (Dayton Ohio)* (2016) 34:2536–47. doi: 10.1002/stem.2412

23. Tan HX, Xiao ZG, Huang T, Fang ZX, Liu Y, Huang ZC. CXCR4/TGF-β1 mediated self-differentiation of human mesenchymal stem cells to carcinoma-associated fibroblasts and promoted colorectal carcinoma development. *Cancer Biol Ther* (2020) 21:248–57. doi: 10.1080/15384047.2019.1685156

24. Zhao L, Ji G, Le X, Luo Z, Wang C, Feng M, et al. An integrated analysis identifies STAT4 as a key regulator of ovarian cancer metastasis. *Oncogene* (2017) 36:3384–96. doi: 10.1038/onc.2016.487

25. Zhu H, Guo S, Zhang Y, Yin J, Yin W, Tao S, et al. Proton-sensing GPCR-YAP signalling promotes cancer-associated fibroblast activation of mesenchymal stem cells. *Int J Biol Sci* (2016) 12:389–96. doi: 10.7150/ijbs.13688

26. Biffi G, Oni TE, Spielman B, Hao Y, Elyada E, Park Y, et al. IL1-induced JAK/STAT signaling is antagonized by TGFβ to shape CAF heterogeneity in pancreatic ductal adenocarcinoma. *Cancer Discov* (2019) 9:282–301. doi: 10.1158/2159-8290.Cd-18-0710

27. Kanzaki R, Pietras K. Heterogeneity of cancer-associated fibroblasts: Opportunities for precision medicine. *Cancer Sci* (2020) 111:2708–17. doi: 10.1111/cas.14537

28. Nomura S. Identification, friend or foe: Vimentin and α-smooth muscle actin in cancer-associated fibroblasts. *Ann Surg Oncol* (2019) 26:4191–2. doi: 10.1245/s10434-019-07894-8

29. Yamao T, Yamashita YI, Yamamura K, Nakao Y, Tsukamoto M, Nakagawa S, et al. Cellular senescence, represented by expression of caveolin-1, in cancer-associated fibroblasts promotes tumor invasion in pancreatic cancer. *Ann Surg Oncol* (2019) 26:1552–9. doi: 10.1245/s10434-019-07266-2

30. Shimizu K, Kirita K, Aokage K, Kojima M, Hishida T, Kuwata T, et al. Clinicopathological significance of caveolin-1 expression by cancer-associated fibroblasts in lung adenocarcinoma. *J Cancer Res Clin Oncol* (2017) 143:321–8. doi: 10.1007/s00432-016-2285-2

31. Kobayashi H, Gieniec KA, Lannagan TRM, Wang T, Asai N, Mizutani Y, et al. The origin and contribution of cancer-associated fibroblasts in colorectal carcinogenesis. *Gastroenterology* (2022) 162:890–906. doi: 10.1053/j.gastro.2021.11.037

32. Zaghdoudi S, Decaup E, Belhabib I, Samain R, Cassant-Sourdy S, Rochotte J, et al. FAK activity in cancer-associated fibroblasts is a prognostic marker and a druggable key metastatic player in pancreatic cancer. *EMBO Mol Med* (2020) 12: e12010. doi: 10.15252/emmm.202012010

33. Elyada E, Bolisetty M, Laise P, Flynn WF, Courtois ET, Burkhart RA, et al. Cross-species single-cell analysis of pancreatic ductal adenocarcinoma reveals antigen-presenting cancer-associated fibroblasts. *Cancer Discov* (2019) 9:1102–23. doi: 10.1158/2159-8290.Cd-19-0094

34. Neuzillet C, Tijeras-Raballand A, Ragulan C, Cros J, Patil Y, Martinet M, et al. Inter- and intra-tumoural heterogeneity in cancer-associated fibroblasts of human pancreatic ductal adenocarcinoma. *J Pathol* (2019) 248:51–65. doi: 10.1002/path.5224

35. Wang Y, Liang Y, Xu H, Zhang X, Mao T, Cui J, et al. Single-cell analysis of pancreatic ductal adenocarcinoma identifies a novel fibroblast subtype associated with poor prognosis but better immunotherapy response. *Cell Discov* (2021) 7:36. doi: 10.1038/s41421-021-00271-4

36. Pelon F, Bourachot B, Kieffer Y, Magagna I, Mermet-Meillon F, Bonnet I, et al. Cancer-associated fibroblast heterogeneity in axillary lymph nodes drives metastases in breast cancer through complementary mechanisms. *Nat Commun* (2020) 11:404. doi: 10.1038/s41467-019-14134-w

37. Su S, Chen J, Yao H, Liu J, Yu S, Lao L, et al. CD10(+)GPR77(+) cancer-associated fibroblasts promote cancer formation and chemoresistance by sustaining cancer stemness. *Cell* (2018) 172:841–56.e16. doi: 10.1016/j.cell.2018.01.009

38. Bartoschek M, Oskolkov N, Bocci M, Lövrot J, Larsson C, Sommarin M, et al. Spatially and functionally distinct subclasses of breast cancer-associated fibroblasts revealed by single cell RNA sequencing. *Nat Commun* (2018) 9:5150. doi: 10.1038/s41467-018-07582-3

39. Patel AK, Vipparthi K, Thatikonda V, Arun I, Bhattacharjee S, Sharan R, et al. A subtype of cancer-associated fibroblasts with lower expression of alpha-smooth muscle actin suppresses stemness through BMP4 in oral carcinoma. *Oncogenesis* (2018) 7:78. doi: 10.1038/s41389-018-0087-x

40. Li X, Sun Z, Peng G, Xiao Y, Guo J, Wu B, et al. Single-cell RNA sequencing reveals a pro-invasive cancer-associated fibroblast subgroup associated with poor clinical outcomes in patients with gastric cancer. *Theranostics* (2022) 12:620–38. doi: 10.7150/thno.60540

41. Li H, Courtois ET, Sengupta D, Tan Y, Chen KH, Goh JJL, et al. Reference component analysis of single-cell transcriptomes elucidates cellular heterogeneity in human colorectal tumors. *Nat Genet* (2017) 49:708–18. doi: 10.1038/ng.3818

42. Hu H, Piotrowska Z, Hare PJ, Chen H, Mulvey HE, Mayfield A, et al. Three subtypes of lung cancer fibroblasts define distinct therapeutic paradigms. *Cancer Cell* (2021) 39:1531–47.e10. doi: 10.1016/j.ccell.2021.09.003

43. Yin Z, Dong C, Jiang K, Xu Z, Li R, Guo K, et al. Heterogeneity of cancer-associated fibroblasts and roles in the progression, prognosis, and therapy of hepatocellular carcinoma. *J Hematol Oncol* (2019) 12:101. doi: 10.1186/s13045-019-0782-x

44. Hussain A, Voisin V, Poon S, Karamboulas C, Bui NHB, Meens J, et al. Distinct fibroblast functional states drive clinical outcomes in ovarian cancer and are regulated by TCF21. *J Exp Med* (2020) 217:e20191094. doi: 10.1084/jem.20191094

45. Chen X, Song E. Turning foes to friends: targeting cancer-associated fibroblasts. *Nat Rev Drug Discov* (2019) 18:99–115. doi: 10.1038/s41573-018-0004-1

46. Papalexi E, Satija R. Single-cell RNA sequencing to explore immune cell heterogeneity. *Nat Rev Immunol* (2018) 18:35–45. doi: 10.1038/nri.2017.76

47. Zhang Q, Lou Y, Yang J, Wang J, Feng J, Zhao Y, et al. Integrated multiomic analysis reveals comprehensive tumour heterogeneity and novel immunophenotypic classification in hepatocellular carcinomas. *Gut* (2019) 68:2019–31. doi: 10.1136/gutjnl-2019-318912

48. Ker HG, Coura-Vital W, Valadares DG, Aguiar-Soares RDO, de Brito RCF, Veras PST, et al. Multiplex flow cytometry serology to diagnosis of canine visceral leishmaniasis. *Appl Microbiol Biotechnol* (2019) 103:8179–90. doi: 10.1007/s00253-019-10068-x

49. Dong LQ, Peng LH, Ma LJ, Liu DB, Zhang S, Luo SZ, et al. Heterogeneous immunogenomic features and distinct escape mechanisms in multifocal hepatocellular carcinoma. *J Hepatol* (2020) 72:896–908. doi: 10.1016/j.jhep.2019.12.014

50. Chen Z, Zhou L, Liu L, Hou Y, Xiong M, Yang Y, et al. Single-cell RNA sequencing highlights the role of inflammatory cancer-associated fibroblasts in bladder urothelial carcinoma. *Nat Commun* (2020) 11:5077. doi: 10.1038/s41467-020-18916-5

51. Wang Y, Lan W, Xu M, Song J, Mao J, Li C, et al. Cancer-associated fibroblast-derived SDF-1 induces epithelial-mesenchymal transition of lung adenocarcinoma *via* CXCR4/β-catenin/PPARδ signalling. *Cell Death Dis* (2021) 12:214. doi: 10.1038/s41419-021-03509-x

52. Wen S, Hou Y, Fu L, Xi L, Yang D, Zhao M, et al. Cancer-associated fibroblast (CAF)-derived IL32 promotes breast cancer cell invasion and metastasis *via* integrin β3-p38 MAPK signalling. *Cancer Lett* (2019) 442:320–32. doi: 10.1016/j.canlet.2018.10.015

53. Ren J, Smid M, Iaria J, Salvatori DCF, van Dam H, Zhu HJ, et al. Cancer-associated fibroblast-derived gremlin 1 promotes breast cancer progression. *Breast Cancer Res* (2019) 21:109. doi: 10.1186/s13058-019-1194-0

54. Wang R, Sun Y, Yu W, Yan Y, Qiao M, Jiang R, et al. Downregulation of miRNA-214 in cancer-associated fibroblasts contributes to migration and invasion of gastric cancer cells through targeting FGF9 and inducing EMT. *J Exp Clin Cancer Res* (2019) 38:20. doi: 10.1186/s13046-018-0995-9

55. Ji Q, Zhou L, Sui H, Yang L, Wu X, Song Q, et al. Primary tumors release ITGBL1-rich extracellular vesicles to promote distal metastatic tumor growth through fibroblast-niche formation. *Nat Commun* (2020) 11:1211. doi: 10.1038/s41467-020-14869-x

56. Hu JL, Wang W, Lan XL, Zeng ZC, Liang YS, Yan YR, et al. CAFs secreted exosomes promote metastasis and chemotherapy resistance by enhancing cell stemness and epithelial-mesenchymal transition in colorectal cancer. *Mol Cancer* (2019) 18:91. doi: 10.1186/s12943-019-1019-x

57. Gascard P, Tlsty TD. Carcinoma-associated fibroblasts: Orchestrating the composition of malignancy. *Genes Dev* (2016) 30:1002–19. doi: 10.1101/gad.279737.116

58. Tao L, Huang G, Wang R, Pan Y, He Z, Chu X, et al. Cancer-associated fibroblasts treated with cisplatin facilitates chemoresistance of lung adenocarcinoma through IL-11/IL-11R/STAT3 signaling pathway. *Sci Rep* (2016) 6:38408. doi: 10.1038/srep38408

59. Gao Y, Li X, Zeng C, Liu C, Hao Q, Li W, et al. CD63(+) cancer-associated fibroblasts confer tamoxifen resistance to breast cancer cells through exosomal miR-22. *Advanced Sci (Weinheim Baden-Wurttemberg Germany)* (2020) 7:2002518. doi: 10.1002/advs.202002518

60. Zhang H, Deng T, Liu R, Ning T, Yang H, Liu D, et al. CAF secreted miR-522 suppresses ferroptosis and promotes acquired chemo-resistance in gastric cancer. *Mol Cancer* (2020) 19:43. doi: 10.1186/s12943-020-01168-8

61. Zhai J, Shen J, Xie G, Wu J, He M, Gao L, et al. Cancer-associated fibroblasts-derived IL-8 mediates resistance to cisplatin in human gastric cancer. *Cancer Lett* (2019) 454:37–43. doi: 10.1016/j.canlet.2019.04.002

62. Wei L, Ye H, Li G, Lu Y, Zhou Q, Zheng S, et al. Cancer-associated fibroblasts promote progression and gemcitabine resistance *via* the SDF-1/SATB-1 pathway in pancreatic cancer. *Cell Death Dis* (2018) 9:1065. doi: 10.1038/s41419-018-1104-x

63. Richards KE, Zeleniak AE, Fishel ML, Wu J, Littlepage LE, Hill R. Cancer-associated fibroblast exosomes regulate survival and proliferation of pancreatic cancer cells. *Oncogene* (2017) 36:1770–8. doi: 10.1038/onc.2016.353

64. Chen PY, Wei WF, Wu HZ, Fan LS, Wang W. Cancer-associated fibroblast heterogeneity: A factor that cannot be ignored in immune microenvironment remodeling. *Front Immunol* (2021) 12:2021.671595. doi: 10.3389/fimmu.2021.671595

65. Costa A, Kieffer Y, Scholer-Dahirel A, Pelon F, Bourachot B, Cardon M, et al. Fibroblast heterogeneity and immunosuppressive environment in human breast cancer. *Cancer Cell* (2018) 33:463–79.e10. doi: 10.1016/j.ccell.2018.01.011

66. Zhao X, Ding L, Lu Z, Huang X, Jing Y, Yang Y, et al. Diminished CD68(+) cancer-associated fibroblast subset induces regulatory T-cell (Treg) infiltration and predicts poor prognosis of oral squamous cell carcinoma patients. *Am J Pathol* (2020) 190:886–99. doi: 10.1016/j.ajpath.2019.12.007

67. Dou D, Ren X, Han M, Xu X, Ge X, Gu Y, et al. Cancer-associated fibroblasts-derived exosomes suppress immune cell function in breast cancer *via*

the miR-92/PD-L1 pathway. *Front Immunol* (2020) 11:2020.02026. doi: 10.3389/fimmu.2020.02026

68. Li Z, Zhou J, Zhang J, Li S, Wang H, Du J. Cancer-associated fibroblasts promote PD-L1 expression in mice cancer cells *via* secreting CXCL5. *Int J Cancer* (2019) 145:1946–57. doi: 10.1002/ijc.32278

69. Huang TX, Tan XY, Huang HS, Li YT, Liu BL, Liu KS, et al. Targeting cancer-associated fibroblast-secreted WNT2 restores dendritic cell-mediated antitumour immunity. *Gut* (2022) 71:333–44. doi: 10.1136/gutjnl-2020-322924

70. Cheng JT, Deng YN, Yi HM, Wang GY, Fu BS, Chen WJ, et al. Hepatic carcinoma-associated fibroblasts induce IDO-producing regulatory dendritic cells through IL-6-mediated STAT3 activation. *Oncogenesis* (2016) 5:e198. doi: 10.1038/oncsis.2016.7

71. Cheng Y, Li H, Deng Y, Tai Y, Zeng K, Zhang Y, et al. Cancer-associated fibroblasts induce PDL1+ neutrophils through the IL6-STAT3 pathway that foster immune suppression in hepatocellular carcinoma. *Cell Death Dis* (2018) 9:422. doi: 10.1038/s41419-018-0458-4

72. Shani O, Vorobyov T, Monteran L, Lavie D, Cohen N, Raz Y, et al. Fibroblast-derived IL33 facilitates breast cancer metastasis by modifying the immune microenvironment and driving type 2 immunity. *Cancer Res* (2020) 80:5317–29. doi: 10.1158/0008-5472.Can-20-2116

73. Özdemir BC, Pentcheva-Hoang T, Carstens JL, Zheng X, Wu CC, Simpson TR, et al. Depletion of carcinoma-associated fibroblasts and fibrosis induces immunosuppression and accelerates pancreas cancer with reduced survival. *Cancer Cell* (2014) 25:719–34. doi: 10.1016/j.ccr.2014.04.005

74. Rhim AD, Oberstein PE, Thomas DH, Mirek ET, Palermo CF, Sastra SA, et al. Stromal elements act to restrain, rather than support, pancreatic ductal adenocarcinoma. *Cancer Cell* (2014) 25:735–47. doi: 10.1016/j.ccr.2014.04.021

75. Brechbuhl HM, Finlay-Schultz J, Yamamoto TM, Gillen AE, Cittelly DM, Tan AC, et al. Fibroblast subtypes regulate responsiveness of luminal breast cancer to estrogen. *Clin Cancer Res* (2017) 23:1710–21. doi: 10.1158/1078-0432.Ccr-15-2851

76. Mizutani Y, Kobayashi H, Iida T, Asai N, Masamune A, Hara A, et al. Meflin-positive cancer-associated fibroblasts inhibit pancreatic carcinogenesis. *Cancer Res* (2019) 79:5367–81. doi: 10.1158/0008-5472.Can-19-0454

77. Fiori ME, Di Franco S, Villanova L, Bianca P, Stassi G, De Maria R. Cancer-associated fibroblasts as abettors of tumor progression at the crossroads of EMT and therapy resistance. *Mol Cancer* (2019) 18:70. doi: 10.1186/s12943-019-0994-2

78. Scott AM, Wiseman G, Welt S, Adjei A, Lee FT, Hopkins W, et al. A phase I dose-escalation study of sibrotuzumab in patients with advanced or metastatic fibroblast activation protein-positive cancer. *Clin Cancer Res* (2003) 9:1639–47.

79. Narra K, Mullins SR, Lee HO, Strzemkowski-Brun B, Magalong K, Christiansen VJ, et al. Phase II trial of single agent Val-boroPro (Talabostat) inhibiting fibroblast activation protein in patients with metastatic colorectal cancer. *Cancer Biol Ther* (2007) 6:1691–9. doi: 10.4161/cbt.6.11.4874

80. Duperret EK, Trautz A, Ammons D, Perales-Puchalt A, Wise MC, Yan J, et al. Alteration of the tumor stroma using a consensus DNA vaccine targeting fibroblast activation protein (FAP) synergizes with antitumor vaccine therapy in mice. *Clin Cancer Res* (2018) 24:1190–201. doi: 10.1158/1078-0432.Ccr-17-2033

81. Fang J, Xiao L, Joo KI, Liu Y, Zhang C, Liu S, et al. A potent immunotoxin targeting fibroblast activation protein for treatment of breast cancer in mice. *Int J Cancer* (2016) 138:1013–23. doi: 10.1002/ijc.29831

82. Murakami M, Ernsting MJ, Undzys E, Holwell N, Foltz WD, Li SD. Docetaxel conjugate nanoparticles that target α-smooth muscle actin-expressing stromal cells suppress breast cancer metastasis. *Cancer Res* (2013) 73:4862–71. doi: 10.1158/0008-5472.Can-13-0062

83. Haubeiss S, Schmid JO, Mürdter TE, Sonnenberg M, Friedel G, van der Kuip H, et al. Dasatinib reverses cancer-associated fibroblasts (CAFs) from primary lung carcinomas to a phenotype comparable to that of normal fibroblasts. *Mol Cancer* (2010) 9:168. doi: 10.1186/1476-4598-9-168

84. Yao Y, Guo Q, Cao Y, Qiu Y, Tan R, Yu Z, et al. Artemisinin derivatives inactivate cancer-associated fibroblasts through suppressing TGF-β signaling in breast cancer. *J Exp Clin Cancer Res* (2018) 37:282. doi: 10.1186/s13046-018-0960-7

85. Albrengues J, Bertero T, Grasset E, Bonan S, Maiel M, Bourget I, et al. Epigenetic switch drives the conversion of fibroblasts into proinvasive cancer-associated fibroblasts. *Nat Commun* (2015) 6:10204. doi: 10.1038/ncomms10204

86. Ford K, Hanley CJ, Mellone M, Szyndralewiez C, Heitz F, Wiesel P, et al. NOX4 inhibition potentiates immunotherapy by overcoming cancer-associated fibroblast-mediated CD8 T-cell exclusion from tumors. *Cancer Res* (2020) 80:1846–60. doi: 10.1158/0008-5472.Can-19-3158

87. Banerjee S, Modi S, McGinn O, Zhao X, Dudeja V, Ramakrishnan S, et al. Impaired synthesis of stromal components in response to minnelide improves vascular function, drug delivery, and survival in pancreatic cancer. *Clin Cancer Res* (2016) 22:415–25. doi: 10.1158/1078-0432.Ccr-15-1155

88. Murphy JE, Wo JY, Ryan DP, Clark JW, Jiang W, Yeap BY, et al. Total neoadjuvant therapy with FOLFIRINOX in combination with losartan followed by chemoradiotherapy for locally advanced pancreatic cancer: A phase 2 clinical trial. *JAMA Oncol* (2019) 5:1020–7. doi: 10.1001/jamaoncol.2019.0892

89. Mazzocca A, Fransvea E, Dituri F, Lupo L, Antonaci S, Giannelli G. Down-regulation of connective tissue growth factor by inhibition of transforming growth factor beta blocks the tumor-stroma cross-talk and tumor progression in hepatocellular carcinoma. *Hepatol (Baltimore Md)* (2010) 51:523–34. doi: 10.1002/hep.23285

90. Ogier C, Colombo PE, Bousquet C, Canterel-Thouennon L, Sicard P, Garambois V, et al. Targeting the NRG1/HER3 pathway in tumor cells and cancer-associated fibroblasts with an anti-neuregulin 1 antibody inhibits tumor growth in pre-clinical models of pancreatic cancer. *Cancer Lett* (2018) 432:227–36. doi: 10.1016/j.canlet.2018.06.023

91. Zhang J, Li S, Zhao Y, Ma P, Cao Y, Liu C, et al. Cancer-associated fibroblasts promote the migration and invasion of gastric cancer cells *via* activating IL-17a/JAK2/STAT3 signaling. *Ann Trans Med* (2020) 8:877. doi: 10.21037/atm-20-4843

92. Zhou Q, Zhou Y, Liu X, Shen Y. GDC-0449 improves the antitumor activity of nano-doxorubicin in pancreatic cancer in a fibroblast-enriched microenvironment. *Sci Rep* (2017) 7:13379. doi: 10.1038/s41598-017-13869-0

93. Sun L, Wang Y, Wang L, Yao B, Chen T, Li Q, et al. Resolvin D1 prevents epithelial-mesenchymal transition and reduces the stemness features of hepatocellular carcinoma by inhibiting paracrine of cancer-associated fibroblast-derived COMP. *J Exp Clin Cancer Res* (2019) 38:170. doi: 10.1186/s13046-019-1163-6

94. Lefort S, Thuleau A, Kieffer Y, Sirven P, Bieche I, Marangoni E, et al. CXCR4 inhibitors could benefit to HER2 but not to triple-negative breast cancer patients. *Oncogene* (2017) 36:1211–22. doi: 10.1038/onc.2016.284

95. Hurwitz HI, Uppal N, Wagner SA, Bendell JC, Beck JT, Wade SM3rd, et al. Randomized, double-blind, phase II study of ruxolitinib or placebo in combination with capecitabine in patients with metastatic pancreatic cancer for whom therapy with gemcitabine has failed. *J Clin Oncol* (2015) 33:4039–47. doi: 10.1200/jco.2015.61.4578

96. Schmid P, Rugo HS, Adams S, Schneeweiss A, Barrios CH, Iwata H, et al. Atezolizumab plus nab-paclitaxel as first-line treatment for unresectable, locally advanced or metastatic triple-negative breast cancer (IMpassion130): updated efficacy results from a randomised, double-blind, placebo-controlled, phase 3 trial. *Lancet Oncol* (2020) 21:44–59. doi: 10.1016/s1470-2045(19)30689-8

97. Roberts EW, Deonarine A, Jones JO, Denton AE, Feig C, Lyons SK, et al. Depletion of stromal cells expressing fibroblast activation protein-α from skeletal muscle and bone marrow results in cachexia and anemia. *J Exp Med* (2013) 210:1137–51. doi: 10.1084/jem.20122344

98. Hanley CJ, Mellone M, Ford K, Thirdborough SM, Mellows T, Frampton SJ, et al. Targeting the myofibroblastic cancer-associated fibroblast phenotype through inhibition of NOX4. *J Natl Cancer Institute* (2018) 110:109–20. doi: 10.1093/jnci/djx121

99. Chauhan VP, Chen IX, Tong R, Ng MR, Martin JD, Naxerova K, et al. Reprogramming the microenvironment with tumor-selective angiotensin blockers enhances cancer immunotherapy. *Proc Natl Acad Sci U.S.A.* (2019) 116:10674–80. doi: 10.1073/pnas.1819889116

100. Feng R, Morine Y, Ikemoto T, Imura S, Iwahashi S, Saito Y, et al. Nab-paclitaxel interrupts cancer-stromal interaction through c-X-C motif chemokine 10-mediated interleukin-6 downregulation *in vitro*. *Cancer Sci* (2018) 109:2509–19. doi: 10.1111/cas.13694

frontiers | Frontiers in Pharmacology

TYPE Original Research
PUBLISHED 23 November 2022
DOI 10.3389/fphar.2022.1056337

OPEN ACCESS

EDITED BY
Qianming Du,
Nanjing Medical University, China

REVIEWED BY
Hao Sun,
China Pharmaceutical University, China
Xiuting Liu,
Washington University in St. Louis, United States

*CORRESPONDENCE
Yuxian Song,
songyuxian1986@126.com
Yanhong Ni,
niyanhong12@163.com
Guowen Sun,
238957@sina.com

SPECIALTY SECTION
This article was submitted to Pharmacology of Anti-Cancer Drugs, a section of the journal Frontiers in Pharmacology

RECEIVED 28 September 2022
ACCEPTED 07 November 2022
PUBLISHED 23 November 2022

CITATION
Wang D, Tian M, Fu Y, Sun Y, Ding L, Zhang X, Jing Y, Sun G, Ni Y and Song Y (2022), Halofuginone inhibits tumor migration and invasion by affecting cancer-associated fibroblasts in oral squamous cell carcinoma. *Front. Pharmacol.* 13:1056337. doi: 10.3389/fphar.2022.1056337

Halofuginone inhibits tumor migration and invasion by affecting cancer-associated fibroblasts in oral squamous cell carcinoma

Danni Wang[1,2], Mei Tian[1,2], Yong Fu[1,2], Yawei Sun[1,2], Liang Ding[1], Xiaoxin Zhang[1], Yue Jing[1], Guowen Sun[2]*, Yanhong Ni[1]* and Yuxian Song[1]*

[1]Central Laboratory of Stomatology, Nanjing Stomatological Hospital, Medical School of Nanjing University, Nanjing, China, [2]Department of Oral and Maxillofacial Surgery, Nanjing Stomatological Hospital, Medical School of Nanjing University, Nanjing, China

Oral squamous cell carcinoma (OSCC) is the most common malignant tumor in the oral and maxillofacial regions, with a high rate of metastasis. Cancer-associated fibroblasts (CAFs) play critical roles in tumor growth, metastasis and invasion, making them attractive therapeutic targets for cancer treatment. As an old anti-coccidiosis drug for poultry, Halofuginone (HF) has also been reported to possess anti-fibrosis and anti-cancer activities in the recent decades. However, whether it works by targeting CAFs in OSCC, and the mechanisms involved remain unclear. In the present study, we observed HF dose-dependently inhibits OSCC-derived CAF viability and proliferation. Meanwhile, HF decreased the expressions of α-SMA, FSP-1 and PDGFRβ, markers of the malignant phenotype of CAFs, both at mRNA and protein levels. Furthermore, functional studies demonstrated that HF dramatically attenuates the promotion effect of CAFs on OSCC cell migration and invasion. Mechanistically, the inhibition of MMP2 secretion and the upstream TGF-β/Smad2/3 signaling pathway played an important role in these processes. In the orthotopic transplanted tongue carcinoma in mice model, we confirmed that HF administration inhibited tumor growth and lymph node metastasis (LNM) with reduced CAF population, MMP2 expression and collagen deposition in tumor. Altogether, these results indicate that HF can inhibit the migration and invasion of OSCC by targeting CAFs, which will provide new ideas for the treatment of OSCC.

KEYWORDS

cancer-associated fibroblasts, halofuginone, tumor migration, tumor invasion, oral squamous cell carcinoma (OSCC)

Introduction

Oral squamous cell carcinoma (OSCC) is the most common malignant tumor in the oral and maxillofacial regions, accounting for approximately 90% of oral malignant tumors (Siegel et al., 2021). At present, clinical treatment of oral squamous cell carcinomas is primarily surgery, and in some cases, combined with chemoradiation or biological therapy. Although the technical level is unceasingly enhanced, the patient's 5-year survival rate does not improve significantly and remains at approximately 60% (Chen S. H. et al., 2021; Mesia et al., 2021). Therefore, further exploration of effective neoadjuvant is urgently needed.

Emerging evidence has demonstrated that the tumor microenvironment (TME) plays a pivotal role in tumor growth, metastasis and invasion and has a profound impact on the therapeutic effect of tumors (Qin et al., 2021). As a principal constituent of the tumor stroma, Cancer-associated fibroblasts (CAFs) play critical roles in the TME (Kalluri, 2016; Ping et al., 2021).

CAFs affect tumor development in a variety of ways, including maintenance of extracellular matrix, angiogenesis, regulation of tumor metabolism, inhibition of antitumor immunity and promotion of chemotherapy resistance (Zhang et al., 2020) (Dumont et al., 2013). Therefore, CAFs as new therapeutic targets for cancer treatment are attracting increasing attention. In OSCC, our studies and others have demonstrated that the density of CAFs is positively correlated with lymph node metastasis, local recurrence and distant metastasis (Li et al., 2015; Wang et al., 2019). Thus, the role of CAFs in promoting the metastasis and invasion of oral squamous cell carcinoma deserves special attention. Therefore, we considered whether a drug could be used to inhibit the interaction between CAFs and tumors to seek a new adjuvant therapy for oral squamous cell carcinoma.

Halofuginone (HF), an alkaloid originally isolated from the Chinese plant Dichroa febrifuga, has been approved by the US FDA in the 1980s for the prevention of coccidiosis in poultry (Daugschies et al., 1998). In recent years, studies have found that HF can inhibit collagen synthesis, inhibit tissue fibrosis and promote wound healing through the TGF-β/Smad2/3 signaling pathway (Luo et al., 2018; Marty et al., 2021). On the other hand, accumulating evidence has suggested HF can affect tumor cell proliferation, apoptosis and metastasis in many kinds of solid tumors, including lung cancer (Demiroglu-Zergeroglu et al., 2020), rectal cancer (Wang C. et al., 2020), breast cancer (Jin et al., 2014) and esophageal squamous cell carcinoma (Wang Y. et al., 2020). A recent study has demonstrated that HF inhibits the progression of pancreatic ductal carcinoma by inhibiting fibrosis (Elahi-Gedwillo et al., 2019). Since fibroblast is the essential initiator of fibrosis, it seems logical to envisage that HF might regulate CAF activities to change the interactions between CAFs and tumor cells so that enhance its anticancer effect. However, whether it works on CAFs in the TME, especially in OSCC, and the mechanism involved remains largely unknown. The present study aims to fill this gap of knowledge by investigating the effects of HF on OSCC derived CAFs and actions of HF-pretreated CAFs on OSCC cells, which will provide new ideas for HF treatment of OSCC.

Materials and methods

Reagents

Halofuginone (Sigma, #64924-67-0, molecular weight: 495.59 g/mol) was dissolved in phosphate buffer solution (PBS) at pH 5.3 at a concentration of 1 mM as a stock solution and diluted to the indicated concentrations with medium before each test.

Cell culture and preparation of conditioned medium

CAFs and NFs (normal fibroblasts) were isolated from the tumor tissues and the adjacent normal tissues of OSCC patients treated at the Nanjing Stomatological Hospital, Medical School of Nanjing University as previously described (Ding et al., 2018; Wang et al., 2019). The study was approved by the ethics committee for clinical study of Nanjing Stomatological Hospital. CAFs and NFs were cultured in fibroblast medium (Cat No. 2301, SclenCell™). For further experiments, CAFs were used between the third and seventh passage. OSCC cell lines HSC3 and HN6 were cultured in complete DMEM medium supplemented with 10% FBS, penicillin (100 U/mL) and streptomycin (0.1 mg/ml).

Conditioned medium (CM) from CAFs was prepared as follow: CAFs were seeded into four dishes, treated with different concentrations of HF (25, 50, 100 nM) or vehicle (PBS, pH = 5.3) for 6 h, the cells were then washed twice with PBS, and cultured in fresh complete media for another 48 h. Cell fragments were removed from the supernatants by centrifugation at 3,000 rpm for 10 min at 4°C. Supernatants were collected and used immediately or stored at −20°C for later use.

Western blotting

Proteins from cells were extracted in RIPA lysis buffer with a mixture of protease and phosphatase inhibitors on ice. The protein concentration of each sample was determined using a BCA protein assay kit (Vazyme, China). Total protein (20 μg) was separated by 4%–20% sodium dodecyl sulfate–polyacrylamide gel electrophoresis and was transferred to polyvinylidene difluoride membrane. Membranes were

blocked at room temperature for 1 h with 5% BSA in Tris-buffered saline, and incubated with primary antibodies at 4°C overnight. After washing, the membranes were incubated at room temperature with HRP-conjugated secondary antibody for 1 h, protein bands were detected by a protein imaging system (Tanon, China). The primary antibodies were as follow: α-SMA (#ab5694) was obtained from the Abcam company. FSP-1 (# 66489), Vimentin (#10366), PDGFRβ (#13449) and MMP2 (#10373) were obtained from Proteintech company. p-Smad2/3 (#8828S), p-AKT (#4060S), p-JNK (#9255S), p-P38 (#4511S), Anti-rabbit IgG, HRP-linked Antibody (#7074), Anti-mouse IgG and HRP-linked Antibody (#7076) were obtained from Cell Signaling Technology.

Immunofluorescence

CAFs were cultured in confocal dishes and treated with HF or not as indicated. Cells were then fixed with 4% paraformaldehyde and permeated with 1%Trition X-100 solution at room temperature. Following three extensive washings with PBS, the samples were blocked with 5% BSA and incubated with primary antibodies at 4°C overnight. After rinsing three times in PBS, the samples were incubated with different secondary antibodies at a 1:400 dilution for 1.5 h at room temperature in the dark, and then the nuclei were stained with DAPI. Samples were visualized using Nikon A1 confocal microscope (Nikon, Japan).

Cell viability assay

CAFs were seeded into 96-well plate (4000 cells per well, in 100 μL) overnight and treated with different concentrations of HF (25, 50, 100, 200, 400 nM) or vehicle for 24 h or 48 h. HSC3 or NH6 cells were seeded into 96-well plate (5000 cells per well, in 100 μL) overnight, and cultured in different treated CM from CAFs for 48 h. Cell counting kit-8 (CCK8) (Dojindo, Japan) was used according to the manufacturer's instruction to detect cell viabilities. Absorbance of 450 nm was measured by a microplate reader Spectra Max M3 (Molecular Devices, United States).

Apoptosis assay

CAFs were seeded into 12-well plate (2×10^5 cells per well) and treated with HF (25, 50, 100 nM) or vehicle for 48 h. To analyze the effect of HF on cell-apoptosis, the CAFs were digested by trypsin (excluding EDTA) and centrifuged at 1,300 rpm, 4°C for 5 min. After washing with PBS, the cells were stained with Annexin-V-FITC/PI (Vazyme, China) according to the manufacturer's instruction. Flow cytometry was performed using FACSCalibur flow cytometer (BD Bioscience, San Diego), and data were analyzed with FlowJo software (Treestar, Inc., San Carlos).

EdU assay

CAFs were plated to 12-well plate and treated with HF (25, 50, 100 nM) or vehicle for 48 h. EdU staining proliferation kit was used according to the manufacturer's instruction (Beyotime, China). Briefly, cells in plates were added with EdU solution and incubated for 2 h and then treated with 4% formaldehyde. After fixation, permeable solution was added and incubated for 10–15 min. After cleaning, 500 μL Click reaction solution was added to each well and incubated at room temperature in dark for 30 min. Cells were observed and photographed under a fluorescence microscope.

Quantitative real-time polymerase chain reaction (qRT-PCR)

After HF-treated CAFs were cultured for 48 h, RNA of CAFs was extracted. RNA was obtained using Trizol reagent following the manufacturer's procedure and then reverse transcribed into cDNA using HiScript III RT SuperMix (Vazyme, China). Subsequently, real-time quantitative PCR was performed using the AceQ® qPCR SYBR® Green Master Mix (Vazyme, China) and Vii7 Real-Time PCR System (Applied Biosystems, CA). The primer sequences used in this study were obtained from commercial sources and are displayed in Table 1.

Wound healing assay

To study the effects of HF on cell migration *in vitro*, a wound healing assay was performed using HSC3 and NH6 cells. Cells were seeded in 6-well plate and grown until the cell confluence reached 90%. Then cells were serum-starved for 12 h. A linear wound was created in the confluent monolayer using a 200-μL pipette tip. After PBS washing, different concentrations of CM were added and mixed 1:1 with normal serum-free media. The trace widths of different treatment groups were observed at 0 h, 8 h, 16 h, and 24 h and photographed and recorded. The time points with the largest differences were taken for results analysis.

Migration and invasion assay

For migration assay, HSC3 or NH6 cells (1×10^5 cells per well) were seeded in the upper chambers of 24-well Transwell plate (with 8 μm pore size, Costar) and starved overnight. CAFs were seeded into another 24-well plate (5×10^4 cells per well) and

TABLE 1 Primers used for real-time quantitative PCR analysis.

Gene	Forward primer	Reverse primer
a-SMA	CCTGTGTTGTGGTTTACACTGG	GGGGGAATTATCTTTCCTGGTCC
FSP-1	GATGAGCAACTTGGACAGCAA	CTGGGCTGCTTATCTGGGAAG
PDGFRβ	AGCACCTTCGTTCTGACCTG	TATTCTCCCGTGTCTAGCCCA
N-Cadherin	TCAGGCGTCTGTAGAGGCTT	ATGCACATCCTTCGATAAGACTG
Vimentin	GACGCCATCAACACCGAGTT	CTTTGTCGTTGGTTAGCTGGT
GAPDH	GGAGCGAGATCCCTCCAAAA	GGCTGTTGTCATACTTCTCATGG

treated with HF (25, 50, 100 nM) or vehicle for 6 h. CAFs were then washed twice with PBS and replaced with fresh complete media. Tumor cells in the Transwell inserts were carefully transferred to the 24-well plate paved with CAFs, and co-cultured for 12 h. For invasion assay, matrigel was spread on the Transwell chamber and co-cultured for 24 h. After 12 h or 24 h of co-culture, tumor cells were fixed with 4% paraformaldehyde, stained with crystal violet, and observed and counted under a microscope.

Xenograft tumor models

Female Balb/c nude mice (4–6 weeks) were kept in standard environment with the unified breeding. All the experiments were approved by the Animal Research Committee of Medical College Affiliated to Nanjing University and conformed to the ethical standards with the guidelines of the National Animal Care and Ethics Institution. A total of 1×10^6 CAFs and 2×10^5 HN6 cells (CAFs and HN6 were mixed at a ratio of 5:1) were injected on the right tongue edge of each mouse to observe tumor formation. After 14 days, 10 mice with successfully established tongue tumor were randomly divided into two groups: the control group (n = 5) and the HF treatment group (n = 5). The treatment group was intraperitoneally injected with 0.5 mg/kg HF every other day for 14 days, and the control group injected with PBS (pH = 5.3). On the 28th day, the mice were sacrificed by cervical dislocation under general anesthesia, and the tongues and cervical lymph nodes were removed. Tissues were soaked overnight in 4% paraformaldehyde, dehydrated conventionally and embedded in paraffin.

Masson staining

Paraffin embedded tumor tissues of mice were cut into 5 μm slices for Masson staining. The distribution of collagen in tumor tissue was observed and photographed under a cell imaging system, and the staining results were analyzed by using ImageJ software.

Immunohistochemistry analysis

Paraffin embedded tumor tissues of mice were cut into 5 μm slices, and the dehydration was reached with the different concentrations of ethanol after being dewaxed in xylene. The sections were subjected to antigen retrieval using 10 mM citrate buffer (92°C for 30 min). Hydrogen peroxide (3%) and BSA (5%) were used to block endogenous peroxidase activity and nonspecific staining for 10 min and 20 min, respectively. Immunohistochemical staining for α-SMA and MMP2 was performed. Protein levels of α-SMA and MMP2 were evaluated according to staining intensity and the percentage of positive cells.

Statistical analysis

All results were expressed as the mean ± S.E.M unless otherwise indicated. Each experiment was repeated at least three times. Data with $p < 0.05$ were considered statistically significant. Analysis of experimental results was performed using GraphPad Prism (GraphPad Software v8.0).

Results

Extraction and phenotypic identification of primary cancer-associated fibroblasts

We first extracted primary CAFs and NFs from the tumor tissue and the adjacent normal tissue of OSCC patients. The morphologies of CAFs and NFs were observed under invert microscope. As shown in Figure 1A, both CAFs and NFs have large and long spindle shapes. Phenotypic identifications of CAFs were then conducted. Western blotting analysis showed that, compared with NFs, CAFs expressed higher level of mesenchymal markers, such as α-SMA, Vimentin and PDGFRβ (Figure 1B). Results of immunofluorescence also showed that CAFs express higher levels of α-SMA and PDGFRβ (Figure 1C).

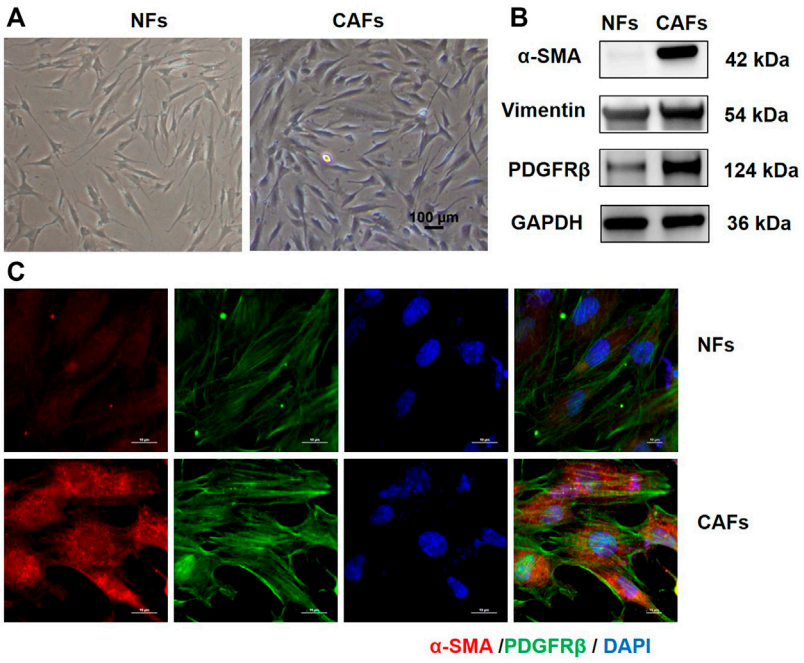

FIGURE 1
Culture and identification of primary tumor-associated fibroblasts. **(A)** Morphology of NFs and CAFs under invert microscope (100×). **(B)** Protein levels of α-SMA, Vimentin and PDGFRβ in NFs and CAFs detected by Western blotting analysis. **(C)** Expression levels of α-SMA and PDGFRβ in NFs and CAFs were observed by immunofluorescence.

Halofuginone decreased CAF proliferation

CAFs were treated with different concentrations of HF (structure was shown in Figure 2B) and their viabilities were tested using the CCK-8 assay. As shown in Figure 2A, HF inhibited CAF cell viability in a dose-dependent manner. Furthermore, EdU assay showed HF inhibited the proliferation of CAFs at 50 and 100 nM (Figure 2C). We further investigated the effect of HF on cell apoptosis. Flow cytometry results showed that only 100 nM HF significantly induced early apoptosis at a ratio of 10% compared with 5% in control group. However, there were no significant differences among low concentration groups and control group either for early or late apoptosis (Figure 2D).

Halofuginone reduced the expressions of CAF phenotypic markers

Activated fibroblasts express high levels of α-SMA, FSP-1, PDGFRβ, N-cadherin and vimentin, which are markers of the malignant phenotype of CAFs. To determine whether HF treatment altered CAF phenotype, we treated CAFs with HF (25, 50, 100 nM) for 24 h or 48 h. The mRNA and protein levels of these markers were detected by using qRT-PCR, western blotting and immunofluorescence assay, respectively. We found that the mRNA levels of these markers didn't change by HF treatment at 24 h (data not shown), while α-SMA, FSP-1, PDGFRβ and vimentin but not N-cadherin decreased significantly at 48 h treatment (Figure 3A). Meanwhile, results of western blotting showed that HF dose-dependently inhibited expression levels of α-SMA, FSP-1 and PDGFRβ but not N-cadherin or vimentin (Figure 3B). The subsequent immunofluorescence assay confirmed these results (Figure 3C).

HF-pretreated CAFs reduced the migration and invasion of OSCC cells

To observe whether HF-treated CAFs could affect the proliferation, migration and invasion of tumor cells, CMs from HF-treated CAFs or the cells (in Transwell) were co-cultured with OSCC cells, then the cell viability, migration and invasion activities were detected. Results of CCK-8 assay showed that different CMs had no significant effect on the proliferation of OSCC cell line HN6 (Figure 4A). However, wound healing assay results showed that the CM collected from 100 nM HF-treated CAFs could inhibit the migration ability of HN6 cells after 8 h of treatment

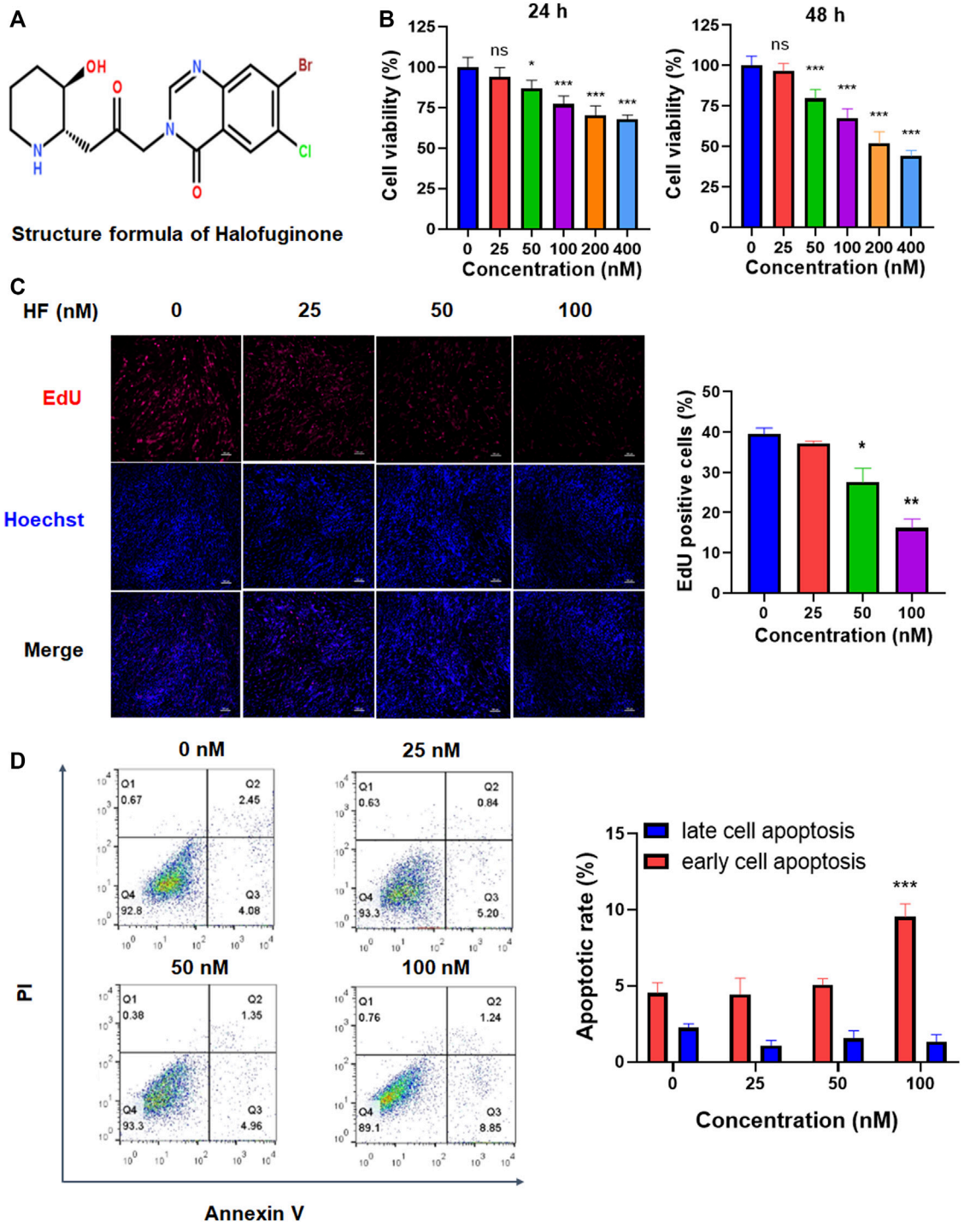

FIGURE 2
The effects of Halofuginone on CAF viability, proliferation and apoptosis. **(A)** Chemical structure of HF. **(B)** CAFs were treated with or without HF (25, 50, 100, 200, 400 nM) for 24 h or 48 h, and cell viability of CAFs was detected by CCK8; **(C)** CAFs were treated with or without HF (25, 50, 100 nM) for 48 h, cell proliferation was detected by EdU staining. **(D)** Cell apoptosis was analyzed by flow cytometry. *:$p < 0.05$, **:$p < 0.01$.

(Figure 4B). Further, transwell migration and invasion experiments also showed that HF-treated CAFs could obviously decrease HN6 cell migration (Figure 4C) and invasion in dose-dependent manners (Figure 4D). The same results were observed in HSC3 cell line (Supplemental Figure S1).

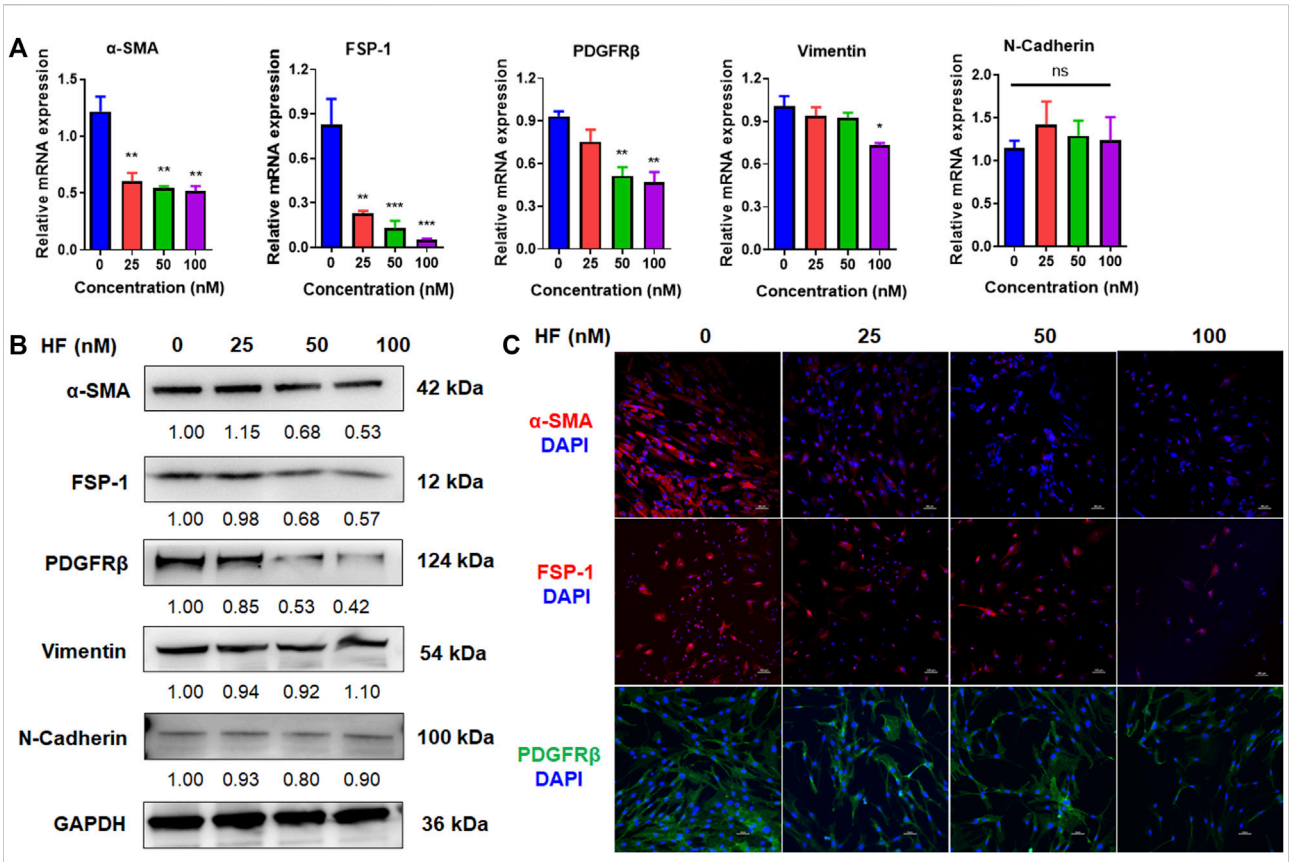

FIGURE 3
Halofuginone inhibited the expressions of CAF phenotypic markers. CAFs were treated with or without HF (25, 50, 100 nM) for 48 h. The mRNA and protein levels of CAF phenotypic markers α-SMA, FSP-1, PDGFRβ, N-cadherin and vimentin were detected by qRT-PCR **(A)** and Western blotting **(B)**, respectively. **(C)** The Protein levels of α-SMA, FSP-1, PDGFRβ were confirmed by immunofluorescence assays. *:$p < 0.05$, **:$p < 0.01$.

Halofuginone inhibited MMP2 expression and TGF-β/Smad2/3 signaling pathway in CAFs

Matrix metalloproteinases 2 (MMP2) is a well-known enzyme synthesized by fibroblasts and controlled ECM degradation and remodeling to influence tumor migration. To investigate whether HF inhibit tumor cell migration and invasion by regulating ECM, we carried out qRT-PCR and western blotting to detect the effect of HF on the expression of MMP2 at the mRNA and protein levels. Results showed that either MMP2 mRNA (Figure 5A) or protein (Figure 5B) level in CAFs was not changed after 6 h treatment of HF, but decreased 24 h later after continuous culture in complete media. TGF-β is commonly high expressed in tumor tissues of OSCC patients and extensively associated with cell migration and tumor metastasis (Lu et al., 2019). Several studies suggest TGF-β increases the synthesis of MMP2 and enhances its activity in tumor cells (Kim et al., 2021). Thus, we tested whether HF affect the TGF-β signaling pathways, including the SMAD-dependent canonical pathway or SMAD-independent non-canonical MAPK and PI3K/AKT signaling pathways (Chen J. et al., 2021). CAFs were treated with or without 50 nM HF followed by stimulation with 10 ng/ml TGF-β for indicated time points to stimulate the activation of related signaling pathways. Results showed that TGF-β activated the phosphorylation of Smad2/3 but not ERK, JNK, p38 or AKT in CAFs. However, HF treatment decreased the phosphorylation of Smad2/3 and upregulated the phosphorylation of ERK1/2 (Figure 5C). Thus, we hypothesized that HF inhibited the proliferation and activation of CAFs through the TGF-β/Smad2/3 signaling pathway which resulted to inhibit tumor cell migration and invasion.

Halofuginone inhibited tumor growth and metastasis *in vivo*

To verify the above findings *in vivo*, we established an orthotopic model of OSCC in nude mice by injecting HN6 and CAFs into the tongue (Figure 6A). As shown in Figure 6B, HF administration dramatically inhibited tumor

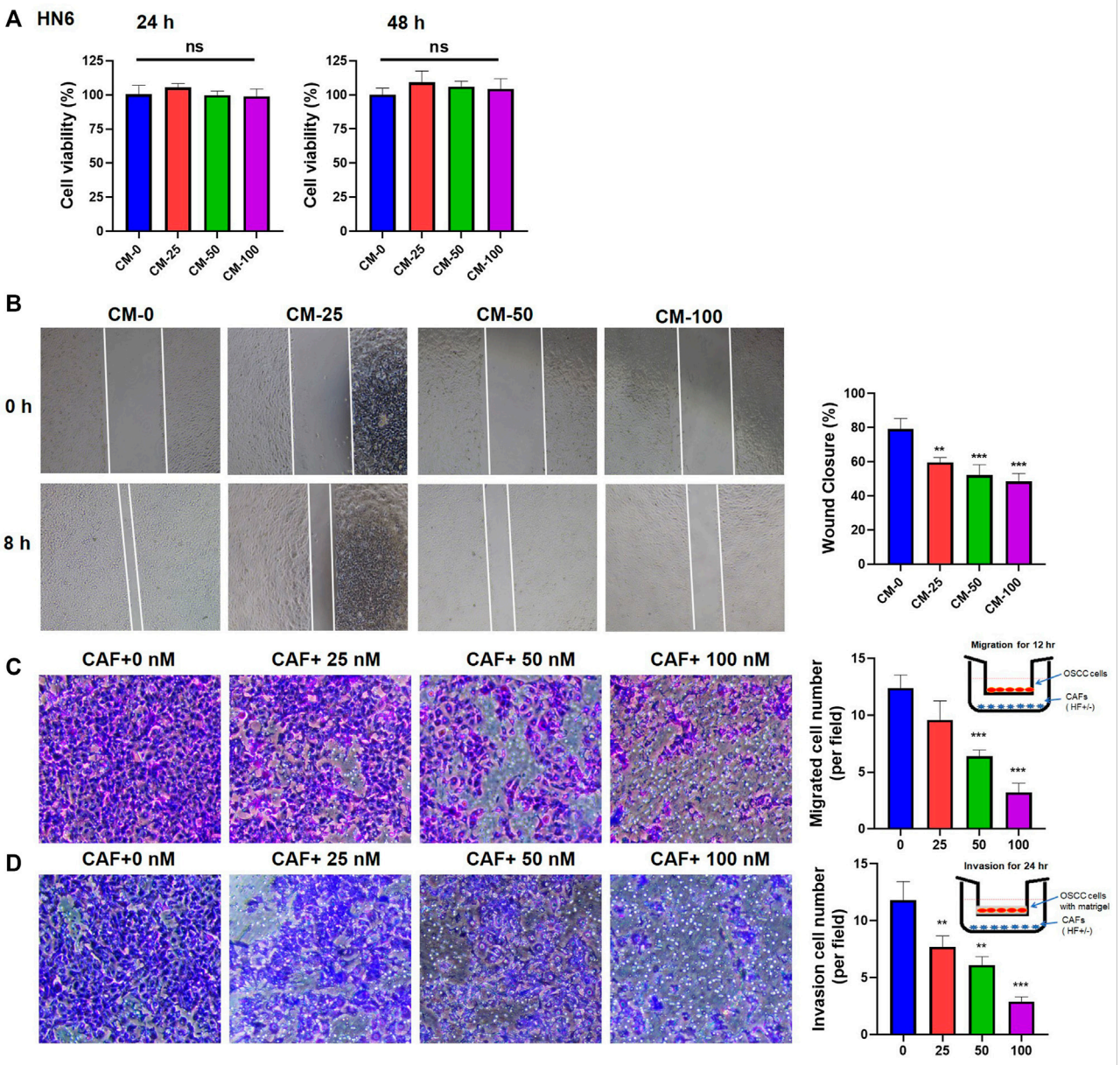

FIGURE 4
Effects of HF-treated CAFs on the proliferation, migration, and invasion of tumor cells. **(A)** CM had no effect on the proliferation of HN6 cells. **(B)** CM treated with high-concentration (100 nM) HF could significantly inhibit the migration of HN6 cells (100×). Transwell experiments showed that HF-treated CAFs significantly inhibit tumor migration **(C)** and invasion **(D)**. *:$p < 0.05$, **:$p < 0.01$, ***:$p < 0.001$.

growth in the tongue (Figure 6B). The mean volume of tumors at day 28 in the mice who received HF (23.93 ± 8.91 mm^3) was significantly decreased compared with control mice (6.69 ± 5.76 mm^3) ($p < 0.01$, Figure 6C). In addition, the percentage of lymph node metastasis (LNM) was also remarkably reduced in HF group (20% LNM^+) compared with control group (80% LNM^+) (Figure 6D). We further performed Masson staining and immunohistochemical staining on tumor tissues. Results showed that HF treatment decreased collagen deposition in tumor stroma, and the expression of α-SMA and MMP2 were also reduced (Figure 6E).

Discussion

Halofuginone is an alkaloid derived from quinazolinone with a low molecular weight that has a significant antifibrotic effect and can inhibit the production of type I collagen and reverse the

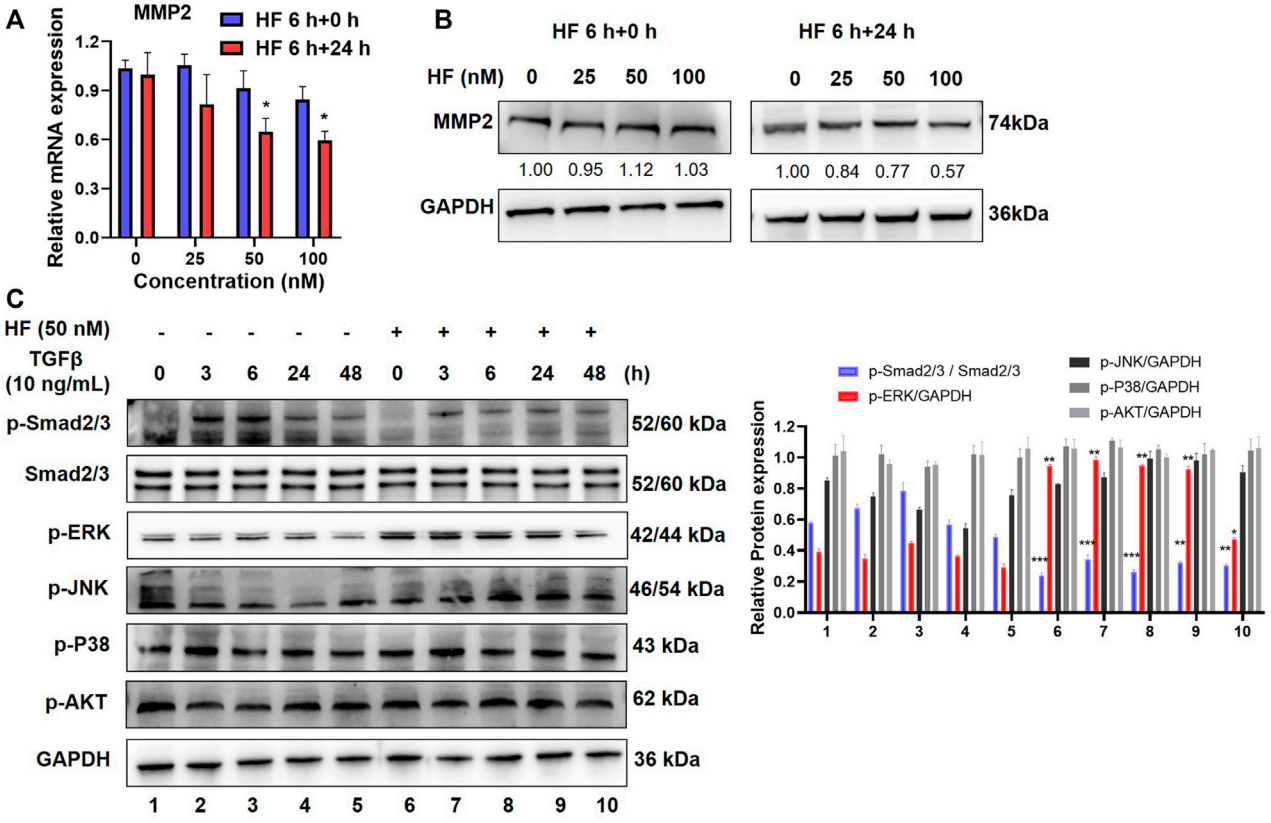

FIGURE 5
Halofuginone inhibited MMP2 expression and TGF-β/Smad2/3 signaling pathway in CAFs. **(A)** CAFs were treated with or without HF (25, 50, 100 nM) for 6 h and replaced with complete media and cultured for further 24 h. The mRNA level of MMP2 in CAFs was detected by qPCR. **(B)** The protein level of MMP2 was detected by Western bloting, and bands were quantified using ImageJ software. Similar results were seen in at least three independent experiments. *:$p < 0.05$. **(C)** CAFs were treated with HF (50 nM) for 48 h with or without TGFβ (10 ng/ml, R&D) stimulation for 3 h, 6 h, 24 h, and 48 h to stimulate the activation of the signaling pathway. Western blotting was used to detect the changes in phosphorylated Smad2/3, ERK, JNK, p38 and AKT protein levels.

fibrosis state (McGaha et al., 2002). Accumulating evidences suggest that halofuginone can induce apoptosis of several kinds of cancer cells and inhibit migration of cancer cells in some ways. Recent studies have also found that HF can inhibit the progression of pancreatic ductal carcinoma by inhibiting CAF activity and breaking the barrier affecting targeted drug delivery (Elahi-Gedwillo et al., 2019). Here, our results demonstrated for the first time that halofuginone dose-dependently inhibits OSCC-derived CAF viability and proliferation. Meanwhile, HF decreases the expressions of α-SMA, FSP-1 and PDGFRβ, markers of the malignant phenotype of CAFs, both at mRNA and protein levels. It seems that HF can partially shift CAFs to a less active phenotype, somewhat like the NF phenotype.

It is widely accepted that CAFs are crucial in the occurrence, development, invasion and metastasis of OSCC (Erdogan and Webb, 2017; Haga et al., 2021). Therefore, it is important to explore whether HF could inhibit the migration and invasion of OSCC cells by affecting CAFs. Our further experiments confirm this hypothesis that HF dramatically attenuates the promotion effect of CAFs on OSCC cell migration and invasion. Furthermore, we have also shown the beneficial effects of HF in the orthotopic transplanted tongue carcinoma mouse mode. We demonstrate that HF can inhibit tumor growth, LNM, collagen deposition and the population of α-SMA positive CAFs, indicating that HF treatment can reduce the proliferation, activation and tumor invasion of CAFs in the tumor region. Although the direct effect of HF on OSCC cells has not been reported yet, and not showed in the present study, we believe that HF can decrease the malignancy of OSCC not only by directly targeting tumor cells but also by targeting CAFs in the tumor microenvironment. Therefore, HF is a suitable candidate for anticancer combination therapy and tumor metastasis inhibition.

When exploring the mechanism of HF effects on CAFs, we find HF inhibits the secretion of MMP2 and the upstream TGF-

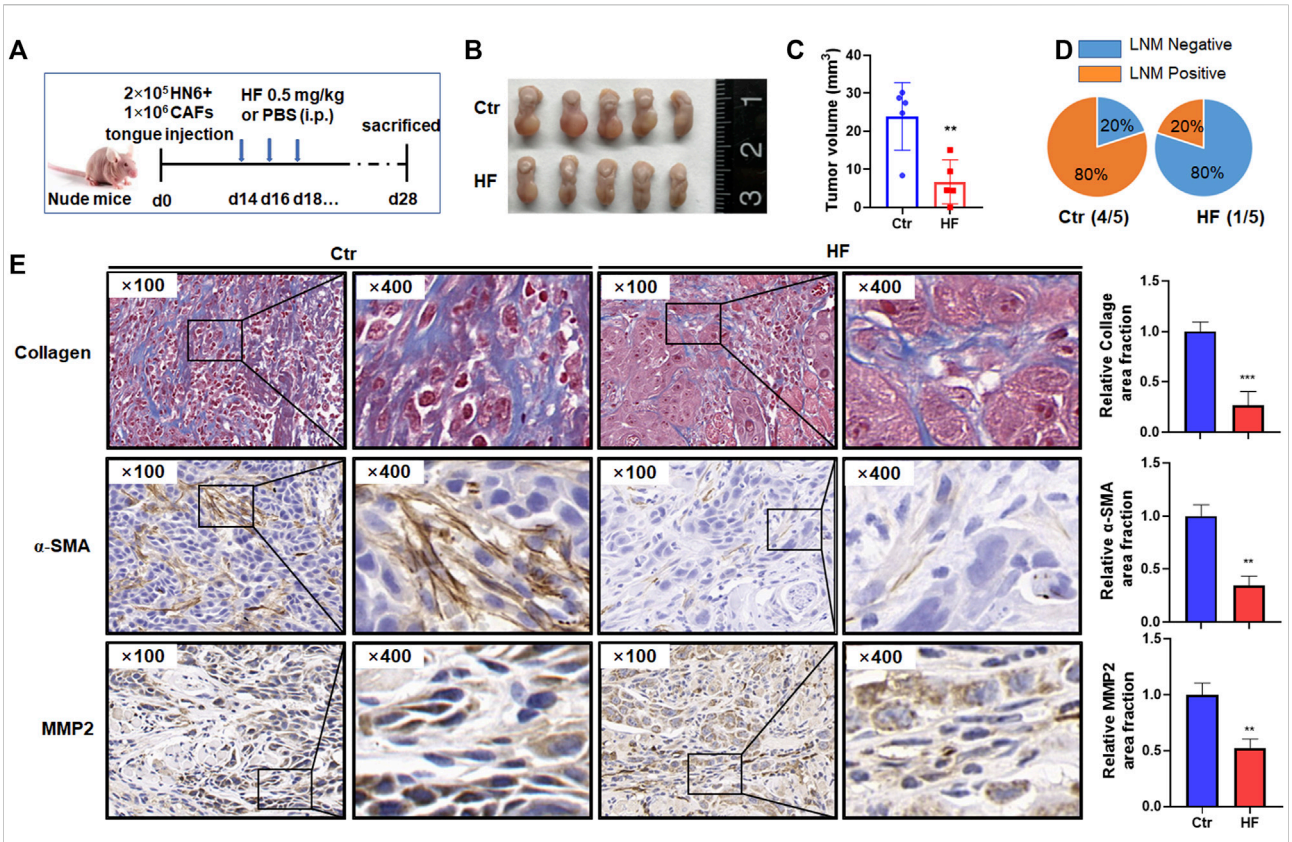

FIGURE 6
Halofuginone decreased tumor growth, LNM, CAF population, MMP2 expression and collagen deposition *in vivo*. **(A)** Experimental design for the *in vivo* study. Female Balb/c nude mice (4–6 weeks) successfully established tongue tumor were randomly divided into two groups: the control group (PBS, n = 5) and the HF treatment group (n = 5). The treatment group was intraperitoneally injected with 0.5 mg/kg HF every other day for 14 days. Tumor measurement **(B,C)** and LNM percentage **(D)** were made after mice were sacrificed on day 28th. **(E)** Masson staining was conducted to determine the collagen deposition in tumor stroma. Immunohistochemistry was used to evaluate the α-SMA and MMP2 protein levels. **:$p < 0.01$, ***:$p < 0.001$.

β/Smad2/3 signaling pathway but active the ERK pathway. In fact, the signaling pathway by which HF affecting on remains controversial. Roffe et al. (2010) found that HF inhibited Smad3 phosphorylation in muscle cells was due, at least in part, to HF-dependent activation of ERK, JNK and p38. Zeng et al. (2017) suggested that HF treatment robustly suppressed the TNF-α-induced phosphorylation of p38 and JNK, but didn't effluence ERK activation in fibroblast-like synoviocytes. However, Li et al. (2021) demonstrated that HF inhibited cancer cell proliferation by downregulating ERK phosphorylation in lung cancer cells. Thus, the effect of HF on ERK phosphorylation in different environments is not the same. Our results demonstrated that HF inhibits the proliferation activity of CAFs and the expression of malignant phenotypic markers through the TGF-β/Smad2/3 signaling pathway. Meanwhile, HF upregulated the phosphorylation of ERK1/2 in CAFs.

Taken together, we believe that HF can inhibit the migration and invasion of OSCC by acting on CAFs. Our results will provide new ideas for HF treatment of postoperative recurrence and metastasis of OSCC.

Data availability statement

The original contributions presented in the study are included in the article/Supplementary Material, further inquiries can be directed to the corresponding authors.

Ethics statement

The studies involving human participants were reviewed and approved by Ethics committee of Nanjing Stomatological Hospital, Medical School of Nanjing University. The patients/participants provided their written informed consent to participate in this study. The animal study was reviewed and approved by Animal Research Committee of Medical College Affiliated to Nanjing University.

Author contributions

DW and YS designed the study and wrote the manuscript. DW, MT, YS, YF, LD, XZ, and YJ did *in vitro* and *in vivo* experiments analyzed the data. YS, YN, and GS revised the manuscript.

Funding

This study was supported by the National Natural Science Foundation of China (No. 82173159, 82002865, 81902759, and 81902754), Nanjing Medical Science and Technique Development Foundation (Nos. YKK20151 and YKK19091) and the Key Research and Development Projects in Jiangsu Province (No. BE2020628).

Conflict of interest

The authors declare that the research was conducted in the absence of any commercial or financial relationships that could be construed as a potential conflict of interest.

Publisher's note

Supplementary material

The Supplementary Material for this article can be found online at: https://www.frontiersin.org/articles/10.3389/fphar.2022.1056337/full#supplementary-material

SUPPLEMENTARY FIGURE S1
Effects of HF-treated CAFs on the proliferation, migration, and invasion of HSC3 cells. **(A)** CM had no effect on the proliferation of HSC3 cells. **(B)** CM treated with high-concentration (100 nM) HF could significantly inhibit the migration of HSC3 cells (100×). Transwell experiments showed that HF-treated CAFs significantly inhibit tumor migration **(C)** and invasion **(D)**. *:$p < 0.05$, **:$p < 0.01$, ***:$p < 0.001$.

References

Chen, J., Ding, Z. Y., Li, S., Liu, S., Xiao, C., Li, Z., et al. (2021a). Targeting transforming growth factor-β signaling for enhanced cancer chemotherapy. *Theranostics* 11 (3), 1345–1363. doi:10.7150/thno.51383

Chen, S. H., Hsiao, S. Y., Chang, K. Y., and Chang, J. Y. (2021b). New insights into oral squamous cell carcinoma: From clinical aspects to molecular tumorigenesis. *Int. J. Mol. Sci.* 22 (5), 2252. doi:10.3390/ijms22052252

Daugschies, A., Gässlein, U., Rommel, M., and Gasslein, U. (1998). Comparative efficacy of anticoccidials under the conditions of commercial broiler production and in battery trials. *Vet. Parasitol.* 76 (3), 163–171. doi:10.1016/s0304-4017(97)00203-3

Demiroglu-Zergeroglu, A., Turhal, G., Topal, H., Ceylan, H., Donbaloglu, F., Karadeniz Cerit, K., et al. (2020). Anticarcinogenic effects of halofuginone on lung-derived cancer cells. *Cell. Biol. Int.* 44 (9), 1934–1944. doi:10.1002/cbin.11399

Ding, L., Ren, J., Zhang, D., Li, Y., Huang, X., Hu, Q., et al. (2018). A novel stromal lncRNA signature reprograms fibroblasts to promote the growth of oral squamous cell carcinoma via LncRNA-CAF/interleukin-33. *Carcinogenesis* 39 (3), 397–406. doi:10.1093/carcin/bgy006

Dumont, N., Liu, B., Defilippis, R. A., Chang, H., Rabban, J. T., Karnezis, A. N., et al. (2013). Breast fibroblasts modulate early dissemination, tumorigenesis, and metastasis through alteration of extracellular matrix characteristics. *Neoplasia* 15 (3), 249–262. doi:10.1593/neo.121950

Elahi-Gedwillo, K. Y., Carlson, M., Zettervall, J., and Provenzano, P. P. (2019). Antifibrotic therapy disrupts stromal barriers and modulates the immune landscape in pancreatic ductal adenocarcinoma. *Cancer Res.* 79 (2), 372–386. doi:10.1158/0008-5472.Can-18-1334

Erdogan, B., and Webb, D. J. (2017). Cancer-associated fibroblasts modulate growth factor signaling and extracellular matrix remodeling to regulate tumor metastasis. *Biochem. Soc. Trans.* 45 (1), 229–236. doi:10.1042/bst20160387

Haga, K., Yamazaki, M., Maruyama, S., Kawaharada, M., Suzuki, A., Hoshikawa, E., et al. (2021). Crosstalk between oral squamous cell carcinoma cells and cancer-associated fibroblasts via the TGF-β/SOX9 axis in cancer progression. *Transl. Oncol.* 14 (12), 101236. doi:10.1016/j.tranon.2021.101236

Jin, M. L., Park, S. Y., Kim, Y. H., Park, G., and Lee, S. J. (2014). Halofuginone induces the apoptosis of breast cancer cells and inhibits migration via downregulation of matrix metalloproteinase-9. *Int. J. Oncol.* 44 (1), 309–318. doi:10.3892/ijo.2013.2157

Kalluri, R. (2016). The biology and function of fibroblasts in cancer. *Nat. Rev. Cancer* 16 (9), 582–598. doi:10.1038/nrc.2016.73

Kim, H., Choi, P., Kim, T., Kim, Y., Song, B. G., Park, Y. T., et al. (2021). Ginsenosides Rk1 and Rg5 inhibit transforming growth factor-β1-induced epithelial-mesenchymal transition and suppress migration, invasion, anoikis resistance, and development of stem-like features in lung cancer. *J. Ginseng Res.* 45 (1), 134–148. doi:10.1016/j.jgr.2020.02.005

Li, H., Zhang, J., Chen, S. W., Liu, L. L., Li, L., Gao, F., et al. (2015). Cancer-associated fibroblasts provide a suitable microenvironment for tumor development and progression in oral tongue squamous cancer. *J. Transl. Med.* 13, 198. doi:10.1186/s12967-015-0551-8

Li, H., Zhang, Y., Lan, X., Yu, J., Yang, C., Sun, Z., et al. (2021). Halofuginone sensitizes lung cancer organoids to cisplatin via suppressing PI3K/AKT and MAPK signaling pathways. *Front. Cell. Dev. Biol.* 9, 773048. doi:10.3389/fcell.2021.773048

Lu, Z., Ding, L., Ding, H., Hao, F., Pu, Y., Wang, Y., et al. (2019). Tumor cell-derived TGF-β at tumor center independently predicts recurrence and poor survival in oral squamous cell carcinoma. *J. Oral Pathol. Med.* 48 (8), 696–704. doi:10.1111/jop.12888

Luo, L., Gao, Y., Yang, C., Shao, Z., Wu, X., Li, S., et al. (2018). Halofuginone attenuates intervertebral discs degeneration by suppressing collagen I production and inactivating TGFβ and NF-κB pathway. *Biomed. Pharmacother.* 101, 745–753. doi:10.1016/j.biopha.2018.01.100

Marty, P., Chatelain, B., Lihoreau, T., Tissot, M., Dirand, Z., Humbert, P., et al. (2021). Halofuginone regulates keloid fibroblast fibrotic response to TGF-β induction. *Biomed. Pharmacother.* 135, 111182. doi:10.1016/j.biopha.2020.111182

McGaha, T. L., Phelps, R. G., Spiera, H., and Bona, C. (2002). Halofuginone, an inhibitor of type-I collagen synthesis and skin sclerosis, blocks transforming-growth-factor-beta-mediated Smad3 activation in fibroblasts. *J. Investig. Dermatol.* 118 (3), 461–470. doi:10.1046/j.0022-202x.2001.01690.x

Mesia, R., Iglesias, L., Lambea, J., Martínez-Trufero, J., Soria, A., Taberna, M., et al. (2021). SEOM clinical guidelines for the treatment of head and neck cancer (2020). *Clin. Transl. Oncol.* 23, 913–921. doi:10.1007/s12094-020-02533-1

Ping, Q., Yan, R., Cheng, X., Wang, W., Zhong, Y., Hou, Z., et al. (2021). Cancer-associated fibroblasts: Overview, progress, challenges, and directions. *Cancer Gene Ther.* 28, 984–999. doi:10.1038/s41417-021-00318-4

Qin, Y., Zheng, X., Gao, W., Wang, B., and Wu, Y. (2021). Tumor microenvironment and immune-related therapies of head and neck squamous cell carcinoma. *Mol. Ther. Oncolytics* 20, 342–351. doi:10.1016/j.omto.2021.01.011

Roffe, S., Hagai, Y., Pines, M., and Halevy, O. (2010). Halofuginone inhibits Smad3 phosphorylation via the PI3K/akt and MAPK/ERK pathways in muscle cells: Effect on myotube fusion. *Exp. Cell. Res.* 316 (6), 1061–1069. doi:10.1016/j.yexcr.2010.01.003

Siegel, R. L., Miller, K. D., Fuchs, H. E., and Jemal, A. (2021). Cancer statistics, 2017. *Ca. Cancer J. Clin.* 71 (1), 7–30. doi:10.3322/caac.21387

Wang, C., Zhu, J. B., Yan, Y. Y., Zhang, W., Gong, X. J., Wang, X., et al. (2020a). Halofuginone inhibits tumorigenic progression of 5-FU-resistant human colorectal cancer HCT-15/FU cells by targeting miR-132-3p *in vitro*. *Oncol. Lett.* 20 (6), 385. doi:10.3892/ol.2020.12248

Wang, Y., Jing, Y., Ding, L., Zhang, X., Song, Y., Chen, S., et al. (2019). Epiregulin reprograms cancer-associated fibroblasts and facilitates oral squamous cell carcinoma invasion via JAK2-STAT3 pathway. *J. Exp. Clin. Cancer Res.* 38 (1), 274. doi:10.1186/s13046-019-1277-x

Wang, Y., Xie, Z., and Lu, H. (2020b). Significance of halofuginone in esophageal squamous carcinoma cell apoptosis through HIF-1α-FOXO3a pathway. *Life Sci.* 257, 118104. doi:10.1016/j.lfs.2020.118104

Zeng, S., Wang, K., Huang, M., Qiu, Q., Xiao, Y., Shi, M., et al. (2017). Halofuginone inhibits TNF-α-induced the migration and proliferation of fibroblast-like synoviocytes from rheumatoid arthritis patients. *Int. Immunopharmacol.* 43, 187–194. doi:10.1016/j.intimp.2016.12.016

Zhang, X., Dong, Y., Zhao, M., Ding, L., Yang, X., Jing, Y., et al. (2020). ITGB2-mediated metabolic switch in CAFs promotes OSCC proliferation by oxidation of NADH in mitochondrial oxidative phosphorylation system. *Theranostics* 10 (26), 12044–12059. doi:10.7150/thno.47901

frontiers | Frontiers in Pharmacology

TYPE Original Research
PUBLISHED 07 December 2022
DOI 10.3389/fphar.2022.1064032

OPEN ACCESS

EDITED BY
Qianming Du,
Nanjing Medical University, China

REVIEWED BY
Jing Ji,
Jiangsu Ocean Universiity, China
Liang Ding,
Nanjing University, China
Bin Dong,
China Pharmaceutical University, China

*CORRESPONDENCE
Jun Zhang,
junzhang301@163.com
Shi-ming Yang,
shm_yang@163.com
Fang-yuan Wang,
fangyuanwang05@163.com

†These authors have contributed equally to this work

SPECIALTY SECTION
This article was submitted to Pharmacology of Anti-Cancer Drugs, a section of the journal Frontiers in Pharmacology

RECEIVED 07 October 2022
ACCEPTED 24 November 2022
PUBLISHED 07 December 2022

CITATION
Xue X-m, Liu Y-y, Chen X-m, Tao B-y, Liu P, Zhou H-w, Zhang C, Wang L, Jiang Y-k, Ding Z-w, Shen W-d, Zhang J, Yang S-m and Wang F-y (2022), Pan-cancer analysis identifies NT5E as a novel prognostic biomarker on cancer-associated fibroblasts associated with unique tumor microenvironment. *Front. Pharmacol.* 13:1064032. doi: 10.3389/fphar.2022.1064032

Pan-cancer analysis identifies NT5E as a novel prognostic biomarker on cancer-associated fibroblasts associated with unique tumor microenvironment

Xin-miao Xue[1,2†], Yu-yang Liu[1,3†], Xue-min Chen[1,2†], Bing-yan Tao[1,3], Peng Liu[1,2], Han-wen Zhou[1,2], Chi Zhang[1,4], Li Wang[1,2], Yu-ke Jiang[1,2], Zhi-wei Ding[1,2], Wei-dong Shen[2], Jun Zhang[3]*, Shi-ming Yang[2]* and Fang-yuan Wang[2]*

[1]Medical School of Chinese People's Liberation Army (PLA), Beijing, China, [2]Senior Department of Otolaryngology-Head & Neck Surgery, Chinese People's Liberation Army (PLA) General Hospital, National Clinical Research Center for Otolaryngologic Diseases, State Key Lab of Hearing Science, Beijing Key Lab of Hearing Impairment Prevention and Treatment, Ministry of Education, Beijing, China, [3]Department of Neurosurgery, Chinese People's Liberation Army (PLA) General Hospital, Beijing, China, [4]The Zhantansi Outpatient Department of Central Medical Branch of People's Liberation Army (PLA) General Hospital Beijing, China

Background: Ecto-5′-nucleotidase (NT5E) encodes the cluster of differentiation 73 (CD73), whose overexpression contributes to the formation of immunosuppressive tumor microenvironment and is related to exacerbated prognosis, increased risk of metastasis and resistance to immunotherapy of various tumors. However, the prognostic significance of NT5E in pan-cancer is obscure so far.

Methods: We explored the expression level of NT5E in cancers and adjacent tissues and revealed the relationship between the NT5E expression level and clinical outcomes in pan-cancer by utilizing the UCSC Xena database. Then, correlation analyses were performed to evaluate the relationship between NT5E expression and immune infiltration level *via* EPIC, MCP-counter and CIBERSORT methods, and the enrichment analysis were employed to identify NT5E-interacting molecules and functional pathways. Furthermore, we conducted single-cell analysis to explore the potential role of NT5E on single-cell level based on the CancerSEA database. Meanwhile, gene set enrichment analysis (GSEA) in single-cell level was also conducted in TISCH database and single-cell signature explorer was utilized to evaluate the epithelial-mesenchymal transition (EMT) level in each cell type.

Results: The expression level of NT5E was aberrant in almost all cancer types, and was correlated with worse prognosis in several cancers. Notably, NT5E overexpression was related to worse overall survival (OS) in pancreatic adenocarcinoma (PAAD), head and neck squamous cell carcinoma (HNSC), mesothelioma (MESO), stomach adenocarcinoma (STAD), uveal melanoma (UVM) and cervical squamous cell carcinoma and endocervical adenocarcinoma (CESC) ($p < 0.01$). NT5E-related immune microenvironment

analysis revealed that NT5E is associated positively with the degree of infiltration of cancer-associated fibroblasts (CAFs) and endothelial cells in most cancers. Enrichment analysis of cellular component (CC) demonstrated the critical part of NT5E played in cell-substrate junction, cell-substrate adherens junction, focal adhesion and external side of plasma membrane. Finally, single-cell analysis of NT5E illuminated that EMT function of CAFs was elevated in basal cell carcinoma (BCC), skin cutaneous melanoma (SKCM), HNSC and PAAD.

Conclusion: NT5E could serve as a potential prognostic biomarker for cancers. The potential mechanism may be related to the upregulated EMT function of CAFs, which provides novel inspiration for immunotherapy by targeting CAFs with high NT5E expression.

KEYWORDS

NT5E, CD73, pan-cancer analysis, cancer-associated fibroblast, immunotherapy, epithelial-mesenchymal transition

Highlights

1) NT5E could serve as an efficient prognostic biomarker in pan-cancer.
2) NT5E expression is positively related to cancer-associated fibroblasts (CAFs) and endothelial cells infiltration in pan-cancer.
3) NT5E is highly expressed in the endothelia cells and CAFs in pan-cancer.
4) CAFs may play an important role in epithelial-mesenchymal transition (EMT) of various tumor species, which may be a novel target for immunotherapy.

1 Introduction

Ecto-5′-nucleotidase (NT5E), namely cluster of differentiation 73 (CD73), is a glycosylphosphatidylinositol-anchored cell surface protein. Encoded by the NT5E gene, CD73 is widely distributed in the human body, including the central nervous system, cardiovascular system, and epithelial tissues (Thompson et al., 2004; Zimmermann et al., 2012; Jeong et al., 2020). Structurally, NT5E consists of three domains, including a glycosylated N-terminal domain and a C-terminal domain, which are responsible for metal binding and the catalytic function respectively, and an alpha helix connecting the aforementioned two domains (Buschette-Brambrink and Gutensohn, 1989; Fini et al., 2003). Functionally, NT5E possesses nucleosidase activity (Sträter, 2006), and could hydrolyze extracellular adenosine monophosphate (AMP) into adenosine (Kordas et al., 2018). Extracellular adenosine plays an important role in modulating inflammation regulation and tumor immunity (Antonioli et al., 2013; Allard et al., 2017a; Kordas et al., 2018; Boison and Yegutkin, 2019), where A_{2A} receptor ($A_{2A}R$)-mediated signaling pathway matters most (Colella et al., 2018). Adenosine can activate the immune suppressive effects, which is characterized by the inhibition of chemotaxis and proliferation function among T cells (Sitkovsky et al., 2004; Allard et al., 2014). Meanwhile, it has been demonstrated that adenosine promotes angiogenesis and inhibits the release of cytokines and the expression of adhesion molecules such as E-selectin (Bouma et al., 1996; Spychala, 2000), hinting that NT5E may be related to cell adhesion function (Henttinen et al., 2003). Furthermore, it has also been proved that NT5E could influence cell adhesion and migration performance by the molecular mechanism of tenascin C, one of the important factors among extracellular matrix (ECM) (Sadej and Skladanowski, 2012). Therefore, NT5E could promote tumor growth not only by accumulating adenosine to inhibit the antitumoral immune responses, but also by facilitating dissemination of cancer cells (Kordas et al., 2018).

According to previous studies, NT5E has been detected among various tumor entities, including melanoma (Sadej et al., 2006a; Sadej et al., 2006b; Wang et al., 2012), triple-negative breast cancer (Allard et al., 2014; Buisseret et al., 2018), colorectal cancer (Liu et al., 2012), and non-small cell lung cancer (Inoue et al., 2017). Furthermore, it is not only expressed on malignant cells, but also on several immune cells such as regulatory T cells (Tregs) (Alam et al., 2009), myeloid-derived suppressor cells (MDSCs) (Ryzhov et al., 2011), dendritic cells (DCs) (Berchtold et al., 1999) and natural killer (NK) cells (Neo et al., 2020), which could result in more obvious accumulation of immunosuppressive adenosine and lead to the downregulation of the T cell immune responses (Saldanha-Araujo et al., 2011), and it has been illustrated that $NT5E^{+}$ NK cells could inhibit T cell activity by upregulating interleukin-10 (IL-10) and transforming growth factor-β (TGF-β) production (Neo et al., 2020). Moreover, adenosinergic $A_{2A}R$

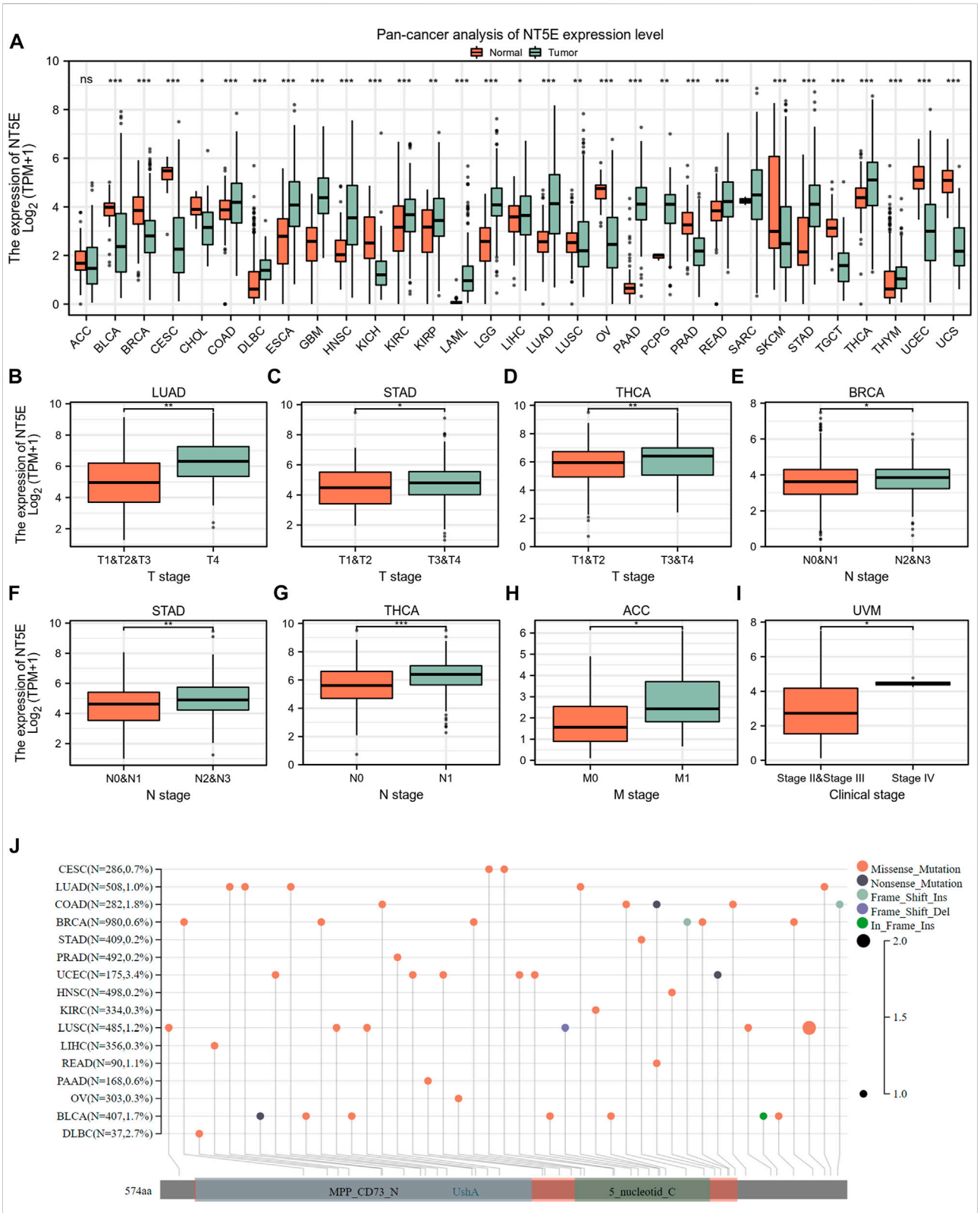

FIGURE 1
Basic information of NT5E. **(A)** The expression level of NT5E between tumor and normal tissues in each cancer based on the integrated data from TCGA and GTEx databases. **(B)** The expression level of NT5E between T1 & T2 & T3 and T4 stage in LUAD. **(C)** The expression level of NT5E between T1 & T2 and T3 & T4 stage in STAD. **(D)** The expression level of NT5E between T1 & T2 and T3 & T4 stage in THCA. **(E)** The expression level of NT5E between N0 & N1 and N2 & N3 stage in BRCA. **(F)** The expression level of NT5E between N0 & N1 and N2 & N3 stage in STAD. **(G)** The expression level of NT5E between N0 and N1 stage in THCA. **(H)** The expression level of NT5E between M0 and M1 stage in ACC. **(I)** The expression level of NT5E between clinical stage II & stage III and clinical stage IV in UVM. **(J)** NT5E abrupt landscape map in pan-cancer study according to the cBioPortal database (ns, $p \geq 0.05$, *$p < 0.05$, **$p < 0.01$, ***$p < 0.001$).

were also expressed on DCs, MDSCs, NK cells, and macrophages, indicating that the function of these regulatory immune cells could also be inhibited by adenosine (Allard et al., 2016; Kalekar et al., 2016; Young et al., 2016; Kalekar and Mueller, 2017).

It has been illustrated that adenosine triphosphate (ATP) concentration is about hundreds of thousands of times higher in the tumor microenvironment (TME) than the non-tumoral extracellular tissues (Zimmermann, 2000; Pellegatti et al., 2008). ATP is hydrolyzed to AMP, and lastly to adenosine by plasma membrane nucleotidases. According to previous studies, adenosine-mediated immunosuppression is a crucial part in the TME (Leone and Emens, 2018), which was constructed by vascular endothelial cells, fibroblast cells, and many types of innate and adaptive immune cells, together with ECM as well as multiple extracellular soluble molecules (cytokines, chemotactic factor, growth factors, etc.) (Binnewies et al., 2018). Furthermore, TME complexity is an important part in the differentiation of cold tumors and hot tumors. The feature of hot tumors is a high T cell infiltration level and abundant immune active molecular signatures, while cold tumors show distinctive characteristic of T cell absence (Gajewski, 2015). Thus, the immunosuppressive environment of cold tumors exhibited resistant to numerous immune checkpoint blockade therapies (Quail and Joyce, 2017).

There are several components correlated with the maintenance of an immunosuppressive environment, including some molecules like TGF-β, epidermal growth factor (EGF) and adenosine (Wei et al., 2022), and several immunosuppressive cells, including Tregs, tumor-associated macrophages (TAMs), endothelial cells, and cancer-associated fibroblasts (CAFs) (Zhu et al., 2022). In particular, CAFs may correlate with the enhancement of tumor phenotypes by regulating cancer cell proliferation and invasion and ECM remodeling (Costa et al., 2014; Gascard and Tlsty, 2016; Gentric et al., 2017). It has been validated that CAFs could secrete a vast amount of cytokines, including hepatocyte growth factor, EGF, connective tissue growth factor, insulin-like growth factor. All these cytokines could function directly on the surrounding cells and facilitate ECM reprogramming. Meanwhile, CAFs also secrete extracellular vesicles, metabolites, ECM components and ECM-remodeling enzymes (Jacob et al., 2012). Consequently, CAFs were considered to play a long-term role in the tumor development from tumorigenesis to cancer metastasis (Cirri and Chiarugi, 2011; Marsh et al., 2013; Kalluri, 2016).

In our previous study, we have concluded that NT5E could serve as an independent prognostic indicator for head and neck squamous cell carcinoma (HNSC) (Chen et al., 2022). Similarly, in pancreas, prostate and bladder cancer, NT5E has also been validated to correlate with tumor development and invasion (Yang et al., 2013; Mandapathil et al., 2018; Koivisto et al., 2019; Zhou et al., 2019; Chen et al., 2022). In detail, for gastric cancer patients, CD73 may serve as a regulator in RICS/RhoA-LIMK-cofilin signaling pathway by its extracellular function in adenosinergic pathway, and then promote β-catenin-induced epithelial-mesenchymal transition (EMT) process, which is correlated with metastasis property of tumor cells (Xu et al., 2020; Goulioumis and Gyftopoulos, 2022). In our study, the enrichment analyses also indicated that NT5E may be related to EMT and metastasis during HNSC progression. Furthermore, HNSC-related immune infiltration analysis and single-cell type analysis revealed that NT5E expression was positively related to CAFs infiltration in HNSC (Chen et al., 2022), which is in line with the previous conclusion that NT5E expression is related to tumor migration and invasion (Costa et al., 2014).

Although there is abundant evidence indicating that the expression level of NT5E is related to clinical outcomes and the prognosis in certain tumors, several questions still remain suspension, including the expression landscape of NT5E among various tumor types, the certain cell types expressing NT5E, and the potential signal pathways consisting NT5E in tumor growth and metastasis. To the best of our knowledge, the pan-cancer analysis of NT5E is still a virgin land. Thus, in this study, we performed NT5E expression analysis and prognosis analysis in pan-cancer, and explored the potential role of NT5E in the TME and the EMT function of CAFs, so as to provide novel clues for immunotherapy against malignant tumors.

2 Materials and methods

2.1 Dataset acquisition and normalization

The data of mRNA expression profile and clinical outcomes of patients (TCGA pan-cancer cohort) or normal tissues (GTEx database) were acquired from the UCSC Xena database (https://xenabrowser.net/datapages/). By applying the transcripts per million (TPM) method, we normalized the raw data. Then we employed log2 (TPM+1) transformation for the subsequent analyses. The information of genomic alteration frequency about NT5E in the 33 cancer types were acquired from the cBioPortal database (http://cbioportal.org).

2.2 NT5E expression analysis

Based on the mRNA expression profile obtained from UCSC Xena database, the NT5E expression level was compared between tumors and corresponding normal tissues. Totally, 31 types of tumors were included in this analysis, except for mesothelioma (MESO) and uveal melanoma (UVM), because of unavailability of corresponding normal tissues data. Besides, NT5E expression in patients stratified by different characteristics were also compared. The R software (Version 3.6.3) was used for statistical analysis with "ggplot2" package adopted for visualization. Moreover, the representative NT5E immunohistochemistry (IHC) staining pictures were retrieved from the Human Protein Atlas (HPA) on line database (http://www.proteinatlas.org).

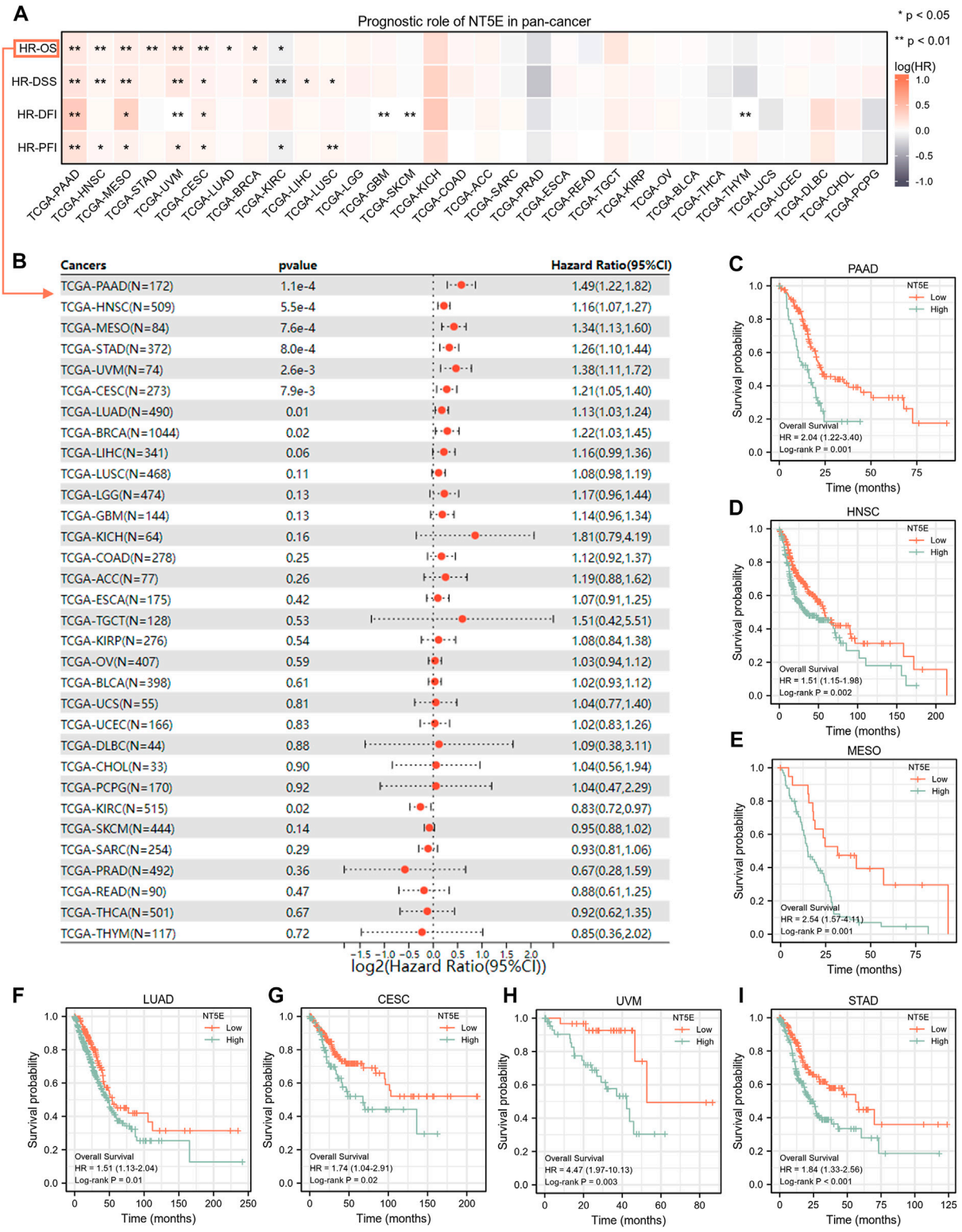

FIGURE 2
(A) the relationship between expression level of NT5E and overall survival (OS), disease-specific survival (DSS), disease-free interval (DFI) and progression-free interval (PFI) through the univariate Cox regression and Kaplan-Meier models. Red represents that NT5E is a risk factor, and gray indicates a protective factor related to prognosis. Only *p* values < 0.05 were shown. **(B)** The forest plot showed the prognostic value of NT5E in cancers using univariate Cox regression method. **(C–I)** Kaplan-Meier overall survival curves of NT5E in PAAD (HR = 2.04; 95% CI = 1.22–3.40; $p = 0.001$) **(C)**, HNSC (HR = 1.51; CI = 1.51–1.98; $p = 0.002$) **(D)**, MESO (HR = 2.54; CI = 1.57–4.11; $p = 0.001$) **(E)**, LUAD (HR = 1.51; CI = 1.13–2.04; $p = 0.01$) **(F)**, CESC (HR = 1.74; CI = 1.04–2.91; $p = 0.02$) **(G)**, UVM (HR = 4.47; CI = 1.97–10.13; $p = 0.003$) **(H)**, and STAD (HR = 1.84; CI= 1.32–2.56; $p < 0.001$) **(I)** (*$p < 0.05$; **$p < 0.01$).

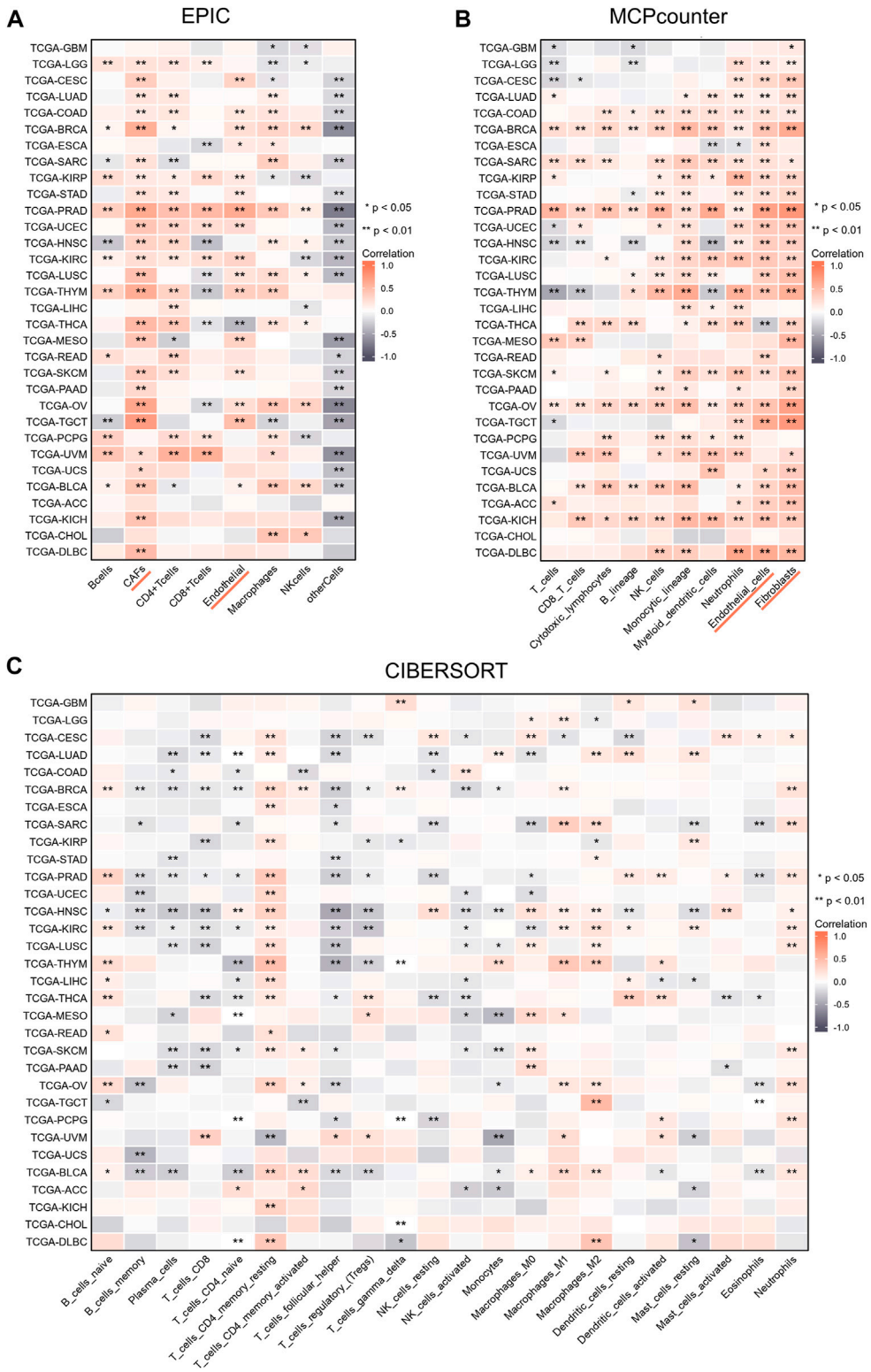

FIGURE 3
(A–C) The relationships of NT5E expression and the infiltration levels of immune cells in cancers based on EPIC **(A)**, MCPcounter **(B)**, and CIBERSORT methods **(C)**. Positive correlation in red and negative correlation in gray. (*$p < 0.05$; **$p < 0.01$).

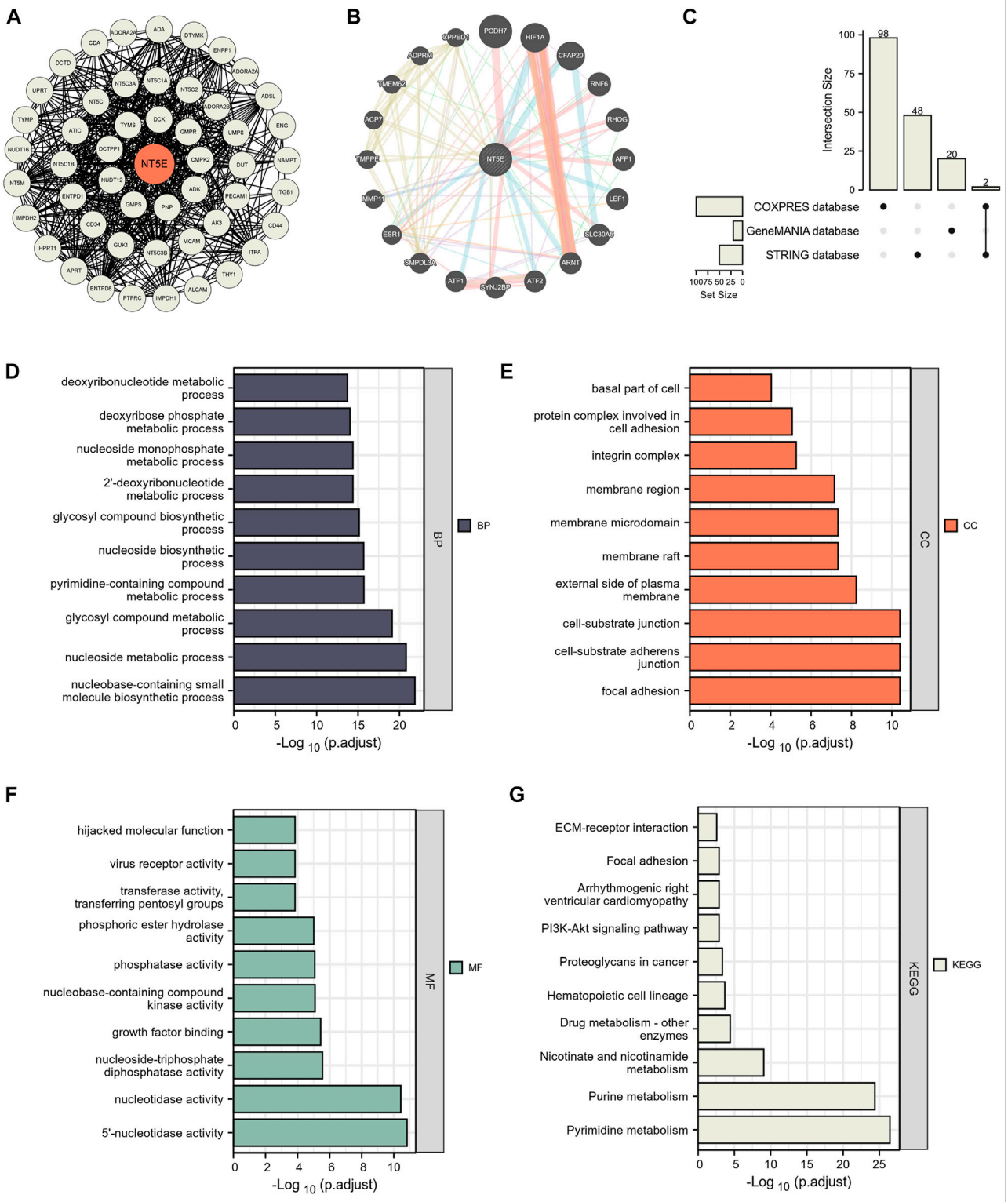

FIGURE 4
NT5E-related gene enrichment analysis. **(A)** We obtained the available experimentally determined NT5E -binding proteins using the STRING database. **(B)** We used the GeneMANIA website to get the 20 genes most closely related to NT5E. **(C)** 168 NT5E related molecules were selected from STRING database, GeneMANIA database and COXPRESdb. **(D–F)** The biological process **(D)**, cell components **(E)**, and molecular function **(F)** involved in NT5E in GO enrichment analyses. **(G)** the KEGG pathways enrichment analysis.

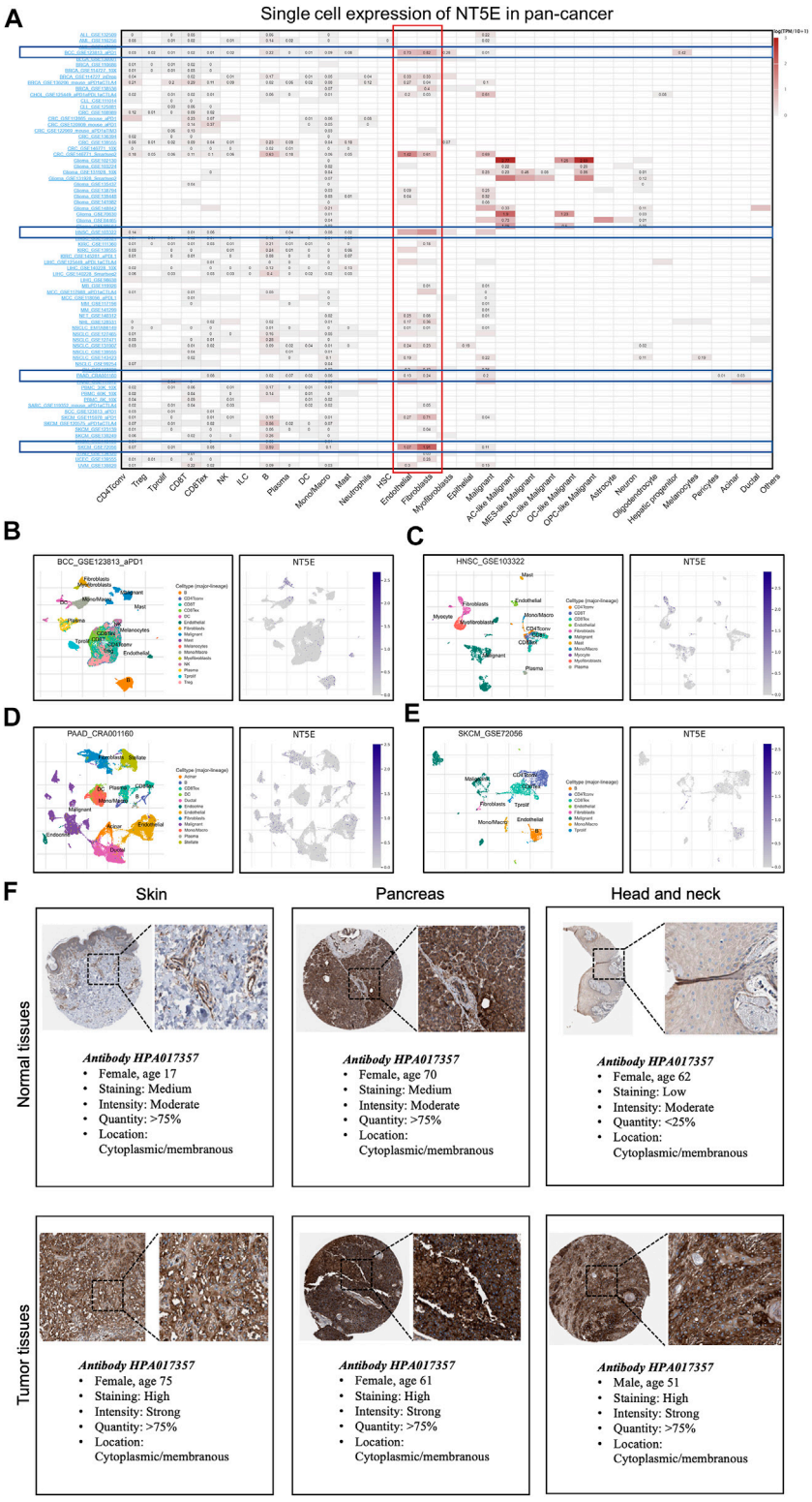

FIGURE 5
(A) Summary of NT5E expression of 33 cell types in 79 single cell databases. **(B–E)** Scatter plot showed the distributions of 10 different cell types (Left) and the NT5E expression levels (Right) of cells in the GSE123813_aPD1 BCC database **(B)**, GSE103322 HNSC database **(C)**, CRA001160 PAAD database **(D)** and GSE72056 SKCM database **(E)**. **(F)** Expression of the NT5E protein in several normal and tumor tissues.

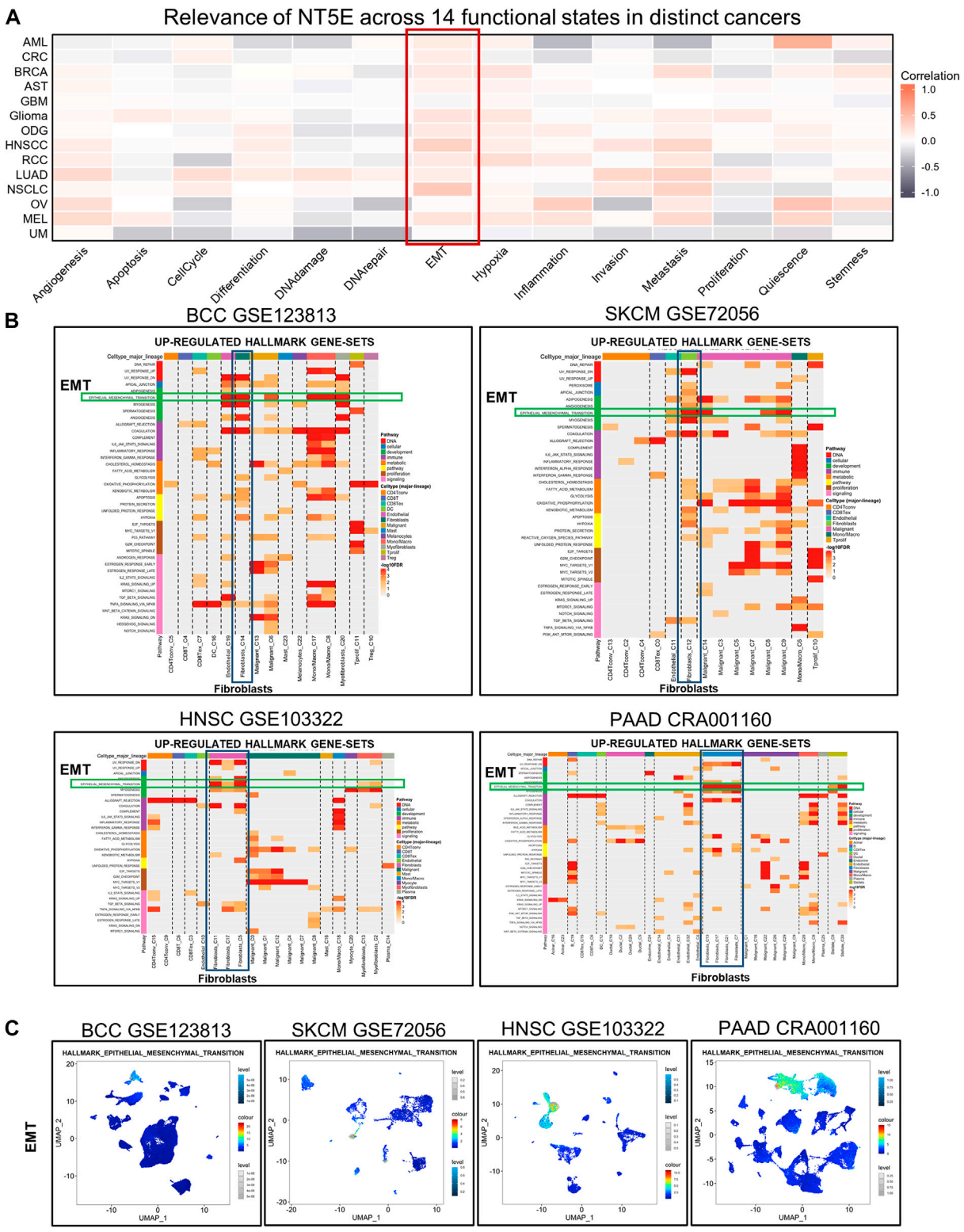

FIGURE 6
(A) Relevance of NT5E across 14 functional states in distinct cancers based on CancerSEA database. **(B)** The UP-REGULATED HALLMARK GENE-SETS enrichment analysis of NT5E in pan-cancer. **(C)** EMT in multiple cell subsets were obtained using the single-cell Signature Explorer function in the GSEA module of TISCH database.

2.3 Single-cell analysis of NT5E

To uncover the potential role of NT5E on single-cell level, we used the CancerSEA database (http://biocc.hrbmu.edu.cn/CancerSEA/home.jsp) to reveal the relationship between NT5E expression level and 14 function status in distinct cancers. Moreover, the Tumor Immune Single-cell Hub (TISCH) database (http://tisch.comp-genomics.org/home/) were employed to quantify the expression level of NT5E in different cell type. Gene set enrichment analysis (GSEA) in single-cell level was also conducted in TISCH database. Up-regulated hallmark gene-sets were visualized in the heatmap. Meanwhile, we used single-cell signature explorer to evaluate the level epithelial mesenchymal transition in each cell type.

2.4 Prognostic value of NT5E in pan-cancer

The prognosis information including overall survival (OS), disease-specific survival (DSS), disease-free interval (DFI) and progression-free interval (PFI) was obtained from the UCSC Xena database (https://xenabrowser.net/datapages/). The continuous variable of NT5E expression profile was utilized in the univariate Cox regression analysis. Meanwhile, the Kaplan–Meier curve was also used to evaluate the prognostic value of NT5E, and the cut-off point with the minimum *p*-value was selected for further analysis. The "survival" package was applied for statistical analysis, and the "survminer" package was used for visualization.

2.5 NT5E-related immune microenvironment analysis

For NT5E-related immune infiltration analysis, three methods (EPIC, MCP-counter, and CIBERSORT) were selected for further analysis. Correlation analyses were utilized to estimate the relationship between NT5E expression and immune infiltration level. All these immune infiltration levels of each sample were directly acquired from the TIMER2.0 database (http://timer.comp-genomics.org/). The heatmap constructed by the "ggplot2" R package was used for results visualization.

2.6 Identification of NT5E related molecules and functional enrichment

The top 50 NT5E-associated proteins were obtained *via* STRING database (https://cn.string-db.org/). Briefly, the parameters were selected as follows: evidence is selected for meaning network edges, all options were included for active interaction sources, and the medium confidence was chosen at 0.4 for minimum required interaction score. The Cytoscape software (Version 3.9.1) was utilized for visualization. Additionally, an NT5E-related gene-gene interaction (GGI) network was constructed using the GeneMANIA database (http://www.genemania.org), and the top 20 genes most closely to NT5E were involved in GGI. Besides, the top 100 co-expressed genes of NT5E were obtained from the COXPRESdb (Obayashi et al., 2019) (https://coxpresdb.jp/). The upset diagram was used to illustrate NT5E-related molecules from these three online databases and "UpSetR" R package was utilized for visualization. Totally, 168 NT5E related molecules were selected to perform enrichment analysis using the R package "clusterProfiler" and the "ggplot2" package was used for visualization.

2.7 Immunofluorescence staining

We collected supraglottic carcinoma specimens from the operating room of Chinese PLA General Hospital. All specimens were fixed with 4% formalin and embedded in paraffin. Seven serial sections with a thickness of 3 mm were made. After using high pressure method for antigen retrieval for 3 min, the sections were blocked with 10% goat serum (C0265, Beyotime, China) for 30 min in thermostat at 37°C, and incubated overnight at 4°C with smooth muscle actin (α-SMA/ACTA2) primary antibody at concentrations of 1:50 (CL594-14395, Proteintech, United States). Then, sections were rinsed with PBS for three times for 10 min each, and incubated with NT5E antibody at 1:50 (CL488-67789, Proteintech, United States) overnight at 4°C. The cy3-labeled goat anti-rabbit IgG (A0516, Beyotime, China) was added and incubated at room temperature for 1 h, followed by counterstaining with DAPI for 8 min. Whole slide imaging was operated by Pannoramic scan system (3DHISTECH, Hungary). The abovementioned procedures were approved by the Ethics Committee of Chinese PLA General Hospital (No. S2021-339-02). All of the patients or their legal guardians gave their informed consent to participate.

2.8 Statistical analysis

The Wilcoxon rank-sum test was employed to detect the statistical significance between two groups. Correlation analysis was analyzed by Spearman's correlation coefficient. All statistical analysis was performed using R software (version 3.6.3), and two-tailed $p < 0.05$ was considered as of statistical significance.

3 Results

3.1 NT5E was aberrantly expressed in pan-cancer

To illuminate the expression landscape of NT5E in cancer, we performed studies comparing NT5E mRNA expression level in cancers and normal tissues *via* TCGA and GTEx databases.

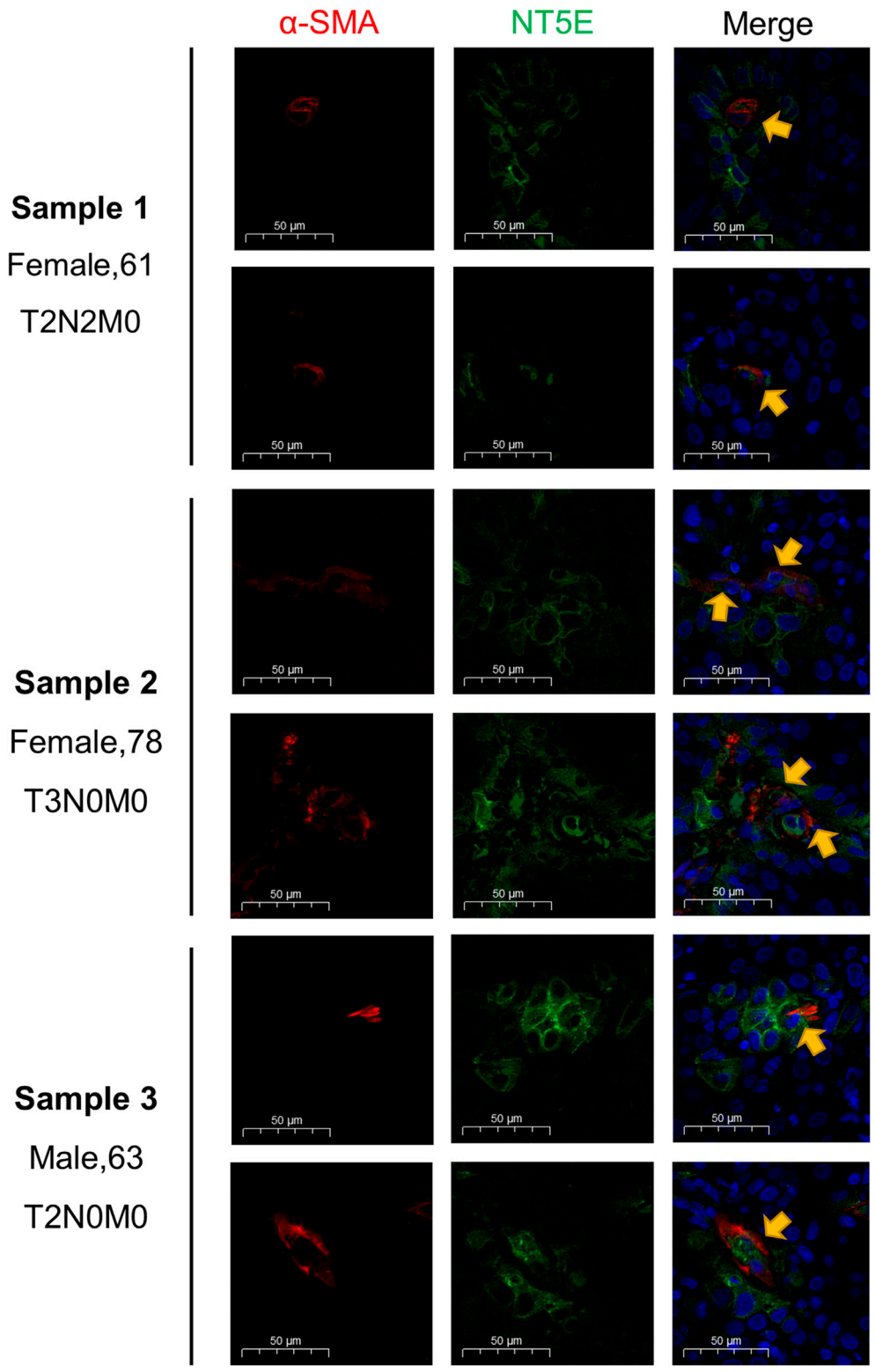

FIGURE 7
Validation of NT5E expression pattern on the supraglottic carcinoma specimens with various TNM-staging. Scale bar = 50 μm. Red stands for α-SMA expression, green stands for NT5E expression, and blue stands for nuclear staining by DAPI.

The results indicated that the expression level of NT5E is significantly aberrant in a variety of cancer types. It was up-regulated in tumoral tissues compared to normal tissues in colon adenocarcinoma (COAD), lymphoid neoplasm diffuse large B-cell lymphoma (DLBC), esophageal carcinoma (ESCA), glioblastoma multiforme (GBM), HNSC, kidney renal clear cell carcinoma (KIRC), kidney renal papillary cell carcinoma (KIRP), acute myeloid leukemia (LAML), brain lower grade glioma (LGG), lung adenocarcinoma (LUAD), pancreatic adenocarcinoma (PAAD), rectum adenocarcinoma (READ), stomach adenocarcinoma (STAD), thyroid carcinoma (THCA) and thymoma (THYM) ($p < 0.001$) (Figure 1A), while down-regulated in bladder Urothelial Carcinoma (BLCA), breast invasive carcinoma (BRCA), cervical squamous cell carcinoma and endocervical adenocarcinoma (CESC), kidney chromophobe (KICH), ovarian serous cystadenocarcinoma (OV), prostate adenocarcinoma (PRAD), skin cutaneous melanoma (SKCM), testicular germ cell tumors (TGCT), uterine corpus endometrial carcinoma (UCEC) and uterine carcinosarcoma (UCS) ($p < 0.001$) (Figure 1A).

Furthermore, in order to illustrate the relationship between NT5E overexpression and tumor progression, we employed studies to analyze the degree of NT5E expression in different pathological stages and revealed an aberrant difference in NT5E expression as the tumor progressed in adrenocortical carcinoma (ACC), uveal melanoma (UVM), LUAD, STAD, BRCA, and THCA. Firstly, NT5E expression is linked to cancer T stage, which was elevated in T4 stage compared with T1 & T2 & T3 stage in LUAD ($p < 0.01$) (Figure 1B), and was higher in T3 & T4 stage than T1 & T2 stage in STAD ($p < 0.05$) and THCA ($p < 0.01$) (Figures 1C,D). Secondly, expression levels of NT5E were also corelated with cancer N stage. We illustrated that the expression level of NT5E up-regulated in N2 & N3 stage in BRCA ($p < 0.05$) and STAD ($p < 0.01$) (Figures 1E,F), and up-regulated in N1 stage compared with N0 stage in THCA ($p < 0.001$) (Figure 1G). Finally, the expression level of NT5E is also different between M0 and M1 stage in ACC ($p < 0.05$) (Figure 1H), and difference between clinical stage II & III and clinical stage IV in UVM ($p < 0.05$) (Figure 1I). And then, we performed genomic alteration analysis of NT5E and the results illuminated that alterations of NT5E across pan-cancer were not universal (Figure 1J). Thus, we hypothesized that it may be more important to study the changes of NT5E expression in transcription levels.

3.2 NT5E could serve as an efficient prognostic biomarker in pan-cancer

We performed studies to validate the potential value of NT5E expression in clinical prognostic among pan-cancer patients derived from TCGA database. According to the univariate Cox regression analysis, NT5E expression was associated with a variety of prognostic indicators in a variety of tumors, and the overexpression of NT5E could strongly predict worse OS in pancreatic adenocarcinoma (PAAD), HNSC, mesothelioma (MESO), STAD, UVM, CESC ($p < 0.01$), LUAD, BRCA and KIRC ($p < 0.05$) (Figures 2A,B). Confounding characteristics selected with $p < 0.05$, we then conducted Kaplan-Meier survival analysis, which suggested that a higher NT5E expression was associated with poor survival outcomes in PAAD [hazard ratio (HR) = 2.04; 95% confidence interval (CI) = 1.22–3.40; $p = 0.001$), HNSC (HR = 1.51; CI = 1.51–1.98; $p = 0.002$), MESO (HR = 2.54; CI = 1.57–4.11; $p = 0.001$), LUAD (HR = 1.51; CI = 1.13–2.04; $p = 0.01$), CESC (HR = 1.74; CI = 1.04–2.91; $p = 0.02$), UVM (HR = 4.47; CI = 1.97–10.13; $p = 0.003$), and STAD (HR = 1.84; CI = 1.32–2.56; $p < 0.001$), emphasizing that overexpression of NT5E is related to poor prognosis in these cancers (Figures 2C–I).

3.3 NT5E expression was positively related to CAFs and endothelial cells infiltration in pan-cancer

We performed studies to analyze the relationship between the infiltration degree of the immune cells and NT5E expression by several algorithms. According to EPIC and MCPcounter algorithms, we observed that NT5E expression was positively related to CAFs and endothelial cells infiltration in almost all cancers (Figures 3A,B; $p < 0.01$). Furthermore, to reveal the relationship between more species immune cells infiltration situation and the expression level of NT5E, we employed related analysis by applying CIBERSORT algorithms, in which there are 22 kinds of cells. The results illustrated that the expression level of NT5E is positively correlated several immune cells infiltration in almost all cancers, such as memory $CD4^+$ T-Cells and M1-polarized macrophages, while negatively related to plasma cells and T follicular helper cells in pan-cancer (Figure 3C).

3.4 NT5E was related to cell adhesion function

We have confirmed that the expression degree of NT5E is corelated with the immune cell infiltration in the TME of several cancers. Thus, it is necessary to further explore the potential function of NT5E in the TME. We obtained numerous proteins that closely contacted with NT5E in functional level through the STRING database, in which the data was verified by experimental evidence. The protein interaction network was exhibited in Figure 4A, and the gene interaction network was exhibited in Figure 4B, which was analysed based on the GeneMANIA website. Furthermore, we performed GO and KEGG enrichment analysis based on 168 NT5E related molecules, which were selected from STRING database, GeneMANIA database and COXPRESdb (Figure 4C). The GO enrichment analysis revealed the biological

process (BP), cellular component (CC) and molecular function (MF), involved in NT5E (Figures 4D–F). Moreover, the result of KEGG enrichment analysis is exhibited in Figure 4G. It's worth noting that the cell components related to NT5E include cytoplasmic vesicle lumen, cell-substrate junction, cell-substrate adherens junction, focal adhesion and external side of plasma membrane (Figure 4E).

3.5 NT5E was highly expressed in the endothelia cells and CAFs in pan-cancer

We performed the single-cell analysis of NT5E to quantify the expression level of NT5E in different cell types (including immune cells, stromal cells, malignant cells, and functional cells), the results also showed that NT5E more likely expressed in the endothelia cells and CAFs in several cancers such as basal cell carcinoma (BCC), HNSC, PAAD and skin cutaneous melanoma (SKCM) (Figure 5A). Furthermore, the scatter plots also illustrated that NT5E is undoubtedly highly expressed in CAFs and endothelia cells in the tumor microenvironment in above four cancers (Figures 5B–E). Moreover, the *in situ* expression of NT5E was further analyzed using HPA databases based on IHC staining, in which NT5E expression is significantly higher in tumor tissues than normal tissues, and this phenomenon is all exhibited in skin, pancreas and head and neck tissues (Figure 5F).

3.6 CAFs might play an important role in epithelial-mesenchymal transition of various tumor species

Moreover, we estimated the cancer biology-related functional states of NT5E at single-cell sequencing level using CancerSEA Portal, the results exhibited that NT5E expression is positively correlated with EMT function in several cancers (Figure 6A). Then, we performed studies to obtain up-regulated Hallmark gene-sets in different cell subsets, and the results suggested that EMT function of CAFs was significantly up-regulated in multiple tumor species, including BCC, SKCM, HNSC, and PAAD (Figure 6B). Furthermore, we also found that the degree of EMT of CAFs cell subsets was higher than that of other cell subsets based on the GSEA module of TISCH database (Figure 6C). These results suggest that CAFs may play an important role in EMT of various tumor species.

3.7 *In-situ* immunofluorescence staining verified the NT5E expression on CAFs in HNSC specimens

The supraglottic carcinoma specimens with various TNM-staging were collected as representatives for HNSC samples, and the staining results were displayed in Figure 7. The expression abundance of NT5E was positively related to T staging. Besides, the immunofluorescence staining results revealed the co-expressed pattern of NT5E and α-SMA, a most commonly used CAFs marker.

4 Discussion

This study is an integrated pan-cancer analysis about the potential prognostic value of NT5E. We reported that the expression level of NT5E was elevated in many tumor types, such as ovarian cancer and colorectal tumor tissues (Gaudreau et al., 2016; Wu et al., 2016). The overexpression of NT5E was also associated with poor prognosis, and was related to tumor development and invasion in pancreas, prostate, bladder and head and neck cancer (Yang et al., 2013; Mandapathil et al., 2018; Koivisto et al., 2019; Zhou et al., 2019; Chen et al., 2022). In this study, not only did we illustrate that NT5E might serve as a negative prognostic biomarker for LUAD, STAD, BRCA and UVM, but also revealed that it is positively correlated with tumor stage in several cancers. The results of immunofluorescence staining, in our study, also uncovered that the expression level of NT5E was positively correlated with T staging in the supraglottic carcinoma, which is considered to belong to the typical HNSC. These results suggested that NT5E might facilitate tumor growth and tumor metastasis.

Tumor metastasis is a complex process manipulated by multiple mechanisms (Pantel and Brakenhoff, 2004; Quail and Joyce, 2013; López-Soto et al., 2017). One of the important mechanisms is that the primary tumors cells invade through the physical barrier, namely the basement membrane, and disseminate *via* the circulation system. In the process of tumor invasion, the epithelial cells also break through the basement membrane and separate from neighboring cells to damage adjacent cell layers. The reason lies in the acquirement of migratory and invasive properties through EMT (Thiery et al., 2009), during which the apical-basal polarity and cell-cell adhesion of epithelial cells were weakened, and thus transited into invasive mesenchymal cells (Du and Shim, 2016). Then, mesenchymal cells could invade through ECM, one of the essential components of TME, which is composed of collagen, elastin, fibronectin, hyaluronic acid, proteoglycans and glycoproteins, undertaking the task to support tissues by encapsulating cells (Otranto et al., 2012; Pickup et al., 2014; Willumsen et al., 2018). In this case, the tumor cells would lose cell-cell adhesion and thus acquire motility. Moreover, it has been reported that the circulating tumor cells, which are important precursors of cancer metastasis, could be allowed to escape from antimetastatic checkpoints to realize distant metastasis by the mechanism of EMT process (Xiang et al., 2022). In our study, the results of enrichment analysis also demonstrated the critical role of NT5E as a regulator of cell-substrate junction, cell-substrate adherens

junction, focal adhesion and external side of plasma membrane, and these functions are closely related to cell polarization and EMT (Thiery and Sleeman, 2006; Baronsky et al., 2017; Venhuizen et al., 2020), which plays an crucial role in cancer progression, especially tumor cell invasion (Son and Moon, 2010). Therefore, the pro-tumor function of NT5E may be related to facilitating the EMT of tumor cells.

Moreover, the metastatic potential of cancer cells is closely dependent on the TME. Notably, CAFs are one of the major components of the tumor stroma contributing significantly to the TME, which were differentiated from stromal fibroblast cells by the stimulation of paracrine growth factors secreted from tumor cells (Kalluri and Zeisberg, 2006; Tejada et al., 2006). Unlike normal stromal fibroblasts, CAFs could facilitate cancer cells survival (Martinez-Outschoorn et al., 2010), growth and progression (Orimo et al., 2005; Giannoni et al., 2010). It has been validated that CAFs secrete a number of cytokines, which could facilitate tumor cells invasion and metastasis by activating several signaling pathways (Ao et al., 2007; Kojima et al., 2010; Karagiannis et al., 2012; Yu et al., 2014; Shien et al., 2017; Gao et al., 2019). In addition, CAFs also play important roles in orchestrating the ECM in almost all cancers. It has been illustrated that ECM remodeling could also facilitate the invasion and migration of cancer cells, and cancer cells with the EMT phenotype make great contribution to this process by producing ECM-degrading proteases (Giannoni et al., 2010; Qiao et al., 2010). In our study, the results of enrichment analysis of NT5E may imply that it may be correlated with EMT during cancer progress. Moreover, we employed studies to gain elevated hallmark gene-sets in different cell subsets, and the results illuminated that EMT function of CAFs was elevated in BCC, SKCM, HNSC, and PAAD. Then, based on the GSEA module of TISCH database, the analysis results, also showed that the degree of EMT of CAFs was higher than that of other cell subsets. These results are consistent with the above conclusion that CAFs make great contribution to maintain tumor growth and development.

According to previous studies, a high level of CAFs infiltration was considered to make great contribute to an unfavorable clinical outcome of patients (Gieniec et al., 2019; Hosein et al., 2020; Piersma et al., 2020). Consequently, there are more and more attentions focused on the therapy targeted-CAFs, which is believed to be one of the complementary treatment strategies for cancer. The first strategy is to deplete CAFs directly by either transgenic technologies or immunotherapies (Özdemir et al., 2015). For example, the previous study revealed that a specific CAF subpopulation (referred to as CAF-S1) expressed NT5E could upregulate the power of Tregs to inhibit the proliferation of effector T cells (Costa et al., 2018; Givel et al., 2018), while this effect could be neutralize after using an anti-CD73 antibody (Magagna et al., 2021). Secondly, some molecules, including all-trans retinoic acid (ATRA) and calcipotriol, could promote CAFs to become normalized and adopt an inactive phenotype (Froeling et al., 2011). Moreover, CAFs could be used as a vehicle to deliver anticancer drugs, including TNF-related apoptosis-inducing ligand (TRAIL) or type I interferon (IFN) (Miao et al., 2017). Finally, the function of CAFs could be inhibited by regulating the activation of targeting crucial signals and effectors, such as chemokine and growth factor pathways (Giannoni et al., 2010; Albrengues et al., 2015). Interestingly, NT5E has also been considered as a novel checkpoint inhibitor target (Allard et al., 2017b). It has been illustrated that overexpression of NT5E could inhibit the immunosurveillance of immune cells, which may be correlated with immune evasion and tumor metastasis (Stagg et al., 2010; Leclerc et al., 2016). Moreover, tumor cell death could result in CAFs-NT5E overexpression *via* an adenosine-adenosinergic $A2_B$ receptor ($A_{2B}R$) mediated feedforward circuit, which could furtherly exacerbate the immunosuppressive environment (Yu et al., 2020). According to the results of our study, NT5E was related positively to the infiltration stage of CAFs in most cancers (Hu et al., 2020), and single-cell analysis also showed that NT5E was mainly expressed on the CAFs in several cancers such as BCC, HNSC, PAAD, and SKCM. Furthermore, in the supraglottic carcinoma specimens, we also illustrated that NT5E was co-expressed with α-SMA, which was one of the myofibroblast markers and expressed on CAFs (Orimo and Weinberg, 2007; Sharon et al., 2013). Thus, NT5E may be a crucial signal related to the activation of CAFs. High-NT5E expressed CAFs could serve as novel targets for immunotherapy. Thus, we performed correlation analyses between immune-related genes and NT5E expression level on pan-cancer level, and uncovered that the expression levels of several immunoinhibitors were positively correlated with NT5E expression, including kinase insert domain-containing receptor (KDR), interleukin-10 receptor B (IL10RB) and transforming growth factor-beta receptor 1 (TGFBR1) (Supplementary Figures S1, S2).

Still and all, there is no doubt that our research also has some limitations. Firstly, because the data used in this study was derived from online databases, which are characterized by open and imprecise, systematic bias may become an inevitable factor. Secondly, pan-cancer analysis is of distinct heterogeneity attributing to different cancer. Thirdly, the findings of the current investigation demand clinical trial-based validation in several cancer patients receiving high-NT5E-expression CAFs-targeting immunotherapies. Finally, more functional experiments such as flow cytometry and single cell RNA-seq are needed to further elucidate CAFs and NT5E contents in specific cancer.

5 Conclusion

In summary, this study is an integrated analysis of NT5E in pan-cancer. We illuminated that NT5E could serve as an efficient prognostic biomarker in pan-cancer, its expression level was positively related to CAFs and endothelial cells infiltration in pan-cancer. Moreover, NT5E is more likely expressed in the endothelia cells and CAFs in pan-cancer, and CAFs may play an important role in EMT of various tumor species. We concluded that the underlying mechanism of the NT5E pro-tumor effect

may be related to the up-regulated EMT function of CAFs, which may provide some information to study immune therapy targeted CAFs and NT5E.

Data availability statement

The original contributions presented in the study are included in the article/Supplementary Materials, further inquiries can be directed to the corresponding author/s.

Author contributions

X-mX, Y-yL, and X-mC undertook the task of conception, study design and bioinformatics analysis. B-yT, PL, H-wZ and CZ interpreted the data. LW, Y-kJ, Z-wD, and W-dS were responsible for acquisition of data. F-yW, S-mY, and JZ were responsible for a final approval of the version to be submitted. All authors contributed to and revised the final manuscript.

Funding

This work was supported by grants from the National key research and development program (Nos. 2019YFC0121302 and 2019YFC0840707) and the Beijing Nova Program (No. Z201100006820133).

Conflict of interest

The authors declare that the research was conducted in the absence of any commercial or financial relationships that could be construed as a potential conflict of interest.

Publisher's note

All claims expressed in this article are solely those of the authors and do not necessarily represent those of their affiliated organizations, or those of the publisher, the editors and the reviewers. Any product that may be evaluated in this article, or claim that may be made by its manufacturer, is not guaranteed or endorsed by the publisher.

Supplementary material

The Supplementary Material for this article can be found online at: https://www.frontiersin.org/articles/10.3389/fphar.2022.1064032/full#supplementary-material

References

Alam, M. S., Kurtz, C. C., Rowlett, R. M., Reuter, B. K., Wiznerowicz, E., Das, S., et al. (2009). CD73 is expressed by human regulatory T helper cells and suppresses proinflammatory cytokine production and Helicobacter felis-induced gastritis in mice. *J. Infect. Dis.* 199 (4), 494–504. doi:10.1086/596205

Albrengues, J., Bertero, T., Grasset, E., Bonan, S., Maiel, M., Bourget, I., et al. (2015). Epigenetic switch drives the conversion of fibroblasts into proinvasive cancer-associated fibroblasts. *Nat. Commun.* 6, 10204. doi:10.1038/Ncomms10204

Allard, B., Beavis, P. A., Darcy, P. K., and Stagg, J. (2016). Immunosuppressive activities of adenosine in cancer. *Curr. Opin. Pharmacol.* 29, 7–16. doi:10.1016/J.Coph.2016.04.001

Allard, B., Longhi, M. S., Robson, S. C., and Stagg, J. (2017). The ectonucleotidases CD39 and CD73: Novel checkpoint inhibitor targets. *Immunol. Rev.* 276 (1), 121–144. doi:10.1111/Imr.12528

Allard, B., Turcotte, M., and Stagg, J. (2014). Targeting CD73 and downstream adenosine receptor signaling in triple-negative breast cancer. *Expert Opin. Ther. Targets* 18 (8), 863–881. doi:10.1517/14728222.2014.915315

Allard, D., Turcotte, M., and Stagg, J. (2017). Targeting A2 adenosine receptors in cancer. *Immunol. Cell Biol.* 95 (4), 333–339. doi:10.1038/Icb.2017.8

Antonioli, L., Blandizzi, C., Pacher, P., and Hasko, G. (2013). Immunity, inflammation and cancer: a leading role for adenosine. *Nat. Rev. Cancer* 13 (12), 842–857. doi:10.1038/Nrc3613

Ao, M., Franco, O. E., Park, D., Raman, D., Williams, K., and Hayward, S. W. (2007). Cross-talk between paracrine-acting cytokine and chemokine pathways promotes malignancy in benign human prostatic epithelium. *Cancer Res.* 67 (9), 4244–4253. doi:10.1158/0008-5472.Can-06-3946

Baronsky, T., Ruhlandt, D., Brückner, B. R., Schafer, J., Karedla, N., Isbaner, S., et al. (2017). Cell-substrate dynamics of the epithelial-to-mesenchymal transition. *Nano Lett.* 17 (5), 3320–3326. doi:10.1021/Acs.Nanolett.7b01558

Berchtold, S., Ogilvie, A. L., Bogdan, C., Muhl-Zurbes, P., Schuler, G., et al. (1999). Human monocyte derived dendritic cells express functional P2X and P2Y receptors as well as ecto-nucleotidases. *FEBS Lett.* 458 (3), 424–428. doi:10.1016/S0014-5793(99)01197-7

Binnewies, M., Roberts, E. W., Kersten, K., Chan, V., Fearon, D. F., Merad, M., et al. (2018). Understanding the tumor immune microenvironment (TIME) for effective therapy. *Nat. Med.* 24 (5), 541–550. doi:10.1038/S41591-018-0014-X

Boison, D., and Yegutkin, G. G. (2019). Adenosine metabolism: Emerging concepts for cancer therapy. *Cancer Cell* 36 (6), 582–596. doi:10.1016/J.Ccell.2019.10.007

Bouma, M. G., Van Den Wildenberg, F. A., and Buurman, W. A. (1996). Adenosine inhibits cytokine release and expression of adhesion molecules by activated human endothelial cells. *Am. J. Physiol.* 270, C522–C529. doi:10.1152/Ajpcell.1996.270.2.C522

Buisseret, L., Pommey, S., Allard, B., Garaud, S., Bergeron, M., Cousineau, I., et al. (2018). Clinical significance of CD73 in triple-negative breast cancer: multiplex analysis of a phase III clinical trial. *Ann. Oncol.* 29 (4), 1056–1062. doi:10.1093/Annonc/Mdx730

Buschette-Brambrink, S., and Gutensohn, W. (1989). Human placental ecto-5'-nucleotidase: Isoforms and chemical crosslinking products of the membrane-bound and isolated enzyme. *Biol. Chem. Hoppe. Seyler.* 370 (1), 67–74. doi:10.1515/Bchm3.1989.370.1.67

Chen, X. M., Liu, Y. Y., Tao, B. Y., Xue, X. M., Zhang, X. X., Wang, L. L., et al. (2022). NT5E upregulation in head and neck squamous cell carcinoma: a novel biomarker on cancer-associated fibroblasts for predicting immunosuppressive tumor microenvironment. *Front. Immunol.* 13, 97. doi:10.3389/Fimmu.2022.975847

Cirri, P., and Chiarugi, P. (2011). Cancer associated fibroblasts: the dark side of the coin. *Am. J. Cancer Res.* 1 (4), 482–497.

Colella, M., Zinni, M., Pansiot, J., Cassanello, M., Mairesse, J., Ramenghi, L., et al. (2018). Modulation of microglial activation by adenosine A2a receptor in animal models of perinatal brain injury. *Front. Neurol.* 9, 605. doi:10.3389/Fneur.2018.00605

Costa, A., Kieffer, Y., Scholer-Dahirel, A., Pelon, F., Bourachot, B., Cardon, M., et al. (2018). Fibroblast heterogeneity and immunosuppressive environment in human breast cancer. *Cancer Cell* 33 (3), 463–479. doi:10.1016/J.Ccell.2018.01.011

Costa, A., Scholer-Dahirel, A., and Mechta-Grigoriou, F. (2014). The role of reactive oxygen species and metabolism on cancer cells and their microenvironment. *Semin. Cancer Biol.* 25, 23–32. doi:10.1016/J.Semcancer.2013.12.007

Du, B., and Shim, J. S. (2016). Targeting epithelial-mesenchymal transition (EMT) to overcome drug resistance in cancer. *Molecules* 21 (7), 965. doi:10.3390/Molecules21070965

Fini, C., Talamo, F., Cherri, S., Coli, M., Floridi, A., Ferrara, L., et al. (2003). Biochemical and mass spectrometric characterization of soluble ecto-5'-nucleotidase from bull seminal plasma. *Biochem. J.* 372 (2), 443–451. doi:10.1042/Bj20021687

Froeling, F. E., Feig, C., Chelala, C., Dobson, R., Mein, C. E., Tuveson, D. A., et al. (2011). Retinoic acid-induced pancreatic stellate cell quiescence reduces paracrine Wnt-β-catenin signaling to slow tumor progression. *Gastroenterology* 141 (4), 1486–1497. doi:10.1053/J.Gastro.2011.06.047

Gajewski, T. F. (2015). The next hurdle in cancer immunotherapy: Overcoming the non-T-cell-inflamed tumor microenvironment. *Semin. Oncol.* 42 (4), 663–671. doi:10.1053/J.Seminoncol.2015.05.011

Gao, Q., Yang, Z., Xu, S., Li, X., Yang, X., Jin, P., et al. (2019). Heterotypic CAF-tumor spheroids promote early peritoneal metastatis of ovarian cancer. *J. Exp. Med.* 216 (3), 688–703. doi:10.1084/Jem.20180765

Gascard, P., and Tlsty, T. D. (2016). Carcinoma-associated fibroblasts: orchestrating the composition of malignancy. *Genes Dev.* 30 (9), 1002–1019. doi:10.1101/Gad.279737.116

Gaudreau, P. O., Allard, B., Turcotte, M., and Stagg, J. (2016). CD73-adenosine reduces immune responses and survival in ovarian cancer patients. *Oncoimmunology* 5 (5), E1127496. doi:10.1080/2162402x.2015.1127496

Gentric, G., Mieulet, V., and Mechta-Grigoriou, F. (2017). Heterogeneity in cancer metabolism: New concepts in an old field. *Antioxid. Redox Signal.* 26 (9), 462–485. doi:10.1089/Ars.2016.6750

Giannoni, E., Bianchini, F., Masieri, L., Serni, S., Torre, E., Calorini, L., et al. (2010). Reciprocal activation of prostate cancer cells and cancer-associated fibroblasts stimulates epithelial-mesenchymal transition and cancer stemness. *Cancer Res.* 70 (17), 6945–6956. doi:10.1158/0008-5472.Can-10-0785

Gieniec, K. A., Butler, L. M., Worthley, D. L., and Woods, S. L. (2019). Cancer-associated fibroblasts-heroes or villains? *Br. J. Cancer* 121 (4), 293–302. doi:10.1038/S41416-019-0509-3

Givel, A. M., Kieffer, Y., Scholer-Dahirel, A., Sirven, P., Cardon, M., Pelon, F., et al. (2018). miR200-regulated CXCL12β promotes fibroblast heterogeneity and immunosuppression in ovarian cancers. *Nat. Commun.* 9 (1), 1056. doi:10.1038/S41467-018-03348-Z

Goulioumis, A., and Gyftopoulos, K. (2022). Epithelial-to-Mesenchymal transition in metastasis: Focus on laryngeal carcinoma. *Biomedicines* 10 (9), 2148. doi:10.3390/Biomedicines10092148

Henttinen, T., Jalkanen, S., and Yegutkin, G. G. (2003). Adherent leukocytes prevent adenosine formation and impair endothelial barrier function by Ecto-5'-nucleotidase/CD73-dependent mechanism. *J. Biol. Chem.* 278 (27), 24888–24895. doi:10.1074/Jbc.M300779200

Hosein, A. N., Brekken, R. A., and Maitra, A. (2020). Pancreatic cancer stroma: an update on therapeutic targeting strategies. *Nat. Rev. Gastroenterol. Hepatol.* 17 (8), 487–505. doi:10.1038/S41575-020-0300-1

Hu, G., Cheng, P., Pan, J., Wang, S., Ding, Q., Jiang, Z., et al. (2020). An IL6-adenosine positive feedback loop between CD73+ γδTregs and CAFs promotes tumor progression in human breast cancer. *Cancer Immunol. Res.* 8 (10), 1273–1286. doi:10.1158/2326-6066.Cir-19-0923

Inoue, Y., Yoshimura, K., Kurabe, N., Kahyo, T., Kawase, A., Tanahashi, M., et al. (2017). Prognostic impact of CD73 and A2A adenosine receptor expression in non-small-cell lung cancer. *Oncotarget* 8 (5), 8738–8751. doi:10.18632/Oncotarget.14434

Jacob, M., Chang, L., and Puré, E. (2012). Fibroblast activation protein in remodeling tissues. *Curr. Mol. Med.* 12 (10), 1220–1243. doi:10.2174/156652412803833607

Jeong, Y. J., Oh, H. K., and Choi, H. R. (2020). Methylation Of The Nt5e Gene Is Associated With Poor Prognostic Factors In Breast Cancer. *Diagn. (Basel)* 10 (11). doi:10.3390/Diagnostics10110939

Kalekar, L. A., and Mueller, D. L. (2017). Relationship between CD4 regulatory T cells and anergy *in vivo*. *J. Immunol.* 198 (7), 2527–2533. doi:10.4049/Jimmunol.1602031

Kalekar, L. A., Schmiel, S. E., Nandiwada, S. L., Lam, W. Y., Barsness, L. O., Zhang, N., et al. (2016). CD4(+) T cell anergy prevents autoimmunity and generates regulatory T cell precursors. *Nat. Immunol.* 17 (3), 304–314. doi:10.1038/Ni.3331

Kalluri, R. (2016). The biology and function of fibroblasts in cancer. *Nat. Rev. Cancer* 16 (9), 582–598. doi:10.1038/Nrc.2016.73

Kalluri, R., and Zeisberg, M. (2006). Fibroblasts in cancer. *Nat. Rev. Cancer* 6 (5), 392–401. doi:10.1038/Nrc1877

Karagiannis, G. S., Poutahidis, T., Erdman, S. E., Kirsch, R., Riddell, R. H., and Diamandis, E. P. (2012). Cancer-associated fibroblasts drive the progression of metastasis through both paracrine and mechanical pressure on cancer tissue. *Mol. Cancer Res.* 10 (11), 1403–1418. doi:10.1158/1541-7786.Mcr-12-0307

Koivisto, M. K., Tervahartiala, M., Kenessey, I., Jalkanen, S., Bostrom, P. J., and Salmi, M. (2019). Cell-type-specific CD73 expression is an independent prognostic factor in bladder cancer. *Carcinogenesis* 40 (1), 84–92. doi:10.1093/Carcin/Bgy154

Kojima, Y., Acar, A., Eaton, E. N., Mellody, K. T., Scheel, C., Ben-Porath, I., et al. (2010). Autocrine TGF-beta and stromal cell-derived factor-1 (SDF-1) signaling drives the evolution of tumor-promoting mammary stromal myofibroblasts. *Proc. Natl. Acad. Sci. U. S. A.* 107 (46), 20009–20014. doi:10.1073/Pnas.1013805107

Kordas, T., Osen, W., and Eichmüller, S. B. (2018). Controlling the immune suppressor: Transcription factors and MicroRNAs regulating CD73/NT5E. *Front. Immunol.* 9, 813. doi:10.3389/Fimmu.2018.00813

Leclerc, B. G., Charlebois, R., Chouinard, G., Allard, B., Pommey, S., Saad, F., et al. (2016). CD73 expression is an independent prognostic factor in prostate cancer. *Clin. Cancer Res.* 22 (1), 158–166. doi:10.1158/1078-0432.Ccr-15-1181

Leone, R. D., and Emens, L. A. (2018). Targeting adenosine for cancer immunotherapy. *J. Immunother. Cancer* 6 (1), 57. doi:10.1186/S40425-018-0360-8

Liu, N., Fang, X. D., and Vadis, Q. (2012). CD73 as a novel prognostic biomarker for human colorectal cancer. *J. Surg. Oncol.* 106 (7), 918–919. doi:10.1002/Jso.23159

López-Soto, A., Gonzalez, S., Smyth, M. J., and Galluzzi, L. (2017). Control of metastasis by NK cells. *Cancer Cell* 32 (2), 135–154. doi:10.1016/J.Ccell.2017.06.009

Magagna, I., Gourdin, N., Kieffer, Y., Licaj, M., Mhaidly, R., Andre, P., et al. (2021). CD73-Mediated immunosuppression is linked to a specific fibroblast population that paves the way for new therapy in breast cancer. *Cancers (Basel)* 13 (23), 5878. doi:10.3390/Cancers13235878

Mandapathil, M., Boduc, M., Netzer, C., Guldner, C., Roessler, M., Wallicek-Dworschak, U., et al. (2018). CD73 expression in lymph node metastases in patients with head and neck cancer. *Acta Otolaryngol.* 138 (2), 180–184. doi:10.1080/00016489.2017.1378436

Marsh, T., Pietras, K., and Mcallister, S. S. (2013). Fibroblasts as architects of cancer pathogenesis. *Biochim. Biophys. Acta* 1832 (7), 1070–1078. doi:10.1016/J.Bbadis.2012.10.013

Martinez-Outschoorn, U. E., Trimmer, C., Lin, Z., Whitaker-Menezes, D., Chiavarina, B., Zhou, J., et al. (2010). Autophagy in cancer associated fibroblasts promotes tumor cell survival: Role of hypoxia, HIF1 induction and NFκB activation in the tumor stromal microenvironment. *Cell Cycle* 9 (17), 3515–3533. doi:10.4161/Cc.9.17.12928

Miao, L., Liu, Q., Lin, C. M., Luo, C., and Wang, Y. (2017). Targeting tumor-associated fibroblasts for therapeutic delivery in desmoplastic tumors. *Cancer Res.* 77 (3), 719–731. doi:10.1158/0008-5472.Can-16-0866

Neo, S. Y., Yang, Y., Record, J., Ma, R., Chen, X., Chen, Z., et al. (2020). CD73 immune checkpoint defines regulatory NK cells within the tumor microenvironment. *J. Clin. Invest.* 130 (3), 1185–1198. doi:10.1172/Jci128895

Obayashi, T., Kagaya, Y., Aoki, Y., Tadaka, S., and Kinoshita, K. (2019). COXPRESdb v7: a gene coexpression database for 11 animal species supported by 23 coexpression platforms for technical evaluation and evolutionary inference. *Nucleic Acids Res.* 47 (D1), D55–D62. doi:10.1093/Nar/Gky1155

Orimo, A., Gupta, P. B., Sgroi, D. C., Arenzana-Seisdedos, F., Delaunay, T., Naeem, R., et al. (2005). Stromal fibroblasts present in invasive human breast carcinomas promote tumor growth and angiogenesis through elevated SDF-1/CXCL12 secretion. *Cell* 121 (3), 335–348. doi:10.1016/J.Cell.2005.02.034

Orimo, A., and Weinberg, R. A. (2007). Heterogeneity of stromal fibroblasts in tumors. *Cancer Biol. Ther.* 6 (4), 618–619. doi:10.4161/Cbt.6.4.4255

Otranto, M., Sarrazy, V., Bonté, F., Hinz, B., Gabbiani, G., and Desmouliere, A. (2012). The role of the myofibroblast in tumor stroma remodeling. *Cell adh. Migr.* 6 (3), 203–219. doi:10.4161/Cam.20377

Özdemir, B. C., Pentcheva-Hoang, T., Carstens, J. L., Zheng, X., Wu, C. C., Simpson, T. R., et al. (2015). Depletion of carcinoma-associated fibroblasts and fibrosis induces immunosuppression and accelerates pancreas cancer with reduced survival. *Cancer Cell* 28 (6), 831–833. doi:10.1016/J.Ccell.2015.11.002

Pantel, K., and Brakenhoff, R. H. (2004). Dissecting the metastatic cascade. *Nat. Rev. Cancer* 4 (6), 448–456. doi:10.1038/Nrc1370

Pellegatti, P., Raffaghello, L., Bianchi, G., Piccardi, F., Pistoia, V., and Di Virgilio, F. (2008). Increased level of extracellular ATP at tumor sites: *in vivo* imaging with plasma membrane luciferase. *Plos One* 3 (7), E2599. doi:10.1371/Journal.Pone.0002599

Pickup, M. W., Mouw, J. K., and Weaver, V. M. (2014). The extracellular matrix modulates the hallmarks of cancer. *EMBO Rep.* 15 (12), 1243–1253. doi:10.15252/Embr.201439246

Piersma, B., Hayward, M. K., and Weaver, V. M. (2020). Fibrosis and cancer: A strained relationship. *Biochim. Biophys. Acta. Rev. Cancer* 1873 (2), 188356. doi:10.1016/J.Bbcan.2020.188356

Qiao, B., Johnson, N. W., and Gao, J. (2010). Epithelial-mesenchymal transition in oral squamous cell carcinoma triggered by transforming growth factor-beta1 is Snail family-dependent and correlates with matrix metalloproteinase-2 and -9 expressions. *Int. J. Oncol.* 37 (3), 663–668. doi:10.3892/Ijo_00000715

Quail, D. F., and Joyce, J. A. (2013). Microenvironmental regulation of tumor progression and metastasis. *Nat. Med.* 19 (11), 1423–1437. doi:10.1038/Nm.3394

Quail, D. F., and Joyce, J. A. (2017). The microenvironmental landscape of brain tumors. *Cancer Cell* 31 (3), 326–341. doi:10.1016/J.Ccell.2017.02.009

Ryzhov, S., Novitskiy, S. V., Goldstein, A. E., Biktasova, A., Blackburn, M. R., Biaggioni, I., et al. (2011). Adenosinergic regulation of the expansion and immunosuppressive activity of CD11b+Gr1+ cells. *J. Immunol.* 187 (11), 6120–6129. doi:10.4049/Jimmunol.1101225

Sadej, R., and Skladanowski, A. C. (2012). Dual, enzymatic and non-enzymatic, function of ecto-5'-nucleotidase (eN, CD73) in migration and invasion of A375 melanoma cells. *Acta Biochim. Pol.* 59 (4), 647–652. doi:10.18388/abp.2012_2105

Sadej, R., Spychala, J., and Skladanowski, A. C. (2006). Ecto-5'-nucleotidase (eN, CD73) is coexpressed with metastasis promoting antigens in human melanoma cells. *Nucleosides Nucleotides Nucleic Acids* 25 (9-11), 1119–1123. doi:10.1080/15257770600894188

Sadej, R., Spychala, J., and Skladanowski, A. C. (2006). Expression of ecto-5'-nucleotidase (eN, CD73) in cell lines from various stages of human melanoma. *Melanoma Res.* 16 (3), 213–222. doi:10.1097/01.Cmr.0000215030.69823.11

Saldanha-Araujo, F., Ferreira, F. I., Palma, P. V., Araujo, A. G., Queiroz, R. H. C., Covas, D. T., et al. (2011). Mesenchymal stromal cells up-regulate CD39 and increase adenosine production to suppress activated T-lymphocytes. *Stem Cell Res.* 7 (1), 66–74. doi:10.1016/J.Scr.2011.04.001

Sharon, Y., Alon, L., Glanz, S., Servais, C., and Erez, N. (2013). Isolation of normal and cancer-associated fibroblasts from fresh tissues by Fluorescence Activated Cell Sorting (FACS). *J. Vis. Exp.* (71), e4425. doi:10.3791/4425

Shien, K., Papadimitrakopoulou, V. A., Ruder, D., Behrens, C., Shen, L., Kalhor, N., et al. (2017). JAK1/STAT3 activation through a proinflammatory cytokine pathway leads to resistance to molecularly targeted therapy in non-small cell lung cancer. *Mol. Cancer Ther.* 16 (10), 2234–2245. doi:10.1158/1535-7163.Mct-17-0148

Sitkovsky, M. V., Lukashev, D., Apasov, S., Kojima, H., Koshiba, M., Caldwell, C., et al. (2004). Physiological control of immune response and inflammatory tissue damage by hypoxia-inducible factors and adenosine A2A receptors. *Annu. Rev. Immunol.* 22, 657–682. doi:10.1146/Annurev.Immunol.22.012703.104731

Son, H., and Moon, A. (2010). Epithelial-mesenchymal transition and cell invasion. *Toxicol. Res.* 26 (4), 245–252. doi:10.5487/Tr.2010.26.4.245

Spychala, J. (2000). Tumor-promoting functions of adenosine. *Pharmacol. Ther.* 87 (2-3), 161–173. doi:10.1016/S0163-7258(00)00053-X

Stagg, J., Divisekera, U., Mclaughlin, N., Sharkey, J., Pommey, S., Denoyer, D., et al. (2010). Anti-CD73 antibody therapy inhibits breast tumor growth and metastasis. *Proc. Natl. Acad. Sci. U. S. A.* 107 (4), 1547–1552. doi:10.1073/Pnas.0908801107

Sträter, N. (2006). Ecto-5'-nucleotidase: structure function relationships. *Purinergic Signal.* 2 (2), 343–350. doi:10.1007/S11302-006-9000-8

Tejada, M. L., Yu, L., Dong, J., Jung, K., Meng, G., Peale, F. V., et al. (2006). Tumor-driven paracrine platelet-derived growth factor receptor alpha signaling is a key determinant of stromal cell recruitment in a model of human lung carcinoma. *Clin. Cancer Res.* 12 (9), 2676–2688. doi:10.1158/1078-0432.Ccr-05-1770

Thiery, J. P., Acloque, H., Huang, R. Y., and Nieto, M. A. (2009). Epithelial-mesenchymal transitions in development and disease. *Cell* 139 (5), 871–890. doi:10.1016/J.Cell.2009.11.007

Thiery, J. P., and Sleeman, J. P. (2006). Complex networks orchestrate epithelial-mesenchymal transitions. *Nat. Rev. Mol. Cell Biol.* 7 (2), 131–142. doi:10.1038/Nrm1835

Thompson, L. F., Eltzschig, H. K., Ibla, J. C., Van De Wiele, C. J., Resta, R., Morote-Garcia, J. C., et al. (2004). Crucial role for ecto-5'-nucleotidase (CD73) in vascular leakage during hypoxia. *J. Exp. Med.* 200 (11), 1395–1405. doi:10.1084/Jem.20040915

Venhuizen, J. H., Jacobs, F. J. C., Span, P. N., and Zegers, M. M. (2020). P120 and E-cadherin: Double-edged swords in tumor metastasis. *Semin. Cancer Biol.* 60, 107–120. doi:10.1016/J.Semcancer.2019.07.020

Wang, H., Lee, S., Nigro, C. L., Lattanzio, L., Merlano, M., Monteverde, M., et al. (2012). NT5E (CD73) is epigenetically regulated in malignant melanoma and associated with metastatic site specificity. *Br. J. Cancer* 106 (8), 1446–1452. doi:10.1038/Bjc.2012.95

Wei, C., Ma, Y., Wang, F., Liao, Y., Chen, Y., Zhao, B., et al. (2022). Igniting hope for tumor immunotherapy: Promoting the "hot and cold" tumor transition. *Clin. Med. Insights. Oncol.* 16, 11795549221120708. doi:10.1177/11795549221120708

Willumsen, N., Thomsen, L. B., Bager, C. L., Jensen, C., and Karsdal, M. A. (2018). Quantification of altered tissue turnover in a liquid biopsy: a proposed precision medicine tool to assess chronic inflammation and desmoplasia associated with a pro-cancerous niche and response to immuno-therapeutic anti-tumor modalities. *Cancer Immunol. Immunother.* 67 (1), 1–12. doi:10.1007/S00262-017-2074-Z

Wu, R., Chen, Y., Li, F., Li, W., Zhou, H., Yang, Y., et al. (2016). Effects of CD73 on human colorectal cancer cell growth *in vivo* and *in vitro*. *Oncol. Rep.* 35 (3), 1750–1756. doi:10.3892/Or.2015.4512

Xiang, Z., Huang, G., Wu, H., He, Q., Yang, C., Dou, R., et al. (2022). SNHG16 upregulation-induced positive feedback loop with YAP1/TEAD1 complex in Colorectal Cancer cell lines facilitates liver metastasis of colorectal cancer by modulating CTCs epithelial-mesenchymal transition. *Int. J. Biol. Sci.* 18 (14), 5291–5308. doi:10.7150/Ijbs.73438

Xu, Z., Gu, C., Yao, X., Guo, W., Wang, H., Lin, T., et al. (2020). CD73 promotes tumor metastasis by modulating RICS/RhoA signaling and EMT in gastric cancer. *Cell Death Dis.* 11 (3), 202. doi:10.1038/S41419-020-2403-6

Yang, Q., Du, J., and Zu, L. (2013). Overexpression of CD73 in prostate cancer is associated with lymph node metastasis. *Pathol. Oncol. Res.* 19 (4), 811–814. doi:10.1007/S12253-013-9648-7

Young, A., Ngiow, S. F., Barkauskas, D. S., Sult, E., Hay, C., Blake, S. J., et al. (2016). Co-Inhibition of CD73 and A2AR adenosine signaling improves anti-tumor immune responses. *Cancer Cell* 30 (3), 391–403. doi:10.1016/J.Ccell.2016.06.025

Yu, M., Guo, G., Huang, L., Deng, L., Chang, C. S., Achyut, B. R., et al. (2020). CD73 on cancer-associated fibroblasts enhanced by the A2B-mediated feedforward circuit enforces an immune checkpoint. *Nat. Commun.* 11 (1), 515. doi:10.1038/S41467-019-14060-X

Yu, Y., Xiao, C. H., Tan, L. D., Wang, Q. S., Li, X. Q., and Feng, Y. M. (2014). Cancer-associated fibroblasts induce epithelial-mesenchymal transition of breast cancer cells through paracrine TGF-β signalling. *Br. J. Cancer* 110 (3), 724–732. doi:10.1038/Bjc.2013.768

Zhou, L., Jia, S., Chen, Y., Wang, W., Wu, Z., Yu, W., et al. (2019). The distinct role of CD73 in the progression of pancreatic cancer. *J. Mol. Med.* 97 (6), 803–815. doi:10.1007/S00109-018-01742-0

Zhu, X., Liang, R., Lan, T., Ding, D., Huang, S., Shao, J., et al. (2022). Tumor-associated macrophage-specific CD155 contributes to M2-phenotype transition, immunosuppression, and tumor progression in colorectal cancer. *J. Immunother. Cancer* 10 (9), e004219. doi:10.1136/Jitc-2021-004219

Zimmermann, H., Zebisch, M., and Sträter, N. (2012). Cellular function and molecular structure of ecto-nucleotidases. *Purinergic Signal* 8 (3), 437–502. doi:10.1007/S11302-012-9309-4

Zimmermann, H. (2000). Extracellular metabolism of ATP and other nucleotides. *Naunyn. Schmiedeb. Arch. Pharmacol.* 362 (4-5), 299–309. doi:10.1007/S002100000309

frontiers | Frontiers in Pharmacology

TYPE Systematic Review
PUBLISHED 09 January 2023
DOI 10.3389/fphar.2022.1095734

OPEN ACCESS

EDITED BY
Qianming Du,
Nanjing Medical University, China

REVIEWED BY
Xinmao Song,
Fudan University, China
Yi Chen,
Guizhou Medical University, China

*CORRESPONDENCE
Haocheng Gou,
15760552907@163.com

SPECIALTY SECTION
This article was submitted to Pharmacology of Anti-Cancer Drugs, a section of the journal Frontiers in Pharmacology

RECEIVED 11 November 2022
ACCEPTED 28 December 2022
PUBLISHED 09 January 2023

CITATION
Yan L, Ren B, Hu R, Zhang H and Gou H (2023), Are PD-1 inhibitors effective for recurrent/metastatic nasopharyngeal carcinoma? Meta-analysis and systematic review.
Front. Pharmacol. 13:1095734.
doi: 10.3389/fphar.2022.1095734

Are PD-1 inhibitors effective for recurrent/metastatic nasopharyngeal carcinoma? Meta-analysis and systematic review

Le Yan[1], Bi Ren[2], Rongqiu Hu[3], Huiping Zhang[1] and Haocheng Gou[4]*

[1]School of Medical and Life Sciences, Reproductive and Women-Children Hospital, Chengdu University of Traditional Chinese Medicine, Chengdu, China, [2]North Sichuan Medical College, Affiliated Hospital of North Sichuan Medical College, Nanchong, China, [3]School of Nursing, Southwest Medical University, Luzhou, China, [4]Department of Otorhinolaryngology Head and Neck Surgery, The Second Clinical Medical College, Nanchong Central Hospital, Nanchong, China

Objective: For metastatic/recurrent nasopharyngeal carcinoma (NPC) patients, a programmed cell death protein 1 (PD-1) is a controversial option. This meta-analysis aimed to investigate the efficacy and safety of PD-1 inhibitors in patients with metastatic/recurrent NPC.

Methods: Electronic databases such as PubMed, Embase, Cochrane library, and Web of Science were manually searched until 1 July 2022, and Stata 15.0 was used to analyze the data.

Result: A total of 10 studies were included, of which three were randomized controlled trials with data, and seven were single-arm studies. For randomized controlled trial (RCT) study, ORR [OR = 1.11, 95% CI (.49, 2.52); p = .812], OS [1-year OR = 1.26, 95% CI (.76, 2.08); p = .367], [2-year OR = 1.04, 95% CI (.39, 2.71); p = .928] in patients with metastatic/recurrent NPC were consistent with PD-1 inhibitor therapy and conventional chemotherapy. However, PD-1 inhibitor had higher 1-year PFS than conventional chemotherapy [OR = 2.16, 95% CI (1.26, 3.70); p = .005]. For single-arm studies, after PD-1 inhibitor therapy, the ORR of patients with recurrent/metastatic NPC reached [ES = 37%, 95 CI (17%–56%)], 1-year OS [ES = 61%, 95% CI (46%–76%)], 2-year [ES = 16%, 95% CI (6%–26%)], and 1-year PFS [ES = 16%,95% CI (12%–20%)].

Conclusion: The efficacy of PD-1 inhibitor monotherapy in patients with metastatic/recurrent nasopharyngeal carcinoma was not significantly different from that of conventional chemotherapy; however, due to the limitations of the included studies, further phase III RCTs are required to corroborate our conclusion.

Systematic Review Registration: https://www.crd.york.ac.uk/prospero/display_record.php?ID=CRD42022342400; Identifier: CRD42022342400.

KEYWORDS

recurrent/metastatic nasopharyngeal carcinoma, PD-1, meta-analysis, adverse event, ICB

1 Introduction

Nasopharyngeal carcinoma (NPC) is a malignant tumor that originates from the nasopharyngeal mucosal epithelium (Chen et al., 2019). The histological types are mostly poorly differentiated or undifferentiated carcinomas. The incidence is high in southern China and North Africa (Beyene et al., 2021; Bossi et al., 2021). According to GLOBOCAN (Bray et al., 2018), the incidence in these regions is 4–25 cases per 1,00,000 people, which is 50–100 times higher than the incidence in the rest of the world. NPC can be divided into three subtypes: keratinizing squamous cell carcinoma, non-keratinizing squamous cell carcinoma, and undifferentiated or poorly differentiated carcinoma (Kang et al., 2020; Yarza et al., 2021). The non-keratinizing subtype of NPC accounts for 95% of NPC endemic areas and 75% in the USA. This unique geographic distribution has been linked to genetic and environmental factors (Chang et al., 2021). NPC is a high radio- and chemo-sensitive tumor type (Lee et al., 2015). NPC is sensitive to both chemoradiation and chemotherapy except in stage I patients (Kang et al., 2020; Tsang et al., 2020). Currently, gemcitabine and/or cisplatin are the standard (first-line) treatments for NPC (Zhang et al., 2019). The 5-year OS of patients with early-stage NPC after receiving standard chemotherapy regimens can be as high as 80% (Dwijayanti et al., 2020); for patients with recurrent or metastatic NPC, the 5-year OS is only 40%–50% (Lee et al., 2019; Sun et al., 2019). Therefore, patients with recurrent/metastatic nasopharyngeal carcinoma are less effective in first-line therapy, and second-and third-line treatment options are limited.

Tumor immunotherapy has the potential to activate the body's immune system while also targeting cancer cells and tumor tissues, making it an essential option for tumor therapy (Riley et al., 2019; Hiam-Galvez et al., 2021). Clinically, immunotherapy can be divided into two categories: the first category refers to active immunotherapy methods, such as adoptive immunotherapy or tumor vaccines (Gohil et al., 2021); the second category refers to the host's natural anti-tumor immune response (Li et al., 2019), immune suppression or escape mechanisms. Blocking the inhibitory pathway of infiltrating T cells reactivates antitumor immune response, known as an immune checkpoint blockade (ICB) (Diesendruck and Benhar, 2017). At present, immune checkpoint inhibitors mainly targeting PD-1 play a role in the process of ICB (Kumar et al., 2020). ICB has become a research hotspot, and the most well-known target molecule in ICB therapy is PD-1. There are many ongoing phase III trials (NCT03427827, NCT04376866, NCT04446663, NCT04447612) to compare the efficacy of PD-1 inhibitors and chemotherapy for metastatic/recurrent NPC, and clinical opinions on PD-1 inhibitors for metastatic/recurrent NPC are inconsistent. The objective of this meta-analysis was to analyze and summarize the currently available data on the efficacy and safety of PD-1 inhibitors alone or in combination with chemotherapy in the treatment of patients with metastatic/recurrent NPC to determine the efficacy of this class of drugs and provide new treatment options for patients and clinicians.

2 Materials and methods

The protocol has been registered in the International Prospective Register of Systematic Reviews database (PROSPERO: CRD42022342400).

2.1 Retrieval strategy

Search PubMed, Embase, Cochrane library, and Web of science for articles published by 1 July 2022, on PD-1 inhibitors for metastatic/recurrent NPC. The search terms are (Nasopharyngeal Carcinoma, Carcinomas, Nasopharyngeal, nasopharyngeal cancer, NPC) and (Checkpoint Blockers, Immune, PD-1 Inhibitors), specific searches strategy of PubMed and Embase see Supplementary Tables S1, S2.

2.2 Inclusion and exclusion criteria

The included population was diagnosed with recurrent nasopharyngeal carcinoma or distant metastasis of nasopharyngeal carcinoma and received PD-1 inhibitor intervention. Randomized controlled studies (RCT) or single-arm studies reporting OS: overall survival, PFS: progression-free survival, ORR: objective response rate were included, and complete response (CR) + partial response (PR) are considered ORR. Conference abstracts, literature reviews, meta-analyses, duplicate publications, animal experiments, case reports, the number of included cases <10, the full text not available, and the data not available were all excluded.

2.3 Data extraction

The extracted data included the investigator's name, publication year, drug type, number of included cases, drug dose, follow-up, median OS, median PFS, and median ORR. The basic information of the studies was extracted independently by two investigators.

2.4 Risk of bias evaluate

For RCTs: the Cochrane to Randomized Clinical Trials Risk of Bias Tool 2.0 (RoB2) was used to assess the risk of bias (Sterne et al., 2019). RoB2 was also paired with two independent investigators. A third investigator performed consensus if two investigators differed on the risk of bias analyzed. The evaluators examined the randomization process, deviations from expected interventions, missing outcome data, choice of outcome measures, and reported outcomes. Therefore, the studies were classified as low, moderate, or high risk of bias (Supplementary Figure S1).

For single arm study: The Newcastle-Ottawa Scale (NOS) (Lo et al., 2014) was used to assess quality. Assessment scores of 0–3, 4–6, and 7–9 represent poor, fair, and good studies, respectively, and any disagreements are resolved by consensus (Supplementary Table S3).

2.5 Data analysis

For randomized controlled trials, Odds ratio (OR) and 95% confidence interval (CI) were used for binary variables such as ORR value, 1-year OS, 2-year OS and 1-year PFS. For single-arm studies, we used effect size (ES) and 95% CI. The random utility model was employed for meta-analysis due to the considerable heterogeneity of treatment types, frequency, and frequency among different studies. Stata software (version 15.0; Stata Corp, College Station, TX, United States) performed statistical analyses and tested for

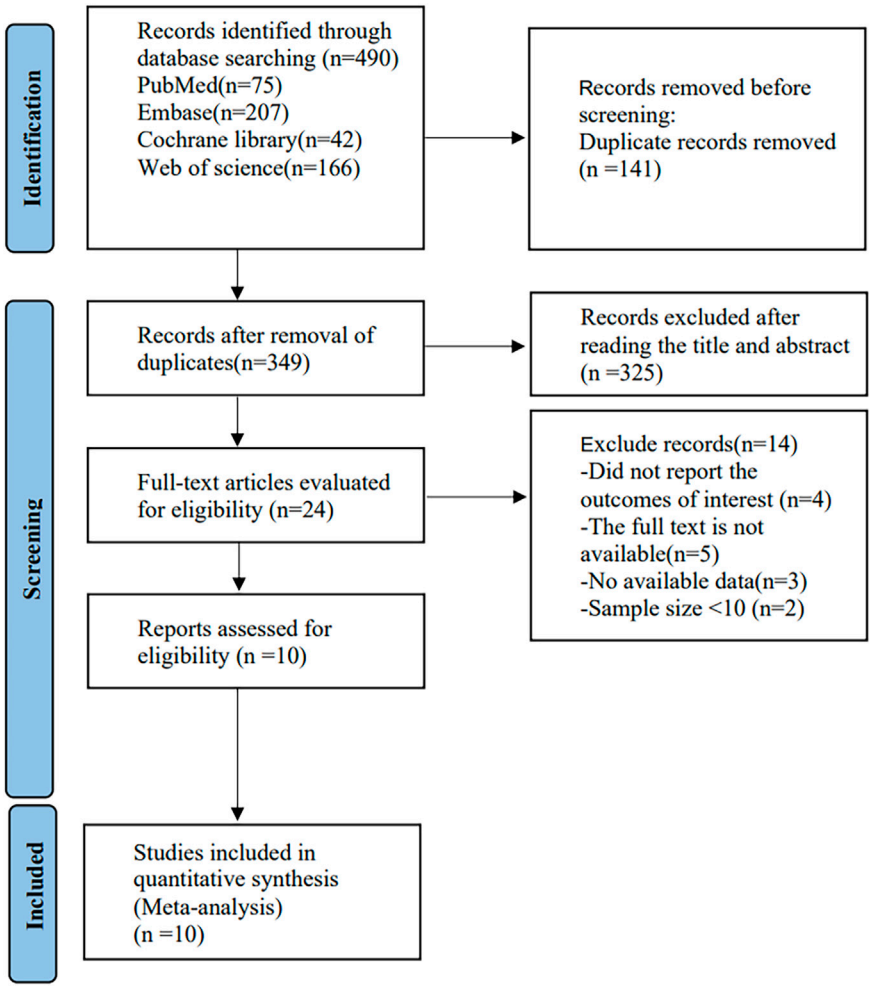

FIGURE 1
Literature screening flowchart.

heterogeneity by I2 values or Q statistics. I2 values of 0%, 25%, 50%, and 75% represent no, low, medium and high heterogeneity, respectively. Sensitivity analyses were undertaken when I2 values were ≥50% to investigate potential sources of heterogeneity; otherwise, the fixed effects model was employed. In addition, publication bias was assessed by Egger's test or Begg's test using the random effects model. Two-sided $p < .05$ was considered statistically significant.

3 Result

3.1 Literature screening and characteristics

Through manual retrieval, a total of 490 articles were obtained, 349 articles were obtained after removing duplicates, 24 articles were obtained by checking the titles and abstracts of the articles, 10 articles (Hsu et al., 2017; Fang et al., 2018; Ma et al., 2018; Sato et al., 2020; Even et al., 2021; Ma et al., 2021; Mai et al., 2021; Wang et al., 2021; Yang et al., 2021; Economopoulou et al., 2022) were finally included in the analysis by reading the full text. See Figure 1.

3.2 Characteristics of literature

A total of 10 studies were included, of which 3 (Even et al., 2021; Mai et al., 2021; Yang et al., 2021) were randomized controlled trials with data, and 7 (Hsu et al., 2017; Fang et al., 2018; Ma et al., 2018; Sato et al., 2020; Ma et al., 2021; Wang et al., 2021; Economopoulou et al., 2022) were single-arm studies. The most used PD-1 inhibitors included: Camrelizumab, Toripalimab, Pembrolizumab, and Nivolumab. There are four studies (Fang et al., 2018; Sato et al., 2020; Mai et al., 2021; Yang et al., 2021) that did not report the median OS, and the specific characteristics of the literature are shown in Table 1.

3.3 Meta analysis for RCT

3.3.1 ORR

A total of three studies involved a total of 672 patients with metastatic/recurrent NPC. There were 360 patients in the PD-1 inhibitor group and 312 patients in the control group (I2 = 77.6%, $p = .012$), indicating higher heterogeneity. Figure 2 [OR = 1.11, 95% CI (.49, 2.52); $p = .812$] suggested that PD-1 inhibitors did not improve

TABLE 1 Literature baseline table.

Study	Year	Type	Sample size (male)	Mean age (years)	Dose	Follow-up (Mo)	Median OS(Mo)	Median PFS(Mo)	Median ORR (%)	Metastatic sites	PD-L1>1%	TNM stage
Randomized controlled trial												
YP Yang	2021	PD-1	T:134 (113)	T:52	Camrelizumab 200 mg Q3W	20	NR	T:9.7	T:87.3	Liver; lung	NR	NR
			C:129 (105)	C:49				C:6.9	C:80.6			
HQ Mai	2021	PD-1	T:146 (124)	T:46	Toripalimab 240 mg Q3W	30	NRE	T:11.7	T:77.4	Liver; lung; bone	T:109	NR
			C:143 (116)	C:51				C:8	C:66.4		C:109	
Even C	2021	PD-1	T:82 (68)	T:51	Spartalizumab (PDR001) 400 mg Q4W	28	T:25.2	T:1.9	T:18.4	Liver; lung	T:78	NR
			C:40 (33)	C:50			C:15.5	C:6.6	C:32.5		C:38	
Single-armed experiment												
P Economopoulou	2022	PD-1	46 (36)	56.3	Nivolumab/pembrolizumab	60	19.1	5.6	26.2	Liver; lung; bone	NR	II-IV
WF Fang	2018	PD-1	93 (75)	45	Camrelizumab 3 mg/kg Q2W	12	NR	5.6	34	Liver; lung	NR	NR
C Hus	2017	PD-1	27 (21)	52	Pembrolizumab 10 mg/kg Q2W	28	16.5	6.5	25.9	Liver; lung; bone; Lymph node	41	II-III
BBY Ma	2018	PD-1	45 (35)	57	Nivolumab 3 mg/kg Q2W	24	17.1	2.8	20.5	Liver; lung; bone; Lymph node	18	NR
YX Ma	2021	PD-1	124 (95)	46	Camrelizumab 10 mg/kg Q2W/ Nivolumab 3 mg/kg Q3W	34	17.1	3.8	29.8	Liver; lung; bone; Lymph node	NR	NR
H Sato	2020	PD-1	12 (10)	58	Nivolumab 3 mg/kg Q2W	20	NR	3.6	16.7	Liver; lung; bone; Lymph node	1	II-IVC
FH Wang	2021	PD-1	190 (158)	46.4	Toripalimab 3 mg/kg Q2W	40	17.4	1.9	20.5	Liver; lung; bone; Lymph node	48	III-IVb

Abbreviation: T, treatment group; C, control group; GP, gemcitabine-cisplatin; MO, months; OS, overall survival; PFS, progression free survival; ORR, objective response rate; NR, not reported; NRE, not reached; Q3W, every 3 weeks.

10.3389/fphar.2022.1095734

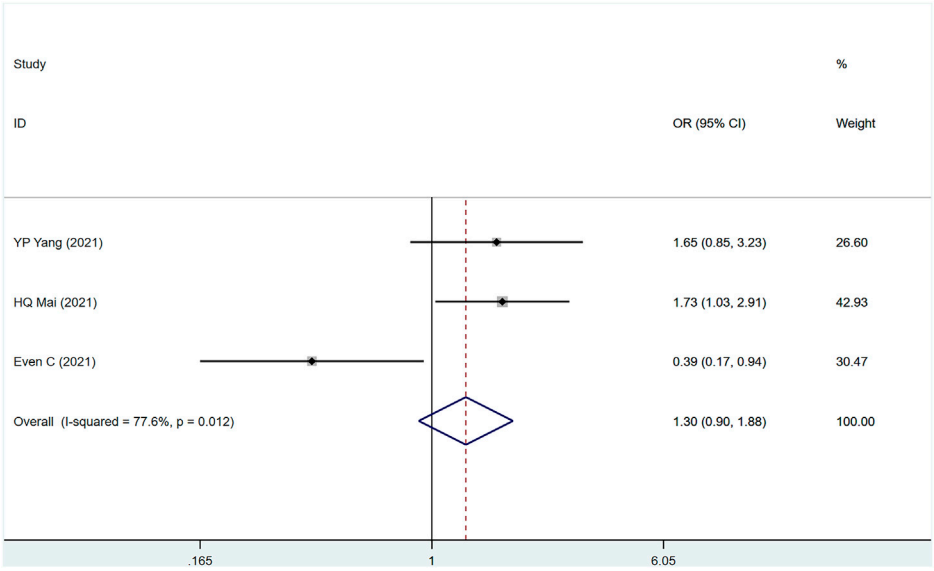

FIGURE 2
Estimated ORR proportion (95% CI) of patients with metastatic/recurrent nasopharyngeal carcinoma after PD-1 treatment forest plot—randomized controlled trial.

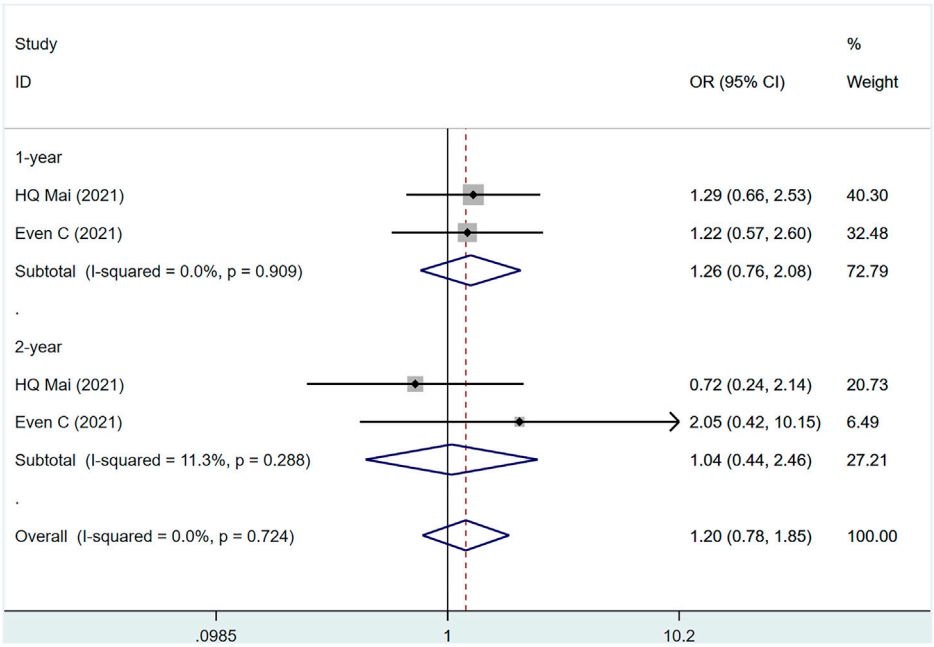

FIGURE 3
Estimated OS proportion (95% CI) of patients with metastatic/recurrent nasopharyngeal carcinoma after PD-1 treatment forest plot—randomized controlled trial.

ORR in patients with metastatic/recurrent NPC. Sensitivity analysis was performed on the deleted studies one by one, and it was found that the potential heterogeneity may originate from Even C (23) (Supplementary Figure S2A). *p*-values for assessing publication bias (Egger test: .294, Begg test: .117) were all >.05, indicating that there is a small possibility that there is no publication bias (Supplementary Table S4).

3.3.2 OS

Two studies (Even et al., 2021; Mai et al., 2021) involved a total of 441 patients, of which 228 were PD-1 and 183 were control group (I2 = 0%, p = .724), suggesting that the heterogeneity is acceptable. Figure 3 shows that PD-1 inhibitors had no effect on 1- and 2-year OS in patients with metastatic/recurrent NPC [1-year OR = 1.26, 95% CI (.76, 2.08); p = .367]; [2-year OR = 1.03, 95% CI (.39, 2.71); p = .928].

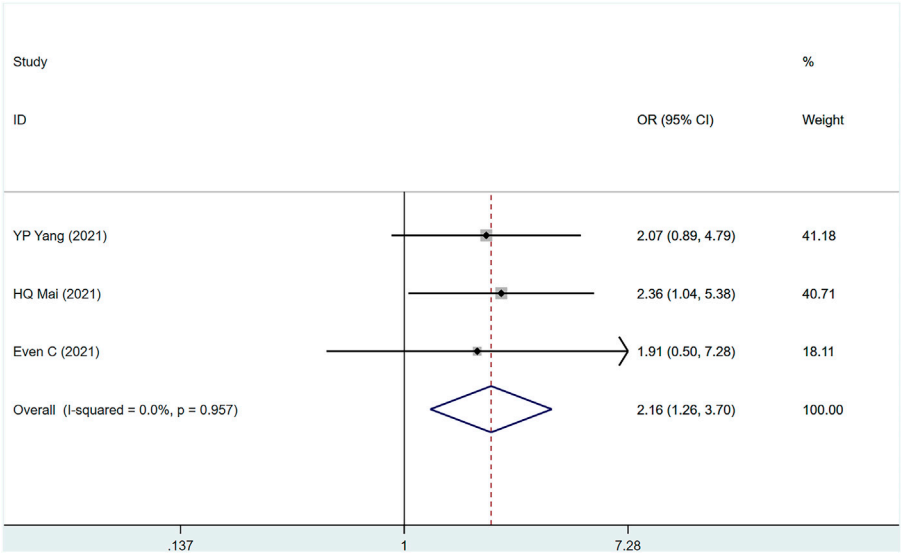

FIGURE 4
Estimated PFS proportion (95% CI) of patients with metastatic/recurrent nasopharyngeal carcinoma after PD-1 treatment forest plot—randomized controlled trial.

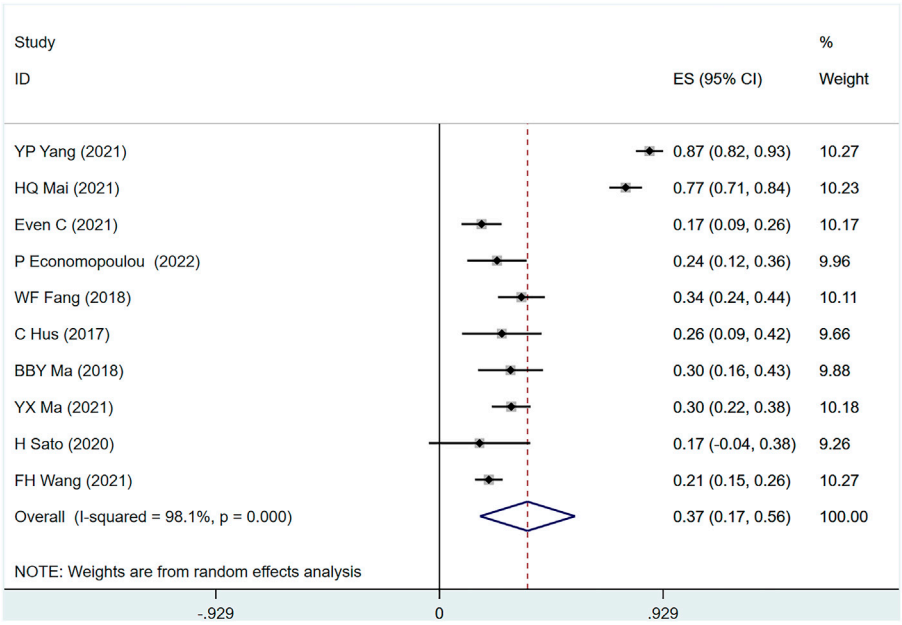

FIGURE 5
Estimated ORR proportion (95% CI) of patients with metastatic/recurrent nasopharyngeal carcinoma after PD-1 treatment forest plot—single arm studies.

p-values for assessing publication bias (Egger test: .718, Begg test: 1.000) were all >.05, indicating that there is a small possibility that there is no publication bias (Supplementary Table S4).

3.3.3 PFS

The three studies (Even et al., 2021; Mai et al., 2021; Yang et al., 2021) involved a total of 604 people, of which 313 were PD-1 and 291 were control group. (I2 = 0%, p = .957), suggesting that the heterogeneity is small. Figure 4 [OR = 2.16, 95% CI (1.26, 3.70); p = .005]; suggests that PD-1 inhibitors can improve the 1-year PFS of metastatic/recurrent NPC patients. *p*-values for assessing publication bias (Egger test: .528, Begg test: 1.040) were all >.05, indicating that there is a small possibility that there is no publication bias (Supplementary Table S4).

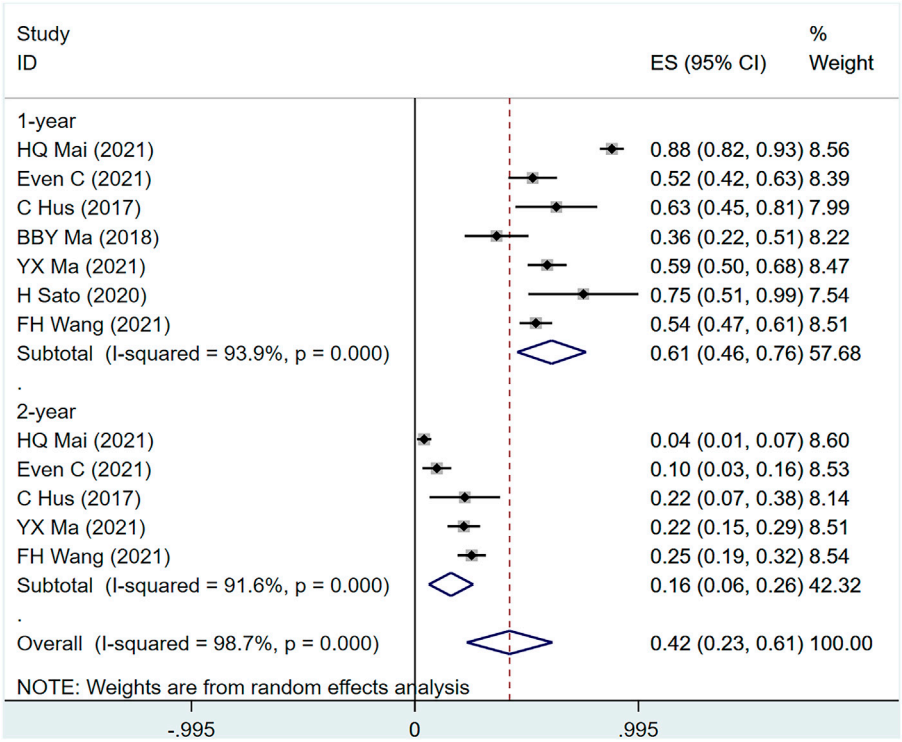

FIGURE 6
Estimated OS proportion (95% CI) of patients with metastatic/recurrent nasopharyngeal carcinoma after PD-1 treatment forest plot—single arm studies.

3.4 Meta analysis for single-arm study

3.4.1 ORR

ORR was mentioned in 10 studies (Hsu et al., 2017; Fang et al., 2018; Ma et al., 2018; Sato et al., 2020; Even et al., 2021; Ma et al., 2021; Mai et al., 2021; Wang et al., 2021; Yang et al., 2021; Economopoulou et al., 2022) involving 894 people, (I2 = 98.1, p = 0) suggesting a large heterogeneity among the included studies. Figure 5 shows ORR in metastatic/recurrent NPC patients treated with PD-1 inhibitors [ES = 37%, 95% CI (17%–56%); p = .00]. Sensitivity analysis indicated that the analysis results were relatively stable (Supplementary Figure S2B), with p > .05 for Egger's and Begg's publication bias assessment (Egger test: .244, Begg test: 0.180), suggesting that there was a small possibility of publication bias (Supplementary Table S4).

3.4.2 OS

OS was mentioned in seven studies including 617 people (I2 = 98.7, p = 0), indicating that the heterogeneity among included studies was large. Figure 6 shows the OS of patients with metastatic/recurrent NPC using PD-1 inhibitors [1-year ES = 61%, 95% CI (46%–76%); p = .00]; [2-year ES = 16%, 95% CI (6%–26%); p = .001]. Sensitivity analysis suggests that the analysis results are relatively stable (Supplementary Figure S2C), with p > .05 for the evaluation of egg's and Begg's in publication bias (Egger test: .196, Begg test: .583), suggesting the possibility of publication bias Less sexual (Supplementary Table S4).

3.4.3 PFS

PFS was mentioned in nine studies (Hsu et al., 2017; Fang et al., 2018; Ma et al., 2018; Sato et al., 2020; Even et al., 2021; Ma et al., 2021; Mai et al., 2021; Wang et al., 2021; Yang et al., 2021) involving 842 people, (I2 = 50.1.7, p = .042) suggesting the heterogeneity among included studies. Figure 7 shows the use of PD-1 inhibitors for PFS in patients with metastatic/recurrent NPC [1-year ES = 16%, 95% CI (12%–20%); p = .00]. Sensitivity analysis indicated that the analysis results were relatively stable (Supplementary Figure S2D), with p > .05 for Egger's and Begg's (Egger test: .074, Begg test: .095), suggesting that there is a small possibility of publication bias (Supplementary Table S4).

3.5 Meta analysis for adverse event

Among the 10 included studies (Hsu et al., 2017; Fang et al., 2018; Ma et al., 2018; Sato et al., 2020; Even et al., 2021; Ma et al., 2021; Mai et al., 2021; Wang et al., 2021; Yang et al., 2021; Economopoulou et al., 2022), the main adverse events were rash, Leukopenia, Anemia, Neutropenia, Vomiting, Thrombocytopenia, Decreased appetite, and Constipation. In any grade ES (rash = 18%, Leukopenia = 66%, Anemia = 36%, Neutropenia = 63%, Vomiting = 62%, Thrombocytopenia = 48%, Reduced appetite = 40%, Constipation = 28%), in grade ≥3 ES (rash = 2%, Leukopenia = 64%, Anemia = 18%, Neutropenia = 31%, Vomiting = 4%, Thrombocytopenia = 24%, and Reduced appetite = 1%) (Supplementary Table S5).

3.6 Survival curve analysis

Combined with the PFS of three randomized controlled trials, the survival curve is shown in Figure 8 [HR = 1.21, 95% CI (1.06, 1.38),

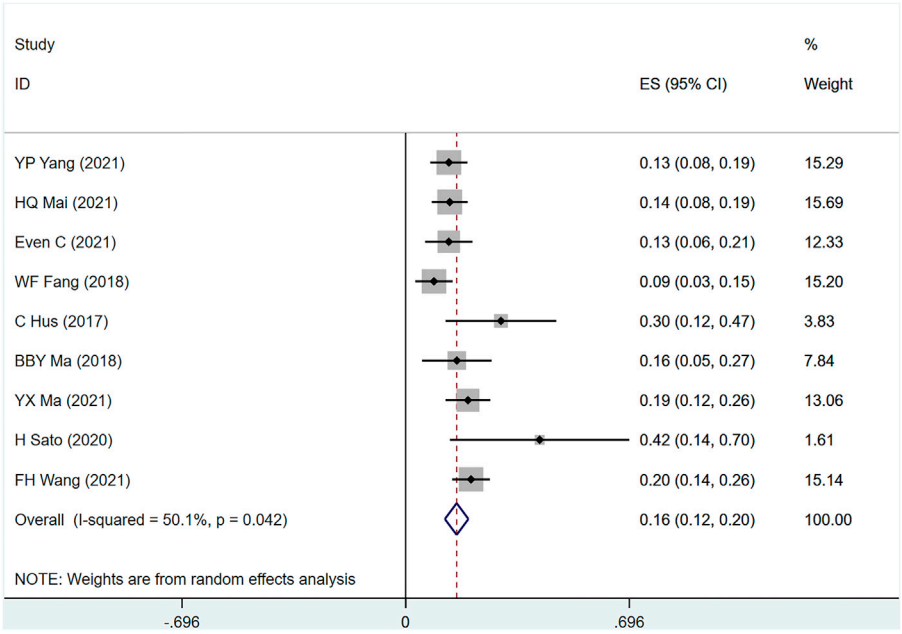

FIGURE 7
Estimated PFS proportion (95% CI) of patients with metastatic/recurrent nasopharyngeal carcinoma after PD-1 treatment forest plot—single arm studies.

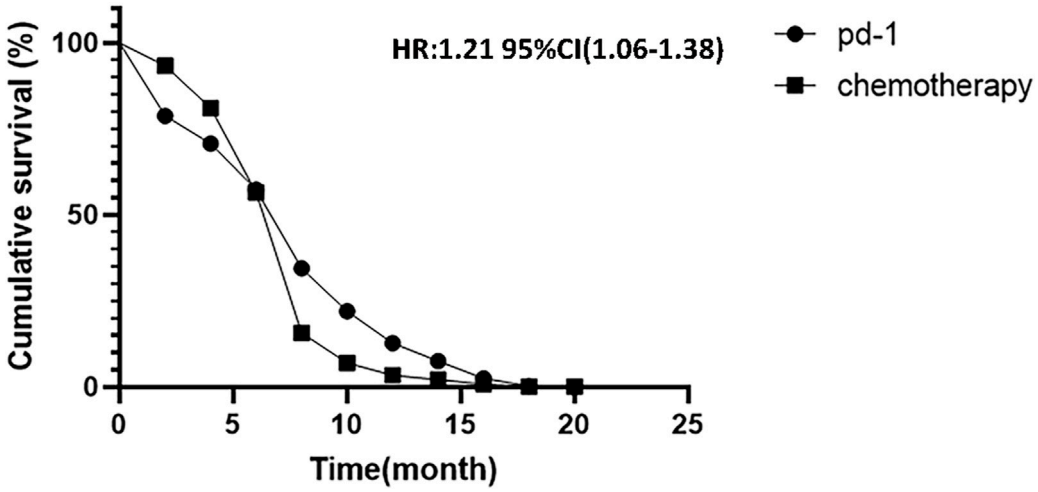

FIGURE 8
Kaplan-Meier analysis of cumulative progression-free survival between PD-1 inhibitors and chemotherapy.

shown in Figure 8. $p = .002$]. This indicates that PD-1 inhibitor showed a significant extension of PFS in patients with PD-1 inhibitor compared to traditional chemotherapy.

4 Discussion

As far as we know, this is not the first meta-analysis on similar topics. Wang et al. (2020) published a similar meta-paper in 2020, but compared with Wang, this study has the following advantages: first, the latest RCTs and single-arm studies were included, and the latest evidence was obtained; second, most of the articles included were conference articles and case reports, and no obvious conclusions were drawn in Wang's paper. Therefore, compared with this paper, our paper has obvious advantages and innovation.

Once the tumor metastasizes, it means that the disease changes from a local disease to a systemic disease (Klein, 2009). The clinical treatment is mainly palliative chemotherapy. However, due to the previous treatment usage of multiple chemotherapeutic medications, drug sensitivity is reduced, and treatment effect is frequently poor (Prada et al., 2013).

Currently, PD-1 is believed to be expressed on activated T cells, B cells, NK cells, and macrophages. Therefore, the use of PD-1 antibodies for the treatment of metastatic/recurrent NPC can enhance the body's immune system. The way of anti-tumor effect, synergistic chemotherapy enhances the therapeutic effect (Kim and Chen, 2016).

For meta-analysis of RCTs, we found that ORR [OR = 1.11, 95% CI (.49, 2.52); p = .812], 1-year OS [OR = 1.26, 95% CI (.76, 2.08); p = .367], and 2-year OS [OR = 1.03, 95% CI (.39, 2.71); p = .928] in patients with metastatic/recurrent NPC were consistent with PD-1 and conventional chemotherapy. This is the first RCT-based conclusion on PD-1 inhibitor therapy for relapsed/metastatic NPC, but we should treat the conclusion with caution because the number of included studies was small, the included study drug was not the same, and the treatment of Even C (23) only used PD-1 inhibitors, while the other two studies used Gemcitabine-cisplatin. However, PD-1 inhibitors outperformed conventional chemotherapy in terms of 1-year PFS [OR = 2.16, 95% CI (1.26, 3.70); p = .005]. Possible explanations include: I) some patients receiving PD-1 inhibitor treatment for a long time after the therapeutic impact was determined to have an advanced disease; and II) some patients receiving follow-up treatment for a longer period after receiving PD-1 inhibitor therapy (Xie et al., 2019; Jiang et al., 2021). With the results of multiple phase III trials (CAPTAIN first, JUPITER 02, and RATIONALE 309), RATIONALE-309 (Zhang et al., 2022) is consistent with the conclusion. 263 eligible metastatic/recurrent NPC patients were randomly assigned 1:1 to receive tislelizumab 200 mg IV or placebo. Results showed that, compared with placebo + chemotherapy, Tislelizumab plus chemotherapy showed a consistent, clinically meaningful improvement in PFS. We believe that PD-1 inhibitors therapy can achieve a breakthrough in the treatment of recurrent or metastatic NPC (Hua et al., 2022; Huang et al., 2022).

For the meta-analysis of single-arm studies, after PD-1 inhibitors therapy, the ORR of patients with recurrent/metastatic NPC reached [ES = 37%, 95% CI (17%–56%)], 1-year OS [ES = 61%, 95% CI (46%–76%)], 2-year [ES = 16%, 95% CI (6%–26%)], and 1-year PFS [ES = 16%, 95% CI (12%–20%)]. This is consistent with the conclusion drawn by Lin and colleagues (Lin et al., 2022). The 12 patients with conventional chemotherapy + PD-1 inhibitors had an overall best ORR of 66.6% and a disease control rate (DCR) as high as 66.6%, the OS in June and December was 87.5% and 63.5%, respectively, and the median OS was not reached. This result suggests that conventional chemotherapy + PD-1 inhibitors treatment can effectively improve the remission rate even if the tumor progresses after PD-1 treatment, and strengthens the evidence that palliative chemotherapy participates in combined immunotherapy after PD-1 resistance. The advantages of combined chemotherapy in cancer were comparable to immune monotherapy. Possible reasons: 1. The combination of chemotherapy and PD-1 inhibitor therapy has a synergistic effect. Chemotherapy can transform "cold tumors" into "hot tumors" by changing the tumor microenvironment, thereby increasing the efficacy of immunotherapy (Herrera et al., 2017). 2. NPC itself is immunogenic, and EBV-infected nasopharyngeal carcinoma cells express target proteins of $CD4^+$ T cells and $CD8^+$ T cells. 3. Combination of the chemotherapy and PD-1 antibody can significantly increase the degree of tumor CTL infiltration and reduce the level of regulatory T cells, thereby significantly prolonging the survival time (Jarzab et al., 2005). The PACIFIC study (Antonia et al., 2017) enrolled 713 patients. In a 2:1 randomization, it was found that use of Durvalumab consolidation therapy after concurrent chemotherapy significantly prolonged the progression-free survival of these patients (17.2 months vs. 5.6 months). This revolutionized the field of radiotherapy combined with immunization. Therefore, we believe that the combined treatment mode of radiotherapy and anti-PD-1 still has clinical practical significance for recurrent and metastatic NPC patients with immune resistance (Theodoraki et al., 2022; Tian et al., 2022). The frequency of associated adverse events, such as nausea, vomiting, and anemia, is not increased in patients with recurrent/metastatic NPC treated with PD-1 inhibitors. The majority of the adverse effects were tolerable in grades 1–2 and may be reduced with appropriate therapy. Thus, adverse effects do not preclude the use of PD-1 inhibitors in metastatic/recurrent NPC (Yang et al., 2022).

There are still some limitations to this study. First: the number of included studies is small, and there are few randomized controlled trials, so there may be an influence on the conclusion. Second: the drug dosage and frequency of drugs used in the included studies were not consistently included in the studies are not consistent. Some studies used combination drugs, but some studies used drugs alone, which may lead to a large potential heterogeneity between studies. Third, despite doing an extensive systematic search of topics and a manual search of relevant articles to retrieve as many eligible papers as possible, it is likely that relevant studies were missed or excluded.

5 Conclusion

According to the available evidence, the efficacy of PD-1 inhibitor monotherapy in patients with metastatic/recurrent nasopharyngeal carcinoma was not significantly different from that of conventional chemotherapy; however, due to the limitations of the included studies, further phase III RCTs are required to corroborate our conclusion.

Data availability statement

The original contributions presented in the study are included in the article/Supplementary Material, further inquiries can be directed to the corresponding author.

Author contributions

LY: Topic proposal, data collection, methodology, software Priya Singh, data curation, writing-original draft preparation. HG: Data collection, essay writing, software analysis. BR: Data collection, software analysis. HPZ and RQH: Data collection.

Acknowledgments

We would like to thank the researchers and study participants for their contributions. HXZ: Data collection, quality assessment. LHQ and LTD: Topic proposal, writing-reviewing and editing.

Conflict of interest

The authors declare that the research was conducted in the absence of any commercial or financial relationships that could be construed as a potential conflict of interest.

Publisher's note

All claims expressed in this article are solely those of the authors and do not necessarily represent those of their affiliated organizations, or those of the publisher, the editors and the reviewers. Any product that may be evaluated in this article, or claim that may be made by its manufacturer, is not guaranteed or endorsed by the publisher.

Supplementary material

The Supplementary Material for this article can be found online at: https://www.frontiersin.org/articles/10.3389/fphar.2022.1095734/full#supplementary-material

References

Antonia, S. J., Villegas, A., Daniel, D., Vicente, D., Murakami, S., Hui, R., et al. (2017). Durvalumab after chemoradiotherapy in stage III non-small-cell lung cancer. *N. Engl. J. Med.* 377 (20), 1919–1929. doi:10.1056/NEJMoa1709937

Beyene, E. T., Ketema, S. G., Alebachew, A. N., Saleh, M. Y., and Gebremariam, T. A. (2021). Descriptive epidemiology of nasopharyngeal carcinoma at tikur anbessa hospital, Ethiopia. *BMC Cancer* 21 (1), 540. doi:10.1186/s12885-021-08311-8

Bossi, P., Chan, A. T., Licitra, L., Trama, A., Orlandi, E., Hui, E. P., et al. (2021). Nasopharyngeal carcinoma: ESMO-EURACAN clinical practice guidelines for diagnosis, treatment and follow-up(†). *Ann. Oncol.* 32 (4), 452–465. doi:10.1016/j.annonc.2020.12.007

Bray, F., Ferlay, J., Soerjomataram, I., Siegel, R. L., Torre, L. A., and Jemal, A. (2018). Global cancer statistics 2018: GLOBOCAN estimates of incidence and mortality worldwide for 36 cancers in 185 countries. *CA Cancer J. Clin.* 68 (6), 394–424. doi:10.3322/caac.21492

Chang, E. T., Ye, W., Zeng, Y. X., and Adami, H. O. (2021). The evolving epidemiology of nasopharyngeal carcinoma. *Cancer Epidemiol. Biomarkers Prev.* 30 (6), 1035–1047. doi:10.1158/1055-9965.EPI-20-1702

Chen, Y. P., Chan, A. T. C., Le, Q. T., Blanchard, P., Sun, Y., and Ma, J. (2019). Nasopharyngeal carcinoma. *Lancet* 394 (10192), 64–80. doi:10.1016/S0140-6736(19)30956-0

Diesendruck, Y., and Benhar, I. (2017). Novel immune check point inhibiting antibodies in cancer therapy-Opportunities and challenges. *Drug Resist Updat* 30, 39–47. doi:10.1016/j.drup.2017.02.001

Dwijayanti, F., Prabawa, A., and Besral, Herawati C. (2020). The five-year survival rate of patients with nasopharyngeal carcinoma based on tumor response after receiving neoadjuvant chemotherapy, followed by chemoradiation, in Indonesia: A retrospective study. *Oncology* 98 (3), 154–160. doi:10.1159/000504449

Economopoulou, P., Pantazopoulos, A., Spathis, A., Kotsantis, I., Kyriazoglou, A., Kavourakis, G., et al. (2022). Immunotherapy in nonendemic nasopharyngeal carcinoma: Real-world data from two nonendemic regions. *Cells* 11 (1), 32. doi:10.3390/cells11010032

Even, C., Wang, H. M., Li, S. H., Ngan, R. K., Dechaphunkul, A., Zhang, L., et al. (2021). Phase II, randomized study of spartalizumab (PDR001), an anti-PD-1 antibody, versus chemotherapy in patients with recurrent/metastatic nasopharyngeal cancer. *Clin. Cancer Res.* 27 (23), 6413–6423. doi:10.1158/1078-0432.CCR-21-0822

Fang, W., Yang, Y., Ma, Y., Hong, S., Lin, L., He, X., et al. (2018). Camrelizumab (SHR-1210) alone or in combination with gemcitabine plus cisplatin for nasopharyngeal carcinoma: Results from two single-arm, phase 1 trials. *Lancet Oncol.* 19 (10), 1338–1350. doi:10.1016/S1470-2045(18)30495-9

Gohil, S. H., Iorgulescu, J. B., Braun, D. A., Keskin, D. B., and Livak, K. J. (2021). Applying high-dimensional single-cell technologies to the analysis of cancer immunotherapy. *Nat. Rev. Clin. Oncol.* 18 (4), 244–256. doi:10.1038/s41571-020-00449-x

Herrera, F. G., Bourhis, J., and Coukos, G. (2017). Radiotherapy combination opportunities leveraging immunity for the next oncology practice. *CA Cancer J. Clin.* 67 (1), 65–85. doi:10.3322/caac.21358

Hiam-Galvez, K. J., Allen, B. M., and Spitzer, M. H. (2021). Systemic immunity in cancer. *Nat. Rev. Cancer* 21 (6), 345–359. doi:10.1038/s41568-021-00347-z

Hsu, C., Lee, S. H., Ejadi, S., Even, C., Cohen, R. B., Le Tourneau, C., et al. (2017). Safety and antitumor activity of Pembrolizumab in patients with programmed death-ligand 1-positive nasopharyngeal carcinoma: Results of the KEYNOTE-028 study. *J. Clin. Oncol.* 35 (36), 4050. doi:10.1200/JCO.2017.73.3675

Hua, Y. H., Dong, R. Z., Jin, T., Jin, Q. F., and Chen, X. Z. (2022). Anti-PD-1 monoclonal antibody combined with anti-VEGF agent is safe and effective in patients with recurrent/metastatic head and neck squamous cancer as second-line or beyond treatment. *Front. Oncol.* 12. doi:10.3389/fonc.2022.781348

Huang, J. L., Chen, S. Y., and Lin, C. S. (2022). Targeting cancer stem cells through epigenetic modulation of interferon response. *J. Personalized Med.* 12 (4), 556. doi:10.3390/jpm12040556

Jarzab, B., Handkiewicz-Junak, D., and Wloch, J. (2005). Juvenile differentiated thyroid carcinoma and the role of radioiodine in its treatment: A qualitative review. *Endocr. Relat. Cancer* 12 (4), 773–803. doi:10.1677/erc.1.00880

Jiang, W., Pan, S., Chen, X., Wang, Z. W., and Zhu, X. (2021). The role of lncRNAs and circRNAs in the PD-1/PD-L1 pathway in cancer immunotherapy. *Mol. Cancer* 20 (1), 116. doi:10.1186/s12943-021-01406-7

Kang, Y., He, W., Ren, C., Qiao, J., Guo, Q., Hu, J., et al. (2020). Advances in targeted therapy mainly based on signal pathways for nasopharyngeal carcinoma. *Signal Transduct. Target Ther.* 5 (1), 245. doi:10.1038/s41392-020-00340-2

Kim, J. M., and Chen, D. S. (2016). Immune escape to PD-L1/PD-1 blockade: Seven steps to success (or failure). *Ann. Oncol.* 27 (8), 1492–1504. doi:10.1093/annonc/mdw217

Klein, C. A. (2009). Parallel progression of primary tumours and metastases. *Nat. Rev. Cancer* 9 (4), 302–312. doi:10.1038/nrc2627

Kumar, P., Saini, S., and Prabhakar, B. S. (2020). Cancer immunotherapy with check point inhibitor can cause autoimmune adverse events due to loss of Treg homeostasis. *Semin. Cancer Biol.* 64, 29–35. doi:10.1016/j.semcancer.2019.01.006

Lee, A. W., Ma, B. B., Ng, W. T., and Chan, A. T. (2015). Management of nasopharyngeal carcinoma: Current practice and future perspective. *J. Clin. Oncol.* 33 (29), 3356–3364. doi:10.1200/JCO.2015.60.9347

Lee, H. M., Okuda, K. S., González, F. E., and Patel, V. (2019). Current perspectives on nasopharyngeal carcinoma. *Adv. Exp. Med. Biol.* 1164, 11–34. doi:10.1007/978-3-030-22254-3_2

Li, X., Wenes, M., Romero, P., Huang, S. C., Fendt, S. M., and Ho, P. C. (2019). Navigating metabolic pathways to enhance antitumour immunity and immunotherapy. *Nat. Rev. Clin. Oncol.* 16 (7), 425–441. doi:10.1038/s41571-019-0203-7

Lin, J., Guo, Q., Guo, Z., Lu, T., Chen, G., Lin, S., et al. (2022). Stereotactic body radiotherapy extends the clinical benefit of PD-1 inhibitors in refractory recurrent/metastatic nasopharyngeal carcinoma. *Radiat. Oncol.* 17 (1), 117. doi:10.1186/s13014-022-02073-8

Lo, C. K., Mertz, D., and Loeb, M. (2014). Newcastle-ottawa Scale: Comparing reviewers' to authors' assessments. *BMC Med. Res. Methodol.* 14, 45. doi:10.1186/1471-2288-14-45

Ma, B. B. Y., Lim, W. T., Goh, B. C., Hui, E. P., Lo, K. W., Pettinger, A., et al. (2018). Antitumor activity of nivolumab in recurrent and metastatic nasopharyngeal carcinoma: An international, multicenter study of the mayo clinic phase 2 consortium (NCI-9742). *J. Clin. Oncol.* 36 (14), 1412–1418. doi:10.1200/JCO.2017.77.0388

Ma, Y., Chen, X., Wang, A., Zhao, H., Lin, Q., Bao, H., et al. (2021). Copy number loss in granzyme genes confers resistance to immune checkpoint inhibitor in nasopharyngeal carcinoma. *J. Immunother. Cancer* 9 (3), e002014. doi:10.1136/jitc-2020-002014

Mai, H. Q., Chen, Q. Y., Chen, D. P., Hu, C. S., Yang, K. Y., Wen, J. Y., et al. (2021). Toripalimab or placebo plus chemotherapy as first-line treatment in advanced nasopharyngeal carcinoma: A multicenter randomized phase 3 trial. *Nat. Med.* 27 (9), 1536–1543. doi:10.1038/s41591-021-01444-0

Prada, C. E., Jousma, E., Rizvi, T. A., Wu, J., Dunn, R. S., Mayes, D. A., et al. (2013). Neurofibroma-associated macrophages play roles in tumor growth and response to pharmacological inhibition. *Acta Neuropathol.* 125 (1), 159–168. doi:10.1007/s00401-012-1056-7

Riley, R. S., June, C. H., Langer, R., and Mitchell, M. J. (2019). Delivery technologies for cancer immunotherapy. *Nat. Rev. Drug Discov.* 18 (3), 175–196. doi:10.1038/s41573-018-0006-z

Sato, H., Fushimi, C., Okada, T., Matsuki, T., Kondo, T., Omura, G. O., et al. (2020). Investigation of the efficacy and safety of nivolumab in recurrent and metastatic nasopharyngeal carcinoma. *Vivo* 34 (5), 2967–2972. doi:10.21873/invivo.12127

Sterne, J. A. C., Savović, J., Page, M. J., Elbers, R. G., Blencowe, N. S., Boutron, I., et al. (2019). RoB 2: A revised tool for assessing risk of bias in randomised trials. *Bmj* 366, l4898. doi:10.1136/bmj.l4898

Sun, X. S., Li, X. Y., Chen, Q. Y., Tang, L. Q., and Mai, H. Q. (2019). Future of radiotherapy in nasopharyngeal carcinoma. *Br. J. Radiol.* 92 (1102), 20190209. doi:10.1259/bjr.20190209

Theodoraki, M. N., Laban, S., and Hoffmann, T. K. (2022). Immunotherapy of head and neck cancer Highlights of the ASCO and ESMO annual meetings 2021. *Hno* 70 (4), 271–277. doi:10.1007/s00106-021-01142-w

Tian, K., Han, J. Q., Wang, Z., and Chen, J. (2022). Immune checkpoint inhibition in first-line treatment for recurrent or metastatic nasopharyngeal carcinoma: A CAPTAIN-1st and JUPITER-02 trial-based cost-effectiveness analysis. *Oral Oncol.* 128, 105842. doi:10.1016/j.oraloncology.2022.105842

Tsang, C. M., Lui, V. W. Y., Bruce, J. P., Pugh, T. J., and Lo, K. W. (2020). Translational genomics of nasopharyngeal cancer. *Semin. Cancer Biol.* 61, 84–100. doi:10.1016/j.semcancer.2019.09.006

Wang, B. C., Cao, R. B., Fu, C., Chen, W. B., Li, P. D., Lin, G. H., et al. (2020). The efficacy and safety of PD-1/PD-L1 inhibitors in patients with recurrent or metastatic nasopharyngeal carcinoma: A systematic review and meta-analysis. *Oral Oncol.* 104, 104640. doi:10.1016/j.oraloncology.2020.104640

Wang, F. H., Wei, X. L., Feng, J., Li, Q., Xu, N., Hu, X. C., et al. (2021). Efficacy, safety, and correlative biomarkers of Toripalimab in previously treated recurrent or metastatic nasopharyngeal carcinoma: A phase II clinical trial (POLARIS-02). *J. Clin. Oncol.* 39 (7), 704–712. doi:10.1200/JCO.20.02712

Xie, F., Xu, M., Lu, J., Mao, L., and Wang, S. (2019). The role of exosomal PD-L1 in tumor progression and immunotherapy. *Mol. Cancer* 18 (1), 146. doi:10.1186/s12943-019-1074-3

Yang, J., Chen, J., Liang, H., and Yu, Y. (2022). Nasopharyngeal cancer cell-derived exosomal PD-L1 inhibits CD8+ T cell activity and promotes immune escape. *Cancer Sci.* 113, 3044–3054. doi:10.1111/cas.15433

Yang, Y. P., Zhou, T., Chen, X. Z., Li, J. A., Pan, J. J., He, X. H., et al. (2021). Efficacy, safety, and biomarker analysis of Camrelizumab in previously treated recurrent or metastatic nasopharyngeal carcinoma (CAPTAIN study). *J. Immunother. Cancer* 9 (12), e003790. doi:10.1136/jitc-2021-003790

Yarza, R., Bover, M., Agulló-Ortuño, M. T., and Iglesias-Docampo, L. C. (2021). Current approach and novel perspectives in nasopharyngeal carcinoma: The role of targeting proteasome dysregulation as a molecular landmark in nasopharyngeal cancer. *J. Exp. Clin. Cancer Res.* 40 (1), 202. doi:10.1186/s13046-021-02010-9

Zhang, L., Yang, Y., Pan, J., Chen, X., Sun, Y., Wang, H., et al. (2022). RATIONALE-309: Updated progression-free survival (PFS), PFS after next line of treatment, and overall survival from a phase 3 double-blind trial of tislelizumab versus placebo, plus chemotherapy, as first-line treatment for recurrent/metastatic nasopharyngeal cancer. *J. Clin. Oncol.* 40 (36), 384950. doi:10.1200/jco.2022.40.36_suppl.384950

Zhang, Y., Chen, L., Hu, G. Q., Zhang, N., Zhu, X. D., Yang, K. Y., et al. (2019). Gemcitabine and cisplatin induction chemotherapy in nasopharyngeal carcinoma. *N. Engl. J. Med.* 381 (12), 1124–1135. doi:10.1056/NEJMoa1905287

frontiers | Frontiers in Pharmacology

TYPE Original Research
PUBLISHED 20 January 2023
DOI 10.3389/fphar.2023.1121586

OPEN ACCESS

EDITED BY
Qianming Du,
Nanjing Medical University, China

REVIEWED BY
Yuxian Song,
Nanjing University, China
Xue-Yan He,
Cold Spring Harbor Laboratory,
United States

*CORRESPONDENCE
Weijun Qin,
qinwj@fmmu.edu.cn
Weihong Wen,
weihongwen@nwpu.edu.cn
Fa Yang,
yangfa@fmmu.edu.cn

†These authors have contributed equally to this work and share first authorship

SPECIALTY SECTION
This article was submitted to Pharmacology of Anti-Cancer Drugs, a section of the journal Frontiers in Pharmacology

RECEIVED 12 December 2022
ACCEPTED 13 January 2023
PUBLISHED 20 January 2023

CITATION
Zhang J, Lu S, Lu T, Han D, Zhang K, Gan L, Wu X, Li Y, Zhao X, Li Z, Shen Y, Hu S, Yang F, Wen W and Qin W (2023), Single-cell analysis reveals the COL11A1^{+} fibroblasts are cancer-specific fibroblasts that promote tumor progression. *Front. Pharmacol.* 14:1121586. doi: 10.3389/fphar.2023.1121586

Single-cell analysis reveals the COL11A1^{+} fibroblasts are cancer-specific fibroblasts that promote tumor progression

Jiayu Zhang[1†], Shiqi Lu[2†], Tong Lu[1†], Donghui Han[1], Keying Zhang[1], Lunbiao Gan[2], Xinjie Wu[2], Yu Li[1], Xiaolong Zhao[1], Zhengxuan Li[1], Yajie Shen[1], Sijun Hu[2], Fa Yang[1*], Weihong Wen[2*] and Weijun Qin[1*]

[1]Department of Urology, Xijing Hospital, Fourth Military Medical University, Xi'an, China, [2]Institute of Medical Research, Northwestern Polytechnical University, Xi'an, China

Background: Cancer-associated fibroblasts (CAFs) promote tumor progression through extracellular matrix (ECM) remodeling and extensive communication with other cells in tumor microenvironment. However, most CAF-targeting strategies failed in clinical trials due to the heterogeneity of CAFs. Hence, we aimed to identify the cluster of tumor-promoting CAFs, elucidate their function and determine their specific membrane markers to ensure precise targeting.

Methods: We integrated multiple single-cell RNA sequencing (scRNA-seq) datasets across different tumors and adjacent normal tissues to identify the tumor-promoting CAF cluster. We analyzed the origin of these CAFs by pseudotime analysis, and tried to elucidate the function of these CAFs by gene regulatory network analysis and cell-cell communication analysis. We also performed cell-type deconvolution analysis to examine the association between the proportion of these CAFs and patients' prognosis in TCGA cancer cohorts, and validated that through IHC staining in clinical tumor tissues. In addition, we analyzed the membrane molecules in different fibroblast clusters, trying to identify the membrane molecules that were specifically expressed on these CAFs.

Results: We found that COL11A1+ fibroblasts specifically exist in tumor tissues but not in normal tissues and named them cancer-specific fibroblasts (CSFs). We revealed that these CSFs were transformed from normal fibroblasts. CSFs represented a more activated CAF cluster and may promote tumor progression through the regulation on ECM remodeling and antitumor immune responses. High CSF proportion was associated with poor prognosis in bladder cancer (BCa) and lung adenocarcinoma (LUAD), and IHC staining of COL11A1 confirmed their specific expression in tumor stroma in clinical BCa samples. We also identified that CSFs specifically express the membrane molecules LRRC15, ITGA11, SPHK1 and FAP, which could distinguish CSFs from other fibroblasts.

Conclusion: We identified that CSFs is a tumor specific cluster of fibroblasts, which are in active state, may promote tumor progression through the regulation on ECM remodeling and antitumor immune responses. Membrane molecules LRRC15, ITGA11, SPHK1 and FAP could be used as therapeutic targets for CSF-targeting cancer treatment.

KEYWORDS

cancer-associated fibroblasts, single-cell RNA sequencing, tumor microenvironment, ECM remodeling, immune response

1 Introduction

Cancer-associated fibroblasts (CAFs) promote tumor invasion, metastasis and drug resistance *via* extracellular matrix (ECM) remodeling, cytokine secretion, and crosstalk with different cells in tumor microenvironment (TME), such as cancer cells, immune cells and stromal cells (Sahai et al., 2020; Biffi and Tuveson, 2021). CAFs are considered attractive targets for cancer treatment (Chen et al., 2021a). However, multiple CAF-targeting strategies failed in clinical trials and in some cases even accelerated tumor progression. For example, chemotherapy combined with CAF-targeting drugs, such as the Hedgehog pathway inhibitor hyaluronidase to decompose hyaluronic acid (hyaluronan, HA) or matrix metalloproteinase 9 (MMP9) inhibitors, did not show synergistic effects, and some combinations even increased adverse effects, such as gastrointestinal (GI) toxicity and thromboembolic (TE) events, in patients with different cancers, including metastatic pancreatic cancer (mPC), colorectal cancer (CRC), ovarian cancers (OVC) and gastric cancer (Kaye et al., 2012; Berlin et al., 2013; Catenacci et al., 2015; De Jesus-Acosta et al., 2020; Van Cutsem et al., 2020; Shah et al., 2021).

CAFs are composed of distinct clusters with different or even opposite functions, the heterogeneity of CAFs may account for the failure of these CAF-targeting treatment in clinical trials (Chen et al., 2021a; Galbo et al., 2021; Hutton et al., 2021). In addition, currently used CAF-targeting molecules are expressed in other cell types or even normal tissues, which may also explain the severe adverse effects of CAF-targeting therapeutic strategies. For example, hyaluronic acid (HA), an ECM component, also commonly exists in various human tissues, which may account for the severe adverse events of hyaluronidase (Garantziotis and Savani, 2019). The diverse origins of CAFs are an important reason for their heterogeneity, and several cell types have been proposed to be the precursors of CAFs, such as normal fibroblasts, mesenchymal stem cells (MSCs), endothelial cells, pericytes, myeloid cells and epithelial cells (Zeisberg et al., 2007; Hosaka et al., 2016; Biffi and Tuveson, 2021; Butti et al., 2021; Tang et al., 2022). In-depth analysis of the differences between these precursor cells and CAFs may provide evidence regarding the origin of CAFs and the mechanism of cell transition.

Single-cell RNA sequencing (scRNA-seq) is an effective way to analyze the heterogeneity of CAFs and the differences between different clusters of CAFs (Qian et al., 2020; Zhang et al., 2020; Olbrecht et al., 2021). The classification of CAFs is based on their different functions, by which, CAFs are commonly divided into matrix CAFs or myo-CAFs (mCAFs), inflammatory CAFs (iCAFs), antigen-presenting CAFs (apCAFs), EMT-like CAFs (eCAFs) and vascular CAFs (vCAFs) (Chen et al., 2020; Zhang et al., 2020). However, these classifications cannot distinguish the fibroblasts that specifically exist in tumor tissues from fibroblasts in normal tissues. Decoding the differences between them could not only elucidate the mechanisms how these fibroblasts promote tumor progression but also provide new therapeutic targets for cancer treatment.

In this study, by analyzing scRNA-seq datasets of multiple cancer types, we compared the differences between fibroblasts that specifically exist in tumor tissues and fibroblasts in normal tissues (Ma et al., 2019; Qian et al., 2020; Steele et al., 2020; Zhang et al., 2020; Affo et al., 2021; Chen et al., 2021b; Olbrecht et al., 2021). We identified that the COL11A1$^+$ fibroblasts only exist in various tumor tissues but not in normal tissues, thus we named them cancer-specific fibroblasts (CSFs). We revealed that CSFs might transform from normal fibroblasts and may promote tumor progression through the regulation on ECM remodeling and antitumor immune responses. We also found that membrane molecules, such as leucine-rich repeat-containing protein (LRRC15), integrin alpha-11 (ITGA11), sphingosine kinase 1 (SPHK1) and fibroblast activation protein (FAP) were specifically expressed in CSFs, which could be used as therapeutic targets in CSF-targeting cancer treatment.

2 Materials and methods

2.1 Datasets of single-cell RNA-sequencing (scRNA-seq)

ScRNA-seq datasets containing tumor tissues (ten datasets across eight tumor types) and adjacent normal tissues (six datasets from five types of normal tissues) were downloaded from the Gene Expression Omnibus (GEO, RRID:SCR_005012) and https://lambrechtslab.sites.vib.be/en/data-access, as shown in Supplementary Table S1.

2.2 Integrated analysis of scRNA-seq datasets

Analysis of scRNA-seq datasets was performed primarily using the Seurat package (v4.0.5) in R (v4.1.0) (Hao et al., 2021). First, we used Seurat package to create individual Seurat Objects from gene expression matrices separately. Genes expressed in fewer than three cells were removed in this process. Second, strict quality control procedures were performed in Seurat. Seurat Objects were filtered to exclude the cells that expressed fewer than 200 genes, more than 6000 or 8000 genes, greater than 20% mitochondrial genes, and more than 0.1% or 1% hemoglobin genes. Third, all Seurat Objects were merged to generate a combined Seurat Object, and the merged Seurat Object was normalized and scaled separately using the NormalizeData and ScaleData functions. The Find Variable Features function was applied to identify the variable genes. Fourth, principal component analysis (PCA) was conducted with the RunPCA function based on the variable genes. After the PCA, we applied Harmony package (v0.1.0) to integrate the merged Seurat Objects and correct batch effects from different samples (Korsunsky et al., 2019). Finally, clustering was conducted using the Find Neighbors and the Find Clusters functions at a resolution = 3 for tumor tissue cells or a resolution = 0.8 for normal tissue cells. Visualization was implemented *via* uniform manifold approximation and projection (UMAP) or t-distributed stochastic neighbor embedding (tSNE).

Marker genes of cell clusters were identified using the Find All Markers function *via* Wilcoxon rank-sum tests. Then, each cell cluster was renamed to the specific cell type according to classical marker genes as follows: B cells (marked with CD79A and MS4A1), plasma cells (marked with CD79A, IGKC and IGLC2), CD4$^+$ T cells (marked with CD3D, CD4 and IL7R), CD8$^+$ T cells (marked with CD3D, CD8A and GZMB), dendritic cells (DCs, marked with CD1C and CD1E), endothelial cells (marked with PECAM1 and vWF), epithelial cells (marked with EPCAM and KRT18), fibroblasts (FBs, marked with COL1A1 and DCN), macrophages (marked with CD68 and CD163), mast cells (marked with CPA3 and KIT), monocytes (marked with CD14 and S100A8), natural killer cells (NK cells, marked with NKG7 and GNLY), and pericytes (marked with CSPG4 and RGS5).

2.3 Construction of the fibroblast atlas

The fibroblast data were extracted from integrated multi-tumor and multi-tissue scRNA-seq datasets. ScRNA-seq data of CAFs and normal fibroblasts were integrated *via* the Harmony package. Merged fibroblasts were divided into six distinct clusters. UMAP was applied to visualize the fibroblast atlas.

2.4 Gene set variation analysis

Gene set variation analysis (GSVA) was performed using the GSVA package (v1.40.1) (Hanzelmann et al., 2013). Specifically, single-sample gene set enrichment analysis (ssGSEA) was used to evaluate the pathway activations of the 50 hallmark gene sets from the Molecular Signatures Database (MSigDB) for each cell.

2.5 Gene regulatory network analysis

To identify the gene regulatory network of each fibroblast cluster, single-cell regulatory network inference and clustering (SCENIC) was performed using pySCENIC (v0.11.2), a Python implementation of the SCENIC pipeline (Van de Sande et al., 2020). First, gene expression matrix was extracted from the Seurat Object of fibroblasts using the Seurat package. Second, co-expression modules were inferred using the method of GRNBoost2 based on gene expression matrix. Third, regulons (i.e., transcription factors and their target genes) were refined from these co-expression modules using cis-regulatory motif discovery (cisTarget). Fourth, the activity of these regulons was quantified in each individual cell *via* AUCell. Finally, the differentially activated regulons of each fibroblast subcluster were identified by using the Wilcoxon rank sum test.

2.6 Pseudotime analysis

Pseudotime analysis was conducted using the Monocle3 package (v1.0.0) (Cao et al., 2019). Single-cell trajectories were calculated using the functions "learn_graph" and "order_cells" based on fibroblast clusters from Seurat. The result of pseudotime analysis was visualized through the UMAP method.

2.7 Cell–cell communication analysis

Cell–cell communication analysis was inferred based on the expression of known ligand–receptor pairs in different cell types *via* the CellChat package (v1.1.3) (Jin et al., 2021). The official workflow was used for further analysis. "Secreted Signaling" pathways were set to the reference database of ligand–receptor pairs. The essential functions "identifyOverExpressedGenes," "identifyOverExpressedInteractions," "projectData," "computeCommunProb," "computeCommunProbPathway," and "aggregateNet" were applied using standard parameters to conduct the primary analysis. The function "netVisualbubble" was used to visualize the result of cell–cell interactions.

2.8 Cell composition deconvolution

We applied CIBERSORTx to perform cell composition deconvolution for TCGA bulk RNA-seq data of tumor tissues and adjacent normal tissues (Newman et al., 2019). Firstly, CIBERSORTx was used to construct a signature gene expression matrix based on the multi-cancer scRNA-seq dataset. Secondly, fragments per kilobase of transcript per million mapped reads (FPKM) values of TCGA bulk RNA-seq data were transformed into transcripts per million reads (TPM) values. Finally, cell proportions of tumor tissues and adjacent normal tissues were evaluated *via* CIBERSORTx based on the TCGA bulk RNA-seq data. The cell types included CSFs, CLDN1$^+$ FBs, CXCL14$^+$ FBs, BAMBI$^+$ FBs, DPT$^+$ FBs, RGS5$^+$ FBs, B cells, CD4$^+$ T cells, CD8$^+$ T cells, endothelial cells, epithelial cells, macrophages, mast cells, monocytes and pericytes.

2.9 Immunohistochemistry (IHC) staining

IHC staining of bladder cancer tissue microarray (HBlaU079Su01, Shanghai Outdo Biotech Company) was performed with COL11A1 polyclonal antibody (1:200, ABP53753, Abbkine) according to standard protocols. Intensity of IHC staining of COL11A1 in tumor tissue was scored by two independent pathologists according to semi-quantitative immunoreactivity scoring (IRS) system. The staining intensity was scored as 0 (negative), 1 (weak), 2 (moderate), and 3 (strong), and the staining extent was quantified as: 0 (negative), 1 (1%–10%), 2 (11%–50%), 3 (51%–80%), and 4 (81%–100%). The staining intensity and extent values were multiplied to get the IHC score (Cheng et al., 2021). The baseline characteristics of enrolled bladder cancer patients showed in Supplementary Table S9.

2.10 Survival analysis

Survival analysis of distinct fibroblast clusters was conducted using the R packages survival (v3.2.13) and survminer (v0.4.9). Patients were divided into CSF-high and CSF-low groups in each cancer type of the TCGA cohort based on the median value of the CSF proportions. The "survfit" function was applied to generate Kaplan–Meier survival plots in different cancer types. In addition, univariable Cox proportional hazards regression analysis was performed *via* the "coxph" function. Survival analysis based on gene expression was performed *via* the Gene Expression Profiling Interactive Analysis (GEPIA, RRID:SCR_018294) platform (Tang et al., 2019).

2.11 Statistical analysis

Statistical analysis was conducted using R (v4.1.0). The Wilcoxon rank-rum test was performed to test the significance for most cases. Statistical significance was defined as a p-value <0.05 (*$p < 0.05$, **$p < 0.01$, ***$p < 0.001$; ns, not significant). Overall survival analysis was performed using the log-rank test.

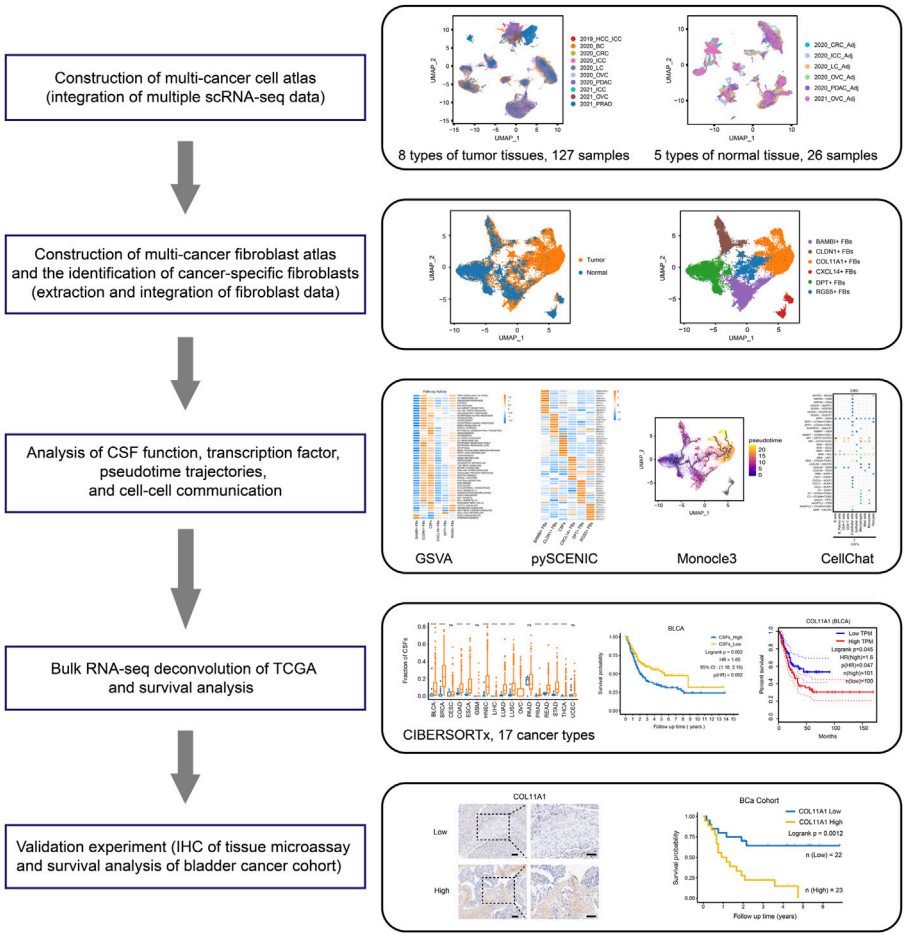

FIGURE 1
Workflow of this study.

2.12 Data and code availability

The scRNA-seq data analyzed in this study were obtained from https://lambrechtslab.sites.vib.be/en/data-access and the GEO (GSE141445, GSE155698, GSE125449, GSE138709, GSE142784, and GSE154170). TCGA bulk RNA-seq datasets with FPKM values and clinical data were obtained from the UCSC Xena platform (Goldman et al., 2020).

All R packages used are available online. Customized code for data analysis and plotting are available on GitHub (https://github.com/jiayu2022/pancancer_caf).

3 Results

3.1 COL11A1$^+$ fibroblasts specifically exist in different tumor tissues

The graphic flowchart summarized the main procedures of present study (Figure 1). To construct a multi-tumor fibroblast atlas, we integrated ten scRNA-seq datasets across eight tumor types, including colorectal cancer (CRC), ovarian cancer (OVC), prostate adenocarcinoma (PRAD), breast cancer (BC), pancreatic ductal adenocarcinoma (PDAC), hepatocellular carcinoma (HCC), lung cancer (LC) and intrahepatic cholangiocarcinoma (ICC) (Ma et al., 2019; Qian et al., 2020; Steele et al., 2020; Zhang et al., 2020; Affo et al., 2021; Chen et al., 2021b; Olbrecht et al., 2021). The multi-tumor cell atlas included 215,871 high-quality cells from 127 tumor samples of 94 patients, and the batch effects across samples were corrected (Supplementary Figure S1A; Supplementary Tables S1, S2). These cells were divided into 13 distinct cell types using classification markers: B cells, plasma cells, CD4$^+$ T cells, CD8$^+$ T cells, DCs, endothelial cells, epithelial cells, fibroblasts, macrophages, mast cells, monocytes, NK cells and pericytes (Figure 2A; Supplementary Figures S1B, C; Supplementary Table S3). Similarly, six scRNA-seq datasets from five types of adjacent normal tissues were also integrated, including lung, ovary, colorectum, pancreas and intrahepatic bile duct. We obtained 65, 807 high-quality cells from 26 normal tissues, and removed the batch effects across samples (Supplementary Figure S1D; Supplementary Tables S1, S2). These cells were also divided into 13 cell types indicated above (Figure 2B; Supplementary Figure S1E, F; Supplementary Table S4).

Then, fibroblast clusters were extracted from the multi-tumor cell atlas and multi-tissue cell atlas separately, re-embedded and re-

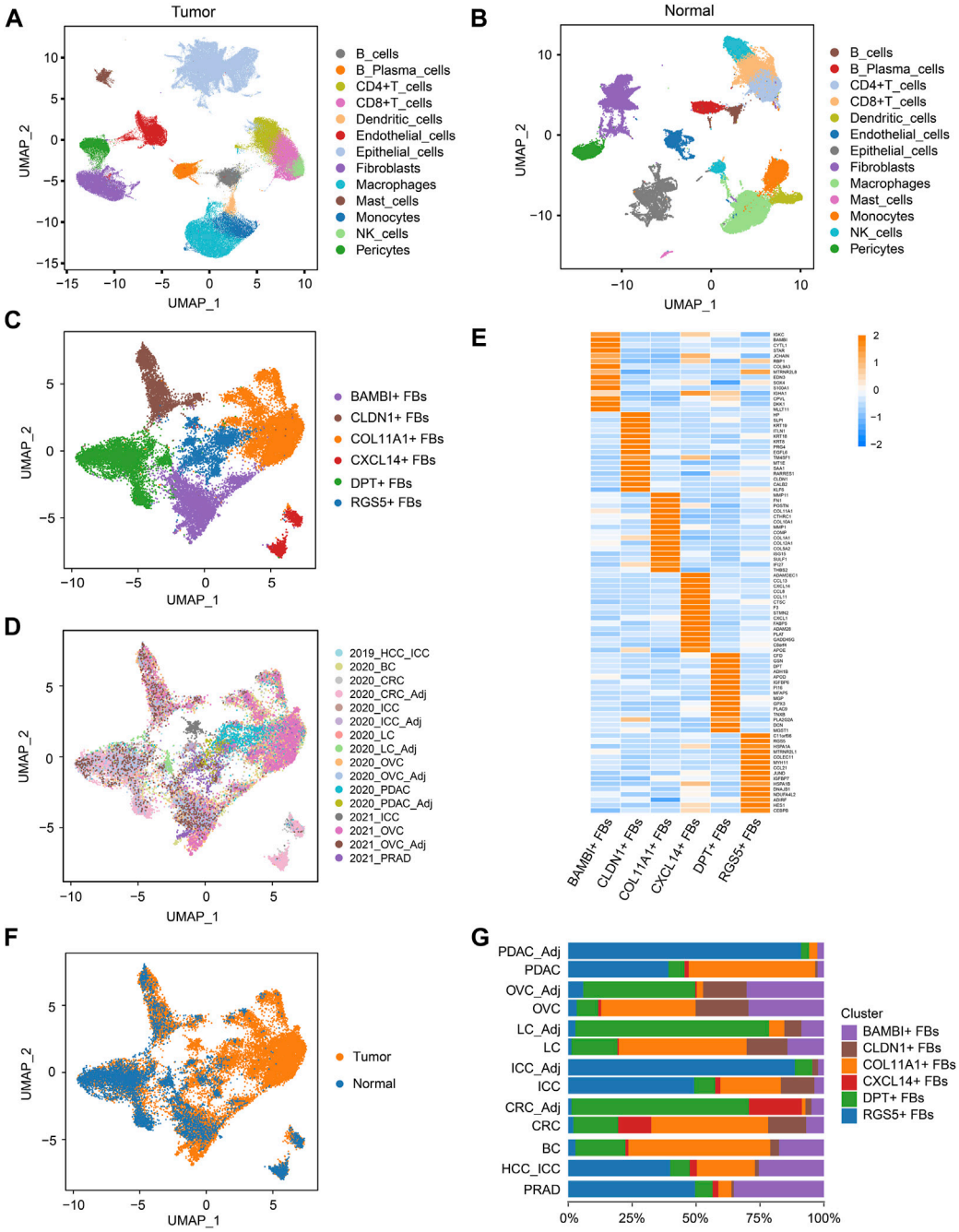

FIGURE 2
COL11A1$^+$ fibroblasts specifically exist in tumor tissues. **(A)**, UMAP visualization of the cell populations in tumor tissues from ten scRNA-seq datasets across eight tumor types. **(B)**, UMAP visualization of the cell populations from six scRNA-seq datasets of five types of normal tissues. **(C)**, UMAP visualization of fibroblast clusters across normal tissues and tumor tissues. Different fibroblast clusters are color-coded. **(D)**, UMAP to depict the tissue origins of the fibroblast clusters. **(E)**, Heatmap to show the top DEGs (Wilcoxon test) in each fibroblast cluster. **(F)**, UMAP to depict the tissue types (tumor or normal tissue) of different fibroblast clusters. **(G)**, Bar plots to show the proportion of different fibroblast clusters in each tissue. DEGs, differentially expressed genes.

clustered to construct the multi-cancer fibroblast atlas, and the bias induced by the cell cycle states was removed (Figures 2C, D; Supplementary Figures S2A, B). In this atlas, 24,662 fibroblasts were divided into six clusters: COL11A1$^+$ fibroblasts (FBs), CLDN1$^+$ FBs, CXCL14$^+$ FBs, BAMBI$^+$ FBs, DPT$^+$ FBs and RGS5$^+$ FBs (Figures 2C, E; Supplementary Figures S2C, D; Supplementary Table S5). Among these clusters, CXCL14$^+$ FBs mainly existed in CRC and normal colorectal tissues, indicating that they were tissue-specific fibroblasts. Notably, COL11A1$^+$ FBs only existed in various tumor tissues but not normal tissues, thus, we named them cancer-specific fibroblasts (CSFs), while other clusters existed in both tumor tissues and normal tissues (Figures 2F, G). According to these results, we speculate that COL11A1$^+$ FBs are CSFs that specifically exist across different cancer types.

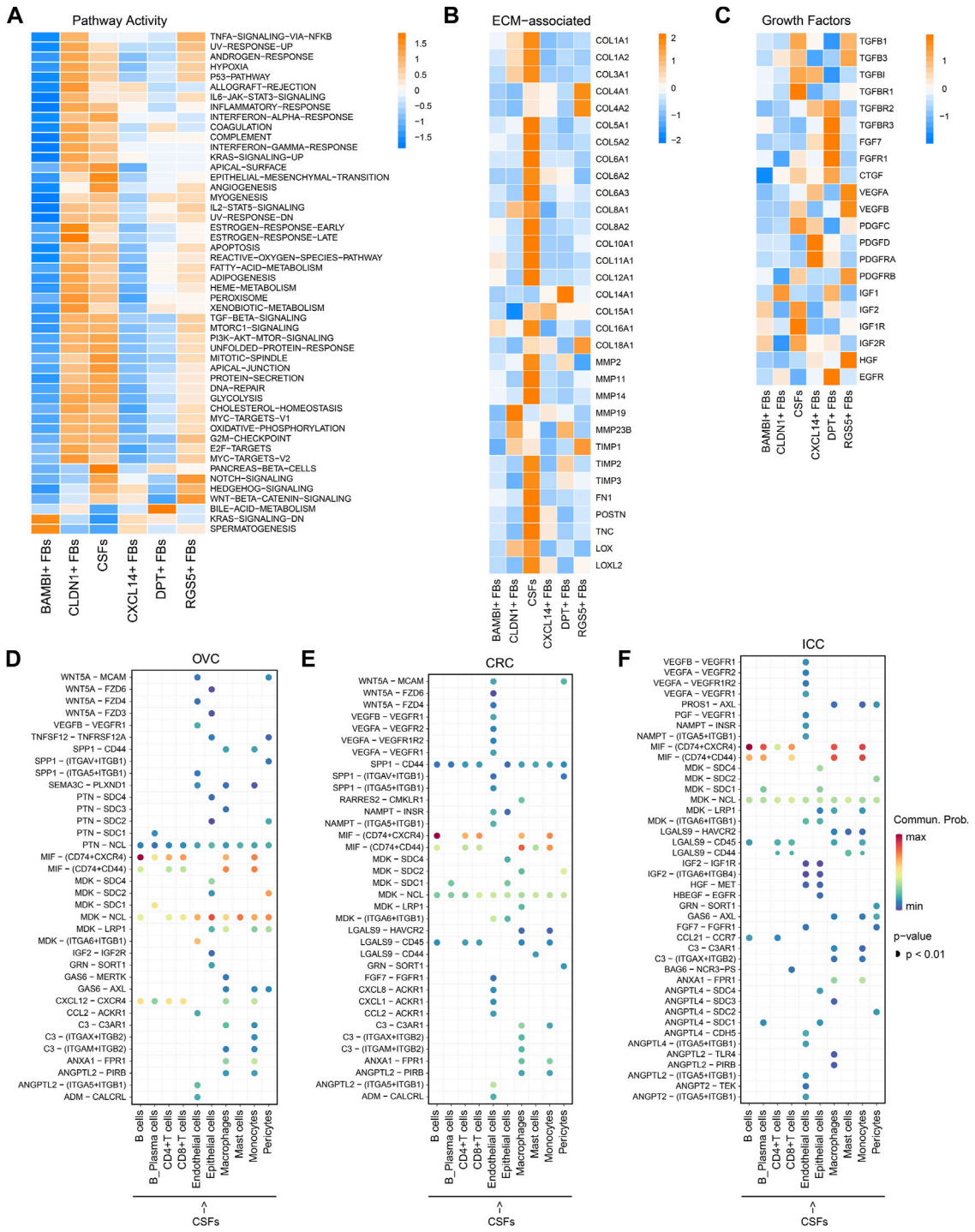

FIGURE 3
CSFs represent a more activated CAFs cluster that may enhance ECM remodeling and inhibit antitumor immune response. **(A)**, Activity of Hallmark pathways (scored per cell by GSVA) in six fibroblast clusters. **(B)**, Heatmap to show the differentially expressed ECM associated genes in six fibroblast clusters. **(C)**, Heatmap to show the differentially expressed growth factors in six fibroblast clusters. **(D–F)**, Interaction analysis to show the enriched receptor-ligand pairs between CSFs and other cell types in OVC **(D)**, CRC **(E)** and ICC **(F)**.

3.2 CSFs represent an activated cluster of CAFs that may enhance ECM remodeling and inhibit antitumor immune response

Next, we investigated the differences between CSFs and other fibroblast clusters. Pathway analysis revealed that CSFs had higher enrichment scores than other fibroblasts in TGF-β signaling and protein secretion pathways. Notch signaling, Hedgehog signaling and Wnt/β-catenin signaling, which have shown to be associated with the maintenance of cell stemness were highly activated in CSFs compared with other fibroblasts except the RGS5^{+} FBs (Figure 3A) (Briscoe and Therond, 2013; Liu et al., 2022; Zhou et al., 2022).

10.3389/fphar.2023.1121586

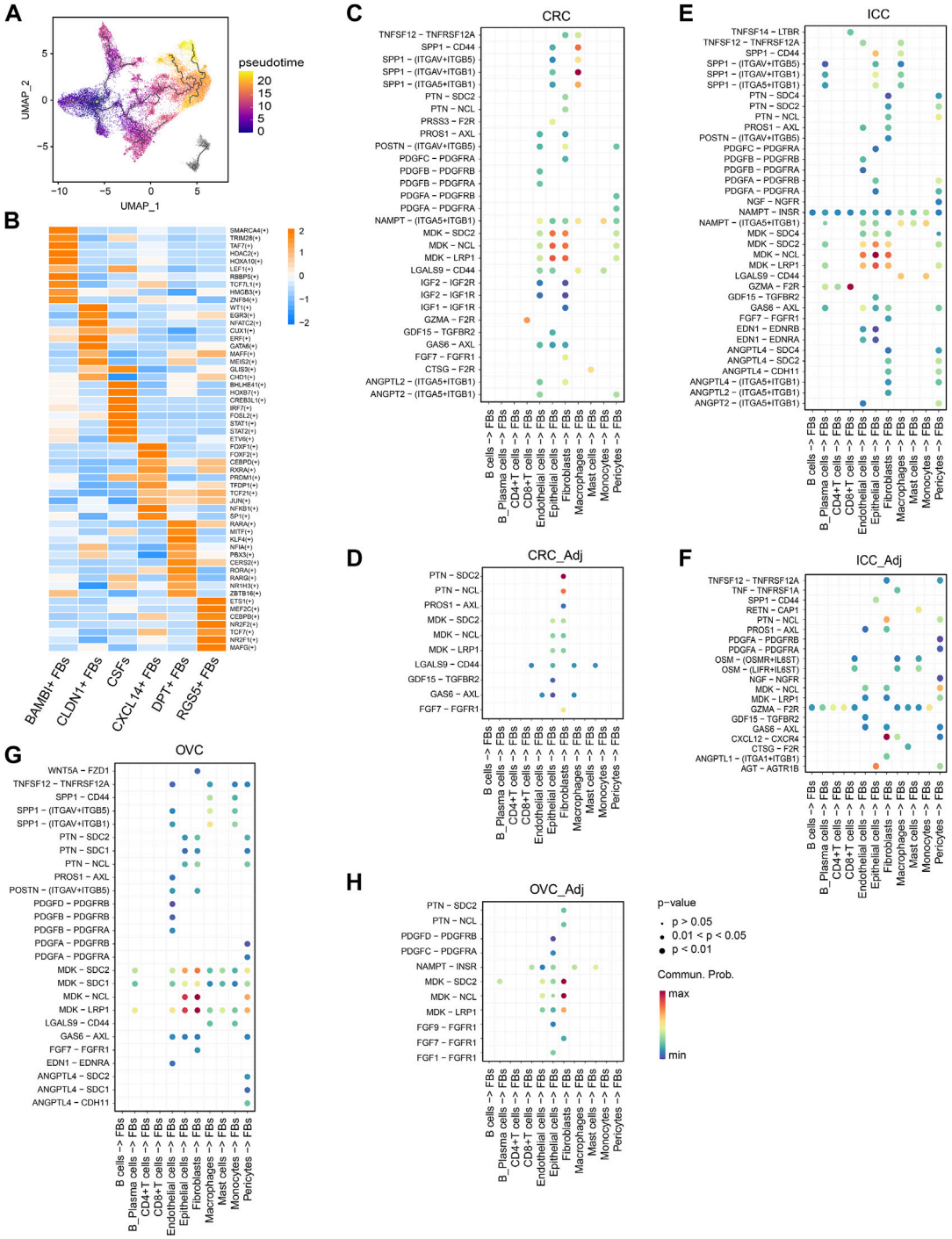

FIGURE 4
CSFs mainly transform from normal fibroblasts. **(A)**, UMAP of fibroblasts to show the projection of Pseudotime trajectory. Pseudotime values code the cell color. **(B)**, Heatmap to show the t-value for the area under the curve score of expression regulation by transcription factors, as estimated by pySCENIC. **(C–H)**, Interaction analysis to show the enriched receptor-ligand pairs between fibroblasts and other cell types in CRC **(C)**, normal colorectal tissues **(D)**, ICC **(E)**, intrahepatic bile ducts **(F)**, OVC **(G)** and normal ovarian tissues **(H)**.

Furthermore, ECM-associated genes, such as multiple collagens, MMPs, tissue inhibitors of metalloproteinases (TIMPs), fibronectin 1 (FN1) and periostin (POSTN), were all highly expressed in CSFs (Figure 3B). In addition, CSFs had high expression of TGF-β and TGF-β receptor type 1 (TGFR-1), indicating the existence of a positive feedback loop in CSFs to maintain their activation state. Similarly, the high expression of insulin-like growth factor 2 (IGF-2) and IGFR-2 indicated that IGF-2 may also promote the proliferation of CSFs in an autocrine manner (Figure 3C). These results indicate that CSFs existed in a more active state than other fibroblasts.

Then, we analyzed the potential communication between CSFs and other cell types using cell-cell communication analysis, and found

that CSFs might interact with T cells and macrophages through the secretion of chemokines such as CXCL12 in OVC, LC, and PDAC (Figure 3D; Supplementary Figures S3A, B). Since CXCL12 may exert immunosuppressive function through inhibiting the infiltration of $CD8^+$ T cells and promoting recruitment of regulatory T cells (Treg), myeloid-derived suppressor cells (MDSC) and macrophages (Garg et al., 2018; Givel et al., 2018; Yu et al., 2019), our findings indicated that CSFs may promote the formation of immunosuppressive microenvironment through the secretion of CXCL12. We also found that the MIF-CD74 pair was highly enriched between CSFs and immune cells, including B cells, $CD4^+$ T cells, $CD8^+$ T cells, macrophages and monocytes, in OVC, CRC and ICC (Figures 3D–F; Supplementary Figures S3A, B). As shown in other studies, the MIF-CD74 pair can suppress the T cell mediated antitumor effect by directly inhibiting T cell activation, or promoting the recruitment of tumor-associated macrophages (TAMs), thus accelerate tumor progression (Balogh et al., 2018; Klemke et al., 2021). Hence, CSFs may inhibit antitumor immune response *via* MIF-CD74 axis. Altogether, CSFs represent an activated cluster of CAFs, which may enhance ECM remodeling and inhibit antitumor immune response.

3.3 CSFs mainly transform from normal fibroblasts

To explore whether CSFs originate from other fibroblast clusters, we conducted pseudotime analysis and found that both DPT^+ FBs and $RGS5^+$ FBs could transform into CSFs. Since DPT^+ FBs and $RGS5^+$ FBs also exist in normal tissues, we speculated that CSFs transform from normal fibroblasts (Figure 4A). We also analyzed the transition of CSFs in separate cancer types, and found that in BC, CRC and OVC, CSFs were mainly transformed from DPT^+ fibroblasts, while in ICC, CSFs were mainly transformed from $RGS5^+$ FBs (Supplementary Figures S4A–D). Then, we analyzed the gene regulatory network to decode the changes in transcription factor (TF) activity during the transition. CSFs showed high activity of CREB3L1, FOSL2, IRF7 and HOXB7 (Figure 4B), among which CREB3L1, FOSL2 and IRF7 had been shown to be strongly involved in fibroblast activation, and HOXB7 could promote the transition of normal fibroblasts to MSCs (Steens et al., 2020; Tabib et al., 2021). These results indicate that CREB3L1, FOSL2, IRF7 and HOXB7 may facilitate the transition of normal fibroblasts to CSFs.

Then, we compared the differences in secreted proteins between tumor tissues and normal tissues to identify the factors that might be responsible for the activation and transition of CSFs. We found that the osteopontin (OPN, encoded by SPP1)-CD44 pair was significantly enriched between macrophages and fibroblasts in different tumor types but was absent in most normal tissues (Figures 4C–H; Supplementary Figures S5A–D). As reported in other studies, OPN/SPP1 could indeed induce the transition of normal fibroblasts into tumor-promoting CAFs (Sharon et al., 2015; Butti et al., 2021). However, in contrast to other reports that showed OPN/SPP1 was highly expressed in tumor cells, our data indicated that OPN/SPP1 was mainly expressed in macrophages (Supplementary Figure S5E). Since it has been well recognized that macrophages are critical for the transition of normal fibroblasts into CAFs (Costa-Silva et al., 2015; Nielsen et al., 2016), our results indicate that macrophages may promote the transition of normal fibroblasts to CSFs through OPN/SPP1-CD44 axis.

3.4 High CSF proportion is associated with poor prognosis in bladder cancer and lung adenocarcinoma

After confirming the existence of CSFs in different tumors, we explored the association between CSF proportion and patients' prognosis. For this purpose, we assessed cell proportions of tumor tissues and adjacent normal tissues in multiple cancer cohorts from TCGA database. CIBERSORTx was used for cell composition deconvolution analysis, with the scRNA-seq dataset of multi-cancer as a reference panel (Supplementary Table S8). Results showed that the proportions of total fibroblasts in most tumor types were similar to or even lower than adjacent normal tissues, which might be caused by the increased proportions of epithelial cells in tumor tissues (Figure 5A). However, the proportions of CSFs were significantly higher in most types of tumor tissues (12 out of 17) than adjacent normal tissues, indicating that CSFs mainly exist in tumor tissues (Figure 5B). Consistently, the expression of COL11A1 in various tumor tissues was significantly higher than adjacent normal tissues (Supplementary Figure S6).

Then, we examined the association between CSF proportion and patients' prognosis, in which patients with different cancer types were divided into two groups based on the proportion of CSFs (high or low) for survival analysis (Supplementary Figure S7). As a control, we also examined whether total fibroblast proportion was associated with patients' prognosis. Results showed that high CSFs proportion was associated with poor prognosis in bladder cancer (BCa) and lung adenocarcinoma (LUAD), while total fibroblast proportion was not associated with clinical outcomes, indicating that CSFs may promote tumor progression in BCa and LUAD (Figures 5C–F).

3.5 Highly expressed ECM-associated genes in CSFs are also associated with patients' prognosis

As previously shown in Figure 3B, compared with other clusters of fibroblasts, CSFs express higher levels of multiple collagens, MMPs, TIMPs, FN1 and POSTN, indicating that CSFs might be involved in ECM remodeling. To evaluate whether CSFs promote tumor progression through ECM remodeling, we studied the association between the highly expressed ECM associated genes in CSFs and patients' prognosis in BCa and LUAD cohorts from TCGA database. Results showed that ECM associated genes, such as POSTN, COL11A1 and COL5A2, were also associated with poor prognosis in BCa and LUAD patients (Figures 6A–F). Furthermore, we performed IHC staining to examine the expression of COL11A1 in clinical BCa samples and verified the specific COL11A1 expression in tumor stroma. We validated that patients with high COL11A1 expression tended to have poor prognosis in our BCa cohort (Figures 6G, H). We also confirmed that these ECM associated genes were mainly expressed in fibroblasts, especially CSFs (Supplementary Figure S8). Our data was consistent with other studies which also showed that POSTN and COL11A1 were more highly expressed in tumor tissues than normal tissues (Raglow and Thomas, 2015; Yu et al., 2018), POSTN could promote cancer stemness in ovarian cancer and head and neck squamous cell carcinoma (HNSCC) (Malanchi et al., 2011; Yu et al., 2018), and COL11A1 could facilitate fibroblast activation through modulating the

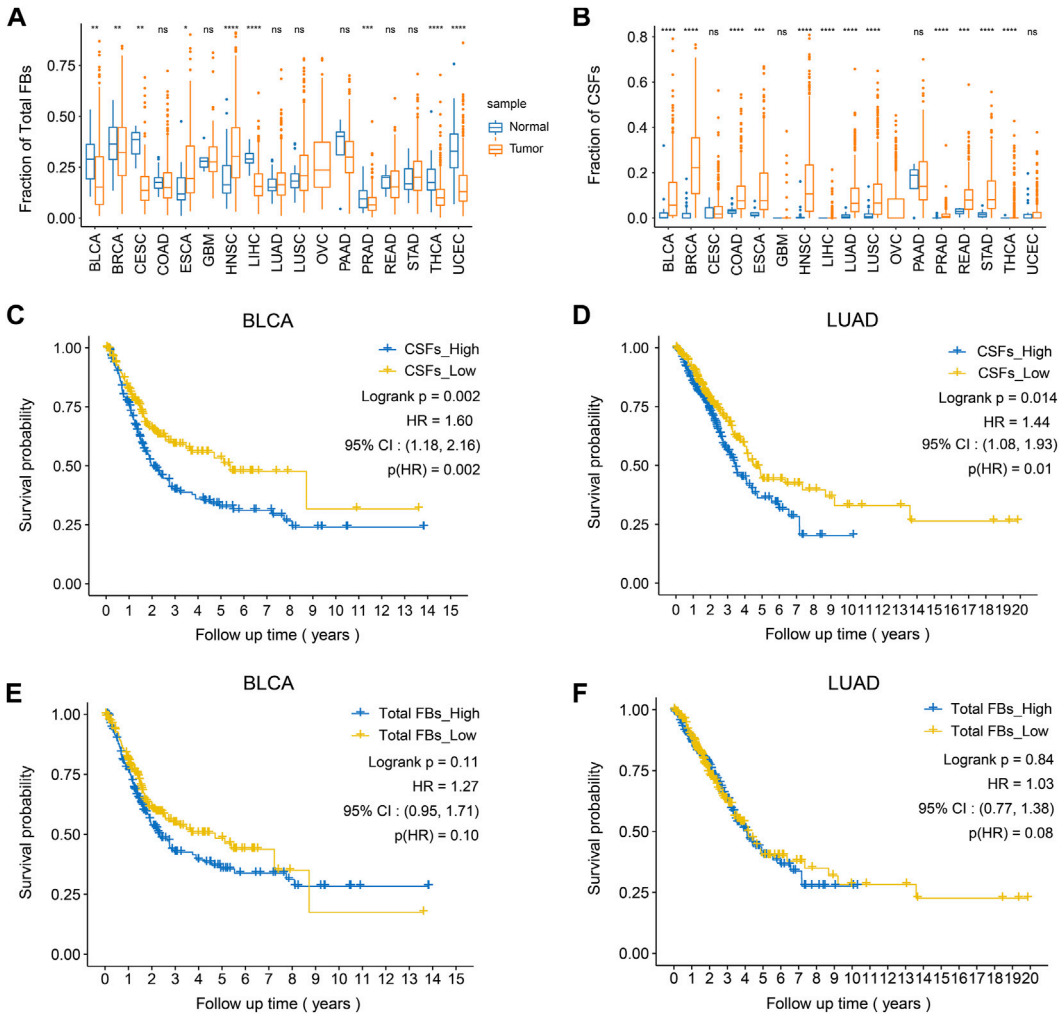

FIGURE 5
High CSFs proportion is associated with poor prognosis in bladder cancer and lung adenocarcinoma. **(A)**, The fractions of total fibroblasts in tumor tissues and normal tissues in 17 TCGA cancer types. **(B)**, The fractions of CSFs in tumor tissues and normal tissues in 17 TCGA cancer types. **(C, D)**, Kaplan-Meier plots to depict the survival of patients with high CSFs or low CSFs in BLCA **(C)** and LUAD **(D)**. **(E, F)**, Kaplan-Meier plots to depict the survival of patients with high or low fibroblasts in BLCA **(E)** and LUAD **(F)**. HR, hazard ratio.

TGF-β pathway and contribute to metastasis and poor clinical outcomes in ovarian cancer (Cheon et al., 2014; Wu et al., 2021). Altogether, these results further confirmed that CSFs may promote tumor progression through enhancing ECM remodeling.

3.6 CSFs specifically express membrane proteins FAP, LRRC15, ITGA11 and SPHK1

Because of the tumor-promoting function, CSFs can be potential targets for cancer treatment. Therefore, identifying the membrane molecules that are specifically expressed on CSFs is critical for CSFs specific targeting. We first examined the expression of classical fibroblast marker genes in different fibroblast clusters. Platelet-derived growth factor receptor alpha (PDGFR-α, encoded by PDGFRA) was specifically expressed in fibroblasts but not in other cell types, but since it was expressed in fibroblasts of both normal tissues and tumor tissues, thus it could be used as a pan-fibroblast marker (Figures 7A, B). We found that, α-smooth muscle actin (α-SMA, encoded by ACTA2), a commonly used marker for CAFs, was not a specific marker for CAFs since it was also highly expressed in pericytes, which was consistent with other previously reported studies (Schadler et al., 2010; Dubrac et al., 2018). In contrast, we found that FAP and PDPN were specifically expressed in fibroblasts in tumor tissues but almost absent in normal tissues, indicating that they could be used as CAFs specific markers in various cancer types (Figures 7A, B). In addition, we found that FAP was mainly expressed in CSFs, very few in other clusters, indicating that it could be an attractive CSFs specific target (Figure 7C).

To find out more CSFs specific membrane molecules for targeting, we also screened the membrane molecules in different fibroblast clusters. We found that LRRC15, ITGA11 and SPHK1 were also specifically expressed on CSFs, but not in other clusters of fibroblasts, indicating that they could also be attractive CSFs specific targets for cancer treatment (Figures 7D, E). Thus, we proposed that FAP, LRRC15, ITGA11 and SPHK1 could be used as markers for CSFs targeting, especially LRRC15 and ITGA11 due to their more specific expression.

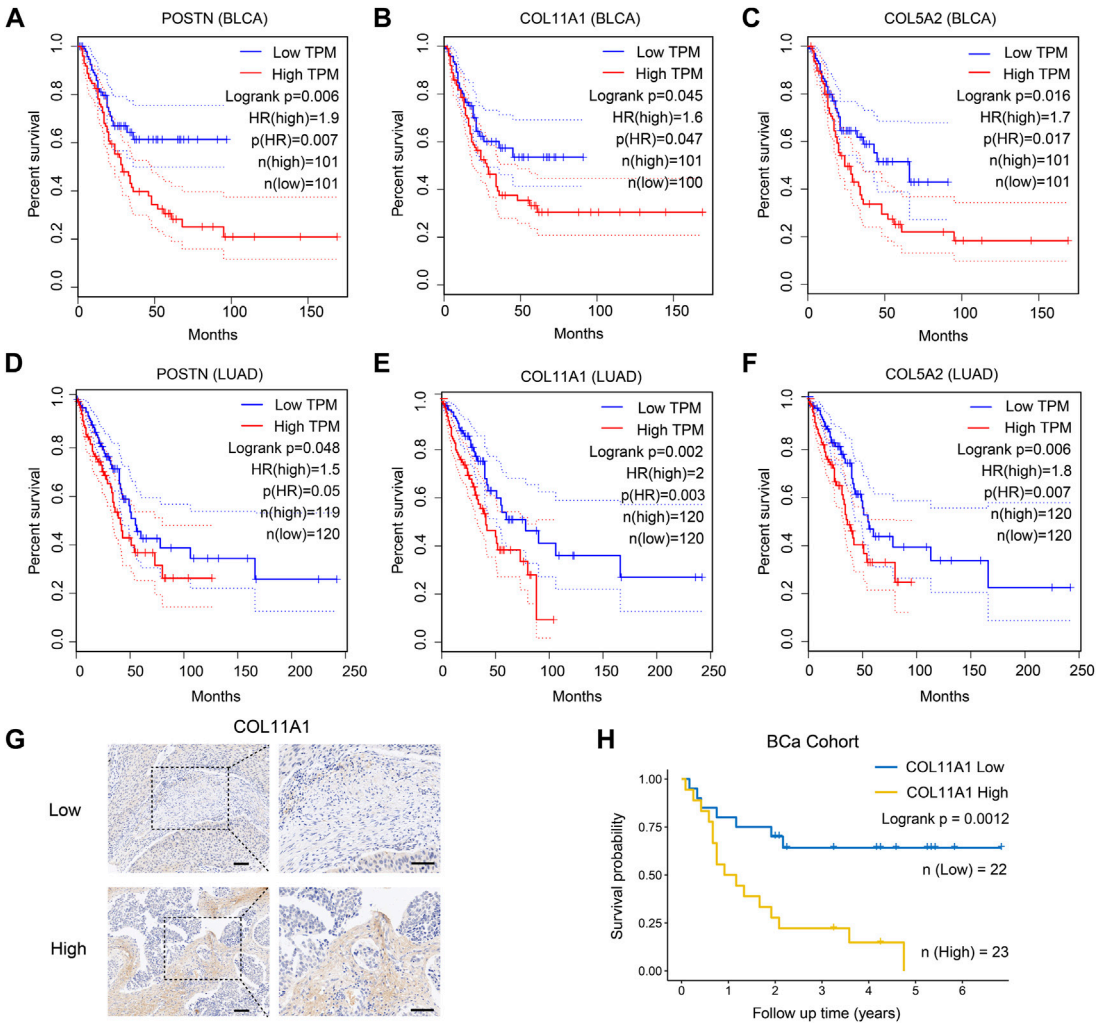

FIGURE 6
ECM associated genes are highly expressed in CSFs and associated with patients' prognosis. **(A–C)**, Overall survival of patients with different expression of the three highly expressed genes in CSFs, including POSTN **(A)**, COL11A1 **(B)** and COL5A2 **(C)** in TCGA BLCA cohort. **(D–F)**, Overall survival of patients with different expression of the three highly expressed genes in CSFs, including POSTN **(D)**, COL11A1 **(E)** and COL5A2 **(F)** in TCGA LUAD cohort. **(G)**, IHC analysis of COL11A1 expression in BCa tissues. Scale bar, 50 μm. **(H)**, Overall survival of patients with different COL11A1 expression in BCa cohort (IHC score ≤1, low expression of COL11A1; IHC score >1, high expression of COL11A1).

Based on all the results, we proposed a working model how CSFs promote tumor progression, that is, CSFs secrete plenty of TGF-β to maintain their activation state and enhance ECM remodeling; CSFs also highly express MIF to inhibit T cell-mediated antitumor immune response; MIF may also induce macrophage to secrete OPN/SPP1, thus further enhance the transition of normal fibroblasts to CSFs (Figure 7F).

4 Discussion

CAFs have long been considered attractive targets for cancer treatment since they can promote tumor progression through ECM remodeling and extensive interactions with other cell types (Sahai et al., 2020; Yang et al., 2020; Chen et al., 2021a; Biffi and Tuveson, 2021). However, clinical trials targeting CAFs have not met the expectations, which might be caused by the heterogeneity of CAFs, since they are composed of distinct clusters that have different even opposite functions (Kim et al., 2014; Yang et al., 2020; Chen et al., 2021a; Biffi and Tuveson, 2021; Chen et al., 2021c; Hutton et al., 2021). Thus, to improve the antitumor efficacy of CAFs targeting strategies, it is of vital important to identify the tumor-promoting CAF clusters and elucidate their function in tumor progression.

ScRNA-seq provides an effective way to study the heterogeneity of CAFs and decode the differences between different CAF clusters (Zhang et al., 2020; Galbo et al., 2021; Olbrecht et al., 2021). Currently, based on scRNA-seq data, CAFs are commonly divided into mCAFs, iCAFs, apCAFs, vCAFs and eCAFs (Chen et al., 2020; Zhang et al., 2020). In addition, some new markers have been identified to classify CAFs into other clusters. For example, Hutton et al. found that in pancreatic cancer, $CD105^{+}$ and $CD105^{-}$ fibroblasts had opposite functions; $CD105^{+}$ fibroblasts could promote tumor progression, while $CD105^{-}$ fibroblasts inhibited tumor growth by enhancing the antitumor immune response. Thus, in their study, CAFs were divided into tumor-promoting CAFs and tumor-suppressing CAFs. In a study of non-small-cell lung cancer

10.3389/fphar.2023.1121586

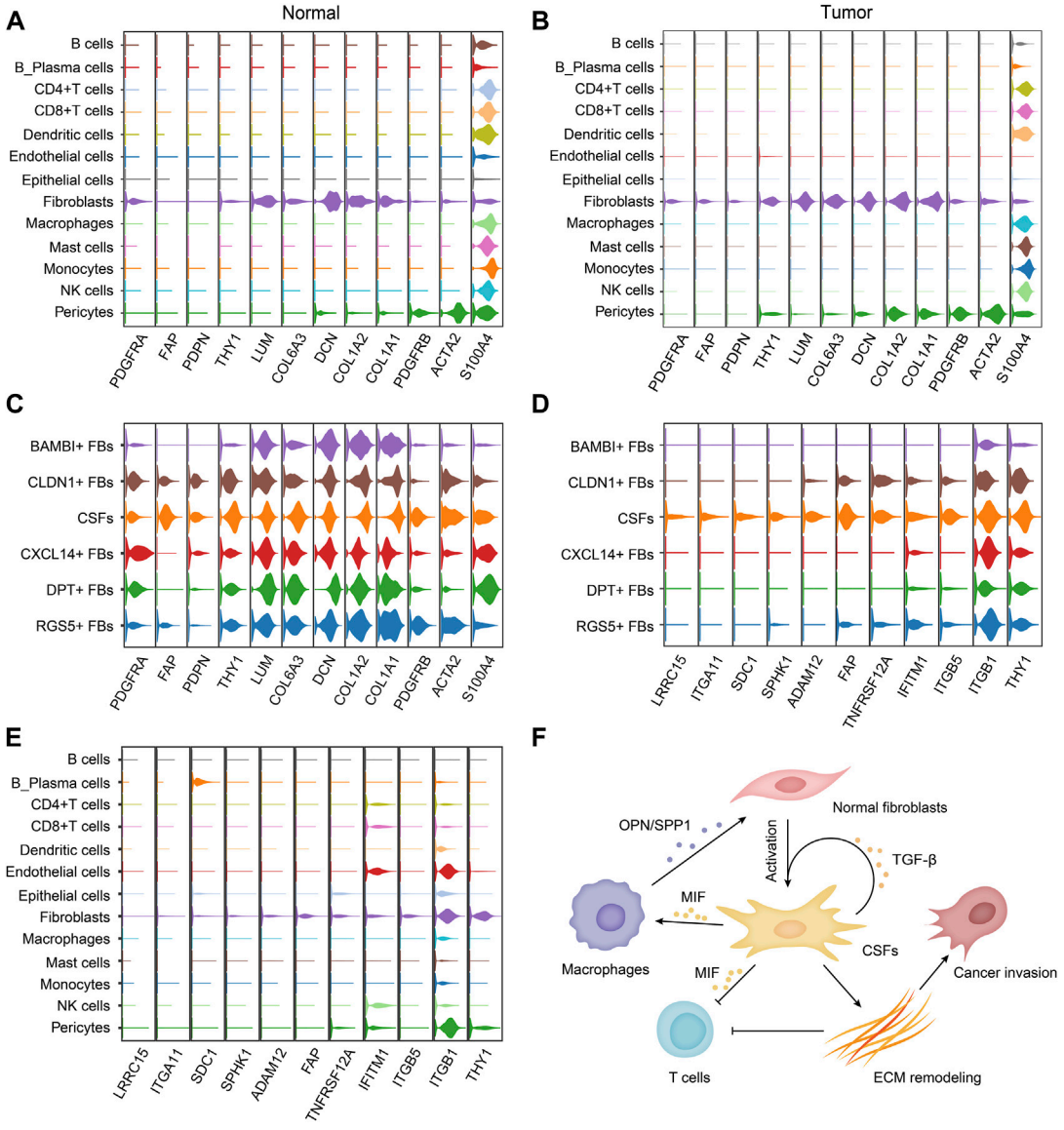

FIGURE 7
CSFs specifically express membrane proteins LRRC15, ITGA11, SPHK1 and FAP. **(A, B)**, Violin plots to show the expression levels of classical fibroblast markers in different cell types of normal tissues **(A)** and tumor tissues **(B)**. **(C)**, Violin plots to show the expression levels of classical fibroblast markers in different fibroblast clusters. **(D, E)**, Violin plots to show the highly expressed surface molecules of CSFs in different fibroblast clusters **(D)** and different cell types **(E)**. **(F)**, Schematic illustration of the proposed mechanism how CSFs promote tumor progression.

(NSCLC), based on their response to tyrosine kinase inhibitors (TKIs), Hu et al. divided CAFs into three clusters with distinctive function (Hu et al., 2021). Although these studies proposed different mechanisms how CAFs promote tumor progression, they did not clarify the differences between fibroblasts that specifically exist in tumor tissues (we called CSFs) and normal fibroblasts. Therefore, it was still difficult to identify therapeutic targets for CSFs. In addition, current studies were mainly performed in mouse models, however, CAF clusters are more complex in human tumors than mouse models. Thus, it's still urgently needed to identify the CSF cluster in human sample.

In this study, by using scRNA-seq data from multiple cancer types, we compared the differences between fibroblasts specifically exist in tumor tissues and normal tissues. We constructed a multi-cancer fibroblast atlas, in which fibroblasts were classified into six clusters: BAMBI$^+$ FBs, CLDN1$^+$ FBs, COL11A1$^+$ FBs, CXCL14$^+$ FBs, DPT$^+$ FBs and RGS5$^+$ FBs. Among these clusters, BAMBI$^+$ FBs have high expression of genes that are related to Wnt signaling pathway, such as BAMBI, SOX4, DKK1 and MDK. CLDN1$^+$ FBs highly express keratins such as KRT8, KRT18 and KRT19, indicating that they are epithelial-to-mesenchymal transition (EMT)-like fibroblasts. CXCL14$^+$ FBs have high expression of chemokines, including CCL8, CCL11, CCL13, CXCL1 and CXCL14, indicating that they are inflammatory fibroblasts. DPT$^+$ FBs have high expression of APOD, DPT, CFD, GSN and MGP, indicating that they are associated with lipid metabolism. RGS5$^+$ FBs have high expression of genes related with vascular development, including RGS5, MYH11 and NOTCH3. Notably, COL11A1$^+$ FBs only existed in

various tumor tissues but not in normal tissues, while other fibroblast clusters existed in both tumor tissues and normal tissues. Thus, we mainly focused on the COL11A1$^+$ FBs and named them CSFs.

Interestingly, one previous study has shown that coordinated overexpression of COL11A1, THBS2 and INHBA in a subset of CAFs was related to high-stage cancers, and this signature only occurred when cancers reached certain stages, for example stage IIIc in ovarian cancer and stage II in colorectal cancer. This subset of CAFs was named metastasis associated fibroblasts (MAFs) (Kim et al., 2010). Then by comparing the gene expression profile at single cell level, the same group further reported that these COL11A1-expressing CAFs were transformed from a particular type of adipose derived stromal/stem cells (ASCs) that also naturally present in the stromal vascular fraction of normal adipose tissue (Zhu et al., 2021). Since ASCs are also kind of normal fibroblasts, since they express fibroblast marker genes, our findings are consistent that CSFs originate from normal fibroblasts. It's more interesting that when analyzing the origin of CSFs in separate cancer types, we found that CSFs were mainly transformed from DPT$^+$ FBs in BC, CRC and OVC, while mainly from RGS5$^+$ FBs in ICC. These results indicated that CSFs may originate from different normal fibroblast clusters in different cancer types.

Some other studies reported that COL11A1 was also involved in the CAF-cancer cell interaction and promote tumor progression through different mechanisms. For example, one study analyzed three large microarray datasets in serous ovarian cancer, and reported a 10-gene signature that are associated with poor OS, which included COL11A1 and could be regulated by TGF-signaling. They also found that COL11A1 expression increased during ovarian cancer progression, and downregulation of COL11A1 in ovarian cancer cells could significantly inhibit tumor growth *in vivo* (Cheon et al., 2014). The same group also found that COL11A1 could be used as a specific marker for activated CAFs, and COL11A1 expression was correlated with tumor stage, tumor grade and patients' outcome in 13 types of carcinomas (Jia et al., 2016). In addition, another study reported that COL11A1 could induce the expression and secretion of TGF-β3 in ovarian cancer cells through NFκB/IGFBP2 axis, which then promote the transformation of ovarian fibroblasts into CAFs, at the same time, COL11A1 could also induce CAFs to secrete IL-6, thus to promote ovarian cancer cell growth and invasion (Wu et al., 2021). Based on these findings that COL11A1 could promote tumor progression, COL11A1 has been considered as a potential therapeutic target for cancer treatment (Liu et al., 2021). Although most studies showed that COL11A1 was mainly expressed in CAFs, yet COL11A1 was also found to be expressed in certain kind of tumor cells, such as the tumor cells of salivary gland cancer (SGC) with intercalated duct origin. This finding indicated that COL11A1-targeted therapy might have particularly high potential in SGC, or could help to categorize tumors in the setting of possible future COL11A1-related therapies (Arolt et al., 2022).

In our study, we aimed to identify the fibroblasts that specifically exist in tumor tissues. Our results showed that COL11A1$^+$ FBs specifically exist in tumor tissues, thus could be considered as CSFs. Then we further analyzed their origin and the potential mechanisms how CSFs promote tumor progression. By using pseudotime analysis, we revealed that these CSFs might transformed from normal fibroblasts. By using pathway analysis, gene regulatory network analysis and cell-cell communication analysis, we found that CSFs exhibited a higher activation state than other fibroblast clusters. The high expression of ECM-associated genes, and TGF-β, TGFR-1, IGF-2 and IGFR-2 in CSFs all indicated that they may control the activation state of CSFs and regulate ECM remodeling. Our data also found that CSFs may be involved in the regulation of antitumor immune response through the secretion of CXCL12 and the interaction between CSFs and immune cells through MIF-CD74 pair. In addition, we found that high proportions of CSFs were associated with poor prognosis in BCa and LUAD, while total fibroblast proportions did not show significant association. Thus, we proposed that CSFs could be effective targets for cancer treatment.

To ensure specific targeting of CSFs, we also tried to identify the membrane molecules that were specifically expressed in CSFs. We found that FAP, LRRC15, ITGA11 and SPHK1 were specifically expressed in CSFs, especially LRRC15 and ITGA11 due to their more specific expression in CSFs. Current studies have shown that some of these molecules have been extensively applied in both preclinical and clinical studies. For example, FAP-targeted PET/CT or PET/MRI has shown diagnostic value in multiple cancers, such as lung cancer, breast cancer, HNSCC and gastric cancer (Backhaus et al., 2022; Kumar et al., 2022; Promteangtrong et al., 2022; Wang et al., 2022). In preclinical studies, the LRRC15-targeting antibody-drug conjugate ABBV-085 showed antitumor effect in breast cancer and ovarian cancer (Purcell et al., 2018; Ray et al., 2022). We believe that strategies targeting ITGA11 and SPHK1 could also have diagnostic and therapeutic value. Besides these membrane molecules, the cytokines that inhibit antitumor immune response or promote the transition of normal fibroblasts to CSFs, such as MIF, SPP1/OPN, could also be considered as therapeutic targets for cancer treatment (as proposed in Figure 7F).

This study also had limitations. First, we only analyzed limited scRNA-seq datasets, including ten datasets across eight tumor types and six datasets from five types of adjacent normal tissues. It is for sure that analysis of more scRNA-seq datasets will obtain more accurate results. Second, the data in this study only came from integrated analysis of scRNA-seq datasets, and the proposed features and functions of CSFs still need to be validated by experimental methods, such as mass cytometry, single-cell proteomics and multiplex staining techniques.

In summary, through comparison between fibroblasts in tumor tissues and normal tissues at single-cell level, we identified that COL11A1$^+$ FBs specifically exist in tumor tissues, but not normal tissues, thus we named them CSFs. We further revealed that CSFs originate from normal fibroblasts. CSFs are in a more active state than other fibroblasts and may promote tumor progression through enhancing ECM remodeling and inhibiting antitumor immune response. We demonstrated that CSFs could be potential targets for cancer treatment, and membrane molecules FAP, LRRC15, ITGA11 and SPHK1 could be used as CSFs specific targets.

Data availability statement

The original contributions presented in the study are included in the article/Supplementary Material; further inquiries can be directed to the corresponding authors.

Ethics statement

Written informed consent was obtained from the individual(s) for the publication of any potentially identifiable images or data included in this article.

Author contributions

JZ, SL, and TL: data collection, data analysis and writing the original draft. JZ, DH, and KZ: methodology. LG, XW, and YL: data interpretation. XZ and ZL: creating figures. YS and SH: literature research and IHC analysis. WQ, WW, and FY: conceptualization and manuscript revision. All authors read and approved the final manuscript.

Funding

This study was supported by the National Natural Science Foundation of China (No. 82173204; 81772734), the Innovation Capability Support Program of Shaanxi (2020PT-021; 2021TD-39), the Natural Science Basic Research Program of Shaanxi (2022JZ-62), and the Fundamental Research Funds for the Central Universities (G2021KY05102).

Acknowledgments

We thank Chao Xu and Shaojie Liu (Department of Urology, Xijing Hospital, Fourth Military Medical University, China) for assistance with data interpretation. We thank Jianming Zeng (Faculty of Health Sciences, University of Macau, China) and all the members of his bioinformatics team, biotrainee, for generously sharing their experience and codes.

Conflict of interest

The authors declare that the research was conducted in the absence of any commercial or financial relationships that could be construed as a potential conflict of interest.

Publisher's note

Supplementary material

The Supplementary Material for this article can be found online at: https://www.frontiersin.org/articles/10.3389/fphar.2023.1121586/full#supplementary-material

References

Affo, S., Nair, A., Brundu, F., Ravichandra, A., Bhattacharjee, S., Matsuda, M., et al. (2021). Promotion of cholangiocarcinoma growth by diverse cancer-associated fibroblast subpopulations. *Cancer Cell* 39 (6), 866–882.e11. doi:10.1016/j.ccell.2021.03.012

Arolt, C., Hoffmann, F., Nachtsheim, L., Wolber, P., Guntinas-Lichius, O., Buettner, R., et al. (2022). Mutually exclusive expression of Col11a1 by cafs and tumour cells in a large pancancer and a salivary gland carcinoma cohort. *Head. Neck Pathol.* 16 (2), 394–406. doi:10.1007/s12105-021-01370-0

Backhaus, P., Burg, M. C., Roll, W., Buther, F., Breyholz, H. J., Weigel, S., et al. (2022). Simultaneous fapi pet/mri targeting the fibroblast-activation protein for breast cancer. *Radiology* 302 (1), 39–47. doi:10.1148/radiol.2021204677

Balogh, K. N., Templeton, D. J., and Cross, J. V. (2018). Macrophage migration inhibitory factor protects cancer cells from immunogenic cell death and impairs anti-tumor immune responses. *PLoS One* 13 (6), e0197702. doi:10.1371/journal.pone.0197702

Berlin, J., Bendell, J. C., Hart, L. L., Firdaus, I., Gore, I., Hermann, R. C., et al. (2013). A randomized phase ii trial of vismodegib versus placebo with folfox or folfiri and bevacizumab in patients with previously untreated metastatic colorectal cancer. *Clin. Cancer Res.* 19 (1), 258–267. doi:10.1158/1078-0432.Ccr-12-1800

Biffi, G., and Tuveson, D. A. (2021). Diversity and biology of cancer-associated fibroblasts. *Physiol. Rev.* 101 (1), 147–176. doi:10.1152/physrev.00048.2019

Briscoe, J., and Therond, P. P. (2013). The mechanisms of Hedgehog signalling and its roles in development and disease. *Nat. Rev. Mol. Cell Biol.* 14 (7), 416–429. doi:10.1038/nrm3598

Butti, R., Nimma, R., Kundu, G., Bulbule, A., Kumar, T. V. S., Gunasekaran, V. P., et al. (2021). Tumor-derived osteopontin drives the resident fibroblast to myofibroblast differentiation through Twist1 to promote breast cancer progression. *Oncogene* 40 (11), 2002–2017. doi:10.1038/s41388-021-01663-2

Cao, J., Spielmann, M., Qiu, X., Huang, X., Ibrahim, D. M., Hill, A. J., et al. (2019). The single-cell transcriptional landscape of mammalian organogenesis. *Nature* 566 (7745), 496–502. doi:10.1038/s41586-019-0969-x

Catenacci, D. V., Junttila, M. R., Karrison, T., Bahary, N., Horiba, M. N., Nattam, S. R., et al. (2015). Randomized phase ib/ii study of gemcitabine plus placebo or vismodegib, a Hedgehog pathway inhibitor, in patients with metastatic pancreatic cancer. *J. Clin. Oncol.* 33 (36), 4284–4292. doi:10.1200/JCO.2015.62.8719

Chen, S., Zhu, G., Yang, Y., Wang, F., Xiao, Y. T., Zhang, N., et al. (2021). Single-cell analysis reveals transcriptomic remodellings in distinct cell types that contribute to human prostate cancer progression. *Nat. Cell Biol.* 23 (1), 87–98. doi:10.1038/s41556-020-00613-6

Chen, Y., Kim, J., Yang, S., Wang, H., Wu, C. J., Sugimoto, H., et al. (2021). Type I collagen deletion in αSMA$^+$ myofibroblasts augments immune suppression and accelerates progression of pancreatic cancer. *Cancer Cell* 39 (4), 548–565.e6. doi:10.1016/j.ccell.2021.02.007

Chen, Y., McAndrews, K. M., and Kalluri, R. (2021). Clinical and therapeutic relevance of cancer-associated fibroblasts. *Nat. Rev. Clin. Oncol.* 18 (12), 792–804. doi:10.1038/s41571-021-00546-5

Chen, Z., Zhou, L., Liu, L., Hou, Y., Xiong, M., Yang, Y., et al. (2020). Single-cell rna sequencing highlights the role of inflammatory cancer-associated fibroblasts in bladder urothelial carcinoma. *Nat. Commun.* 11 (1), 5077. doi:10.1038/s41467-020-18916-5

Cheng, Y., Mo, F., Li, Q., Han, X., Shi, H., Chen, S., et al. (2021). Targeting Cxcr2 inhibits the progression of lung cancer and promotes therapeutic effect of cisplatin. *Mol. Cancer* 20 (1), 62. doi:10.1186/s12943-021-01355-1

Cheon, D. J., Tong, Y., Sim, M. S., Dering, J., Berel, D., Cui, X., et al. (2014). A collagen-remodeling gene signature regulated by tgf-beta signaling is associated with metastasis and poor survival in serous ovarian cancer. *Clin. Cancer Res.* 20 (3), 711–723. doi:10.1158/1078-0432.CCR-13-1256

Costa-Silva, B., Aiello, N. M., Ocean, A. J., Singh, S., Zhang, H., Thakur, B. K., et al. (2015). Pancreatic cancer exosomes initiate pre-metastatic niche formation in the liver. *Nat. Cell Biol.* 17 (6), 816–826. doi:10.1038/ncb3169

De Jesus-Acosta, A., Sugar, E. A., O'Dwyer, P. J., Ramanathan, R. K., Von Hoff, D. D., Rasheed, Z., et al. (2020). Phase 2 study of vismodegib, a Hedgehog inhibitor, combined with gemcitabine and nab-paclitaxel in patients with untreated metastatic pancreatic adenocarcinoma. *Br. J. Cancer* 122 (4), 498–505. doi:10.1038/s41416-019-0683-3

Dubrac, A., Kunzel, S. E., Kunzel, S. H., Li, J., Chandran, R. R., Martin, K., et al. (2018). Nck-dependent pericyte migration promotes pathological neovascularization in ischemic retinopathy. *Nat. Commun.* 9 (1), 3463. doi:10.1038/s41467-018-05926-7

Galbo, P. M., Zang, X., and Zheng, D. (2021). Molecular features of cancer-associated fibroblast subtypes and their implication on cancer pathogenesis, prognosis, and immunotherapy resistance. *Clin. Cancer Res.* 27 (9), 2636–2647. doi:10.1158/1078-0432.Ccr-20-4226

Garantziotis, S., and Savani, R. C. (2019). Hyaluronan biology: A complex balancing act of structure, function, location and context. *Matrix Biol.* 78-79, 781–7910. doi:10.1016/j.matbio.2019.02.002

Garg, B., Giri, B., Modi, S., Sethi, V., Castro, I., Umland, O., et al. (2018). NFκB in pancreatic stellate cells reduces infiltration of tumors by cytotoxic T cells and killing of cancer cells, via up-regulation of CXCL12. *Gastroenterology* 155 (3), 880–891. doi:10.1053/j.gastro.2018.05.051

Givel, A. M., Kieffer, Y., Scholer-Dahirel, A., Sirven, P., Cardon, M., Pelon, F., et al. (2018). Mir200-Regulated Cxcl12β promotes fibroblast heterogeneity and

immunosuppression in ovarian cancers. *Nat. Commun.* 9 (1), 1056. doi:10.1038/s41467-018-03348-z

Goldman, M. J., Craft, B., Hastie, M., Repecka, K., McDade, F., Kamath, A., et al. (2020). Visualizing and interpreting cancer genomics data via the Xena platform. *Nat. Biotechnol.* 38 (6), 675–678. doi:10.1038/s41587-020-0546-8

Hanzelmann, S., Castelo, R., and Guinney, J. (2013). Gsva: Gene set variation analysis for microarray and rna-seq data. *BMC Bioinforma.* 14 (1), 7. doi:10.1186/1471-2105-14-7

Hao, Y., Hao, S., Andersen-Nissen, E., Mauck, W. M., 3rd, Zheng, S., Butler, A., et al. (2021). Integrated analysis of multimodal single-cell data. *Cell* 184 (13), 3573–3587.e29. doi:10.1016/j.cell.2021.04.048

Hosaka, K., Yang, Y., Seki, T., Fischer, C., Dubey, O., Fredlund, E., et al. (2016). Pericyte-fibroblast transition promotes tumor growth and metastasis. *Proc. Natl. Acad. Sci. U. S. A.* 113 (38), E5618–E5627. doi:10.1073/pnas.1608384113

Hu, H., Piotrowska, Z., Hare, P. J., Chen, H., Mulvey, H. E., Mayfield, A., et al. (2021). Three subtypes of lung cancer fibroblasts define distinct therapeutic paradigms. *Cancer Cell* 39 (11), 1531–1547.e10. doi:10.1016/j.ccell.2021.09.003

Hutton, C., Heider, F., Blanco-Gomez, A., Banyard, A., Kononov, A., Zhang, X., et al. (2021). Single-cell analysis defines a pancreatic fibroblast lineage that supports anti-tumor immunity. *Cancer Cell* 39 (9), 1227–1244.e20. doi:10.1016/j.ccell.2021.06.017

Jia, D., Liu, Z., Deng, N., Tan, T. Z., Huang, R. Y., Taylor-Harding, B., et al. (2016). A col11a1-correlated pan-cancer gene signature of activated fibroblasts for the prioritization of therapeutic targets. *Cancer Lett.* 382 (2), 203–214. doi:10.1016/j.canlet.2016.09.001

Jin, S., Guerrero-Juarez, C. F., Zhang, L., Chang, I., Ramos, R., Kuan, C. H., et al. (2021). Inference and analysis of cell-cell communication using cellchat. *Nat. Commun.* 12 (1), 1088. doi:10.1038/s41467-021-21246-9

Kaye, S. B., Fehrenbacher, L., Holloway, R., Amit, A., Karlan, B., Slomovitz, B., et al. (2012). A phase ii, randomized, placebo-controlled study of vismodegib as maintenance therapy in patients with ovarian cancer in second or third complete remission. *Clin. Cancer Res.* 18 (23), 6509–6518. doi:10.1158/1078-0432.Ccr-12-1796

Kim, E. J., Sahai, V., Abel, E. V., Griffith, K. A., Greenson, J. K., Takebe, N., et al. (2014). Pilot clinical trial of Hedgehog pathway inhibitor gdc-0449 (vismodegib) in combination with gemcitabine in patients with metastatic pancreatic adenocarcinoma. *Clin. Cancer Res.* 20 (23), 5937–5945. doi:10.1158/1078-0432.CCR-14-1269

Kim, H., Watkinson, J., Varadan, V., and Anastassiou, D. (2010). Multi-cancer computational analysis reveals invasion-associated variant of desmoplastic reaction involving inhba, Thbs2 and Col11a1. *BMC Med. Genomics* 3, 51. doi:10.1186/1755-8794-3-51

Klemke, L., De Oliveira, T., Witt, D., Winkler, N., Bohnenberger, H., Bucala, R., et al. (2021). Hsp90-Stabilized mif supports tumor progression via macrophage recruitment and angiogenesis in colorectal cancer. *Cell Death Dis.* 12 (2), 155. doi:10.1038/s41419-021-03426-z

Korsunsky, I., Millard, N., Fan, J., Slowikowski, K., Zhang, F., Wei, K., et al. (2019). Fast, sensitive and accurate integration of single-cell data with Harmony. *Nat. Methods* 16 (12), 1289–1296. doi:10.1038/s41592-019-0619-0

Kumar, V., Ramnarayanan, K., Sundar, R., Padmanabhan, N., Srivastava, S., Koiwa, M., et al. (2022). Single-cell atlas of lineage states, tumor microenvironment, and subtype-specific expression programs in gastric cancer. *Cancer Discov.* 12 (3), 670–691. doi:10.1158/2159-8290.CD-21-0683

Liu, J., Xiao, Q., Xiao, J., Niu, C., Li, Y., Zhang, X., et al. (2022). Wnt/β-catenin signalling: Function, biological mechanisms, and therapeutic opportunities. *Signal Transduct. Target Ther.* 7 (1), 3. doi:10.1038/s41392-021-00762-6

Liu, Z., Lai, J., Jiang, H., Ma, C., and Huang, H. (2021). Collagen xi alpha 1 chain, a potential therapeutic target for cancer. *FASEB J.* 35 (6), e21603. doi:10.1096/fj.202100054RR

Ma, L., Hernandez, M. O., Zhao, Y., Mehta, M., Tran, B., Kelly, M., et al. (2019). Tumor cell biodiversity drives microenvironmental reprogramming in liver cancer. *Cancer Cell* 36 (4), 418–430. doi:10.1016/j.ccell.2019.08.007

Malanchi, I., Santamaria-Martinez, A., Susanto, E., Peng, H., Lehr, H. A., Delaloye, J. F., et al. (2011). Interactions between cancer stem cells and their niche govern metastatic colonization. *Nature* 481 (7379), 85–89. doi:10.1038/nature10694

Newman, A. M., Steen, C. B., Liu, C. L., Gentles, A. J., Chaudhuri, A. A., Scherer, F., et al. (2019). Determining cell type abundance and expression from bulk tissues with digital cytometry. *Nat. Biotechnol.* 37 (7), 773–782. doi:10.1038/s41587-019-0114-2

Nielsen, S. R., Quaranta, V., Linford, A., Emeagi, P., Rainer, C., Santos, A., et al. (2016). Macrophage-secreted granulin supports pancreatic cancer metastasis by inducing liver fibrosis. *Nat. Cell Biol.* 18 (5), 549–560. doi:10.1038/ncb3340

Olbrecht, S., Busschaert, P., Qian, J., Vanderstichele, A., Loverix, L., Van Gorp, T., et al. (2021). High-grade serous tubo-ovarian cancer refined with single-cell rna sequencing: Specific cell subtypes influence survival and determine molecular subtype classification. *Genome Med.* 13 (1), 111. doi:10.1186/s13073-021-00922-x

Promteangtrong, C., Siripongsatian, D., Jantarato, A., Kunawudhi, A., Kiatkittikul, P., Yaset, S., et al. (2022). Head-to-Head comparison of (68)Ga-Fapi-46 and (18)F-fdg pet/ct for evaluation of head and neck squamous cell carcinoma: A single-center exploratory study. *J. Nucl. Med.* 63 (8), 1155–1161. doi:10.2967/jnumed.121.262831

Purcell, J. W., Tanlimco, S. G., Hickson, J., Fox, M., Sho, M., Durkin, L., et al. (2018). Lrrc15 is a novel mesenchymal protein and stromal target for antibody-drug conjugates. *Cancer Res.* 78 (14), 4059–4072. doi:10.1158/0008-5472.CAN-18-0327

Qian, J., Olbrecht, S., Boeckx, B., Vos, H., Laoui, D., Etlioglu, E., et al. (2020). A pan-cancer blueprint of the heterogeneous tumor microenvironment revealed by single-cell profiling. *Cell Res.* 30 (9), 745–762. doi:10.1038/s41422-020-0355-0

Raglow, Z., and Thomas, S. M. (2015). Tumor matrix protein collagen XIα1 in cancer. *Cancer Lett.* 357 (2), 448–453. doi:10.1016/j.canlet.2014.12.011

Ray, U., Jung, D. B., Jin, L., Xiao, Y., Dasari, S., Sarkar Bhattacharya, S., et al. (2022). Targeting Lrrc15 inhibits metastatic dissemination of ovarian cancer. *Cancer Res.* 82 (6), 1038–1054. doi:10.1158/0008-5472.CAN-21-0622

Sahai, E., Astsaturov, I., Cukierman, E., DeNardo, D. G., Egeblad, M., Evans, R. M., et al. (2020). A framework for advancing our understanding of cancer-associated fibroblasts. *Nat. Rev. Cancer* 20 (3), 174–186. doi:10.1038/s41568-019-0238-1

Schadler, K. L., Zweidler-McKay, P. A., Guan, H., and Kleinerman, E. S. (2010). Delta-like ligand 4 plays a critical role in pericyte/vascular smooth muscle cell formation during vasculogenesis and tumor vessel expansion in ewing's sarcoma. *Clin. Cancer Res.* 16 (3), 848–856. doi:10.1158/1078-0432.Ccr-09-1299

Shah, M. A., Bodoky, G., Starodub, A., Cunningham, D., Yip, D., Wainberg, Z. A., et al. (2021). Phase iii study to evaluate efficacy and safety of andecaliximab with Mfolfox6 as first-line treatment in patients with advanced gastric or gej adenocarcinoma (Gamma-1). *J. Clin. Oncol.* 39 (9), 990–1000. doi:10.1200/jco.20.02755

Sharon, Y., Raz, Y., Cohen, N., Ben-Shmuel, A., Schwartz, H., Geiger, T., et al. (2015). Tumor-derived osteopontin reprograms normal mammary fibroblasts to promote inflammation and tumor growth in breast cancer. *Cancer Res.* 75 (6), 963–973. doi:10.1158/0008-5472.Can-14-1990

Steele, N. G., Carpenter, E. S., Kemp, S. B., Sirihorachai, V. R., The, S., Delrosario, L., et al. (2020). Multimodal mapping of the tumor and peripheral blood immune landscape in human pancreatic cancer. *Nat. Cancer* 1 (11), 1097–1112. doi:10.1038/s43018-020-00121-4

Steens, J., Unger, K., Klar, L., Neureiter, A., Wieber, K., Hess, J., et al. (2020). Direct conversion of human fibroblasts into therapeutically active vascular wall-typical mesenchymal stem cells. *Cell Mol. Life Sci.* 77 (17), 3401–3422. doi:10.1007/s00018-019-03358-0

Tabib, T., Huang, M., Morse, N., Papazoglou, A., Behera, R., Jia, M., et al. (2021). Myofibroblast transcriptome indicates Sfrp2hi fibroblast progenitors in systemic sclerosis skin. *Nat. Commun.* 12 (1), 4384. doi:10.1038/s41467-021-24607-6

Tang, P. C., Chung, J. Y., Xue, V. W., Xiao, J., Meng, X. M., Huang, X. R., et al. (2022). Smad3 promotes cancer-associated fibroblasts generation via macrophage-myofibroblast transition. *Adv. Sci.* 9 (1), e2101235. doi:10.1002/advs.202101235

Tang, Z., Kang, B., Li, C., Chen, T., and Zhang, Z. (2019). Gepia2: An enhanced web server for large-scale expression profiling and interactive analysis. *Nucleic Acids Res.* 47 (W1), W556–W60. doi:10.1093/nar/gkz430

Van Cutsem, E., Tempero, M. A., Sigal, D., Oh, D. Y., Fazio, N., Macarulla, T., et al. (2020). Randomized phase iii trial of pegvorhyaluronidase alfa with nab-paclitaxel plus gemcitabine for patients with hyaluronan-high metastatic pancreatic adenocarcinoma. *J. Clin. Oncol.* 38 (27), 3185–3194. doi:10.1200/JCO.20.00590

Van de Sande, B., Flerin, C., Davie, K., De Waegeneer, M., Hulselmans, G., Aibar, S., et al. (2020). A scalable scenic workflow for single-cell gene regulatory network analysis. *Nat. Protoc.* 15 (7), 2247–2276. doi:10.1038/s41596-020-0336-2

Wang, L., Tang, G., Hu, K., Liu, X., Zhou, W., Li, H., et al. (2022). Comparison of 68ga-fapi and 18f-fdg pet/ct in the evaluation of advanced lung cancer. *Radiology* 303 (1), 191–199. doi:10.1148/radiol.211424

Wu, Y. H., Huang, Y. F., Chang, T. H., Chen, C. C., Wu, P. Y., Huang, S. C., et al. (2021). COL11A1 activates cancer-associated fibroblasts by modulating TGF-β3 through the NF-κB/IGFBP2 axis in ovarian cancer cells. *Oncogene* 40 (26), 4503–4519. doi:10.1038/s41388-021-01865-8

Yang, F., Wei, Y., Han, D., Li, Y., Shi, S., Jiao, D., et al. (2020). Interaction with Cd68 and regulation of Gas6 expression by endosialin in fibroblasts drives recruitment and polarization of macrophages in hepatocellular carcinoma. *Cancer Res.* 80 (18), 3892–3905. doi:10.1158/0008-5472.CAN-19-2691

Yu, B., Wu, K., Wang, X., Zhang, J., Wang, L., Jiang, Y., et al. (2018). Periostin secreted by cancer-associated fibroblasts promotes cancer stemness in head and neck cancer by activating protein tyrosine kinase 7. *Cell Death Dis.* 9 (11), 1082. doi:10.1038/s41419-018-1116-6

Yu, X., Wang, D., Wang, X., Sun, S., Zhang, Y., Wang, S., et al. (2019). Cxcl12/Cxcr4 promotes inflammation-driven colorectal cancer progression through activation of rhoa signaling by sponging mir-133a-3p. *J. Exp. Clin. Cancer Res.* 38 (1), 32. doi:10.1186/s13046-018-1014-x

Zeisberg, E. M., Potenta, S., Xie, L., Zeisberg, M., and Kalluri, R. (2007). Discovery of endothelial to mesenchymal transition as a source for carcinoma-associated fibroblasts. *Cancer Res.* 67 (21), 10123–10128. doi:10.1158/0008-5472.Can-07-3127

Zhang, M., Yang, H., Wan, L., Wang, Z., Wang, H., Ge, C., et al. (2020). Single-cell transcriptomic architecture and intercellular crosstalk of human intrahepatic cholangiocarcinoma. *J. Hepatology* 73 (5), 1118–1130. doi:10.1016/j.jhep.2020.05.039

Zhou, B., Lin, W., Long, Y., Yang, Y., Zhang, H., Wu, K., et al. (2022). Notch signaling pathway: Architecture, disease, and therapeutics. *Signal Transduct. Target Ther.* 7 (1), 95. doi:10.1038/s41392-022-00934-y

Zhu, K., Cai, L., Cui, C., de Los Toyos, J. R., and Anastassiou, D. (2021). Single-cell analysis reveals the pan-cancer invasiveness-associated transition of adipose-derived stromal cells into col11a1-expressing cancer-associated fibroblasts. *PLoS Comput. Biol.* 17 (7), e1009228. doi:10.1371/journal.pcbi.1009228

frontiers | Frontiers in Pharmacology

TYPE Review
PUBLISHED 14 March 2023
DOI 10.3389/fphar.2023.1113378

OPEN ACCESS

EDITED BY
Bin Liu,
Jiangsu Ocean Universiity, China

REVIEWED BY
Yan Chen,
Guizhou Medical University, China
Zhi Xu,
Nanjing Drum Tower Hospital, China
Ping Liu,
Affiliated Hospital of Guizhou Medical University, China

*CORRESPONDENCE
Qianming Du,
duqianming@njmu.edu.cn
Rong Hu,
ronghu@cpu.edu.cn
Chao Liu,
liuchaogermany@sina.cn

†These authors have contributed equally to this work and share first authorship

SPECIALTY SECTION
This article was submitted to Pharmacology of Anti-Cancer Drugs, a section of the journal Frontiers in Pharmacology

RECEIVED 01 December 2022
ACCEPTED 23 February 2023
PUBLISHED 14 March 2023

CITATION
Zhang C, Fei Y, Wang H, Hu S, Liu C, Hu R and Du Q (2023), CAFs orchestrates tumor immune microenvironment—A new target in cancer therapy? *Front. Pharmacol.* 14:1113378. doi: 10.3389/fphar.2023.1113378

CAFs orchestrates tumor immune microenvironment—A new target in cancer therapy?

Chunxue Zhang[1†], Yuxiang Fei[2†], Hui Wang[1], Sheng Hu[3], Chao Liu[2*], Rong Hu[4*] and Qianming Du[5*]

[1]School of Basic Medicine and Clinical Pharmacy, China Pharmaceutical University, Nanjing, China, [2]Department of Pharmacy, Nanjing First Hospital, Nanjing Medical University, Nanjing, China, [3]College of Pharmacy, Xinjiang Medical University, Urumqi, China, [4]State Key Laboratory of Natural Medicines, Department of Physiology, China Pharmaceutical University, Jiangsu Nanjing, China, [5]General Clinical Research Center, Nanjing First Hospital, Nanjing Medical University, Nanjing, China

Cancer immunotherapy has opened a new landscape in cancer treatment, however, the poor specificity and resistance of most targeted therapeutics have limited their therapeutic efficacy. In recent years, the role of CAFs in immune regulation has been increasingly noted as more evidence has been uncovered regarding the link between cancer-associated fibroblasts (CAFs) and the evolutionary process of tumor progression. CAFs interact with immune cells to shape the tumor immune microenvironment (TIME) that favors malignant tumor progression, a crosstalk process that leads to the failure of cancer immunotherapies. In this review, we outline recent advances in the immunosuppressive function of CAFs, highlight the mechanisms of CAFs-immune cell interactions, and discuss current CAF-targeted therapeutic strategies for future study.

KEYWORDS

tumor microenvironment, cancer-associated fibroblasts, immune cells, CAF-targeted therapy, cancer

1 Introduction

Cancer, a major global public health problem, is the second leading cause of death (Deo et al., 2022). The process of cancer progression is accompanied by dynamic changes in the microenvironment, forming the tumor microenvironment (TME) (Duan et al., 2020). TME is capable of inducing tumor immunosuppression, metastasis, drug resistance, and response to targeted therapies, which is one of the major causes of cancer treatment failure (Bejarano et al., 2021). The TME is a highly complex, dynamically evolving, finely regulated system composed of tumor cells, infiltrating immune cells, cancer-associated fibroblasts (CAFs), endothelial cells, lipid cells, extracellular matrix (ECM), and multiple signaling molecules. CAFs, a major component of TME, have been shown to originate from various cellular precursors types, such as tissue-resident fibroblasts, bone marrow mesenchymal stem cells, and pericytes (Hinshaw and Shevde, 2019). Numerous studies have demonstrated that CAFs promote tumor cell proliferation, drug resistance, and invasive metastasis by participating in a variety of biological processes, and are involved in exogenous pathways such as angiogenesis, ECM remodeling, and epithelial-mesenchymal transition (Feng et al., 2022). Therefore, understanding the nature of CAFs and their functional mechanisms in cancer development is beneficial for finding new cancer treatment strategies.

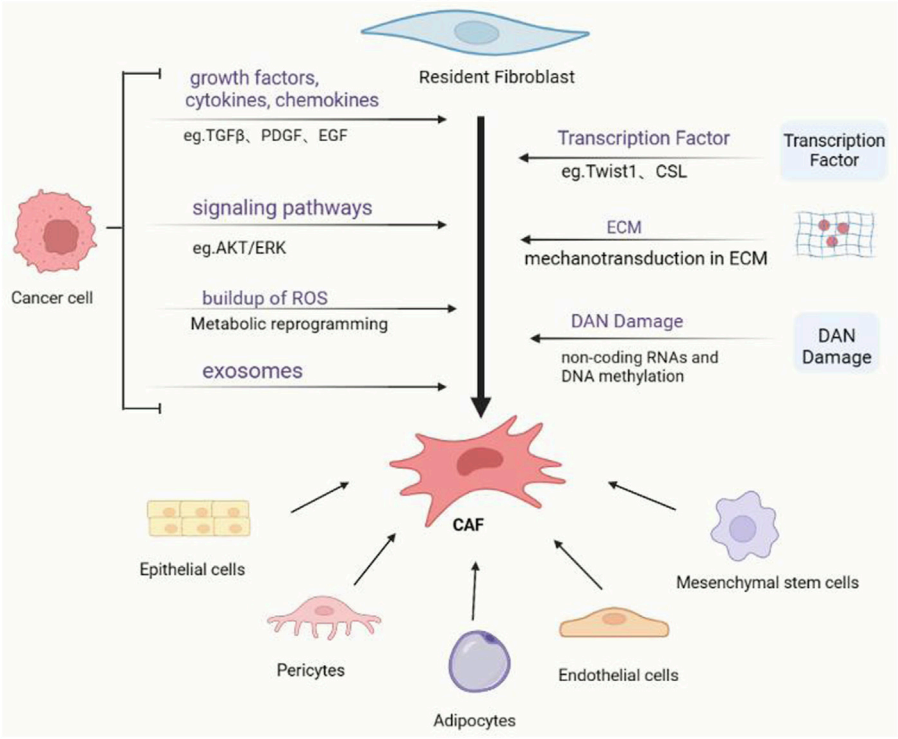

FIGURE 1
Cancer-associated fibroblasts (CAFs) and their activation mechanisms. Various progenitor cells can give rise to cancer-associated fibroblasts *via* diverse pathways. The most researched process is the activation of local fibroblasts, which can be triggered by a variety of triggers, including tumor-secreted proteins and physical TME features.

A growing body of clinical evidence demonstrates the superior efficacy of cancer immunotherapy in many tumor types (Riley et al., 2019). Modulation of the immune system by immune checkpoint inhibitors (ICIs), such as anti-CTLA4, has led to remission in a wide range of tumors (Riley et al., 2019). Despite these successes, immunotherapy still has inevitable limitations for most cancer patients, such as drug resistance and limited applicability (O'Donnell et al., 2019). Studies have shown that the complexity and diversity of the immune environment of the tumor microenvironment have important implications for immunotherapy (Barrett and Puré, 2020; Kockx et al., 2021). As major components of the tumor immune microenvironment, infiltrating immune cells can be both pro-tumor (Tumor-associated macrophages, TAM) and anti-tumor (Cytotoxic $CD8^+$ T cells), and the ratio of these two populations play an important role in tumor progression (Lin et al., 2019; Woan and Miller, 2019). Therefore, the tumor immune microenvironment (TIME) plays a key role in cancer immunotherapy. Numerous studies indicate that CAFs regulate immune infiltration and affect TIME composition, and influence the outcome of cancer immunotherapy (Barrett and Puré, 2020). CAFs control the infiltration and phenotypic alterations of immune cells as well as influence their spatial movement within the tumor to promote immune regulation (Xiang et al., 2022). For example, CAFs can induce immunosuppressive cells such as regulatory T cells (Treg cells) and myeloid-derived suppressor cells (MDSCs) by secreting various cytokines including CXCL12 and other effector molecules, suppressing the immune function of immune effector cells and cytotoxic T lymphocytes ultimately create a TIME for immune tolerance that is conducive to tumor progression (Mao et al., 2021). Therefore, understanding the interactions between CAFs and immune cells can identify the mechanism of immunosuppression of CAFs more accurately, thus discovering effective therapy targeting CAFs, which can improve the success rate of immunotherapy. This review describes the research progress on immunosuppressive mechanisms mediated by CAFs from the perspective of CAFs-immune cell interactions in TME, concludes the major CAF-based targeted immunotherapy technologies, and discusses the shortcomings of current CAF-targeted therapies for future study.

2 Origins and activators of CAFs

The origin of CAFs is difficult to determine because of the lack of unique biomarkers that are not expressed in any other cells (Figure 1). Most scientists believe that fibroblasts are derived from primitive mesenchymal cells, whereas CAFs are derived from activated fibroblasts in local tissues (Arina et al., 2016). CAFs have also been found to originate from other cells, such as mesenchymal stem cells (MSCs), epithelial cells, pericytes, adipocytes, and endothelial cells (Simon and Salhia, 2022).

CAFs in the tumor stroma can be identified by their shape as well as specific identification markers. The production of a-smooth muscle (α-SMA) is commonly used to activate cancer-associated

fibroblasts (Nurmik et al., 2020). a-SMA is the most commonly used maker for identifying CAFs (Nurmik et al., 2020). Fibroblast activation protein (FAP) is a membrane protein that is expressed specifically in CAFs induced by many types of human epithelial carcinoma cells (Chen and Song, 2019). CAFs contain the proteins fibroblast-specific protein 1 (FSP1), vimentin, and platelet-derived growth factor receptor (PDGFR) (Chen and Song, 2019). They could be indicators of cancer-related fibrillogenic cell activity.

Tissue-resident fibroblasts are typically activated by cytokines secreted by tumor cells and other stromal cells, such as specifically transforming growth factor beta (TGFβ), platelet-derived growth factor (PDGF), basic fibroblast growth factor (bFGF), epithelial growth factor (EGF), connective tissue growth factor (CTGF), hepatocyte growth factor (HGF) and vascular endothelial growth factor (VCAM-1) (Mao et al., 2021). TGFβ is a multifunctional cytokine that affects cell proliferation, differentiation, and migration. It is thought to be the most efficient cytokine for eliciting CAF activation. TGFβ activates the TGF-β/Smad classical pathway directly, decreasing αSMA expression and increasing contractile cytoskeleton activity (Liu et al., 2016). Resident fibroblasts can stimulate CAF transformation by directly activating the TGFβ-/Smad classical pathway *via* autocrine TGF-β to regulate *a*-SMA expression (Peng et al., 2022). Protein kinase B (AKT) and extracellular signal-regulated kinase (ERK) pathways activation can also influence *a*-SMA expression (Kuzet and Gaggioli, 2016; Foglia et al., 2019). TGFβ can also indirectly activate Smad2-mediated TGF-β-driven transformation from fibroblasts to CAFs in gastric cancer *via* upregulation of lactose lectin-1 (galectin-1, Gal1) expression in fibroblasts *via* the PI3K/Akt axis (Zheng et al., 2016). Chloride intracellular channel 4 (CLIC4) is a protein that highly upregulated during TGF-β-induced fibroblasts differentiation into activated fibroblasts and is thought to be important in the TGF-β signaling pathway (Shukla et al., 2014). The specific mechanism is that TGF-β promotes fibroblast transformation through CLIC4-mediated p38 map kinase activation upregulating the expression of CAF markers (Shukla et al., 2014).

MSCs transdifferentiate into CAFs through activating tumor cell and stromal cell-secreted transforming growth factor beta-1 (TGFβ-1) and C-X-C chemokine ligand (CXCL) 16 (Jung et al., 2013; Barcellos-de-Souza et al., 2016; Jiang et al., 2016; Ganguly et al., 2020). MSCs generated from bone marrow can be transformed into myofibroblasts in mouse fibrotic liver *via* the sphingosine kinase/sphingosine 1 phosphate receptor axis by TGF-β1 (Yang et al., 2012; Chandra Jena et al., 2021). When activated with TGFβ-1, human adipose tissue-derived stem cells (HASCs) transdifferentiate into CAFs with a fibroblastic phenotype (α-smooth muscle actin and tenascin-C expression) (Jotzu et al., 2011; de Araújo Farias et al., 2018). However, less evidence supports these origins, and their relevance to other types of tumors is limited.

In addition to the regulatory molecules mentioned above, inflammatory cytokines in TME such as chemokines (CXL), interleukins (IL), interferons (IFN), and tumor necrosis factors (TNF) not only govern CAF activation but also directly or indirectly promote tumor growth (Rollins, 2006; Mhaidly and Mechta-Grigoriou, 2020). TNF stimulates CAFs to produce C-C motif chemokine ligand2 (CCL2), C-C motif chemokine ligand 5 (CCL5), C-C motif chemokine ligand 7 (CCL7), C-X-C motif chemokine ligand 8 (CXCL8), C-X-C motif chemokine ligand 12 (CXCL12), C-X-C motif chemokine ligand 14 (CXCL14), and C-X-C motif chemokine ligand 16 (CXCL16), which activate ERK and AKT signaling pathways through focal mucin kinase (FAK), increasing the transcriptional activity of downstream -catenin and NF-κB. Interleukin-1 (IL-1), interleukin-6 (IL-6), interleukin-8 (IL-8), or IFN interact with receptors on the surface of CAFs such as IL6-R and CXC receptor 2 (CXCR2). CAFs express IL6-R, CXCR2, and other receptors that activate Janus kinase/signal transducer and activator of transcription (JAK1/STAT3), Rho-associated kinases (ROCK), or AKT/ERK1/2 signaling pathways to activate CAFs, increase myosin contractility, and ECM (Prabhavathy et al., 2014; Kuzet and Gaggioli, 2016). Many transcription factors, including Notch signaling transcriptional repressor (CBF1/RBP-J/suppressor of hairless/LAG-1, CSL) and recombinant human activating transcription factor-3 (ATF3), can operate as mediators of CAF activation (Kim et al., 2017). Twist-related protein 1 (Twist1) and paired related homeobox 1 (Prrx1) are specific transcription factors that positively regulate CAFs activation. The study confirmed that Twist1-Prrx1-TNC can form a positive feedback loop to induce the activation of CAFs (Yeo et al., 2018). In addition, CD44, a cell surface molecule expressed by MSCs, can also induce the activation of CAFs by up regulating Twist transcription (Spaeth et al., 2013; Hu et al., 2022). Myristoylated alanine-rich protein kinase C substrate (MARCKS), the forkhead box F1 gene (FoxF1), and the zinc finger transcription factor (snail 1) by activating AKT/Twist1 signaling to upregulate αSMA and PDGFR, the release of paracrine factors such as FGF-2 and HGF is promoted, resulting in the activation of CAFs and tumor (Saito et al., 2010; Stanisavljevic et al., 2015; Yang et al., 2016a).

The transformation of local fibroblasts into CAFs is also triggered by the buildup of reactive oxygen species (ROS). By increasing the expression of growth factors such as PDGF and TGF-β, ROS regulates the communication between cancer cells and fibroblasts, subsequently triggering the release of chemokines such as CXCL12 (Costa et al., 2014). Additionally, CAF activation is influenced by radiation therapy-induced DNA damage, tumor-derived exosomes, and ECM (Calvo et al., 2013; Hellevik and Martinez-Zubiaurre, 2014; Giusti et al., 2018).

3 CAF-mediated regulation of the innate anti-tumor immune response

3.1 Interaction between CAFs and tumor-associated macrophages

Tumor-associated macrophages (TAMs) are heterologous cell populations with distinct functional phenotypes due to their flexibility; they are classified as M1 or M2 based on their functional differentiation state and immune response (Arvanitakis et al., 2022). M1 types are involved in T helper type 1 (Th1) cells responses, activated by cytokines such as interferon-gamma (IFN-γ), tumor necrosis factor (TNF-α), or lipopolysaccharide (LPS), and are characterized by the secretion of pro-inflammatory molecules and reactive ROS (Grivennikov et al., 2010; Yang et al., 2020). M2 types are involved in T helper type 2 (Th2) cells immune responses which promote tissue repair,

angiogenesis promotion, immunosuppressive factors secretion, inhibit cytotoxic T cell killing, and promote tumor cell invasion and metastasis and ECM remodeling (Grivennikov et al., 2010; Yang et al., 2020). Now, some studies show that TAM cells rarely show true M1 or M2 phenotypes (Locati et al., 2020; Mao et al., 2021). This means that this binary classification is not a good way to understand how complicated these cells are. Some researchers try to get around this problem by putting macrophages into different groups (like M2a, M2b, and M2c instead of M2) or by using more general terms (such as M1-like and M2-like, rather than M1 and M2) (Szulc-Kielbik and Kielbik, 2012). But making changes to these definitions might not be enough to cover all of the complexity of TAM.

CAFs and TAMs are essential components of the tumor microenvironment, coordinating pro-tumor inflammation (Tajaldini et al., 2022). TAMs are the most abundant innate immune cell type in the vicinity of densely populated areas of CAF, suggesting a close relationship between TAMs and CAFs (Gunaydin, 2021). In addition to their roles in monocyte recruitment and TAM differentiation, there are numerous studies suggesting that the interaction between CAFs and TAMs promotes cancer growth and the activation of immunosuppressive macrophages to generate an immunosuppressive environment (Raskov et al., 2021). CAFs and M2-polarized macrophages play a synergistic role in the progression of prostate cancer, as evidenced by an examination of patients with prostate cancer at various clinical stages (Comito et al., 2014). A similar pattern of CAF-promoted macrophage recruitment and TAM differentiation for cancer progression has also been found in other cancer types. In pancreatic ductal adenocarcinoma (PDAC), CAFs were able to produce the TAM phenotype in part *via* released M-CSF and incerased ROS generation in monocytes, and CAFs-induced M2 macrophages greatly promoted the proliferation, migration, and invasion of pancreatic tumor cells (Zhang et al., 2017). In colorectal cancer, Haaglim Cho et al. demonstrated that CAF production of GM-CSF and IL6 in response to cancer cell stimulation induced human monocytes to differentiate into pro-invasive M2-like macrophages (Yeo et al., 2018). Andersson et al. discovered that CAFs induce TAM phenotypic transition from M1 to M2 by releasing high amounts of interleukin-33 (IL-33), which leads to cancer metastasis *via* the IL-33/NF-Bκ/MMP9/laminin axis (Andersson et al., 2018). In oral squamous cell carcinoma (OSCC), XingLia et al. found that CAFs stimulates monocyte differentiation into M2 macrophages *via* the CXCL12/CXCR4 pathway (Li et al., 2019). These polarized M2 macrophages then promoted the formation of CSC-like cells in OSCC, leading to increased proliferation and decreased apoptosis in OSCC(57). *In vitro* investigations conducted by Shuhai Chen and colleagues revealed that CAF enhances macrophage M2 polarization and CAF-secreted CXCL12 causes TAMs to release plasminogen activator inhibitor-1 (PAI-1), hence promoting HCC progression (Chen et al., 2021). Ran Zhang et al. found that knocking down G protein-coupled receptor 30 (GPR30) in CAFs reduced CXCL12 expression and thus inhibited macrophage migration, as well as that macrophages had attenuated M2 polarization, downregulated M2-like marker expression, and inhibited prostate cancer (PCa) cell invasion by reducing IL-6 secretion (Zhang et al., 2021). Furthermore, CAF-derived Chitinase 3-like 1, associated with inflammatory disease, has been reported to contribute to tumor growth in breast cancer with high infiltration of M2-polarised macrophages and TH2-type immune responses (Cohen et al., 2017). C-C chemokine ligand 2 (CCL2), derived from FSP1 CAF enhances inflammatory response in skin tumors by increasing monocyte recruitment, which promotes cancer development (Zhang et al., 2011). More importantly, CAFs may be associated with the establishment of an immunosuppressive environment through the induction of immunosuppressive macrophages. The current study found a significant relationship between the number of TAMs and the CAFs grade in breast cancer (Gok Yavuz et al., 2019). High grade CAF tissues contained more CD163 or CD206 macrophages, according to research by Betul Gok Yavuz and colleagues (Gok Yavuz et al., 2019). Additionally, fewer CD163 or CD206 macrophages were linked to low CAF grade (Gok Yavuz et al., 2019). Betul Gok Yavuz et al.(2019) also identified the role of CAFs on monocyte recruitment and macrophage polarisation in breast cancer and induced immunosuppressive PD-1^{+} TAM to shape the tumor microenvironment. CAF attracts monocytes in colorectal cancer by secreting IL-8 and promotes the polarization and recruitment of macrophage M2. M2 polarized macrophages collaborate with CAF to inhibit natural killer (NK) cell function and protect CRC cells from NK cell-mediated killing (Zhang et al., 2019). In a recent article, the authors demonstrated that co-culture with triple-negative breast cancer (TNBC)derived CAFs resulted in the reprogramming of blood monocytes to immunosuppressive $STAB1^{+}TREM2^{high}$ lipid-associated macrophages (LAM), thereby inhibiting T cell activation and proliferation, thereby inducing an immunosuppressive microenvironment (Timperi et al., 2022). Next, CAFs derived from (lung squamous cell carcinoma) LSCC were shown to promote $CCR2^{+}$ monocyte migration, prompting their transformation into immunosuppressive myeloid-derived suppressor cells (MDSCs), and decrease $CD8^{+}$ T cell proliferation and IFN production. The immunosuppressive role of CAF-induced MDSCs might be reversed by targeting CCR2 to reduce monocyte migration and IDO1 or NOX to inhibit ROS generation, hence disrupting CAF-monocyte interactions (Xiang et al., 2020). Furthermore, some studies have shown that M2 TAMs can activate CAFs, hence promoting tumor growth. Macrophage-determined components may promote the transformation of resident hepatic stellate cells into myofibroblasts, resulting in a fibrotic environment in pancreatic ductal adenocarcinoma liver metastases (Nielsen et al., 2016). Osteopontin (OPN) has been identified as a crucial molecule involved in CAF and TAM interactions in HCC. TAMs in the TME release OPN, a chemokine-like phosphorylated glycoprotein. TAM-secreted OPN promotes OPN secretion from CAFs, which increases cancer cell malignancy by upregulating proliferation, ECM degradation, and migration (Tokuda et al., 2021). Additionally, TAM is capable of influencing CAF. It has been observed that TAMs promote neuroblastoma growth by inducing the proliferation and invasion of CAF-like bone marrow mesenchymal stem cells. Activated CAF also increase TAM activity, establishing a positive feedback loop that promotes cancer growth and an immunosuppressive microenvironment (Hashimoto et al., 2016).

Among the different cells present in TME, TAMs, and CAFs have been shown to operate the tissues that make up the ECM to regulate angiogenesis, tumor metastasis, and drug resistance with

significant value (Monteran and Erez, 2019). It has been demonstrated that TAM and CAF in the TME establish a barrier with the ECM to isolate the action of drugs and even inhibit the killing action of immune cells, resulting in a poor prognosis and the failure of chemotherapeutic drug treatment (Tajaldini et al., 2022). Given the synergistic relationship between CAFs and TAMs in the TME in promoting cancer development, strategies to alter the polarization phenotype of TAMs should also consider the synergistic effects of CAFs, thereby contributing to a more effective antitumor immune response. Accordingly, the co-focusing of CAFs and TAMs is viewed as a choice to be thought of.

3.2 Interaction between CAFs and tumor-associated neutrophils (TANs)

Neutrophils were initially considered the first responders of the innate immune system against extracellular pathogens (Lehrer et al., 1988; Schoen et al., 2022). However, current evidence suggests that neutrophils are not only involved in the regulation of the innate and adaptive immune systems but can polarize toward different phenotypes in response to environmental signals (Hedrick and Malanchi, 2022). On the one hand, N1 TANs exhibit antitumor activity mediated by direct or indirect tumor cell lysis, while on the other hand, N2 TANs have a prominent role in growth, invasion, angiogenesis, and metastasis in various cancer types (Hedrick and Malanchi, 2022). TGF-β plays an important role in neutrophil proliferation plasticity, driving the acquisition of the N2 phenotype (Piccard et al., 2012; Arvanitakis et al., 2021; Mahmud et al., 2022). Additionally, the N2 phenotype is linked to the production of neutrophil extracellular traps (NETs), complexes made of DNA and granule proteins that are released in response to stimulation. NETs contain proteins including matrix metallopeptidase-9 (MMP-9) and histonectin G that promote tumor growth (Brinkmann et al., 2004; Jaillon et al., 2007; Demkow, 2021; Segal et al., 2022).

According to the current report, CAFs may be involved in the recruitment polarization of TANs and induce the immunosuppressive properties of TANs. For instance Cancer-associated fibroblasts infiltrating HCC(HCC-CAFs) recruit peripheral blood neutrophils by the SDF1a/CXCR4 pathway. CAFs infiltrating HCC induce TANs survival and activation, as reflected by increased expression of CD66b, programmed death ligands 1 (PD-L1), IL-8, TNF, and C-C chemokine ligand 22 (CCL22) and decreased expression of CD62L. Also, HCC-CAFs cause $PDL1^{+}$ neutrophils formation through the IL6 signaling transducer and transcriptional activator STAT3-PD-L signaling cascade (Cheng et al., 2018). This stops T cells from working and makes it easier for HCC to spread. Several other studies have also shown that CAFs may be involved in the polarization of TANs. It has been demonstrated that the CAF-expressed cytokine receptor CXCR2 is essential for the recruitment of neutrophils into malignancies. It is possible that CAFs may help TANs move in a way that depends on CXCR2 (Li et al., 2015). In a recent study, Song et al. (2021) investigated the interrelationship between CAFs, HCC cells, and TANs, which is mediated by a cytokine network. The scientists found that the cardiotrophin-like cytokine factor 1 (CLCF1)-CXCL6/TGFβ-axis, as well as the contemporaneous recruitment of N2 TANs, had a role in the control of cancer stemness in a cohort of HCC clinical samples, leading to the poor prognosis of HCC patients. CLCF1, which was made by CAFs, caused tumor cells to make more CXCL6 and TGF-β, which worked on tumor cells to make them more stem-like and on TANs to cause N2 polarization. Next, CAFs were found to induce neutrophil extracellular traps modulates tumor growth. Munir et al. (2021) discovered that neutrophils are frequently limited to CAF-rich areas in primary mouse pancreatic and skin (melanoma) cancers, hinting that there may be crosstalk between the two populations. Through a ROS-dependent mechanism, CAF-secreted amyloid promotes the formation of tumor-associated NETs (t-NETs) *via* CD11b (Munir et al., 2021). Inhibiting the treatment of t-NETs or reducing the generation of amyloid by CAFs can halt tumor growth and restore the antitumor status of neutrophils invading the tumor (Munir et al., 2021). In addition, gastric cancer mesenchymal stem cells (GC-MSCs) and neutrophils interact bidirectionally, according to Zhu et al. (2014) GC-MSCs can stimulate neutrophil chemotaxis and activation through IL-6-mediated STAT3-ERK1/2 axis and activated TANs can promote MSCs becoming CAFs.

In conclusion, CAF may be involved in the recruitment of polarized TANs and the induction of immunosuppressive properties, but the number of articles on the interaction of CAF with TANs is limited, and the specific mechanism of CAF-TAN interaction is not well understood and needs further study.

3.3 Interaction between CAFs and natural killer (NK) cells

There are various types of NK cells. Humans have two main subtypes: $CD56^{bright}CD16^{dim}$ and $CD56^{dim}CD16^{bright}$. The latter subtype, mature NK cells, is more cytotoxic to its targets than the former (Ran et al., 2022). CD56 is a recognized NK cell marker. CD16 is a marker of activated and mature NK cells (Ran et al., 2022). Whether NK cells are active is determined by the expression of activating or inhibitory receptors on the cell surface.

CAFs reduce NK cells activation receptor, IFN-γ, TNF-α, perforin and granzyme B expression by secreting various cytokines, chemokines and MMPs to reduce NK cell toxicity (Li et al., 2013; Huang et al., 2019). For example, MMP secreted by CAFs in the melanoma microenvironment reduced the expression of NKG2D ligand (MICA/B) in NK cells, which further inhibited the killing of tumor cells by NK cells (Ziani et al., 2017). CAFs secrete IDO or PGE2 to reduce NKG2D expression in NK cells, creating an unresponsive state in antitumor immunity (Balsamo et al., 2009; Li et al., 2012). Substantial studies have proven that TGFβ can reduce the cytotoxic actions of NK cells by decreasing the expression of the activating receptors NKG2D, NKp30, and NKp44 on NK cells (Trotta et al., 2008; Ziani et al., 2017; Han et al., 2018; Lim et al., 2019). By controlling the expression of the ligands associated with NK cell activation receptors on tumor cells, CAFs can also subtly inhibit the activity and functionality of NK cells. A decrease in poliovirus receptor (PVR, a ligand of an NK-activating receptor) expression on the cell surface is essential for the CAF-mediated inhibition of NK cells killing activities. Meanwhile, NK cell-mediated cleavage of CAFs was observed in a variety of tumor

types. Pancreatic stellate cells (PSCs) are CAFs subpopulations found in PDAC (94). Through interactions between NKG2D and MICA/B, NK cells can target activated PSCs and mediate PSCs lysis (Bachem et al., 2005). However, only a few studies have examined the impact of NK cells on CAFs, and more research is required to clarify how this interaction develops.

3.4 Interaction between CAFs and mast cells (MCs)

Mast cells, which develop from CD34/CD117 pluripotent hematopoietic stem cells, are tissue-resident sentinel cells that, upon activation, produce a vast array of chemokines and cytokines. MC1 (meaning anti-tumorigenic) produce granzyme B, IL-9, and histamine, which induce dendritic cells (DCs) maturation and inhibit murine tumor growth. MC2 (meaning pro-tumorigenic) produces VEGFs, FGF, MMP-9, TGF-β, and cytokines (IL-1, IL-6, and IL-13) (Varricchi et al., 2019).

Mast cells and stellate cells, a CAF precursor, have complex relationships. *In vitro*, Ma et al. (2013) discovered that PSC can stimulate and proliferate mast cells. Mast cells, on the other hand, can stimulate CAF synthesis in the TGF-β2-STAT6 non-dependent route by secreting IL-13 and trypsin-like proteases. In breast cancer, MCs promote ECM destruction and myofibroblast differentiation through MMP and trypsin secretion, thus contributing to tumor aggressiveness and metastatic spread (Mangia et al., 2011). Mast cell-derived trypsin indirectly enhances CAF-induced morphological changes in prostate epithelium *via* the tumor microenvironment (Pereira et al., 2019). CAFs recruit mast cells. Gene microarray analysis identified CXCL12 as the primary estrogen-driven target gene in CXCL12, while CAFs recruited mast cells in a CXCR4-dependent manner *via* CXCL12 (Ellem et al., 2014). To date, the interactions between mast cells and CAFs in TME are still poorly understood and need further study.

3.5 Interaction between CAFs and dendritic cells (DCs)

Among all immune cells, DCs are the most potent antigen-presenting cells (APCs) in the immune system and are central players of the adaptive immune response (Lee and Radford, 2019). DCs can be conventional (cDC) or plasmacytoid (pDC) based on their ontogeny (Wculek et al., 2020). According to DCs development, it might be immature or mature. Most immature DCs live on mucosal surfaces, while skin and solid organs operate as antigen sentinels. These DCs express fewer MHC I and II, T cell co-stimulating factors, and adhesion molecules (Wculek et al., 2020). Recent researches have illustrated that CAFs can influence the differentiation of monocytes into DCs as well as maturation, antigen presentation, and immune responses.

According to pertinent studies, CAF-derived TGF-β (Weber et al., 2005; Travis and Sheppard, 2014), VEGF (Gabrilovich et al., 1996; Huang et al., 2007) and inflammatory cytokine (Chomarat et al., 2000; Park et al., 2004) are reimplicated in restraining DCs function and maturation. TGF-β (Gabrilovich et al., 1996; Huang et al., 2007) mediates the downregulation of MHC class II molecules and costimulatory molecules in dendritic cells, inhibiting dendritic cell antigen presentation and activating the cytotoxic T-cell response. CAFs-produced IL-6 induces a tolerogenic phenotype in hepatocellular carcinoma DCs, increases tumor infiltration of immunosuppressive regulatory T cells (Tregs) (CD4CD25Foxp3), and decreases IFN-γ production by CD8 T cells (Cheng et al., 2016). Furthermore, tryptophan 2,3-dioxygenase (TDO2) secreted by CAFs inhibited the differentiation and function of DCs in a transplantable model of lung cancer, whereas TDO2 inhibition increased DC function and T cell responses (Silzle et al., 2004). In a recent study, WNT2 secreted by CAFs was found to inhibit the *in vitro* differentiation and immunostimulatory activity of DCs (Huang et al., 2022a). In primary OSCC tumors, WNT2 CAFs and CD8 T cells correlated negatively. Anti-WNT2 mAb restored anti-tumour T-cell responses and increased active DC in mouse OSCC and CRC syngeneic cancer models (Huang et al., 2022a). By inhibiting CAFs-derived WNT2, DC differentiation and antitumor T cell responses were restored. WNT2 produced by CAFs suppressed anti-tumor T cell responses mediated by DC *via* SOCS3/p-JAK2/p-STAT (110).

However, the detailed mechanisms by which CAF influences DCs development, maturation, and function are not yet understood, based on the existing evidence.

4 Interaction between CAFs and adaptive immune cells in the TME

4.1 Direct interaction between CAFs and T lymphocytes

When activated, naive CD4 T cells differentiate into various T helper (Th) subpopulations, the most common of which are Th1, Th2, and Th17 cells (Ruterbusch et al., 2020). CD4 Th1 cells mediate the immune response to viral infections and malignancies. In addition to antitumor $CD8^+$ T cells, they are an important source of IFN-γ, which has direct antitumor effects (Zhu and Zhu, 2020). Th2 cells activate and maintain humoral or antibody-mediated immune responses against extracellular parasites, bacteria, allergens, and toxins (Zhu and Zhu, 2020). A predominantly Th1 response is associated with a better prognosis in human tumors such as colorectal, breast, brain cancers, whereas Th2 is linked to a worse prognosis for pancreatic and colorectal malignancies (Chraa et al., 2019).

Direct and indirect evidence suggests that CAFs recruit and balance CD4 effector T cell subsets to promote Th2 responses at the expense of Th1 responses. *In vivo* studies using the breast cancer 4T1 model depleted FAP CAFs by DNA vaccines led to increased expression of IL-2 and IL-7 (inducing Th1 cell differentiation) and decreased expression of IL-4 and IL-6 (inducing Th2 cell differentiation) in tumor homogenates, indicating that CAFs regulate the transition from Th1 to Th2 mediated immunity (Liao et al., 2009). TNF and IL-1 stimulate CAF in human pancreatic tumors to produce thymic stromal lymphopoietin (TSLP), which indirectly promotes Th2 cells by acting on dendritic cells. Specifically, TSLP increases Th2 recruitment through stimulated dendritic cell production of C-C motif chemokine ligand 17 (CCL17) and CCL2, naive CD4 T cells to

polarize to the Th2 phenotype (measured by IL-13 production), thereby increasing Th2 numbers (De Monte et al., 2011). There is less evidence that CAF and Th17 interact, and it is less clear what role Th17 cells play in the immune system's ability to fight cancer. In a recent study, CAFs in the colorectal area made RANTES and MCP-1 to attract Th17s instead of other T helper subpopulations (Su et al., 2010). This was made possible by TLR3 signaling to CAFs (Su et al., 2010). Also, CAFs helped naive CD4 T cells turn into Th17 cells by letting out IL-1, IL-6, IL-23, and TGFβ, which was partly caused by contact (Su et al., 2010). These studies demonstrate that CAFs may contribute to the establishment of a fraction of immunosuppressive helper T cells that is less cytotoxic.

Tregs serve a vital function in maintaining immune system homeostasis. Tregs interact positively with CAFs, cancer cells, and negatively with cytotoxic T lymphocytes (CTL) and natural killer cells (Ohue and Nishikawa, 2019). The possibility of interactions between CAFs and Treg cells has been demonstrated in numerous researches. In 2013, Kinoshita et al. (2013) revealed that the existence of Tregs coexisting with CAFs is correlated with poor lung adenocarcinoma patient outcomes. Sharma et al. (2005) reported a potential interaction between CAFs and Tregs *via* COX-2 production of CAFs in the lung or pancreatic cancer leading to their emission of PGE-2, which is known to stimulate Foxp3 expression. Liao et al. (2009) focused on FAP$^+$ CAFs and showed that their depletion in breast tumors is connected with reduced Tregs Ozdemir et al. (2014) reduced *a*-SMA$^+$ CAFs in pancreatic cancer animal models and detected an increase in CD4$^+$FoxP3$^+$ Tregs. In addition, CAFs excel in recruiting and inducing Tregs due to their strong secretory activity and capacity to release immunosuppressive cytokines. For instance, Chang et al. discovered that CCL5, a factor that CAFs can release, increases Tregs migration into tumors, and that blocking CCR5 signaling and knocking down CCL5 in tumor cells reduced Treg infiltration and slowed tumor progression in a mouse model of colorectal cancer (Chang et al., 2012). Other molecules such as Vascular endothelial growth factor A (VEGF-A) (Bourhis et al., 2021), C-C motif chemokine ligand 1 (CCL1) (Kuehnemuth et al., 2018), CCL2 (Kadomoto et al., 2021), CCL22 (Anz et al., 2015) and other factors have also been shown to be involved in promoting the recruitment and infiltration of Treg cells. CAFs not only increase Treg cells recruitment and infiltration, but they also promote their transformation and immunosuppression. For instance, in head and neck malignancies, TGFβ released by CAFs promotes T cells death and Tregs polarization, creating an immunosuppressive milieu (Takahashi et al., 2015). Julie Jacobs et al. (2018) examined the prognostic value of CD70 expression in CRC tissues using immunohistochemistry, as well as its interaction with fibroblast markers and Tregs. The involvement of CD70-positive CAF in migration and immune evasion was determined by *in vitro* experiments. Functionally, CD70-positive CAFs stimulated the frequency of naturally occurring Tregs and encouraged migration. Moreover, CAF altered the immunosuppressive TIL population of TME by secreting high levels of IL6, which decreased CD8 $^+$ TILs while increasing Foxp3$^+$ TILs (Kato et al., 2018). Recently, using single-cell RNA sequencing, HuocongHuang et al. determined that antigen-presenting CAF (ap-CAF) originates from mesothelial cells and that ap-CAF induces naive CD4 T cells to form regulatory T cells in an antigen-specific transformation manner, induces Treg immunosuppressive function and suppresses CD8$^+$ T cell function (Huang et al., 2022b).

All the above results indicate that CAFs may have an effect on Tregs in TME, leading to their recruitment and differentiation. Determining whether CAFs cause immunosuppression in the TME through interaction with Tregs and the precise mechanism of this process would undoubtedly contribute to a greater comprehension of the antitumor immune response.

CD8$^+$ T cells, which are also known as CTLs, are responsible for mediating cytotoxic actions (St Paul and Ohashi, 2020). This is mostly done by making tumor cells go through a process called apoptosis, which is thought to be the most important part of antitumor immunity (St Paul and Ohashi, 2020).

Numerous studies indicate that CAF lowers the ability of CD8$^+$ T lymphocytes to kill tumor cells by reducing T cell penetration into the tumor, preventing T cell trafficking in the microenvironment, and lowering cytotoxic activity (Freeman and Mielgo, 2020). When activated in the TME, CAF may block the recruitment of CD8$^+$ T lymphocytes from the periphery to the tumor by secreting many cytokines and chemokines that result in immunosuppression. The CXCL12-CXCR4 chemokine axis is the most well-known of these mechanisms. T cells express the CXCL12 receptor, which FAPCAFs in the TME generate. This binding keeps TIL in the tumor stroma and stops them from getting to areas of the tumor with cancer cells (Wang et al., 2022). For instance, CXCL12 generation by activated CAF in PDAC increases migration of peripheral CD8$^+$ T cells to active CAF in the peritumor stromal region, resulting in a concentration of CD8$^+$ T cells in the pan-mesenchymal compartment and decreased recruitment to the tumor islets (Ene-Obong et al., 2013). In preclinical research on PDAC, inhibition of CXCR4 at both the pharmacological and genetic levels led to the rapid buildup of CD8$^+$ T cells in tumors and a reduction in tumor growth (Feig et al., 2013). A new inflammatory CAF (iCAF) subpopulation was discovered in a recent study that used single cell RNA-sequencing to examine stromal cell populations in patients with TNBC(135). Genes in the CXCL12-CXCR4 chemoattractant pathway were turned up by iCAFs, and the presence of iCAFs was strongly linked to the failure and exclusion of CD8$^+$ T cells (Kocher et al., 2020). Furthermore, CAF can reduce CD8$^+$ T cell recruitment and inhibit their cytotoxic activity against tumor cells by releasing IL-6 and TGF-β. When co-inoculated with CAFs and tumor cells, Kato et al. demonstrated that tumor growth was more prominent in immunocompetent mice than immunodeficient nude mice, indicating that CAFs may aid tumor growth by modifying the immune response. Furthermore, the rejection of CD8$^+$ T cells by CAFs is dependent on IL-6, and inhibiting IL-6 results in a substantial shift from FoxP3 to CD8$^+$ T cells in the TIL population (Kato et al., 2018). It has been demonstrated that increased CAF-derived TGF-β secretion is associated with decreased CD8$^+$ T cell accumulation in metastatic colorectal cancer and urothelial cancer as well as diminished sensitivity to immune checkpoint medications (Thomas and Massagué, 2005; Tauriello et al., 2018). Inhibition of CAF-derived TGF-β enhanced T cell density inside the tumor parenchyma in both of these malignancies, restored the effectiveness of checkpoint inhibition, and decreased metastatic burden.

In addition to CAF-secreted elements that directly influence CD8$^+$ T cell control of migration and function in TME, it has been

discovered that dense ECM structures can impede $CD8^+$ T cell intratumoral migration (Vyas and Demehri, 2022).

4.2 CAFs inhibit T lymphocyte infiltration through ECM

The ability of activated CAFs to abnormally deposit ECM proteins such as fibronectin, collagen, and hyaluronan as well as matrix breakdown enzymes is a crucial characteristic of these cells (Tian et al., 2019). This prevents T-cell contact-dependent death of tumor cells in several solid cancers. CAFs were found to reduce the number of tumor-infiltrating $CD8^+$ T lymphocytes by altering ECM composition. It was found that $CD8^+$ T cells tend to gather in the stromal parts of these tumors, which have a much sparser network of fibrin and collagen fibrils than the islets of the tumor, which are surrounded by dense networks of collagen and fibrin fibers that run in parallel. The same result was found in ovarian cancer (Bougherara et al., 2015). CAFs made from activated tissue-resident stellate cells kept $CD8^+$ T lymphocytes away from the tumor in stromal compartments in human tissue sections and a mouse model of pancreatic cancer, which was linked to a shorter survival time (Ene-Obong et al., 2013). In the same way, focal adhesion kinase, non-receptor tyrosine kinases, and enhanced stromal collagen 1 deposition were shown to be activated in pancreatic cancers, which led to inadequate $CD8^+$ cytotoxic T cell infiltration. In mouse pancreatic cancer, blocking focal adhesion kinase 1 increased the number of $CD8^+$ T cells and decreased the amount of collagen and CAFs (Jiang et al., 2016). NADPH oxidase 4 (NOX4), a TGFβ-1 downstream target that generates reactive ROS, can regulate the transition of fibroblasts to myofibroblasts. In a mouse model of CAF-rich tumors, silencing NOX4 or blocking it with drugs prevents TGFβ-driven differentiation of CAF into myofibroblasts and downregulates functional markers of fully differentiated CAF, such as αSMA and collagen 1 (141). Tumor hypoxia is one more element that affects how many solid tumors have less $CD8^+$ T cell infiltration (Mortezaee and Majidpoor, 2021). In response to hypoxia, CAFs release a variety of angiogenic factors, including VEGF, which decreases the expression of cell adhesion molecules on endothelial cells, such as intercellular cell adhesion molecule (ICAM)-1/2 (Pietras and Ostman, 2010). Insufficient cell adhesion molecules, it is hard for peripheral $CD8^+$ T-cells to move through the vascular system and reach the tumor site (Slaney et al., 2014).

4.3 CAFs inhibit T lymphocyte function by upregulating the expression of immune checkpoint molecules

Lower effector function and reduced proliferative capacity are two characteristics of antitumor T cell dysfunction, which is partly brought on by the overexpression of immunological checkpoint molecules (Lakins et al., 2018). CAFs have the ability to directly kill $CD8^+$ T lymphocytes and express immunological checkpoint molecules such as PD-L1 and PD-L2 in their cells. (Lakins et al., 2018). Lakins et al. (2018) found that by increasing both PD-L2 and Fas ligands, CAFs from mouse lung adenocarcinoma and melanoma tumors can directly kill tumor-specific $CD8^+$ T-cells, which helps the tumor stay alive. Fibroblasts from biopsies of melanoma patients show upregulation of both PD-L1 and PD-L2, which bind to the PD-1 receptor and directly counteract $CD8^+$ T cell function (Khalili et al., 2012). In the same context, it was discovered that PD-L1 and PD-L2 were elevated in pancreatic cancer CAF expression and that CAF encourages the development of co-suppressive immune checkpoint receptors (such as PD-1) in proliferating T cells, which results in T cell malfunction (Gorchs et al., 2019). Melanoma-associated fibroblast-derived soluble factors significantly downregulated CD69 expression on the surface of activated $CD8^+$ T cells and reduced granzyme B production and release. Melanoma-associated fibroblasts (MAFs) were also discovered to selectively dysregulate many immunological checkpoint regulators on $CD8^+$ T cells. The MAF-derived soluble factors increase the number of BTLA-positive and TIGIT-positive $CD8^+$ T cells by a large amount, interfere with intracellular CTL signaling, and make CTL less effective (Érsek et al., 2021). However, the underlying mechanism by which CAF promotes upregulation of suppressive immune checkpoints on $CD8^+$ T cells is not fully understood.

4.4 CAFs inhibit T lymphocyte function by interfering with antigen presentation

It has also been demonstrated that CAFs suppress the T cell receptor (TCR) to decrease the proliferation and function of CD8 T cells, hence interfering with the antigen detection and activation process. For example, both *in vitro* and mouse models of pancreatic cancer showed that CAF-derived βig-h3 protein (also known as TGF-βi) had an inhibiting effect on tumor-specific CD8 T cells by acting directly on them (Goehrig et al., 2019). βIg-h3 interacts with CD61 on $CD8^+$ T cells, causing Hic-5 protein to bind to Y505-phosphorylated Lck and inhibit TCR signaling, which inhibited tumor-specific $CD8^+$ T-cell activation (Goehrig et al., 2019). Additionally, preventing professional APC and/or interfering with antigen expression can indirectly prevent $CD8^+$ T cells from performing their cytotoxic activity. CAFs stop DCs or NK cells from presenting antigens by interfering with their normal development. They also cause immunosuppressive subpopulations and immune checkpoint expression, which makes it harder for effector T cells to fight tumors. For example, human hepatocellular carcinoma-derived CAFs can secrete IL-6, which upregulates the activation of the STAT3 signaling pathway in DCs and creates a regulatory DC (rDC) phenotype that can't prime and activate T lymphocytes (Cheng et al., 2016).

4.5 CAFs inhibit T lymphocyte function through metabolic reprogramming

In recent years, there has been a growing body of data indicating CAF metabolic reprogramming provides an additional mechanism for inhibiting cytotoxic T cell function inside TME. For instance, it has been demonstrated that purinergic nucleosides produced by tumor-educated MSCs isolated from human cervical cancer (CeCa)

patients inhibit the proliferation, activation, and effector activities of $CD8^+$ T lymphocytes (de Lourdes Mora-García et al., 2016). Glycolytic CAFs release lactate to act on $CD4^+$ T cells, decreasing Th1 and increasing Tregs (Comito et al., 2019). Because cancer cells are able to utilise lactate and pyruvate that is generated by CAFs, the activity of effector T cells is inhibited without an impact on the survival of cancer cells. This is because CAFs that glycolyze glucose diminish ambient glucose levels in the TME (Comito et al., 2019). The presence of CAFs inhibits the activity of CTL and reveals a vital role for arginase. In melanoma, CAF-derived soluble factors boost l-arginase activity and CXCL12 release, while also decreasing the amount of CD69 seen on activated CTL. The absence of $CD8^+$ T lymphocytes in solid tumors may be due to the high levels of CXCL12 produced by CAFs, which might function as a chemoattractant and explain this phenomenon (Érsek et al., 2021).

In conclusion, CAFs promote immune suppression in the TME by promoting the cancer-promoting phenotype shift of naive T cells by boosting the function of immune inhibitory T lymphocytes, dampening the activity of effector T lymphocytes, interference with antigen presentation and metabolic reprogramming. There is a dearth of research into the impact of T lymphocytes on CAFs, which could be an exciting new area of study.

4.6 Interaction between CAFs and MDSCs

In addition of influencing immune responses to tolerate tumors, MDSCs support a number of neoplastic progression-related processes, including tumor angiogenesis, cancer stemness, and metastatic spread (Khaled et al., 2013).

Clinical data shows that CAFs play an immunosuppressive role associated with MDSCs. By releasing different cytokines and chemokines in the TME, CAFs can change how MDSCs are recruited and activated. Earlier studies have described the effect of CAF-secreted CXCL16 on monocyte aggregation in triple-negative (TN) breast cancer (Allaoui et al., 2016). Many studies have shown that CAFs can activate the signaling pathway molecule STAT3 by secreting IL6, leading to the conversion of monocyte precursors into MDSCs (Kim et al., 2012; Mace et al., 2013). Recent studies on esophageal squamous cell carcinoma, for instance, have underlined the significance of CAF-secreted IL-6 in the production of MDSCs and demonstrated that CAF-derived exosome-filled microRNA-21 (miR-21) also generates mononuclear MDSCs (M-MDSCs) by activating STAT3 signaling (Zhao et al., 2021). CXCL12 in the tumor microenvironment is mostly produced by CAF and plays a crucial function in attracting myeloid cells and supporting an immunosuppressive phenotype; inhibition of CXCL12 or its receptor CXCR4 lowers the amount of MDSC in the tumor (Obermajer et al., 2011; Feig et al., 2013). It was discovered that CAFs from hepatocellular carcinoma impact T cell development and function, as well as the patient's overall longevity, by enticing monocytes to the TME by releasing CXCL12 and driving them to transform into MDSCs by activating STAT3 through IL-6 (Deng et al., 2017). Moreover, CAF, which is a significant source of CCL2, can also activate the STAT3 signaling pathway to increase MDSCs recruitment and promote tumor progression. Xuguang Yang et al. used a mouse liver tumor model to show that FAP CAFs are a major source of CCL2 and that CAF increases MDSCs recruitment *via* STAT3-CCL2 signaling to promote tumor growth (Yang et al., 2016b). A recent study found that LSCC-derived CAFs promote CCR2+ monocyte recruitment by secreting CCL2, which polarizes monocytes to the MDSCs phenotype, thereby inhibiting $CD8^+$ T cell proliferation and IFN-γ production. The CAFs-MDSCs axis effect could be eliminated by inhibiting CCR2 and scavenging ROS, elucidating a potential therapeutic pathway to reverse CAF-mediated immunosuppression (Xiang et al., 2020). In addition to increasing MDSCS recruitment and activation to promote an immunosuppressive phenotype, a recent study showed that CAFs can regulate MDSCs function to enhance cancer stemness. The results of the study showed that CAF increased the expression and activity of 5-lipoxygenase (5-LO) in MDSCs by secreting IL-6 and IL-33, which greatly contributed to the efficiency of tumor sphere formation and stemness marker gene expression in intrahepatic cholangiocarcinoma (ICC) cells (Lin et al., 2022).

5 CAF targeting strategies

With further research and understanding of CAF-mediated suppression of the immune response, there has been a revival of interest in targeting CAFs for treatment in recent years. As shown previously, it is now well established that CAFs can play immunomodulatory roles: they can promote tumor progression directly or indirectly by increasing the content of suppressive immune cells and counteracting effector immune cell functions; and by participating in ECM remodeling and metabolic reprogramming to create an immune tolerance microenvironment. Because of their role in creating an immunosuppressive microenvironment during tumor growth, CAFs are now being considered potential therapeutic targets for the treatment of cancer and have also demonstrated the potential of CAF-targeting strategies in combination with immunotherapy. Table 1 briefly summarizes the CAF-targeted therapeutic strategies in clinical and preclinical studies. In clinical and preclinical studies, Table 1 gives a brief summary of the current ways that CAFs are treated. Different strategies are being investigated, including CAF activation and functional suppression, direct CAF depletion, combined with CAF-induced ECM remodeling limitation.

5.1 Suppressing CAF activation and function by targeting associated effector molecules

CAF exhibits phenotypic flexibility, and that certain of its phenotypes may be tumor suppressive, according to recent research. As a result, it is possible to reprogram CAF to a dormant or even immunologically licensed phenotype.

Ene-Obong et al. (2013) discovered that in PDAC, quiescent PSC suppressed malignant progression of PDAC cells by upregulating apoptosis and suppressing Wnt-linked protein signaling through the expression of secreted frizzled-related protein 4 (SFRP4). This finding raises the possibility of indirectly targeting malignant cells by controlling tumor-tumor crosstalk. Notably, co-engagement of all-trans retinoic acid (ATRA) with

TABLE 1 CAF-related targeting modalities in preclinical or clinical studies.

Suppressing CAF activation and function by targeting associated effector molecules							
Target	Drugs name	Mechanisms	Combination therapy	Therapeutic effects	Cancer models	Status	Ref
Vitamin Ametabolism	All-trans retinoic acid (ATRA)	Retinol levels restoration, PSC de-activation	Gemcitabine	Increases T-cell infiltration	PDAC	Phase Ib	Kocher et al. (2020)
Vitamin D receptor	Calcipotriol	PSC de-activation	Gemcitabine	Revers chemoresistance	PDAC	Preclinical	Sherman et al. (2014)
Hedgehog	Sonidegib	Inhibits hedgehog signaling through SMO inhibition	Docetaxel	Inhibits tumor growth	TBNC	Phase I/II	Ruiz-Borrego et al. (2019)
NOX1/4	GKT137831 (setanaxib)	Inhibition and of CAFs formation	None	Increases T-cell infiltration	CRC	Preclinical	Ruiz-Borrego et al. (2019)
TGF-βR2/ PD-L1	M7824	TGF-βR2 inhibition	None	Reduces tumor infiltration Tregs inhibits tumor development	PDAC	Preclinical	Ravi et al. (2018)
TGFBR1	Galunisertib	Prevents CAF activation and immunosuppression	Gemcitabine	Prolongs patients' survival with minimal added toxicity	PDAC	Phase I/II	Herbertz et al. (2015)
TGF-β	Fresolimumab	Neutralizing TGF-β	None	Extend overall survivability	Breast cancer	Phase II	Formenti et al. (2018)
CXCR4	AMD3100 (plerixafor)	Inhibit CXCL12 production; prevents signaling from CAFs to immune cells	Anti-PD-L1 therapy	Promotes T-cell accumulation and eliminates cancer cells	CRC and PDAC	Preclinical	Biasci et al. (2020)
CCL2-CCR2	PF-04136309	CCL2-CCR2 signaling axis inhibition	FOLFIRINOX	Restricts immune suppression and improves clinical prognosis	PDAC	Phase Ib	Nywening et al. (2016)
IL-6	Tocilizumab	IL-6-JAK/ STAT3 inhibition	None	Increases anticancer immunity	PDAC	Preclinical	Goumas et al. (2015)
JAK	Ruxolitinib	JAK-STA3 inhibition	Capecitabine	Inhibits tumor-promoting inflammation	Metastatic pancreatic cancer	Phase II	Hurwitz et al. (2015)
WNT2	WNT2 monoclonal antibody	WNT2 inhibition	PD-1 monoclonal antibody	Restore anti-tumor T cell reaction and increase the number of active DC	OSCC and CRC	Preclinical	Huang et al. (2022a)
Depleting CAFs directly by targeting surface markers							
FAP enzyme inhibition	DNA vaccine	Inhibits FAP enzymatic activity	Doxorubicin	Increase CD8T cell infiltration	CRC	Preclinical	Loeffler et al. (2006)
	OMTX705		Pembrolizumab	Increased infiltration of $CD8^+$ cytotoxic T cells	PDAC	Preclinical	Fabre et al. (2020)
	^{177}Lu-FAP-2286		None	Activation of immune cells	CRC	Phase I	Baum et al. (2022)
a-SMA-targeted nanoparticles	Cellax	Inhibits *a*-SMA enzymatic activity	None	Increases anti-stromal action and tumor inhibition	PDAC and breast cancer	Preclinical	Murakami et al. (2013)
Targeting CAF-derived ECM proteins							
;LOX	BAPN	LOX and LOXL inhibition	None	Anti-crosslinking and inhibites tumor growth and metastasis	Breast Cancer	Preclinical	Levental et al. (2009)
LOXL2	Simtuzumab	LOXL2 inhibition	None	Anti-crosslinking and inhibites tumor growth and metastasis	Breast Cancer	Preclinical	Grossman et al. (2016)
Hyaluronic acid	PEGPH20	Tumor stromal hyaluronan-targeted depletion	Nab-paclitaxel/ Gemcitabine	Prolongs patients' survival with less systematic side effect	PDAC	Phase II	Hingorani et al. (2018)

(Continued on following page)

TABLE 1 (*Continued*) CAF-related targeting modalities in preclinical or clinical studies.

Suppressing CAF activation and function by targeting associated effector molecules							
Target	Drugs name	Mechanisms	Combination therapy	Therapeutic effects	Cancer models	Status	Ref
FAK	VS-4718	FAK inhibition	None	Decreases fibrosis and immunosuppressive cell populations	PDAC	Phase I	Jiang et al. (2016)

PSC quiescence has been demonstrated to boost intratumoral $CD8^+$ T cells and improve survival. ATRA and gemcitabine-nab-paclitaxel combination therapy has been tried in phase I clinical studies and is currently being investigated in phase Ib trials (Kocher et al., 2020). The vitamin D receptor (VDR), which regulates PSC transcriptional activity and can convert PSC into a dormant state, is likewise a viable therapeutic approach for targeting CAFs (Sherman et al., 2014). In mice with spontaneous PDAC, calcipotriol, a ligand of the VDR family, enhanced chemotherapy response and decreased tumor development. It also decreased inflammation and fibrosis in mouse pancreatitis and the interstitium of human tumors (Sherman et al., 2014). Cazet et al. (2018) investigated the TNBC model and discovered that Hedgehog-dependent CAF activation and ECM remodeling supported the establishment of CSC ecotopes, hence resulting in docetaxel resistance. This work suggests that treatment strategies targeting the Hedgehog pathway are feasible. In phase I and phase II clinical trials with an inhibitor of the hedgehog signaling system (sonidegib) in conjunction with docetaxel, three out of twelve TNBC patients with distant metastases benefited from the combination therapy (Ruiz-Borrego et al., 2019). The NOX1/4 inhibitor GKT137831 (setanaxib) stops or turns around CAF differentiation in tumors. It also helps $CD8^+$ T-cells move into tumors and overcomes anti-PD-1 therapies (Ford et al., 2020).

As mentioned above, CAFs promote immune escape by secreting relevant effectors, so targeting important CAF-related effector molecules as well as signaling pathways seems to be a more practical strategy to slow down the development of CAF and immune cell contacts during immunosuppression-induced TME. Several preclinical and clinical investigations have demonstrated that targeting the immune functions of CAF might boost immunotherapeutic efficacy.

The activation of CAF and the interaction of CAF with immune cells are both significantly influenced by TGF-β (Angioni et al., 2021). It makes sense to target this pathway by inhibiting TGF-β, which has been done using a number of methods, such as TGF-β mRNA-directed agents, antibodies, fusion proteins, and small molecule kinase inhibitors against TGFBRs (Ciardiello et al., 2020). For example, poor anti-PD-L1 efficacy in advanced uroepithelial carcinoma has been associated with a facilitative effect of TGF-β1 signaling on $CD8^+$ T-cell tumor exclusion. Combined administration of TGF-β blocking antibodies and anti-PD-L1 antibodies on mouse tumor models improved treatment responsiveness and improved T cell infiltration in tumors (Mariathasan et al., 2018). In preclinical investigations, bifunctional fusion proteins that target PD-L1 and TGF-β have demonstrated anticancer efficacy. The anti-CTLA4-TGFβ-R2 molecule is more effective than ipilimumab (an anti-CTLA-4 antibody), at inhibiting tumor progression and decreasing tumor-infiltrating Treg cells (Ravi et al., 2018). Galunisertib, a TGFBR1 kinase inhibitor chosen for its reasonably safe toxicological profile, started clinical trials more than a decade ago (Herbertz et al., 2015). In phase I studies, intermittent dosing was demonstrated to be well-tolerated, suggesting a therapeutic window. A number of clinical trials have since tested the safety of galunisertib alone or in combination with other chemotherapeutic drugs, with acceptable findings (Ciardiello et al., 2020; Kim et al., 2021). A monoclonal antibody called fresolimumab is capable of neutralizing all three TGFβ isoforms. High-dose fresolimumab led to a longer OS than low-dose fresolimumab when used in conjunction with radiation in patients with breast cancer who had distant metastases (Formenti et al., 2018). It is clear from the above that FAP-derived CXCL12 inhibits the accumulation of CD8T cells in tumors in the tumor microenvironment (Feig et al., 2013). By inhibiting the CXCL12-CXCR4 signaling pathway, AMD3100 (plerixafor), a CXCR4 inhibitor, has been shown to diminish CAF-mediated immunosuppression and boost the response to anti-PD-1 immunotherapy (Biasci et al., 2020). In the mouse breast cancer models, genetic deletion of CXCR4 in stromal cells expressing the αSMA marker decreased fibrosis, increased T-cell infiltration, and enhanced sensitivity to checkpoint inhibition (Chen et al., 2019). The CXCL-CXCR2 axis was inhibited, which inhibited tumor angiogenesis and prolonged survival. The infiltration of MDSCs, neutrophils, and $ARG\text{-}1^+$ TAMs was significantly reduced, while apoptotic tumor cells and $iNOS^+$ M1-like TAMs increased significantly (Sano et al., 2019). CCR2 inhibitor (PF-04136309) dramatically decreased the number of tumor-infiltrating macrophages and Treg cells while boosting the number of effector T lymphocytes in the TME, consequently enhancing pancreatic cancer antitumor immunity (Nywening et al., 2016). Additionally, there are treatment approaches that target the key pathways triggered by CAF, such as the IL6-JAK1/2-STAT pathway (Mace et al., 2013). Tocilizumab, a humanized anti-IL-6R monoclonal antibody, shown substantial anticancer effects in numerous forms of cancer in preclinical tests (Goumas et al., 2015). In a double-blind phase II study of the JAK1/JAK2 inhibitor ruxolitinib in conjunction with capecitabine, patients with MPC (multiple primary malignancies) exhibited improved tolerability and a longer life expectancy (Hurwitz et al., 2015). Recently, it was found that using WNT2 monoclonal antibody with PD-1 monoclonal antibody significantly restored intra-tumor anti-tumor T cell responses and improved anti-PD-1 efficacy in mouse OSCC and CRC homologous tumor

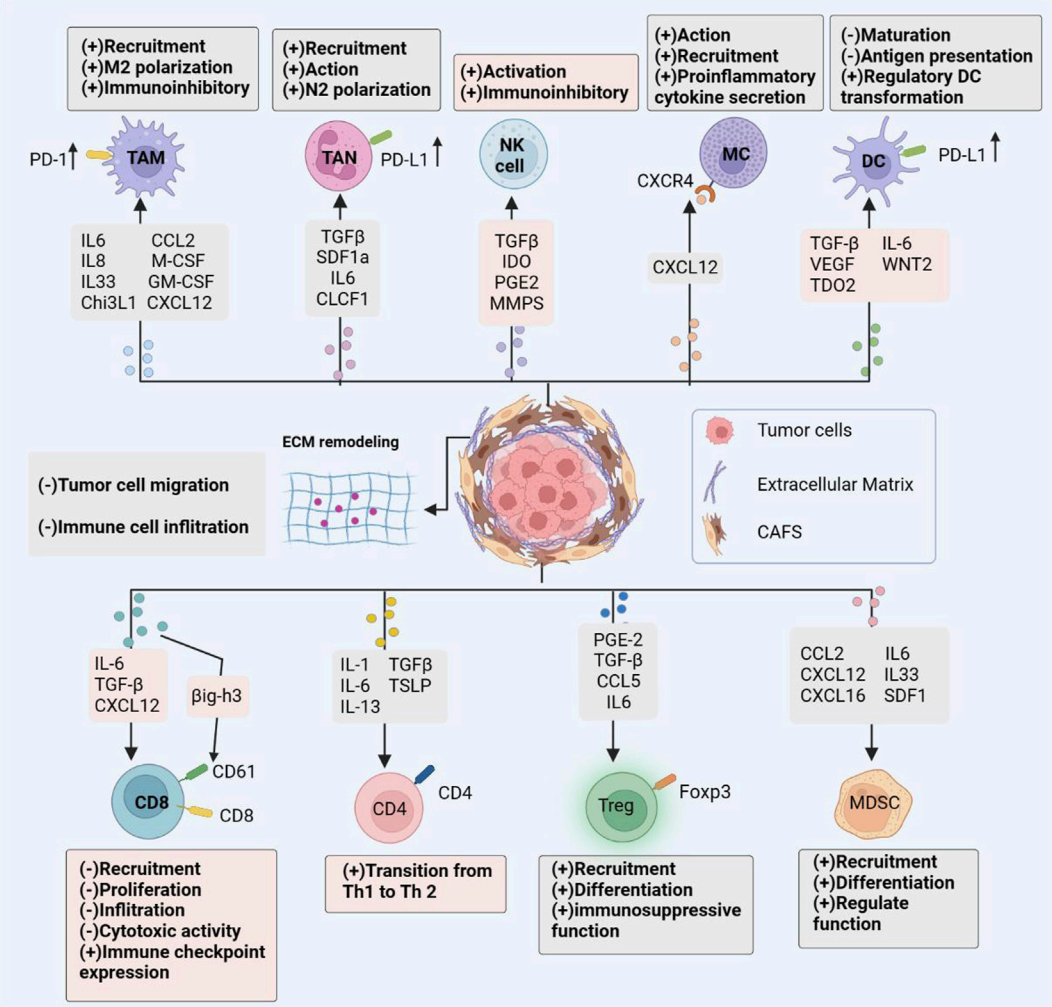

FIGURE 2
CAF immune Effects. Cancer-associated fibroblasts interact with the immune microenvironment in tumors, influencing the majority of immune cell populations and resulting to an immunosuppressive tumor microenvironment. By secreting an array of chemokines, cytokines, and other effector molecules, CAFs modulate immune cell-mediated antitumor immunity. Promoting the recruitment, activation, and immunosuppressive effects of immunosuppressive cells; limiting the cytotoxic activity and cytokine production of effector immune cells such as natural killer (NK) cells and cytotoxic T lymphocytes (CTL).

models by increasing the number of active DCs (Huang et al., 2022a).

5.2 Depleting CAFs directly by targeting surface markers

Currently, CAF is eliminated primarily by targeting CAF surface markers such as FAP, *a*-SMA, and PDFR. Although CAF marker inhibitors are the primary kind of CAF depletion therapy, the absence of CAF-specific markers and the adverse effects of this method have hampered their practical application.

In mouse models of colon and breast cancer, it has been shown that killing FAP^+ CAFs by $CD8^+$ T lymphocytes prevents primary tumor development and metastasis (Lo et al., 2015). In a pioneering investigation, an oral DNA vaccine targeting FAP targets was shown to drastically decrease primary tumor cell proliferation and neovascularization, considerably boost intra-tumor medication absorption, and minimize metastasis in colon and breast cancers by killing tumor-associated fibroblasts (Loeffler et al., 2006). Although FAP-specific CAR-T cells can all produce limited anti-tumor effects, they also produce serious side effects, such as bone marrow toxicity (Lee et al., 2022). OMTX705 is a first-in-class antibody–drug conjugate (ADC) that targets the tumor microenvironment with FAP-dependent cytotoxic activity. It has showed effectiveness in mouse models and a spectrum of solid malignancies, with the potential to increase $CD8^+$T cell infiltration and activity when paired with therapeutically relevant medications (Fabre et al., 2020). FAP-2286 is a therapeutic and diagnostic agent comprised of a FAP-binding peptide with high affinity for human FAP protein and radionuclide labeling. In initial clinical studies, it showed promise for ameliorating the unpleasant symptoms of invasive adenocarcinoma and was well tolerated (Baum et al., 2022). Docetaxel conjugate nanoparticules that target αSMA

stromal cells in a mouse model of breast cancer suppress the growth of metastases (Murakami et al., 2013). In contrast, in a pancreatic cancer model using mice transgenic for αSMA thymidine kinase, elimination of αSMA myofibroblasts resulted in more aggressive tumors and decreased animal survival (Özdemir et al., 2014). In addition, myofibroblast-depleted mice showed suppressed immune surveillance with elevated CD4 Foxp3 Tregs along with resistance to anti-CTLA-4 immunotherapy (Rhim et al., 2014). It is evident from the above that CAF does not fully express either *a*-SMA or FAP, which poses a significant obstacle to the precise strategy of CAF-based therapy.

5.3 Targeting CAF-derived ECM proteins

CAF-rich tumor Stroma is abundant in collagen, fibronectin, and proteoglycans, which encase and restrict the mobility of T cells (Evanko et al., 2012). Consequently, several CAF-targeted treatments reduce the associated fibrotic products and restrict ECM remodeling by inhibiting the fibrotic signal pathway. The modified ECM mitigates the inhibitory influence of the TME on tumor recruitment of immune effector cells and increases anti-tumor immunity (McCarthy et al., 2018). The LOX and LOXL enzymes were the target of preclinical investigations involving *ß*-aminopropionitrile (BAPN), which greatly decreased tumor fibrosis and restored cellular function, but their toxicity precluded their use in clinical trials (Belhabib et al., 2021). In preclinical trials, simtuzumab suppressed tumor cell proliferation and metastasis by targeting LOXL2, which regulated the structure of collagen; nevertheless, clinical trials were unsuccessful (Grossman et al., 2016). Enzymatic hydrolysis of HA is an additional method for decreasing tumor interstitial pressure (TIFP). To improve intratumoral medication delivery and synergistic tumor therapy. Based on preclinical research, anti-HA therapy using the vascular enzyme hyaluronidase was employed to destroy tumor cells by lowering TIFP, boosting vascular permeability, and promoting gemcitabine transport efficiency (Maloney et al., 2019). In a similar way, combining PEGPH20 with nab-paclitaxel/gemcitabine increased PFS in untreated patients with metastatic PDAC, especially those with high levels of HA (189). FAK inhibitors target integrin signal transduction. By reducing FAK signaling pathway activation, VS-4718 lowers fibrosis and immunosuppressive cells and increases pancreatic tumor sensitivity to chemotherapy and immunotherapy (Jiang et al., 2016). Although certain medicines targeting fibrosis-activated signaling pathways and fibrosis-related products had promise in preclinical models, they failed to enhance survival in patients with multiple advanced malignancies in clinical trials.

5.4 Discussion on CAF targeting strategy

However, many of the current strategies for targeting CAFs as immunotherapy have been clinically ineffective. First, as previously mentioned, the lack of specific markers for CAF means that current CAF-targeted therapies must address the insurmountable challenge of simultaneously improving antitumor efficacy and reducing systemic side effects. Second, most of the current preclinical studies have been conducted with overall CAFs, with insufficient understanding of the functions of CAFs in tumors, ignoring their high heterogeneity in tumor development. It has been demonstrated that different subtypes of CAFs have different functions in tumor immune regulation because of the high heterogeneity of CAFs. For example, pCAFs (Cancer-promoting CAFs) inhibit antitumor immunity mainly by expressing FAP-α or *a*-SMA multiplex, while rCAFs (Cancer-restraining CAFs) inhibit pancreatic cancer growth with Meflin (glycosylphosphatidylinositol-anchored protein) as a biomarker (Takahashi et al., 2021). The discovery of the tumor suppressive function of specific subgroups of CAFs provides a potential explanation for the failure of clinical trials targeting immunotherapy with CAFs. Therefore, preclinical studies are needed to determine whether the targeted subpopulations of CAFs function as fully immunosuppressed before applying immunotherapeutic strategies for CAFs. For example, the transcriptome and proteome of relevant CAF subgroups were studied in depth using technologies such as single-cell sequencing to analyze the immunosuppressive functions of specific CAFs to identify the exact targeting mediators. In addition, CAFs cells are more susceptible to phenotypic transformation than tumor cells and exist in a complex tumor microenvironment, so standard methods for cancer drug screening may be less applicable to CAFs. Therefore, suitable *in vivo* and *in vitro* models are needed to screen for effective targets of CAFs. These challenges may be the reason why CAF-targeted therapies are rarely put into clinical use. Future research on these issues still needs to be intensively studied to find more precise and effective molecular targets for CAFs.

6 Conclusion and outlook

In recent years, evidence showing the role and significance of CAFs in tumorigenesis, progression, immunosuppression, and drug resistance in a variety of malignancies has increased. As key components of the TME, CAFs are closely associated with the TME as well as the whole host in a context-dependent manner with phenotypic and functional heterogeneity. This paper illustrates the relationship between CAFs and immune cells, where CAFs not only directly influence the activity of immune cells, but also alter the ECM within TME and induce metabolic reprogramming. The interaction between cancer-associated fibroblasts and immune cells has a significant impact on the regulation of tumor growth.

As previously described, this review summarizes the mechanism of interaction between CAFs and immune cells in TME. CAFs induce the formation of immunosuppressive microenvironment by secreting a series of cytokines that have direct effects on immune cells, specifically by inducing the recruitment and activation of TAMs, TANs, CD4T cells, tregs, MCs, MDSCs cells; inducing TAMs, TANs cells polarization to an immunosuppressive phenotype; and inhibition of CD8T cell and NK cell activity and function. In addition, CAFs can also secrete ECM proteins to induce ECM remodeling to inhibit CD8T cell infiltration; upregulate the expression of immune checkpoint molecules to directly kill CD8 T cells; inhibit TCR to hinder CD8 T cell proliferation and activation; and metabolic reprogramming to inhibit CD8 T cell proliferation and activity,

thus indirectly leading to an immunosuppressive microenvironment. Although research on CAFs is expanding, there are still significant gaps in the therapeutic efficacy of targeted CAFs in clinical trials. The main CAF targeting strategies currently available are through the following pathways: 1) inhibition of CAF activation and function by targeting relevant effector molecules; 2) direct depletion of CAF by targeting surface markers; and 3) targeting CAF-derived ECM proteins. The mechanism of interaction between CAFs and immune cells is summarized in Figure 2. Numerous pre-clinical studies failed to detect any appreciable anti-tumor effects or significantly increase patient survival. The clinical failure of CAF-targeted therapy may be due to the following reasons; lack of specific markers and systemic side effects of targeted drugs; ignoring the highly heterogeneous nature of CAFs, with some subpopulations belonging to tumor suppressor phenotypes, targeting overall CAFs cannot achieve good clinical results; inapplicable drug screening methods; difficulty of *in vitro* models to restore the complex tumor microenvironment conditions.

Future research focusing on the heterogeneity of CAFs is needed to identify the functions and specific mechanisms of specific subpopulations of CAFs through single cell sequencing to elucidate their clinical importance and impact on cancer development in order to find effective targeted immunotherapies and mediators. Second, the complicated tumor microenvironment (hypoxia, acidic microenvironment, anomalies in tumor vascularity, etc.,) necessitates the employment of appropriate *in vivo* and *in vitro* study models that are more useful for research. Current research foci on CAFs in carcinogenesis and treatment resistance are primarily focused on subgroup analyses and functional studies because the majority of solid tumors have many CAFs subgroups.

Author contributions

CZ, CL, RH, and QD conceived the research for this report and designed the structure of the paper. CZ and YF wrote the manuscript. CZ, SH, and HW was responsible for the drawings and tables. CL, RH, and QD proofread the paper, supervised the results of the paper and approved the submission. All authors agreed to the publication of the final version of this manuscript.

Funding

This work was supported by the Natural Science Foundation of China (No. 82172558, 82273971, 82204394), the Distinguished Young Scholars of Nanjing (JQX20008).

Conflict of interest

The authors declare that the research was conducted in the absence of any commercial or financial relationships that could be construed as a potential conflict of interest.

Publisher's note

References

Allaoui, R., Bergenfelz, C., Mohlin, S., Hagerling, C., Salari, K., Werb, Z., et al. (2016). Cancer-associated fibroblast-secreted CXCL16 attracts monocytes to promote stroma activation in triple-negative breast cancers. *Nat. Commun.* 7, 13050. doi:10.1038/ncomms13050

Andersson, P., Yang, Y., Hosaka, K., Zhang, Y., Fischer, C., Braun, H., et al. (2018). Molecular mechanisms of IL-33-mediated stromal interactions in cancer metastasis. *JCI insight* 3 (20), e122375. doi:10.1172/jci.insight.122375

Angioni, R., Sánchez-Rodríguez, R., Viola, A., and Molon, B. (2021). TGF-B in cancer: Metabolic driver of the tolerogenic crosstalk in the tumor microenvironment. *Cancers* 13 (3), 401. doi:10.3390/cancers13030401

Anz, D., Rapp, M., Eiber, S., Koelzer, V. H., Thaler, R., Haubner, S., et al. (2015). Suppression of intratumoral CCL22 by type i interferon inhibits migration of regulatory T cells and blocks cancer progression. *Cancer Res.* 75 (21), 4483–4493. doi:10.1158/0008-5472.CAN-14-3499

Arina, A., Idel, C., Hyjek, E. M., Alegre, M. L., Wang, Y., Bindokas, V. P., et al. (2016). Tumor-associated fibroblasts predominantly come from local and not circulating precursors. *Proc. Natl. Acad. Sci. U. S. A.* 113 (27), 7551–7556. doi:10.1073/pnas.1600363113

Arvanitakis, K., Koletsa, T., Mitroulis, I., and Germanidis, G. (2022). Tumor-associated macrophages in hepatocellular carcinoma pathogenesis, prognosis and therapy. *Cancers* 14 (1), 226. doi:10.3390/cancers14010226

Arvanitakis, K., Mitroulis, I., and Germanidis, G. (2021). Tumor-associated neutrophils in hepatocellular carcinoma pathogenesis, prognosis, and therapy. *Cancers* 13 (12), 2899. doi:10.3390/cancers13122899

Bachem, M. G., Schünemann, M., Ramadani, M., Siech, M., Beger, H., Buck, A., et al. (2005). Pancreatic carcinoma cells induce fibrosis by stimulating proliferation and matrix synthesis of stellate cells. *Gastroenterology* 128 (4), 907–921. doi:10.1053/j.gastro.2004.12.036

Balsamo, M., Scordamaglia, F., Pietra, G., Manzini, C., Cantoni, C., Boitano, M., et al. (2009). Melanoma-associated fibroblasts modulate NK cell phenotype and antitumor cytotoxicity. *Proc. Natl. Acad. Sci. U. S. A.* 106 (49), 20847–20852. doi:10.1073/pnas.0906481106

Barcellos-de-Souza, P., Comito, G., Pons-Segura, C., Taddei, M. L., Gori, V., Becherucci, V., et al. (2016). Mesenchymal stem cells are recruited and activated into carcinoma-associated fibroblasts by prostate cancer microenvironment-derived TGF-β1. *Stem cells Dayt. Ohio)* 34 (10), 2536–2547. doi:10.1002/stem.2412

Barrett, R., and Puré, E. (2020). Cancer-associated fibroblasts: Key determinants of tumor immunity and immunotherapy. *Curr. Opin. Immunol.* 64, 80–87. doi:10.1016/j.coi.2020.03.004

Baum, R. P., Schuchardt, C., Singh, A., Chantadisai, M., Robiller, F. C., Zhang, J., et al. (2022). Feasibility, biodistribution, and preliminary dosimetry in peptide-targeted radionuclide therapy of diverse adenocarcinomas using (177)Lu-FAP-2286: First-in-Humans results. *J. Nucl. Med. official Publ. Soc. Nucl. Med.* 63 (3), 415–423. doi:10.2967/jnumed.120.259192

Bejarano, L., Jordão, M. J. C., and Joyce, J. A. (2021). Therapeutic targeting of the tumor microenvironment. *Cancer Discov.* 11 (4), 933–959. doi:10.1158/2159-8290.CD-20-1808

Belhabib, I., Zaghdoudi, S., Lac, C., Bousquet, C., and Jean, C. (2021). Extracellular matrices and cancer-associated fibroblasts: Targets for cancer diagnosis and therapy? *Cancers* 13 (14), 3466. doi:10.3390/cancers13143466

Biasci, D., Smoragiewicz, M., Connell, C. M., Wang, Z., Gao, Y., Thaventhiran, J. E. D., et al. (2020). CXCR4 inhibition in human pancreatic and colorectal cancers induces an integrated immune response. *Proc. Natl. Acad. Sci. U. S. A.* 117 (46), 28960–28970. doi:10.1073/pnas.2013644117

Bougherara, H., Mansuet-Lupo, A., Alifano, M., Ngô, C., Damotte, D., Le Frère-Belda, M. A., et al. (2015). Real-time imaging of resident T cells in human lung and ovarian

carcinomas reveals how different tumor microenvironments control T lymphocyte migration. *Front. Immunol.* 6, 500. doi:10.3389/fimmu.2015.00500

Bourhis, M., Palle, J., Galy-Fauroux, I., and Terme, M. (2021). Direct and indirect modulation of T cells by VEGF-A counteracted by anti-angiogenic treatment. *Front. Immunol.* 12, 616837. doi:10.3389/fimmu.2021.616837

Brinkmann, V., Reichard, U., Goosmann, C., Fauler, B., Uhlemann, Y., Weiss, D. S., et al. (2004). Neutrophil extracellular traps kill bacteria. *Sci. (New York, NY)* 303 (5663), 1532–1535. doi:10.1126/science.1092385

Calvo, F., Ege, N., Grande-Garcia, A., Hooper, S., Jenkins, R. P., Chaudhry, S. I., et al. (2013). Mechanotransduction and YAP-dependent matrix remodelling is required for the generation and maintenance of cancer-associated fibroblasts. *Nat. Cell Biol.* 15 (6), 637–646. doi:10.1038/ncb2756

Cazet, A. S., Hui, M. N., Elsworth, B. L., Wu, S. Z., Roden, D., Chan, C. L., et al. (2018). Targeting stromal remodeling and cancer stem cell plasticity overcomes chemoresistance in triple negative breast cancer. *Nat. Commun.* 9 (1), 2897. doi:10.1038/s41467-018-05220-6

Chandra Jena, B., Sarkar, S., Rout, L., and Mandal, M. (2021). The transformation of cancer-associated fibroblasts: Current perspectives on the role of TGF-β in CAF mediated tumor progression and therapeutic resistance. *Cancer Lett.* 520, 222–232. doi:10.1016/j.canlet.2021.08.002

Chang, L. Y., Lin, Y. C., Mahalingam, J., Huang, C. T., Chen, T. W., Kang, C. W., et al. (2012). Tumor-derived chemokine CCL5 enhances TGF-β-mediated killing of CD8(+) T cells in colon cancer by T-regulatory cells. *Cancer Res.* 72 (5), 1092–1102. doi:10.1158/0008-5472.CAN-11-2493

Chen, I. X., Chauhan, V. P., Posada, J., Ng, M. R., Wu, M. W., Adstamongkonkul, P., et al. (2019). Blocking CXCR4 alleviates desmoplasia, increases T-lymphocyte infiltration, and improves immunotherapy in metastatic breast cancer. *Proc. Natl. Acad. Sci. U. S. A.* 116 (10), 4558–4566. doi:10.1073/pnas.1815515116

Chen, S., Morine, Y., Tokuda, K., Yamada, S., Saito, Y., Nishi, M., et al. (2021). Cancer-associated fibroblast-induced M2-polarized macrophages promote hepatocellular carcinoma progression via the plasminogen activator inhibitor-1 pathway. *Int. J. Oncol.* 59 (2), 59. doi:10.3892/ijo.2021.5239

Chen, X., and Song, E. (2019). Turning foes to friends: Targeting cancer-associated fibroblasts. *Nat. Rev. Drug Discov.* 18 (2), 99–115. doi:10.1038/s41573-018-0004-1

Cheng, J. T., Deng, Y. N., Yi, H. M., Wang, G. Y., Fu, B. S., Chen, W. J., et al. (2016). Hepatic carcinoma-associated fibroblasts induce Ido-producing regulatory dendritic cells through IL-6-mediated STAT3 activation. *Oncogenesis* 5 (2), e198. doi:10.1038/oncsis.2016.7

Cheng, Y., Li, H., Deng, Y., Tai, Y., Zeng, K., Zhang, Y., et al. (2018). Cancer-associated fibroblasts induce PDL1+ neutrophils through the IL6-STAT3 pathway that foster immune suppression in hepatocellular carcinoma. *Cell death Dis.* 9 (4), 422. doi:10.1038/s41419-018-0458-4

Chomarat, P., Banchereau, J., Davoust, J., and Palucka, A. K. (2000). IL-6 switches the differentiation of monocytes from dendritic cells to macrophages. *Nat. Immunol.* 1 (6), 510–514. doi:10.1038/82763

Chraa, D., Naim, A., Olive, D., and Badou, A. (2019). T lymphocyte subsets in cancer immunity: Friends or foes. *J. Leukoc. Biol.* 105 (2), 243–255. doi:10.1002/JLB.MR0318-097R

Ciardiello, D., Elez, E., Tabernero, J., and Seoane, J. (2020). Clinical development of therapies targeting TGFβ: Current knowledge and future perspectives. *Ann. Oncol. official J. Eur. Soc. Med. Oncol.* 31 (10), 1336–1349. doi:10.1016/j.annonc.2020.07.009

Cohen, N., Shani, O., Raz, Y., Sharon, Y., Hoffman, D., Abramovitz, L., et al. (2017). Fibroblasts drive an immunosuppressive and growth-promoting microenvironment in breast cancer via secretion of Chitinase 3-like 1. *Oncogene* 36 (31), 4457–4468. doi:10.1038/onc.2017.65

Comito, G., Giannoni, E., Segura, C. P., Barcellos-de-Souza, P., Raspollini, M. R., Baroni, G., et al. (2014). Cancer-associated fibroblasts and M2-polarized macrophages synergize during prostate carcinoma progression. *Oncogene* 33 (19), 2423–2431. doi:10.1038/onc.2013.191

Comito, G., Iscaro, A., Bacci, M., Morandi, A., Ippolito, L., Parri, M., et al. (2019). Lactate modulates CD4(+) T-cell polarization and induces an immunosuppressive environment, which sustains prostate carcinoma progression via TLR8/miR21 axis. *Oncogene* 38 (19), 3681–3695. doi:10.1038/s41388-019-0688-7

Costa, A., Scholer-Dahirel, A., and Mechta-Grigoriou, F. (2014). The role of reactive oxygen species and metabolism on cancer cells and their microenvironment. *Seminars cancer Biol.* 25, 23–32. doi:10.1016/j.semcancer.2013.12.007

de Araújo Farias, V., Carrillo-Gálvez, A. B., Martín, F., and Anderson, P. (2018). TGF-β and mesenchymal stromal cells in regenerative medicine, autoimmunity and cancer. *Cytokine & growth factor Rev.* 43, 25–37. doi:10.1016/j.cytogfr.2018.06.002

de Lourdes Mora-García, M., García-Rocha, R., Morales-Ramírez, O., Montesinos, J. J., Weiss-Steider, B., Hernández-Montes, J., et al. (2016). Mesenchymal stromal cells derived from cervical cancer produce high amounts of adenosine to suppress cytotoxic T lymphocyte functions. *J. Transl. Med.* 14 (1), 302. doi:10.1186/s12967-016-1057-8

De Monte, L., Reni, M., Tassi, E., Clavenna, D., Papa, I., Recalde, H., et al. (2011). Intratumor T helper type 2 cell infiltrate correlates with cancer-associated fibroblast thymic stromal lymphopoietin production and reduced survival in pancreatic cancer. *J. Exp. Med.* 208 (3), 469–478. doi:10.1084/jem.20101876

Demkow, U. (2021). Neutrophil extracellular traps (NETs) in cancer invasion, evasion and metastasis. *Cancers* 13 (17), 4495. doi:10.3390/cancers13174495

Deng, Y., Cheng, J., Fu, B., Liu, W., Chen, G., Zhang, Q., et al. (2017). Hepatic carcinoma-associated fibroblasts enhance immune suppression by facilitating the generation of myeloid-derived suppressor cells. *Oncogene* 36 (8), 1090–1101. doi:10.1038/onc.2016.273

Deo, S. V. S., Sharma, J., and Kumar, S. (2022). GLOBOCAN 2020 report on global cancer burden: Challenges and opportunities for surgical oncologists. *Ann. Surg. Oncol.* 29 (11), 6497–6500. doi:10.1245/s10434-022-12151-6

Duan, Q., Zhang, H., Zheng, J., and Zhang, L. (2020). Turning cold into hot: Firing up the tumor microenvironment. *Trends cancer* 6 (7), 605–618. doi:10.1016/j.trecan.2020.02.022

Ellem, S. J., Taylor, R. A., Furic, L., Larsson, O., Frydenberg, M., Pook, D., et al. (2014). A pro-tumourigenic loop at the human prostate tumour interface orchestrated by oestrogen, CXCL12 and mast cell recruitment. *J. pathology* 234 (1), 86–98. doi:10.1002/path.4386

Ene-Obong, A., Clear, A. J., Watt, J., Wang, J., Fatah, R., Riches, J. C., et al. (2013). Activated pancreatic stellate cells sequester CD8+ T cells to reduce their infiltration of the juxtatumoral compartment of pancreatic ductal adenocarcinoma. *Gastroenterology* 145 (5), 1121–1132. doi:10.1053/j.gastro.2013.07.025

Érsek, B., Silló, P., Cakir, U., Molnár, V., Bencsik, A., Mayer, B., et al. (2021). Melanoma-associated fibroblasts impair CD8+ T cell function and modify expression of immune checkpoint regulators via increased arginase activity. *Cell. Mol. life Sci. CMLS* 78 (2), 661–673. doi:10.1007/s00018-020-03517-8

Evanko, S. P., Potter-Perigo, S., Bollyky, P. L., Nepom, G. T., and Wight, T. N. (2012). Hyaluronan and versican in the control of human T-lymphocyte adhesion and migration. *Matrix Biol. J. Int. Soc. Matrix Biol.* 31 (2), 90–100. doi:10.1016/j.matbio.2011.10.004

Fabre, M., Ferrer, C., Domínguez-Hormaetxe, S., Bockorny, B., Murias, L., Seifert, O., et al. (2020). OMTX705, a novel FAP-targeting ADC demonstrates activity in chemotherapy and pembrolizumab-resistant solid tumor models. *Clin. cancer Res. official J. Am. Assoc. Cancer Res.* 26 (13), 3420–3430. doi:10.1158/1078-0432.CCR-19-2238

Feig, C., Jones, J. O., Kraman, M., Wells, R. J., Deonarine, A., Chan, D. S., et al. (2013). Targeting CXCL12 from FAP-expressing carcinoma-associated fibroblasts synergizes with anti-PD-L1 immunotherapy in pancreatic cancer. *Proc. Natl. Acad. Sci. U. S. A.* 110 (50), 20212–20217. doi:10.1073/pnas.1320318110

Feng, B., Wu, J., Shen, B., Jiang, F., and Feng, J. (2022). Cancer-associated fibroblasts and resistance to anticancer therapies: Status, mechanisms, and countermeasures. *Cancer Cell Int.* 22 (1), 166. doi:10.1186/s12935-022-02599-7

Foglia, B., Cannito, S., Bocca, C., Parola, M., and Novo, E. (2019). ERK pathway in activated, myofibroblast-like, hepatic stellate cells: A critical signaling crossroad sustaining liver fibrosis. *Int. J. Mol. Sci.* 20 (11), 2700. doi:10.3390/ijms20112700

Ford, K., Hanley, C. J., Mellone, M., Szyndralewiez, C., Heitz, F., Wiesel, P., et al. (2020). NOX4 inhibition potentiates immunotherapy by overcoming cancer-associated fibroblast-mediated CD8 T-cell exclusion from tumors. *Cancer Res.* 80 (9), 1846–1860. doi:10.1158/0008-5472.CAN-19-3158

Formenti, S. C., Lee, P., Adams, S., Goldberg, J. D., Li, X., Xie, M. W., et al. (2018). Focal irradiation and systemic TGFβ blockade in metastatic breast cancer. *Clin. cancer Res. official J. Am. Assoc. Cancer Res.* 24 (11), 2493–2504. doi:10.1158/1078-0432.CCR-17-3322

Freeman, P., and Mielgo, A. (2020). Cancer-associated fibroblast mediated inhibition of CD8+ cytotoxic T cell accumulation in tumours: Mechanisms and therapeutic opportunities. *Cancers* 12 (9), 2687. doi:10.3390/cancers12092687

Gabrilovich, D. I., Chen, H. L., Girgis, K. R., Cunningham, H. T., Meny, G. M., Nadaf, S., et al. (1996). Production of vascular endothelial growth factor by human tumors inhibits the functional maturation of dendritic cells. *Nat. Med.* 2 (10), 1096–1103. doi:10.1038/nm1096-1096

Ganguly, D., Chandra, R., Karalis, J., Teke, M., Aguilera, T., Maddipati, R., et al. (2020). Cancer-associated fibroblasts: Versatile players in the tumor microenvironment. *Cancers* 12 (9), 2652. doi:10.3390/cancers12092652

Giusti, I., Di Francesco, M., D'Ascenzo, S., Palmerini, M. G., Macchiarelli, G., Carta, G., et al. (2018). Ovarian cancer-derived extracellular vesicles affect normal human fibroblast behavior. *Cancer Biol. Ther.* 19 (8), 722–734. doi:10.1080/15384047.2018.1451286

Goehrig, D., Nigri, J., Samain, R., Wu, Z., Cappello, P., Gabiane, G., et al. (2019). Stromal protein βig-h3 reprogrammes tumour microenvironment in pancreatic cancer. *Gut* 68 (4), 693–707. doi:10.1136/gutjnl-2018-317570

Gok Yavuz, B., Gunaydin, G., Gedik, M. E., Kosemehmetoglu, K., Karakoc, D., Ozgur, F., et al. (2019). Cancer associated fibroblasts sculpt tumour microenvironment by recruiting monocytes and inducing immunosuppressive PD-1(+) TAMs. *Sci. Rep.* 9 (1), 3172. doi:10.1038/s41598-019-39553-z

Gorchs, L., Fernández Moro, C., Bankhead, P., Kern, K. P., Sadeak, I., Meng, Q., et al. (2019). Human pancreatic carcinoma-associated fibroblasts promote expression of Co-inhibitory markers on CD4(+) and CD8(+) T-cells. *Front. Immunol.* 10, 847. doi:10.3389/fimmu.2019.00847

Goumas, F. A., Holmer, R., Egberts, J. H., Gontarewicz, A., Heneweer, C., Geisen, U., et al. (2015). Inhibition of IL-6 signaling significantly reduces primary tumor growth and recurrencies in orthotopic xenograft models of pancreatic cancer. *Int. J. cancer* 137 (5), 1035–1046. doi:10.1002/ijc.29445

Grivennikov, S. I., Greten, F. R., and Karin, M. (2010). Immunity, inflammation, and cancer. *Cell* 140 (6), 883–899. doi:10.1016/j.cell.2010.01.025

Grossman, M., Ben-Chetrit, N., Zhuravlev, A., Afik, R., Bassat, E., Solomonov, I., et al. (2016). Tumor cell invasion can Be blocked by modulators of collagen fibril alignment that control assembly of the extracellular matrix. *Cancer Res.* 76 (14), 4249–4258. doi:10.1158/0008-5472.CAN-15-2813

Gunaydin, G. (2021). CAFs interacting with TAMs in tumor microenvironment to enhance tumorigenesis and immune evasion. *Front. Oncol.* 11, 668349. doi:10.3389/fonc.2021.668349

Han, B., Mao, F. Y., Zhao, Y. L., Lv, Y. P., Teng, Y. S., Duan, M., et al. (2018). Altered NKp30, NKp46, NKG2D, and DNAM-1 expression on circulating NK cells is associated with tumor progression in human gastric cancer. *J. Immunol. Res.* 2018, 6248590. doi:10.1155/2018/6248590

Hashimoto, O., Yoshida, M., Koma, Y., Yanai, T., Hasegawa, D., Kosaka, Y., et al. (2016). Collaboration of cancer-associated fibroblasts and tumour-associated macrophages for neuroblastoma development. *J. pathology* 240 (2), 211–223. doi:10.1002/path.4769

Hedrick, C. C., and Malanchi, I. (2022). Neutrophils in cancer: Heterogeneous and multifaceted. *Nat. Rev. Immunol.* 22 (3), 173–187. doi:10.1038/s41577-021-00571-6

Hellevik, T., and Martinez-Zubiaurre, I. (2014). Radiotherapy and the tumor stroma: The importance of dose and fractionation. *Front. Oncol.* 4, 1. doi:10.3389/fonc.2014.00001

Herbertz, S., Sawyer, J. S., Stauber, A. J., Gueorguieva, I., Driscoll, K. E., Estrem, S. T., et al. (2015). Clinical development of galunisertib (LY2157299 monohydrate), a small molecule inhibitor of transforming growth factor-beta signaling pathway. *Drug Des. Dev. Ther.* 9, 4479–4499. doi:10.2147/DDDT.S86621

Hingorani, S. R., Zheng, L., Bullock, A. J., Seery, T. E., Harris, W. P., Sigal, D. S., et al. (2018). Halo 202: Randomized phase II study of PEGPH20 plus nab-paclitaxel/gemcitabine versus nab-paclitaxel/gemcitabine in patients with untreated, metastatic pancreatic ductal adenocarcinoma. *J. Clin. Oncol. official J. Am. Soc. Clin. Oncol.* 36 (4), 359–366. doi:10.1200/JCO.2017.74.9564

Hinshaw, D. C., and Shevde, L. A. (2019). The tumor microenvironment innately modulates cancer progression. *Cancer Res.* 79 (18), 4557–4566. doi:10.1158/0008-5472.CAN-18-3962

Hu, D., Li, Z., Zheng, B., Lin, X., Pan, Y., Gong, P., et al. (2022). Cancer-associated fibroblasts in breast cancer: Challenges and opportunities. *Cancer Commun. Lond. Engl.* 42 (5), 401–434. doi:10.1002/cac2.12291

Huang, H., Wang, Z., Zhang, Y., Pradhan, R. N., Ganguly, D., Chandra, R., et al. (2022). Mesothelial cell-derived antigen-presenting cancer-associated fibroblasts induce expansion of regulatory T cells in pancreatic cancer. *Cancer Cell* 40 (6), 656–673.e7. doi:10.1016/j.ccell.2022.04.011

Huang, Q., Huang, M., Meng, F., and Sun, R. (2019). Activated pancreatic stellate cells inhibit NK cell function in the human pancreatic cancer microenvironment. *Cell. Mol. Immunol.* 16 (1), 87–89. doi:10.1038/s41423-018-0014-2

Huang, T. X., Tan, X. Y., Huang, H. S., Li, Y. T., Liu, B. L., Liu, K. S., et al. (2022). Targeting cancer-associated fibroblast-secreted WNT2 restores dendritic cell-mediated antitumour immunity. *Gut* 71 (2), 333–344. doi:10.1136/gutjnl-2020-322924

Huang, Y., Chen, X., Dikov, M. M., Novitskiy, S. V., Mosse, C. A., Yang, L., et al. (2007). Distinct roles of VEGFR-1 and VEGFR-2 in the aberrant hematopoiesis associated with elevated levels of VEGF. *Blood* 110 (2), 624–631. doi:10.1182/blood-2007-01-065714

Hurwitz, H. I., Uppal, N., Wagner, S. A., Bendell, J. C., Beck, J. T., Wade, S. M., 3rd, et al. (2015). Randomized, double-blind, phase II study of ruxolitinib or placebo in combination with capecitabine in patients with metastatic pancreatic cancer for whom therapy with gemcitabine has failed. *J. Clin. Oncol. official J. Am. Soc. Clin. Oncol.* 33 (34), 4039–4047. doi:10.1200/JCO.2015.61.4578

Jacobs, J., Deschoolmeester, V., Zwaenepoel, K., Flieswasser, T., Deben, C., Van den Bossche, J., et al. (2018). Unveiling a CD70-positive subset of cancer-associated fibroblasts marked by pro-migratory activity and thriving regulatory T cell accumulation. *Oncoimmunology* 7 (7), e1440167. doi:10.1080/2162402X.2018.1440167

Jaillon, S., Peri, G., Delneste, Y., Frémaux, I., Doni, A., Moalli, F., et al. (2007). The humoral pattern recognition receptor PTX3 is stored in neutrophil granules and localizes in extracellular traps. *J. Exp. Med.* 204 (4), 793–804. doi:10.1084/jem.20061301

Jiang, H., Hegde, S., Knolhoff, B. L., Zhu, Y., Herndon, J. M., Meyer, M. A., et al. (2016). Targeting focal adhesion kinase renders pancreatic cancers responsive to checkpoint immunotherapy. *Nat. Med.* 22 (8), 851–860. doi:10.1038/nm.4123

Jotzu, C., Alt, E., Welte, G., Li, J., Hennessy, B. T., Devarajan, E., et al. (2011). Adipose tissue derived stem cells differentiate into carcinoma-associated fibroblast-like cells under the influence of tumor derived factors. *Cell. Oncol. Dordr.* 34 (1), 55–67. doi:10.1007/s13402-011-0012-1

Jung, Y., Kim, J. K., Shiozawa, Y., Wang, J., Mishra, A., Joseph, J., et al. (2013). Recruitment of mesenchymal stem cells into prostate tumours promotes metastasis. *Nat. Commun.* 4, 1795. doi:10.1038/ncomms2766

Kadomoto, S., Izumi, K., and Mizokami, A. (2021). Roles of CCL2-CCR2 Axis in the tumor microenvironment. *Int. J. Mol. Sci.* 22 (16), 8530. doi:10.3390/ijms22168530

Kato, T., Noma, K., Ohara, T., Kashima, H., Katsura, Y., Sato, H., et al. (2018). Cancer-associated fibroblasts affect intratumoral CD8(+) and FoxP3(+) T cells via IL6 in the tumor microenvironment. *Clin. cancer Res. official J. Am. Assoc. Cancer Res.* 24 (19), 4820–4833. doi:10.1158/1078-0432.CCR-18-0205

Khaled, Y. S., Ammori, B. J., and Elkord, E. (2013). Myeloid-derived suppressor cells in cancer: Recent progress and prospects. *Immunol. Cell Biol.* 91 (8), 493–502. doi:10.1038/icb.2013.29

Khalili, J. S., Liu, S., Rodríguez-Cruz, T. G., Whittington, M., Wardell, S., Liu, C., et al. (2012). Oncogenic BRAF(V600E) promotes stromal cell-mediated immunosuppression via induction of interleukin-1 in melanoma. *Clin. cancer Res. official J. Am. Assoc. Cancer Res.* 18 (19), 5329–5340. doi:10.1158/1078-0432.CCR-12-1632

Kim, B. G., Malek, E., Choi, S. H., Ignatz-Hoover, J. J., and Driscoll, J. J. (2021). Novel therapies emerging in oncology to target the TGF-β pathway. *J. Hematol. Oncol.* 14 (1), 55. doi:10.1186/s13045-021-01053-x

Kim, D. E., Procopio, M. G., Ghosh, S., Jo, S. H., Goruppi, S., Magliozzi, F., et al. (2017). Convergent roles of ATF3 and CSL in chromatin control of cancer-associated fibroblast activation. *J. Exp. Med.* 214 (8), 2349–2368. doi:10.1084/jem.20170724

Kim, J. H., Oh, S. H., Kim, E. J., Park, S. J., Hong, S. P., Cheon, J. H., et al. (2012). The role of myofibroblasts in upregulation of S100A8 and S100A9 and the differentiation of myeloid cells in the colorectal cancer microenvironment. *Biochem. biophysical Res. Commun.* 423 (1), 60–66. doi:10.1016/j.bbrc.2012.05.081

Kinoshita, T., Ishii, G., Hiraoka, N., Hirayama, S., Yamauchi, C., Aokage, K., et al. (2013). Forkhead box P3 regulatory T cells coexisting with cancer associated fibroblasts are correlated with a poor outcome in lung adenocarcinoma. *Cancer Sci.* 104 (4), 409–415. doi:10.1111/cas.12099

Kocher, H. M., Basu, B., Froeling, F. E. M., Sarker, D., Slater, S., Carlin, D., et al. (2020). Phase I clinical trial repurposing all-trans retinoic acid as a stromal targeting agent for pancreatic cancer. *Nat. Commun.* 11 (1), 4841. doi:10.1038/s41467-020-18636-w

Kockx, M. M., McCleland, M., and Koeppen, H. (2021). Microenvironmental regulation of tumour immunity and response to immunotherapy. *J. pathology* 254 (4), 374–383. doi:10.1002/path.5681

Kuehnemuth, B., Piseddu, I., Wiedemann, G. M., Lauseker, M., Kuhn, C., Hofmann, S., et al. (2018). CCL1 is a major regulatory T cell attracting factor in human breast cancer. *BMC cancer* 18 (1), 1278. doi:10.1186/s12885-018-5117-8

Kuzet, S. E., and Gaggioli, C. (2016). Fibroblast activation in cancer: When seed fertilizes soil. *Cell tissue Res.* 365 (3), 607–619. doi:10.1007/s00441-016-2467-x

Lakins, M. A., Ghorani, E., Munir, H., Martins, C. P., and Shields, J. D. (2018). Cancer-associated fibroblasts induce antigen-specific deletion of CD8 (+) T Cells to protect tumour cells. *Nat. Commun.* 9 (1), 948. doi:10.1038/s41467-018-03347-0

Lee, I. K., Noguera-Ortega, E., Xiao, Z., Todd, L., Scholler, J., Song, D., et al. (2022). Monitoring therapeutic response to anti-FAP CAR T cells using [18F]AlF-FAPI-74. *Clin. cancer Res. official J. Am. Assoc. Cancer Res.* 28 (24), 5330–5342. doi:10.1158/1078-0432.CCR-22-1379

Lee, Y. S., and Radford, K. J. (2019). The role of dendritic cells in cancer. *Int. Rev. Cell Mol. Biol.* 348, 123–178. doi:10.1016/bs.ircmb.2019.07.006

Lehrer, R. I., Ganz, T., Selsted, M. E., Babior, B. M., and Curnutte, J. T. (1988). Neutrophils and host defense. *Ann. Intern. Med.* 109 (2), 127–142. doi:10.7326/0003-4819-109-2-127

Levental, K. R., Yu, H., Kass, L., Lakins, J. N., Egeblad, M., Erler, J. T., et al. (2009)., 139. Fig1, 891–906. doi:10.1016/j.cell.2009.10.027Matrix crosslinking forces tumor progression by enhancing integrin signaling*Cell*5

Li, L., Xu, L., Yan, J., Zhen, Z. J., Ji, Y., Liu, C. Q., et al. (2015). CXCR2-CXCL1 axis is correlated with neutrophil infiltration and predicts a poor prognosis in hepatocellular carcinoma. *J. Exp. Clin. cancer Res. CR* 34, 129. doi:10.1186/s13046-015-0247-1

Li, T., Yang, Y., Hua, X., Wang, G., Liu, W., Jia, C., et al. (2012). Hepatocellular carcinoma-associated fibroblasts trigger NK cell dysfunction via PGE2 and Ido. *Cancer Lett.* 318 (2), 154–161. doi:10.1016/j.canlet.2011.12.020

Li, T., Yi, S., Liu, W., Jia, C., Wang, G., Hua, X., et al. (2013). Colorectal carcinoma-derived fibroblasts modulate natural killer cell phenotype and antitumor cytotoxicity. *Med. Oncol. N. Lond. Engl.* 30 (3), 663. doi:10.1007/s12032-013-0663-z

Li, X., Bu, W., Meng, L., Liu, X., Wang, S., Jiang, L., et al. (2019). CXCL12/CXCR4 pathway orchestrates CSC-like properties by CAF recruited tumor associated macrophage in OSCC. *Exp. Cell Res.* 378 (2), 131–138. doi:10.1016/j.yexcr.2019.03.013

Liao, D., Luo, Y., Markowitz, D., Xiang, R., and Reisfeld, R. A. (2009). Cancer associated fibroblasts promote tumor growth and metastasis by modulating the tumor immune microenvironment in a 4T1 murine breast cancer model. *PloS one* 4 (11), e7965. doi:10.1371/journal.pone.0007965

Lim, S. A., Kim, J., Jeon, S., Shin, M. H., Kwon, J., Kim, T. J., et al. (2019). Defective localization with impaired tumor cytotoxicity contributes to the immune escape of NK cells in pancreatic cancer patients. *Front. Immunol.* 10, 496. doi:10.3389/fimmu.2019.00496

Lin, Y., Cai, Q., Chen, Y., Shi, T., Liu, W., Mao, L., et al. (2022). CAFs shape myeloid-derived suppressor cells to promote stemness of intrahepatic cholangiocarcinoma through 5-lipoxygenase. *Hepatol. Baltim. Md)* 75 (1), 28–42. doi:10.1002/hep.32099

Lin, Y., Xu, J., and Lan, H. (2019). Tumor-associated macrophages in tumor metastasis: Biological roles and clinical therapeutic applications. *J. Hematol. Oncol.* 12 (1), 76. doi:10.1186/s13045-019-0760-3

Liu, J., Chen, S., Wang, W., Ning, B. F., Chen, F., Shen, W., et al. (2016). Cancer-associated fibroblasts promote hepatocellular carcinoma metastasis through chemokine-activated hedgehog and TGF-β pathways. *Cancer Lett.* 379 (1), 49–59. doi:10.1016/j.canlet.2016.05.022

Lo, A., Wang, L. S., Scholler, J., Monslow, J., Avery, D., Newick, K., et al. (2015). Tumor-promoting desmoplasia is disrupted by depleting FAP-expressing stromal cells. *Cancer Res.* 75 (14), 2800–2810. doi:10.1158/0008-5472.CAN-14-3041

Locati, M., Curtale, G., and Mantovani, A. (2020). Diversity, mechanisms, and significance of macrophage plasticity. *Annu. Rev. pathology* 15, 123–147. doi:10.1146/annurev-pathmechdis-012418-012718

Loeffler, M., Krüger, J. A., Niethammer, A. G., and Reisfeld, R. A. (2006). Targeting tumor-associated fibroblasts improves cancer chemotherapy by increasing intratumoral drug uptake. *J. Clin. investigation* 116 (7), 1955–1962. doi:10.1172/JCI26532

Ma, Y., Hwang, R. F., Logsdon, C. D., and Ullrich, S. E. (2013). Dynamic mast cell-stromal cell interactions promote growth of pancreatic cancer. *Cancer Res.* 73 (13), 3927–3937. doi:10.1158/0008-5472.CAN-12-4479

Mace, T. A., Ameen, Z., Collins, A., Wojcik, S., Mair, M., Young, G. S., et al. (2013). Pancreatic cancer-associated stellate cells promote differentiation of myeloid-derived suppressor cells in a STAT3-dependent manner. *Cancer Res.* 73 (10), 3007–3018. doi:10.1158/0008-5472.CAN-12-4601

Mahmud, Z., Rahman, A., Mishu, I. D., and Kabir, Y. (2022). Mechanistic insights into the interplays between neutrophils and other immune cells in cancer development and progression. *Cancer metastasis Rev.* 41 (2), 405–432. doi:10.1007/s10555-022-10024-8

Maloney, E., DuFort, C. C., Provenzano, P. P., Farr, N., Carlson, M. A., Vohra, R., et al. (2019). Non-invasive monitoring of stromal biophysics with targeted depletion of hyaluronan in pancreatic ductal adenocarcinoma. *Cancers* 11 (6), 772. doi:10.3390/cancers11060772

Mangia, A., Malfettone, A., Rossi, R., Paradiso, A., Ranieri, G., Simone, G., et al. (2011). Tissue remodelling in breast cancer: Human mast cell tryptase as an initiator of myofibroblast differentiation. *Histopathology* 58 (7), 1096–1106. doi:10.1111/j.1365-2559.2011.03842.x

Mao, X., Xu, J., Wang, W., Liang, C., Hua, J., Liu, J., et al. (2021). Crosstalk between cancer-associated fibroblasts and immune cells in the tumor microenvironment: New findings and future perspectives. *Mol. cancer* 20 (1), 131. doi:10.1186/s12943-021-01428-1

Mariathasan, S., Turley, S. J., Nickles, D., Castiglioni, A., Yuen, K., Wang, Y., et al. (2018). TGFβ attenuates tumour response to PD-L1 blockade by contributing to exclusion of T cells. *Nature* 554 (7693), 544–548. doi:10.1038/nature25501

McCarthy, J. B., El-Ashry, D., and Turley, E. A. (2018). Hyaluronan, cancer-associated fibroblasts and the tumor microenvironment in malignant progression. *Front. Cell Dev. Biol.* 6, 48. doi:10.3389/fcell.2018.00048

Mhaidly, R., and Mechta-Grigoriou, F. (2020). Fibroblast heterogeneity in tumor micro-environment: Role in immunosuppression and new therapies. *Seminars Immunol.* 48, 101417. doi:10.1016/j.smim.2020.101417

Monteran, L., and Erez, N. (2019). The dark side of fibroblasts: Cancer-associated fibroblasts as mediators of immunosuppression in the tumor microenvironment. *Front. Immunol.* 10, 1835. doi:10.3389/fimmu.2019.01835

Mortezaee, K., and Majidpoor, J. (2021). The impact of hypoxia on immune state in cancer. *Life Sci.* 286, 120057. doi:10.1016/j.lfs.2021.120057

Munir, H., Jones, J. O., Janowitz, T., Hoffmann, M., Euler, M., Martins, C. P., et al. (2021). Stromal-driven and Amyloid β-dependent induction of neutrophil extracellular traps modulates tumor growth. *Nat. Commun.* 12 (1), 683. doi:10.1038/s41467-021-20982-2

Murakami, M., Ernsting, M. J., Undzys, E., Holwell, N., Foltz, W. D., and Li, S. D. (2013). Docetaxel conjugate nanoparticles that target α-smooth muscle actin-expressing stromal cells suppress breast cancer metastasis. *Cancer Res.* 73 (15), 4862–4871. doi:10.1158/0008-5472.CAN-13-0062

Nielsen, S. R., Quaranta, V., Linford, A., Emeagi, P., Rainer, C., Santos, A., et al. (2016). Macrophage-secreted granulin supports pancreatic cancer metastasis by inducing liver fibrosis. *Nat. Cell Biol.* 18 (5), 549–560. doi:10.1038/ncb3340

Nurmik, M., Ullmann, P., Rodriguez, F., Haan, S., and Letellier, E. (2020). In search of definitions: Cancer-associated fibroblasts and their markers. *Int. J. cancer* 146 (4), 895–905. doi:10.1002/ijc.32193

Nywening, T. M., Wang-Gillam, A., Sanford, D. E., Belt, B. A., Panni, R. Z., Cusworth, B. M., et al. (2016). Targeting tumour-associated macrophages with CCR2 inhibition in combination with FOLFIRINOX in patients with borderline resectable and locally advanced pancreatic cancer: A single-centre, open-label, dose-finding, non-randomised, phase 1b trial. *Lancet Oncol.* 17 (5), 651–662. doi:10.1016/S1470-2045(16)00078-4

O'Donnell, J. S., Teng, M. W. L., and Smyth, M. J. (2019). Cancer immunoediting and resistance to T cell-based immunotherapy. *Nat. Rev. Clin. Oncol.* 16 (3), 151–167. doi:10.1038/s41571-018-0142-8

Obermajer, N., Muthuswamy, R., Odunsi, K., Edwards, R. P., and Kalinski, P. (2011). PGE(2)-induced CXCL12 production and CXCR4 expression controls the accumulation of human MDSCs in ovarian cancer environment. *Cancer Res.* 71 (24), 7463–7470. doi:10.1158/0008-5472.CAN-11-2449

Ohue, Y., and Nishikawa, H. (2019). Regulatory T (Treg) cells in cancer: Can Treg cells be a new therapeutic target? *Cancer Sci.* 110 (7), 2080–2089. doi:10.1111/cas.14069

Özdemir, B. C., Pentcheva-Hoang, T., Carstens, J. L., Zheng, X., Wu, C. C., Simpson, T. R., et al. (2014). Depletion of carcinoma-associated fibroblasts and fibrosis induces immunosuppression and accelerates pancreas cancer with reduced survival. *Cancer Cell* 25 (6), 719–734. doi:10.1016/j.ccr.2014.04.005

Park, S. J., Nakagawa, T., Kitamura, H., Atsumi, T., Kamon, H., Sawa, S., et al. (2004), IL-6 regulates *in vivo* dendritic cell differentiation through STAT3 activation. *J. Immunol. Baltim. Md 1950)* 173 (6), 3844, doi:10.4049/jimmunol.173.6.3844

Peng, D., Fu, M., Wang, M., Wei, Y., and Wei, X. (2022). Targeting TGF-β signal transduction for fibrosis and cancer therapy. *Mol. cancer* 21 (1), 104. doi:10.1186/s12943-022-01569-x

Pereira, B. A., Lister, N. L., Hashimoto, K., Teng, L., Flandes-Iparraguirre, M., Eder, A., et al. (2019). Tissue engineered human prostate microtissues reveal key role of mast cell-derived tryptase in potentiating cancer-associated fibroblast (CAF)-induced morphometric transition *in vitro*. *Biomaterials* 197, 72–85. doi:10.1016/j.biomaterials.2018.12.030

Piccard, H., Muschel, R. J., and Opdenakker, G. (2012). On the dual roles and polarized phenotypes of neutrophils in tumor development and progression. *Crit. Rev. oncology/hematology* 82 (3), 296–309. doi:10.1016/j.critrevonc.2011.06.004

Pietras, K., and Ostman, A. (2010). Hallmarks of cancer: Interactions with the tumor stroma. *Exp. Cell Res.* 316 (8), 1324–1331. doi:10.1016/j.yexcr.2010.02.045

Prabhavathy, D., Vijayalakshmi, R., Kanchana, M. P., and Karunagaran, D. (2014). HPV16 E2 enhances the expression of NF-κB and STAT3 target genes and potentiates NF-κB activation by inflammatory mediators. *Cell. Immunol.* 292 (1-2), 70–77. doi:10.1016/j.cellimm.2014.09.005

Ran, G. H., Lin, Y. Q., Tian, L., Zhang, T., Yan, D. M., Yu, J. H., et al. (2022). Natural killer cell homing and trafficking in tissues and tumors: From biology to application. *Signal Transduct. Target. Ther.* 7 (1), 205. doi:10.1038/s41392-022-01058-z

Raskov, H., Orhan, A., Gaggar, S., and Gögenur, I. (2021). Cancer-associated fibroblasts and tumor-associated macrophages in cancer and cancer immunotherapy. *Front. Oncol.* 11, 668731. doi:10.3389/fonc.2021.668731

Ravi, R., Noonan, K. A., Pham, V., Bedi, R., Zhavoronkov, A., Ozerov, I. V., et al. (2018). Bifunctional immune checkpoint-targeted antibody-ligand traps that simultaneously disable TGFβ enhance the efficacy of cancer immunotherapy. *Nat. Commun.* 9 (1), 741. doi:10.1038/s41467-017-02696-6

Rhim, A. D., Oberstein, P. E., Thomas, D. H., Mirek, E. T., Palermo, C. F., Sastra, S. A., et al. (2014). Stromal elements act to restrain, rather than support, pancreatic ductal adenocarcinoma. *Cancer Cell* 25 (6), 735–747. doi:10.1016/j.ccr.2014.04.021

Riley, R. S., June, C. H., Langer, R., and Mitchell, M. J. (2019). Delivery technologies for cancer immunotherapy. *Nat. Rev. Drug Discov.* 18 (3), 175–196. doi:10.1038/s41573-018-0006-z

Rollins, B. J. (2006). Inflammatory chemokines in cancer growth and progression. *Eur. J. cancer* 42 (6), 760, doi:10.1016/j.ejca.2006.01.002

Ruiz-Borrego, M., Jimenez, B., Antolín, S., García-Saenz, J. A., Corral, J., Jerez, Y., et al. (2019). A phase Ib study of sonidegib (LDE225), an oral small molecule inhibitor of smoothened or hedgehog pathway, in combination with docetaxel in triple negative advanced breast cancer patients: GEICAM/2012-12 (EDALINE) study. *Investig. new drugs* 37 (1), 98–108. doi:10.1007/s10637-018-0614-9

Ruterbusch, M., Pruner, K. B., Shehata, L., and Pepper, M. (2020). *In vivo* CD4+ T cell differentiation and function: Revisiting the Th1/Th2 paradigm. *Annu. Rev. Immunol.* 38, 705–725. doi:10.1146/annurev-immunol-103019-085803

Saito, R. A., Micke, P., Paulsson, J., Augsten, M., Peña, C., Jönsson, P., et al. (2010). Forkhead box F1 regulates tumor-promoting properties of cancer-associated fibroblasts in lung cancer. *Cancer Res.* 70 (7), 2644–2654. doi:10.1158/0008-5472.CAN-09-3644

Sano, M., Ijichi, H., Takahashi, R., Miyabayashi, K., Fujiwara, H., Yamada, T., et al. (2019). Blocking CXCLs-CXCR2 axis in tumor-stromal interactions contributes to survival in a mouse model of pancreatic ductal adenocarcinoma through reduced cell invasion/migration and a shift of immune-inflammatory microenvironment. *Oncogenesis* 8 (2), 8. doi:10.1038/s41389-018-0117-8

Schoen, J., Euler, M., Schauer, C., Schett, G., Herrmann, M., Knopf, J., et al. (2022). Neutrophils' extracellular trap mechanisms: From physiology to pathology. *Int. J. Mol. Sci.* 23 (21), 12855. doi:10.3390/ijms232112855

Segal, B. H., Giridharan, T., Suzuki, S., Khan, A. N. H., Zsiros, E., Emmons, T. R., et al. (2022). Neutrophil interactions with T cells, platelets, endothelial cells, and of course tumor cells. *Immunol. Rev.* doi:10.1111/imr.13178

Sharma, S., Yang, S. C., Zhu, L., Reckamp, K., Gardner, B., Baratelli, F., et al. (2005). Tumor cyclooxygenase-2/prostaglandin E2-dependent promotion of FOXP3 expression and CD4+ CD25+ T regulatory cell activities in lung cancer. *Cancer Res.* 65 (12), 5211–5220. doi:10.1158/0008-5472.CAN-05-0141

Sherman, M. H., Yu, R. T., Engle, D. D., Ding, N., Atkins, A. R., Tiriac, H., et al. (2014). Vitamin D receptor-mediated stromal reprogramming suppresses pancreatitis and enhances pancreatic cancer therapy. *Cell* 159 (1), 80–93. doi:10.1016/j.cell.2014.08.007

Shukla, A., Edwards, R., Yang, Y., Hahn, A., Folkers, K., Ding, J., et al. (2014). CLIC4 regulates TGF-β-dependent myofibroblast differentiation to produce a cancer stroma. *Oncogene* 33 (7), 842–850. doi:10.1038/onc.2013.18

Silzle, T., Randolph, G. J., Kreutz, M., and Kunz-Schughart, L. A. (2004). The fibroblast: Sentinel cell and local immune modulator in tumor tissue. *Int. J. cancer* 108 (2), 173–180. doi:10.1002/ijc.11542

Simon, T., and Salhia, B. (2022). Cancer-associated fibroblast subpopulations with diverse and dynamic roles in the tumor microenvironment. *Mol. cancer Res. MCR* 20 (2), 183–192. doi:10.1158/1541-7786.MCR-21-0282

Slaney, C. Y., Kershaw, M. H., and Darcy, P. K. (2014). Trafficking of T cells into tumors. *Cancer Res.* 74 (24), 7168–7174. doi:10.1158/0008-5472.CAN-14-2458

Song, M., He, J., Pan, Q. Z., Yang, J., Zhao, J., Zhang, Y. J., et al. (2021). Cancer-associated fibroblast-mediated cellular crosstalk supports hepatocellular carcinoma progression. *Hepatol. Baltim. Md)* 73 (5), 1717–1735. doi:10.1002/hep.31792

Spaeth, E. L., Labaff, A. M., Toole, B. P., Klopp, A., Andreeff, M., and Marini, F. C. (2013). Mesenchymal CD44 expression contributes to the acquisition of an activated fibroblast phenotype via TWIST activation in the tumor microenvironment. *Cancer Res.* 73 (17), 5347–5359. doi:10.1158/0008-5472.CAN-13-0087

St Paul, M., and Ohashi, P. S. (2020). The roles of CD8(+) T cell subsets in antitumor immunity. *Trends Cell Biol.* 30 (9), 695–704. doi:10.1016/j.tcb.2020.06.003

Stanisavljevic, J., Loubat-Casanovas, J., Herrera, M., Luque, T., Peña, R., Lluch, A., et al. (2015). Snail1-expressing fibroblasts in the tumor microenvironment display mechanical properties that support metastasis. *Cancer Res.* 75 (2), 284–295. doi:10.1158/0008-5472.CAN-14-1903

Su, X., Ye, J., Hsueh, E. C., Zhang, Y., Hoft, D. F., and Peng, G. (2010). Tumor microenvironments direct the recruitment and expansion of human Th17 cells. *J. Immunol.* 184(3), 1630, doi:10.4049/jimmunol.0902813

Szulc-Kielbik, I., and Kielbik, M. (2012). Tumor-associated macrophages: Reasons to Be cheerful, reasons to Be fearful. *Exp. Suppl.* 113, 107, doi:10.1007/978-3-030-91311-3_4

Tajaldini, M., Saeedi, M., Amiriani, T., Amiriani, A. H., Sedighi, S., Mohammad Zadeh, F., et al. (2022). Cancer-associated fibroblasts (CAFs) and tumor-associated macrophages (TAMs); where do they stand in tumorigenesis and how they can change the face of cancer therapy? *Eur. J. Pharmacol.* 928, 175087. doi:10.1016/j.ejphar.2022.175087

Takahashi, H., Sakakura, K., Kawabata-Iwakawa, R., Rokudai, S., Toyoda, M., Nishiyama, M., et al. (2015). Immunosuppressive activity of cancer-associated fibroblasts in head and neck squamous cell carcinoma. *CII* 64 (11), 1407–1417. doi:10.1007/s00262-015-1742-0

Takahashi, M., Kobayashi, H., Mizutani, Y., Hara, A., Iida, T., Miyai, Y., et al. (2021). Roles of the mesenchymal stromal/stem cell marker meflin/islr in cancer fibrosis. *Front. Cell Dev. Biol.* 9, 749924. doi:10.3389/fcell.2021.749924

Tauriello, D. V. F., Palomo-Ponce, S., Stork, D., Berenguer-Llergo, A., Badia-Ramentol, J., Iglesias, M., et al. (2018). TGFβ drives immune evasion in genetically reconstituted colon cancer metastasis. *Nature* 554 (7693), 538–543. doi:10.1038/nature25492

Thomas, D. A., and Massagué, J. (2005). TGF-beta directly targets cytotoxic T cell functions during tumor evasion of immune surveillance. *Cancer Cell* 8 (5), 369–380. doi:10.1016/j.ccr.2005.10.012

Tian, C., Clauser, K. R., Öhlund, D., Rickelt, S., Huang, Y., Gupta, M., et al. (2019). Proteomic analyses of ECM during pancreatic ductal adenocarcinoma progression reveal different contributions by tumor and stromal cells. *Proc. Natl. Acad. Sci. U. S. A.* 116 (39), 19609–19618. doi:10.1073/pnas.1908626116

Timperi, E., Gueguen, P., Molgora, M., Magagna, I., Kieffer, Y., Lopez-Lastra, S., et al. (2022). Lipid-associated macrophages are induced by cancer-associated fibroblasts and mediate immune suppression in breast cancer. *Cancer Res.* 82 (18), 3291–3306. doi:10.1158/0008-5472.CAN-22-1427

Tokuda, K., Morine, Y., Miyazaki, K., Yamada, S., Saito, Y., Nishi, M., et al. (2021). The interaction between cancer associated fibroblasts and tumor associated macrophages via the osteopontin pathway in the tumor microenvironment of hepatocellular carcinoma. *Oncotarget* 12 (4), 333–343. doi:10.18632/oncotarget.27881

Travis, M. A., and Sheppard, D. (2014). TGF-β activation and function in immunity. *Annu. Rev. Immunol.* 32, 51–82. doi:10.1146/annurev-immunol-032713-120257

Trotta, R., Dal Col, J., Yu, J., Ciarlariello, D., Thomas, B., Zhang, X., et al. (2008), TGF-beta utilizes SMAD3 to inhibit CD16-mediated IFN-gamma production and antibody-dependent cellular cytotoxicity in human NK cells. *J. Immunol. Baltim. Md 1950*) 181 (6), 3784, doi:10.4049/jimmunol.181.6.3784

Varricchi, G., de Paulis, A., Marone, G., and Galli, S. J. (2019). Future needs in mast cell biology. *Int. J. Mol. Sci.* 20 (18), 4397. doi:10.3390/ijms20184397

Vyas, M., and Demehri, S. (2022). The extracellular matrix and immunity: Breaking the old barrier in cancer. *Trends Immunol.* 43 (6), 423–425. doi:10.1016/j.it.2022.04.004

Wang, Z., Moresco, P., Yan, R., Li, J., Gao, Y., Biasci, D., et al. (2022). Carcinomas assemble a filamentous CXCL12-keratin-19 coating that suppresses T cell-mediated immune attack. *Proc. Natl. Acad. Sci. U. S. A.* 119 (4), e2119463119. doi:10.1073/pnas.2119463119

Wculek, S. K., Cueto, F. J., Mujal, A. M., Melero, I., Krummel, M. F., and Sancho, D. (2020). Dendritic cells in cancer immunology and immunotherapy. *Nat. Rev. Immunol.* 20 (1), 7–24. doi:10.1038/s41577-019-0210-z

Weber, F., Byrne, S. N., Le, S., Brown, D. A., Breit, S. N., Scolyer, R. A., et al. (2005). Transforming growth factor-beta1 immobilises dendritic cells within skin tumours and facilitates tumour escape from the immune system. *CII* 54 (9), 898–906. doi:10.1007/s00262-004-0652-3

Woan, K. V., and Miller, J. S. (2019). Harnessing natural killer cell antitumor immunity: From the bench to bedside. *Cancer Immunol. Res.* 7 (11), 1742–1747. doi:10.1158/2326-6066.CIR-19-0404

Xiang, H., Ramil, C. P., Hai, J., Zhang, C., Wang, H., Watkins, A. A., et al. (2020). Cancer-associated fibroblasts promote immunosuppression by inducing ROS-generating monocytic MDSCs in lung squamous cell carcinoma. *Cancer Immunol. Res.* 8 (4), 436–450. doi:10.1158/2326-6066.CIR-19-0507

Xiang, X., Niu, Y. R., Wang, Z. H., Ye, L. L., Peng, W. B., and Zhou, Q. (2022). Cancer-associated fibroblasts: Vital suppressors of the immune response in the tumor microenvironment. *Cytokine & growth factor Rev.* 67, 35–48. doi:10.1016/j.cytogfr.2022.07.006

Yang, L., Chang, N., Liu, X., Han, Z., Zhu, T., Li, C., et al. (2012). Bone marrow-derived mesenchymal stem cells differentiate to hepatic myofibroblasts by transforming growth factor-β1 via sphingosine kinase/sphingosine 1-phosphate (S1P)/S1P receptor axis. *Am. J. pathology* 181 (1), 85–97. doi:10.1016/j.ajpath.2012.03.014

Yang, Q., Guo, N., Zhou, Y., Chen, J., Wei, Q., and Han, M. (2020). The role of tumor-associated macrophages (TAMs) in tumor progression and relevant advance in targeted therapy. *Acta Pharm. Sin. B* 10 (11), 2156–2170. doi:10.1016/j.apsb.2020.04.004

Yang, X., Lin, Y., Shi, Y., Li, B., Liu, W., Yin, W., et al. (2016). FAP promotes immunosuppression by cancer-associated fibroblasts in the tumor microenvironment via STAT3-CCL2 signaling. *Cancer Res.* 76 (14), 4124–4135. doi:10.1158/0008-5472.CAN-15-2973

Yang, Z., Xu, S., Jin, P., Yang, X., Li, X., Wan, D., et al. (2016). MARCKS contributes to stromal cancer-associated fibroblast activation and facilitates ovarian cancer metastasis. *Oncotarget* 7 (25), 37649–37663. doi:10.18632/oncotarget.8726

Yeo, S. Y., Lee, K. W., Shin, D., An, S., Cho, K. H., and Kim, S. H. (2018). A positive feedback loop bi-stably activates fibroblasts. *Nat. Commun.* 9 (1), 3016. doi:10.1038/s41467-018-05274-6

Zhang, A., Qian, Y., Ye, Z., Chen, H., Xie, H., Zhou, L., et al. (2017). Cancer-associated fibroblasts promote M2 polarization of macrophages in pancreatic ductal adenocarcinoma. *Cancer Med.* 6 (2), 463–470. doi:10.1002/cam4.993

Zhang, J., Chen, L., Xiao, M., Wang, C., and Qin, Z. (2011). FSP1+ fibroblasts promote skin carcinogenesis by maintaining MCP-1-mediated macrophage infiltration and chronic inflammation. *Am. J. pathology* 178 (1), 382–390. doi:10.1016/j.ajpath.2010.11.017

Zhang, R., Qi, F., Zhao, F., Li, G., Shao, S., Zhang, X., et al. (2019). Cancer-associated fibroblasts enhance tumor-associated macrophages enrichment and suppress NK cells function in colorectal cancer. *Cell death Dis.* 10 (4), 273. doi:10.1038/s41419-019-1435-2

Zhang, R., Zong, J., Peng, Y., Shi, J., Du, X., Liu, H., et al. (2021). GPR30 knockdown weakens the capacity of CAF in promoting prostate cancer cell invasion via reducing macrophage infiltration and M2 polarization. *J. Cell. Biochem.* 122, 1173–1191. doi:10.1002/jcb.29938

Zhao, Q., Huang, L., Qin, G., Qiao, Y., Ren, F., Shen, C., et al. (2021). Cancer-associated fibroblasts induce monocytic myeloid-derived suppressor cell generation via IL-6/exosomal miR-21-activated STAT3 signaling to promote cisplatin resistance in esophageal squamous cell carcinoma. *Cancer Lett.* 518, 35–48. doi:10.1016/j.canlet.2021.06.009

Zheng, L., Xu, C., Guan, Z., Su, X., Xu, Z., Cao, J., et al. (2016). Galectin-1 mediates TGF-β-induced transformation from normal fibroblasts into carcinoma-associated fibroblasts and promotes tumor progression in gastric cancer. *Am. J. Transl. Res.* 8 (4), 1641–1658.

Zhu, Q., Zhang, X., Zhang, L., Li, W., Wu, H., Yuan, X., et al. (2014). The IL-6-STAT3 axis mediates a reciprocal crosstalk between cancer-derived mesenchymal stem cells and neutrophils to synergistically prompt gastric cancer progression. *Cell death Dis.* 5 (6), e1295. doi:10.1038/cddis.2014.263

Zhu, X., and Zhu, J. (2020). CD4 T helper cell subsets and related human immunological disorders. *Int. J. Mol. Sci.* 21 (21), 8011. doi:10.3390/ijms21218011

Ziani, L., Safta-Saadoun, T. B., Gourbeix, J., Cavalcanti, A., Robert, C., Favre, G., et al. (2017). Melanoma-associated fibroblasts decrease tumor cell susceptibility to NK cell-mediated killing through matrix-metalloproteinases secretion. *Oncotarget* 8 (12), 19780–19794. doi:10.18632/oncotarget.15540

frontiers | Frontiers in Pharmacology

TYPE Original Research
PUBLISHED 27 June 2023
DOI 10.3389/fphar.2023.1136960

OPEN ACCESS

EDITED BY
Qianming Du,
Nanjing Medical University, China

REVIEWED BY
Zhi Xu,
Nanjing Drum Tower Hospital, China
Xiuting Liu,
Washington University in St. Louis, United States

*CORRESPONDENCE
Zhang Tao,
zhangt10@126.com
Hu Xueyu,
huxueyu@fmmu.edu.cn
Wang Zhe,
wangzhe@fmmu.edu.cn

†These authors have contributed equally to this work and share first authorship

RECEIVED 03 January 2023
ACCEPTED 09 June 2023
PUBLISHED 27 June 2023

CITATION
Zhihao Z, Cheng J, Xiaoshuang Z, Yangguang M, Tingyu W, Yongyong Y, Zhou Y, Jie Z, Tao Z, Xueyu H and Zhe W (2023), Cancer-associated fibroblast infiltration in osteosarcoma: the discrepancy in subtypes pathways and immunosuppression.
Front. Pharmacol. 14:1136960.
doi: 10.3389/fphar.2023.1136960

Cancer-associated fibroblast infiltration in osteosarcoma: the discrepancy in subtypes pathways and immunosuppression

Zhang Zhihao[1†], Ju Cheng[1†], Zuo Xiaoshuang[1†], Ma Yangguang[1], Wu Tingyu[1], Yang Yongyong[1], Yao Zhou[1], Zhou Jie[1], Zhang Tao[2*], Hu Xueyu[1*] and Wang Zhe[1*]

[1]Department of Orthopedics, Xijing Hospital, Air Force Military Medical University, Xi'an, Shaanxi, China, [2]Department of Radiation Oncology, National Cancer Center, National Clinical Research Center for Cancer, Cancer Hospital, Chinese Academy of Medical Science and Peking Union Medical College, Beijing, China

Introduction: Osteosarcoma (OS), the primary malignant bone tumor, has a low survival rate for recurrent patients. Latest reports indicated that cancer-associated fibroblasts (CAFs) were the main component of tumor microenvironment, and would generate a variable role in the progression of tumors. However, the role of CAFs is still few known in osteosarcoma.

Methods: The processed RNA-seq data and the corresponding clinical and molecular information were retrieved from the Cancer Genome Atlas Program (TCGA) database and processed data of tumor tissue was obtained from Gene Expression Omnibus (GEO) database. Xcell method was used in data processing, and Gene set variation analysis (GSVA) was used to calculates enrichment scores. Nomogram was constructed to evaluate prognostic power of the predictive model. And the construction of risk scores and assessment of prognostic predictive were based on the LASSO model.

Results: This study classified Cancer Genome Atlas (TCGA) cohort into high and low CAFs infiltrate phenotype with different CAFs infiltration enrichment scores. Then TOP 9 genes were screened as prognostic signatures among 2,488 differentially expressed genes between the two groups. Key prognostic molecules were CGREF1, CORT and RHBDL2 and the risk score formula is: Risk-score = CGREF1*0.004 + CORT*0.004 + RHBDL2*0.002. The signatures were validated to be independent prognostic factors to predict tumor prognosis with single-factor COX and multi-factor COX regression analyses and Norton chart. The risk score expression of risk score model genes could predict the drug resistance, and significant differences could be found between the high and low scoring groups for 17-AAG, AZD6244, PD-0325901 and Sorafenib.

Discussion: To sum up, this article validated the prediction role of CAF infiltration in the prognosis of OS, which might shed light on the treatment of OS.

KEYWORDS

osteosarcoma, cancer-associated fibroblasts, cancer genome atlas, immune infiltration, drug resistance

1 Introduction

OS is one of the most prevalent primary malignant bone tumors, which occurs principally in kids, teenagers and young adults (Keil, 2020). Operative resection and combined chemotherapy treatment can cure about 70% of patients, and the 5-year survival rate of patients with limited osteosarcoma has increased significantly in the past decades (Kansara et al, 2014; Robison and Hudson, 2014). However, as a highly aggressive tumor, the 5-year survival rate for patients with recurrent and metastatic OS remains at approximately 20%, virtually constant for the past 30 years (Kansara et al, 2014). Therefore, the treatment of osteosarcoma still requires the application of new therapies.

It has been shown that the tumor microenvironment is actively involved in tumor progression (Liotta and Kohn, 2001; Mueller and Fusenig, 2004). The activated mesenchymal cells, CAFs, are a major component of the tumor microenvironment (Chen and Song, 2019). Compared to normal fibroblasts, multiple protein markers are overexpressed in CAFs depending on the tumor type such as α-smooth muscle actin (α-SMA) or fibroblast activation protein (FAP) (Kalluri and Zeisberg, 2006). CAFs could interact with tumor cells by releasing secreted proteins such as transforming growth factor β (TGF-β), insulin-like growth factor (IGF) and interleukin-6 (IL-6), regulating immune feedback or remodeling of the extracellular matrix, etc. (Ishii et al, 2016). Meanwhile, it was demonstrated that the composition of CAFs is heterogeneous, different degrees of CAFs activation would generate different subgroups of CAFs and play a variable role in the progression of tumors (Wang et al, 2021).

OS is a low immunogenic tumor that is less likely to induce an immune response in the host by contrast to immunotherapy effective cancers such as malignant melanoma and lung cancer (Yahiro and Matsumoto, 2021). Immunogenicity is determined by what is known as the tumor mutation burden (TMB), i.e., the accumulation of mutations in the tumor. As a type of sarcoma, OS has a low TMB value. Immunogenicity will largely determine the effectiveness of immunotherapy, and low immunogenicity of OS would result in fewer immune cells tumor-infiltrating and tumor-specific T-cells, making immunotherapy ineffective (Wang et al, 2019a; Yahiro and Matsumoto, 2021). Over the past few decades, the tumor microenvironment has been recognized as a rich target for anti-tumor therapy (Turley et al, 2015), Numerous preclinical studies have also shown that CAFs could be a potential promising target for anti-tumor immunotherapy (Kalluri, 2016; Ziani et al, 2018; Kobayashi et al, 2019).

In osteosarcoma, the studies on the role of CAFs are still few in quantity. Here, as detailed flow chart of this study demonstrated, data derived from TCGA and GEO were divided into high and low fibroblast groups according to CAFs infiltration enrichment scores, and patients in the high fibroblast group had significantly longer OS survival time than those in the low fibroblast group, they differed significantly in stromal and immune-related scores. Then, differentially expressed genes (DEGs) were further screened and enriched for pathways in the GO database of MF, BP, CC, and KEGG, and most of the differentially expressed genes were found to be enriched for immune-related pathways. Next, based on univariate COX regression analysis, 9 genes significantly associated with overall patient survival were screened and identified as fibroblast-related risk markers, and three of them were screened as prognostic molecules. Assigning prognostic molecules with different weights, the risk score of each sample was calculated and samples were divided into high risk and low risk groups based on the median, and the prognostic difference between them was verified using ROC curves. The risk score could be used as an independent predictor of prognosis. For patients with higher risk scores, there was a tendency for higher tumor microenvironment scores and significantly altered tumor hallmark pathway genes. Finally, comparing the IC50 of the drugs, there was a significant difference in the drug sensitive profile between the high and low scoring groups.

2 Materials and methods

2.1 Dataset and source

In this study, we used TCGA (https://portal.gdc.cancer.gov/) and GEO (https://www.ncbi.nlm.nih.gov/geo) (GSE21257 and GSE39058) platforms for data analysis, and the data of the two platforms were used respectively. First, the processed RNA-seq data (88 samples, 85 survival data) and the corresponding clinical and molecular information were retrieved from the TCGA database. After excluding 90% of the NA fields in clinical information, race, gender, age, and site_of_resection_or_biopsy were selected as clinical characters, 85 patients from TCGA cohort were included. The analysis was performed by TCGA data for subtype exploration, prognosis-related gene screening and prognostic model construction. Then we validated the prognostic model using GEO microarray data. Processed data of tumor tissue from patients with osteosarcoma was downloaded from NCBI GEO with accession code GSE39058 and GSE2125. Age, gender, and recurrence were selected as clinical characters in GSE39058 cohort and metastases, and huvos.grade for GSE2125 cohort. Data from the two cohorts of the GEO platform were merged by the COMBAT function in the R sva package. The same type of clinical information (age, gemder) was combined in a clinical correlation analysis. Each of the GSE39058 and GSE2125 cohorts corresponded probes to genes based on information from their corresponding microarrays, and empty vector probes were removed. If multiple probes corresponded to one gene, we selected the median of these probes as the expression level of that gene. As a result, 95 patients from GSE39058 and GSE2125 cohort were included in our study. The flow chart of the experiment could be found in Figure 1.

2.2 Data preprocessing

The downloaded TCGA expression profile data in FRKM format was converted to TPM format. The EPIC, MCP-counter, and Xcell methods were used to calculate the percentage of immune cell infiltration in each sample. The results of the K-M analysis and the one-way COX analysis were compared between above three methods and the Xcell method was selected as it had the best results. To analyze the differences between patients with high CAF scores and low CAF scores, we used the median of the CAF score-based cohort to divide the patients into the high CAF and low CAF groups to reduce the bias caused by the different numbers in the two groups.

2.3 GSVA pathway analysis

GSVA (Gene set variation analysis) is a non-parametric, unsupervised algorithm that calculates enrichment scores for specific gene sets in each sample without pre-grouping the

samples. By using the MSigDB-hallmark gene as the reference gene set and set p-value to <0.05, we performed GSVA and implemented using package clusterProfiler in R. The commonly activated or suppressed pathways were identified.

2.4 Nomogram construction

Clinical information and risk scores including age, gender and tissue origin included in the TCGA cohort were selected for nomogram development, the prognostic risk score models were built using the RMS package. Performance of the model was validated in the TCGA cohort using time-dependent calibration curves and Harrell's concordance index (C-index) to assess the prognosis validity of the model.

2.5 Identification of prognosis-related genes

COX regression analysis and K-M survival analysis were performed to identify the genes which might related to overall survival in database and evaluated the contribution of the genes, $p < 0.05$ was considered as statistically significant. The analysis was conducted with the package of survival and survminer.

2.6 Constructing risk scores and prognostic predictive assessments based on the lasso model

Interactions between genes might form covariate gene clusters, we use R/Bioconductor's lars and glmnet R language package for Lasso regression to reduce the impact of this covariation and improve the accuracy and interpretability of the model. Then we used cross-validation to determine the corresponding parameters in order to obtain a suitable model within the existing models. Based on the obtained model, we calculated the risk score (Risk score = $\sum_{i=1}^{N} coef_i * expr_i$) for each patient, in which N is the number of genes selected, $expr_i$ is the expression value of each gene and $coef_i$ is the multivariate COX regression coefficient. The cohort was divided into low-risk and high-risk groups based on the median risk score, and survival analysis was performed between the two groups using the Kaplan-Meier progression. ROC curves were plotted to predict prognostic 1-, 3-, and 5-year survival rates for patients with osteosarcoma using the survivalroc R package.

2.7 Differential gene analysis and pathway annotation

Data from the TCGA cohort were formatted using the read count package and differential analysis was performed using the deseq2 R package to screen for differential genes between high and low risk scores (p-value <0.01 and abs (log_2FoldChange) > 1). Differential analysis was performed on the GEO microarray data via the limma package and screened the differential genes as described above. Gene set enrichment analysis (GSEA) was performed using the clusterProfiler R language package, with the using of "h.all.v7.0.entrez.gmt" as the reference gene set. p-values were adjusted using the Benjamini and Hochberg methods, and p-values <0.05 were considered as statistic significant.

2.8 Drug resistance assessment by CAFs score

Firstly, based on the expression profile matrix of 471 cell lines downloaded from Cancer Cell Line Encyclopedia (CCLE), the CAFs scores in each cell line sample were calculated by CAFs score model, then the cohort in each sample was divided into high-CAFs group and low-CAFs group based on median, then the resistance IC50 assessment of 471 samples with 24 drugs was corelated, and whether there was a significant difference in drug resistance between the two groups was tested by Wilcoxon signed rank test.

2.9 Cell culture and CCK-8 test

HOS and MG-63 cells were purchased from Meisen Cell Technology Co., Ltd. Cells were cultured in Dulbecco's modified Eagle medium (DMEM) (Gibco, United States) containing 10% fetal bovine serum and 100 units/mL penicillin-streptomycin. The viability of cells after treatment with 17-AAG (MCE, United States), AZD6244 (MCE, United States), PD-0325901 (MCE, United States), Sorafenib (MCE, United States) was determined using Cell Counting Kit-8 (CCK-8) kit (Beyotime, China). HOS and MG-63 cells were inoculated in 96-well cell culture plates at a density of 5×10^4 cells/mL and incubated for 24 h to make cells adhere to the wall. Cells were then treated with 17-AAG, AZD6244, PD-0325901, and Sorafenib at a concentration of 1 μM for 72 h, respectively. Then 10% CCK-8 solution was added, and incubated for 2 h at 37°C. Cell viability after different drug interventions was determined by measuring absorbance values measured at 450 nm on an automated detector (BioTek, United States). All cells were incubated in an incubator at 37°C with 5% CO_2.

2.10 Immunohistochemistry (IHC)

To further validate the expression of the three predicted genes, six pairs of paraffin-embedded osteosarcoma tissues and adjacent tissues were collected for IHC analysis. The study was approved by the Institutional Review Board of the First Affiliated Hospital of the Air Force Military Medical University, and all patients signed an informed consent form. All tissue sections were dewaxed, antigen-repaired, blocked, incubated with primary antibodies and secondary antibodies, and antibodies used included CGREF1 (ABclonal, A14844), RHBDL2 (GeneTex, GTX46323) and CORT (santa, sc-393108). Finally, the sections were stained using the DAB kit (CWBIO, CW 2035S) and hematoxylin. Protein expression of the three molecularly stained sections in each sample was observed by microscopy, and the positive rate relative to paracancer tissue for each IHC stained section was calculated using ImageJ software.

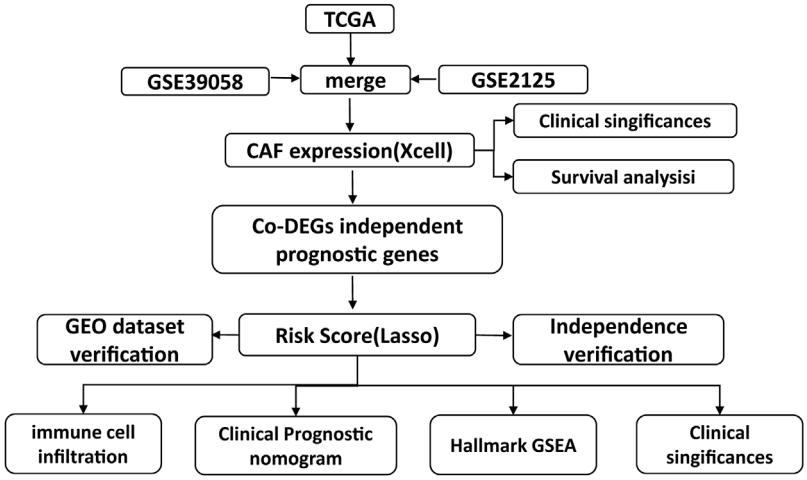

FIGURE 1
Flow chart of the experiment.

2.11 Statistical analysis

The version of the R used in this paper was R version 4.1.0 (2021-05-18)—"Camp Pontanezen". The Wilcox method was used to analyze the scoring tests between the two groups and kruskal test was used to test for three or more groups. In the statistical plots, difference of $p < 0.05$ was considered as significant.

3 Results

3.1 Identification of CAFs infiltrate phenotype and analysis of clinical features

Firstly, after obtaining CAFs infiltration enrichment scores from the TCGA cohort and applying the cut-off grouping as the median, K-M survival analysis showed a significant difference in prognostic survival between the two groups, with the high group having a better prognosis [HR (hazard rate): 2.13 (4.81-0.94)] (Figure 2A). Using univariate and multivariate Cox regression analysis with clinical information, the CAFs were shown to be independent prognostic factors ($p < 0.05$, Figures 2B,C). We further analyzed the correlation between CAFs enrichment score and other immune cell infiltration and immune correlation scores (Figure 2D), which showed a significant positive correlation between CAFs and Stroma Score, a significant positive correlation between CAFs and chondrocytes in osteosarcoma tissue, and a significant negative correlation with Th1_cells and pro_B-cells.

3.2 Correlation between the differences in clinical characteristics of CAFs and ESTIMATE algorithm scores

In view of the crucial roles of the CAFs in tumor progression, we further analyzed the correlation between the differences in CAFs between clinical characteristics and ESTIMATE algorithm scores (Figure 3). The results showed that there were significant differences in StromalScore and ESTIMATEScore between the groups with high and low CAFs infiltrate phenotype. We also found that the low CAFs infiltration group has a higher tumor cell purity.

3.3 Screening of CAF candidate markers and functional analysis

2,488 differentially expressed genes between the two groups were identified in TCGA, with 637 significantly upregulated and 1851 downregulated (Figure 4A). The expression heat map of the differential genes was shown in Figure 4B. The enrichment results of MF, BP, CC in the GO and KEGG showed that most of the differential genes were enriched in immune-related pathways: B cell mediated immunity, humoral immune response, etc. (Figures 4C–F).

3.4 Construction and validation of prognostic signatures of CAFs

Based on the differential gene expression profiles screened above, we used one-way COX regression analysis to screen prognostic signatures associated with patient prognosis, and TOP 9 genes including AOC4P, BMP8B, CGREF1, CORT, CPNE5, CTAGE14P, DUX4L27, GANT14, and GJA5 were selected (Figure 5A). The results of K-M survival analysis demonstrated the prognostic differences of genes [AOC4P, HR: 0.36 (0.76-0.17); BMP8B, HR: 0.35 (0.73-0.17); CGREF1, HR:0.3 (0.62-0.14); CORT, HR: 0.29 (0.6-0.14); CPNE5, HR: 0.34 (0.71-0.16); CTAGE14P, HR: 0.35 (0.74-0.17); DUX4L27, HR: 0.36 (0.75-0.17); GANT14, HR: 0.22 (0.46-0.1); and GJA5, HR: 2.85 (5.91-1.36)], the risk signatures could predict the prognosis of OS patients in most cases (Figure 5A). Then we constructed a regression model with the LASSO algorithm based on the above prognosis-related CFA markers, and the result showed the confidence interval under each lambda (Figure 5B).

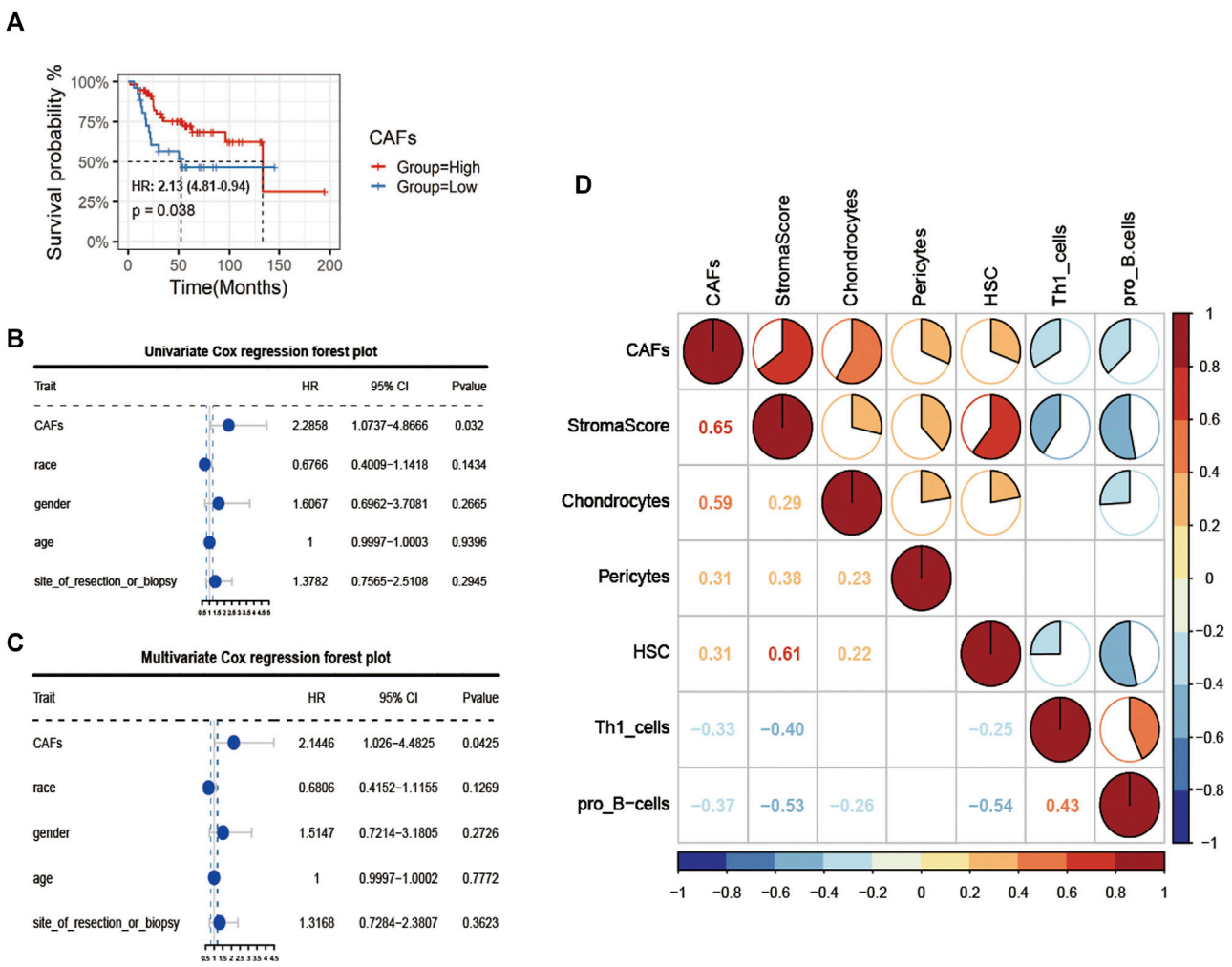

FIGURE 2
Identification of CAFs infiltration phenotype and analysis of clinical features. **(A)** K-M survival analysis between high and low CAFs score patient groups. **(B, C)** Univariate COX regression and multivariate COX regression analysis of factors including CAFs. **(D)** Correlation analysis of CAFs with immune indexes and immune-related cells.

Then we modified the parameters of the LASSO regression model by cross-validation (Figure 5C). Based on the results of the above prognostic predictors, we selected three gene signatures CGREF1, CORT and RHBDL2 as key prognostic molecules and calculated a risk score for each sample based on the weight threshold of each signature, the risk score formula in LASSO-Cox regression analysis is: Risk-score = CGREF1*0.004 + CORT*0.004 + RHBDL2*0.002. In addition, we analyzed risk scores and prognostic assessments using multifactorial COX survival analysis using the TCGA database and GEO database respectively and plotted forest plots (Supplementary Figure S1). The analysis showed that CGREF1 in both GEO database and TCGA database and RHBDL2 in TCGA database showed promising predictions. Then we classified patients into high and low risk score groups using the median as the threshold (Figure 5D). Furthermore, the accuracy of risk score as a prognostic factor for OS was validated through ROC curve analysis using TCGA training set sample, the results of the survival analysis showed that there were significant differences between patients in groups with high and low scores (Figure 5E), Finally, the results were validated on a validation set cohort obtained by combining GSE21257 and GSE39058, which showed a significant difference in prognostic survival between the high and low risk score groups (Figures 5F–I). We then validated of gene expression in tissue of osteosarcoma patients. We demonstrated the results by IHC experiments, and observed that CGREF1, CORT and RHBDL2 proteins expression were high in the tissue of osteosarcoma patients, while the proteins were lowly expressed in normal tissue (Supplementary Figure S2).

3.5 CAFs signature could be used as an independent prognostic factor to predict tumor prognosis

We analyzed the correlation between CAF risk score and clinical characteristics, The results showed that as the risk score increased, the incidence of tumor metastasis increased correspondly, and there was a strong positive correlation between them, whereas the risk score was less correlated with other clinical differential

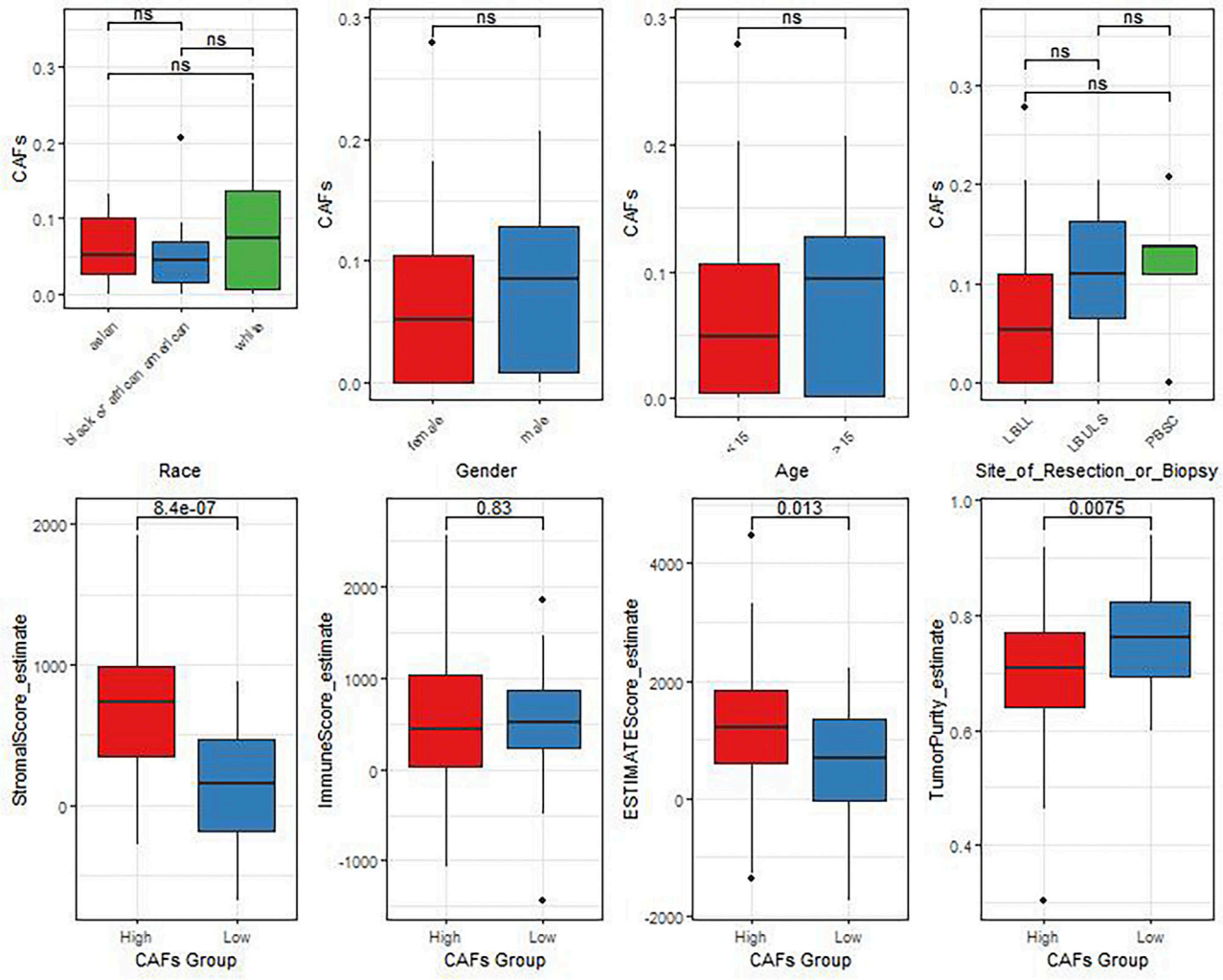

FIGURE 3
The differences of CAFs among patients with different clinical characteristics evaluated by the ESTIMATE algorithm.

characteristics, we then performed single-factor COX and multi-factor COX regression analyses based on the TCGA data set and the patients' clinical characteristics to verify whether the CAF risk score could be used as an independent predictor of prognosis (Figures 6A, B). In addition, the Norton chart results showed that the CAF risk score had the greatest weighting and stronger prognostic power (Figures 6C, D). Above results showed that the CAF score could be used as an independent predictor of prognosis.

3.6 CAFs prognostic signature correlates with immune infiltration and tumor development

We explored the relationship between CAF risk score groupings and each tumor microenvironment cell (immune cells and stromal cells) and each immune score, and characterized its expression with a heat map, which showed that CAF infiltration did not correlate exactly positively with risk score, but patients with high-risk score had relatively low CAF infiltration (Figure 7A). Finally, based on the gene expression data profile of the high and low risk score groups, the R package clusterprofiler was used to enrich for 50 tumor-associated hallmark pathways, and we observed significant changes in the regulation of genes in the tumor-associated pathways (Figure 7B). In addition, we also analyzed the correlational relationship of the CAFs scores and the immune cells infiltration biomarker and immune suppression biomarkers using TCGA database (Figure 3S), and found a significant negative correlation between CAFs and CD 8, CD 25, and CD 206.

3.7 CAFs prognosis signature-associated drug resistance assessment

Finally, we assessed the relationship between risk score and drug resistance in cell lines. From the CCLE (https://sites.broadinstitute.org/ccle)

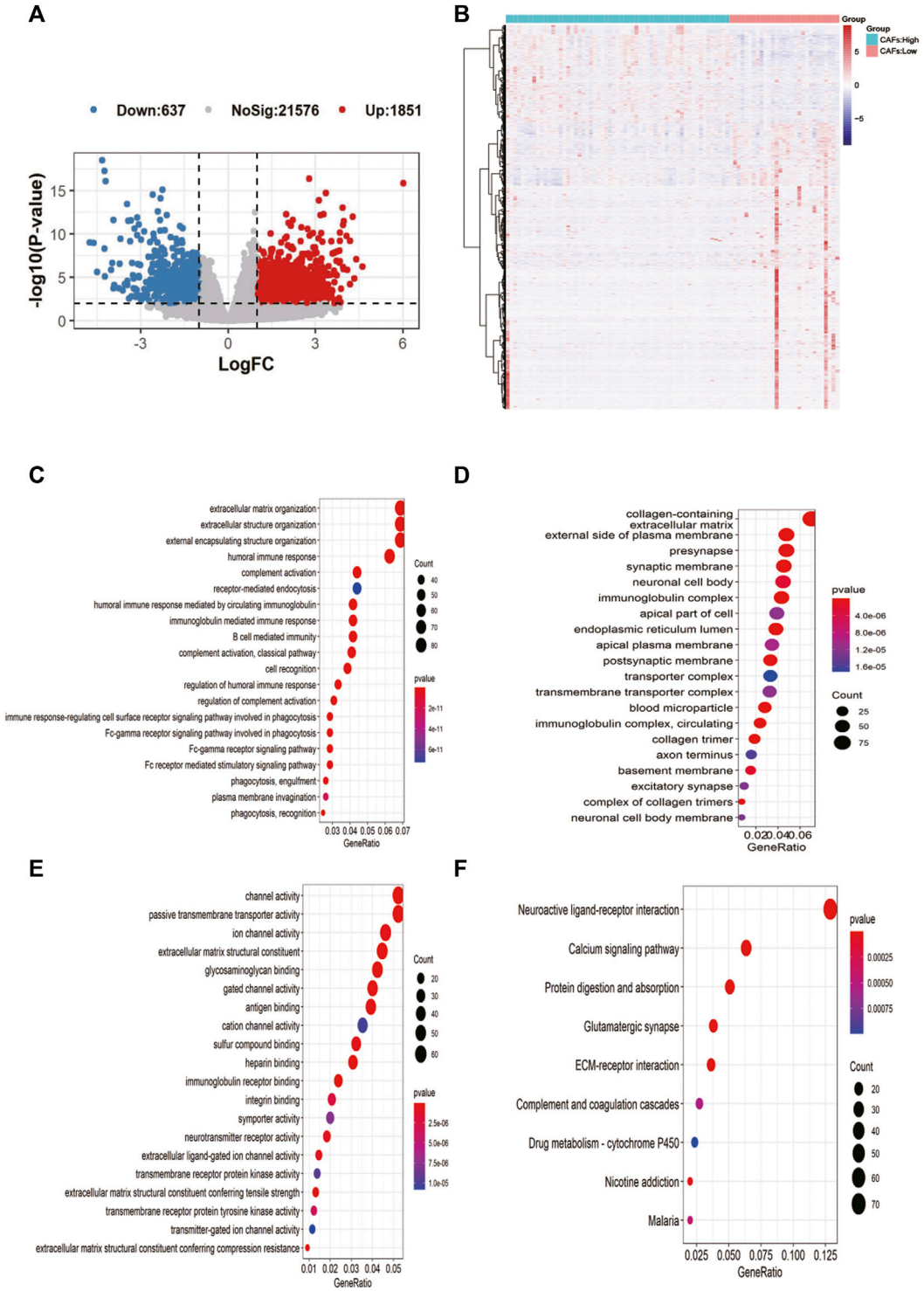

FIGURE 4
Screening of candidate gene markers of CAFs and functional analysis. **(A)** Volcano plot of differentially expressed genes between high and low CFAs score groups. **(B)** Expression profiles of differentially expressed genes between high and low CFAs score groups. **(C–E)**: Enrichment results for BP, MF, and CC pathways in the GO database. **(F)** Results of pathway enrichment in KEGG.

we downloaded information on 471 cell lines with expression profile data and resistance information (IC50) to 24 drugs, showing significant differences between the high and low scoring groups for 17-AAG, AZD6244, PD-0325901 and Sorafenib, there were significant differences between the high and low risk score groups (Figure 8A). We also analyzed the relationship between the expression of risk score model genes (RHBDL2, CORT, CGREF1) and drug resistance; we screened for significant

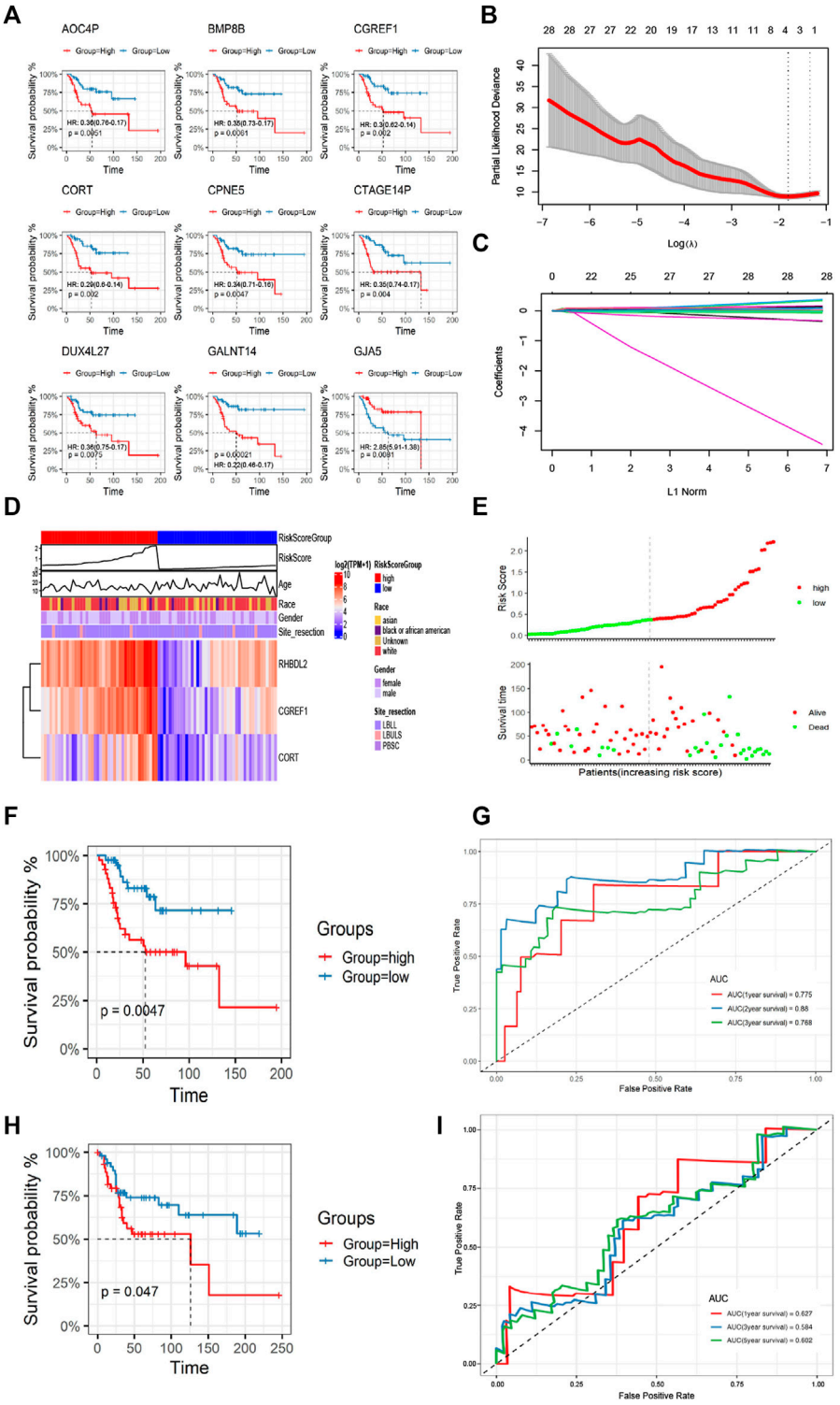

FIGURE 5
Construction and validation of CAFs prognostic signatures. **(A)** K-M survival analysis of Top 9 prognostic signatures. **(B)** A LASSO regression model was constructed using 28 candidate genes. **(C)** LASSO regression parameters were adjusted by cross validation. **(D, E)** Differences in the distribution of risk scores and prognostic signatures expression between high-risk and low-risk score groups. **(F, G)** The CAFs prognostic signatures were verified by K-M survival analysis and ROC curve drawing using TCGA training set. **(H, I)** The GSE21257 and GSE39058 cohorts were used for K-M survival analysis and ROC curve to verify the CAFs prognostic signatures.

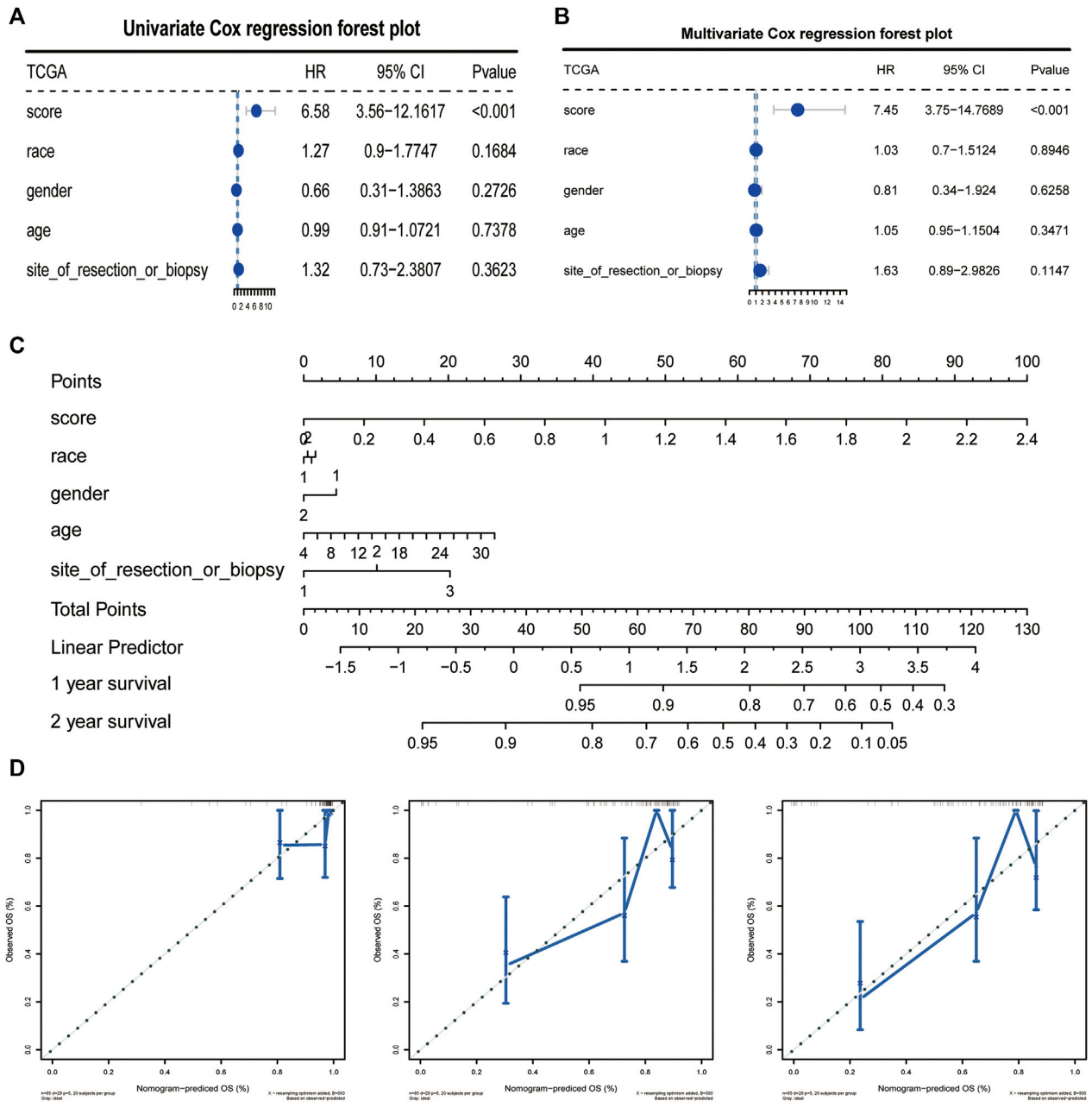

FIGURE 6
CAFs prognostic signatures could be used as an independent prognostic factor for OS. **(A, B)** CAFs risk score could be an independent prognostic factor confirmed by univariate and multivariate COX retrospective analyses. **(C)** Norton plot with clinical information. **(D)** Correction curves for one, three and 5 years.

differences in IC50 drug response between the high and low scoring groups based on median expression (Figures 8B–D); Finally, we observed a correlation between the IC50 response and gene expression, which confirmed the above findings (Figure 8E). To further validate the drug sensitivity in osteosarcoma cells, we used CCK-8 to measure the cellular viability. We demonstrate that the cell viability of HOS and MG63 cell lines was marked suppressed after 17-AAG, AZD6244, PD-0325901 and Sorafenib induction (Supplementary Figure S2).

5 Discussion

In recent years, numerous studies have shown that CAFs could play a regulatory role in tumors such as pancreatic and colorectal cancers by affecting stromal-tumor cell interactions, immune feedback, angiogenesis, and extracellular matrix remodeling (Kobayashi et al, 2019). Previous studies have reported a regulatory role of CAFs in the progression of osteosarcoma (Wang et al, 2019b; Zhao et al, 2021); however,

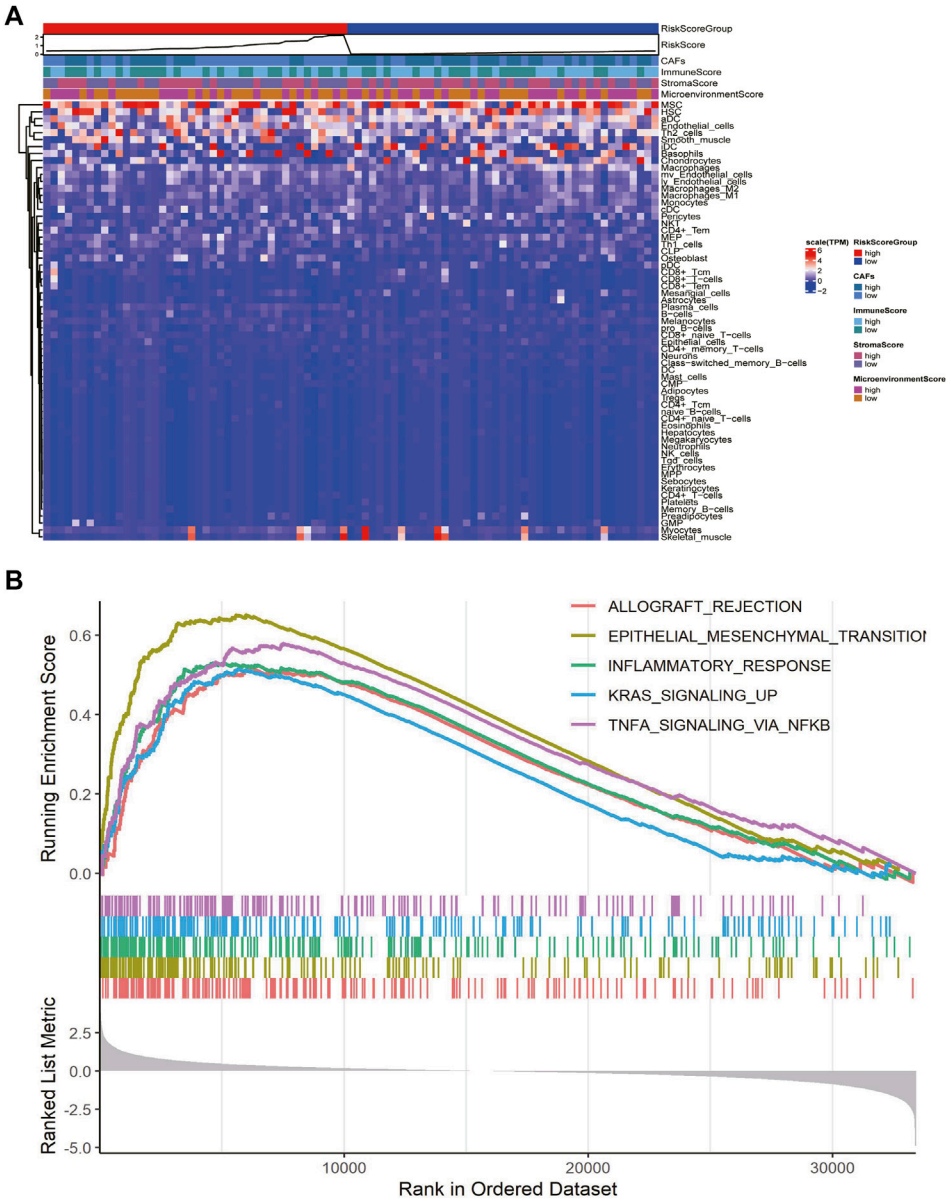

FIGURE 7
CAFs prognostic signatures associated with immune infiltration and tumor progression. **(A)** Heatmaps of immune cells and immune scores corresponding to high and low risk scores of CAFs. **(B)** Results of hallmark pathway enrichment between high and low score groups.

studies on the overall function of CAFs in osteosarcoma are still limiting.

In the current study, we examined the role of CAF infiltration and clustering in predicting osteosarcoma prognosis. Based on XCELL calculation of enrichment scores and grouping by median scores, interestingly, we show for the first time that CAF high infiltration group has a better prognosis, and this difference may come from the dual pro-tumorigenic and tumor-suppressive roles of CAFs exhibited simultaneously in different tumor microenvironments (Wang et al, 2021). Our results also showed that the enrichment score of CAFs was positively and significantly correlated with stromal cell score and chondrocyte content, implying that CAFs might occupy a dominant position in the stromal component of osteosarcoma. Although studies surrounding the role of CAFs in tumors have gradually increased in recent years, there are few studies on the role of CAFs in the prognostic evaluation of osteosarcoma. In the present study, we evaluated that the high infiltration of CAFs plays a role in the prognosis of osteosarcoma, and the results suggest that CAFs risk score is an independent factor influencing the progression of osteosarcoma.

We identified numerous transcriptomic alterations and enrichment pathways in the CAFs highly infiltrated group compared with the low group. Enrichment by GO database and KEGG database showed that immune-related pathways such as B cell mediated immunity, humoral immune response are potentially critical pathways. We construct a survival risk model using CORT molecules, which are closely related to immune response (McCormick et al, 2015), and obtained good tumor risk prognosis, highlighting the potential role of immune-related

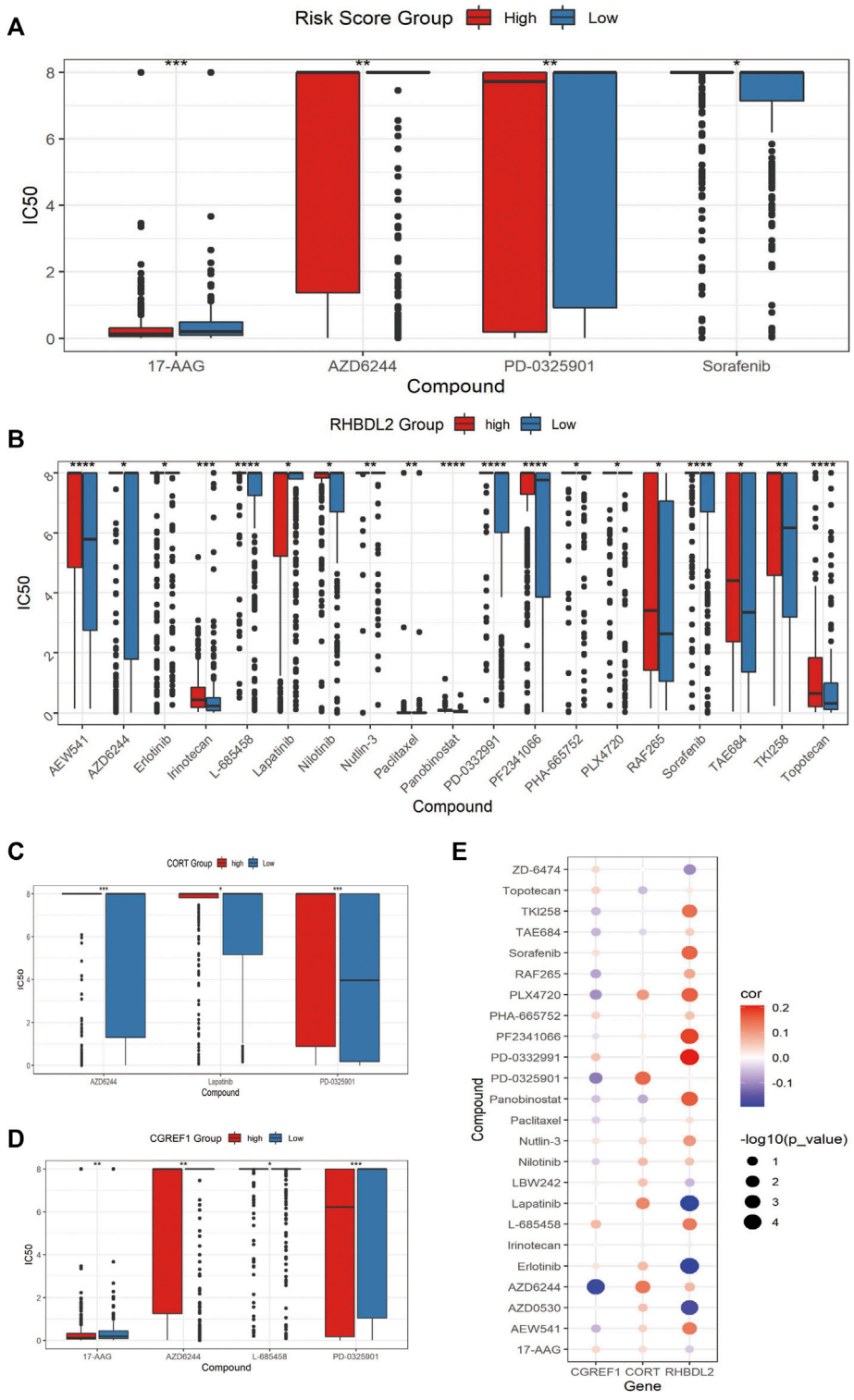

FIGURE 8
Assessment of associated resistance for CAFs prognostic signatures. **(A)** Drugs with significantly differentially in IC50 expression between high-risk and low-risk groups. **(B–D)**: Drugs with differential IC50 between high and low expression groups of RHBDL2, CORT, and CGREF1. **(E)** Correlation between RHBDL2, CORT, and CGREF1 expression and drug sensitivity.

pathways in the progression of osteosarcoma. In addition, whether greater benefit could be obtained with intervention of specific immune pathway inhibitors deserves to be further investigated.

Increasing evidence suggests that CAFs infiltrating in tumors might break down immunosuppression in tumors and further enhance tumor response to immunotherapy. Several current therapeutic strategies

targeting CAFs include direct depletion of CAFs by immunotherapy targeting cell surface markers; normalizing activated CAFs; and targeting CAFs secreted extracellular matrix proteins or their associated signals (Chen and Song, 2019; Liu et al, 2019). Nanodrugs selectively target CAFs has also been shown to enhance infiltration of cytotoxic T-cells thereby to suppress tumor proliferation (Zhen et al, 2017). Studies have shown that the synergistic effect of immune checkpoint molecules and targeted CAFs may enhance the immunotherapeutic response by modulating the immunosuppressive environment (Feig et al, 2013). Our study indicates that CAFs in the extracellular matrix may be involved in the induction and formation of immune microenvironment during osteosarcoma progression and induce the phenotypic transformation of the tumor. Therefore, a better understanding of the interaction between CAFs and antitumor immunity would be beneficial for the establishment of effective immunotherapy. The emerging approaches such as single-cell RNA sequencing (Moncada et al, 2020) and spatial transcriptome (Xu et al, 2021) could provide a more comprehensive understanding of the spatial and temporal dynamics of CAFs interactions with tumor and immune cells and their specific roles in the osteosarcoma stroma.

With the function of producing inflammatory ligands, grown factors and extracellular matrix which could facilitate the tumor growth, resistance to treatment and immune escape, CAFs are always considered as the factor that promote tumorigenesis (Kalluri, 2016). However, with the establishment of new co-culture model and the development of single-cell RNA-sequencing (scRNA-seq) techniques, the subpopulation of CAFs has been found (Öhlund et al, 2017; Elyada et al, 2019; Hu et al, 2022). Öhlund et al (2017) found two different subclasses of CAFs. One group is distributed around tumor cells and highly expresses α-smooth muscle actin (α-SMA), which can produce connective tissue-forming matrix and is named myofibroblast CAFs (myCAFs). The other group is located far from the tumor cells, which is low in α-SMA expression and can secrete inflammatory factors such as IL-6, and is called inflammatory CAFs (iCAFs). In addition, based on scRNA-seq analysis, the study of Elyada et al identified three different CAFs subsets in pancreatic ductal adenocarcinoma. In addition to myCAFs and iCAFs which are previously identified, antigen presenting CAFs (apCAFs) that can utilize cell-expressed MHC II complexes and CD74 for antigen presentation have also been identified, which can present antigen to T-cells and play an anti-tumor role (Elyada et al, 2019). In this study, we found a prediction role of CAFs in the prognosis of OS, a further investigation might be need to clarify the prediction function of each subpopulation of CAFs in OS prognosis with the application of scRNA-seq analysis.

There are limitations present in the present study. First, we did not perform experiments to validate the relationships between CAFs and immune cells which were estimated by purely bioinformatic methods. Whether the conclusions obtained can be consistent with the real world should be viewed with caution. In the study, to reduce the possible bias brought by the analytical approach to CAFs, we scored CAFs using ordered categorical variables, resulting in a more consistent high CAF group or low CAF group. In this study, the data were processed by the XCELL computational algorithm after screening the MCPCOUNTER, XCELL, and EPIC algorithms, and the type abundance of cells was quantified by database-based cell labeling or deconvolution of cell mixtures based on gene expression matrices, and the above-mentioned methods allowed comparison between samples with identical cell types. In addition, multiple datasets from TCGA and GEO were used in this study to make the results obtained more robust, so the conclusions drawn in this study can still provide implications for interpreting the clinical and biological significance of CAFs. Second, large tumor tissues are a mixture of tumor cells themselves, stromal cells and immune cells as a whole, and transcriptomic changes and pathway alterations in each composed of them still need more experimental studies in the future. Meanwhile, this paper's description of the role of CAFs on the clinical characteristics, clinical prognosis and prediction of the immune microenvironment of patients did not consider the subtypes and the spatial-temporal heterogeneity of CAFs. As there is a lack of universal markers for CAFs (Mueller and Fusenig, 2004; Biffi and Tuveson, 2021), the panorama of CAFs is difficult to be observed. ScRNA-seq technology has provided new insights in recent years. The identification of CAF subtypes in osteosarcoma using scRNA-seq technology has been reported (Huang et al, 2022). It is expecting that the gaps in this research area would be filled soon.

Data availability statement

The original contributions presented in the study are included in the article/Supplementary Material, further inquiries can be directed to the corresponding authors.

Author contributions

HX, WZ, and ZT proposed the idea of the study, ZZ, JC, ZX, and MY carried out the analysis and statistical work of the paper, WT, YY, YZ, and ZJ performed the experiment for the work. HX and WZ provided instructions for the article. All authors contributed to the article writing and approved the submitted version.

Conflict of interest

The authors declare that the research was conducted in the absence of any commercial or financial relationships that could be construed as a potential conflict of interest.

Publisher's note

Supplementary material

The Supplementary Material for this article can be found online at: https://www.frontiersin.org/articles/10.3389/fphar.2023.1136960/full#supplementary-material

SUPPLEMENTARY FIGURE S1
Forest plots for assessments of risk scores and prognostic effect using multifactorial COX survival analysis for genes in TCGA database **(A)** and GEO database **(B)**.

SUPPLEMENTARY FIGURE S2
Validation of candidate genes and drug sensitivity. **(A–C)**: Validation of expression level of CGREF1, CORT and RHBDL2 in osteosarcoma and para-cancer tissue by IHC analysis. **(D–E)**: Verification of the sensitivity for 17-AAG, AZD6244, PD-0325901 and Sorafenib in HOS and MG63 cell lines by testing the cellular viability with CCK-8 measurement.

SUPPLEMENTARY FIGURE S3
The correlational relationship of the CAFs scores and the markers of immune cells infiltration and immune suppression. **(A)**: Correlation analysis on the CAFs score and the expression level of immune cells infiltration biomarker CD 8; **(B–D)**: Correlation analysis on the CAFs score and the expression level of immune suppression biomarker CD 4, CD 25, and CD 206.

References

Biffi, G., and Tuveson, D. A. (2021). Diversity and biology of cancer-associated fibroblasts. *Physiol. Rev.* 101 (1), 147–176. doi:10.1152/physrev.00048.2019

Chen, X., and Song, E. (2019). Turning foes to friends: Targeting cancer-associated fibroblasts. *Nat. Rev. Drug Discov.* 18 (2), 99–115. doi:10.1038/s41573-018-0004-1

Elyada, E., Bolisetty, M., Laise, P., Flynn, W. F., Courtois, E. T., Burkhart, R. A., et al. (2019). Cross-species single-cell analysis of pancreatic ductal adenocarcinoma reveals antigen-presenting cancer-associated fibroblasts. *Cancer Discov.* 9 (8), 1102–1123. doi:10.1158/2159-8290.CD-19-0094

Feig, C., Jones, J. O., Kraman, M., Wells, R. J., Deonarine, A., Chan, D. S., et al. (2013). Targeting CXCL12 from FAP-expressing carcinoma-associated fibroblasts synergizes with anti-PD-L1 immunotherapy in pancreatic cancer. *Proc. Natl. Acad. Sci. U. S. A.* 110 (50), 20212–20217. doi:10.1073/pnas.1320318110

Hu, B., Wu, C., Mao, H., Gu, H., Dong, H., Yan, J., et al. (2022). Subpopulations of cancer-associated fibroblasts link the prognosis and metabolic features of pancreatic ductal adenocarcinoma. *Ann. Transl. Med.* 10 (5), 262. doi:10.21037/atm-22-407

Huang, X., Wang, L., Guo, H., Zhang, W., and Shao, Z. (2022). Single-cell transcriptomics reveals the regulative roles of cancer associated fibroblasts in tumor immune microenvironment of recurrent osteosarcoma. *Theranostics* 12 (13), 5877–5887. doi:10.7150/thno.73714

Ishii, G., Ochiai, A., and Neri, S. (2016). Phenotypic and functional heterogeneity of cancer-associated fibroblast within the tumor microenvironment. *Adv. Drug Deliv. Rev.* 99 (Pt B), 186–196. doi:10.1016/j.addr.2015.07.007

Kalluri, R. (2016). The biology and function of fibroblasts in cancer. *Nat. Rev. Cancer* 16 (9), 582–598. doi:10.1038/nrc.2016.73

Kalluri, R., and Zeisberg, M. (2006). Fibroblasts in cancer. *Nat. Rev. Cancer* 6 (5), 392–401. doi:10.1038/nrc1877

Kansara, M., Teng, M., Smyth, M., and Thomas, D. (2014). Translational biology of osteosarcoma. *Nat. Rev. Cancer* 14 (11), 722–735. doi:10.1038/nrc3838

Keil, L. (2020). Bone tumors: Primary bone cancers. *FP Essent.* 493, 22–26.

Kobayashi, H., Enomoto, A., Woods, S. L., Burt, A. D., Takahashi, M., and Worthley, D. L. (2019). Cancer-associated fibroblasts in gastrointestinal cancer. *Nat. Rev. Gastroenterol. Hepatol.* 16 (5), 282–295. doi:10.1038/s41575-019-0115-0

Liotta, L. A., and Kohn, E. C. (2001). The microenvironment of the tumour-host interface. *Nature* 411 (6835), 375–379. doi:10.1038/35077241

Liu, T., Han, C., Wang, S., Fang, P., Ma, Z., Xu, L., et al. (2019). Cancer-associated fibroblasts: An emerging target of anti-cancer immunotherapy. *J. Hematol. Oncol.* 12 (1), 86. doi:10.1186/s13045-019-0770-1

McCormick, G. L., Shea, K., and Langkilde, T. (2015). How do duration, frequency, and intensity of exogenous CORT elevation affect immune outcomes of stress? *Gen. Comp. Endocrinol.* 222, 81–87. doi:10.1016/j.ygcen.2015.07.008

Moncada, R., Barkley, D., Wagner, F., Chiodin, M., Devlin, J. C., Baron, M., et al. (2020). Integrating microarray-based spatial transcriptomics and single-cell RNA-seq reveals tissue architecture in pancreatic ductal adenocarcinomas. *Nat. Biotechnol.* 38 (3), 333–342. doi:10.1038/s41587-019-0392-8

Mueller, M. M., and Fusenig, N. E. (2004). Friends or foes - bipolar effects of the tumour stroma in cancer. *Nat. Rev. Cancer* 4 (11), 839–849. doi:10.1038/nrc1477

Öhlund, D., Handly-Santana, A., Biffi, G., Elyada, E., Almeida, A. S., Ponz-Sarvise, M., et al. (2017). Distinct populations of inflammatory fibroblasts and myofibroblasts in pancreatic cancer. *J. Exp. Med.* 214 (3), 579–596. doi:10.1084/jem.20162024

Robison, L., and Hudson, M. (2014). Survivors of childhood and adolescent cancer: Life-long risks and responsibilities. *Nat. Rev. Cancer* 14 (1), 61–70. doi:10.1038/nrc3634

Turley, S. J., Cremasco, V., and Astarita, J. L. (2015). Immunological hallmarks of stromal cells in the tumour microenvironment. *Nat. Rev. Immunol.* 15 (11), 669–682. doi:10.1038/nri3902

Wang, J. W., Wu, X. F., Gu, X. J., and Jiang, X. H. (2019b). Exosomal miR-1228 from cancer-associated fibroblasts promotes cell migration and invasion of osteosarcoma by directly targeting SCAI. *Oncol. Res.* 27 (9), 979–986. doi:10.3727/096504018X15336368805108

Wang, S., He, Z., Wang, X., Li, H., and Liu, X. S. (2019a). Antigen presentation and tumor immunogenicity in cancer immunotherapy response prediction. *Elife* 8, e49020. doi:10.7554/eLife.49020

Wang, Z., Yang, Q., Tan, Y., Tang, Y., Ye, J., Yuan, B., et al. (2021). Cancer-associated fibroblasts suppress cancer development: The other side of the coin. *Front. Cell Dev. Biol.* 9, 613534. doi:10.3389/fcell.2021.613534

Xu, R., Zhou, X., Wang, S., and Trinkle, C. (2021). Tumor organoid models in precision medicine and investigating cancer-stromal interactions. *Pharmacol. Ther.* 218, 107668. doi:10.1016/j.pharmthera.2020.107668

Yahiro, K., and Matsumoto, Y. (2021). Immunotherapy for osteosarcoma. *Hum. Vaccin Immunother.* 17 (5), 1294–1295. doi:10.1080/21645515.2020.1824499

Zhao, A., Zhao, Z., Liu, W., Cui, X., Wang, N., Wang, Y., et al. (2021). Carcinoma-associated fibroblasts promote the proliferation and metastasis of osteosarcoma by transferring exosomal LncRNA SNHG17. *Am. J. Transl. Res.* 13 (9), 10094–10111.

Zhen, Z., Tang, W., Wang, M., Zhou, S., Wang, H., Wu, Z., et al. (2017). Protein nanocage mediated fibroblast-activation protein targeted photoimmunotherapy to enhance cytotoxic T cell infiltration and tumor control. *Nano Lett.* 17 (2), 862–869. doi:10.1021/acs.nanolett.6b04150

Ziani, L., Chouaib, S., and Thiery, J. (2018). Alteration of the antitumor immune response by cancer-associated fibroblasts. *Front. Immunol.* 9, 414. doi:10.3389/fimmu.2018.00414

Frontiers in Pharmacology

Explores the interactions between chemicals and living beings

The most cited journal in its field, which advances access to pharmacological discoveries to prevent and treat human disease.

Discover the latest Research Topics

See more →

Frontiers

Avenue du Tribunal-Fédéral 34
1005 Lausanne, Switzerland
frontiersin.org

Contact us

+41 (0)21 510 17 00
frontiersin.org/about/contact